

**Connections in  
Steel  
Structures III**

**Behaviour, strength & design**

**Edited by  
Reidar Sjørbøvde  
André Colson  
Riccardo Zandonini**

**Pergamon**

CONNECTIONS  
IN  
STEEL STRUCTURES  
III

Behaviour, Strength and Design

### **Elsevier Titles of Related Interest**

TANAKA & CRUSE

Boundary Element Methods in Applied Mechanics

CHRYSSOSTOMIDIS

BOSS '94, Behaviour of Offshore Structures (3 Volume Set)

GODOY

Thin-Walled Structures with Structural Imperfections: Analysis and Behavior

OEHLERS & BRADFORD

Composite Steel and Concrete Structural Members: Fundamental Behaviour

OLHOFF & ROZVANY

Structural and Multidisciplinary Optimization

SHANMUGAM & CHOO

4th Pacific Structural Steel Conference - Structural Steel (3 Volume Set)

### **Related Journals**

*Free specimen copy gladly sent on request: Elsevier Science Ltd, The Boulevard, Langford Lane, Kidlington, Oxford, OX5 1GB, U.K.*

Advances in Engineering Software

Composite Structures

Computers and Structures

Construction and Building Materials

Engineering Analysis with Boundary Elements

Engineering Failure Analysis

Engineering Structures

Finite Elements in Analysis and Design

International Journal of Solids and Structures

Journal of Constructional Steel Research

Marine Structures

Mathematical and Computer Modelling

Ocean Engineering

Reliability Engineering and System Safety

Soil Dynamics and Earthquake Engineering

Structural Engineering Review

Thin-Walled Structures

CONNECTIONS  
IN  
STEEL STRUCTURES  
III

Behaviour, Strength and Design

Proceedings of the Third International Workshop

held at

Hotel Villa Madruzzo

Trento, Italy

29 - 31 May 1995

*Edited by*

Reidar Bjorhovde

University of Pittsburgh, Pittsburgh, Pennsylvania, U.S.A.

André Colson

Ecole Nationale Supérieure des Arts et Industries de Strasbourg

Strasbourg, France

Riccardo Zandonini

University of Trento, Trento, Italy

Pergamon



- U.K. Elsevier Science Ltd, The Boulevard, Langford Lane,  
Kidlington, Oxford. OX5 1GB, England
- U.S.A. Elsevier Science Inc., 660 White Plains Road, Tarrytown, New  
York, 10591-5153, U.S.A.
- JAPAN Elsevier Science Japan, Tsunashima Building Annex, 3-20-12  
Yushima, Bunkyo-ku, Tokyo 113, Japan

---

Copyright © 1996 Elsevier Science

*All Rights Reserved. No part of this publication may be reproduced,  
stored in a retrieval system or transmitted in any form or by any means;  
electronic, electrostatic, magnetic tape, mechanical photocopying,  
recording or otherwise, without prior permission in writing from the  
publisher.*

First edition 1996

**Library of Congress Cataloging in Publication Data**

A catalogue record for this title is available from the Library of Congress.

**British Library Cataloguing in Publication Data**

A catalogue record for this title is available from the British Library.

ISBN 0-08-042821-5

## CONTENTS

Foreword	xi
Introductory Notes	xv
Reidar Bjorhovde (USA), André Colson (France) and Riccardo Zandonini (Italy)	
<b>COMPOSITE CONNECTIONS</b>	
Finite Element Modeling of Partially Restrained Beam-to-Girder Connections Clinton O. Rex and W. Samuel Easterling (USA)	1
Influence of Slip of the Shear Connection on Composite Joint Behaviour Jean-Marie Aribert (France)	11
The Use of a Rolled Wide-Flange as a Bridge Support Bearing Joseph M. Ales Jr. and Joseph A. Yura (USA)	23
Prediction Method for Moment-Rotation Behaviour of Composite Beam to Steel Column Connection Ping Ren (Luxembourg) and Michel Crisinel (Switzerland)	33
Performance of Mixed Connections under Combined Loads Yasuhiro Ohtani, Yuhshi Fukumoto and Bunzo Tsuji (Japan)	47
Experimental Behaviour of Semi-Rigid Connections in Frames F. Benussi (Italy), D.A. Nethercot (England) and R. Zandonini (Italy)	57
<b>SPECIAL CONNECTIONS</b>	
Connection Between Steel Beams and Concrete Filled R.H.S. Based on the Stud Technique (Threaded Stud) Didier Vandegans and Josè Janss (Belgium)	67
Design of Bolted Connections with Injection Bolts A.M. (Nol) Gresnigt and J.W.B. (Jan) Stark (The Netherlands)	77
Welded Connections in Thin Cold-Formed Rectangular Hollow Sections Xiao-Ling Zhao and Gregory Hancock (Australia)	89
Seismic Performance of CFT Column-to-WF Beam Moment Connections James M. Ricles, Le-Wu Lu, Took K. Sooi and G. Vermaas (USA)	99
Fatigue Behaviour of Mis-Matched Butt Welded Heavy I-Beams and the Rotation Capacity of Joints Made of QST-Steel Ömer Bucak (Germany), Friedrich Mang (Germany) and Lex Stammet (Luxembourg)	115

The Static Strength and Behaviour of Uniplanar and Multiplanar Connections between I-Beams and RHS Columns L.H. Lu and J. Wardenier (The Netherlands)	127
The Static Strength and Behaviour of Multiplanar I-Beam to Tubular Column Connections Loaded with In-Plane Bending Moments G.D. de Winkel and J. Wardenier (The Netherlands)	137
<b>DESIGN METHODS</b>	
Design Methods for Truss and Bracing Connections W.A. Thornton (USA)	149
Steel Moment Connections According to Eurocode 3. Simple design aids for rigid and semi-rigid joints J.P. Jaspart (Belgium)	159
Strength of Moment End-Plate Connections with Multiple Bolt Rows at the Beam Tension Flange Thomas M. Murray and Jeffrey T. Borgsmiller (USA)	169
Stiffened Seated Connections on Column Webs Duane S. Ellifritt, Thomas Sputo and Andrew S. Miller (USA)	179
Partial Fixity from Simple Beam Connections S.A. Ioannides (USA)	191
Estimates of Ductility Requirements for Simple Shear Connections W.A. Thornton (USA)	201
Plastic Design of Semi-Rigid Frames Roberto T. Leon and Jerod J. Hoffman (USA)	211
Eurocode 4 and Design of Composite Joints David Anderson (England)	223
Mechanical Modeling of Semi-Rigid Joints for the Analysis of Framed Steel and Composite Structures F. Tschemmernegg (Austria) and G. Queiroz (Brazil)	237
Proposal of the Stiffness Design Model of the Column Bases František Wald, Zdeněk Sokol (Czech Republic) and Martin Steenhuis (The Netherlands)	249
<b>MODELLING OF CONNECTIONS</b>	
Modelling Composite Connection Response B. Ahmed, T.Q. Li and D.A. Nethercot (England)	259

Moment-Rotation Model of Steel-to-Concrete End-Plate Connections László Dunai, Sándor Adány (Hungary) and Yuhshi Fukumoto (Japan)	269
Some Basic Principles for Semi-Rigid Concept André Colson (France)	279
Behaviour and Modeling of Top & Seat and Top & Seat and Web Angle Connections Antonello De Luca (Italy)	289
<b>FRAME BEHAVIOUR</b>	
Characteristic Semi-Rigid Connection Relationships for Frame Analysis and Design Donald W. White and Wai-Fah Chen (USA)	299
Large-Scale Tests on Steel Frames with Semi-Rigid Connections. Effect of Beam-Column Connections and Column-Bases Miklós Iványi (Hungary)	309
Influence of Structural Frame Behaviour on Joint Design Stephane Guisse and Jean-Pierre Jaspert (Belgium)	321
Reliability of Steel Structures with Semi-Rigid Connections A. Sellier, A. Mébarki, A. Colson (France) and R. Bjorhovde (USA)	331
Evaluation on Static and Dynamic Structural Coefficient of Steel Frames with Semi-Rigid Joints Via Numerical Simulations Dan Dubina, Daniel Grecea and Raul Zaharia (Romania)	349
<b>CYCLIC RESPONSE</b>	
Seismic Loading of Moment End-Plate Connections: Some Preliminary Results Thomas M. Murray and Ronald L. Meng (USA)	361
Low Cycle Fatigue Testing of Semi-Rigid Beam-to-Column Connections Luis Calado (Portugal) and Carlo Castiglioni (Italy)	371
Development of Interim Recommendations for Improved Welded Moment Connections in Response to the Northridge Earthquake Michael D. Engelhardt, Thomas A. Sabol, Riyad S. Aboutaha and Karl H. Frank (USA)	381
Post-Earthquake Stability of Steel Moment Frames with Damaged Connections Abolhassan Astaneh-Asl (USA)	391

**DESIGN STANDARDS**

Serviceability Limit State for Cold-Formed Steel Bolted Connections Roger A. LaBoube, Wei-Wen Yu and Jeffrey L. Carril (USA)	403
An Attempt of Codification of Semirigidity for Seismic Resistant Steel Structures Federico M. Mazzolani and Vincenzo Piluso (Italy)	413
Advances in Connection Design in the United States Charles J. Carter (USA)	423
Criteria for the Use of Preloaded Bolts in Structural Joints J.W.B. (Jan) Stark (The Netherlands)	431
The Stiffness Model of revised Annex J of Eurocode 3 Klaus Weynand (Germany), Jean-Pierre Jaspart (Belgium) and Martin Steenhuis (The Netherlands)	441
Safety Considerations of Annex J of Eurocode 3 Markus Feldmann, Gerhard Sedlacek and Klaus Weynand (Germany)	453
Design of Fillet Welds in Rectangular Hollow Section T,Y and X Connections Using New North American Code Provisions Jeffrey A. Packer (Canada)	463
Requirements and Capabilities for Composite Connections in Non-Sway Frames David A. Nethercot (England)	473
The Use of the Iso Bolts, in Accordance with the European Standards Eugène Piraprez (Belgium)	483
<b>STATE OF PRACTICE</b>	
From Design Drawings to Structure. The Role of the Fabricator's Engineer in Developing Connections in USA Lawrence A. Kloiber (USA)	493
PR Connections in Design Practice Arvind V. Goverdhan and Stanley D. Lindsey (USA)	505
Strength and Installation Characteristics of Tension Control Bolts Geoffrey L. Kulak and Scott T. Undershute (Canada)	515
Economic Comparisons between Simple and Partial Strength Design of Braced Steel Frames David Anderson and Mahmood Md Tahir (England)	527

## Contents

ix

A Review of Connection Research and Development in the UK D.B. Moore (England)	535
Performance of Moment Resisting Steel Frames in the January 17 1994 Northridge Earthquake James O. Malley (USA)	553
<b>CONNECTIONS IN AUSTRALIA</b>	
Connection Research, Design and Practice in Australia Gregory Hancock, Arun Syam, Bruce Chapman and Tim Hogan (Australia)	563
<b>CURRENT RESEARCH NEEDS FOR CONNECTIONS IN STEEL STRUCTURES</b>	
Research Topics for Composite Connections; Special Connections; Design Methods; Modelling of Connections; Frame Behaviour; Cyclic Response; Design Standards; State of Practice	577
<b>APPENDIX</b>	
Attendees of the Third International Workshop on Connections In Steel Structures	583
<b>AUTHOR INDEX</b>	589
<b>KEYWORD INDEX</b>	591

**The Third International Workshop**

on

**Connections in Steel Structures**

was sponsored by

**American Institute of Steel Construction**

Chicago, Illinois, U S A

**Commission of European Communities**

through the

**COST C1 Project**

**European Convention for Constructional Steelwork**

Brussels, Belgium

**Department of Structural Mechanics and Design Automation  
University of Trento**

Trento, Italy

## FOREWORD

This book is the Proceedings of the *Third International Workshop on Connections in Steel Structures: Behaviour, Strength and Design*, held at the Hotel Villa Madruzzo in Trento, Italy, during the period 29-31 May, 1995, under the auspices of the Department of Structural Mechanics and Design Automation of the University of Trento. The First International Workshop was held at Ecole Normale Supérieure de Cachan, in Cachan, France, 25-27 May, 1987, and its Proceedings was published by Elsevier Applied Science Publishers in 1988. The Second International Workshop was held at the Westin William Penn Hotel in Pittsburgh, Pennsylvania, USA, during the period 10-12 April, 1991, under the auspices of the Department of Civil Engineering of the University of Pittsburgh. The Proceedings was published by the American Institute of Steel Construction in 1992.

The workshop organizers wish to express their sincere thanks to the organizations that made the workshop possible through co-sponsor support and other assistance. Thus, the keen interest of the American Institute of Steel Construction and the Commission of European Communities, through the COST C1 project, directed by Professor André Colson, and the European Convention for Constructional Steelwork, is much appreciated.

The Department of Structural Mechanics and Design Automation of the University of Trento was the official host of the workshop, through its Head, Professor Riccardo Zandonini. Extensive logistical and other support was provided by the department, in particular through the work of Mrs. Rosanna Veronesi and research associate Claudio Bernuzzi.

A number of the workshop participants served as technical session chairmen and reporters. In particular, the efforts of Messrs. Donald W. White, Purdue University; David Anderson, University of Warwick; and Jean Pierre Jaspart, University of Liege, who accepted the demanding assignments as Research Reporters for the workshop, are acknowledged.

The support and technical contributions of the participants, without which the workshop would not have been possible, are sincerely acknowledged and appreciated. It is hoped that the kind of international cooperation that has been facilitated by the First, Second and Third International Workshops will continue to enhance research and development efforts in steel structures worldwide.

Trento, Italy

August, 1995

Reidar Bjorhovde

André Colson

Riccardo Zandonini

## INTRODUCTORY NOTES

**Reidar Bjorhovde**

Chairman  
Department of Civil and Environmental Engineering  
University of Pittsburgh  
Pittsburgh, Pennsylvania, U S A

**Andre Colson**

Director  
Ecole Nationale Supérieure des Arts et Industries de Strasbourg  
Strasbourg, France

**Riccardo Zandonini**

Head  
Department of Structural Mechanics and Design Automation  
University of Trento  
Trento, Italy

The success of the First and Second International Workshops on Connections in Steel Structures provided the impetus for the Third. The first was held in 1987; this event was conceived by Messrs. Bjorhovde, Brozzetti and Colson, and following the invitation of 40 internationally recognized research and design experts in the area of steel structures and connections, 37 individuals accepted the challenge to present state-of-the-

art reports on this important specialty of the structural engineering profession. Representing 15 countries, these researchers and their colleagues presented a total of 41 papers, co-authored by 76 individual authors. The Proceedings of the 1987 workshop, which was held in Cachan, near Paris, France, document the technical papers as well as the discussions and the research needs that presented themselves at the time.

The second workshop was held in Pittsburgh, Pennsylvania, USA, in 1991. Using the same type of attendance by invitation only format, 60 internationally recognized research, design and fabricated steel construction experts accepted the challenge to present state-of-the-art reports. Representing 19 countries, these researchers and their colleagues presented a total of 60 papers, authored or co-authored by 81 individuals. A number of the papers were the result of true international cooperation, with authors coming from different countries. The Proceedings of the 1991 workshop document the technical papers as well as the discussions and the research needs that presented themselves at the time.

Preparing for the third workshop, it was decided to retain the format of attendance by invitation only. The original rationale was that restricted participation would allow for the most advanced topics to be considered, without the need to bring everyone to a common base of knowledge, so to speak. In other words, by gathering expert only, it was felt that it would be possible to move the farthest and fastest in the assessments of ongoing research, developments, and research needs. The first and second workshops proved this format to be an unqualified success, so much so that since then, a number of restricted attendance workshops have been held, dealing with many and diverse subject areas.

A total of 53 internationally recognized experts were invited to participate in the third workshop, and 51 accepted the challenge, representing 18 countries. 52 papers with 92 authors and co-authors were submitted; these represent the primary contents of this book.

In the initial planning of the workshop program, some of the subject areas addressed in 1987 and 1991 obviously had such broad interest that it would be important to consider what further progress had been made. Thus, sessions on connection modeling, cyclic response and frame behaviour were selected. Similarly, subjects in the general area of semi-rigid connections continue to be important. Much work over the past 4 years has been dedicated to the development of design code criteria and practical implementation; a total of four sessions were organized to address such issues. Finally, research on connections for composite construction has continued in several centers around the world; one of the workshop sessions dealt with these topic.

As was done for the first and second workshops, Research Reporters monitored all technical sessions for suggestions for needed research and development. The topics that were identified are presented in the last section of this book; they indicate the state-of-the-art as well as the broader outlook on the future of steel construction, considering connections as key elements.

Technical Papers on

**COMPOSITE CONNECTIONS**

## FINITE ELEMENT MODELING OF PARTIALLY RESTRAINED BEAM-TO-GIRDER CONNECTIONS

Clinton O. Rex<sup>1</sup>

W. Samuel Easterling<sup>2</sup>

### Abstract

In recent years the design of steel framed composite floor systems has been controlled more often by serviceability criteria than by strength. It has been suggested that a partially continuous composite floor system would improve serviceability limit states; and that, partially restrained beam-to-girder connections are the key to such a floor system (Rex and Easterling 1994). A research project aimed at developing design methods and criteria for partially restrained beam-to-girder connections and partially continuous floor systems is currently in progress at Virginia Polytechnic Institute and State University (VPI). This paper focuses on a finite element modeling technique that is being used to predict the moment-rotation behavior of various beam-to-girder connections. This method relies heavily on the behavior models of various connection sub-elements (bolts, welds, etc...). These connection sub-element models are also discussed.

### 1. INTRODUCTION

In many cases concrete floor systems are chosen over steel framed composite floor systems in design situations where the overall floor depth is limited. Shallow concrete floor systems can be designed to meet both strength and serviceability design criteria while still remaining economical. Shallow steel framed composite floor systems can meet strength design criteria and remain economical thanks to advancements in composite beam design and the availability of low cost high strength steel. However, in many cases these systems are unable to meet serviceability design criteria while still remaining economical.

One possible method to improve both the strength and serviceability design aspects of a steel framed composite floor system is to design the system as partially continuous. The key to designing a partially continuous floor system lies in the design and analysis of the beam-to-girder connections. A research project investigating the design and analysis of partially

---

<sup>1</sup> Via Doctoral Fellow in the Charles E. Via, Jr. Department of Civil Engineering, Virginia Polytechnic Institute and State University, Blacksburg, VA, USA

<sup>2</sup> Associate Professor in the Charles E. Via, Jr. Department of Civil Engineering, Virginia Polytechnic Institute and State University, Blacksburg, VA, USA

restrained steel and composite beam-to-girder connections is currently in progress at Virginia Polytechnic and State University (VPI).

To date, four full scale composite beam-to-girder connections have been constructed and tested to failure (Rex and Easterling 1994). These four connections are shown schematically in Fig. 1. Connection #1 is a standard single plate shear connection which is commonly used in the United States. To enhance the moment resistance of beam-to-girder connections, both before and after concrete hardens, it was believed that the details of the connections would have to be changed from typical, currently used, details. Connections #2 through #4 represent varying degrees of departure from the typical connections. The results of the tests showed that these simple connections could develop significant rotational restraint and thus justified additional development.

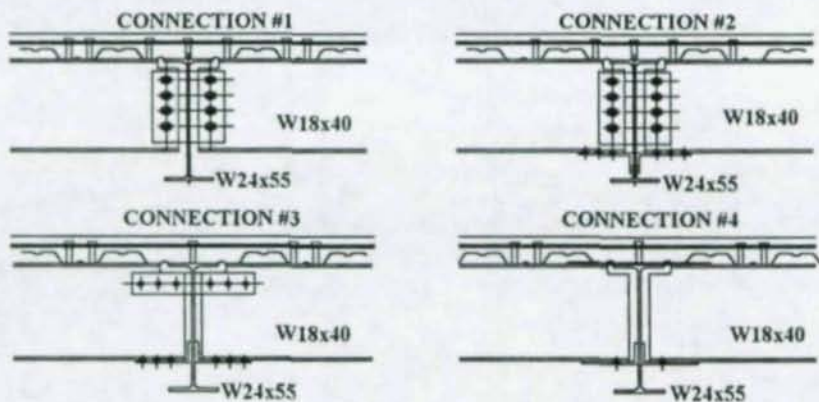


Figure 1 Partially Restrained Composite Beam-To-Girder Connections Tested

An analytical technique to model the moment-rotation behavior of the connections is needed to develop design methods and recommendations for partially restrained beam-to-girder connections. Currently, non-linear finite element analysis is being used.

## 2. FINITE ELEMENT MODELING

Finite element analysis is currently being used to model the partially restrained beam-to-girder connections. Certain simplifications have been adopted so that the finite element models do not become excessively complex. First, the three dimensional connection behavior is reduced to a two dimensional problem by ignoring out-of-plane effects. This is a common assumption made in most research involving connections. Second, the two dimensional problem is then further simplified by using only one dimensional finite elements placed in two dimensional space. The elements used are beam, truss, and non-linear spring elements. Beam elements are used to represent the beam and rigid links. Truss elements are used to represent reinforcing steel, concrete, and steel plates. Non-linear springs are used to represent shear studs, bolts, and welds. Schematics of the finite element models of Connections #1 through #4 are shown in Fig. 2.

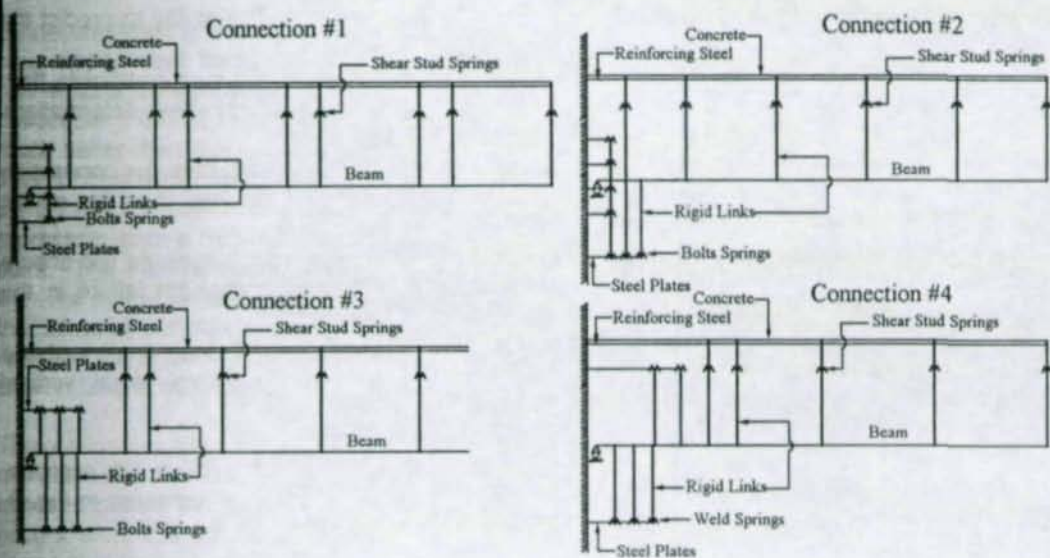


Figure 2 Finite Element Models Of Partially Restrained Beam-To-Girder Connections

Clearly these models have many assumptions and simplifications incorporated into them. Aside from ignoring out of plane effects (such as shear lag in the slab and instabilities in the steel) many in plane effects have been ignored as well. First, the flexural contribution of the concrete slab to the overall rotational resistance of the connection is considered negligible. Second, it is assumed that the composite deck remains in contact with the top flange of the beam at all times (i.e. no slab uplift). Third, shear deformations of the beam are ignored and the beam is assumed to remain elastic. Finally, the vertical shear strength of the connection is assumed sufficient to ensure that a shear strength failure at the connection does not occur and that vertical shear deformation at the connection is small. These assumptions are justified as follows.

- Ignoring shear lag in composite slab: The results of the tests so far showed that within a 60-in. design strip that shear lag was not significant.
- Ignoring instabilities in the steel: Connection #1 failed as a result of distortional buckling of the section; but, subsequent connections and connections that are currently being developed all have some restraint on the bottom flange (such as a seat angle) and buckling of this type has been eliminated. Connection #4 ultimately failed in web crippling. Connections similar to Connection #4 are no longer being considered. In general, proper connection design details will ensure that instabilities do not occur.
- Ignoring flexural contribution of slab: The center of rotation for the connections tested to date was near or below the centerline of the bare steel beam. This places the reinforced composite slab in almost pure tension. As a result, the axial stiffness of the slab is far more dominant than the flexural stiffness of the slab when considering the overall connection behavior.
- Neglecting slab uplift: Because the composite slab is attached to the steel beam with welded headed shear studs the slab cannot separate from the beam without first failing one of the shear studs. This will typically only occur after significant rotational

deformations have occurred and the connection is near failure. The ability to predict the behavior of the connection beyond failure is not of current interest.

- Ignoring shear deformations of beam: The beams in partially continuous composite floor systems are going to be long and shallow. This is a situation in which shear deformations are known to have little effect.
- Assuming beam remains elastic: Currently it is believed that the beam-to-girder connection will be detailed such that the connection moment capacity will be less than the elastic moment capacity of the beam.
- Assuming connection has sufficient shear strength: Proper design guidelines will ensure that a shear strength failure does not occur prior to a moment strength failure in the connection.
- Assuming vertical deformation at the connection is negligible: Proper design of the connection to ensure proper shear strength should also ensure relatively small vertical deformations.

Despite the fact that the connections tested to date violated some of the above assumptions, analytical and experimental results generally compared very favorably, as indicated in Fig. 3, with three notable exceptions.

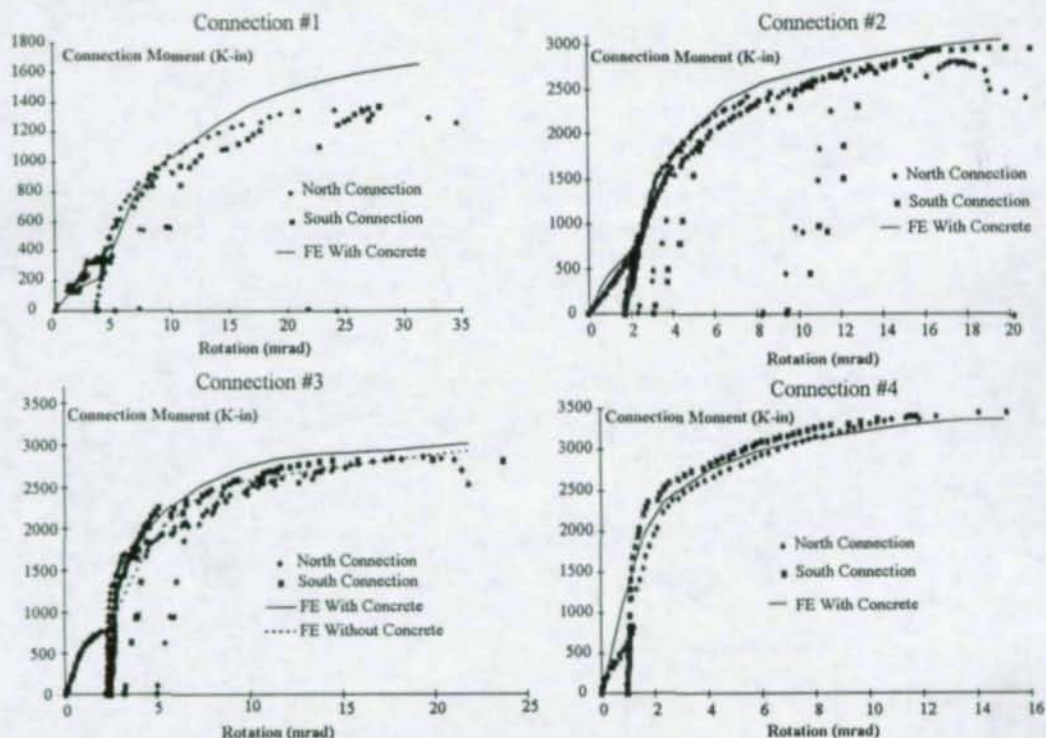


Figure 3 Finite Element Model Results Vs. Test Data

First, the analytical stiffness for the non-composite connection behavior of Connection #1 is not as stiff as that measured during testing. The authors are currently not sure of the reason for this deviation. Possible reasons include bad load measurement for this stage of the

connection loading and stiffening effects of materials not accounted for in the model such as pour stops, steel decking and reinforcing steel in the wet concrete. Because later steel connections were much stiffer than Connection #1 these stiffening effects were probably less noticeable. This is more fully discussed by Rex (1994). Second, the model response was much stiffer than the measured response in the latter stages of the test on Connection #1. This is because Connection #1 failed as a result of distortional buckling of the section. Once the buckling began the connection response softened. Because nothing in the model currently represents such a response it would be expected that the two behaviors would diverge at this point. The third notable difference is the non-composite connection behavior of Connection #4. The model behavior was much stiffer than the measured behavior. It is currently believed that some of this difference may be a result of the method used to measure the experimental rotations. It is believed the accuracy of measurement was insufficient to measure the very small rotations associated with this rather stiff steel connection.

The reader should note that both the data and the models have two stages of behavior. These represent the two stages of connection loading associated with construction loads (loading imposed before the composite slab hardens) and subsequent imposed loading (loading that occurs after the composite slab has hardened). The ability to design and analyze the connection for both stages of behavior is very important.

Another important assumption in the finite element modeling is that we have the ability to predict the behavior of the fundamental elements of the connection (bolts, welds, etc...). These fundamental elements are referred to as "sub-elements". The term "elements" has been reserved for connection parts that are combinations of the sub-elements such as a seat angle connection and a reinforced composite slab. Clearly the ability to predict the behavior of the connection as a whole is directly linked to the ability to predict the behavior of the connection sub-elements. So the question arises, how well can we predict the behavior of the various connection sub-elements?

### 3. SUB-ELEMENT MODELS

Connection sub-elements are essentially the materials and fasteners used in any non-composite or composite connection. This section summarizes current models used to predict the behavior of sub-elements and points out where some of these may need additional consideration before being used in general modeling of partially restrained beam-to-girder connections. Schematics of the load-deformation behavior and the stress-strain behavior incorporated into the finite element models are presented in Fig. 4.

Usually, the ability to predict the strength of a connection sub-element is the first problem to solve. Then, based on the predicted strength, a method to predict the load-deformation or stress-strain behavior is developed. For brevity, the focus of the following paragraphs is on *methods of predicting the load-deformation or stress-strain behavior of the connection sub-elements.*

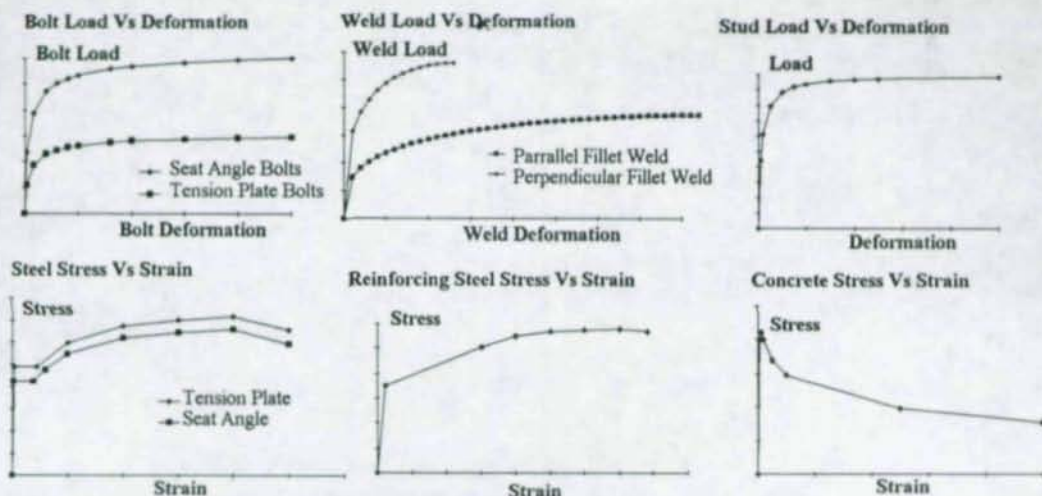


Figure 4 Behavior Of Connection Sub-Elements Used In Finite Element Models

### 3.1 Bolts

The 1994 Load and Resistance Factor Design (LRFD) Manual (*Manual of 1994*) uses the following equation to predict the load-deformation behavior of high strength bolts.

$$R = R_{ult} (1 - e^{-\mu \Delta})^{\lambda} \quad \text{Eq(1)}$$

Where:

$\Delta$  = Total deformation of fastener and bearing deformation of the connected material (in.)

$\mu = 10$

$\lambda = 0.55$

$R_{ult}$  = Ultimate shear strength of a single fastener

$e$  = Base of natural logarithm

The form of the equation was originally developed by Fisher (1965), while the values of the coefficients were determined by Crawford and Kulak (1971) based on six single bolt shear tests. The bolts in these shear tests were fully tensioned A325 3/4-in. bolts placed in double shear and the test specimen was loaded in compression.

Despite the fact that the coefficients of Eq 1 are based on only six tests, the equation is used to predict the bolt load-deformation behavior in the eccentrically loaded connection design aids in the LRFD Manual (*Manual of 1994*). This is done without regard to bolt diameter, whether the bolt is in single or double shear, whether the elements being bolted together are in compression or tension, whether the failure mode of the bolt is shear of the bolt or bearing tearout of the plate, and other parameters that could be associated with this type of element.

To better determine the load-to-deformation behavior of bolted plates in single shear, Richard, et al (1980) conducted a series of 126 bolt tests. These tests consisted of fully tensioned single bolts being placed in single shear and the plates were loaded in tension. Thirty different combinations of plate thicknesses, plate strengths, bolt diameters, edge distances, and bolt strengths were studied. Three typical failure modes were observed in the elemental tests;

shear failure of the bolt, bearing failure of the plate, transverse tension tearing of the plates. Linear regression analyses were performed to determine coefficients for an equation that could be used for additional analytical modeling. This equation is referred to as the Richard Formula and the coefficients determined from the regression analysis are  $K_p$ ,  $R_o$ , and  $n$ . The equation is given by:

$$R = \frac{\Delta K_1}{\left[ 1 + \left( \frac{\Delta K_1}{R_o} \right)^n \right]^{\frac{1}{n}}} + \Delta K_p \quad \text{Eq (2)}$$

Where:

$\Delta$  = Total bolt and plate deformation

$K_1 = K - K_p$

$K = 2E \frac{t_1 t_2}{t_1 + t_2}$  = initial stiffness of the response

$t_1, t_2$  = Plate thickness of the two attached plates

$E$  = Modulus of elasticity for the attached plates

$K_p$  = Plastic stiffness of the response

$R_o$  = The Y-axis intercept of the plastic response

$n$  = Curve fitting parameter

These coefficients were determined on a case by case basis and a general method of predicting the load-deformation behavior of bolts in single shear was never developed.

It is currently believed that the load-deformation behavior of bolts in single shear has a significant impact on the moment-rotation behavior of partially restrained beam-to-girder connections. To better understand this behavior, a series of single bolt tests is currently being conducted at VPI. However, the results of Richard's tests were used in the connection finite element models previously discussed.

### 3.2 Fillet Welds

The 1993 LRFD Specification (*Load and* 1993) uses the following equation to predict the load-deformation behavior of fillet welds.

$$\frac{P}{P_\theta} = f(\rho) \quad \text{Eq (3)}$$

Where:

$P_\theta$  = Strength of weld loaded at angle  $\theta$

$f(\rho) = [\rho(1.9 - 0.9\rho)]^{0.3}$

$\rho = \Delta/\Delta_u$

$\Delta$  = Deformation of the weld element in direction of loading

$\Delta_u = 0.209(\theta+2)^{-0.32} d$  = Deformation at ultimate load of fillet weld

$d$  = Leg size of fillet weld

This equation was developed by Lesik and Kennedy (1990) based on the research by Miazga and Kennedy (1989). It is currently believed that this equation predicts the load-deformation

behavior of fillet welds with sufficient accuracy for finite element modeling of the partially restrained beam-to-girder connections. Consequently, this model was used in the connection finite element models previously discussed.

### 3.3 Shear Studs

Rounded headed shear studs are currently the most common shear connector used in composite beams. Two of the most commonly used analytical models to predict the load-deformation behavior of these shear connectors are:

$$Q = Q_{sol} \left[ \frac{80 \delta}{1 + 80 \delta} \right] \quad \text{Eq (4)}$$

$$Q = Q_{sol} [1 - e^{-10\delta}]^{2/5} \quad \text{Eq (5)}$$

Where:

Q = Load on shear stud

$Q_{sol}$  = Ultimate strength of shear stud

$\delta$  = Deformation (in.)

Eq 4 and Eq 5 were developed by Buttry (1965) and by Ollgaard, et al (1971) respectively for continuously loaded shear studs in solid slabs. It is uncertain at this time whether either of these equations have sufficient accuracy for use in finite element modeling of partially restrained connections. A large data base of push-out tests conducted at VPI (Sublett, et al 1992; Lyons, et al 1994) is currently being reviewed to evaluate the load-deformation behavior for rounded headed shear studs in steel deck. Eq 4 was used to estimate the load-deformation behavior of shear studs in the finite element models of the partially restrained beam-to-girder connections discussed previously.

### 3.4 Mild and Reinforcing Steel

Partially restrained connections should have sufficient rotational ductility to allow proper moment redistribution in partially continuous composite floor systems. It is therefore desirable in most instances to design the connection so that yielding of the steel connection elements occurs prior to any sudden strength or instability failures. To assure that yielding does occur before a sudden failure, it is necessary to consider actual (or at least average) yield stress rather than the minimum specified yield stress.

Recent mill surveys of rolled beams showed that the mean yield stress of A36 (minimum specified yield stress of 36 ksi) steel is approximately 48 ksi (AISC 1994). Mill test data of standard deformed reinforcing steel reviewed by Mirza and MacGregor (1979) showed that the mean yield stress of grade 60 bars (minimum specified yield stress of 60 ksi) was 71 ksi.

In addition to considering more accurate estimates of the steel yield stress, reasonable estimates of the full stress-strain behavior are believed to be necessary. This is based on the fact that reinforcing steel starts into the strain hardening region very soon after yield and that the ductility of the connection at failure may be limited by the available ductility of both reinforcing and mild steel. Methods of estimating the stress-strain behavior based on the yield stress are currently being considered. Measured stress-strain behavior from coupon tests was

used in the finite element modeling of the partially restrained beam-to-girder connections discussed previously.

### 3.5 Concrete Behavior

Most efforts to model composite partially restrained connections to date have typically ignored tension behavior of the concrete. Review of the moment-rotation behavior of Connection #3 in Fig. 3 shows that including the tension behavior of the concrete provides a better estimate of the connection behavior up to the point where the moment in the connection is near the ultimate capacity of the connection. In this latter region the tension stiffening model used for post concrete cracking behavior appears to slightly over predict the connection stiffness. A two stage model of concrete tension behavior given by Collins and Mitchell (1991) was used in the finite element models of the beam-to-girder connections discussed previously.

## 4. CONCLUSION

Partially restrained steel and composite beam-to-girder connections are currently being investigated. A simplified finite element analysis technique has been shown to model the moment-rotation behavior of these connections with reasonable accuracy. This technique relies heavily on the ability to determine and analytically represent the behavior of the fundamental connection elements (connection sub-elements). Review of current methods to predict the sub-element behavior shows that there is a need to further develop some of these methods before they can be used for general modeling of connections. Future investigations will concentrate on the behavior of the connection sub-elements. This behavior will then be used to further investigate partially restrained beam-to-girder connections so that proper design procedures and recommendations can be developed.

## 5. ACKNOWLEDGEMENTS

This research was made possible through the generous financial support of The American Institute of Steel Construction, The American Iron and Steel Institute, and The National Science Foundation (# MSS-9222064). The writers would like to thank the project advisory committee of Dick Heagler (United Steel Deck), Matt Henderson (Commercial Erectors), Barry Barger (Southern Iron Works), and Kurt Swensson (Stanley D. Lindsey and Associates) for their helpful suggestions. The suggestions and technical assistance provided by Professor T. M. Murray are gratefully acknowledged.

## 6. REFERENCES

- AISC Advisory Subcommittee on SMRF Research (1994). "Earthquake Update, AISC Technical Bulletin No. 2: Interim Observations & Recommendations On Steel Moment Resisting Frames," *Modern Steel Construction*, **34**(12), 22-31.
- Buttry, K. E. (1965). "Behavior of Stud Shear Connectors in Lightweight and Normal-Weight Concrete," *MS Thesis, University of Missouri*
- Collins, M. P. and Mitchell, D. (1991). *Prestressed Concrete Structures*, Prentice Hall, 142-154.
- Crawford, S. F. and Kulak, G. L. (1971). "Eccentrically Loaded Bolted Connections," *Journal of the Structural Division*, **97**(ST3), 765-783.
- Fisher, J. W. (1965). "Behavior of Fasteners and Plates With Holes," *Journal of the Structural Division*, **91**(ST6), 265-286.
- Lesik, D. F. and Kennedy, D. J. L. (1990). "Ultimate Strength of Fillet Welded Connections Loaded in Plane," *Canadian Journal of Civil Engineering*, **17**(1), 55-67.
- Load and Resistance Factor Design Specification for Structural Steel Buildings*, (1993). American Institute of Steel Construction, Chicago, Illinois.
- Lyons, J. C., Easterling, W. S. and Murray, T.M. (1994). "Strength Of Headed Shear Studs," Vols. I and II, Report CE/VPI-ST 94/07, Virginia Polytechnic Institute and State University, Blacksburg, VA.
- Manual of Steel Construction; Volume 2, LRFD* (1994)
- Miazga, G. S. and Kennedy, D. J. L. (1989). "Behavior of Fillet Welds As A Function Of The Angle Of Loading," *Canadian Journal of Civil Engineering*, **16**, 583-599.
- Mirza, S. A. and MacGregor, J. G. (1979). "Variability of Mechanical Properties of Reinforcing Bars," *Journal of the Structural Division*, **105**(ST5), 921-937.
- Ollgaard, J. G., Slutter, R. G., and Fisher, J. W. (1971). "Shear Strength of Stud Connectors in Lightweight and Normal Weight Concrete." *AISC Engineering Journal*, **8**(2), 55-64.
- Rex, C.O. (1994). "Behavior of Composite Semi-Rigid Beam-to-Girder Connections," Master Thesis, Virginia Polytechnic Institute and State University, Blacksburg, VA.
- Rex, C.O. and Easterling, W. S. (1994). "Semi-Rigid Composite Beam-to-Girder Connections," Proceedings of the National Steel Construction Conference, Pittsburgh, AISC, 6.1-6.20.
- Richard, R. M., Gillett, P. E., Kriegh, J. D., and Lewis, B. A. (1980). "The Analysis & Design of Single-plate Framing Connections," *AISC Engineering Journal*, 2nd Qtr., 38-52.
- Sublett, C. N., Easterling, W. S. and Murray, T.M. (1992). "Strength Of Welded Headed Studs In Ribbed Metal Deck On Composite Joists," Report No. CE/VPI-ST 92/03, Virginia Polytechnic Institute and State University, Blacksburg, VA, 257 pages.

## INFLUENCE OF SLIP OF THE SHEAR CONNECTION ON COMPOSITE JOINT BEHAVIOUR

Jean-Marie Aribert

### Abstract

Test results on flush end plate composite joints with different degrees of shear connection are reported and commented with regard to modelling aspects. A numerical simulation using an original finite element is then performed, which illustrates the important influence of interface slip even when the shear connection is full. Finally, an attempt of simplified analytical procedure is proposed to determine the moment-rotation curve of a composite joint taking account of the interface slip explicitly.

### 1 - INTRODUCTION

It is recognized in a lot of studies (for example, see the synthesis [1]) that interface slip between concrete slab and steel beam may affect substantially the behaviour of a composite joint ; intuitively, this slip effect will be magnified when the composite beam adjacent to the joint is in partial shear interaction. Moreover, for a configuration of double-sided beam-to-column joint with approximate symmetrical loading, the interface slip may contribute to the joint rotation as the most important component. Unfortunately, it seems that no full-range elasto-plastic analysis is yet available to determine simply an equivalent translational spring reproducing the slip component with good accuracy near the steelwork joint. To our knowledge, the first elaborate approach on this topic was developed by JOHNSON and LAW [2] ; they evaluated the elastic stiffness of a composite joint at the end of a cantilever, using the elastic partial interaction theory developed by NEWMARK et al[3] and neglecting the tensile resistance of concrete. But these authors did not provide any general procedure for the determination of the moment-rotation curve of a composite joint, so that the scope of their approach is relatively limited.

In a more recent paper [4], ANDERSON and NAJAFI assumed that the slip at the joint depends initially on the nearest shear connector to the column ; under increasing load, this alone connector provides resistance to slip until it becomes plastic - Additional loading is then assumed to be resisted by the next shear connector deforming elastically, and so forth. Such an assumption does not appear well comprehensive in so far as any calculation (by using a numerical model for example) demonstrates clearly that the end slip at any stage is the resultant of all the deformations along a significant length of composite beam interface.

Also, TSCHEMMERNEGG et al [5] point out the need to consider interface slip in the design of composite joints, affirming that the stiffness of the associated translational spring " can be obtained from the system calculation" (item 4.2.3.1. of [5]) ; but no practical procedure is given by these authors to do that.

In the present paper, some basic ideas are presented briefly, which may be useful to make progress in the relevant problem. First, conclusions are deduced from tests carried out in Rennes [6,7], only considering the case of beam-to-column joints with bolted flush end plates (because of the limited content of the paper).

Then, numerical simulations using an original finite element are performed for joints having similar characteristics as the tested ones ; in addition, these joints are simulated when being subject to other conditions of working and loading than the experimental ones. Finally, a simplified analytical procedure is proposed to determine with good accuracy the full-range moment-rotation curve of a composite joint in which the rotation component due to slip cannot be neglected.

## 2 - CONCLUSIONS FROM TESTS

Reference is made here to particular tests called A2, C1, C2 and C3 which are extracted from a research program already presented in papers [6, 7]. As a reminder, the specimens were major axis joints and a symmetrical cruciform arrangement with two cantilevers was used to test them, as shown in figure 1.

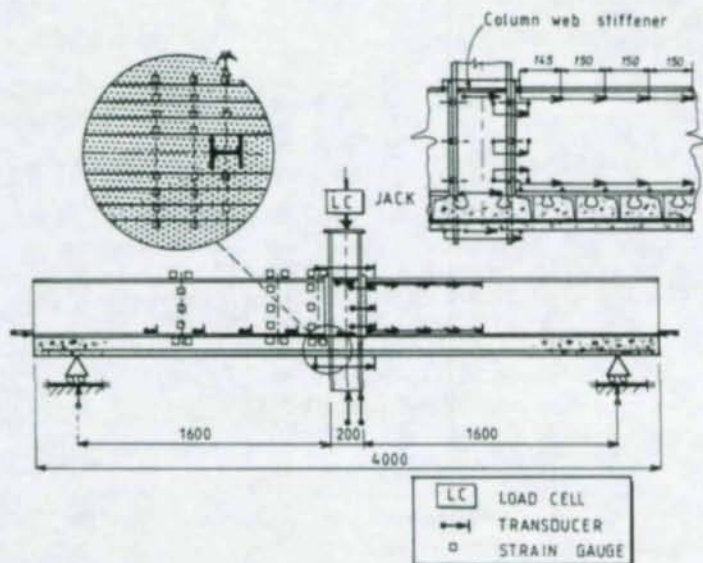


Figure 1 - Arrangement of specimens and instrumentation.

Common characteristics to the tested specimens were :

- beam : IPE 360, and column : HEB 200 in steel grade S235 ;
- bolted flush end plate (grade S235) with :
  - dimensions : 15 mm thick, 200 mm wide, 400 mm deep ;
  - 3 rows of H.S. bolts of 18 mm diameter and grade 10.9 ;
- welded transverse stiffeners in the compression zone of the column web, perfectly aligned with the corresponding beam flange ;
- composite slab with ribs transverse to the steel beam and dimensions : 120 mm deep overall, 1000 mm wide ;
- reinforcement consisting only of one layer of rebars of high ductility and grade S500 (located 88 mm above the upper flange of the steel beam) ;
- concrete of strength class C30.

Other characteristics peculiar to each specimen are collected in table 1 (symbol N is the number of shear connectors in each cantilever).

Test	Shear connectors	Steel profiled sheeting	Degree of connection	Reinforcement
A2	Welded headed studs $\phi$ 19 mm (Nelson)	Hi-Bond 55 (1.2 mm thick)	More than full (N=9)	10 rebars $\phi$ 8 mm
C1	Cold-formed angles 80x60x24.3 (Hilti HVB 80)	Cofrastra 40 (0.8 mm thick)	More than full (N=17)	14 rebars $\phi$ 8 mm
C2	"	"	Full (N=12)	"
C3	"	"	Partial (N=8)	"

Table 1

Bending moments were calculated at the column face, resulting from the jacking forces. Rotations were deduced from the vertical displacements measured through the centroid of the column cross-section; the part due to flexural bending of the composite beam was subtracted from this displacement to determine the specific rotation of the connection alone. The so-obtained moment-rotation curves for the composite joints A2, C1, C2 and C3 are given in figure 2; in fact, these curves are envelope curves resulting from several successive loadings and unloadings so that they show a realistic rotational stiffness in the serviceability domain due to premature cracking of the concrete near the column flange. In comparison with the above-mentioned curves, it is also given in figure 2 the moment-rotation curve of the bare steelwork joint, deduced from a reference test (without slab) called A1.

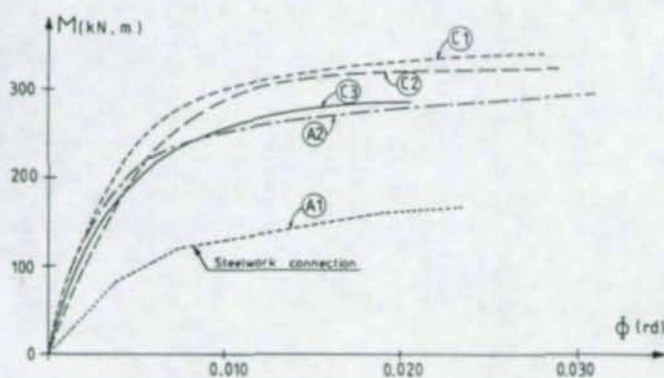


Figure 2 - Experimental moment-rotation curves

With regard to the rotation capacity of the joints, the failure mode was fracture of tension bolts for test A1, fracture of rebars for tests A2 and C1, and fracture of shear connectors for tests C2 and C3.

As additional instrumentation, a lot of strain gauge measures on all the rebars allowed to investigate the distribution of axial forces in reinforcement at different composite cross-sections near the column (figure 1).

The main conclusions are:

(i) All rebars within the total width of the slab participate approximately equally in resisting tension. This observation tends to prove that the effective width of slab in hogging moment region is at least equal to the quarter distance between points of zero bending moment, in spite of the semi-continuous effect produced by the composite joint.

(ii) The variation of the total tensile force in the rebars close to the joint versus loading is affected by the degree of shear connection, as shown in figure 3. Degrees of shear connection greater than unity (see tests A2, C1 and possibly C2) cause greater force in the rebars at intermediate stages of loading; but the final force in the rebars is independent of the precise degree of connection because their plastic resistance can be reached. On the contrary, for partial shear connection (see test C3), the plastic resistance of the rebars cannot be

developed. Moreover, independently of the degree of connection, all the curves show a sudden change of slope at low loading due to concrete cracking whose nature appears much more severe than in continuous beams.

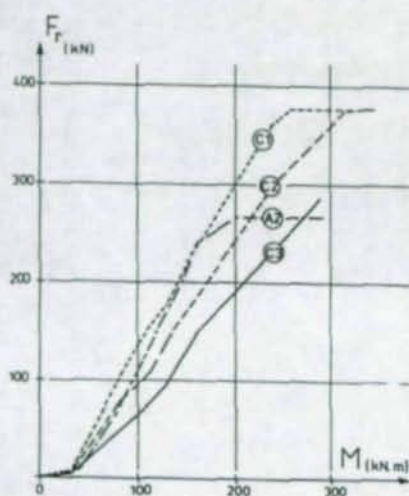


Figure 3 - Total tensile force in the rebars

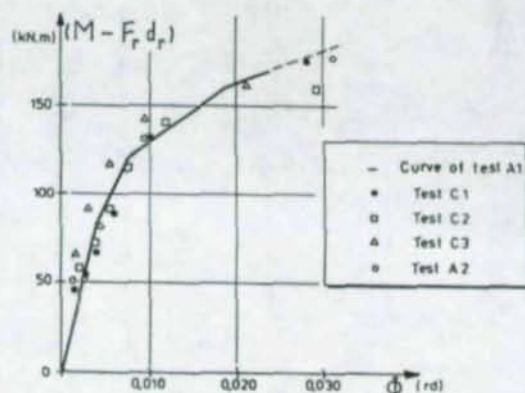


Figure 4 - Contribution of the steelwork joint.

(iii) For the concerned tests, the moment-rotation response of the steelwork part of composite joint resembles closely that of the bare steel joint. Using values picked up on the available curves  $(M-\Phi)$  and  $(F_r-M)$  in figures 2 and 3, corresponding values of the moment  $M_a^*$  of the steelwork part can be calculated from the relationship :

$$M_a^*(\Phi) = M(\Phi) - F_r(\Phi)d_r \quad (1)$$

where  $d_r$  is the lever arm between the layer of rebars and the mid-thickness of the compression flange. In figure 4, the so-calculated values  $M_a^*(\Phi)$  are compared with the curve  $M_a(\phi)$  of reference test A1 (without slab) ; there is in rather good agreement with the curve, which tends to confirm the intrinsic behaviour of the steelwork part.

An explanation of this experimental result may be the following :

- for the bare steel joint (see figure 5-a), assuming the bolt-row number  $i$  subject to the internal force  $F_i$  and the centre of compression of the end plate located at the mid-thickness of the compression flange, the moment  $M_a$  applied to the joint is equal to :

$$M_a = \sum_{i=1}^n F_i y_i \quad (2)$$

where  $y_i$  is the lever arm of the bolt-row number  $i$ .

- For the associated composite joint (see figure 5.b), assuming the same joint rotation  $\Phi$  and the same position of the compression and the rotation centres as previously, the value of moment  $M_a^*$  applied to the steelwork part depends on the point of end plate where it is considered. For example, at the rotation centre (R.C.) of the composite joint, this value is :

$$M_a^* = \sum_{i=1}^n F_i y_i + F_r e$$

hence :

$$M_a^* = M_a + F_r e \quad (3)$$

where  $e$  is the eccentricity between the rotation centre and the compression centre. When  $e$  is small, which can be reasonably assumed for joints with transverse stiffeners in the column web, relationship (3) gives then the result :  $M_a^* = M_a$ . When the eccentricity is not negligible and may depend on the level of loading, it is worth noting that the contribution of the steelwork part to the moment of the composite joint can be evaluated again using the principle of the « component method » of Annex J in Eurocode 3.

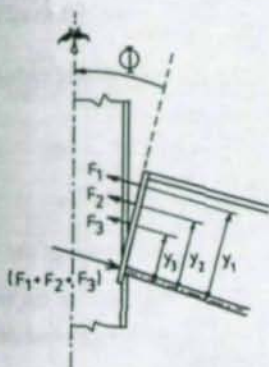


Figure 5.a - Internal forces in the bare steel joint.

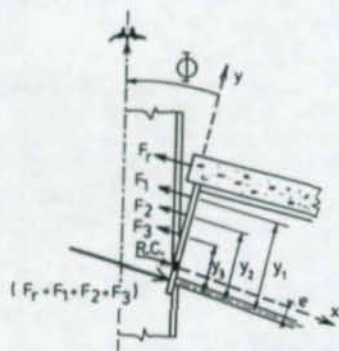


Figure 5.b - Internal forces in the composite joint.

### 3 - NUMERICAL SIMULATION

#### 3.1 Numerical procedure

ARIBERT et al [8] have formulated a finite element for composite beams taking account of interface slip and possible semi-continuous rotation at one of the element ends ; semi-continuity may be due to occurrence of local buckling or to fastening of the element to a semi-rigid joint. Uplift being neglected, only four degrees of freedom are used at each end of the composite beam element (axial and transverse displacements for steel part, axial displacement for slab, and common rotation), as shown in figure 6-a. To simulate interaction with a semi-rigid joint, the composite beam element is fastened to an intermediate spring element of zero length including three components (see figure 6-b) :

- (i) a rotational spring with variable stiffness  $k_{\Phi}$  to control the sum  $(M_a^* + M_b)$  of the internal moments applied to the steel beam and the concrete slab ;
- (ii) a translational spring with variable stiffness  $k_b$  to control the axial force in the slab ;
- (iii) a rigid truss element in front of the rotation centre of the composite joint (see figure 5-b) ; the node of the adjacent steel beam element being translated from the centroid of the steel section to the position of the rotation centre, it is easy to satisfy the kinematic condition :  $u_j^{(a)} = 0$ .

At any level of loading, an iterative procedure must be introduced to determine the unknown values of stiffnesses  $k_{\Phi}$  and  $k_b$ . At iteration number  $\ell$  based on known values  $k_{\Phi}^{(\ell-1)}$  and  $k_b^{(\ell-1)}$ , the calculated rotation of the joint :

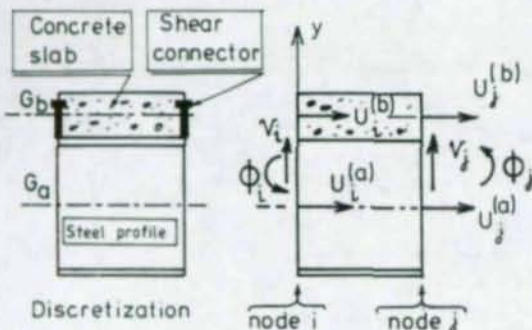


Figure 6.a - Composite beam finite element

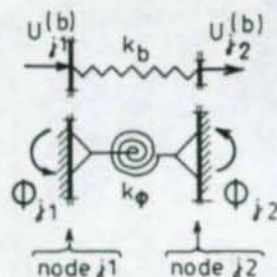


Figure 6.b - Intermediate spring element

$$\Phi^{(\ell)} = \Phi_{j2}^{(\ell)} - \Phi_{j1}^{(\ell)}$$

leads to rectify the rotational stiffness so that relationship (3) for moment-rotation behaviour of the steelwork part is satisfied at best ; hence a new value  $k_{\Phi}^{(\ell)}$ . Moreover,  $k_b$  may be adopted here as the usual axial stiffness of the slab element (essentially the rebars) filling up the space defined by the column mid-depth.

### 3.2 Simulation

A numerical simulation has been performed on cantilever tests C1\*, C2\* and C3\* relatively similar to the above-presented tests C1, C2 and C3, considering the same global arrangement as in figure 1 and the measured properties of the materials :

- for structural steel :  $f_y = 310 \text{ N/mm}^2$  ,  $f_u = 435 \text{ N/mm}^2$  ;
- for concrete :  $f_{ck} = 30 \text{ N/mm}^2$  ;
- for reinforcing steel :  $f_{ry} = 540 \text{ N/mm}^2$  ,  $\epsilon_{ru} = 0.08$ .

But the following simplified assumptions have been adopted to make the further interpretation easier :

- the stress-strain diagram of reinforcing steel is elastic-perfectly plastic, and the tensile resistance of concrete is neglected.
- The force-slip curve of the shears connectors (cold-formed angles) consists of two branches : a first branch starting from the origin with a constant slope equal to  $k_c = 70 \text{ kN/mm}$  ; a second branch, which is horizontal, corresponds to the shear resistance of a connector,  $P_R = 30 \text{ kN}$  , and is limited to the ultimate slip capacity  $s_u = 7 \text{ mm}$  .
- The shear connectors are spaced uniformly.
- The rotation centre of the composite joints is located at the mid-thickness of the compression flange ( $e = 0$ ).

In consequence of the above assumptions for the shear connectors which are clearly ductile according to Eurocode 4 [9], the degree of shear connection  $N/N_f$  can be specified without ambiguity, namely 1.34 for case C1\* , 0.95 for case C2\* and 0.63 for case C3\* .

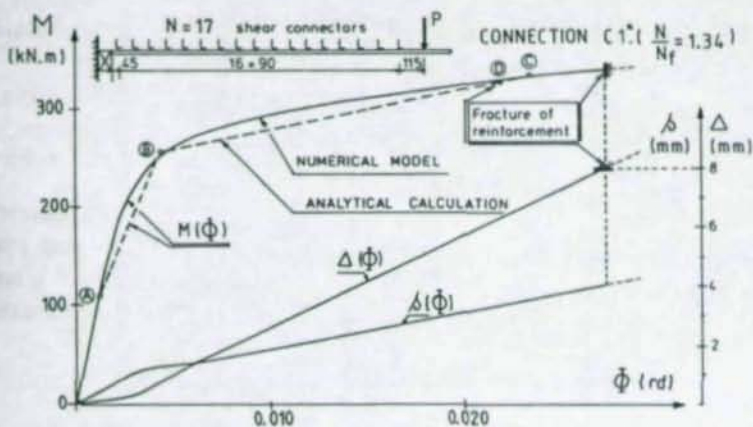


Figure 7 - Curves of moment, slip and extension of rebars versus rotation for joint C1\*.

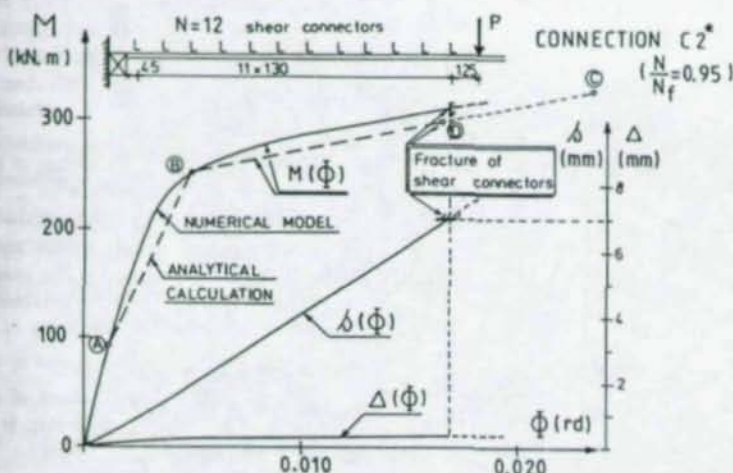


Figure 8 - Curves of moment, slip and extension of rebars versus rotation for joint C2\*.

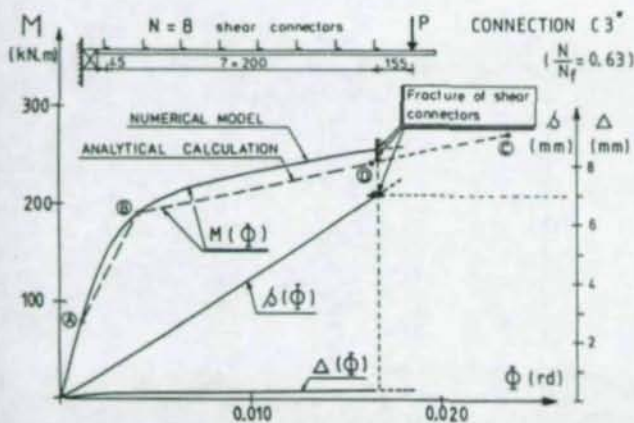


Figure 9 - Curves of moment, slip and extension of rebars versus rotation for joint C3\*.

As results of the numerical simulation, figures 7, 8 and 9 corresponding respectively to joints  $C1^*$ ,  $C2^*$  and  $C3^*$  show the moment-rotation curves  $M(\Phi)$  in continuous line and also the curves  $s(\Phi)$  and  $\Delta(\Phi)$  where  $s$  is the contribution of end slip to the joint rotation and  $\Delta$  that due to extension of the rebars.

Even for  $N/N_f = 1.34$ , the contribution of slip to the rotation is significant, remaining about 33% when the rotation capacity is reached due to fracture of the rebars. For partial shear connection, even for  $N/N_f = 0.95$ , the contribution of slip becomes predominant at any stage of loading; in this case, the rotation capacity is systematically the consequence of fracture of the shear connectors.

The previous conclusions should be considered realistic, comparing the ideal joints  $C1^*$ ,  $C2^*$  and  $C3^*$  with the tested ones  $C1$ ,  $C2$  and  $C3$ ; there is a close similarity between their failure modes and main properties of curves  $M(\Phi)$ , as initial rotational stiffness, ultimate resistance moment and rotation capacity. In particular, it is recommended that the cracked section should be used to evaluate the initial rotational stiffness of a composite joint in hogging moment region.

### 3.3 Simulation of other arrangements

In the previous simulation, the shear connectors were ideally assumed to be spaced uniformly along the cantilever length. Another simulation has been performed keeping the same number  $N$  of shear connectors but spacing them differently; so, the density of connectors in the four ribs of steel sheeting by the side of the joint has been adopted twice that in the other ribs. For all the joints  $C1^*$ ,  $C2^*$  and  $C3^*$ , it has been observed that this new arrangement has negligible influence on the moment-rotation curves, which may be explained by the highly-ductile behaviour of the shear connectors.

In addition, to investigate possible differences of behaviour when the joints are included in a beam of building, a composite beam of 10 metre span has been considered, introducing successively the joints  $C1^*$ ,  $C2^*$  and  $C3^*$  at both ends (any rotation of the end supports being restrained, but translational displacement allowed). The spacing of shear connectors has been kept the same as in paragraph 3.2, leading to a total number of connectors equal to 110, 76 and 50 in the beams with joints  $C1^*$ ,  $C2^*$  and  $C3^*$  respectively. The beams have been subject to uniformly distributed loading which is more significant for buildings than concentrated loads. Comparisons of behaviour of the joints in the beams and the cantilevers are shown in figures 10, 11 and 12.

For high degree of shear connection (see figure 10 dealing with  $C1^*$ ), the  $M(\Phi)$  response is virtually unchanged, although the end slip is slightly higher owing to occurrence of a steep gradient of the slip distribution along the interface very close to the joint; moreover, the rotation capacity of the joint is slightly increased in consequence of the corresponding reduction of extension of the rebars.

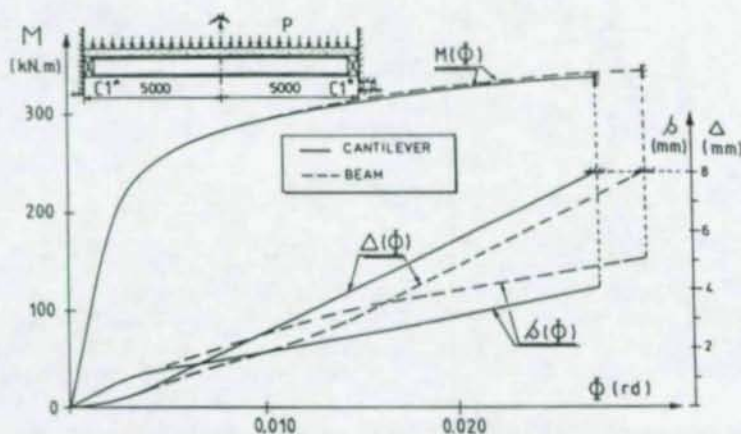


Figure 10 - Behaviour of joint  $C1^*$  in a beam

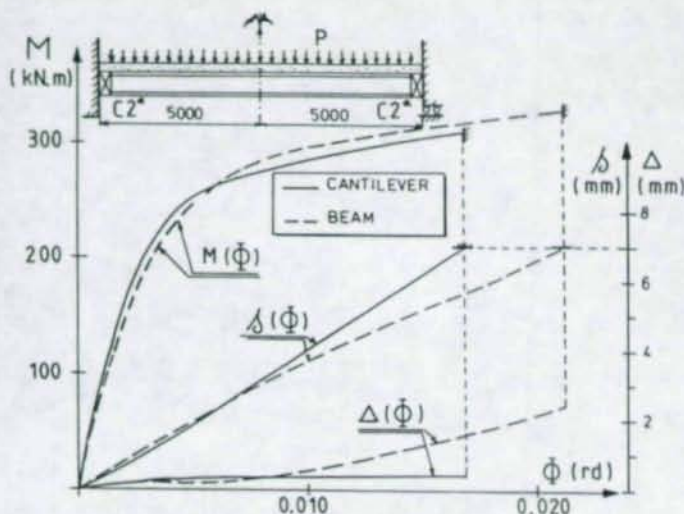


Figure 11 - Behaviour of joint C2\* in a beam

The same observation is valid again for the  $M(\Phi)$  response of the joint C2\* (see figure 11), although the end slip and the extension of the rebars change in reverse order. For low degree of shear connection (see figure 12 dealing with C3\*), even a more favourable  $M(\Phi)$  curve is observed in the beam; the reason of this increase of resistance moment is the higher force  $F_r$  in the rebars which is supplied by redistribution of the longitudinal shear force from the ends of the connection towards the middle.

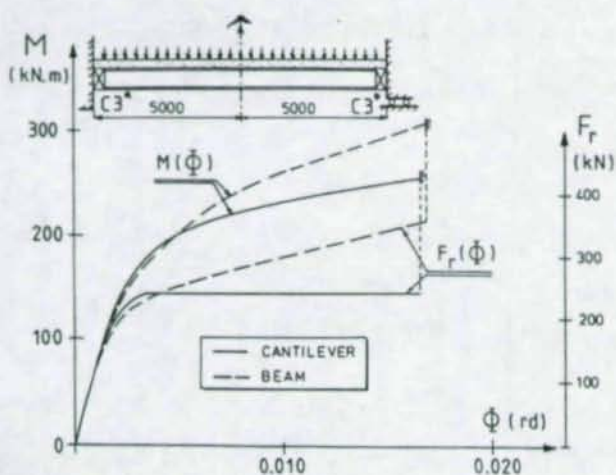


Figure 12 - Behaviour of joint C3\* in a beam

Finally, it seems possible to conclude that the cantilever arrangement with a triangular distribution of bending moment is suitable to characterize the moment-rotation curves of composite joints; generally, the so-obtained curves are accurate enough for practice and on safe side. Moreover, it is recommended to adopt the cantilever span equal to 15% of the beam span.

## 4 - SIMPLIFIED ANALYTICAL PROCEDURE

For the type of composite joint considered up to now with ductile shear connectors, a simplified analytical procedure is proposed hereafter to evaluate the moment-rotation curve. The application of this procedure is illustrated in figures 7, 8 and 9 by the tri-linear curves OABD which appear in very good agreement with the numerical curves. Points A, B and D can be determined as follows :

(i) Point A : It corresponds to the first yielding of the shear connection. Assuming cracked composite cross-sections and founding upon the elastic interaction theory [3], four equations are used which concern :

- the end slip at the joint :

$$s = \frac{a}{k_c} \left[ \frac{M}{(1+\alpha)d\ell} - C \cdot \sqrt{\beta} \cdot \text{ch} \sqrt{\beta} \ell \right] \quad (4)$$

- the tensile force in the rebars at the joint :

$$F_r = \frac{M}{(1+\alpha)d} - C \text{ sh } \sqrt{\beta} \ell \quad (5)$$

- the rotation of the joint (here assuming :  $e = 0$ ) :

$$\Phi = (\Delta + s) / d_r \quad (6)$$

- and the moment applied to the joint (see equation (1)) :

$$M = M_a(\Phi) + F_r d_r \quad (7)$$

In these equations,  $\ell$  is the cantilever span,  $d$  is the distance between the rebars and the centroid of the steel section,  $k_c$  and  $a$  are respectively the stiffness and the spacing of the shear connectors, and :

$$\alpha = E_a I_a / (d^2 E_r A_r) \quad , \quad \beta = (1+\alpha) k_c d^2 / (a E_a I_a)$$

where  $E_a$  and  $E_r$  are the moduli of elasticity of structural steel and reinforcing steel,  $I_a$  is the second moment of area of the steel section, and  $A_r$  is the effective area of the rebars. In addition, for elastic behaviour of the rebars, the extension  $\Delta$  is given by :

$$\Delta = F_r \ell_r / (E_r A_r) \quad , \quad \text{with : } \ell_r = h_c / 2 \quad (8)$$

where  $h_c$  is the column depth.

The unknown coefficient  $C$  for a given value of  $s$  may be calculated by means of a short iterative procedure, for example in the following order :

$$M \xrightarrow{\text{Eq.(4)}} C \xrightarrow{\text{Eq.(5)}} F_r \xrightarrow{\text{Eq.(6) and (8)}} \Phi \xrightarrow{\text{Eq.(7)}} M.$$

The final results for the elastic limit slip  $s^{(A)} = 0.42$  mm are collected in table 2.

TEST	C [N]	$F_r^{(A)}$ [N]	$\Phi^{(A)}$ [rd]	$M^{(A)}$ [kN.m]
C1*	-2600	187300	$1.27 \times 10^{-3}$	110
C2*	-4145	155480	$1.21 \times 10^{-3}$	95
C3*	-6090	124105	$1.16 \times 10^{-3}$	80

Table 2

(ii) **Point B**: It corresponds to the stage of maximum interaction force between the rebars and the steel beam. So:

$$F_r^{(B)} = A_r f_{ry} \quad \text{when: } N / N_f > 1 \quad ; \quad (9)$$

$$F_r^{(B)} = N \cdot P_R \quad \text{when: } N / N_f < 1 \quad , \quad (10)$$

where  $P_R$  is the shear resistance of a connector. Moreover, the end slip is magnified owing to the elastoplastic behaviour of the shear connection. Practically it may be assumed:

$$s^{(B)} = s^{(A)} \left( F_r^{(B)} / F_r^{(A)} \right) \times 2 \quad . \quad (11)$$

Equations (6), (8) and (7) are valid again.

(iii) **Point D**: As a preliminary, the point C corresponding to the rotation capacity  $\Phi_a$  of the bare steel joint is determined (the moment  $M^{(C)}$  is given immediately by equation (7)). Then, point C is replaced by point D on the straight line BC if fracture occurs in the rebars or in the shear connection before reaching rotation  $\Phi_a$ . The rotation associated with point D may be calculated on the safe side by:

$$\Phi^{(D)} = \left( \Delta_u + s^{(B)} \right) / d_r \quad \text{when: } N / N_f > 1 \quad , \quad (12)$$

with:  $\Delta_u = \epsilon_{ru} \cdot \ell_r$  (ultimate extension of the rebars) ;

$$\Phi^{(D)} = \left( \Delta^{(B)} + s_u \right) / d_r \quad \text{when: } N / N_f < 1 \quad , \quad (13)$$

where  $s_u$  is the slip capacity of the shear connectors.

## 5 - CONCLUSION

The present investigation based on observations from tests and numerical simulations is a help to analyse better the contribution of interface slip to the rotation of composite joints which appears relatively important even for full shear connections. The arrangement of cantilever to characterize the moment-rotation curve of the joints has been demonstrated significant for practical design. Considering ductile shear connectors and double-sided composite joints with symmetrical loading, a simplified analytical approach has been proposed to evaluate the moment-rotation behaviour in the shape of a tri-linear curve. It is likely that this approach could be generalized without great difficulty to other types of joints, for example single-sided joints by adding the rotation component due to the shear of web panel, also joints with unstiffened column web by taking account of the variable position of the rotation centre of joints (use of the eccentricity  $e$  in equations (6) and (7)), and possibly cleated joints (assuming no slip in bolt holes).

## REFERENCES

- [1] ZANDONINI, R., Semi-rigid composite joints. In *Structural Connections : Stability and Strength* (ed. R. Narayanan). Elsevier Applied Science, London, 1989, pp. 63-120.
- [2] JOHNSON, R.P. and LAW, C.L.C., Semi-rigid joints for composite frames. *Proc. Int. Conf. on Joints in Structural Steelwork* (ed. J.H. Howlett et al.). Pentech Press, London, 1981, pp. 3.3-3.19.
- [3] NEWMARK, N.M., SIESS, C.P. and VIEST, I.M., Tests and analysis of composite beams with incomplete interaction. *Proc. Soc. Exp. Stress Anal.*, 9(1), 1951, pp. 75-92.
- [4] ANDERSON, D. and NAJAFI, A.A., Performance of composite connections : major axis end plate joints. *J. Construct. Steel Research* 31, 1994, pp. 31-57.
- [5] TSCHEMMERNEGG, F., BRUGGER, R., HITTENBERGER, R., WIESHOLZER, J., HUTER, M., SCHAUR, B. Ch., BADRAN, M.Z., Zur Nachgiebigkeit von Verbundknoten, *Der Stahlbau* 63-H.12, 1994 und 64-H.1, 1995.
- [6] ARIBERT, J.M and LACHAL, A., Experimental investigation of composite connections and global interpretation. COST C1 Workshop in Strasbourg, Oct. 1992.
- [7] ARIBERT, J.M., LACHAL, A., MUZEAU, J.P. and RACHER, P., Recent tests on steel and connections in France. COST C1 Workshop in Pragua, Oct. 1994.
- [8] ARIBERT, J.M., RAGNEAU, E. et XU, H., Développement d'un élément fini de poutre mixte acier-béton intégrant les phénomènes de glissement et de semi-continuité avec éventuellement voilement local. *Construction Métallique*, n° 2, 1993, p. 31-49.
- [9] CEN, Design of composite steel and concrete structures. EVN 1994-1-1, Oct. 1992.

## THE USE OF A ROLLED WIDE-FLANGE AS A BRIDGE SUPPORT BEARING

Joseph M. Ales Jr.<sup>1</sup>

Joseph A. Yura<sup>2</sup>

### Abstract

The design of the connection between an integral steel cap girder and a concrete pier in a bridge structure requires careful attention to detail. The bearings will be subject not only to vertical dead and live loads but also to imposed displacements, such as rotation caused by alternate span vehicle loading and horizontal translation caused by temperature-induced expansion and contraction of the superstructure. Though a bearing can be designed fairly easily to resist vertical loads, complex designs and details are often required to accommodate the imposed displacements. A simple and cost-effective detail has been developed; in place of a machined rocker bearing, a rolled wide-flange section is used. The research presented herein describes the results of tests pertaining to the use of the rolled wide-flange section as a bridge support bearing.

### 1. INTRODUCTION

#### 1.1 Problem Statement

Rocker bearings have been used as part of the connection between a concrete pier and a steel cap girder supporting continuous steel bridge girders. Figure 1 is a photo of a typical connection and a

---

<sup>1</sup>Design Engineer, Walter P. Moore and Associates, Inc., 201 East Kennedy Blvd., Suite 300, Tampa, Florida, 33602, USA

<sup>2</sup>Warren S. Bellows Centennial Professor in Civil Engineering, The University of Texas at Austin, Department of Civil Engineering, Austin, Texas, 78712, USA

schematic drawing is shown in Figure 2. Twin bearings at each concrete pier are designed to resist moments in the transverse direction caused by eccentric truck traffic, as shown in Figure 3. In the longitudinal direction (the direction parallel to traffic flow) the rocker bearing combined with long anchor bolts are designed to produce an ideal pin support so that the continuous longitudinal bridge girders are not restrained at the pier. The main reason for the free rotation concept is to avoid fatigue in the steel cap girder details caused by alternate span loading. This connection, which is essentially a fixed support in the transverse direction and a pinned support in the longitudinal direction, is fairly complex and costly. A research project was undertaken to determine experimentally the static strength, the fatigue strength, and the stiffness of the connection in both the transverse and longitudinal directions. The primary objective of the research was to develop a simpler and more cost-effective connection. The new detail that was developed uses a wide-flange section as a bearing in place of the machined rocker. This paper presents the results of the phase of the research concerned with the use of a wide-flange section as a bearing support.



Figure 1 Connection Between Integral Steel Cap Girder and Concrete Pier

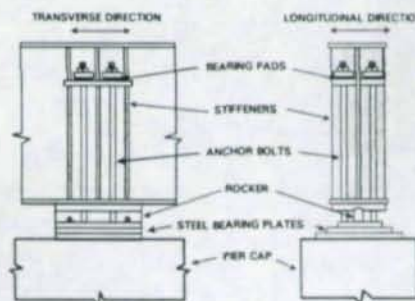


Figure 2 Connection with Rocker Bearing

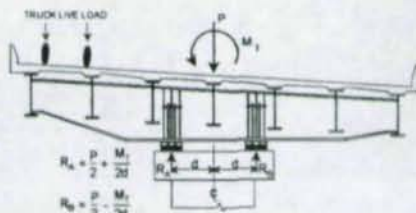


Figure 3 Vertical Loads on Bearings

## 1.2 Longitudinal Direction Behavior

The bearing must support the compressive load associated with the bridge live and dead loads. In the longitudinal direction, the cap girder is subject to rotation caused by the longitudinal girders. If the connection restrains the rotation, moments and forces will be produced in the cap girder, the connections, and in the pier. The resisting moment is proportional to the rotational stiffness of the connection. The center of rotation of a cap girder that is free to rotate is about the neutral axis of the longitudinal girders. Since the bearings are located near the bottom flange of the cap girder and are not coincident with the center of rotation, a horizontal displacement is produced at the bearings. This is shown in Figure 4. Additional horizontal displacement will be produced by the expansion and contraction of the superstructure caused by temperature changes.

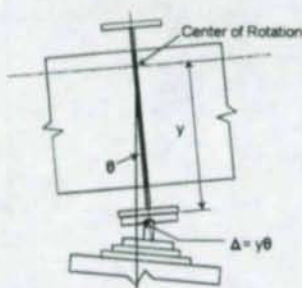


Figure 4 Horizontal Displacement of Bearing

## 1.3 Replacement of Rocker with Rolled Wide-Flange Section

A comparison of the connection using the rocker bearing and the connection with the wide-flange bearing is shown in Figure 5. The wide-flange section is simpler and less expensive than the machined rocker bearing and it provides a positive connection between the steel cap girder and the concrete pier cap, eliminating the need for the anchor bolts. Though the wide-flange section does not allow free rotation, the web should be less stiff with respect to horizontal translation than the rocker bearing. The tests on the wide-flange sections were used to determine compressive strength and out-of-plane stiffness and fatigue strength and led to the development of a design procedure.

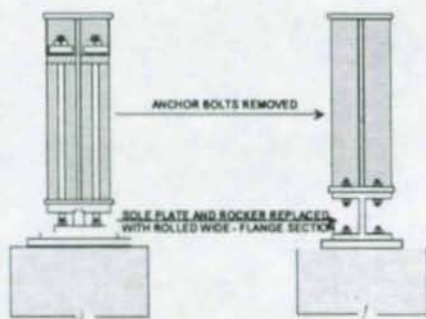


Figure 5 Comparison of Existing Connection and New Connection, Longitudinal Direction

## 2. COMPRESSIVE STRENGTH OF WIDE-FLANGE SECTION

### 2.1 Test Program and Test Setup

Three sizes of wide-flange sections were selected as bearing specimens for the compression tests. The sizes were a representative sample of the standard sections classified as the W12 and W14 column sections in the AISC Manual of Steel Construction (AISC, 1989). The sizes tested were W12X87, W12X152, and W12X230 (W310X310X129, 226, 342). The material used was A572 Grade 50, Yield strength  $F_y = 50$  ksi (345 MPa). The primary variable for the compression tests was the slenderness ratio of the web. The slenderness ratio of the web was defined as the height of the web between the flanges,  $h$ , divided by the radius of gyration of the web,  $r$ . The range of the slenderness ratio for the W12 and W14 sections varies from 14 to 80 for web thicknesses between 0.5 in. (13 mm) and 2 in. (51 mm). Nine tests were conducted; the average measured values of the web thicknesses were 0.51 in. (13.0 mm) for the W12X87 specimens, 0.89 in. (22.6 mm) for the W12X152 specimens, and 1.30 in. (33.0 mm) for the W12X230 specimens. The slenderness ratios of the test specimens varied from 28 to 71. An additional variable was considered, the length of the bearing. Two lengths of bearings were tested, 24 in. (607 mm) and 36 in. (914 mm), to determine whether the length of the bearing had any effect on the buckling stress. Replicate specimens were tested for each category. The length effect was examined using the W12X87 bearings

A schematic of the test setup is shown in Figure 6. The bottom platform supported a half section of a concrete pier cap and the top platform supported a 2 million pound (8900 kN) capacity hydraulic ram. A steel bearing plate transferred the compression load from the test specimen into the pier cap section. It was assumed in the original design of the loading frame that the test specimens would fail in the fixed-fixed buckling model; in this failure mode, the top and bottom flanges are restrained from both rotating and translating. The frame, however, lacked sufficient stiffness to prevent lateral sway of the top flange of the test specimen. The instrumentation used on the specimens consisted of strain gages, linear potentiometers, and servo inclinometers. Whitewash was applied to each specimen to accentuate the yield lines.

## 2.2 Compressive Strength of Bearing Web

The results of the bearing compression tests are shown in Figure 7 as a plot of the non-

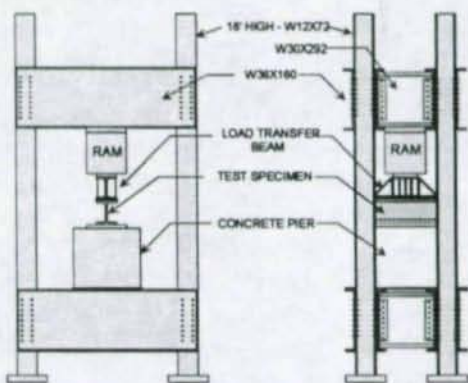


Figure 6 Schematic of Test Frame

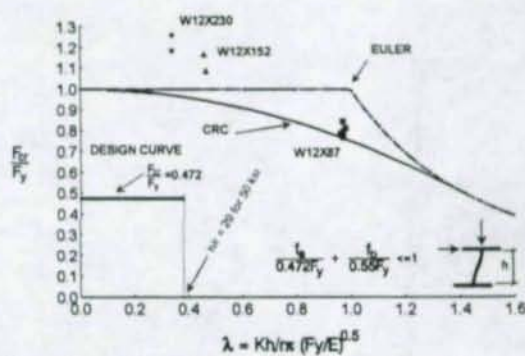


Figure 7 Non-Dimensionalized Buckling Stress vs. Slenderness Parameter

dimensionalized buckling stress vs. the slenderness parameter; an effective length factor of 1 is used. The critical buckling stress,  $F_{cr}$ , is defined as the maximum static load divided by the area of the web. All of the specimens failed in the sway mode. A graph showing the non-dimensional axial stress vs. the top flange lateral deflection for the W12X230 specimens is shown in Figure 8. The failure loads of the specimens in each group are repeatable and the length of the specimen, which was varied in the W12X87 group, had no effect on the results. All of the specimens buckled in the inelastic range and strain hardening occurred in the W12X152 and the W12X230 groups. A photo of a failed specimen is shown in Figure 9.

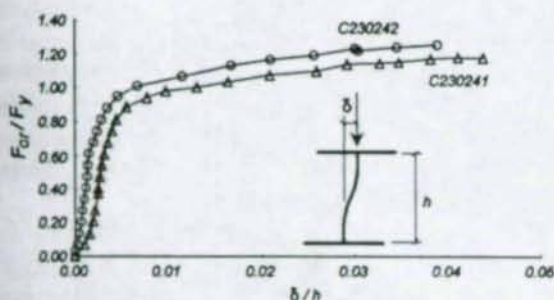


Figure 8 Non-Dimensionalized Axial Stress vs. Lateral Deflection, W12X230 Specimens

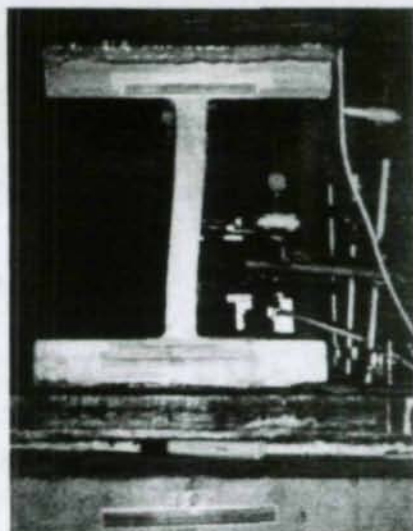


Figure 9 W12X230 Specimen  
P = 1800 Kips (8000 kN)

The bearing web will not be subject to axial loading only; the horizontal forces due to temperature change and live load rotation will produce bending in the web. The design of members for combined bending and axial loading is governed by an interaction equation. The AASHTO allowable stress design specification (AASHTO, 1992) requires the check of two interaction equations, one of which governs for failure due to instability and one which governs for yield failure. The high compressive loads in bridge bearings will necessitate the use of wide-flange sections with thick webs and correspondingly low slenderness ratios. The test results showed that for webs with low slenderness ratios, buckling occurred in the strain hardening range. Therefore, it seems reasonable to base the design on yielding. To ensure that yielding will always control the design, the slenderness ratio of the wide-flange will be limited such that general yield failure will occur prior to buckling failure. If the allowable compressive stress is  $0.472F_y$  (a safety factor of 2.12 is used) and the effective length factor of the web is set to one, the limiting slenderness ratio becomes

$$\frac{h}{r} \leq 1.22 \sqrt{\frac{E}{F_y}} \quad (1)$$

where E is the modulus of elasticity. If  $F_y = 50$  ksi (345 MPa) the maximum slenderness ratio is 29.

Since  $r = t / \sqrt{12}$  for a rectangular section, the limiting slenderness ratio can be converted to a minimum thickness limit. If the allowable bending stress is set to  $0.55F_y$ , the interaction equation to be used for the design of the bearing web is

$$\frac{f_a}{0.472 F_y} + \frac{f_b}{0.55 F_y} \leq 1 \quad ; \quad t_w \geq 2.85 h \sqrt{\frac{F_y}{E}} \quad (2)$$

### 2.3 Behavior of Bearing Flange

The compressive loads in steel bridge bearings are typically transferred to the concrete pier through bearing plates, which are designed based on the assumption of uniform stress distribution in the concrete. This assumption is valid only if the bearing plate is flexurally very stiff in relation to the concrete; this is typically not the case and the result is a very conservative design. The flange of the rolled wide-flange section acts as a bearing plate to distribute the concentrated web load to either another bearing plate or directly to the concrete. The load in the web is a point load applied to the center of the flange and since the flange is not infinitely stiff it will bend, in a manner similar to a beam on an elastic foundation.

Figure 10 shows the ratio of the end deflection of the plate to the center of the plate vs. the quantity  $\beta l$ , where  $\beta$  is a measure of the modulus of reaction of the concrete to the flexural stiffness of the beam (or plate) and  $l$  is the length of the plate. The graph shows that as the beam becomes less flexurally stiff, i.e. the length increases, the stress distribution in the concrete becomes less uniform. At a certain length the ends of the plate begin resisting tension; since a bearing plate is not designed to resist tension, a portion of the plate becomes ineffective. This behavior was confirmed during the compression tests through the use of strain gages placed on the bearing plate. The stress in the plate as calculated based on a uniform stress distribution was many times larger than the recorded stress. The tests also showed that the concrete bearing stress can reach several times its allowable value (for the tests,  $0.6 f_c$ ) with no signs of distress. A design procedure was developed for determining the required thickness for the bearing plate based on a modelling of the bearing plate as a beam on an elastic foundation.

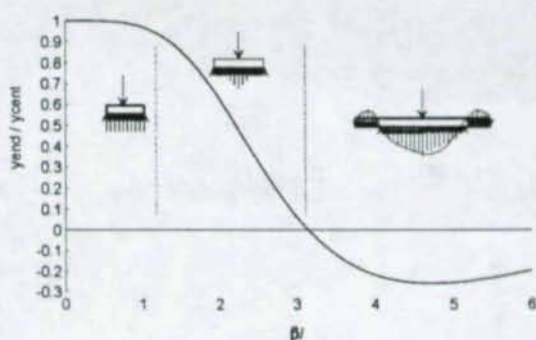


Figure 10 Ratio of End Deflection to Center Deflection vs.  $\beta l$

## 3. OUT-OF-PLANE FATIGUE STRENGTH OF WIDE-FLANGE SECTIONS

### 3.1 Test Variables

The bridge bearings will be subject to out-of-plane distortion due to horizontal movements and rotations. The primary horizontal movement is due to contraction and expansion caused by temperature changes. This movement, however, is not considered likely to cause fatigue damage. Fatigue damage is caused by the movements and forces produced by the cyclic live loading of truck traffic, which produces a horizontal displacement, as well as a rotation, at the bearing location (shown in Figure 4).

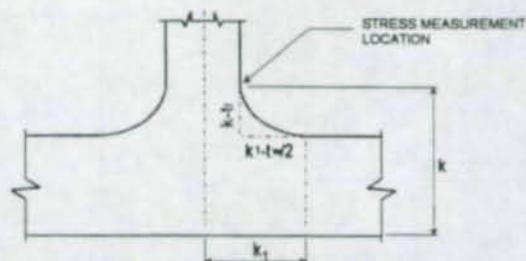


Figure 11 Location of Maximum Stress

The maximum stress in the bearing occurs at the intersection of the web and the flange, as shown in Figure 11. Rolled structural shapes have an approximate parabolic fillet transition from the web to the flange. Stress risers will be present in this transitional area, the magnitude of which will depend on the geometry of the transition. A sharper transition will produce a larger stress riser. Fatigue cracks may develop at these stress riser locations. The edges of the fillet are defined by two dimensions,  $k-t_f$  and  $k_1-t_w/2$ . There is not much variation in these dimensions for the W12 and W14 sections. The fatigue specimens comprised the same three sizes that were tested in the compression tests. The objective of the fatigue tests was to determine if a wide-flange section, when subject to cyclic out-of-plane shear distortion, would exhibit a fatigue life consistent with an AASHTO category A detail. The category A detail encompasses details described as "Plain material, Base metal with rolled or cleaned surfaces". The allowable stress range is 24 ksi (165 MPa) for an infinite life rating. Since a category A fatigue detail rarely controls the design of a bridge detail, a classification of the wide-flange section as such would simplify the design procedure by eliminating the requirement of checking for fatigue. Given that the allowable stress range for a category A detail for infinite life is 24 ksi (165 MPa), the fatigue specimens were tested at stress ranges above this value, 30 ksi, 40 ksi, and 50 ksi (207, 276 and 345 MPa).

### 3.2 Test Program

The test frame, shown in Figure 12, was designed to simulate the horizontal displacement caused by the longitudinal girder rotation. The individual test specimens were 12 in. (305 mm) wide. In most cases, two specimens were tested simultaneously, located symmetrically above and below the load application point. The top flange of the upper specimen and the bottom flange of the lower specimen were bolted to the test frame and were restrained from

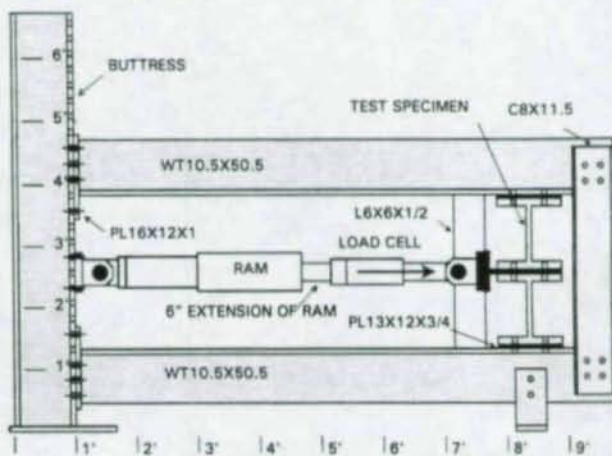


Figure 12 Schematic of Fatigue Test Setup

rotation and displacement. The bottom flange of the upper specimen and the top flange of the lower specimen were bolted together, but separated by a 1 in. (25 mm) thick loading plate. The loading plate was attached to a hydraulic ram that applied a constant amplitude sinusoidal load. The two specimens were free to translate, but not to rotate, at the load application point. Some tests were also conducted with only one specimen in the lower position. These tests were necessary to produce a 40 ksi (276 MPa) stress range in the W12X230 (W310X310X342) specimens and in the single specimen tests a rotation as well as a horizontal displacement was produced.

Strain gages were used to measure the stress ranges at the anticipated peak tensile stress locations, assumed as the point of tangency of the web and the fillet, or the dimension  $k$  from the bottom flange. The constant amplitude, sinusoidal cyclic load was applied by means of a closed-loop hydraulic system. A load controller was used to define the mean load and the tensile load range. The minimum load was set to produce a minimum stress of approximately +4 ksi (28 MPa) for the fillets in tension. The load frequency varied from 3.0 Hz to 4.5 Hz and the number of cycles was recorded by a counter. Limits were placed on the load so that the system would turn off if a limit was exceeded. A fatigue crack typically activated the limit mechanism. If no fatigue crack occurred at 2 million cycles, the specimens were loaded to a 4 million cycle limit. If no fatigue crack occurred at the 4 million cycle limit, the stress range was increased and loading continued at this higher stress range until a failure occurred.

### 3.3 Test Results

The results of the fatigue tests are shown in Figure 13 as a log-log plot of the stress range vs. the

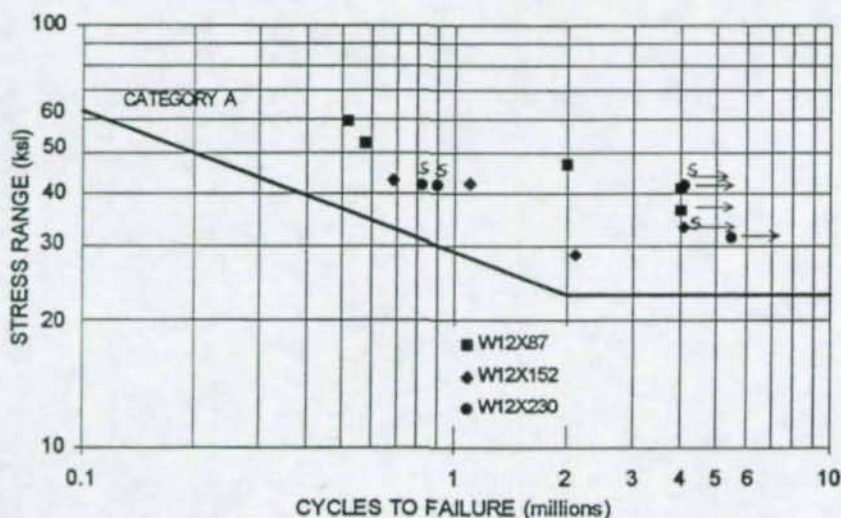


Figure 13 Stress Range vs. Number of Cycles to Failure

number of cycles to failure. One data point represents the results from each group of fillets. The data points for the fillets that did not fail are accompanied by an arrow. Superimposed on the graph is the equation for the category A detail. In all cases, the experimental data points lie above the category A boundary. The data points for the tests in which only one specimen was tested are indicated by an asterisk. The results do not seem to be influenced by the test configuration. In all cases, the crack initiated at some point within the center two-thirds of the web. There was usually more than one crack initiation site and typically more than one crack plane. The cracks usually occurred just above or just below the anticipated cracking plane (at distance  $k$  from the outer surface of the flange) and the crack propagated as an ellipse. In some cases the crack was visually observed before the loading system shut down. The specimens typically went through a few hundred thousand cycles from the time the crack was observed to the time it propagated through most of the thickness of the web or to the edge of the specimen. The fatigue life of a cracked specimen was taken either as the cycle count at the time the crack was visually observed or the last observed cycle count before the system shut down (this was usually the case if the specimen failed during the night). There is not much apparent difference in the performances of the different sections, though the W12X87 (W310X310X129) sections had longer fatigue lives for higher stress ranges than the other two sections. This may be because the size of the fillet, which has dimensions ( $k_1-t_w/2$ ,  $k-t_f$ ) that are larger than the web thickness, provides a smoother transition from the web to the flange and therefore has a smaller stress concentration. Experimental thermoelastic stress analyses, conducted during the fatigue testing, showed no obvious stress concentrations in the fillets of any of the specimens. It should also be noted that all of the W12X87 (W310X310X129) and W12X152 (W310X310X226) specimens that failed had a peak stress above the yield stress. A photo of a cracked specimen is shown in Figure 14.



Figure 14 Fatigue Crack in W12X152 Specimen

#### 4. CONCLUSIONS

The research presented in this paper showed that a rolled wide-flange section can be used as a bridge support bearing. A simple interaction equation is used to design the bearing for static strength and the fatigue tests showed that a rolled wide-flange can be classified as a category A detail when subject to out-of-plane shear distortion. Also described in a qualitative manner was the behavior of the flange as it acts as a bearing plate to distribute the web load to the concrete. The flange acts more as a beam on an elastic foundation than as a rigid plate. The primary advantages of the wide-flange section

compared with the rocker detail are its simplicity and cost-effectiveness.

## REFERENCES

AASHTO, *Standard Specifications for Highway Bridges*, 15th Edition, American Association of State Highway and Transportation Officials: Washington, D. C., 1992.

AISC, *Manual of Steel Construction, Allowable Stress Design*, 9th Edition, American Institute of Steel Construction: Chicago, IL, 1989.

## CONVERSIONS

1 ft = .3048 m : 1 in = 25.4 mm : 1 lb = .453 kg : 1 kip = 4.448 kN : 1 ksi = 6.895 MPa

# PREDICTION METHOD FOR MOMENT - ROTATION BEHAVIOUR OF COMPOSITE BEAM TO STEEL COLUMN CONNECTION

Ping Ren<sup>1</sup>

Michel Crisinel<sup>2</sup>

## Abstract

The moment-rotation relationship of a composite connection is the end product of a complex interaction between the composite beam and the steel column, through the steelwork connection and the reinforced-concrete slab.

Based on numerical analysis and experimental study, simplified calculation methods to predict rotational stiffness and moment resistance of composite connections have been developed. The simplified spring model includes the steelwork connection, the horizontal shear connection and the reinforced-concrete slab. Applications of the proposed prediction methods validated using the test results are the following :

1. Calculation of the moment redistribution for composite frames, considering the partial-strength end connections and using the predicted moment resistance.
2. Calculation of the beam deflections in composite frames, considering the semi-rigidity of end connections and using the predicted rotational stiffness.

## 1. INTRODUCTION

Joints in composite structures comprise the following load transfer components (Figure 1):

- steel beam and column via the steelwork connection (endplate, cleats, bolts, etc.)
- reinforced-concrete slab and decking (if used).

At present it is customary in structural frame design, to simplify actual beam and column connections and assume that they behave as ideally fully rigid or pinned. The ideally pinned connection implies that no moment will be transmitted between the

<sup>1</sup>Dr, Commercial Intertech, Diekirch-Luxembourg (former Ph. D. Student at ICOM EPFL)

<sup>2</sup>Section Manager, ICOM-Steel Structures, Swiss Federal Institute of Technology (EPFL), Lausanne

beam and the column, and the fully rigid connection implies that no relative rotation will occur between the beam and the column. Although, it is recognised that even pinned connections possess some ability to resist moment, and rigid connections also have some flexibility, these two ideal assumptions are rarely encountered in real structures.

In this study, connection types have been limited to the double web cleat and the flush end plate connections. These two types of connections are typical pinned and semi-rigid connections, they are also the most common connections used in Switzerland (Figure 1).

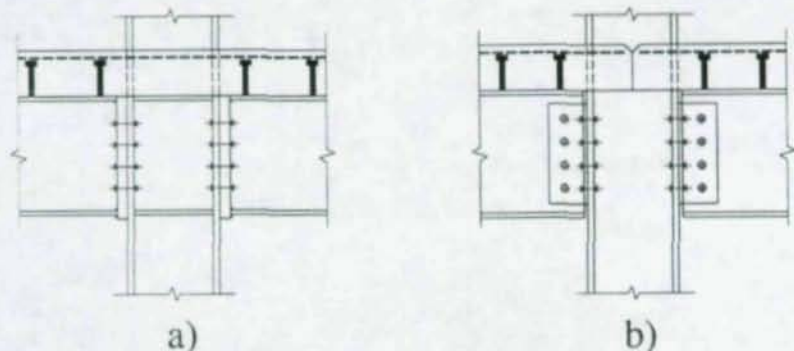


Figure 1 - Composite joints with typical steelwork connections

The performance of frames being strongly influenced by the behaviour of the connections, there are advantages to consider their semi-rigid behaviour in the design, which can lead to more economical structures and to a more reasonable estimation of the structure strength.

Composite connections can achieve significant stiffness and strength being provided by the longitudinal reinforcement placed continuously in the slab. According to the European prestandard for composite steel-concrete structures (Eurocode 4, 1992), semi-rigid composite connections are allowed. However, no application rules are given for the calculation of moment resistance, rotational stiffness or rotation capacity of composite semi-rigid connections. In addition no application rules are given for analysis of frames with such connections, existing methods are not sufficiently developed to be included in this code and the prediction of moment-rotation characteristics for composite connections is not well established.

The main problems existing when modelling the composite connection behaviour are the steelwork connection under bending moment and axial compression, the slip between the slab and the steel beam, the reinforced-concrete slab under tension, the interaction between the reinforcing bar and the concrete, the interaction of slab with column, etc.

Based on above consideration, the objectives of the study carried out at ICOM-EPFL (Ren, 1995) were as follows:

- To develop a numerical model which can analyse the non-linear composite joint behaviour, taking into account the flexibilities governing the composite joint characteristics.
- To conduct experimental investigation of bare steel connections and composite connections for supporting the proposed numerical model.
- To identify the relative importance of the parameters affecting the composite connection behaviour.
- To develop simplified methods to predict the key values required for the design of composite connections.

The present contribution emphasizes especially the development of this simplified prediction method.

## 2. THEORETICAL AND EXPERIMENTAL INVESTIGATIONS

A numerical model to analyse the non-linear composite joint behaviour including all the flexibilities governing the characteristics of this type of joint has been developed ((Ren & Crisinel, 1994, Ren, 1995). By incorporating this numerical model into an existing composite beam analysis program COMPCAL (Ren & Crisinel, 1992), a new program COJOINT has been developed to simulate the semi-rigid behaviour of composite joints. The program COJOINT has been verified with 14 tests of specimens having a wide range of member geometries, types of steelwork connections, degrees of shear interaction and ratios of reinforcement. The comparisons demonstrated a very good moment-rotation agreement between the tests and the numerical simulations. The relative importance of the parameters affecting the composite joint behaviour has been identified by a parametric study with the use of the program COJOINT.

Two series of tests have been conducted (Ren & Crisinel, 1994). The first series (bare steel beam-to-column connection tests) involving 11 individual specimens was initially carried-out to assess the interaction between bending and normal forces as well as the contribution of the steelwork connection to the composite connection behaviour. The second series (three composite joint tests) was then performed in order to understand the influence of the slab on the steel connection behaviour with respect to the amount of reinforcement used in the slab and different types of steelwork connections.

### 3. MOMENT-ROTATION RELATIONSHIP

For the analysis of structures, the characteristics of composite connection moment-rotation curves should be known. For design purposes, the characteristic curve is divided by a safety factor. For simplification, this design curve is often replaced by a tri-linear diagram as shown in Figure 2. The three properties needed for the design are:

- the moment resistance,  $M_{cj}$  (calculated plastic moment of the composite connection),
- the rotational stiffness,  $S_j$  (secant stiffness of moment-rotation curves which corresponds to the elastic bending moment of the "cracked" composite connection cross-section). It is assumed that, at this moment, the concrete is cracked, the reinforcement is in the elastic state and the steelwork is in the elastic state (rigid connections) or in the elasto-plastic state (flexible connections).
- the rotation capacity  $\theta_u$  (defined here as the rotation achieved before the resistance moment falls below its plastic value  $M_{cj}$  as shown in Figure 2).

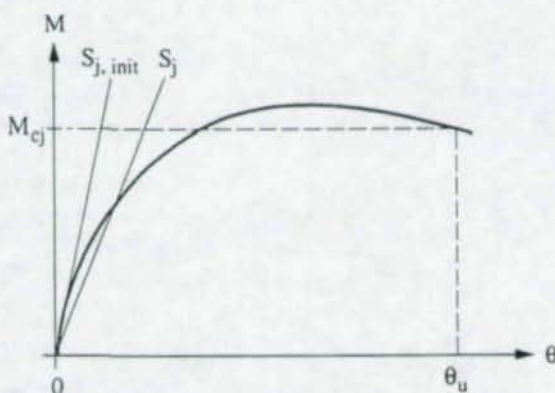


Figure 2 - Main properties for moment-rotation curve

The proposed prediction method is based on a mechanical model, and the key elements of the composite connection are simulated by a spring system. The important parameters which influence the moment-rotation behaviour of a composite joint and partial shear interaction can be included in this method .

Figure 3a shows a composite connection with an applied moment  $M$ . In the connection cross-section, this moment is represented by two component moment  $M_{slab}$  and  $M_{conn}$ , plus a couple of forces  $F_s$  and  $F_c$ . The following simplifications are made :

- The moment  $M_{slab}$  taken by the slab is ignored.
- The tensile force  $F_s$  is acting in the reinforcement.
- The compressive force  $F_c$  and the bending moment  $M_{conn}$ , are acting at the neutral axis of the steelwork connection.

The equilibrium of the system is written as follows :

$$M = F_s \cdot z + M_{\text{conn.}} \quad (1)$$

$$F_s = F_c \quad (2)$$

$z$  : distance between the neutral axis of steelwork connection and the axis of the reinforcement.

At initial elastic state, it is assumed that the compression centre of the steelwork connection is located at the bottom flange of the steel beam for the flush end plate connection (Figure 3b), and at the lower bolt row level for the double web cleat connection. This further assumption can be expressed as follows :

$$M_{\text{conn.}} = F_c \cdot e \quad (3)$$

$e$  : distance between the neutral axis of the steelwork connection and the compression centre (bottom flange of the steel beam in case of flush end plate connection).

Substituting the Equations (2) and (3) into (1), this one can be written in the following form :

$$M = F_s \cdot z + F_c \cdot e = F_s(y_s + y_c) \quad (4)$$

$y_s$  : distance between the axis of the reinforcement and the interface

$y_c$  : distance between the bottom flange of the beam and the interface

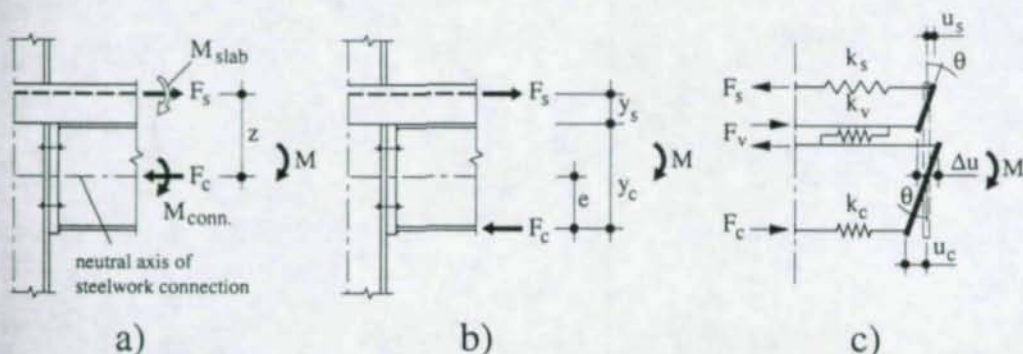


Figure 3 - Simplified spring mechanism for a composite joint

For modelling the deformation of this composite connection, a spring system shown in Figure 3c is used. A tension spring is used to simulate the behaviour of the reinforced-concrete slab in tension. A compression spring is used to simulate that of the steelwork connection in compression. A horizontal shear spring is used to simulate the behaviour of shear interaction between the concrete slab and the steel beam. This shear interaction is provided by the shear connectors of the composite beam. It is equal to the transferring force between the slab and the steel beam.

If there is no interface slip between the slab and the steel beam (full shear interaction), the spring stiffness of the shear interaction should be equal to infinity. If there is no shear interaction between the slab and the steel beam, the spring stiffness should be equal to zero. Each component has its proper equilibrium condition.

Each spring can be assumed to be elastic or elastic-plastic. In Figure 3c,  $k_s$  is the tension stiffness of the reinforced-concrete slab,  $k_c$  is the compression stiffness of the steelwork connection, and  $k_v$  is the stiffness of the shear connectors.  $\Delta u$  is the interface slip between the slab and the steel beam. After deformation, the cross-sections of the reinforced-concrete slab and the steel beam are assumed to remain in plane with the same rotation.

From the Figure 3c, the interface slip between the slab and the steel beam can be written as :

$$\Delta u = -u_c - u_s + \theta (y_c + y_s) \quad (5)$$

$u_s$ ,  $u_c$  and  $\Delta u$  are, respectively, the deformation of the springs representing the reinforced-concrete slab, the steelwork connection and the horizontal shear interaction. They can be written in the following form :

$$\left. \begin{aligned} u_s &= \frac{F_s}{k_s} \\ u_c &= \frac{F_c}{k_c} \\ \Delta u &= \frac{F_v}{k_v} \end{aligned} \right\} \quad (6)$$

$F_v$  is the shear interaction force transferred from the reinforced-concrete slab to the steelwork connection.

Substituting Equation (6) into Equation (5), and considering the equilibrium condition of forces  $F_v = F_s = F_c$ , the following relation can be obtained :

$$\left. \begin{aligned} \frac{F_v}{k_v} &= -\frac{F_c}{k_c} - \frac{F_s}{k_s} + \theta (y_c + y_s) \\ F_s \left( \frac{1}{k_v} + \frac{1}{k_c} + \frac{1}{k_s} \right) &= \theta (y_c + y_s) \end{aligned} \right\} \quad (7)$$

Replacing the above Equation into Equation (4), the moment is calculated as follows :

$$M = \frac{(y_c + y_s)^2}{\frac{1}{k_v} + \frac{1}{k_s} + \frac{1}{k_c}} \theta \quad (8)$$

This can be expressed in the form of rotational stiffness as follows:

$$S_j = \frac{M}{\theta} = \frac{(y_c + y_s)^2}{\frac{1}{k_v} + \frac{1}{k_s} + \frac{1}{k_c}} \quad (9)$$

- If the springs represent the elastic "uncracked" behaviour of the connection cross-section, the initial stiffness  $S_{j,init}$  can be defined (Figure 2).
- If the springs represent the plastic "cracked" behaviour of the connection cross-section at moment resistance  $M_p$ , the rotation capacity  $\theta_u$  at the ultimate limit state can be determined.
- If the springs are assumed to represent an elasto-plastic behaviour, for a given design moment, the rotational stiffness  $S_j$  at serviceability limit state can be determined.

#### 4. PREDICTION OF ROTATIONAL STIFFNESS AT SERVICEABILITY LIMITE STATE

From Equation (9), calculation of the rotational stiffness of the composite connection can be converted to determine the stiffnesses of the tension spring of the reinforced-concrete slab, the compression spring of the steelwork connection and the shear interaction spring of the connectors. Knowledge obtained from experimental results on bare steel connections and from numerical calculation results of the internal force-deformation relations is required.

##### Stiffness of reinforced-concrete slab

The stiffness of the slab is given by :

$$k_s = \frac{E_s A_s}{L} \quad (10)$$

$E_s$  : modulus of elasticity of the reinforcement (mesh and reinforcing bars)

$A_s$  : section area of the reinforcement

$L$  : length of the slab element with the extension  $u_s$ .  $L$  is calculated using the following formula, which consider the effect of cracking of the concrete (see Ren, 1995) :

$$L = 2 \eta l_r = 2 \eta (60 + 1.3 k \cdot s) \quad (11)$$

$\eta$  : coefficient depending on the cohesive characteristic between the reinforcement and the concrete, normally approximated as 0.35

$l_r$  : length of transmission of the cohesive force between steel bar and concrete

- $k$  : coefficient equal to 1.0 in the case of pure tension and 0.5 in the case of simple bending (slab is the case)  
 $s$  : spacing distance between the reinforcement (mesh and reinforcing bars)

### Stiffness of shear connectors between slab and steel beam

The load-slip behaviour is determined using "push-out" tests of connectors. The typical load-slip behaviour of welded shear connectors is shown in Figure 4.

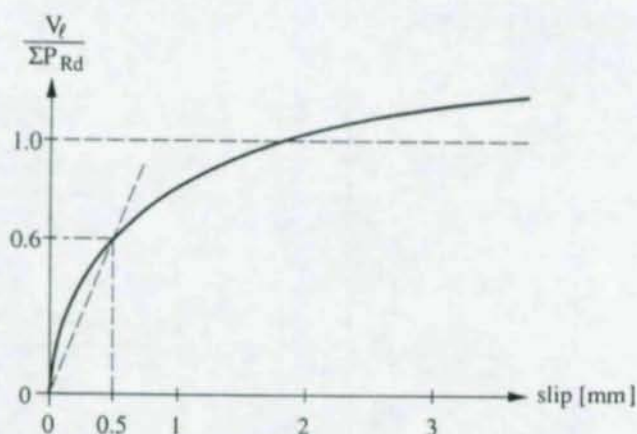


Figure 4 - Typical load-slip behaviour of welded stud shear connectors

It is assumed that at the serviceability limit state, when the corresponding shear interaction force is 0.6 the ultimate shear force, the slip at the interface is approximately equal to 0.5 mm for welded shear connector, see Figure 4 (Bucheli & Crisinel, 1983). The stiffness of the shear interaction is then expressed as follows :

If  $V_l = F_s < \Sigma P_{Rd}$ , representing a full shear interaction, then

$$k_v = \frac{0.6 F_s}{\Delta u} \quad (12)$$

If  $V_l = F_s \geq \Sigma P_{Rd}$  representing partial shear interaction, then

$$k_v = \frac{0.6 \Sigma P_{Rd}}{\Delta u} \quad (13)$$

- $\Sigma P_{Rd}$  : resistance of the sum of the shear connectors placed over the composite beam length of hogging moment  
 $F_s$  : tension resistance of the reinforced-concrete slab  
 $\Delta u$  : interface slip at serviceability limit state (taken here as 0.5 mm for welded shear connectors, see Figure 4)  
 $V_l$  : total longitudinal shear force

### Axial stiffness of steelwork connection

The simplified elastic stiffness equations for these connections are proposed as follows :

For double web cleat connection,

$$k_c = \frac{E_a A_\ell}{L} \quad (14)$$

- $E_a$  : modulus of elasticity of structural steel  
 $A_\ell$  : lateral bearing area of the beam web ( $A_\ell = n t_{wb} \cdot d$ )  
 $L$  : length of the connection element ( $L = hc/2$ )  
 $n$  : row number of bolts  
 $t_{wb}$  : thickness of the beam web  
 $d$  : bolt diameter  
 $h_c$  : height of the column cross-section

For flush end plate connection, the stiffness is taken as the smaller of the following two values:

$$k_c = \frac{E_a A_{wc}}{L} \quad \text{or} \quad k_c = \frac{E_a A_{ab}}{L} \quad (15)$$

$$\begin{aligned}
 A_{wc} &= b_{\text{eff}} \cdot t_{wc} \\
 b_{\text{eff}} &= \{2(t_p + t_{fc}) + t_{fb}\} \cdot 2
 \end{aligned}
 \quad \left. \vphantom{\begin{aligned} A_{wc} \\ b_{\text{eff}} \end{aligned}} \right\} \quad (16)$$

- $A_w$  : effective compression area of the column web  
 $A_{ab}$  : cross section area of the steel beam  
 $b_{\text{eff}}$  : effective length of the column web  
 $t_{fb}$  : thickness of the beam flange  
 $t_{fc}$  : thickness of the column flange  
 $t_p$  : thickness of end plate  
 $t_{wc}$  : thickness of the column web

For double web cleat connections, the steelwork connection may reach the plastic stage at the serviceability state. The proposed stiffness in the plastic stage is as follows:

$$k_c' = \frac{E_a' A_\ell}{L} \quad (17)$$

- $E_a'$  : strain-hardening modulus of structural steel taken as  $0.06 E_a$

### Rotational stiffness of composite connections

Applying the above three kinds of individual stiffness calculation methods to Equation (9), the predicted rotational stiffness of composite connections can be calculated. Some problems particular to different types of connection should be noted :

- For the joint with a double web cleat connection, and at serviceability limit states, the steelwork connection is probably yielded and the beam does not touch the column. The plastic compression stiffness of the steelwork connection should also be calculated. The rotational stiffness of the composite connection can be recalculated from Equation (9), substituting the elastic stiffness of steelwork connection by the plastic stiffness from Equation (17).
- For the joint with a flush end plate connection, the location of centroid of compression  $y_c$  can be considered at the lower flange level of steel beam. For the joint with a double web cleat connection,  $y_c$  can be considered at the lower bolt row level. The location of centroid of tension can be considered at the same level as the reinforcement.

## 5. PREDICTION OF MOMENT RESISTANCE

The proposed method is based on an existing one (Xiao et al, 1992), but has been modified for the calculation of the compressive capacity of the steelwork connection, and extended to double web cleat connections.

### Flush end plate connection

The moment resistance calculation, in the case of a flush end plate connection, is based on the failure mode being controlled by the tension resistance of the reinforcement,  $F_{t,s}$ . It is assumed that full shear interaction is provided between the slab and the steel beam. The tension resistance of bolt row,  $F_{t,1}$ , is determined as described in Annex J of Eurocode 3 [6]. The available compression resistance at the compressive zone of the steelwork connection,  $F_{cc}$ , is determined by the critical section of the beam flange or the effective column web. This approach is illustrated in Figure 5a.

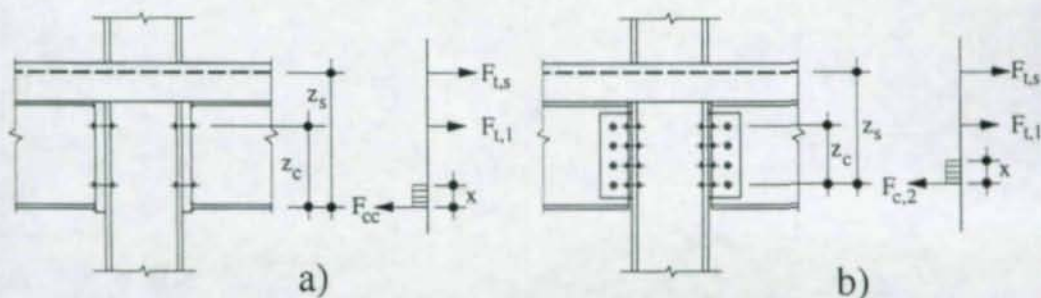


**Figure 5** - Plastic analysis of moment resistance of composite joints with (a) flush end plate connection and (b) double web cleat connection

The moment resistance of a composite connection,  $M_{cj}$ , is predicted using the following equations:

(a) If  $F_{t,s}/F_{cc} \geq 1$  :

$$x = \frac{F_{t,s} - F_{cc}}{t_{wb} \cdot f_{yb}} \quad (18)$$

$$M_{cj} = F_{t,s} \cdot z_s - (F_{t,s} - F_{cc}) \left( \frac{x}{2} + \frac{t_{fb}}{2} \right) \quad (19)$$

(b) If  $F_{t,s}/F_{cc} < 1$  and  $F_{t,s} + F_{t,1} - F_{cc} \geq 0$  :

$$x = \frac{F_{t,s} + F_{t,1} - F_{cc}}{t_{wb} \cdot f_{yb}} \quad (20)$$

$$M_{cj} = F_{t,s} \cdot z_s + F_{t,1} \cdot z_c - (F_{t,s} + F_{t,1} - F_{cc}) \left( \frac{x}{2} + \frac{t_{fb}}{2} \right) \quad (21)$$

$F_{t,s}$  : tension resistance of the reinforcement

$$F_{t,s} = A_s \cdot f_{ys} \quad (22)$$

$F_{cc}$  : compression resistance at the compressive zone of the steelwork connection taken as the smaller of the following two values:

$$\left. \begin{aligned} F_{c,fb} &= b_{fb} \cdot t_{fb} \cdot f_{yb} \\ F_{c,wc} &= f_{yc} \cdot t_{wc} \cdot b_{eff} \end{aligned} \right\} \quad (23)$$

$F_{t,1}$  : tension resistance of the bolts, as given in Annex J of Eurocode 3

$f_{ys}$  : yield strength of reinforcement steel

$f_{yb}$  : yield strength of beam steel

$f_{yc}$  : yield strength of column steel

$b_{eff}$  : effective width of the column web in compression, as given in Annex J of Eurocode 3

Other symbols are given in Figure 5a.

### Double web cleat connection

A similar procedure as that of flush end plate connections is adopted for the prediction of the moment resistance of the double web cleat composite connections. Figure 5b represents the tension and compression resistances in the composite connection section. It is assumed that the centre of compression is located at the lower row of bolts.  $F_{t,1}$  is the tension resistance in the higher row of bolts and  $F_{c,2}$  is the compression resistance of the lower row of bolts. The bearing resistance of bolts

on the beam web, the shear and tension resistances of bolts are determined according to Eurocode 3.

The moment resistance of a composite connection  $M_{Cj}$  is predicted using the following equations:

(a) If  $F_{t,s}/F_{c,2} \geq 1$ :

$$x = \frac{F_{t,s} - F_{c,2}}{t_{wb} \cdot f_{yb}} \quad (24)$$

$$M_{Cj} = F_{t,s} \cdot z_s - (F_{t,s} - F_{c,2}) \left( \frac{x}{2} \right) \quad (25)$$

(b) If  $F_{t,s}/F_{c,2} < 1$ :

$$x = \frac{F_{t,s} + F_{t,1} - F_{c,2}}{t_{wb} \cdot f_{yb}} \quad (26)$$

$$M_{Cj} = F_{t,s} \cdot z_s + F_{t,1} \cdot z_c - (F_{t,s} + F_{t,1} - F_{c,2}) \left( \frac{x}{2} \right) \quad (27)$$

## 6. ROTATION CAPACITY

Equation (8) gives the relationship of the moment-rotation of a composite connection. It can be written in the following form :

$$\theta = \frac{\frac{1}{k_v} + \frac{1}{k_s} + \frac{1}{k_c}}{(y_c + y_s)^2} M \quad (28)$$

For a given moment, the corresponding rotation can be determined. At ultimate limit states, the moment resistance of the composite connection can be calculated as described above. If it is assumed that the reinforced-concrete slab is at the plastic cracked state, the stiffness of the slab can be calculated from Equation (10). The shear connectors can be assumed to have reached its maximum slip, the corresponding stiffness of the shear connectors can be calculated from Equations (12) or (13). The steelwork connection is not the critical factor for causing failure of the composite connection, its stiffness can still be calculated from Equation (14). After calculating the three stiffnesses and the moment resistance of the composite connection, the rotation capacity may be determined from Equation (28).

## 7. COMPARISON OF PREDICTION WITH TEST RESULTS

A typical comparison between predicted and tested M- $\theta$  relationship is shown in Figure 6. The numerical calculation result is also shown in this figure.

The comparison of the moment-rotation curves obtained by the prediction method and the tests has been made using 12 experimental specimens. A generally good agreement has been found between the predicted behaviour and the test results. The predicted rotational stiffness does usually correspond to moments equal to 0.5 to 0.7 times the maximal moment. Therefore, this predicted rotational stiffness can be regarded as the stiffness of composite connections at the serviceability limit state. The predicted moment resistance can be regarded as the maximum moment of the composite connections at the ultimate limit state.

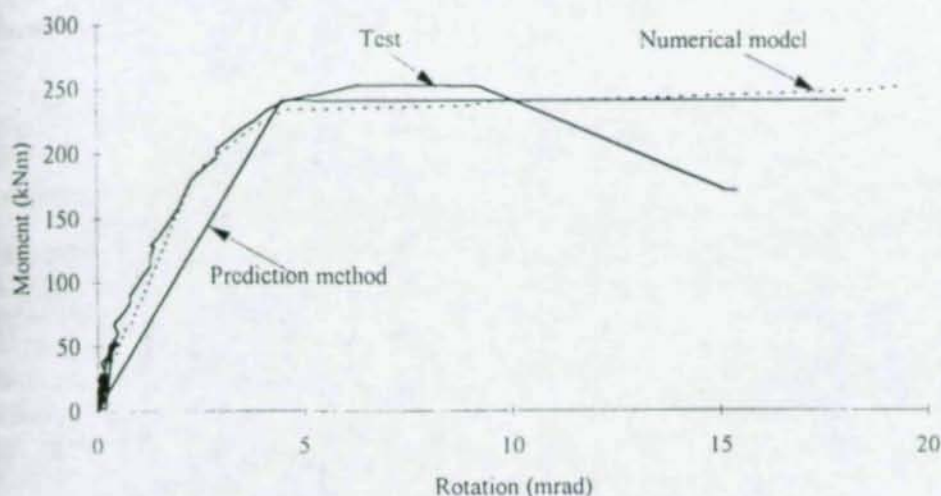


Figure 6 - Comparison for test No.1 (specimen CP01)

## 8. CONCLUSIONS

Having conducted a numerical analysis and an experimental study, simplified calculation methods have been developed for the design of composite connections to predict the rotational stiffness at the serviceability limit state and the moment resistance at the ultimate limit state. The prediction methods have been validated using test results. These methods can be used for the following practical design applications :

- For the ultimate limit state, calculating the moment redistribution for composite frames, considering the partial-strength end connections, using the predicted moment resistance.
- For the serviceability limit state, calculating the deflections of beams in composite frames, considering the semi-rigid end connections, using the predicted rotational stiffness.

## REFERENCES

- BUCHELI P. and CRISINEL M., "Poutres mixtes dans le bâtiment", Centre Suisse de la Construction Métallique (SZS), Publication SZS-A3, Zurich, 1983.
- EUROCODE 3, "Design of steel structures, Part 1.1 General rules and rules for buildings, Revised Annex J: "Joints in building frames", ENV 1993-1-1:1992/pr A2 : 1994, Comité Européen de Normalisation (CEN), Brussels, 1992.
- EUROCODE 4 "Design of composite steel - concrete structures". ENV 1994-1-1:1992, Comité Européen de Normalisation (CEN), Brussels, 1992.
- REN P. and CRISINEL M., "Non-linear analysis of composite members - A new version of the program CompCal, theory, user guide and comparison", Publication ICOM 280, Ecole polytechnique fédérale, Lausanne, 1992.
- REN P. and CRISINEL M., "Effect of reinforced concrete slab on the moment-rotation behaviour of standard steel beam-to-column joints", 2nd Workshop COST C1, Prague, 1994.
- REN, P. "Numerical modelling and experimental analysis of steel beam-to-column connections allowing for the influence of reinforced-concrete slabs", Thesis EPFL No 1369, Ecole polytechnique fédérale, Lausanne, 1995.
- XIAO R., NETHERCOT D. A. and CHOO B.-S., "Moment resistance of composite connections in steel and concrete", Proceedings of the first world conference on constructional steel design, Acapulco, Mexico, November 1992.

## PERFORMANCE OF MIXED CONNECTIONS UNDER COMBINED LOADS

Yasuhiro Ohtani<sup>1</sup>

Yuhshi Fukumoto<sup>2</sup>

Bunzo Tsuji<sup>3</sup>

### Abstract

Steel-concrete mixed connection is studied. The type of connection is endplate type. The connection is proposed for jointing steel members. To clarify the performance of the connection, series of experiments are carried out. Through the experimental observation, capability are examined.

### 1. INTRODUCTION

On site work, bolted joint is usually used for connecting steel members of structures. Since the manufacturing tolerance allowed to the bolted joint is the same in spite of size of the structure, difficulty may arise when large structures are built up or erected on site. It must be of great interest to develop a method of connection which allows larger tolerance in the field work without any degradation of performance compared with the bolted joint.

Adaption of steel-concrete mixed type joint may be one of the solutions to the above issue. The basic concept of the joint is an usage of reinforced concrete instead of bolts for the connection. Since concrete can take any shape by nature, fairly larger tolerance allowed on site work is possible. The connection can be designed so as to have smooth transmission of forces from one member to the other, and to have certain capacity required. In addition, sufficient ductility may also be expected if the mutual restraint due to the interaction of steel and concrete materials is effectively used.

---

<sup>1</sup>Associate Professor, Kobe University, Rokkodai, Nada, Kobe, 657 Japan.

<sup>2</sup>Professor, Osaka University, Suita, Osaka, 565 Japan.

<sup>3</sup>Professor, Kobe University, Rokkodai, Nada, Kobe, 657 Japan.

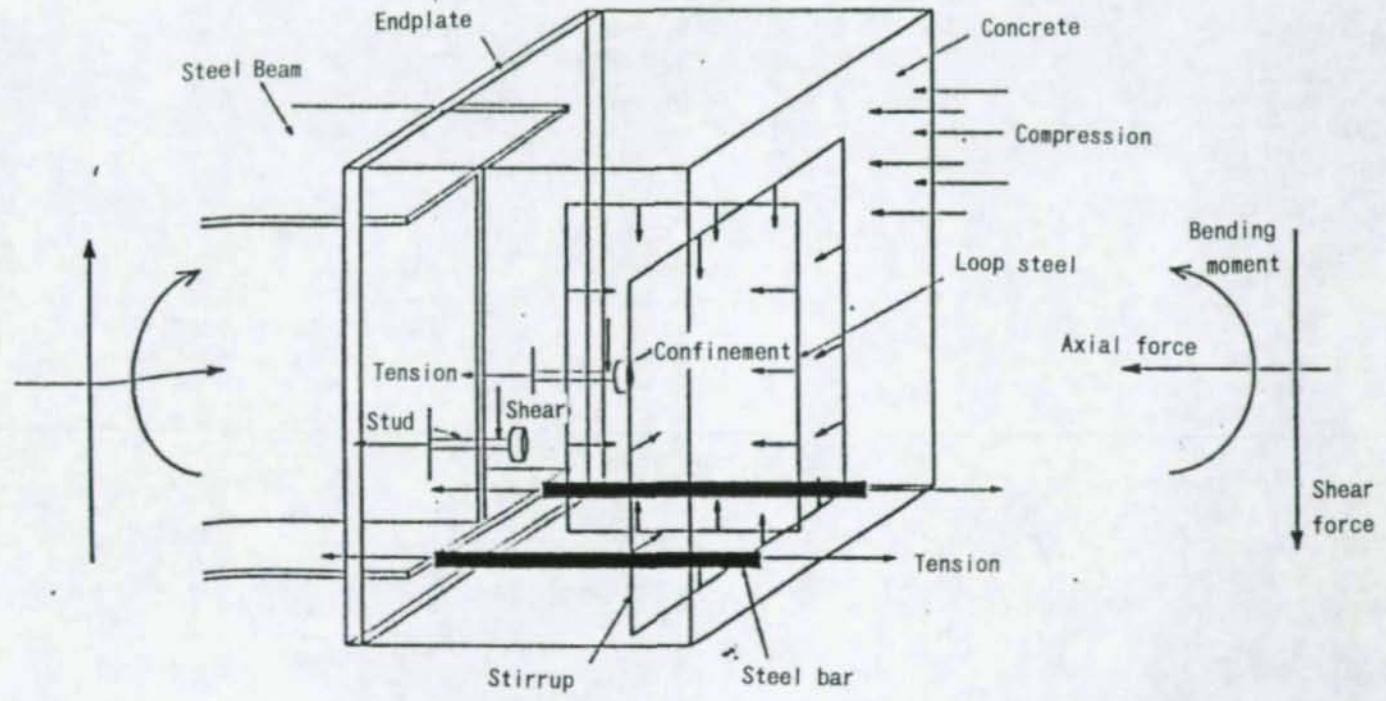


Fig.1 Mixed Connection

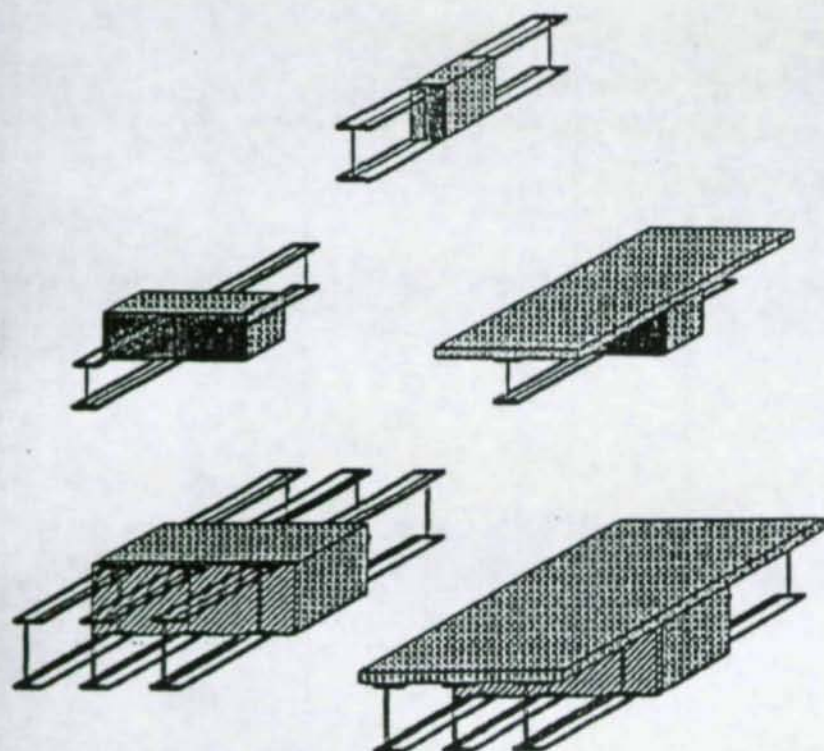


Fig.2 Beam-to-Beam Joint Specimens

Table 1 Parameters

Category	Item	Notations used in name of specimen
Main beam	Type of beam	C : Composite beam S : Steel beam
	Number of beams	1 : Single beam 3 : Three beams
Connection profile	Type of arrangement of steel bars (Fig.3)	1 : Inside (flush) 2 : Outside (extended) 3 : Equally both side (extended) 4 : Not equally both side (extended)
	Width of RC segment	W : Widened None : Same as frange width
Loading condition	Type of loading	M : Bending moment Q : Shear load N : Thrust
	Direction or procedure	P : Positive moment direction N : Negative moment direction C : Cyclic loading
Stress distribution	Tensile elements	R : Rebars in slab None : Steel bars

In this study, the mixed connection which consists of steel endplates and a reinforced concrete segment is proposed for the joint of steel members. Since the performance of the connection affects on the behaviour as well as the strength of the whole structure, the study is dedicated to clarify the performance of the connection. To this end, experimental study as well as analytical study were carried out. In this paper, some results and findings through the series of experiments will be reported.

Herein, mixed connections of beam-to-beam joints are mainly treated. Therefore, experiments were carried on beam type specimens, in which the connection are subjected to pure bending or bending and shear combined loads. A mixed type connection can also be found in a hybrid frame systems, in which, for instance, concrete columns and steel beams are connected. Since the results obtained herein may not be specific but fundamental, those can also be utilized for the evaluation of the structure in which mixed connections are used in beam-to-column joints.

## 2. EXPERIMENT ON ENDPLATE TYPE MIXED CONNECTION

### 2.1 Series of Specimens

Fig.1 shows the schematic view of the steel-concrete mixed type connection treated in this study. The type of connection used was so-called endplate type. A steel endplate was welded at the end of a steel beam, then the reinforced concrete was placed. The experiments were carried out on beam type specimens. As shown in Fig.2, the mixed type of connection was used in the several beam-to-beam joint specimens, where single or multiple number of steel or composite beams were longitudinally connected by reinforced concrete segment. Since resultants must be transmitted through the connection from one side of beams to the other, suitable amount of reinforcing steels and headed stud anchors were placed in the connection.

Fifteen specimens were prepared and tested. Parameters considered were, as shown in Table 1, type of beam, number of beams, type of endplate, arrangement of steel bars, size of connection, loading condition, etc. Series of the specimens are listed with combination of parameters in Table 2. Among these parameters, the arrangement of steel bars is related with the type of endplate as shown in Fig.3. For flush endplate type, steel bars can be placed only inside the flanges (Type-1). For extended endplate type, three types of arrangement are used; steel bars are placed only outside the flanges in Type-2, steel bars are placed equally both side of the flanges in Type-3, and steel bars are placed not equally both side of the flanges in Type-4. The arrangement of steel bars is also related with the type of beam and with the loading condition. If composite beams are used, no steel bar is placed at the endplate in the slab side, but placed in the other side. For the specimen subjected to only one side loading, no steel bar is placed in compression side. In these cases, type of the arrangement is referred to the side where bars are placed.

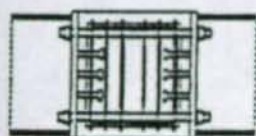
### 2.2 Experimental Results

The series of the experiments were carried in several steps. The specimens can be categorized to five groups as follows, (Fig.4)

- 1) Single composite beam specimens under bending and shear combined loads. (8 spcs.)

Table 2 Series of Specimens

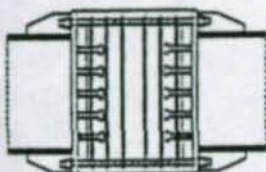
No.	Specimen	Beam		Connection		Loading		Stress
		Type	No.	Steel bars	Width	Type	Direct.	Tensile
1	S1-1-(M+N)C	Steel	1	Type-1		M,N	Cyclic	
2	S1-2-(M+N)C	Steel	1	Type-2		M,N	Cyclic	
3	S1-3-(M+N)C	Steel	1	Type-3		M,N	Cyclic	
4	S1-4W-(M)P	Steel	1	Type-4	Wide	M	Positive	
5	S1-4W-(M+Q)P	Steel	1	Type-4	Wide	M,Q	Positive	
6	S3-4W-(M+Q)P	Steel	3	Type-4	Wide	M,Q	Positive	
7	C1-1-(M)P	Composite	1	Type-1		M	Positive	
8	C1-1-(M+Q)P	Composite	1	Type-1		M,Q	Positive	
9	C1-1W-(M)P	Composite	1	Type-1	Wide	M	Positive	
10	C1-1W-(M)NR	Composite	1	Type-1	Wide	M	Negative	Slab bar
11	C1-1W-(M+Q)P	Composite	1	Type-1	Wide	M,Q	Positive	
12	C1-1W-(M+Q)NR	Composite	1	Type-1	Wide	M,Q	Negative	Slab bar
13	C1-4W-(M)P	Composite	1	Type-4	Wide	M	Positive	
14	C1-4W-(M)NR	Composite	1	Type-4	Wide	M	Negative	Slab bar
15	C3-4-(M+Q)NR	Composite	3	Type-4		M,Q	Negative	Slab bar



Type-1

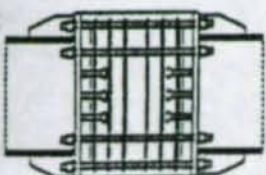
Flush endplate type

Steel bars are placed only inside the flanges



Type-2

Steel bars are placed only outside the flanges



Type-3

Steel bars are placed equally both side of the flanges

Type-4

Steel bars are placed not equally both side of the flanges

Fig.3 Arrangement of Steel Bars

- 2) Multiple composite beam specimens under bending and shear combined loads. (1 spec.)
- 3) Single beam specimens under thrust and bending combined loads. (3 specs.)
- 4) Single beam specimens under bending and shear combined loads. (2 specs.)
- 5) Multiple beam specimens under bending and shear combined loads. (1 spec.)

Details of each test procedure can be found other place, herein only a brief summary is drawn. Except for the specimen group 3), most of all specimens were tested under pure bending or bending and shear combined loads. All of the specimens were tested under elastic loading first, then loaded to the failure. In table 3, peak loads at failure of each specimen are listed. Failure mode of each specimen is also listed in the table. The failure of this type of structures may fall into three categories, that is, a) failure of the beam due to yielding or buckling of flange, b) failure of the reinforced concrete segment due to yielding of steel bars, crush or shear failure of concrete, and c) failure of the endplate due to yielding. Peak loads were estimated using the material test data, and listed in Table 3 for comparison. The peak loads were calculated assuming that capacity of the reinforced concrete segment can be estimated by the strength formula for reinforced concrete beam. From the comparison with experimental data, good agreement are obtained for a single beam specimen if failure occurs in concrete segment.

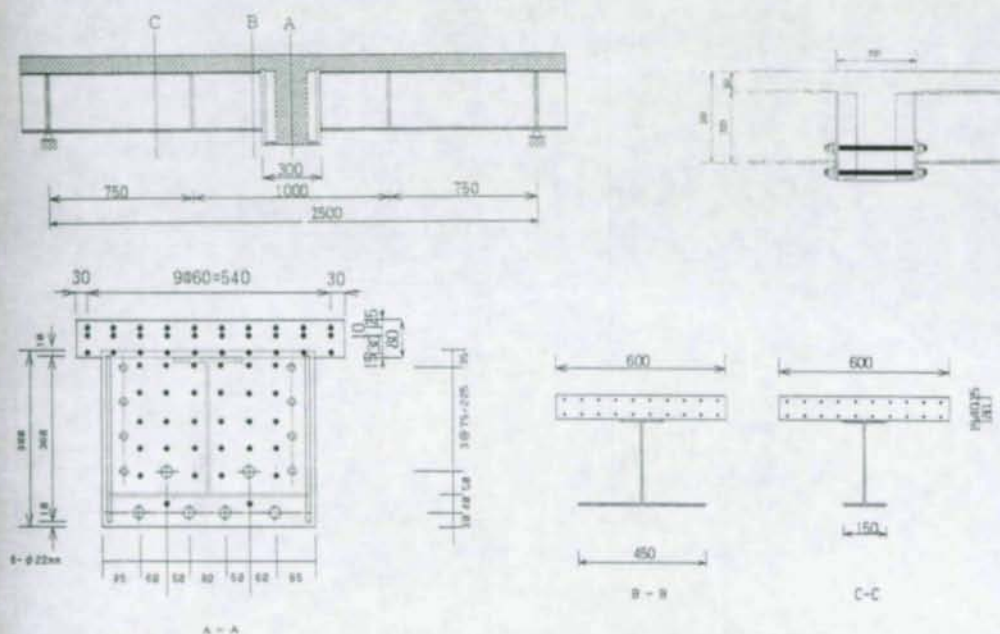
There exist significant relative rotation between endplates when flush endplates are used. The relative rotation must be due to the behaviour of the endplate, concrete, and steel bars. From the experimental observation, it is found that initial rotational stiffness depend on the magnitude of the axial forces. The gap between an endplate and concrete segment is mainly due to the local deformation of the endplate. This gap causes discontinuous rotation, and sometimes makes significant influence to the structural behaviour.

### 3. SOME REMARKS

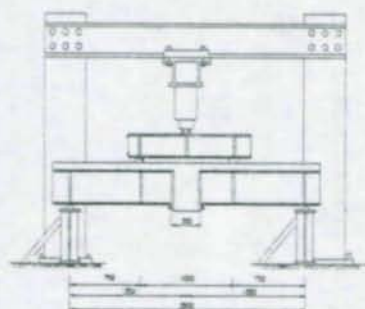
Steel-concrete mixed type of connection was investigated. Through the series of experimental studies, performance of the connection was examined. It is confirmed that strength requirement can be fulfilled. Since its behaviour is somewhat semirigid, appropriate treatment of the connection will be a subject.

### REFERENCES

1. Y.Ohtani, T.Satoh, Y.Fukumoto, S.Matsui, and A. Nanjou, "Performance of Connection in Continued System of Simple Composite Girders", Proceeding of 4th ASCCS Intl. Conf., STEEL-CONCRETE COMPOSITE STRUCTURE, 438-441, 1994.
2. Research Report "Experimental Study on Mechanical Behavior of Connection in Continued Simple Composite Girders," Hanshin Express Way Public Co., 1991

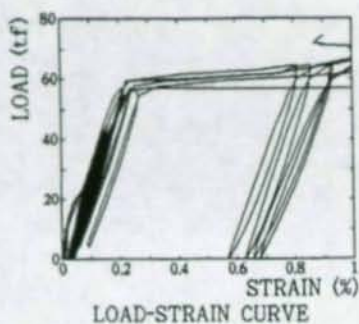


(a) Specimen

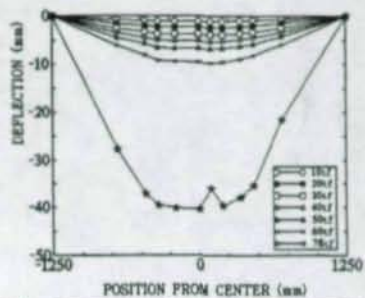


(b) EQUIPMENT FOR LOADING

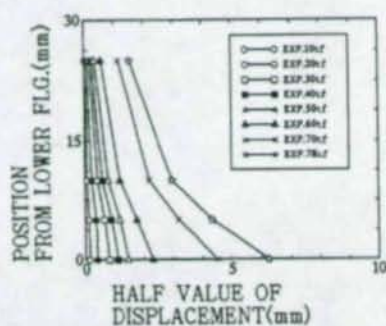
Fig.4 Series of Experimental and Analytical Study  
Specimen C1-4W-(M)P



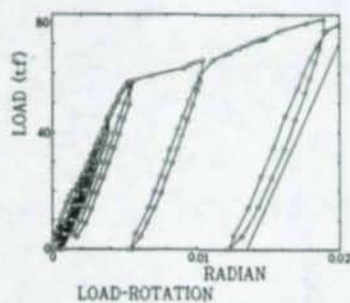
(c) BOLT



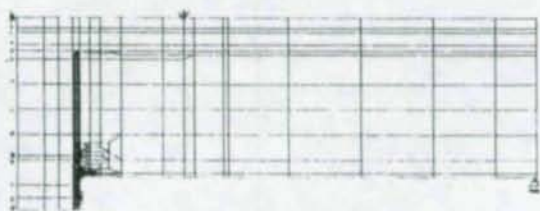
(d) DISTRIBUTION OF DEFLECTION



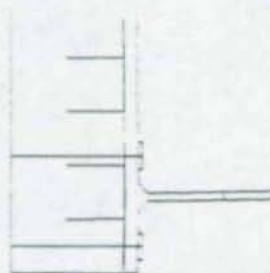
(e) DEFORMATION OF END-PLATE



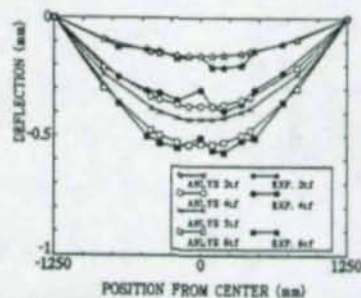
(f) ROTATION OF END-PLATE



(g) MODEL



(h) LOCAL BEHAVIOR



(i) COMPARISON BETWEEN EXPERIMENTAL RESULTS AND ANALYTICAL RESULTS

Fig.4

Table 3 Comparison of Test Results and Calculated Values

No.	Specimen	Calculated Values		Test Results (Peak Loads)		Comparison of Peak Loads		Failure mode
		M <sub>cu</sub> (tfm)	Q <sub>cu</sub> (tf)	M <sub>p</sub> (tfm)	Q <sub>p</sub> (tf)	M <sub>p</sub> /M <sub>cu</sub>	Q <sub>p</sub> /Q <sub>cu</sub>	
1	S1-1-(M+N)C	12		10.5		0.89		Yield of endplate
2	S1-2-(M+N)C	13		12.8		0.97		Crush of concrete
3	S1-3-(M+N)C	19		18.0		0.93		Crush of concrete
4	S1-4W-(M)P	15		13.1		0.88		Crush of concrete
5	S1-4W-(M+Q)P	15		15.0		1.00		Crush of concrete
6	S3-4W-(M+Q)P	-29		-23.9		0.80		Yield of steel bars
7	C1-1-(M)P	53		37.5		0.71		Yield of endplate
8	C1-1-(M+Q)P	53	32	37.7	32.8	0.71	1.03	Shear failure of concrete segment
9	C1-1W-(M)P	68		66.8		0.98		Crush of slab concrete
10	C1-1W-(M)NR	-22		-26.8		1.21		Local buckling of flange
11	C1-1W-(M+Q)P	68	61	72.5	63.0	1.06	1.03	Diagonal crack and crush of concrete
12	C1-1W-(M+Q)NR	-40	-62	-41.4	-36.0	1.04	0.58	Yield of steel bars
13	C1-4W-(M)P	26		28.9		1.10		Crush of slab concrete
14	C1-4W-(M)NR	-40		-40.0		1.00		Crush of concrete
15	C3-4-(M+Q)NR	-69		-53.7		0.78		Failure of slab

## Experimental behaviour of Semi-Rigid connections in Frames

F Benussi<sup>1</sup>

D A Nethercot<sup>2</sup>

R Zandonini<sup>3</sup>

### Abstract

Records of tests on composite frames and subassemblages have been examined and data extracted on the performance of the composite connections. These results are also compared and contrasted with the behaviour of similar types of connections as observed in isolated connection tests. Reasons for differences in connection behaviour for the two types of testing environment are presented and discussed.

### 1. Introduction

During the past twenty years more than 150 tests have been performed worldwide on composite connections (Nethercot and Zandonini, 1994). The results have formed the basis for methods to predict the key measures of joint performance of: moment capacity  $M_c$ , rotational stiffness  $K$  and rotation capacity  $\Phi_u$ . In parallel with these studies, methods have been developed for the analysis and design of composite frames that recognize the true semi-rigid and/or partial strength character of virtually all practical forms of beam to column connection.

To date, however, little opportunity has existed to validate the theoretical work on frames against suitable experimental studies. In addition, it has generally been accepted that the performance of composite joints tested in isolation is representative of the behaviour of similar joints, when functioning as part of a complete structure. Although this second point has been largely substantiated in the case of bare steel construction (Davison et al., 1987), certain "peculiarities" have been observed in the records of full frame tests e.g. the influence of column web flexibility on the unloading stiffness for minor axis connections noted by Gibbons, Kirby and Nethercot (1995).

Only a very limited amount of data exists on the performance of composite

---

<sup>1</sup>Associate Professor, Dept. of Civil Engineering, University of Trieste, Italy

<sup>2</sup>Professor, Dept. of Civil Engineering, University of Nottingham, United Kingdom

<sup>3</sup>Professor, Dept of Structural Mechanics, University of Trento, Italy

connections when tested as part of a more extensive arrangement. Leon (1987) has reported some tests on subassemblages in which sway of the columns was possible, while Jarrett (1993) has tested a series of non-sway sub-frames. Such is the extent and complexity of the problem though, that many important issues were not covered by this work.

The authors have for several years been engaged in research into the behaviour of composite connections, with the aim of extending the recent advances in appreciation of the true role of connections in bare steel construction into the area of composite frames. Several series of connections tests have been completed in Nottingham, Trento and Trieste, some numerical modelling of connections has been undertaken in these centres and methods have been developed for the analysis and design of composite frames.

Therefore it was natural, when planning the most recent phases of this work to see whether some aspects could be conducted in collaboration. When configuring a comprehensive study at Nottingham, involving joint, subassemblage and frame tests, plus associated theoretical work, it became clear that undertaking the subassemblage testing in partnership with the Trento and Trieste teams provided an attractive way of enhancing the overall value of the project. In addition, the Italian group would then be able to input the large frame tests that were to be conducted at BRE as part of the Nottingham study. The resulting arrangements saw the subassemblage testing conducted in Trieste, with advice on the design of the test specimens and the instrumentation to be used being provided from Nottingham.

This paper describes the planning of the Trieste tests and presents some of the preliminary findings. It also gives a very brief indication of the range of results that have been obtained from the BRE frame tests.

## 2. Subassemblage Tests

The geometrical configuration and loading of the two subassemblages designed as part of the experimental study to be conducted in Trieste are illustrated in figure 1. Beam spans, member sizes and connection detailing were selected in order to satisfy the prime requirement of consistency among the different activities of the general research project: i.e. to achieve conditions as close as possible to the frames and limited frames tested at BRE, with reference also to the main features of the expected response, within the restraints imposed by the testing rig and by the use of European sections. The subassemblages differ only for the overall configuration: frame SCS consists of two equal bays of 5m span, while frame UCS has unequal spans of 3.5m and 7m span respectively. Both frames are statically indetermined systems; joints are the weaker component and tests were hence expected to provide useful data on the redistribution capabilities in composite semi-continuous beams as allowed by joint inelastic response. The remarkably asymmetrical configuration of the latter frame should enable further investigation of the contribution of the web panel shear

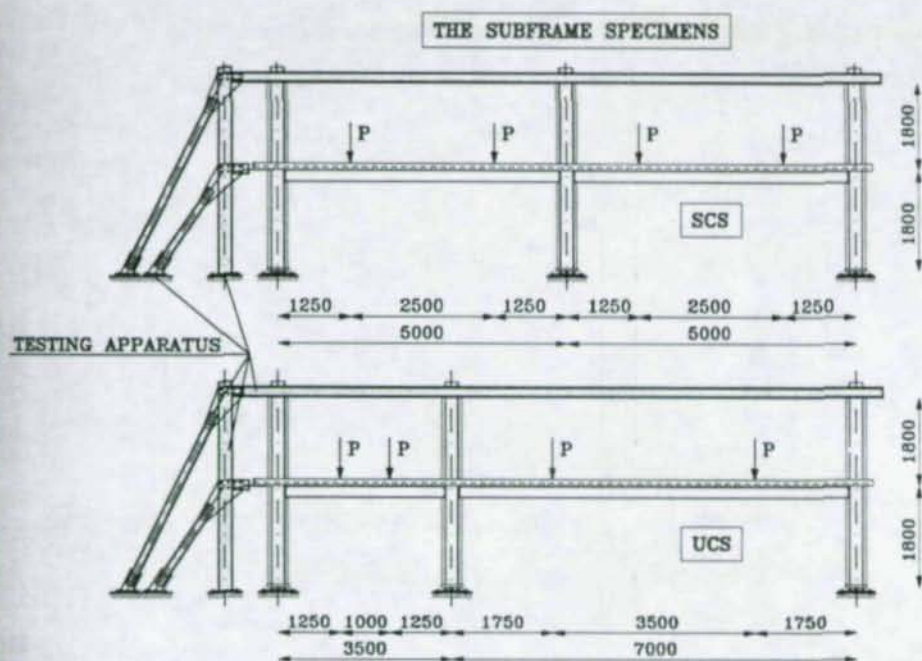


Fig. 1

deformation to the overall joint behaviour.

The extension of the slab beyond the external columns ensures a sufficient anchorage of the longitudinal rebars in accordance to Eurocode 2 (1994); additional trimming bars were used to allow for the formation of a more advantageous slab to column force transfer mechanism.

The key components of the frame response were monitored during the test, and data were logged for an extensive evaluation of the main features of the behaviour; instrumentation comprised of 42 inductive transducers, 156 strain gauges and 7 inclinometers arranged as shown in figure 2. The rotation of the joints was both measured by inclinometers and determined via displacement transducers (LVDTs B in fig.2). The determination of the pattern of moment, and of its evolution during the loading process is made possible by the strain measurements at different beam and column locations. Strain gauges also enable detection of possible yielding in the members (rebars and steel sections) and in the column web panel. Finally, measurement of the deflection at seven locations and of the rotation at two cross sections permits appraisal of the evolution of the beam responses with particular reference to the beam curvature in the positive and negative regions of moments.

Presently, the symmetrical frame (SCS) has been tested, and a first evaluation of the results has been attempted. Preliminary findings are here briefly reported.

Loads were applied in subsequent steps and, at each step, were increased after the specimen deformations fully stabilized. The loading history comprised of several loading cycles with unloading to the zero load condition in order to get a more thorough understanding of the structural behaviour.

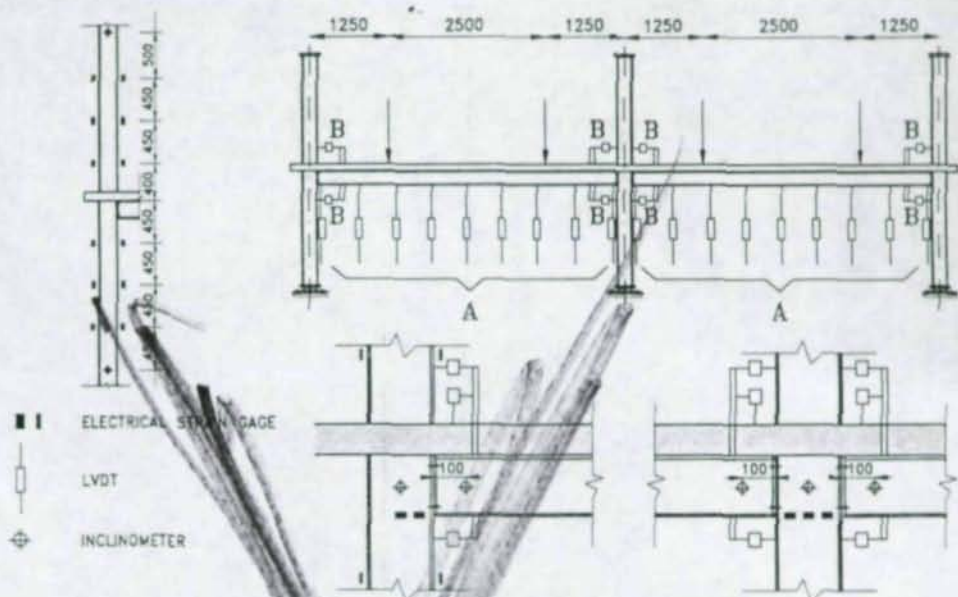


Fig. 2

The monitoring of the different joint component showed that internal joints enter first the plastic range, due to the almost simultaneous yielding of the inner rebars and of the column panel zone in compression. As a consequence, a rather rapid decrease of joint stiffness was observed and a significant moment redistribution process started, which led to the formation of a plastic hinge at the inner load location of the right bay (Fig. 3). Collapse was then attained due to local buckling which occurred at the plastic hinge (Fig. 4).

Despite the important plastic deformations, joints were not involved in the failure mode, and did not show any evidence of particular distress.

Their rotation capacity proved more than sufficient to ensure achievement of the beam plastic failure condition. It is interesting to note that the moment rotation curves obtained for the internal and external joints (Fig. 5) showed a remarkable similarity, with internal joints exhibiting a plateau at a lower moment level mainly due to the

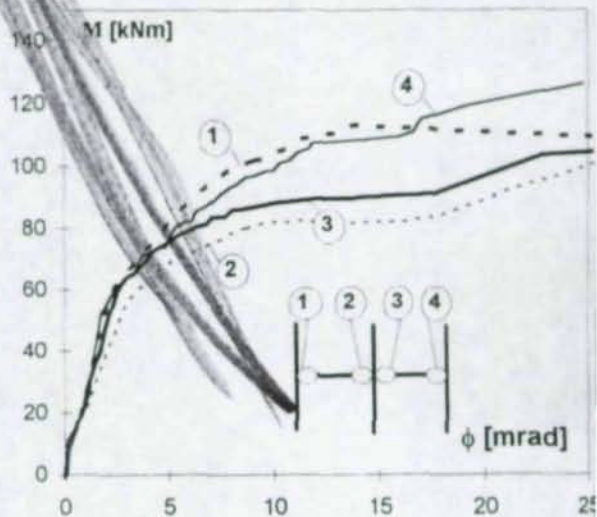


Fig. 5

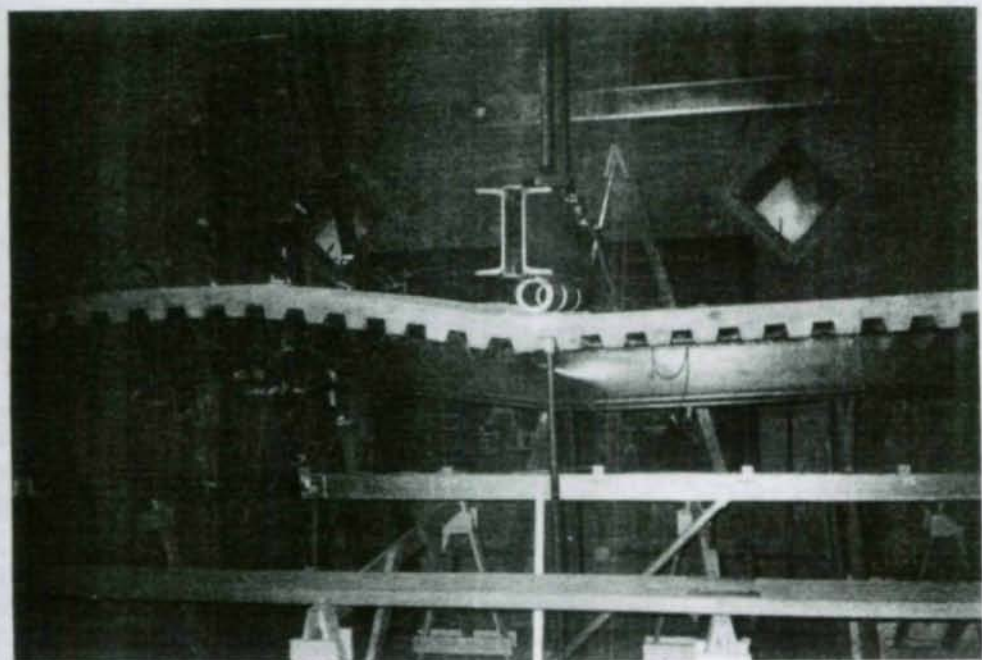


Fig. 3

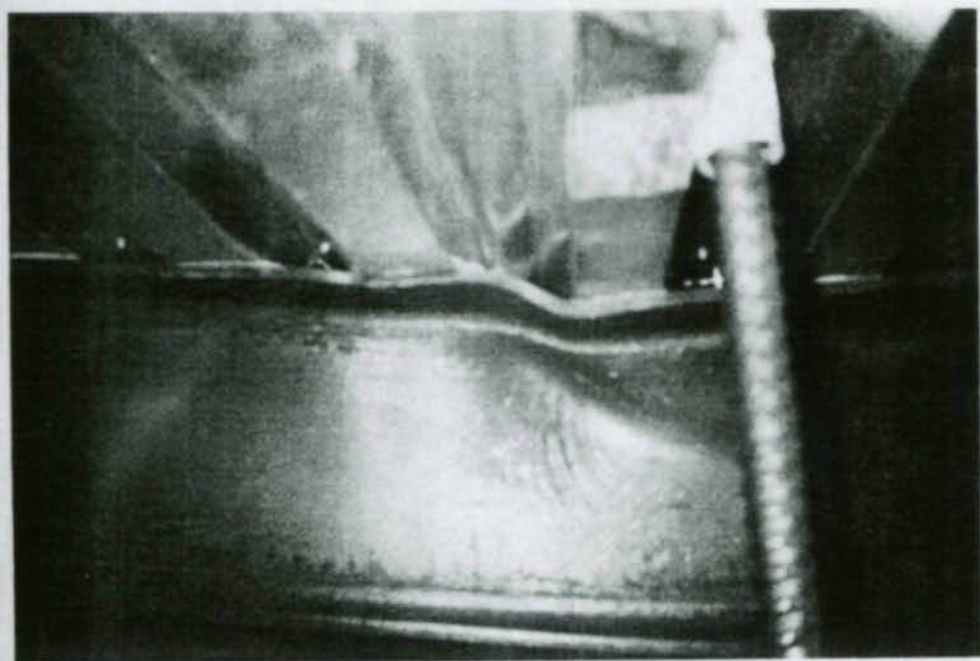


Fig. 4

column web yielding in compression. The anchorage detailing with trimming bars as suggested by Davison (1990) confirmed a more than satisfactory behaviour. Finally, earlier cracking of the nodal zones indicated a remarkable influence of the slab shrinkage. When testing the second subframe, the rebar deformations will hence be monitored since the concrete pouring in order to have a quantitative appraisal of the shrinkage effect.

### 3. Frame Tests

Full details of the test frames, instrumentation and method of testing have been reported elsewhere (Li *et al.*, 1995a). Essentially the arrangement comprised of the pair of 2-span, 2-storey frames illustrated in Fig. 6. Loading could be applied independently to primary and/or secondary beams, as well as to selected columns. Measurements were made of beam deflections, connection rotations and by means of comprehensive strain measurements, of the pattern of moments within the frame at all load levels. For the measurement of connection rotations a combination of 26 "hanging dumb-bell" devices (Moore *et al.*, 1993) and 26 electronic levels was used to monitor the 8 internal connections - at which 3 separate devices were required - and the 20 external connections - at which 2 inclinometers were sufficient.

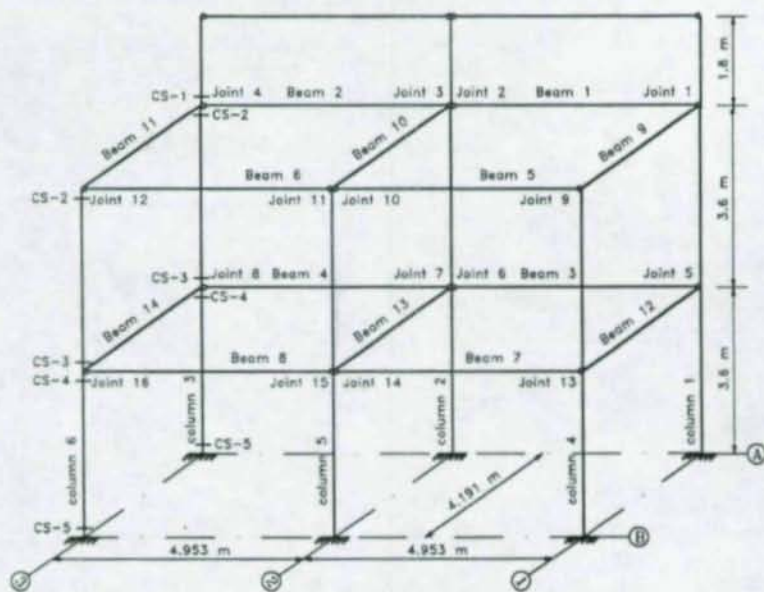


Fig. 6

The two frames were tested separately and in both cases it was observed that - although attainment of the maximum applied load was governed by a particular event - large vertical deflection of beam 1 accompanied by flange buckling adjacent to connection 2 for frame A, Fig. 7, and failure of beam 8 due to local crushing of the concrete slab outside the column at connection 16 for frame B, Fig. 8 - several



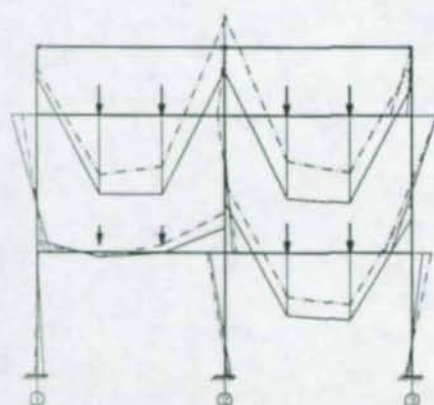
Fig. 7



Fig. 8

components were near the limit of their capacity. It was therefore possible to make direct comparisons between the performance of key components as observed in other isolated tests or as predicted by calculation and the performance in the full frame environment (Li *et al.*, 1995b).

Figure 9 compares the distribution of moments in frame A at failure with that predicted by an elastic analysis that assumes rigid connections and uses then cracked beam section properties throughout. It is clear that whilst the flush endplate form of beam to column connection shown in Fig. 10 did not provide sufficient moment capacity to match the requirements of full continuity, nor did the frame behave as if the beams were simply supported. Clearly the actual structure functioned in a semi-rigid and partial strength fashion.



(e) Test moment diagram and rigid connection moment diagram

Fig. 9

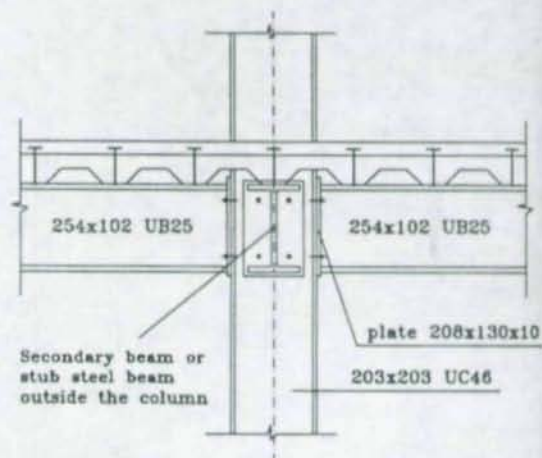


Fig. 10

Detailed comparisons of the moment-rotation characteristics obtained from several joints in the two frames with the results of isolated connection tests on equivalent arrangements (Li *et al.*, 1995c; Li *et al.*, 1995d) are given as Fig. 11 and 12. These show performance in the frame tests to be generally inferior, with a range of behaviours being obtained. Several reasons may be advanced for this:

- (i) For the external column connections, the column rotations prevented development of the full connection moment capacities.
- (ii) The high shear forces at the connections in the frame will have led to somewhat smaller connection moment capacities in the frame as demonstrated by the analyses by Li *et al.* (1995c).
- (iii) The inevitable unbalanced loading in the frame test may have contributed to the smaller connection moment capacities, with the unexpected twisting force on the composite beams causing the connection regions in the frames to exhibit premature

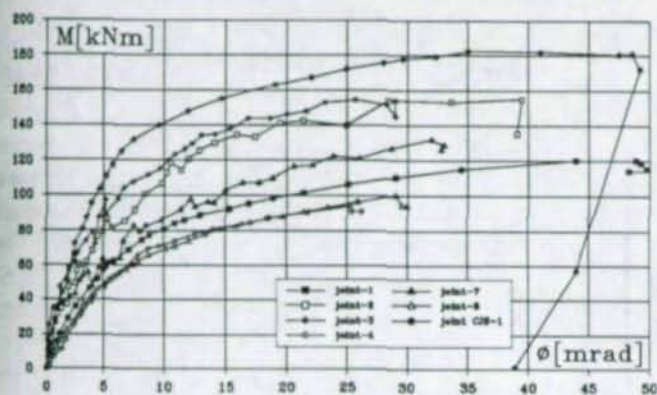


Fig. 11

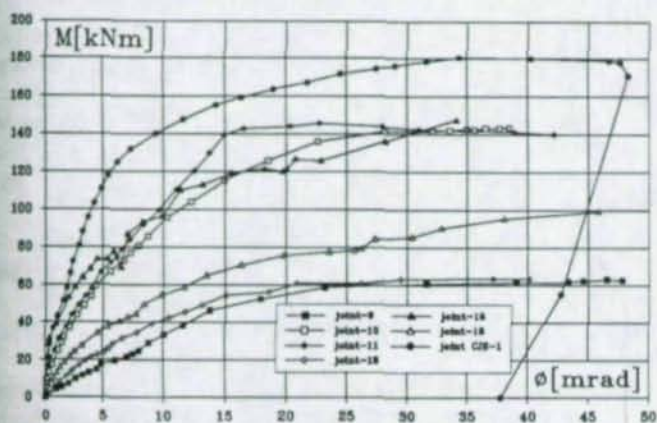


Fig. 12

#### 4. Conclusions

Two recent series of full-scale tests on composite frames and composite sub-assemblages have been used as the basis for an examination of the performance of composite connections when tested in a frame environment. Thus information on the semi-rigid and partial strength nature of the connection has been extracted from the full test histories. These have permitted direct comparisons to be drawn between the performance of connections when tested in isolation and when functioning as part of a complete structure. Reasons for these differences have been proposed. In the case of the composite frame tests the observed connection behaviour was generally inferior to that seen in the related connection tests, principally because additional loading came onto the connections as a result of the full frame action.

Finally, the subassemblage test confirmed the the joint rotation capacity is sufficiently high to ensure the plastic collapse of the beam to be achieved.

local buckling on one side of the beam bottom flange. This kind of behaviour was not observed in the isolated joint tests (Li et al., 1995d).

(iv) The lower connection stiffness from the frame test could have been caused by some degree of overestimation of the connection rotations, since it was impossible to measure the column rotations at the centre of the joints as was done for the isolated joint tests. As the connection rotation was obtained by taking the difference between beam end rotation and column rotation, the connection rotation may have been overestimated and the connection stiffness underestimated in the frame test.

### Acknowledgements

Grant for the English research project was provided by the EPSRC (formerly SERC) in the UK, while MURST funded the Italian work and CNR (Italian Research Council) supported the cooperative work in the framework of the Progetti Bilaterali programme. The considerable assistance provided by BRE during the conduct of the frame test, especially through the contributions of Dr. N Jarrett and Dr. D Moore is acknowledged. Steel for the frame tests was supplied as free issue by the British Steel. The Authors wish to acknowledge as well the contributions of Dr. T.Q Li and Dr. B.S. Choo of Nottingham University, of Dr. C. Bernuzzi and Dr. F. Gadotti of Trento University and Dr. S. Noe' of Trieste University.

### References

- Nethercot D A and Zandonini R, 1994, "Recent Studies of the Behaviour of Semi-rigid Composite Connections", American Society of Civil Engineers Structural Conference, Atlanta, April.
- Davison J B, Kirby P A and Nethercot D A, 1987, "Semi-rigid Connections in Isolation & in Frames", Connections in Steel Structures, Behaviour, Strengths and Design, eds. Bjorhovde, Brozzetti & Colson, Elsevier Applied Science, pp. 195-202.
- Gibbons C, Kirby P A and Nethercot D A, 1995, "The Experimental Behaviour of Semi-rigid Connections in Braced Steel Frames", The Structural Engineer, (under review).
- Leon R T and Ammerman D J, 1987, "Semi-rigid Composite Steel Frames", AISC Engineering Journal, Fourth Quarter, pp. 147-155.
- Jarrett N, 1993, "Tests on Four Composite Steel and Concrete Sub frames" Final Research Report, Geotechniques and Structures Group, Building Research Establishment.
- CEN 1994, "Eurocode 2 - Design of Concrete Structures"
- Li T Q, Moore D B and Nethercot D A, 1995a, "The Experimental Behaviour of a Full-Scale, Semi-Rigidly Connected Composite Frame: Overall Considerations" (in preparation)
- Moore D B, Nethercot D A and Kirby P A, 1993, "Testing Steel Frames at Full Scale", The Structural Engineer, Vol. 71 Nos 23 and 24, December, pp. 418-427.
- Li T Q, Moore D B and Nethercot D A, 1995b, "The Experimental Behaviour of Full-Scale, Semi-Rigidly Connected Composite Frame: Derailed Appraisal." (in preparation).
- Li T Q, Nethercot D A and Choo B S, 1995c, "Behaviour of Flush End Plate Composite Connections with Unbalanced Moment and Variable Shear Moment Rotations: Part 2: Prediction of Moment Capacity", Journal of Constructional Steel Research, (in press).
- Li T Q, Nethercot D A and Choo B S, 1995d, "Behaviour of Flush End Plate Composite Connections with Unbalanced Moment and Variable Shear/Moment Rotations: Part 1: Experimental Behaviour", Journal of Constructional Steel Research, (in press).
- Davison J.B., Lam D., Nethercot D.A., 1990, "Semi-Rigid Action of Composite Joints", The Structural Engineer, Vol. 68, No. 24, December, pp. 489-498.

Technical Papers on

**SPECIAL CONNECTIONS**

# CONNECTION BETWEEN STEEL BEAMS AND CONCRETE FILLED R.H.S. BASED ON THE STUD TECHNIQUE (THREADED STUD).

Didier Vandegans <sup>1</sup>

José Janss <sup>2</sup>

## Abstract

This paper shows that the component method, described in Annex J of Eurocode 3 can be applied in the case of studded joints, by using different existing models. Numerical simulations make it possible to determine the deformation of the bended face of the section, where the studs are fixed. Therefore the curves of behaviour of these joints can be drawn and compared with the experimental curves.

## 1. INTRODUCTION

The concrete-filled R.H.S. technique (Rectangular Hollow Section) has many advantages in the building domain. The bearing load, the stiffness of joints between beams and the column and the fire stability are increased, the floor space required is smaller, the aesthetic is improved, the maintenance is easier, and in comparison with concrete column, no shuttering is needed.

The stiffness of joints with steel beams or mixed steel-concrete beams, and their resistance to bending moment are relatively high. The exploitation of these characteristics during the frame analysis will reduce costs or will result in a significant saving of materials.

In order to calculate the resistance of different joint elements, certain codes or models are developed. However, no model exists to determine the deformability of the face of the hollow section while it is in bending.

---

<sup>1</sup> Engineer, CRIF Steel Construction Department, 6 Quai Banning 4000 Liège, Belgium

<sup>2</sup> Engineer, Head of CRIF Steel Construction Department, ibidem

The aim of this paper is to show that, with the rules given in Annex J of Eurocode 3, based on the component method, with different design models and with numerical simulations, it is possible to determine the characteristics of the behaviour curve of joints between a I-beam and a concrete filled R.H.S.

## 2. THE STUD TECHNIQUE.

The presence of concrete within the hollow section make it impossible to fix a connection element with bolts on the face of this section. The stud technique is useful to solve this problem. This technique consists in welding with the help of a special gun, a threaded stud on the face of the section on which the connection is to be realised. The other elements of the connection are fixed at the studs with nuts, as done for classical bolts. The studs are then subjected to traction and shearing, as for usual joints. The studs to be used are threaded studs with reduced base. So, the welds have approximately the same diameter as the threaded part.

## 3. TEST PROGRAM.

Eight tests have been effected in the laboratory. The aim was to have 4 different joint configurations. Two tests with the same characteristics have been effected for each configuration. These tests are as follows (see figure 1) :

- Test n° 1 : web cleated joint;
- Test n° 2 : extended end-plate joint;
- Test n° 3 : flush end-plate joint;
- Test n° 4 : flange cleated joint.

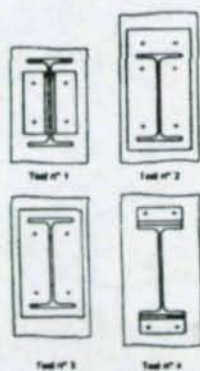


Figure 1

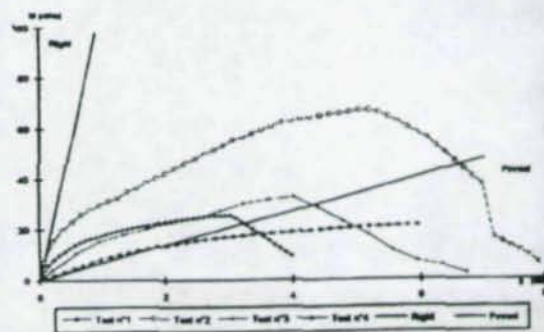


Figure 2

The comparison between the experimental curves and the field in which the joints can be considered as rigid or pinned shows that joint number 1, with web cleats, has the same characteristics as a perfect pin (see figure 2). Then, let's go on with the other joints.

#### 4. METHOD OF CALCULATION USED.

##### 4.1. Annex J of EC3 method.

For the design of the joint, the approach described in Annex J of Eurocode 3 is used. This is based on the component method, which considers a joint not as a unit, but as a set of individual components each with its own strength and stiffness. Annex J allows to calculate the characteristics of the following components :

- end-plate in bending;
- flange cleats in bending;
- flange of the beam in compression;
- web of the beam in tension;
- flange of the beam in bearing;
- bolts in shearing;
- studs in tension.

##### 4.2 Navaux model.

An earlier research made by NAVAUX in CRIF in Belgium has established some design rules for the resistance of the face of the rectangular hollow section. These rules cover the following modes of failure :

- shearing of the face of the section

$$N_{max} \leq 0,95 \cdot \pi \cdot d \cdot t \cdot \frac{f_{yt}}{\sqrt{3}} / \gamma_{mo} \quad (1)$$

- lamellar pull out

$$N_{max} \leq 0,95 \cdot \frac{\pi \cdot d^2}{4} \cdot f_{yt} / \gamma_{mo} \quad (2)$$

$f_{yt}$  is the yield strength of the hollow section,  $t$  is the thickness of the face,  $d$  is the nominal diameter of the studs and  $\gamma_{mo}$  the partial safety factor.

### 4.3 Gomez model.

In order to calculate the resistance of the bended face of the R.H.S, the so called "Gomez Model" is used. Gomez has studied the weak axes beam to column joints and has deduced a model to design the web of the column. A part of this model predicts a local failure of the web of the column due to the bolts in tension. He substitutes the plastic mechanism of the web by an equivalent rectangle of  $b \times c$  dimensions as shown on figure 3.

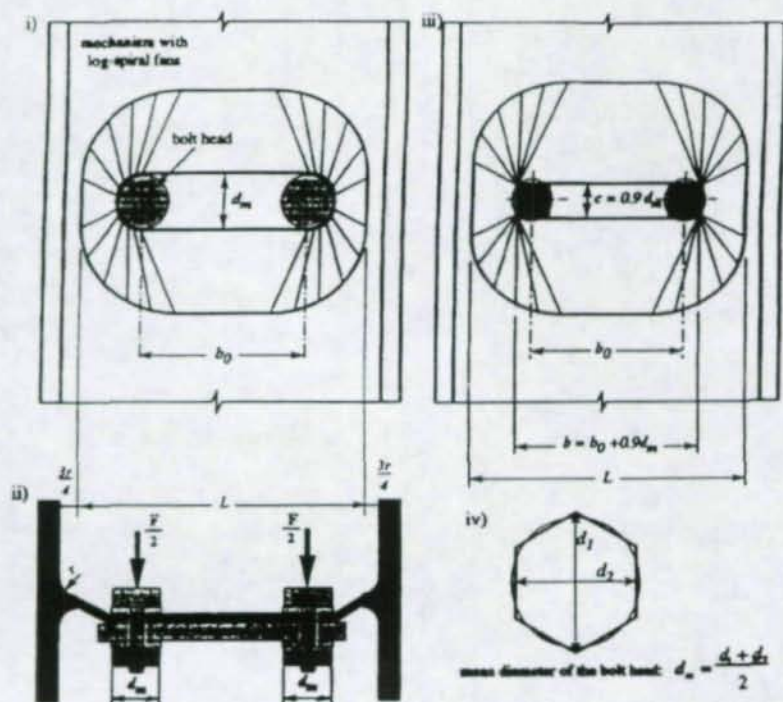


Figure 3 : Local mechanism for bolted connection:

- i) yield line pattern
- ii) section view
- iii) yield line pattern for equivalent rectangle  $b \times c$
- iv) mean diameter of the bolt head ( or nut )

The local resistance of the web is :

$$F_{local} = M_{pl} \cdot \alpha \cdot k \quad (3)$$

in which  $M_{pl}$  is the plastic moment of the web.

$$M_{pl} = \frac{1}{4} I_w^2 f_{yw} \quad (4)$$

$$\alpha = \frac{1}{1 - b/L} \left( \pi \sqrt{1 - b/L} + 2c/L \right) \quad (5)$$

$$k = \begin{cases} 1 & \text{if } (b+c)/L \geq 0,5 \\ 0,7 + 0,6 (b+c)/L & \text{if } (b+c)/L \leq 0,5 \end{cases} \quad (6)$$

The validity range of this model is as follows :

$$\begin{cases} b/L < 0,8 \\ 0,7 \leq h/(L-b) \leq 10 \end{cases} \quad (7)$$

Extending this model to the bended face of the rectangular hollow section leads to good results when only one row of two studs is present. However, the model is not applicable as it is for joints with more than one row of studs because global plastical mechanisms can modify the diagram of plastification.

#### 4.4 Numerical simulations.

So far, no model exists to deduce the deformability of the bended face of the hollow section. Numerical simulations have been done with a program of non-linear finite elements, in order to find a numerical value of the deformation.

### 5. HYPOTHESES.

During the calculation, the following elements have been considered:

1. The presence of concrete stiffens the sheared part of the connection very strongly and increase the compression zone resistance of the joint considerably. Because of lack of information, it is not possible to calculate with a high degree of precision the resistance to shearing and compression and the corresponding deformations. But it is obvious that the resistances which would have been found are largely higher than those of the other components, and in addition, the deformability of these zones is extremely low.
2. Lateral faces of the section are submitted to traction forces, acting on a defined length corresponding of the length of the efforts diffusion. The value of this length of diffusion cannot be determined with a high degree of precision. However, let's consider that the "web" of the R.H.S. is largely over-dimensioned in comparison with its equivalent in a I-beam. The reason is that, in this case, the faces of the section have the same thickness, as opposed to the difference in thickness between the flanges and the web of an I-beam. In addition, adherence may occur between the lateral faces and the concrete. Therefore, this source of deformation is supposed to be negligible.

3. When pulled out by the stud, the face of the section come out of its plane. The angles of the rectangular section are rigid, and thus, while the section is empty, the deformation of one face is followed by a deformation of the other lateral faces, as shown on the figure 4.

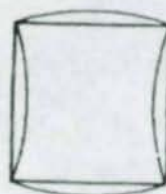


Figure 4

The presence of concrete within the hollow section prevents these lateral faces from deforming and therefore diminishes the deformation of the face connected to the studs when they are submitted to traction. This fact stiffens this component, and therefore, during the numerical simulations, the face of the section is modelised by means of a infinitely long plate, imbedded on 2 faces and subjected to two "concentrated" forces. The reason why a numerical simulation has to be done is that, to our knowledge, no analytical solutions are available.

## 6. RESULTS OF THE CALCULATION.

Without giving all the details, the results of the stiffness and resistance calculation are given in table 1, as well as the corresponding mode of failure.

	$M_{Rd}$ (in kN.m)	$M_u^{exp}$ (in kN.m)	Failure mode	$S_{ji}^{calc}$ (in kN.m/deg)
Test n° 2	37.5	67.1	Face of the section	78.97
Test n° 3	16.5	33.15	"	34.85
Test n° 4	17.7	25.5	Cleat	37.23

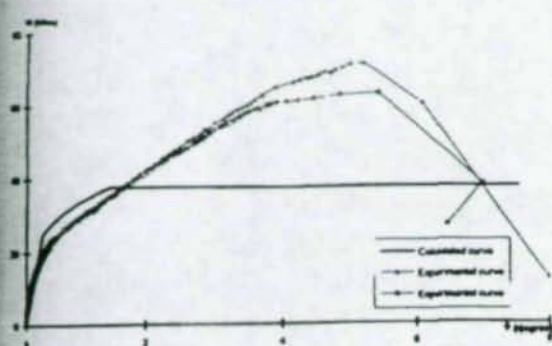
Table n° 1

Figure 5 shows the experimental curves and their equivalent given by calculation, following the rules given in Annex J of Eurocode 3. These figures show that the component method can be extended to this sort of connection without any difficulties.

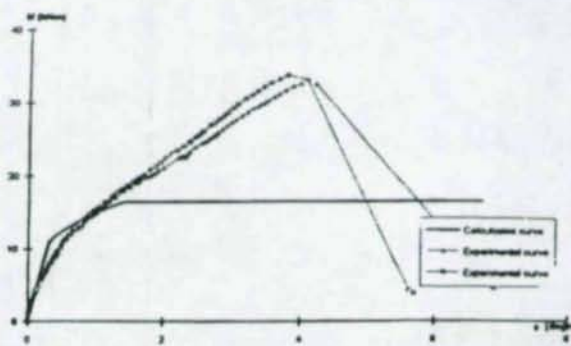
Few remarks can be expressed :

1. As already said, the Gomez model cannot be applied as it is for extended end-plate joints. New development should be done in this direction.

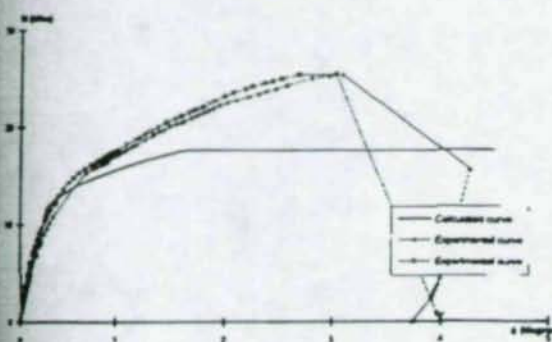
- The view of the curves shows that the calculation of the initial stiffness correspond with the experimentation. 3D simulations have confirm the hypothesis n° 2 which says that the deformation of the lateral faces of the section can be neglectable.
- The experimental results bring out the development of membrane efforts in the bended face of the section. Because of the importance of these membrane efforts, the ratio between initial stiffness  $S_{ji}$  and secant stiffness  $S_{js}$ , and between the elastic moment,  $M_e$  and the design moment resistance  $M_{Rd}$ , as defined in Annex J of Eurocode 3, should be modified, for this sort of connection.



i) Test n° 2 : Extended end plate



ii) Test n°3 : Flush end plate



iii) Test n°4 : Flange cleats

Figure 5 : Experimental and calculated curves

The formulas given in Annex J are as follows :

$$S_j = \frac{E \cdot z^2}{\mu \cdot \sum_i \frac{1}{k_i}} \quad (8)$$

where  $E$  = the Young modulus;  
 $z$  = the lever arm of the external forces;  
 $k_i$  = the stiffness of the individual components;  
 $\mu$  = the stiffness ratio.

$$\mu = \left[ 1,5 \frac{M_{j,Sd}}{M_{j,Rd}} \right]^\psi \quad (9)$$

and  $\psi = 2,7$  for welded and bolted end-plate joints;  
 $= 3,1$  for flange cleated joints.

For the determination of the secant stiffness  $S_{jS}$ ,  $M_{j,Sd}$  equals  $M_{j,Rd}$  and thus

$$\mu = (1,5)^\psi \quad (10)$$

$$\text{and } S_{jS} = S_{ji} / \mu \quad (11)$$

Comparing the value of  $S_{jS}$  (calculated according to Annex J and deriving from the value of the initial stiffness  $S_{ji}$  deduced from the calculation and numerical simulations) and the measurements on the experimental curve, leads to the following results :

	$S_{ji}$ (in kN.m/deg)	$S_{jS}^{EC3}$ (in kN.m/deg)	$S_{jS}^{exp.}$ (in kN.m/deg)	$S_{ji}/S_{jS}^{exp.}$
Test n°2	78.97	26.43	*****	*****
Test n°3	34.85	11.66	14.36	2.43
Test n°4	37.23	10.59	16.80	2.21

Table n° 2

In a first approximation and in order to simplify, it's possible to give the following ratio :

$$M_e = M_{Rd}/3 \quad (12)$$

$$S_{jS} = S_{ji}/\mu \text{ with } \mu \approx 2,3 \quad (13)$$

The figure 6 shows the calculated curves derived from these values. Obviously, further tests should be carried out in order to confirm this observation and to give a more accurate value for the suggestion.

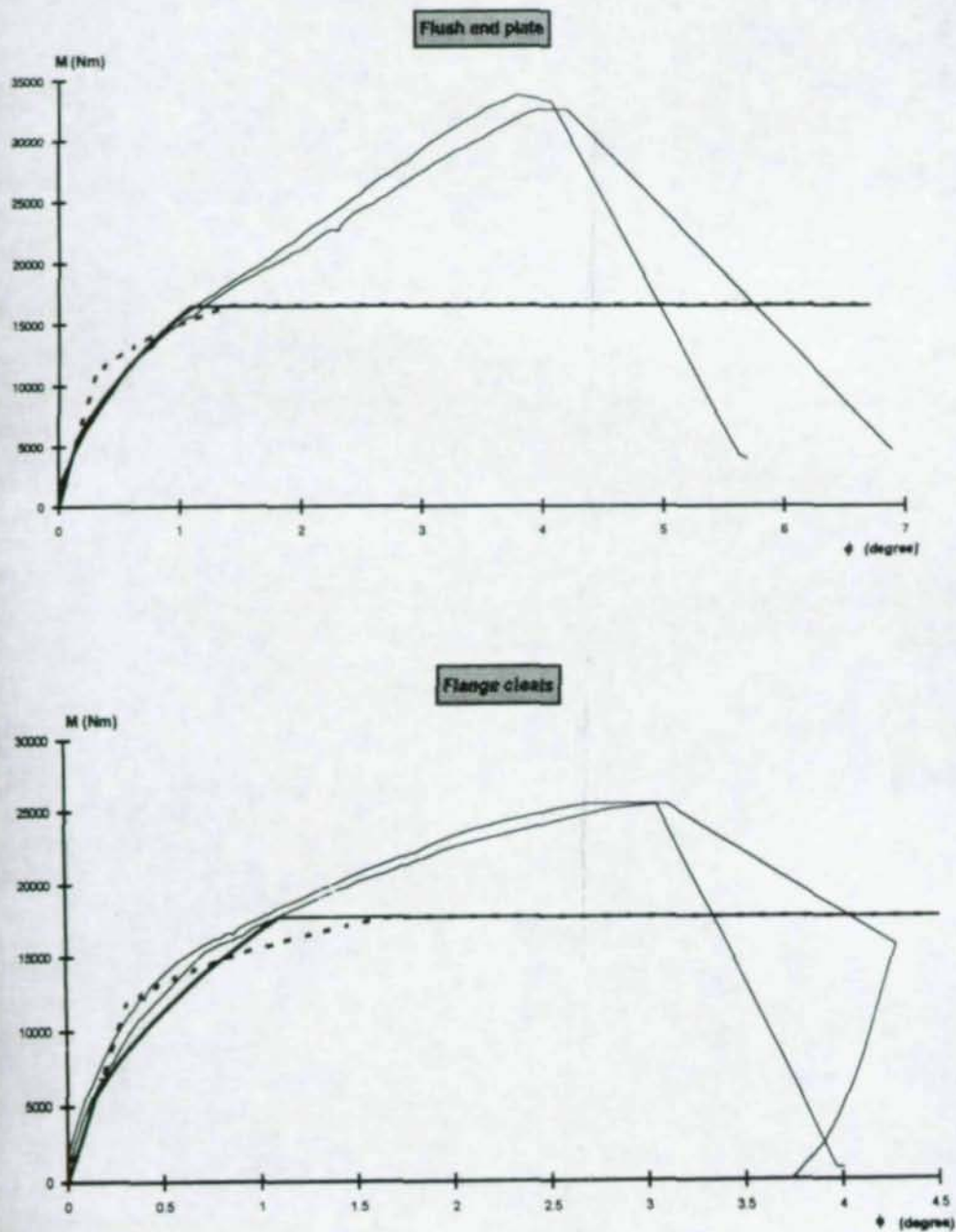


Figure 6

## 7. CONCLUSIONS.

The stud technique makes it easy to build a connection between a I-beam and a R.H.S. column filled with concrete. Reliable design models exist to determine a design value of the joint with one row of studs in tension. In the case of more than one row of studs, the adaptation of the Gomez model will produce a complete model for the design resistance.

The component method described in Annex J of Eurocode 3 can be extended to this sort of connection, without any difficulties, what is of great interest. However, small changes should be made in the assembly procedure of the different components.

The concrete within the hollow section reduces the deformation of the faces and consequently of the joint.

The only component for which the deformation cannot be derived analytically is the bended face of the section. Numerical simulations have shown that it is possible to find the initial stiffness of the joint with a good degree of precision, by neglecting the deformations of the lateral faces of the rectangular section.

## 8. REFERENCES

- [1] EUROCODE 3 : Design of steel structure , Part 1-1 ; General rules and rules for building , ENV 1993-1-1, 1992. Annex J : Joints in building frame , 1994.
- [2] Gomez F.C.T., Jaspart J.P., Maquoi R., "COST project C1 - Semi-rigid behaviour : Behaviour of minor-axes joints and 3-D joints" - Proceedings of COST C1 Workshop, Prague, October 1994.
- [3] Jaspart J.P., "Le boulon dans la construction métallique, perspectives d'avenir" CRIF, Belgium, 1994.
- [4] Maquoi R., Naveau X., Rondal J., "Beam-column welded stud connections". Journal of constructional steel research, Vol. 4 n° 1 - CRIF, Belgium, 1984.

## DESIGN OF BOLTED CONNECTIONS WITH INJECTION BOLTS

A.M. (Nol) Gresnigt<sup>1)</sup>

J.W.B. (Jan) Stark<sup>2)</sup>

### Abstract

Injection bolts are bolts in which the cavity produced by the clearance between the bolt and the wall of the hole is completely filled up with a two component resin. Injection bolts may be used in shear connections where slip is not allowed as an alternative for fitted bolts and for high strength friction grip bolts. Injection bolts are a reliable and relatively cheap fastener for repair and strengthening of existing structures. Also in new structures injection bolts are successfully applied. In the paper examples of successful applications are presented. Also the design rules and the method of installation are shortly discussed.

### 1. INTRODUCTION

Filling of the clearance of an injection bolt is carried out through a small hole in the head of the bolt. After injection and full curing of the resin, the connection is slip resistant. Shear load is transferred through bearing and shear of the bolt.

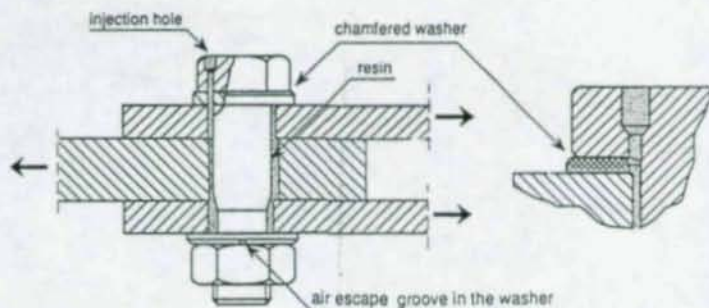


Figure 1: Injection bolt in a double lap joint.

<sup>1)</sup> Senior Lecturer Steel Structures, Faculty of Civil Engineering, Delft University of Technology, The Netherlands.

<sup>2)</sup> Professor Steel Structures, Faculty of Civil Engineering, Delft University of Technology, and Deputy Director TNO Building and Construction Research, Rijswijk, The Netherlands.

Injection bolts can be manufactured from normal standard structural bolts. The bolts and washers are adapted to enable the injection of the resin.

Design rules and rules for execution of injection bolts are laid down in recent ECCS recommendations (ECCS, 1994) and in the draft European rules for execution of steel structures (prENV 1090-1, 1995). Section 4 gives details. Research carried out in the Stevin Laboratory of the Delft University of Technology and experience in practice for more than 25 years are the basis of these design rules and rules for execution.

## 2. ADVANTAGES AND COSTS OF INJECTION BOLTS

### 2.1 Advantages

Compared to other mechanical fasteners, injection bolts have several advantages. A distinction is made between the application in existing structures and in new structures. It is pointed out that in many cases the advantages apply both for repair and strengthening of existing structures, as well as for new structures.

#### Repair and strengthening of existing structures

- *Solution for connections with a low slip factor.* The slip factor for riveted plates is usually very low. The application of new rivets is virtually impossible because of the lack of equipment and skilled labour. Injection bolts have proven to be a good solution for the repair of riveted structures (e.g. old railway bridges). Another possibility are fitted bolts. However, as indicated before, fitted bolts are expensive compared to injection bolts. Injection bolts may be installed in standard holes: 2 to 3 mm bigger than the nominal bolt diameter.
- *Good design resistance in bearing.* Assuming a reasonable ratio between the thickness of the plates and the diameter of the bolts, the design resistance in bearing is usually quite sufficient to replace faulty rivets.
- *No internal corrosion.* Since the resin completely fills the cavity, internal corrosion is avoided (also important for new structures).

#### Application in new structures

- *No slip in case of overload.* In connections with high strength friction grip bolts, slip due to overload is possible. With injection bolts, sudden slip is not possible.
- *Good design resistance in bearing.* Assuming a reasonable ratio between the thickness of the plates and the diameter of the bolts, the design resistance in bearing is of the same magnitude as the slip resistance of high strength friction grip bolts.
- *Compact connections.* If the desired load transfer per bolt is very high (e.g. because the available space for bolts in the connection is small), preloaded injection bolts may offer the solution. As the design resistance of a preloaded injection bolt is the sum of its slip resistance and the bearing resistance of the resin, the number of bolts in a connection will be lower.
- *No special requirements for the contact surfaces and no controlled tightening.* For high strength friction grip bolts special requirements are necessary for the contact surfaces to achieve a satisfactory slip factor. If corrosion prevention is necessary,

the paint to be used has to guarantee the desired slip factor. With non-preloaded injection bolts, slip can be avoided without any special preparation of the contact surfaces. Also the possibility to avoid the necessary calibration and tightening procedures for HSFG bolts may be an incentive to apply non-preloaded injection bolts.

## 2.2 Costs

Because of the costs, injection bolts should only be applied where the advantages justify to do so. The costs of injection bolts consist of:

- a. The purchase of the bolts themselves (standard 10.9 or 8.8 bolts);
- b. The preparation of the bolts and washers (drilling a hole in the bolts head and preparing the special washers, see section 5.1);
- c. The resin, the preparation of the resin and the injection (section 5.2 and 5.3);
- d. The holes must be dry during injection (weather conditions, shelter from rain);
- e. Dismantling is not easy, unless special arrangements are made in advance, e.g. the application of a special separation liquid to prevent bonding of the resin to the bolt and the walls of the hole.

In The Netherlands injection bolts and washers are available from stock (bolt suppliers), ready for use. However, adapting standard bolts and washers can also easily be carried out in the workshop.

Because the injection equipment is cheap and the amount of resin per bolt is limited, the material costs for injection are low. The labour costs for injection per bolt, depend on:

- a. The total number of bolts to be injected;
- b. The number of bolts per connection;
- c. The accessibility of the bolts;
- d. The size and length of the bolts.

Roughly, the labour time for injection varies between 1 and 2 minutes per bolt. When injection bolts are used, the number of bolts in a connection will be less, thereby reducing the costs for holes and bolts. Further, the possibility of larger hole clearances may facilitate erection and consequently also reduce costs.

## 3. EXAMPLES OF SUCCESSFUL APPLICATIONS

### 3.1 Replacement of faulty rivets

Since 1970 it has been standard practice in The Netherlands to repair old railway bridges and road bridges with injection bolts. Also the Hoogovens blast furnace works and other companies use injection bolts for repair of their crane girders.

At present in Germany (Aachen University), studies are in progress to repair old bridges in the eastern part with injection bolts. A German translation is made of the ECCS recommendations (ECCS, 1994).



Figure 2: Riveted bridges in Rotterdam, where injection bolts were used to replace faulty rivets.

### 3.2 Bridge in Curaçao

During erection of this bridge (1967), it collapsed because of the rupture of high strength anchoring bars, see figures 3 and 4.

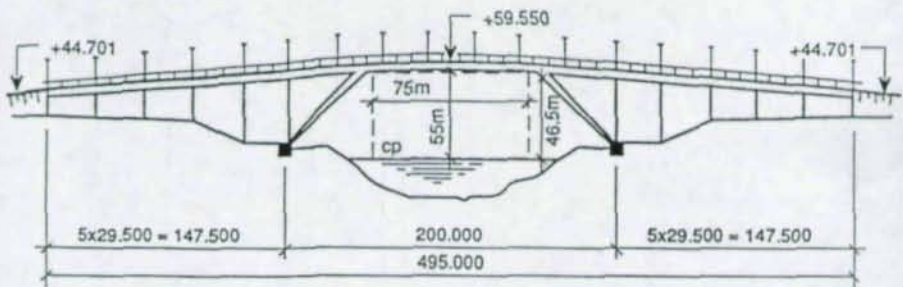


Figure 3: Bridge in Curaçao.

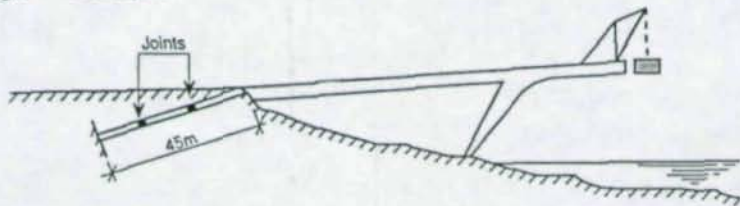


Figure 4: Sketch of the bridge in Curaçao during construction with the steel plates in the anchoring system.

It appeared that the workmen had positioned these high strength bars in the concrete anchoring block by tack welding them to the concrete reinforcing bars. Brittle fracture during erection of the main span was the result. When the bridge was rebuilt, instead of the anchoring bars steel plates were used. The total thickness was 140 mm (25 + 30 + 30 + 30 + 25 mm).

Fitted bolts M29 x 180 were specified for the connections. Displacements had to be prevented at all times. However, during installation of these bolts, mistakes in the position of the bolt holes were revealed. Reaming would be very costly and time consuming. So it was decided to apply injection bolts M27 x 180. The injection of 1500 bolts took only 6 days. After completion of the bridge, the anchor plates were removed and several bolts were checked. It was found that all the cavities due to the bolt clearances were completely filled.

### 3.3 Windmill

During starting and stopping, the connection between the gearbox and the base plate which connects it to the windmill, has to transmit high forces. These forces caused slip when the bolted connection was made with high strength friction grip bolts M39. After some time the bolts became loose. This problem was solved by installing injection bolts. It should be noted that in this type of application dismantling may be necessary at some time.

### 3.4 New bridges

For the Dutch railways it is standard practice to use preloaded injection bolts in their new bridges. Advantages are the resistance against shock loading, the fatigue resistance and the resistance against internal corrosion. The compactness of the connections is also an important factor. In addition, (preloaded) injection bolts are frequently used for new road bridges.

### 3.5 New crane girders

Due to frequent load reversals (tension-to-compression) and occasional overloading (shock loads), preloaded bolts may become loose. In such cases, Hoogovens blast furnace works and other companies with heavy crane traffic use preloaded injection bolts.

### 3.6 New storm surge barrier

In the new storm surge barrier in the waterway between Rotterdam and the North Sea, a great number of M80, M72, M64 and M56 preloaded 8.8 injection bolts are used for the connections in the main hinge (diameter 10 meters) and in the connection between the hinge and the arms. The total thickness of the main plate package is 340 mm.

The main reasons for the choice for preloaded injection bolts were the assurance that slip and internal corrosion were completely ruled out and furthermore the increase in the design resistance per bolt, compared to traditional high strength friction grip bolts.



Figure 5: Artists impression of the new storm surge barrier called: "Maeslant kering". The width of the waterway is 360 meters; the height of the wall is 22 meters, and the length of the arms is 237 meters.

### 3.7 New stadium for AJAX Amsterdam

In the new football stadium for AJAX Amsterdam, injection bolts are applied for the steel structure of the movable roof. This roof is normally open, but it can be closed if weather conditions are bad. The main reason for this application is the requirement that under no circumstances any deformations in the connections are allowed.

## 4. DESIGN RULES

### 4.1 Bearing resistance of the resin

Since resins are susceptible to creep deformation if the bearing stress is too high, the bearing stress has to be kept within certain limits. Several resins were tested. The best resin appeared to be the two component resin "Araldit", manufactured by Ciba-Geigy (SW 404 with hardener HY 404). Some years ago, Ciba Geigy changed the recipe of the hardener, because the HY 404 hardener appeared toxic. The new hardener is called: HY 2404. Creep tests have demonstrated that a safe design value for the bearing stress is:  $f_{b;resin} = 130 \text{ N/mm}^2$ . This means that in case of bolts with standard nominal hole clearances (e.g. for bolts M12 - M24: 2 mm), the maximum creep at a bearing stress of  $130 \text{ N/mm}^2$ , is less than 0.3 mm. This is the same limit as is used in rivets and HSFG connections. Short duration higher bearing stresses virtually have no influence on the creep behaviour. The ECCS recommendations and prENV 1090 give rules for the determination of the design bearing stress in case other resins are selected.

## 4.2 Design rules for static loading

As already indicated before, injection bolts may be non-preloaded (load transfer through bearing and shear of the bolt) and also preloaded (load transfer through bearing and shear of the bolt and through friction between the connected plates). The ECCS recommendations give design rules for both types of shear connections.

### Bearing + shear

No pre-loading or special provisions for contact surfaces are required. The design ultimate shear load shall not exceed the design shear resistance of the bolt, nor the design bearing resistance of the resin. The design bearing resistance of the resin per injection bolt can be calculated as follows (ECCS, 1994):

- Serviceability limit state:

$$F_{b,Rd,ser,resin} = \frac{1.0 k_s d t \beta f_{b,resin}}{\gamma_{Ms,ser}} \quad (1)$$

- Ultimate limit state:

$$F_{b,Rd,ult,resin} = \frac{1.2 k_s d t \beta f_{b,resin}}{\gamma_{Ms,ult}} \quad (2)$$

where:

- $\beta$  = factor depending on the thickness ratio of the plates.
- $\gamma_{Ms,ser}$  = 1.0.
- $\gamma_{Ms,ult}$  = 1.0.
- $k_s$  = 1.0 for holes with standard nominal clearances as specified in 7.5.2 (1) of Eurocode 3: Part 1.1.
- $k_s$  = 1.0 -  $m \cdot 0.10$  for holes with greater clearances than the above standard nominal clearance.
- $m$  = the extra clearance above the standard nominal clearance (in mm). In the case of short slotted holes not longer than specified in 7.5.2 (9) of Eurocode 3: Part 1.1,  $m = 0.5$  times the difference between the length and the width of the hole.

Remarks:

- a. The bearing resistance of the resin  $f_{b,resin}$  is the long duration bearing resistance where the displacement due to creep is not greater than 0.3 mm.
- b. As short duration loads have only limited influence on the displacement due to creep, it is reasonable to use a higher value for the design bearing resistance at ultimate limit state.
- c. Because sudden collapse of the structure due to failure of the resin cannot occur, it is recommended to take  $\gamma_{Ms,ser} = \gamma_{Ms,ult} = 1.0$ .
- d. No test results are available for long slotted holes, so no  $k_s$  value is given for such holes.

## Design example:

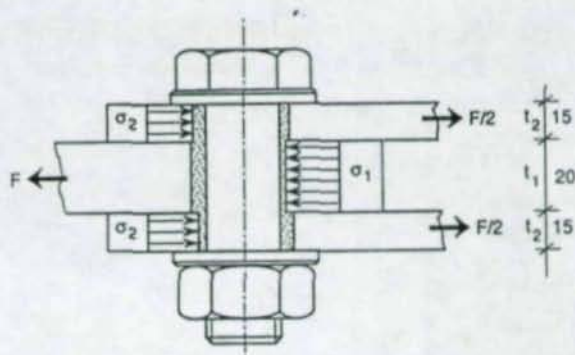


Figure 6: Injection bolt in a double lap joint. Bolts M20, grade 10.9. Steel S355 (Fe 355, Fe 510). Holes 22 mm (standard nominal clearance).

**Bearing resistance of the resin**

- Serviceability limit state:

$$\beta = \frac{2}{3} \left(1 + \frac{t_2}{t_1}\right) = \frac{2}{3} \left(1 + \frac{15}{20}\right) = 1.17$$

$$F_{b,Rd,ser,resin} = 1.0 \cdot 1.0 \cdot 20 \cdot 20 \cdot 1.17 \cdot 130 = 61 \text{ kN}$$

- Ultimate limit state:

$$F_{b,Rd,ult,resin} = 1.2 \cdot 1.0 \cdot 20 \cdot 20 \cdot 1.17 \cdot 130 = 73 \text{ kN}$$

**Shear resistance of the bolt (Eurocode 3, 1992), shear plane passes through the shank of the bolt)**

$$F_{v,Rd} = \frac{0.5 f_{ub} A_s}{\gamma_{Mb}} = \frac{0.5 \cdot 1000 \cdot 314}{1.25} = 126 \text{ kN}$$

$$\text{For 2 planes: } F_{v,Rd} = 2 \cdot 126 = 252 \text{ kN}$$

**Bearing + shear and friction**

Preloaded high strength injection bolts with controlled tightening in conformity with (prENV 1090-1, 1995) shall be used. The design ultimate shear load shall not exceed the design shear resistance of the bolt, nor the design bearing resistance of the steel plates (calculated for a connection without resin).

- *Serviceability limit state:* Only those load cases according to 2.3.4 of (Eurocode 3, 1992) where resistance to slip is required, shall be considered. The design serviceability shear load shall not exceed the sum of the design slip resistance of the connection and the design bearing resistance of the resin.
- *Ultimate limit state:* The design ultimate shear load shall not exceed the design slip resistance of the connection plus the design bearing resistance of the resin.

**Remarks:**

- The above requirements follow the classification in 6.5 of Eurocode 3, part 1.1.
- Because in the ultimate limit state, the design slip resistance of the connection plus

the design bearing resistance of the resin can exceed the design shear resistance of the bolt, the design shear resistance of the bolt shall also be checked.

- c. In the case of relatively long bolts (diameter of the bolts small compared to the thickness of the plates), the bending deformation of the bolt may cause a very uneven bearing stress distribution. These uneven bearing stresses will result in additional creep deformation. The design rules for the bearing resistance of the resin in the ECCS recommendation are only valid for bolts with  $l/d \leq 3$  ( $l$  = total thickness of the plates;  $d$  = diameter of the bolt). For longer bolts, only the bearing resistance for  $l = 3d$  may be taken into account. For more details, see (Gresnigt, 1994), where also attention is paid to the combination of preload, shear and bending moment in the bolt. It is shown that with the design rules in the ECCS recommendations, yielding of the bolt material will not occur and consequently no loss of preload will happen.
- d. In the design examples in (ECCS, 1994), it is demonstrated that in case of preloaded injection bolts, the bearing resistance of injection bolts gives considerable extra strength compared to traditional HCFG bolts.

### 4.3 Design rules for fatigue loading

#### Non-preloaded injection bolts

Non-preloaded connections with injection bolts are comparable to the situation in old riveted structures (virtually no load transfer by friction). In fatigue tests never any damage of the resin was detected. Failure always occurred in the connected plates or in the bolts. Since short duration high bearing stresses do not cause noticeable creep, occasional overloading does not need to be taken into account. For more details, see the ECCS recommendations (ECCS, 1994) or Eurocode 3, part 2 on Bridge Design (Eurocode 3, draft ENV 1993-2, 1994).

#### Preloaded injection bolts

Since load transfer through friction is stiffer than load transfer through bearing (compared to the stiffness of steel, the resin has a relatively low modulus of elasticity), the fatigue load is considered to be taken by the friction. In this case, the bearing resistance can be utilized for the static part of the load transfer.

Design examples for non-preloaded and for preloaded injection bolts can be found in the ECCS recommendations.

## 5. INSTALLATION

### 5.1 Preparation of the bolts and washers

Guidelines for installation are given in the ECCS recommendations and in prENV 1090-1. In the head of the bolt, a small hole is drilled. Under the head, a hardened washer is placed where the inner diameter is at least 0.5 mm larger than the diameter of the bolt, and where the inner side is machined to guarantee easy passage and distribution of the resin. Under the nut, a ring with a groove is mounted to let the air escape.

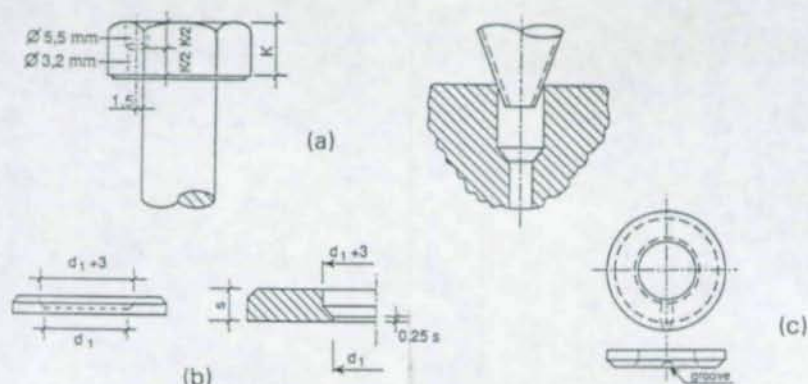


Figure 7: Preparation of (a) the bolt head, (b) the washer under the head and (c) the washer under the nut.

## 5.2 Equipment

The equipment can be either a hand driven or an air driven injection pistol, as frequently used in the building industry, see figure 8. Particularly for longer bolts or where large quantities of bolts to be injected consecutively, air driven equipment is recommended.



Figure 8: Air driven injection pistol.

## 5.3 Injection and curing

Viscosity, pot life and curing time depend on the temperature. If the temperature is too low, preheating of the resin may be necessary to obtain sufficient viscosity. If the temperature is too high, the resin may flow out after the injection has stopped. Simple modelling clay may be used to avoid this. The Araldit as mentioned before, has a pot life at  $20^{\circ}\text{C}$  between 15 and 20 minutes, and a curing time at  $20^{\circ}\text{C}$  of about 24 hours to obtain full bearing resistance. If shorter curing times are required, heating of the connection to e.g.  $50^{\circ}\text{C}$  will speed up curing time to about 4 hours. This may be important in the repair of riveted railway bridges.

## 5.4 Quality control

Guidelines for quality control are given in (ECCS, 1994). Checks may comprise conformity, bolt installation, bolt tightening, the absence of water in the cavities and the curing time. To demonstrate that the installation procedure and equipment is able to fill the clearance completely, an assembly of perspex plates can be injected.

## 6. CONCLUSIONS

The main conclusions are:

- a. Based on extensive research and long duration experience in practice, injection bolts have proven to be a reliable and relatively cheap means for repair and strengthening of existing structures.
- b. Injection bolts behave almost the same as fitted bolts. However, they are much cheaper, especially in thick plate packages, where reaming of the holes may be very expensive.
- c. Preloaded injection bolts have a greater design resistance than traditional HSFG bolts. Therefore the application of preloaded injection bolts reduces the number of bolts and enables more compact connections.
- d. In some applications, injection may be applied to secure that sudden slip in case of overloading is absolutely ruled out.
- e. It is expected that the design rules and guidelines for execution as laid down in the recently published ECCS recommendations and in (prENV 1090-1, 1995) will be an important help for the application of injection bolts in other countries.

## REFERENCES

- ECCS, (1994). *European recommendations for bolted connections with injection bolts*. ECCS publication No. 79, Brussels.
- Eurocode 3, ENV 1993-1-1, (1992). *Design of Steel structures. Part 1.1 - General Rules and Rules for Buildings*.
- Eurocode 3, draft ENV 1993-2, (1994). *Design of Steel structures. Part 2 - Bridges (annex 6.1)*.
- prENV 1090-1, (1995). *Execution of Steel Structures. Part 1 - General Rules and Rules for Buildings*.
- Bouwman L.P., (1970). *Voorlopig overzicht van een onderzoek naar de invloed van het opvullen met epoxy-hars van de ruimte tussen boutsteel en gatwand bij verbindingen met diverse deklagen* (Preliminary survey of the research on injection bolts). TU-Delft, Stevin report 6-70-7.
- Bouwman L.P., Den Boer C., (1972). *Vermoeingsonderzoek welijzersen proefstukken met injectie-voorspanbouten voor de spoorbrug te Culemburg* (Research into the fatigue resistance of wrought iron test samples with preloaded injection bolts for the railway bridge in Culemburg). TU-Delft, Stevin report 6-72-12.
- Bouwman L.P., (1982). *De invloed van opwarmen op de uithardingsnelheid van injectiehars bij injectiebouten* (The influence of preheating on the curing speed of resin for injection bolts). TU-Delft, Stevin report 6-82-8.
- Bouwman L.P., Munter H.L.N., (1989). *Onderzoek naar de vermoeingssterkte van enkelsnede verbindingen met injectiebouten* (Research into the fatigue resistance of simple lap joints with only two plates, one shear plane through the bolt, with injection bolts). TU-Delft, Stevin report 6-89-49.
- Gresnigt A.M., (1994). *Influence of the bolt length in connections with injection bolts and results of creep tests on Araldit SW 404 / HY 2404*. TU-Delft, Stevin report 6-94-02.
- Kluwen H., (1981). *Onderzoek naar het gedrag van injectiebouten indien deze worden toegepast ter vervanging van klinknagels in bestaande constructies* (Research into the behaviour of injection bolts if they are applied to substitute rivets in existing structures). TU-Delft, Stevin report 6-81-9.

## WELDED CONNECTIONS IN THIN COLD-FORMED RECTANGULAR HOLLOW SECTIONS

Xiao-Ling Zhao<sup>1</sup>  
Gregory Hancock<sup>2</sup>

### Abstract

The paper describes welded connection tests which were performed on C450L0 Rectangular Hollow Sections. The thickness of the RHS sections varied from 1.6 mm to 3.0 mm. Butt welds, transverse fillet welds and longitudinal fillet welds were tested. The test configuration was the same as that used by the authors in a previous research project on welds in C350L0 RHS members. The test results are compared with existing Australian and American design formulae. The test results are also compared with the proposed design rules for welds in RHS members derived from the previous research project on C350L0 RHS members. The reliability analysis method is used to calibrate the existing and proposed design rules.

### 1. INTRODUCTION

Cold-Formed Square and Rectangular Hollow Sections (SHS and RHS) with a thickness less than 3 mm are manufactured and used in structures in Australia (Tubemakers, 1994). The limit states Australian Standard AS4100-1990 (SAA, 1990) only applies to steel which is 3 mm or thicker. Tubular sections less than 3 mm thick cannot be designed to this standard but must be designed to the Australian Cold-Formed Steel Structures Standard AS1538-1988 (SAA, 1988), which is a permissible stress code. The member design rules in AS4100-1990 have been found to be appropriate for sections, including C450L0 RHS, less than 3 mm thick by the research summarised in Zhao and Hancock (1991, 1992a, 1992b). However, the design rules for welded connections less than 3 mm thick may be inappropriate. The thickness limits for the design of welded connections in various standards vary from 3.0 mm to 4.6 mm. The design rules for welded connections in AS1538-1988 are the same as those in the AISI Specification (AISI, 1986), which were based on testing performed by Peköz and McGuire (1981) on sheet steel. Similar research on welded sheet steel was also performed by Stark and Soetens (1980), which has been adopted in Eurocode 3-Part 1.3 (1992). Since they were derived for sheet steel, these design rules may be inappropriate when applied to RHS sections.

<sup>1</sup>Lecturer, Department of Civil Engineering, Monash University, Clayton, VIC 3168, Australia

<sup>2</sup>BHP Steel Professor of Steel Structures, School of Civil and Mining Engineering, University of Sydney, NSW 2006, Australia

Tests have been performed on welds in C350L0 RHS members and proposed design rules have been given for butt welds, transverse fillet welds and longitudinal fillet welds (Zhao and Hancock, 1993a,1993b,1994a). However, the proposed design rules may be inappropriate to C450L0 RHS members which have higher material strength and have different statistical data of material and fabrication. The purpose of this paper is to verify whether the proposed design rules are applicable to C450L0 RHS members. The 450 refers to the nominal yield stress of 450 MPa and the L0 refers to the impact properties at 0°C as specified in AS1163-1991 (SAA, 1991a).

Section Number (1)	Nominal ( $D \times B \times t$ ) (2)	Measured ( $D \times B \times t$ ) (3)	$A$ ( $mm^2$ ) (4)	$\sigma_{yta}$ (MPa) (5)	$\sigma_{uta}$ (MPa) (6)	$\sigma_{yto}$ (MPa) (7)	$\sigma_{uto}$ (MPa) (8)
D1	75 × 75 × 3.0	75.20 × 75.20 × 2.95	830	397	492	491	529
D2	75 × 75 × 2.5	75.20 × 75.15 × 2.46	700	425	493	452	506
D3	50 × 50 × 3.0	50.15 × 50.15 × 2.95	535	456	518	498	543
D4	50 × 50 × 2.5	50.10 × 50.25 × 2.46	454	383	459	473	511
D5	50 × 50 × 2.0	50.20 × 50.15 × 1.95	366	386	472	484	527
D6	50 × 50 × 1.6	50.30 × 50.15 × 1.59	303	386	487	466	524
D7	75 × 50 × 3.0	75.20 × 50.10 × 2.95	682	458	495	501	544
D8	75 × 50 × 2.5	75.25 × 50.05 × 2.46	577	466	521	511	567
D9	75 × 50 × 2.0	75.20 × 50.50 × 1.94	463	432	488	486	527
MEAN	-	-	-	421	492	485	531
COV	-	-	-	0.0761	0.0375	0.0360	0.0327

Table 1: Cross-Section Dimensions and Material Properties

In this paper, welded connection tests were performed on cold-formed RHS sections of Grade C450L0. The thickness of the sections tested ranged from 1.6 mm to 3.0 mm. Butt welds, transverse fillet welds and longitudinal fillet welds were tested. The test configuration was the same as that used by the authors in the previous research project on welds in C350L0 RHS members. The test results are compared with existing Australian and American design formulae. The test results are also compared with the proposed design rules for welds in RHS members given by Zhao and Hancock (1994a). The reliability index ( $\beta$ ) is checked for the design rules using FOSM (First Order Second Moment) mean value method (Ellingwood et al (1980)).

## 2. MATERIAL PROPERTIES AND WELDING PROCEDURES

The cold-formed SHS and RHS sections used in the tests were supplied by Tubemakers of Australia Limited. These sections were manufactured by a unique cold forming process which included in-line galvanising. They were similar to those described in earlier column and beam tests (Zhao and Hancock, 1992a, 1992b). The nominal and measured section sizes of RHS selected are presented in Table 1.

It was found by Zhao and Hancock (1992a, 1992b, 1992c) that a variation of yield stress existed around C450L0 RHS sections. Variation in stress around the RHS sections was studied by taking tensile coupons from the adjacent face (i.e., a face adjacent to the face containing the seam) and the opposite face (i.e., a face opposite the face containing the seam). The 0.2 percent proof stress was used for the yield stress of all coupons. The test results are summarised in Table 1. It can be found from Table 1 that the yield stress ( $\sigma_{yto}$ ) and tensile strength ( $\sigma_{uto}$ ) of the opposite faces are 15 percent and 7.9 percent higher on average than those of the adjacent faces ( $\sigma_{yta}$ ,  $\sigma_{uta}$ ) as a result of the forming process. The measured tensile strength ( $X_u$ ) of the weld metal is 527.6 MPa.

The welding procedures used in this project were prequalified according to Section 4 of the Australian Standard AS1554.1-1991 (SAA, 1991b), which is similar to Section 5 of AWS D1.1-92 (AWS, 1992). The prequalification of all the welding procedures was reported in detail in Zhao and Hancock (1994b).

### 3. TESTS OF BUTT WELDS

#### 3.1 Tests of Butt Welds

Butt weld tests are called Type B in this paper. The test configuration of butt welds was the same as that used by Zhao and Hancock (1993a, 1994a). A butt weld connection is shown in Figure 1(a). The dimensions  $C_1$  and  $C_2$  are about three times the dimension  $D$  such that the effect of the fillet weld in the end connection on the butt weld may be ignored. The weld length  $2D$  was chosen to ensure that the end connection part is stronger than the RHS section. The 20 mm thick plate is connected to a pin-ended connection. The load is applied through the pin-ended connection. All the tests were carried out in a 2000 kN capacity DARTEC servo-controlled testing machine. The test procedures were the same as those reported in Zhao and Hancock (1993a).

The dominant failure mode found in the tests was tube failure in the heat affected zone. The failure mode was different from that observed in the tests of C350L0 RHS members, where tube tearing along the seam of the section was observed. No significant necking of RHS sections occurred at the failure cross-section, whereas significant necking of RHS sections was observed in the tests of C350L0 RHS members. This may be because C450L0 RHS sections are stronger but less ductile than C350L0 RHS sections.

#### 3.2 Design of Butt Welds

It was proposed by Zhao and Hancock (1993a) that the complete penetration butt weld of C350L0 tubes may be designed in accordance with the tension member rule in AISI-1991 (AISI, 1991) with a capacity (resistance) factor of 0.95 or the tension member rule in AS4100-1990 with a capacity (resistance) factor of 0.90. For AISI-1991, the tension member rule is based on yielding of the parent metal ( $F_y A$ ). For AS4100-1990, the tension member rule is governed by the lesser of  $F_y A$  and  $0.85 F_u A$ . The tensile yield stress and

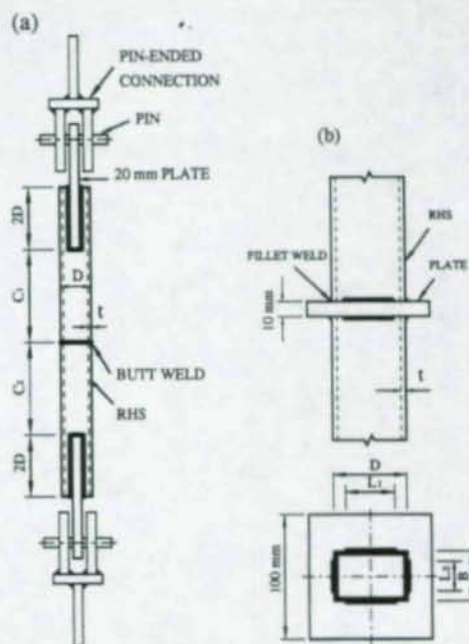


Figure 1: Welded Connections (a) Butt Welds, (b) Transverse Fillet Welds

tensile strength of the opposite face have been used in the calculations. This is more conservative than using values for the adjacent faces for the purpose of establishing design rules.

The statistical parameters of resistance and load used in the reliability analyses were reported in detail in Zhao and Hancock (1994b). A target reliability index of  $\beta_o = 2.5$  is recommended for cold-formed members by the American Iron and Steel Institute (AISI, 1990) when using the FOSM method. It was found by Zhao and Hancock (1994b) that the values of reliability index for the AISI-1991 design model and the AS4100-1990 design model are generally higher than the target value of 2.5 given in AISI (1990), although the values for AISI-1991 fall below 2.5 at low and high  $\frac{D_n}{D_n + L_n}$  ratios. Consideration should be given to including a tension rule based on  $F_u$  rather than  $F_y$  in the AISI specification.

#### 4. TRANSVERSE FILLET WELDS

##### 4.1 Tests of Transverse Fillet Welds

Transverse fillet weld tests are called Type TP in this paper. The length of the fillet welds in Type TP was chosen to be short enough so that weld failure occurred in the tests. The test configuration of the fillet weld test specimens were the same as those of the butt welded connection except for the tested region which is shown in Figure 1(b). The load was applied through the same pin-ended connections used in the Type B tests. The measured

yield stress of the 10 mm plate is 376 MPa and the measured tensile strength is 502 MPa. All the tests were carried out in a 2000 kN capacity DARTEC servo-controlled testing machine. The test procedures were similar to those for Type B tests.

The actual weld lengths and weld sizes (leg lengths) were measured. The measured leg lengths were found to be oversized. The consistent oversize of weld leg length is in agreement with the trend in variation in weld size found in previous international test series (Pham and Bennetts, 1983, Zhao and Hancock, 1993a). The dominant failure mode in the Type TP tests was weld failure in shear across the throat, which was the same as that observed in the tests of transverse fillet welds in C350L0 RHS members.

## 4.2 Design of Transverse Fillet Welds

### 4.2.1 Design rules based on weld metal strength

The design model for transverse fillet welds in AS4100-1990 is based on shear capacity of weld metal ( $0.6X_u aL$ ) with a capacity (resistance) factor of 0.80. It was found by Zhao and Hancock (1993a, 1994a) that the AS4100-1990 design rule was conservative for transverse fillet welds in C350L0 RHS members. A proposed design formula ( $0.6X_u aL[0.75 + 0.5(t/a)]$ ) was given by Zhao and Hancock (1993a, 1994a) for transverse fillet welds, which was a function of the ratio of tube thickness ( $t$ ) to the weld throat thickness ( $a$ ). The proposed formula gives a higher design strength than that given by AS4100-1990. The design strength of transverse fillet welds in the American Institute of Steel Construction Specification has now been increased from  $0.6X_u aL$  in AISC (1986) to  $1.5 \times 0.6X_u aL$  in AISC (1993) with the same capacity (resistance) factor of 0.75. The reliability index ( $\beta$ ) versus  $\frac{D_n}{D_n + L_n}$  curves are plotted in Figure 2(a). It can be seen that the values of reliability index for AS4100-1990 and the proposed design rule by Zhao and Hancock (1993a) are much higher than the target value of 3.5 for cold-formed connections specified in AISI (1990). The predictions of AISC-1993 also produce adequate values of reliability index.

### 4.2.2 Design rules based on parent metal strength

When the thickness of the parent metal is less than or equal to 3.81 mm, the design rules for transverse fillet welds in AISI-1989 (AISI, 1989) and AISI-1991 are based on ultimate strength of the parent metal. When the thickness of the parent metal is greater than 3.81 mm, the strength of the weld metal should be checked. The design rule in AS1538-1988 is the same as that in AISI-1989 with a cut off value of 3.0 mm. It was proposed by Zhao and Hancock (1993a) that the thickness limits (3.81 mm for the AISI specification and 3.0 mm for the Australian Standard AS1538-1988) above which the weld strength must be checked should be reduced to 2.5 mm. Comparisons of the current test results and the AISI specification (Zhao and Hancock, 1994) confirmed the proposal that the weld metal strength should be checked when tube thickness is greater than or equal to 2.5 mm. A proposed design formula ( $F_u t L [1.70 - t/a]$ ) was given by Zhao and Hancock (1993a) for transverse fillet welds, which was a function of the ratio of tube thickness ( $t$ ) to the weld throat thickness ( $a$ ).

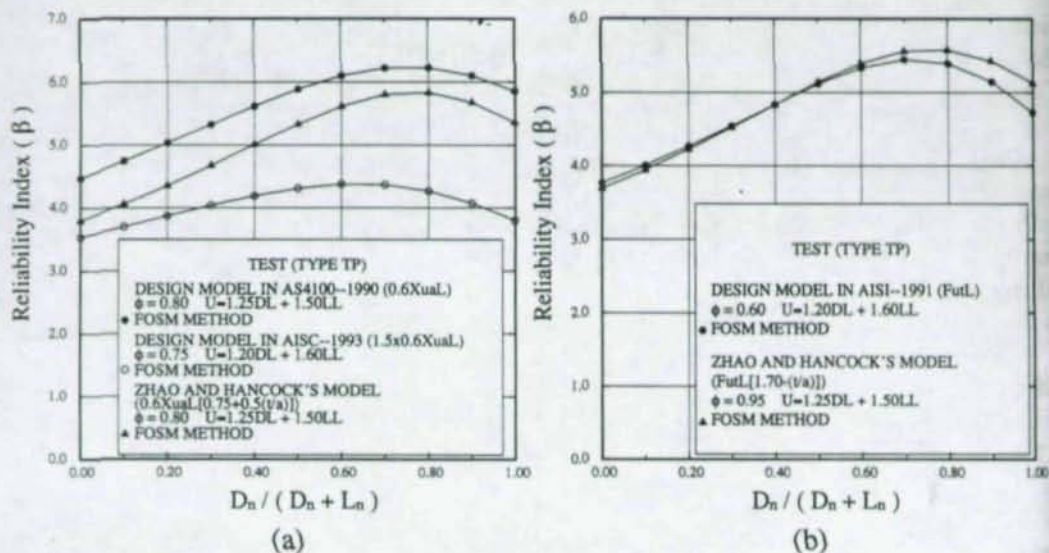


Figure 2: Reliability Index Versus  $\frac{D_n}{D_n + L_n}$  for Transverse Fillet Welds (a) Design Models based on Weld Metal Strength, (b) Design Models based on Parent Metal Strength

The reliability index ( $\beta$ ) versus  $\frac{D_n}{D_n + L_n}$  curves are plotted in Figure 2(b). It is interesting to note that although AISI-1991 produces adequate values of reliability index, the predictions of AISI-1989 (working stress code) produce an inadequate factor of safety when tube thickness is greater than or equal to 2.5 mm. This is due to the low capacity (resistance) factor of 0.60 used in AISI-1991. The values of reliability index for the proposed rule given by Zhao and Hancock (1993a) are higher than the target value of 3.5 given in AISI (1990).

## 5. LONGITUDINAL FILLET WELDS

### 5.1 Tests of Longitudinal Fillet Welds

One end of the specimen was welded to a 20 mm plate which was connected to a pin-ended connection. This is the same as that used in the butt weld tests and transverse fillet weld tests. The other end (the region under test) was also the same except that a 10 mm plate was used and the weld length was shorter.

Four types of tests on the longitudinal fillet welds in C350L0 RHS members were described in Zhao and Hancock (1993b, 1994a), where the tube thickness, the weld length, the end return welds around the end of the 10 mm plate and the orientation of the RHS section were the main parameters varied. It was found by Zhao and Hancock (1993b, 1994a) that the weld capacity of specimens with end returns was about 9 to 14 percent higher than that of specimens without end return welds. It was proposed that end returns should be

considered as a requirement in design as specified in AISC-1993, AWS D1.1-1992 (AWS (1992)) and Eurocode 3 Part 1.1 (1992). Therefore only specimens with end return welds were tested in the current project. It was also found by Zhao and Hancock (1993b, 1994a) that the weld capacity of specimens with welds applied in the opposite face was about 8 to 10 percent higher than that of specimens with welds applied in the adjacent faces. Therefore only specimens with welds applied in the adjacent faces (weaker case) were tested in the current project. These longitudinal fillet weld tests are called Type EY. For each section size, two different lengths of weld were applied. The weld length was chosen to be not long enough to fail the whole RHS cross-section.

The failure mode observed in test Type EY was tube failure in the heat affected zone adjacent to the end return weld. This failure model was the same as that observed in the tests of longitudinal fillet welds (Type EY) in C350L0 RHS members.

## 5.2 Design of Longitudinal Fillet Welds

### 5.2.1 Design rules based on weld metal strength

The design models for longitudinal fillet welds with or without end returns in AS4100-1990 and AISC-1993 with end returns are based on shear capacity of weld metal ( $0.6X_u aL$ ) with capacity (resistance) factors of 0.80 and 0.75 respectively. The reliability index ( $\beta$ ) versus  $\frac{D_n}{D_n+L_n}$  curves are plotted in Figure 3(a). It can be seen that the values of the reliability index for AS4100-1990 are higher than the target value of 3.5 for cold-formed connections specified in AISI (1990) when  $\frac{D_n}{D_n+L_n} > 0.10$ . The values of reliability index for AISC-1993 are higher than those for AS4100-1990 because of the lower capacity (resistance) factor of 0.75 used.

### 5.2.2 Design rules based on parent metal strength

The design models for longitudinal fillet welds in AISI-1989, AS1538-1988 and AISI-1991 are based on the ultimate strength of the parent metal with a consideration of the effect of the weld length, which was derived by Peköz and McGuire (1981). The reduction factor ( $1 - \frac{0.01L_w}{t}$ ) derived by Peköz and McGuire (1981) was not confirmed by the tests of longitudinal fillet welds in C350L0 RHS members as described in Zhao and Hancock (1993b). It was found by Zhao and Hancock (1994) that the reduction factor was not confirmed by the current tests on C450L0 RHS members. A proposed design formula ( $0.75F_u tL$ ) was given by Zhao and Hancock (1993b, 1994a) for longitudinal fillet welds. A capacity factor of 0.72 was proposed by Zhao and Hancock (1993b, 1994a) for the design of longitudinal fillet welds with end returns in C350L0 RHS members. The reliability index ( $\beta$ ) versus  $\frac{D_n}{D_n+L_n}$  curves are plotted in Figure 3(b). It can be seen that the capacity factor of 0.72 seems too high for the design of longitudinal fillet welds with end returns in C450L0 RHS members. The values of reliability index based on a capacity factor of 0.64 seem to be satisfactory, although a lower value may be necessary for welds without end returns. The capacity factor of 0.64 is higher than that of 0.55 used in AISI-1991.

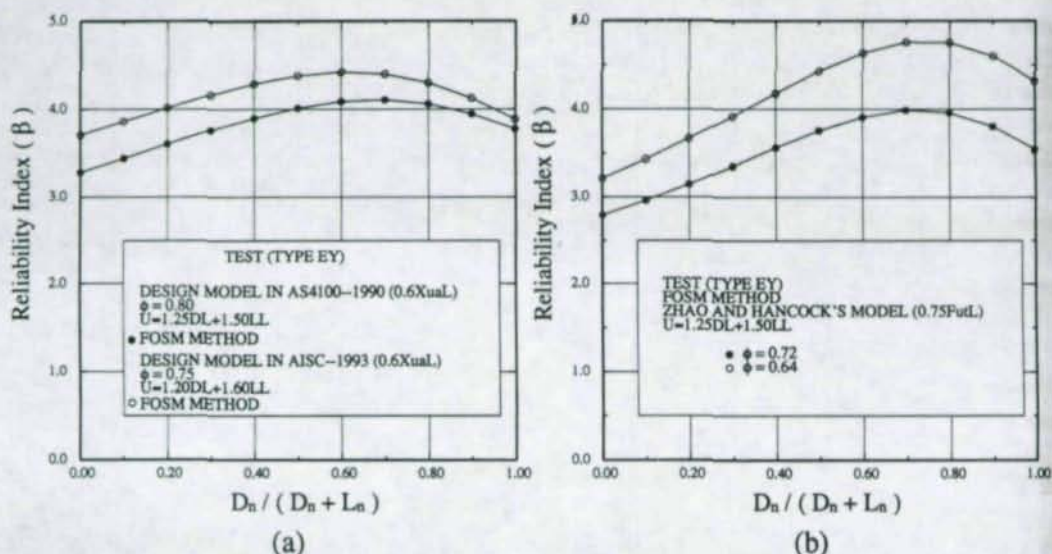


Figure 3: Reliability Index Versus  $\frac{D_n}{D_n + L_n}$  for Longitudinal Fillet Welds (a) Design Models based on Weld Metal Strength, (b) Design Models based on Parent Metal Strength

## 6. CONCLUSIONS

- Complete penetration butt welds in C450L0 members were tested under a static tension load. The dominant failure model was tube failure in the heat affected zone with a lower ductility observed than for tests on C350L0 members. It can be concluded that the complete penetration butt weld may be designed in accordance with the tension member rule in AISI-1991 with a capacity (resistance) factor of 0.95 or tension member rule in AS4100-1990 with a capacity (resistance) factor of 0.90. It is suggested that the AISI-1991 specification include a rule based on  $F_u$  to increase reliability for high strength steel sections.
- Transverse fillet welds (Type TP) in C450L0 members were tested under a static tension load. The dominant failure mode in the Type TP tests was found to be weld shear across the throat. The predictions in AS4100-1990 were found conservative for design of transverse fillet welds. The proposed design model by Zhao and Hancock (1993a) based on weld metal strength and the AISC-1993 specification produced adequate values of reliability index. When the tube thickness is greater than or equal to 2.5 mm, the design rules in AISI-1989 and AS1538-1988 become unsafe, and the weld metal strength should be checked. The AISI-1991 specification produced adequate values of reliability index because of the low capacity (resistance) factor of 0.60 used. The proposed design model by Zhao and Hancock (1993a, 1994a) based on parent metal strength produced adequate values of reliability index.
- Longitudinal fillet welds (Type EY) in C450L0 members were tested under a static tension load. End return welds were applied in all the specimens. The welds were

applied in the adjacent faces of the RHS sections. The failure mode was found to be tube failure in the heat affected zone adjacent to the end return weld. The values of reliability index for AS4100-1990 where a capacity factor of 0.80 was used were higher than the target value of 3.5 when  $\frac{D_n}{D_n+L_n} > 0.10$ . The values of reliability index for AISI-1993 were higher than those for AS4100-1990 because of the lower capacity (resistance) factor of 0.75 used. The reduction factor, as a function of  $(L_w/t)$ , was not confirmed in the current test series. For the proposed design model by Zhao and Hancock (1993b, 1994a) based on parent metal tensile strength, the capacity factor of 0.72 seems too high for the design of longitudinal fillet welds in C450L0 RHS members. The values of reliability index based on a capacity factor of 0.64 seems to be satisfactory.

## 7. REFERENCES

- AISC (1986), *Load and Resistance Factor Design Specification for Structural Steel Buildings*, American Institute of Steel Construction, Chicago, Ill.
- AISC (1993), *Load and Resistance Factor Design Specification for Structural Steel Buildings*, American Institute of Steel Construction, Chicago, Ill.
- AISI (1989), "Specification for the Design of Cold-Formed Steel Structural Members", August 19, 1986 edition, with December 11, 1989 Addendum, *Report CF 89-1*, American Iron and Steel Institute, Washington, D.C.
- AISI (1990), "Commentary on the Load and Resistance Factor Design Specification for Cold-Formed Steel Structural Members", *Report CF 90-2*, August, American Iron and Steel Institute, Washington D.C.
- AISI (1991), American Iron and Steel Institute, *Load and Resistance Factor Design Specification for Cold-Formed Steel Structural Members*, Washington, D.C.
- AWS (1992), *Structural Welding Code - Steel, ANSI/AWS D1.1-92*, 13th edition, American Welding Society Inc., Miami, Fla.
- Ellingwood, B. et al (1980), "Development of a Probability Based Load Criterion for American National Standard A58: Building Code Requirements for Minimum Design Loads in Buildings and Other Structures", NBS No.577, Washington D.C.
- Eurocode 3 Part 1.1 (1992), *Design of Steel Structures: Part 1.1 - General Rules and Rules for Buildings*, DD ENV, 1993-1-1, Eurocode 3 Editorial Group.
- Eurocode 3 Part 1.3 (1992), *Design of Steel Structures: Part 1.3 - Cold-Formed Thin Gauge Members and Sheeting*, CEN/TC 250/SC3-PT1A, Eurocode 3 Editorial Group.
- Peköz, T. and McGuire, W. (1981), "Sheet Steel Welding", *J. Struct. Div.*, ASCE, Vol.107, No.8, pp.1657-1673.

- Pham, L. and Bennetts, I. D. (1983), "Reliability of Fillet Weld Design", *Civil Engineering Transaction*, IEAust., Vol.CE26, No.2, pp.119-124.
- SAA (1988), *Cold-Formed Steel Structures Code*, Australian Standard AS1538, Standards Assoc. of Australia, Sydney.
- SAA (1990), *Steel Structures*, Australian Standard AS4100, Standards Assoc. of Australia
- SAA (1991a), *Structural Steel Hollow Sections*, Australian Standard AS1163, Standards Association of Australia, Sydney.
- SAA (1991b), *Structural Steel Welding (known as the SAA Structural Steel Welding Code)*, Part 1: Welding of Steel Structures, Australian Standard AS1554.1, Standards Association of Australia, Sydney.
- Stark, J.W.B. and Soetens, F. (1980), "Welded Connections in Cold-Formed Sections", *Procs*, 5th Int. Specialty Conference on Cold-Formed Steel Structures, St. Louis, MO.
- Tubemakers (1994), *Design Capacity Tables for DuraGal Steel Hollow Sections*, Tubemakers of Australia Ltd., Struct. Products Div., Newcastle, NSW.
- Zhao, X. L. and Hancock, G. J. (1991), "Tests to Determine Plate Slenderness Limits for Cold-Formed Rectangular Hollow Sections of Grade C450", *J. Australian Institute of Steel Construction*, Vol.25, No.4, pp.2-16.
- Zhao, X. L. and Hancock, G. J., (1992a), "Tests to Determine the Reliability of Stub Columns of DuraGal RHS", Investigation Report, S916, Centre for Advanced Structural Engineering, The University of Sydney, Sydney, Australia.
- Zhao, X. L. and Hancock, G. J., (1992b), "Tests to Determine the Reliability of Beams of DuraGal RHS", Investigation Report, S917, The University of Sydney, Sydney
- Zhao, X. L. and Hancock, G. J., (1992c), "Tests on Rectangular Hollow Sections to Investigate the Effect of Variation of Yield Stress Around a Section", Investigation Report, S885, Centre for Advanced Structural Engineering, The University of Sydney, Sydney.
- Zhao, X. L. and Hancock, G. J., (1993a), "Tests and Design of Butt Welds and Transverse Fillet Welds in Thin Cold-Formed RHS Members", *Research Report*, No. R681, School of Civil and Mining Engineering, The University of Sydney, Sydney.
- Zhao, X. L. and Hancock, G. J., (1993b), "Tests and Design of Longitudinal Fillet Welds in Thin Cold-Formed RHS Members", *Research Report*, R682, School of Civil and Mining Engineering, The University of Sydney, Sydney, Australia.
- Zhao, X. L. and Hancock, G. J. (1994a), "Tests and Design of Butt Welds and Fillet Welds in Thin Cold-Formed RHS Members", *Tubular Struct. VI*, Balkema, Rotterdam, 465-472.
- Zhao, X. L. and Hancock, G. J., (1994b), "Tests and Design of Butt Welds and Fillet Welds in DuraGal RHS Members", *Research Report*, R702, School of Civil and Mining Engineering, The University of Sydney, Sydney, Australia.

# SEISMIC PERFORMANCE OF CFT COLUMN-TO-WF BEAM MOMENT CONNECTIONS

James M. Ricles<sup>1</sup>

Le-Wu Lu<sup>2</sup>, Took K. Sooi<sup>3</sup>, and G. Vermaas<sup>4</sup>

## Abstract

This paper describes ongoing research associated with the seismic behavior of moment connections for CFT column-to-WF beam framing systems. The objective of this multiphase research program is to assess the force transfer mechanism in these type of connections, examining the effect various structural details have on this mechanism, as well as on the connection's strength, stiffness, and ductility. The first phase of the program has been devoted towards assessing the shear capacity of the panel zone in a CFT under simulated seismic lateral load conditions. The results from tests show that a CFT panel zone possess exceptional ductility, including specimens without interior diaphragms. In addition, a capacity equation based on the superposition of the shear strength contribution of the steel tube and concrete core within the panel zone provides a prediction that agrees reasonably well with specimen strength. The second phase of the program is also discussed, which is currently in progress and associated with full-scale structural connection subassembly tests.

## 1. INTRODUCTION

The combining of structural steel and concrete to form composite members results in a structural system that has many attributes. These include the inherent mass, stiffness, damping and economy of concrete, and the speed of erection, strength, long-span capability, and light weight of structural steel. In high-rise structures large axial forces can accumulate in the columns. In addition, inter-story drift can control the design of such structures. *Composite columns are an appealing solution to deal with these issues.* Typical high-rise composite construction involves perimeter moment resisting frames (MRFs) with composite columns, which are either a structural steel shape encased in reinforced concrete or concrete filled tubes (CFTs). The spandrel beams for

---

<sup>1</sup>Associate Professor, <sup>2</sup>Professor, <sup>3</sup>Research Engineer, <sup>4</sup>Research Assistant, Lehigh University, ATLSS Engineering Research Center, 117 ATLSS Drive H Building, Bethlehem, Pennsylvania 18015-4729.

the MRF are typically wide flange (WF) steel sections. Practical applications for composite columns can also be found in low-rise construction, such as in warehouses or industrial buildings. This paper focuses on composite construction which involves CFT columns, which emphasis on the moment connections which join the columns and spandrel beams to form a seismic resistant perimeter MRF.

The advantage of using CFT composite columns is that the steel tube provides a permanent formwork for the concrete placement, thereby expediting construction. In addition, the steel provides confinement to the concrete inside the tube, whereas the concrete inhibits local buckling from occurring in the steel tube. The result is a composite member possessing exceptional axial and lateral stiffness, strength, and ductility. Shown in Figure 1 is an elevation of a 20-story MRF, which is adopted as the prototype for this research study. This MRF is a perimeter frame for a typical office building, and is assumed to exist in a seismic zone 4 within the United States. Both a wide flange column (e.g. non-composite) and a CFT column system were designed for the purpose of comparison. Both systems possessed steel spandrel beams with moment connections to the columns. The beams and columns of both systems were designed according to AISC LRFD Provisions ("American", 1994) in conjunction with NEHRP Seismic Provisions (NEHRP, 1991). The CFT columns were designed with a 55 MPa nominal compressive strength concrete. The profiles for factored inter-story drift under NEHRP stipulated seismic loading is included in Figure 1. Both the CFT column and WF column MRF designs were found to be controlled by drift criteria per NEHRP (1991), which stipulates that the factored inter-story drift  $\delta$  must be within the limit of 1.5%, where

$$\delta = C_d \delta_{el} \quad (1)$$

in which  $\delta_{el}$  is the inter-story drift from an elastic lateral seismic load analysis and  $C_d$  is a displacement amplification factor ( a value of  $C_d=5.5$  was used, as stipulated by NEHRP for ductile MRFs). A comparison of the two designs (the beam and column sizes are summarized in Figure 1) for the building indicates that although the total weight of the CFT column system is 81% greater than that of the WF column system due to the additional weight of the concrete, the former has a total structural steel weight that is 22% less than the latter. This reduced weight of steel in the CFT column system represents a cost savings.

A critical component of the perimeter MRF CFT column system is the moment connections between the steel WF spandrel beams and CFT columns. Under lateral seismic loading to the MRF these connections are susceptible to large forces, including a large shear in the joints' panel zones as illustrated in Figure 2. The panel shear is the result of larger beam flange forces that are transferred into the connection. To deal with the large beam flange forces, CFT construction in Japan has traditionally involved the use of interior or exterior steel plate diaphragms in the connection, as shown in Figure 3, to provide stiffening of the tube and a force path for the beam flange forces. While the use of diaphragms may improve performance and avoid premature connection

failure, their incorporation into CFT moment connections is expensive to fabricate, particularly when interior diaphragms are utilized. Consequently, the saving accrued from reduced steel weight may be lost, or even exceeded, in CFT column systems when interior diaphragms are used in moment connections.

To evaluate the need for diaphragms in seismic resistant moment connections in CFT column systems, a research program has been pursued at Lehigh University. This research program consists of several phases of study, and has as its overall objective to investigate the force transfer mechanism in CFT column-to-WF beam moment connections under seismic loading. The research is to examine the effect various structural details have on the force transfer mechanism, and on the connection's strength, stiffness, and ductility. Based on the results of experimental testing and analysis, the research program has as a goal to provide recommendations for design details for moment connections that provide good performance under seismic conditions, and are economical to fabricate.

The first phase of this program involved an experimental investigation concerned with the shear-deformation characteristics of CFT panel zones. Included was the development and assessment of a capacity model for predicting panel zone shear capacity. The second phase of this research program, which is currently in progress, involves the testing of large scale structural connection subassemblies under lateral cyclic loading. Presented herein are the results from the first phase of work, and a description of the structural subassemblage test program conducted under the second phase.

## 2. CFT PANEL ZONE STUDY

Under lateral loading, the shear developed in the panel zone of a CFT-to-beam moment connection is resisted by both the steel tube and concrete. The concrete resistance to panel zone shear is by the development of a diagonal compression strut, as shown in Figure 1, having the inclination angle (or strut angle) of  $\alpha$ . One of purposes of the panel zone test was to assess the effect the interior diaphragm has on the compression strut. In addition to the diaphragm, other details which can conceivably affect the panel zone's behavior include: the width-to-thickness ( $b/t$ ) ratio of the steel tube in the panel zone; compression strut angle  $\alpha$ ; concrete compressive strength; and steel tube's yield stress. To study some of these effects, four CFT panel zone specimens were designed and tested.

A summary of the test matrix containing the four test specimens is given in Table 1. The details considered as parameters among the specimens were: interior diaphragms;  $b/t$  ratio; and compression strut angle  $\alpha$ . The effects of these parameters on shear capacity

were studied by changing the details of the panel zone in accordance with Table 1. Specimen 1 of the test matrix was the only specimen which had a set of diaphragms, each diaphragm being placed inside the steel tube where simulated beam flange forces were applied to the outside wall of the specimen. Specimen 2 was identical to Specimen 1, except the former did not have any diaphragms. The  $b/t$  ratios of Specimens 3 and 4 were both increased from that of Specimens 1 and 2. While the nominal  $b/t$  ratio was the same for Specimens 3 and 4, Specimen 4 had a larger strut angle, which was accomplished by making Specimen 4 of greater length. The measured material properties for the steel tube's yield stress ( $\sigma_y$ ) and ultimate stress ( $\sigma_u$ ), as well as the concrete compressive strength  $f'_c$  are given in Table 2.

The testing scheme shown in Figure 4 was developed to simulate local force conditions applied to a panel zone, including compression beam flange forces and column axial force. The applicability of the results from tests using this setup to connections which do not have diaphragms, and in which the beam tension flange forces are applied to the wall of the steel tube, is questionable. However, subsequent tests in the second phase of the research program will have details that result in only the compression flange force being applied to the panel for specimens which omit the diaphragms. The test setup for the panel zone test shown in Figure 4 resulted in two panel zones being created in each test specimen, by providing end reactions to a transverse applied load  $H$  at midspan. The magnitude of the end reaction thus was equal to the shear  $V$  developed in the panel zone. The load  $H$  and reactions were applied using rollers in conjunction with 50 mm and 100 mm wide bearing plates placed across the specimen's width at its ends and midspan, respectively. The bearing plates were each 12 mm thick. A constant axial compressive load  $P$  was applied in the horizontal direction to both ends of the specimen to simulate column axial force effects. Both ends of the test specimen were restrained from rotating. The axial force  $P$  was 890 kN in Specimens 1 and 2, and 712 kN in Specimens 3 and 4. The magnitude of  $P$  was equivalent to one-half the nominal squash load  $N_o$  (e.g.  $P=0.5N_o$ ), defined in accordance with AIJ Provisions ("Architectural", 1987):

$$N_o = \frac{1}{3}A_c f'_c + \frac{2}{3}A_s \sigma_y \quad (2)$$

In Equation (2)  $A_c$  and  $A_s$  is equal to the cross sectional area of the concrete core and the steel tube, respectively. Prior to testing, each specimen was instrumented in order to measure strain in the panel zone of the steel tube, displacement under the applied transverse load  $H$ , and end rotation.

The shear-deformation ( $V-\gamma$ ) response of the specimens are shown plotted in Figure 5, where they have been superimposed in order to evaluate the effects of the various panel zone structural parameters. Typical response of a specimen during testing involved an initial linear relationship between  $V$  and  $\gamma$ . As yielding developed in the steel tube of the panel zone under shear, a softening of the panel zone's stiffness occurred, which became quite noticeable as the applied shear  $V$  surpassed the shear capacity  $V_p$ , which corresponded to specimen plastic shear capacity of the steel tube. This is

apparent in Figure 5 for all specimens. With continued loading, the stiffness continued to decrease until it became zero, at which the specimen capacity  $V_{exp}$  had been reached. The shear capacity  $V_{exp}$  of each specimen is summarized in Table 3. Specimen 1 had a 30% greater capacity than corresponding Specimen 2, which is apparent in Figure 5(a) as well as Table 3. The additional strength achieved in Specimen 1 is attributed to the presence of its interior diaphragms, which enhanced the concrete compression strut's strength  $V_c$  by increasing the concrete strength and compression strut width through additional confinement. Specimen 2 was found to have a 20% greater capacity than Specimen 3 (see Figure 5(b)). This increase in strength is mainly attributed to the greater shear strength  $V_s$  of the steel tube of Specimen 2. Specimens 3 and 4 had a capacity  $V_{exp}$  of 589 kN and 578 kN, implying that the difference in strut angle  $\alpha$  of 45 and 56 degrees did not significantly affect specimen capacity.

Continued imposed deformation during testing saw all specimens develop exceptional ductility, with an increase in strength under large displacements occur as tension membrane action developed which provided additional resistance. All specimens eventually developed a local outward buckling in the panel zones. For Specimens 2, 3, and 4 this occurred at a shear deformation of approximately  $\gamma=0.05$  to 0.06 radians, taking the form of an outward uniform bulging of the panels. The interior diaphragms in Specimen 1 enabled a greater shear deformation  $\gamma$  of approximately 0.15 radians to develop before local buckling occurred along a diagonal of the panel zone. This diagonal local buckling resembled that which has been found to occur in stiffened panels of plate girders subjected to shear. The presence of the concrete inside the steel tube enabled the specimens to all develop significant post buckling strength and ductility.

A shear capacity model was developed in order to attempt to predict the shear strength of the test specimens. The formulation for the model was based on superimposing the shear strengths of the steel tube ( $V_s$ ) and that of the concrete ( $V_c$ ) to arrive at the panel zone's total shear capacity ( $V_{total}$ ), as illustrated in Figure 6, and where:

$$V_{total} = V_s + V_c \quad (3)$$

Since shear yielding occurred in the steel tube prior to local buckling, the steel contribution was based on considering the von Mises yield criterion for metals, where

$$V_s = \frac{1}{\sqrt{3}} \sigma_y A_w \quad (4)$$

in which  $A_w$  is the web area of the steel tube that creates the steel panel zone (e.g.  $A_w=2bt$ ). To evaluate the contribution of the concrete's shear strength  $V_c$ , three different models were examined, namely: (1) Strut Model A; (2) Strut Model B; and, (3) ACI Model. Strut Model A and B were both based on the concept of the strut and tie model for reinforced concrete (MacGregor, 1992). The component of the concrete strut force that is parallel to the imposed joint shear  $V$  determines  $V_c$ . The capacity of the concrete

strut provides the maximum strut resisting force. Strut Model A assumes that the crushing strength of the strut depends on the concrete compressive strength  $f'_c$  and the strut width  $B_s = S \cos \alpha$ , where  $S$  is the effective bearing width along the depth of the panel for the beam compressive flange forces. The expression for the concrete shear resistance  $V_c$  for Strut Model A is given in Figure 7(a), which includes formulations for panel zones with and without interior diaphragms. The expression for  $V_c$  when interior diaphragms exist in the panel zone was based on doubling the width  $B_s$  of the compression strut. In the expressions for  $V_c$  in Figure 7 the variable  $B$  refers to the width of the CFT, which is normal to the plane of the panel zone and to which the beam flanges would be connected.

The formulation for Strut Model B is associated with a compression strut width  $B_s$  which is based on the geometry of a 45 degree hydrostatic prism in the concrete (see Figure 7(b)). This prism is created by the bearing stresses imposed to the column by the beam compression flanges. Assuming the strength of the compression strut is proportional to  $0.85f'_c$ , the shear strength contribution  $V_c$  to the panel zone's shear capacity becomes the expressions given in Figure 7(b). The expression on the right hand side of Figure 7(b) accounts for the presence of interior diaphragms, and is based on assuming a secondary compression field develops in the concrete core at an inclined angle of  $\beta$ . This secondary compression field develops near the corners of the panel, which undergo a closure by shear deformation. The angle  $\beta$  is that which is perpendicular to the principal direction of the diagonal tension in the panel zone, where it can be shown that:

$$\sin^2 \beta = 0.5 \left[ 1 - \frac{\frac{d}{b}}{\sqrt{1 + \left(\frac{d}{b}\right)^2}} \right] \quad (5)$$

in which  $d$  and  $b$  are the height and width of the panel zone.

The equations from the ACI Specification (ACI 1989) were used to estimate the concrete contribution  $V_c$  for the ACI Model. The expressions for  $V_c$  for panel zones both with and without interior diaphragms are given in Figure 7(c), where for diaphragms the concrete joint shear strength is based on a higher degree of concrete confinement. For CFT connections without diaphragms, the joint was assumed to be related to the case described in the ACI Specification consisting of confinement on two opposite faces of the joint.

A comparison of the predicted shear capacity  $V_{total}$  of the panel zone of each of the four test specimens with their corresponding experimental capacity  $V_{exp}$  is given in Table 3. The comparison includes the predicted capacity using  $V_c$  based on the various concrete models discussed above. The ratio of the predicted joint shear capacity to experimental capacity ( $V_{total}/V_{exp}$ ) was found to have a mean of 1.01 and 0.99 using Strut Model A and B, respectively. The mean value for the ratio of  $V_{total}/V_{exp}$  using the ACI Model for  $V_c$  was

found to be 1.11, indicating that the contribution of the concrete is overestimated by the adapted ACI criteria. Overall, Strut Model B provided the best estimate for  $V_{total}$ , having a coefficient of variation of 3.1% compared to 7.5% for Strut Model A.

### 3. CONNECTION STRUCTURAL SUBASSEMBLAGE STUDY

To further the understanding of the force transfer mechanism, and to study cyclic lateral load effects, large-scale connection subassembly tests are currently being conducted under the second phase of the research program. The subassembly is a cruciform test specimen, consisting of a CFT column, steel wide flange spandrel beams, and the joint comprised of a moment resisting connection. A schematic of a test specimen placed in the test setup is shown in Figure 8(a). The ends of the beams and column correspond to the midspan and midheight of the spandrel beams and CFT columns, respectively, of the prototype perimeter MRF subjected to lateral load (see Figure 8(b)). In the test setup the column is loaded axially by a constant gravity load of 2224 kN, while subjecting the top of the column to a cyclic loading history by the use of a horizontally placed actuator. The lateral loading history corresponds to successive sets of cyclic displacements of increasing amplitude. The column and beam sizes correspond to a 406 mm by 406 mm concrete filled steel tube and a W24x62 wide flange steel beam, respectively. The nominal concrete compressive strength is 55 MPa that fills the steel tube. These CFT and spandrel beam sizes and lengths correspond to a full-scale version of the members in a lower floor of the prototype perimeter MRF (see Figure 1).

The initial set of test specimens have their connection details shown in Figures 9, 10, and 11, where they are referred to as Connections 1, 2, 3, and 4. Among the test specimens, different details were used in order to assess their effect on connection and subassembly performance. In all of these test specimens the nominal b/t ratio of the steel tube is 32. The joints of the test specimens were designed, using the above joint shear capacity model in conjunction with Strut Model B, to resist the moments and shears developed under plastic hinging of the beams. In the event that during the course of testing the joint is successful in providing sufficient ductility through yielding in the beam, additional tests will be conducted by subsequently strengthening the beams of these specimens in order to force inelastic response in the panel zone of the joint to assess its strength and ductility under cyclic loading.

Connection 1 consists of structural details with an interior set of diaphragms placed at the flange height of the beams. This specimen is to provide a reference for comparing the performance of other test specimens which do not have interior diaphragms. As shown in Figure 9, the diaphragms for Connection 1 are welded along all four edges. The beam flanges were welded to the column using full penetration flux cored arc welding. In Connection 1, as well as the other three test specimens, the shear tab was welded and bolted to the beam web using five-A325 25 mm diameter bolts. The

placement of fillet welds along the shear tab, as shown in Figure 9, was required in accordance with AISC LRFD seismic design provisions ("American" 1994), since the plastic section modulus of the flanges accounted for less than 70% of the plastic moment capacity  $M_p$  of the beam. In addition, in all specimens twelve-16 mm diameter, 102 mm long shear studs were used to transfer the beam's gravity load to the concrete.

The details of Connection 2 are similar to Connection 1, except that the diaphragm in the former is welded along only three of its edges. The detail for Connection 2 has applications suited for CFT construction involving steel box column fabrication using plates. The fourth edge of the diaphragm, which is normally welded using the expensive technique of electro-slag welding in box-column fabrication to close the cross section, was omitted in order to evaluate the effects of this omission on connection performance. In the test program reported herein structural tubing was used for the column, in lieu of box column sections fabricated from plates in order to reduce costs.

Connection 3 has no interior diaphragms, using structural tees as shown in Figure 10 to stiffen the steel tube and activate the panel zone by establishing a more direct force transfer mechanism between the beam flanges and the panel zone. The details of Connection 4, shown in Figure 11, utilizes high strength bolts and end plates (the latter is identified as PL 3/4 x 7 1/4 x 16 in Figure 11) to provide anchorage for the tension beam flange forces, creating a diagonal compression strut in the concrete within the panel zone under lateral frame loading. The shear resistance of the steel tube is activated by the shear deformation developed in the panel zone. During fabrication, the end plates are tack welded to the column and the bolt holes drilled in the shop. To reduce prying action in the high strength bolts as well as increase the stiffness of the connection, washer plates (identified as PL 3/4 x 3 3/4 x 16 in Figure 11) are used. These plates are placed behind the nuts and do not require any welding.

Prior to conducting the tests, which will occur in the near future, each of the specimens will be fully instrumented. The instrumentation will enable the strains in the beam flanges and the steel tube, both in and outside the panel zone, to be measured. In addition, the shear deformations in the panel zone, beam and column displacement, and applied loads will be measured. These measurements will enable the shear force-deformation ( $V$ - $\gamma$ ) relationship of the panel zone to be determined, as well as beam moment-rotation, and lateral load-interstory drift response. In addition, the measurements will enable the effective lateral stiffness of the CFT column under combined axial load and moment to be obtained.

As part of the second phase of the research project, additional tests are to be conducted involving the above structural connection subassemblies. These tests will include details that will omit the shear studs, as well as study the performance of specimens that have weaker panel zones in which the  $b/t$  ratio of the steel tube is larger. To complement the experimental studies, analytical studies are currently commencing, involving inelastic time history analysis of CFT column MRFs subjected to seismic loading. In addition, nonlinear finite element analyses are being conducted of the local joint region to assess the force transfer mechanism.

#### 4. SUMMARY AND CONCLUSIONS

An ongoing research program on the subject of the seismic performance of moment connections for CFT column MRF systems has been presented. This study includes panel zone tests of one half-scale specimens, as well as full-scale structural joint subassembly tests. The results of the completed tests on the CFT panel zone specimens indicates that while interior diaphragms may enhance a panel zone's shear capacity by increasing the contribution of the concrete, panel zone specimens without interior diaphragms also performed well under monotonic load and had exceptional ductility. The shear capacity of the specimens was found to correlate well with joint capacity strength equations that were based on superimposing the shear strength of the steel tube and the concrete core in the joint region, where the latter is based on a strut model. The testing of the structural connection subassemblies will provide additional information when completed, particularly related to cyclic load effects, beam attachment details, and the contribution of the connection to the behavior of the subassembly.

#### 5. ACKNOWLEDGMENTS

The research program reported herein is supported by various sponsors. These include: ATLSS Engineering Research Center at Lehigh University, American Institute of Steel Construction, American Iron and Steel Institute, Bethlehem Steel Corporation, Hollow Structural Sections Institute, the National Science Foundation, and Nippon Steel Corporation. The financial support and donation of materials by the sponsors is gratefully acknowledged. The authors would also like to thank Seung Eun Suh of Cornell University, who assisted in conducting the panel zone experiments while participating in the NSF Research Experiences for Undergraduates Program at ATLSS. The opinions expressed in this paper are those of the authors and do not necessarily reflect the views of the sponsors.

#### 6. REFERENCES

- 1) American Concrete Institute. (1989) "Building Code Requirements for Reinforced Concrete (ACI 318-89) and Commentary-ACI 318R-89," Detroit, Michigan.

- 2) Architectural Institute of Japan. (1987) "Standard for Structural Calculation of Steel Reinforced Concrete Structures," Tokyo, Japan.
- 3) American Institute of Steel Construction. (1994) "Load and Resistant Factored Design," 2nd Edition, *Manual of Steel Construction*, Chicago, Illinois.
- 4) MacGregor, J.G. (1992) "Reinforced Concrete - Mechanics and Design," Prentice-Hall, Inc. Englewood Cliffs, New Jersey.
- 5) National Earthquake Hazards Reduction Program - NEHRP. (1991) "Recommended Provisions for the Development of Seismic Regulations for New Buildings," Building Seismic Safety Council, Federal Emergency Management Agency, Washington, D.C.

Table 1 CFT Panel Zone Test Specimen Matrix

Specimen	Diaphragm	t (mm)	b/t	d (mm)	$\alpha$ (deg)
1	Yes	5.8	35	406	45
2	No	5.8	35.1	406	45
3	No	4.4	46	406	45
4	No	4.4	45.7	610	56

Table 2 CFT Panel Zone Specimen Material Properties

Specimen	Nominal Dimensions (mm x mm x mm)	$\sigma_y$ (MPa)	$\sigma_u$ (MPa)	$f'_c$ (MPa)
1,2	203 x 203 x 6.3	412	520	39
3,4	203 x 203 x 4.5	377	462	39

Table 3 CFT Panel Zone Specimen Capacity

Specimen	$V_{exp}$ (kN)	$V_s/V_{exp}$	$\frac{V_{exp} - V_s}{V_{exp}}$	$V_{total}/V_{exp}$		
				Strut A	Strut B	ACI
1	923	0.59	0.41	1.05	0.99	1.0
2	712	0.76	0.24	1.07	1.04	1.16
3	589	0.65	0.35	1.01	0.97	1.15
4	578	0.66	0.34	0.90	0.98	1.12

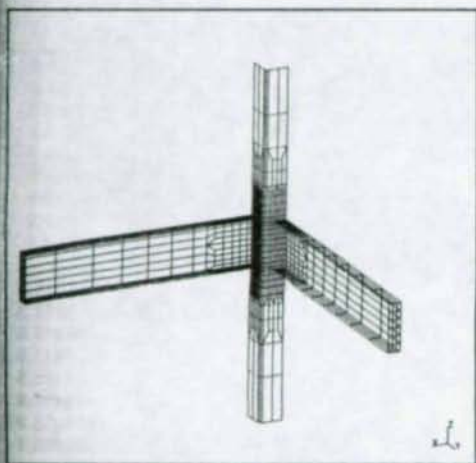


Figure 1 Typical finite element mesh for a multiplanar connection

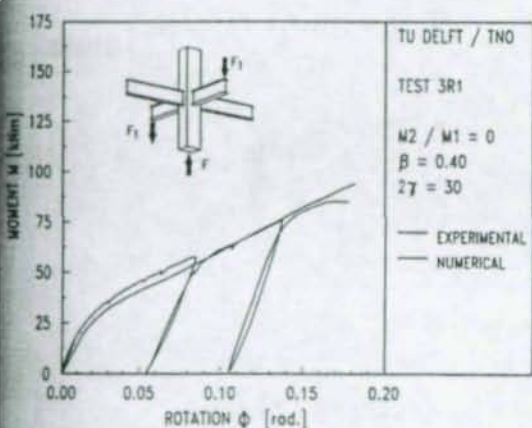


Fig. 2 Calibration of numerical model with experiment for 3R1

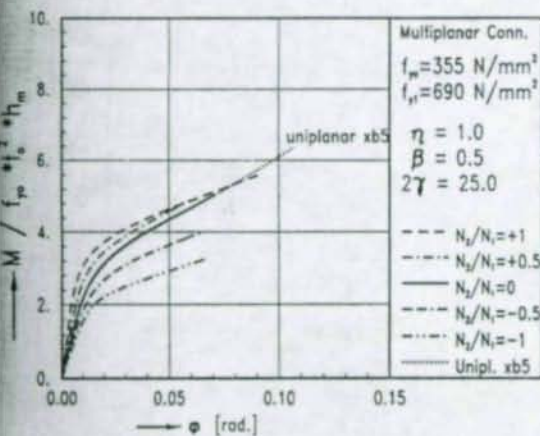


Fig. 3 Moment - rotation curves for xb5 and xxb5

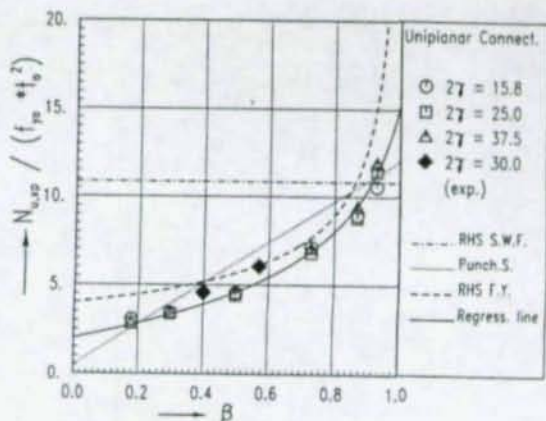


Fig. 4 The strength of uniplanar plate to RHS column connection

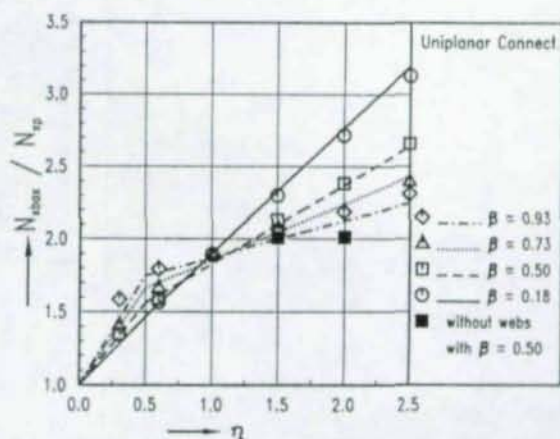


Fig. 5 The effect of the second flange and web

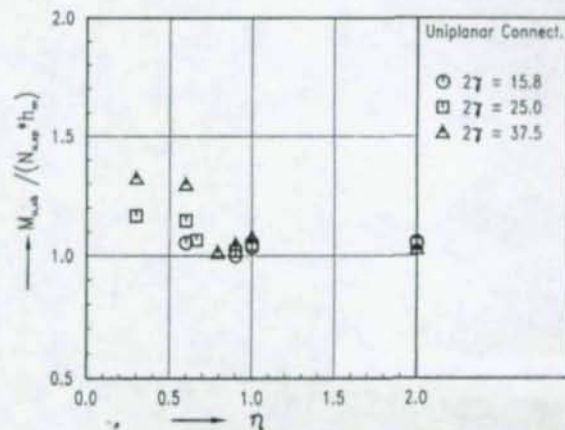


Fig. 6 Comparison of I-beam to RHS with plate to RHS connections

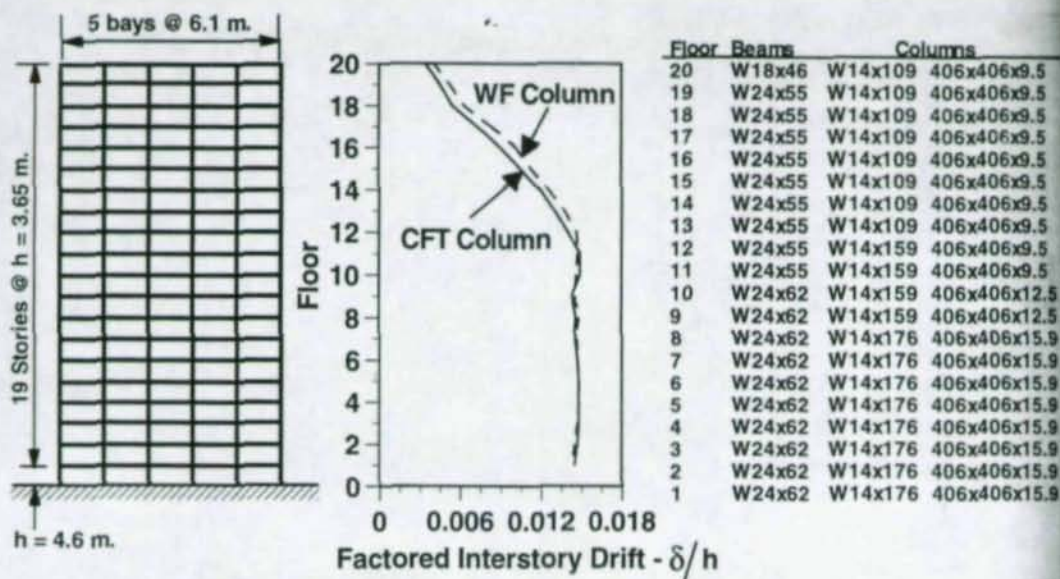


Figure 1 Prototype Perimeter Moment Resisting Frame for CFT and WF Column Systems.

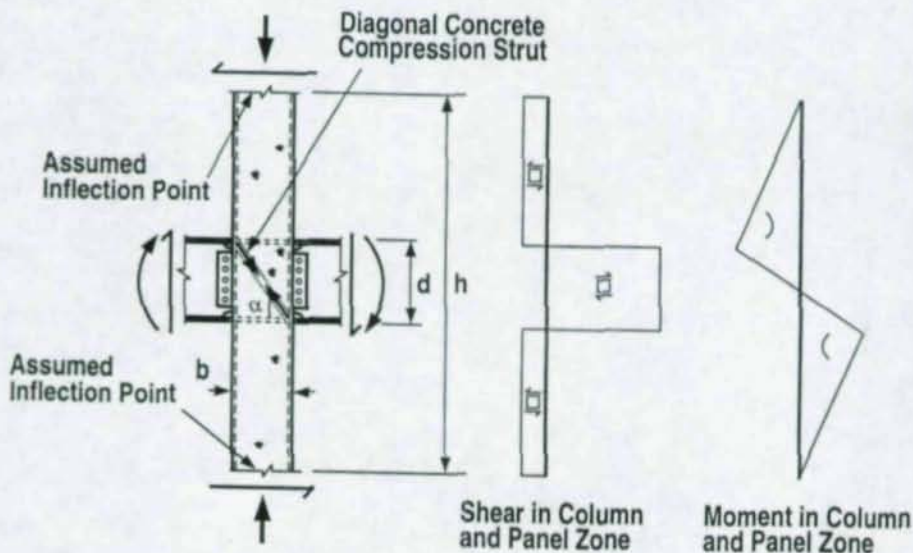


Figure 2 Shear and Moment in Panel Zone Due to Seismic Lateral Loading.

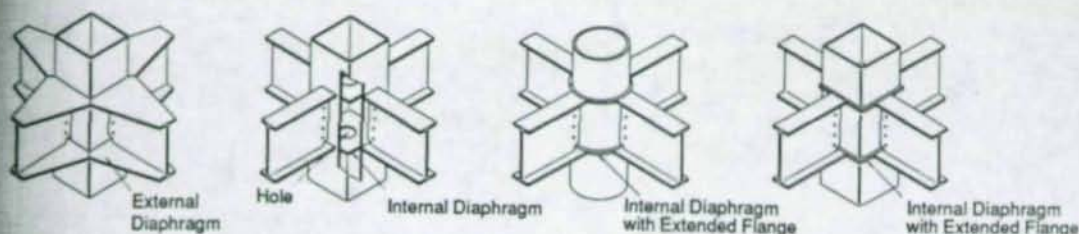


Figure 3 Typical Japanese CFT Column-to-Beam Moment Connections (AIJ, 1987).

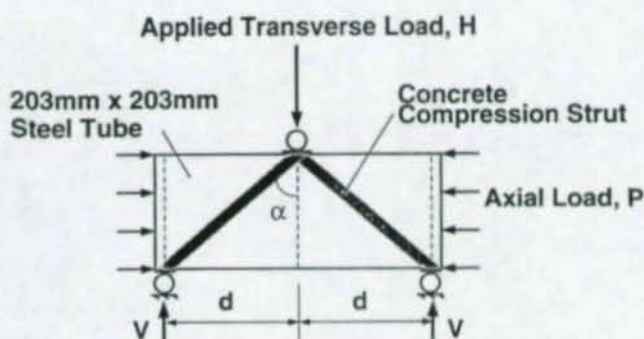


Figure 4 Experimental Setup for CFT Panel Zone Test.

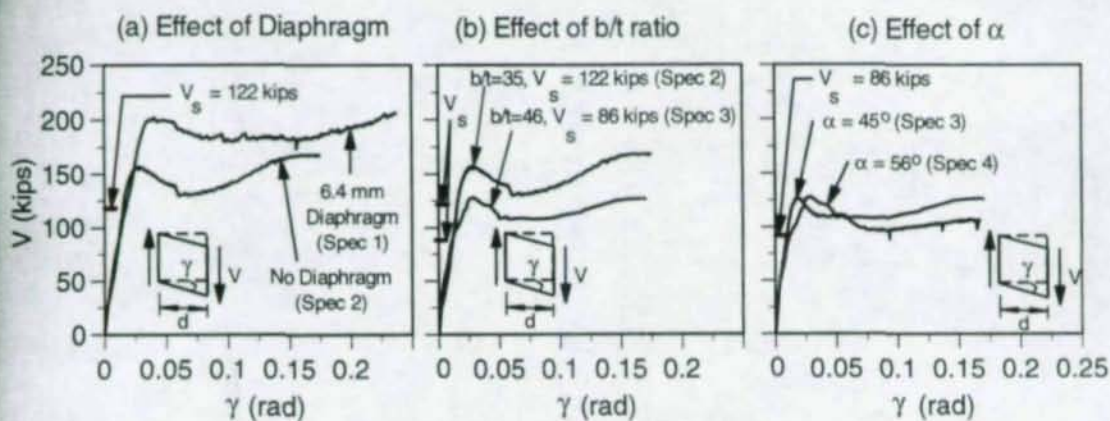


Figure 5 Shear -Deformation ( $V$ - $\gamma$ ) Response of Panel Zone Specimens.

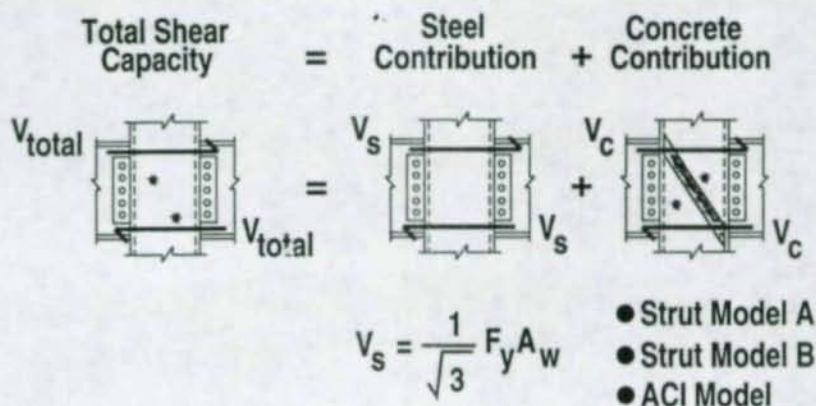
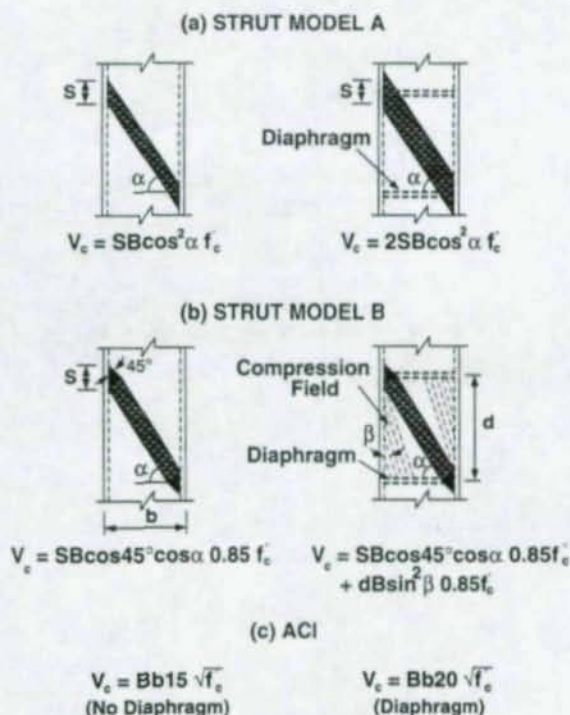


Figure 6 Panel Zone Shear Capacity - Superposition of Steel and Concrete Strengths.



Note: B is the out-of-plane dimension of the column

Figure 7 Various Models for Determining Contribution of Concrete Joint Shear Capacity.

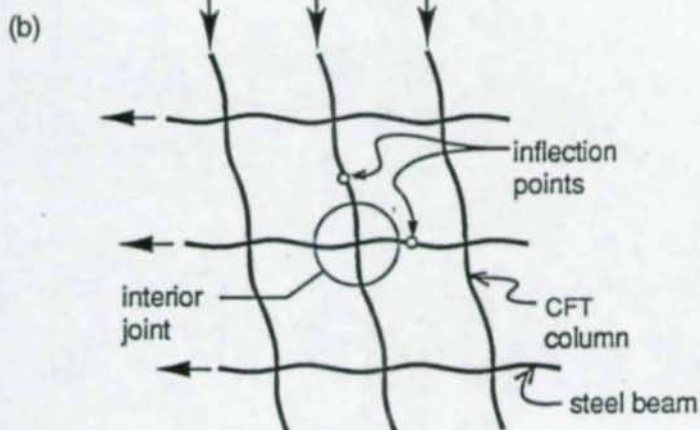
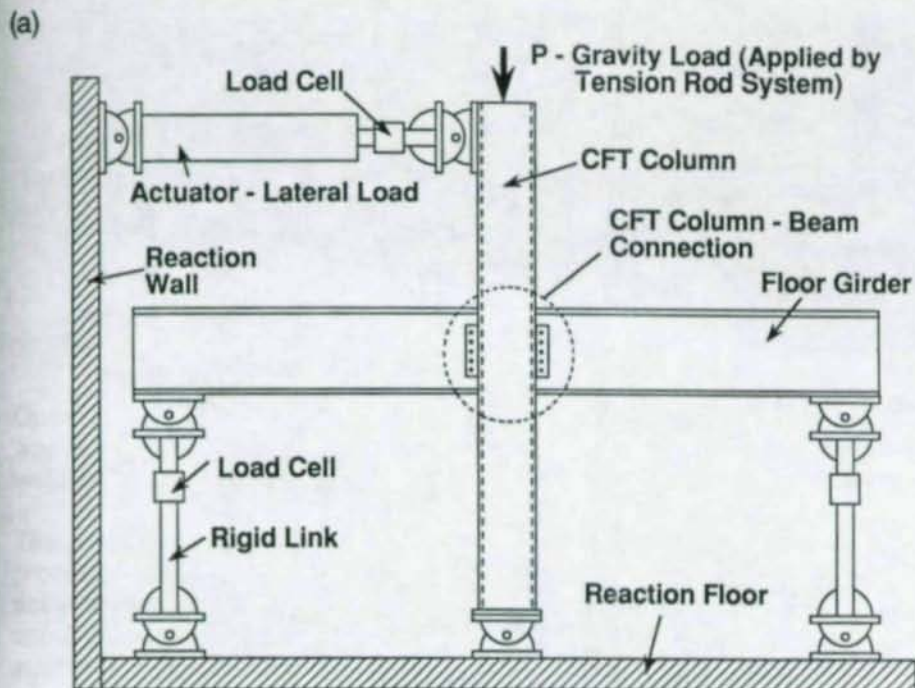


Figure 8 (a) Experimental Structural Subassembly Setup for Cyclic Connection Tests, of (b) Prototype Composite Interior CFT Joint.

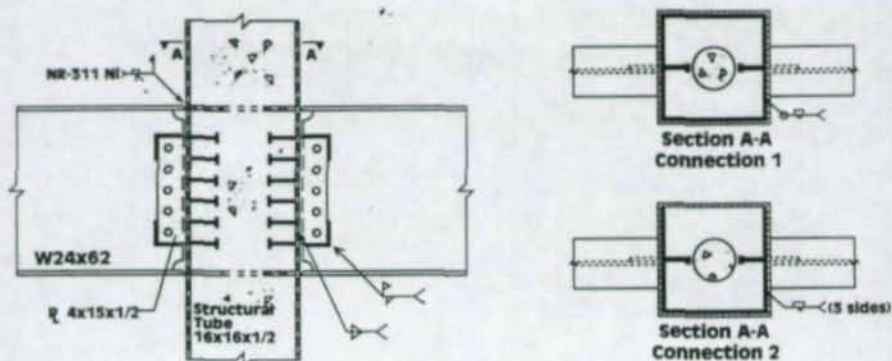


Figure 9 Test Specimen Connection Details - Connections 1 &amp; 2.

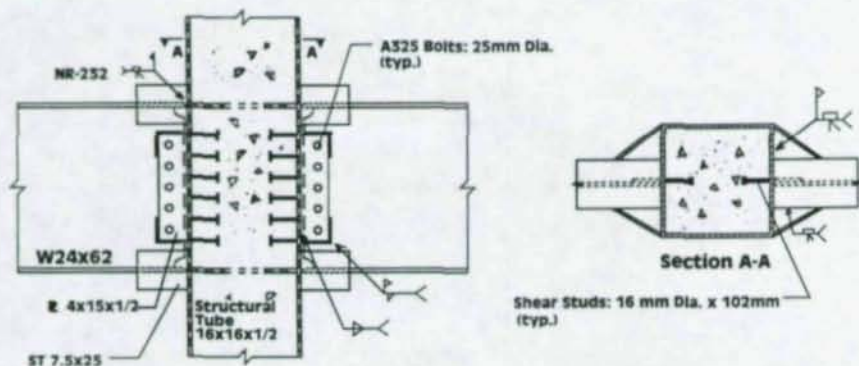


Figure 10 Test Specimen Connection Details - Connection 3.

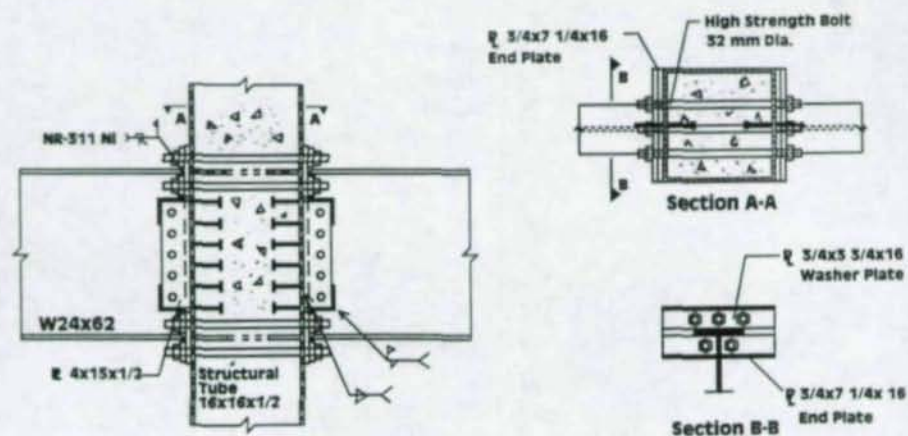


Figure 11 Test Specimen Connection Details - Connection 4.

# FATIGUE BEHAVIOUR OF MIS-MATCHED BUTT WELDED HEAVY I-BEAMS AND THE ROTATION CAPACITY OF JOINTS MADE OF QST-STEEL

Ömer Bucak<sup>1</sup>  
Friedrich Mang<sup>2</sup>  
Lex Stammet<sup>3</sup>

## Abstract

Quenched and self-tempered (QST) rolled steel sections combine in an economical way high yield strength, outstanding toughness at low temperatures and excellent weldability, three properties formerly thought to be incompatible.

The present paper gives in a first part a short description of the QST production process of rolled beams as well as the fabrication properties and test results on full-scale tests on butt welded rolled I-sections. After an analysis of the test results it could be found for the welding of large thickness sections with a minimum yield strength of 460 MPa to use a different type of stick electrodes => mis matching. The second part presents tests on frame work joints, made of high strength QST-steels.

## 1 INTRODUCTION

The tendency of the market demands towards products with greater thickness and higher yield strength, gave the impulse to develop new steels. Furthermore, it is of key importance for safety and economical use to achieve a good toughness at low temperature together with an improved weldability.

Under the conditions of conventional rolling methods it is not attainable to combine great thicknesses with high yield strength. Relatively large additions of alloying elements would be necessary, which decrease weldability and toughness at low temperatures whereas production and fabrication costs would be raised to a hardly competitive level (Fig. 1).

The challenge of producing rolled sections with a high yield strength in an economical way, outstanding toughness at low temperatures and excellent weldability got mastered by the development of a new process, namely the quenching and self-tempering (QST). This process has been brought to industrial maturity in the last years by ARBED on its GREY heavy section mill at Differdange (Luxembourg).

<sup>1</sup> Dr.-Ing., University of Karlsruhe, Kaiserstr. 12, D-76128 Karlsruhe

<sup>2</sup> Prof. Dr.-Ing., University of Karlsruhe, Kaiserstr. 12, D-76128 Karlsruhe

<sup>3</sup> Dipl.-Ing., Arbed Recherches, Esch-sur-Alzette, Luxembourg

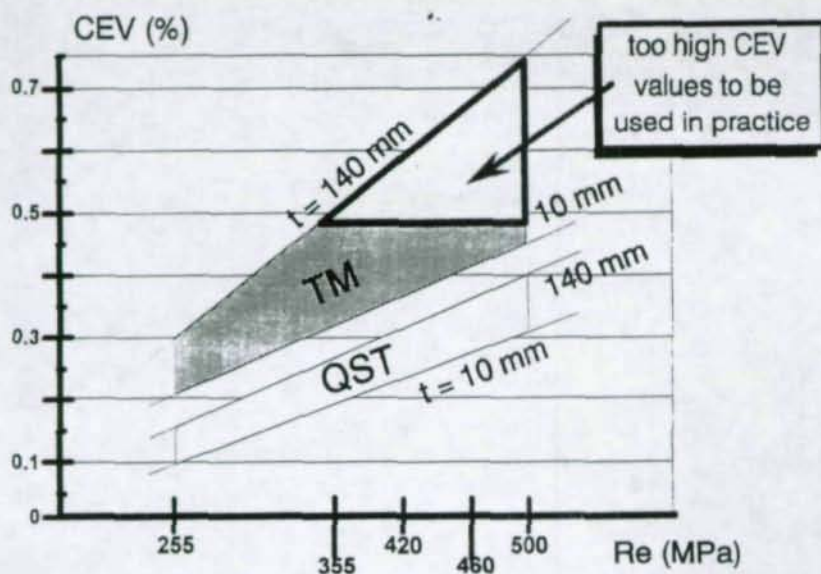


Fig. 1 Chemical Composition of Steel Grades

The QST-technology led to a new generation of high-strength structural shapes with extremely low carbon equivalent values (Fig. 2), combining the above mentioned beneficial properties with a high competitiveness due to reduced production and fabrication costs.

## 2 DESCRIPTION OF THE QST PROCESS

Conventional thermomechanical (TM) rolling has enabled to produce, for a medium range of product thickness and yield strengths, easily weldable steel qualities with good toughness properties at low temperatures.

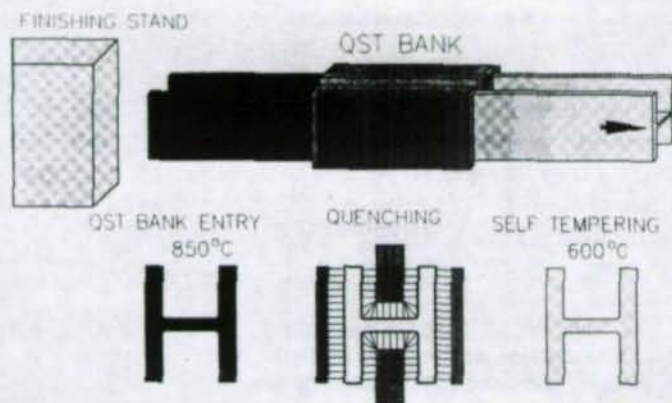


Fig. 2 QST Treatment of Beams

In a QST process, using water and the rolling heat as working substances, an intense water cooling is applied to the whole surface of the section directly after the last rolling pass. Cooling is interrupted before the core is affected by quenching and the outer layers are tempered by the flow of heat from the core of the surface. Fig. 2 illustrates schematically the treatment. At the exit of the finishing stand directly at the entry of the cooling bank temperatures are typically at 850°C. After cooling over the whole surface of the section, a self-tempering temperature of 600°C is achieved.

### 3 MECHANICAL AND TECHNOLOGICAL PROPERTIES OF HISTAR SECTIONS

Fig. 1 summarizes the relationships between chemical composition, product thickness and tensile properties for the conventional TM rolling route and the new combined TM/QST process. Based on this relationship, the new HISTAR proprietary grades have been created. Compared to the conventional TM rolling route the combined TM/QST process offers decisive advantages:

- a substantial reduction of the alloy content of the standard steel grades like FeE 355 ( $R_e \geq 355$  MPa), leading to an important increase of toughness and weldability.
- the possibility for an economical production of heavy rolled sections with a flange thickness up to 140 mm in high-strength steel grades like Fe E 460 ( $R_e \geq 460$  MPa), that could not be obtained until now without a serious drop in toughness and weldability.

The QST treatment lowers considerably the transition temperature from ductile to brittle fracture behaviour. With respect to yield strength and toughness, it is now possible to produce directly in the rolling heat beams with the tensile properties of an Fe E 460 ( $R_e \geq 460$  MPa) in thicknesses up to 140 mm combined with temperatures for a guaranteed CVN-toughness down to -50°C. Fabrication tests have shown that all HISTAR beams can be cold worked under the same conditions as classical material. However, oxycutting of QST beams is much easier, especially for the thicker shapes and higher grades, as it does not need any preheating to avoid cracking.

### 4 WELDABILITY EVALUATION OF HISTAR BEAMS

A major aim of the weldability investigations was to study the influence of the cooling time  $t_{8/5}$  between 800°C and 500°C on HAZ toughness and strength. In order to obtain a wide range of  $t_{8/5}$  times heat input and beam thickness were varied. In order to evaluate their weldability under the above mentioned conditions, QST beams were butt welded with various methods currently used in steel construction. The welds have been performed **without preheating** on shapes up to 125 mm thickness in steel FeE 355 ( $R_e \geq 355$  MPa) and FeE 460 ( $R_e \geq 460$  MPa). The very favourable results have already been reported previously (2), (3), (4) and (10).

In all cases the beam flanges were cut off, grinded and butt welded together. In order to simulate butt welding conditions for beams, strong backs were used for maintaining the cut-off flanges during welding. This method reflects best the heavily restrained situation of the flanges during butt welding. Sampling was always performed at the 1/6 flange width position. This position has been chosen by all major standards and reflects best the average properties of a beam.

An American wide flange section W 14" x 16" x 311 lbs (W 360 x 410 x 463) with a flange thickness of 57 mm was used. The 2 flanges were grinded longitudinally at the 1/6 position. After fixing the strong backs, the assemblies were welded with two different processes using three heat inputs. The first weldment was realized by flux cored arc welding (FCAW) with a welding energy of 0,8 kJ/mm whilst the two other assemblies were welded by submerged arc welding (SAW) with welding energies of 3,5 and 5,0 kJ/mm respectively. Due to the very low CEV of 0,34%, combined with a reduced carbon content of 0,085 % C, **preheating was not necessary** for neither of the three weldments.

- At cross weld tensile tests all ruptures of the specimens occurred outside of the weld area.
- The results of the CVN tests show that toughness at -40°C remains on a very high level in all positions of the weld and no drop of the absorbed energy can be detected.
- The results of the bend tests show a good deformation behaviour of the weld area in all cases.
- For all welding conditions and on both specified positions (coarse grain HAZ and subcritical HAZ) CTOD values are high showing a large margin from the usually required minimum value.

Based on the test results as well as on computer simulations, it is not necessary to preheat HISTAR material in order to prevent a loss of toughness of the HAZ, whereas for the conventional material preheating temperatures can reach 200°C. These charts are valid for the normal range of heat inputs (0.8 to 6.0 kJ/mm), provided that low hydrogen filler metal and auxiliary products are used.

## 5 COMPARATIVE STUDY OF STICK ELECTRODES FOR WELDING GRADE FeE 460 ( $R_e \geq 460$ MPa)

This investigation has been carried out to compare the fatigue behaviour of different welds using 5 electrodes from different producers for butt welding sections with large flange thickness. The results should enable to select the electrode with the best performance for welding grade FeE 460.

American wide flange section W 36" x 16.5" x 439 lbs (W 920 x 420 x 653) with a flange thickness of 62 mm, in grade HISTAR 460 was tested (fig. 3). The chemistry is typically marked by a low CEV value of 0.36%.

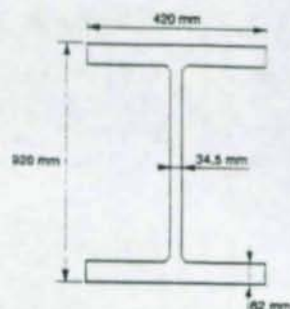
Table 1 below shows the designations of the different electrodes and the welding procedure. The criteria for the selection of the electrodes were:

- yield and tensile strength,

- good impact toughness at low temperature,
- basic electrodes and low hydrogen content,
- commercial availability.

Section Size: W 36 x 16,5 x 439

Metric Weight: 653 kg/m



Chemical Composition (Product Analysis) in Weight %

C	Si	Mn	P	S	Al	Nb	V	Cr	Cu	Ni	Mo	CE
0,103	0,192	1,44	0,029	0,012	0,029	0,046	0,000	0,04	0,08	0,05	0,010	0,36

Tensile- and Impact Test Results

Re (MPa)	Rm (MPa)	A5d (%)	CVN <sub>L</sub> (J)	
			T = -40°C	T = -60°C
529	673	19,6	99	82

Fig. 3 Base Material Histar 460

Table 1

### Welding Electrodes

Electrode	Electrode designation DIN	Re (MPa)	Rm (MPa)	A5d (%)	CVN (J) at -40°C
A	EY 55 54 Mn B H 10 20	600	680	24	50 (-30°C)
B	E 51 55 B 10	470	530	33	120
C	E 51 55 B 10	470-530	570-630	30	60
D	SY42 76 1 Ni B H5	> 460	540-640	> 25	> 100
E	EY 50 75 Mn1 Ni B	> 510	590-690	> 23	> 100

A gap has been cut in the flange to web junction to allow a continuous weld over the whole flange width. The welding has been carried out in the horizontal position, using a welding energy of 1 kJ/mm **without any preheating**.

For each type of electrode, one assembly has been welded. The sample positions and results from chemical analysis, tensile-, impact- and CTOD tests are reported in Fig. 4. The specimens were located at the standard 1/6 flange width position.

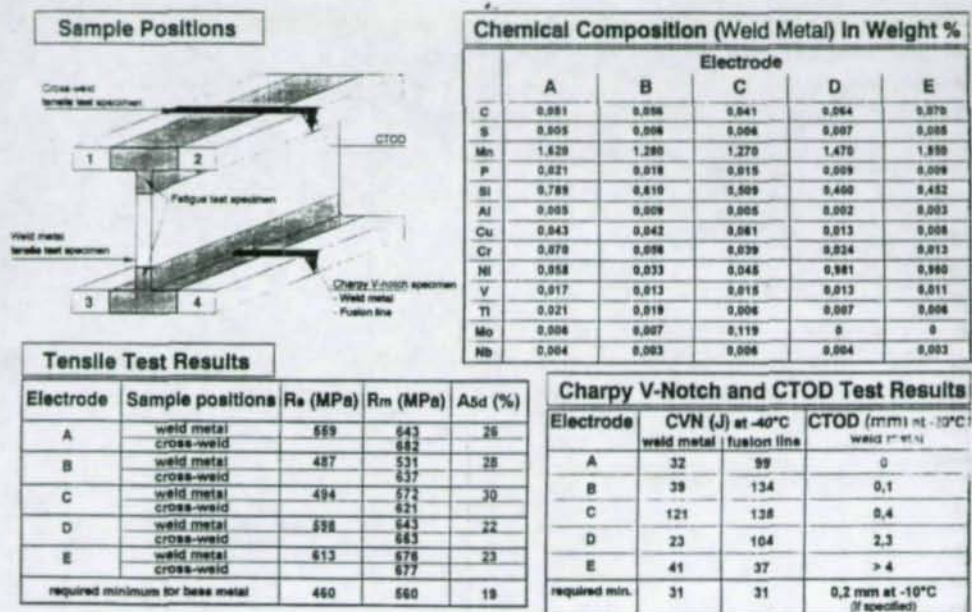


Fig. 4 Weld characterization

The chemical composition showed a 1% nickel content for types D and E and for type C a higher molybdenum content compared to the other electrodes.

In the tensile tests, except for type A, the deposit metals met the properties specified by manufacturers. All assemblies met the minimum yield (460 MPa) and tensile strength (560 MPa) required for the base material. The acceptance criteria in welding procedure qualifications, namely that the actual strength of the cross-weld specimen has to exceed the required minimum strength of the base material, was satisfied in all cases. For types B, C and D the rupture of the cross-weld specimen occurred in the weld metal. The actual tensile strength of the weld metal was generally slightly inferior to that of the base metal.

Impact tests have been performed at the fusion line and in weld metal. All types, except type D, exceeded in both positions the requirement of the base metal of 31 J at -40°C. The specified values by the manufacturers were only achieved by weld metal C.

CTOD tests of the weld metal have been performed in supplement to common requirements. The results of types C, D and E exceeded, if specified, the normally required minimum CTOD value of 0.2 mm at -10°C even at the test temperature of -20°C.

Three point bend fatigue tests have been performed to evaluate the behaviour of the electrodes when fatigue is expected. For all types, the cracking has been initiated in the weld metal. The results of types C, D and E exhibited a fatigue behaviour satisfying the requirement of Eurocode 3 for detail category 112, i.e. minimum of 100 000 loading cycles, whereas types A and B failed to meet these criteria.

### 6 Full-Scale Fatigue Tests

Based on the results described in 5 and in view of economic aspects, the electrode with the designation C has been chosen for the welding of full-scale specimens. The reasons for the experimental investigations on full-scale test specimens are as follows:

- check of the validity of the data determined on the test specimens HE 300 B and HE 400 M of grade Fe 510,
- determination of the crack initiation,
- determination of the crack growth,
- confirmation of the small-scale tests.

For root welding, an electrode with lower strength and for the filling and final runs a more high-strength electrode has been chosen.

The results of the last investigations have been recorded in Fig. 5 and compared with previous tests on the HE 300 B and HE 400 M sections, corresponding to steel grade Fe 510-DD1. A good agreement or a slight improvement of the results from the test specimens of the steel grade QST can be seen.

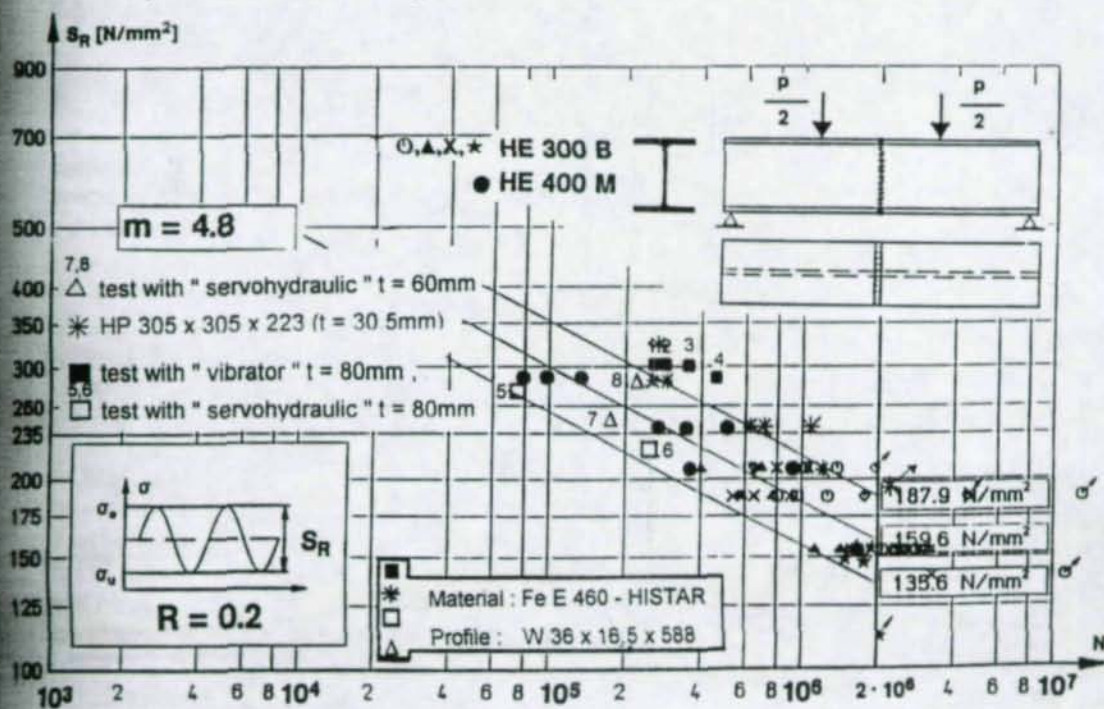


Fig. 5 But Weld Specimens without Holes

The cracks started in the web-flange transition area (fig. 6) and first progressed faster in the web and then into the flange.

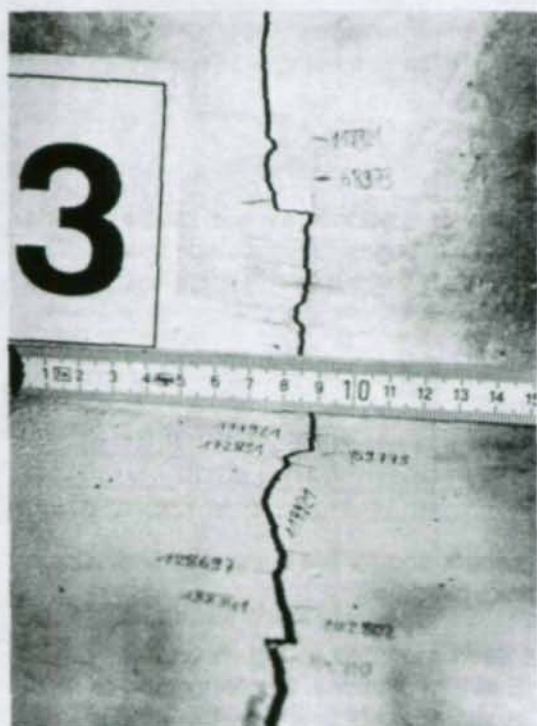


Fig. 6 Fatigue cracks

This type of crack development points at a very high welding residual stress in the neck area of the section since this area has been welded last. Fig. 7 shows the chosen weld preparation. The welding of the hole has been carried out because of the better power flow under load. In investigations on smaller sections (for ex. HE 400 M), the cracks started from the external edge of the flange in tension with the same weld preparation and welding and spread in both directions. It can be seen as very positive that all test specimens showed a very long crack growth behaviour and that it did not result in a brittle failure despite a bigger thickness. The results of the crack surface evaluation will be given at a later time since they are being processed at present.

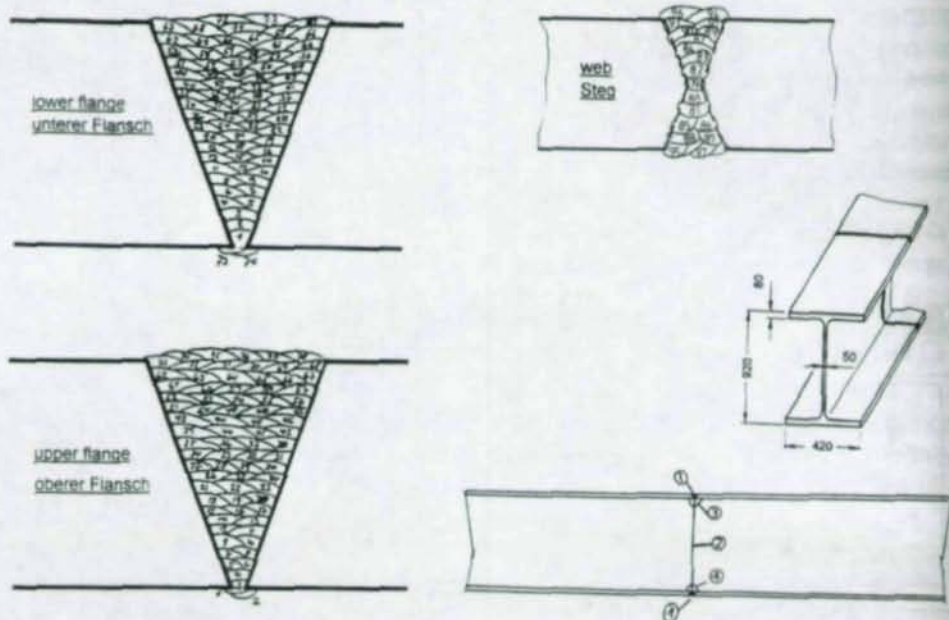


Fig. 7 Weld preparation

Fig. 8 shows the crack propagation rate for thick-walled butt welded I-shapes. The test specimens need a long time from the first visible crack until the end of the test.

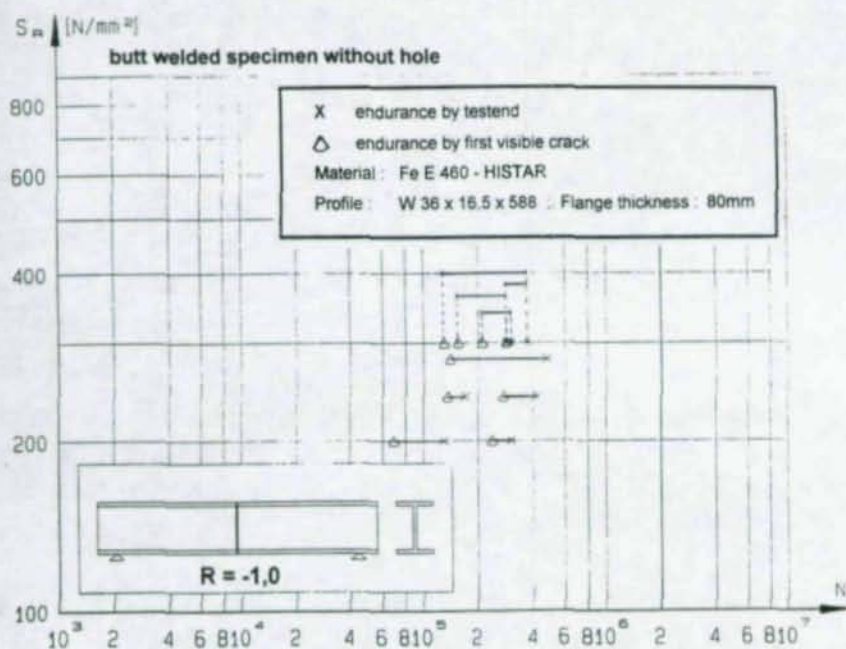


Fig. 8 Crack propagation results on full scale tests

## 7 Future Work on the Fatigue Behaviour of QSt-Quality

Based on the good results determined from the investigations and assessment of the crack initiation point as well as the course of the crack propagation, similar welding with electrodes of a different strength is to be carried out.

As a new proposal, the

Upper flange: layers 1 to 8 and the

Lower flange: layers 60 to 73 and

the slot welding will be carried out with low-strength electrodes (see fig. 7).

In this case, the level of the maximum tensile residual stresses will be able to reach the level of the corresponding value of the strength of the low strength electrodes. Furthermore, the residual stresses will decrease through local plastification under first loading. Since the low-strength electrodes also show a better toughness, this will have a favourable effect on the resistance against crack initiation. New tests will be started in the second half of 1995.

A further demand for investigation is the behaviour of stick electrodes with 1% Ni. It has to be considered that they cost 3 times as much compared to the electrode types investigated here.

In consideration of the fact that the costs for additional materials, e.g. electrodes, normally amount to about 5-10% of the overall costs for such a butt weld, such types of electrodes can be used as well.

A further possibility for a better fatigue life is given by the selection of the welding sequence. In this way, the crack initiation will start later at higher endurance.

## 8 Tests on Framework Joints

For applying higher loads or for large-scale spaces without any inside columns, frameworks and/or Vierendeel girders made of open profiles are used. For this, profiles with a bigger wall thickness and with cramped cross section are applied. Due to the local load application, it is intended to reinforce the joint area. The basic idea starts from the fact that the stiffeners induce the bending moment (separated in couples of forces) into the central web area (ribbing of the joint area) as a continuation of the chords of the web member.

This type of usual stiffening is proved for lightweight and medium weight profiles and has the following series disadvantages for heavy profiles:

- the weld volume of a connection grows quadratically with the plate thickness => a bigger number of welding layers is necessary => the production costs increase,
- the volume of the single welding passes becomes very small with an increasing plate thickness compared to the basic material => hardness increases and possible micro cracks,
- triaxial residual stress conditions occur and may lead to failure also for existing cracks.

These disadvantages can be avoided if so-called lamellated frame joints are produced instead of thick chord stiffeners and a reinforced shear field. Lamellar frame joints are produced by welding relatively thin plates parallel to the profile webs by a thin weld (Fig. 9).

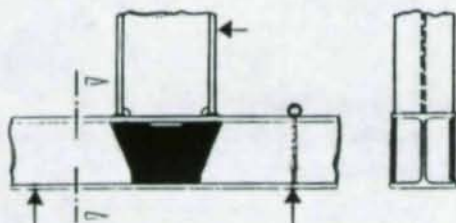


Fig. 9 Lamellated frame joints

In the scope of a building project, such lamellated frame joints have been investigated experimentally at the "Versuchsanstalt für Stahl, Holz und Steine" (Testing Centre for Steel, Timber and Masonry) of the University of Karlsruhe. In parallel, FE calculations have been carried out by Dr. Wippel/Dr. Maier [9].

### Tests on T-joints (for example joints in the middle of a Vierendeel girder)

With this test series, joints of a Vierendeel girder and the rotation capacity of the welded joint are to be investigated.

The joints to be investigated have been composed of profile HE 500 B (chord member) and HE 700 M (vertical member) and have been welded corresponding to their strength (Fe E 460).

For experimental reasons, 2 test specimens have been installed simultaneously into the testing machine (fig. 10), so that a symmetrical experimental set-up was possible. In order to obtain as much information as possible from the tests, one of the joints has been produced **without** stiffeners and tested as reference specimen. With a maximum load of 2350 kN, the first plastic deformations occurred in the joint area, e.g. the whole design area plastified.

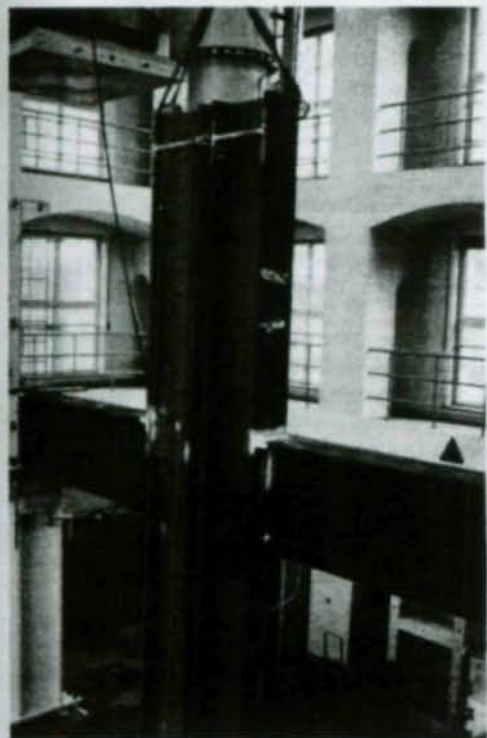


Fig. 10 T-joints made of open profiles in the 50 MN testing machine

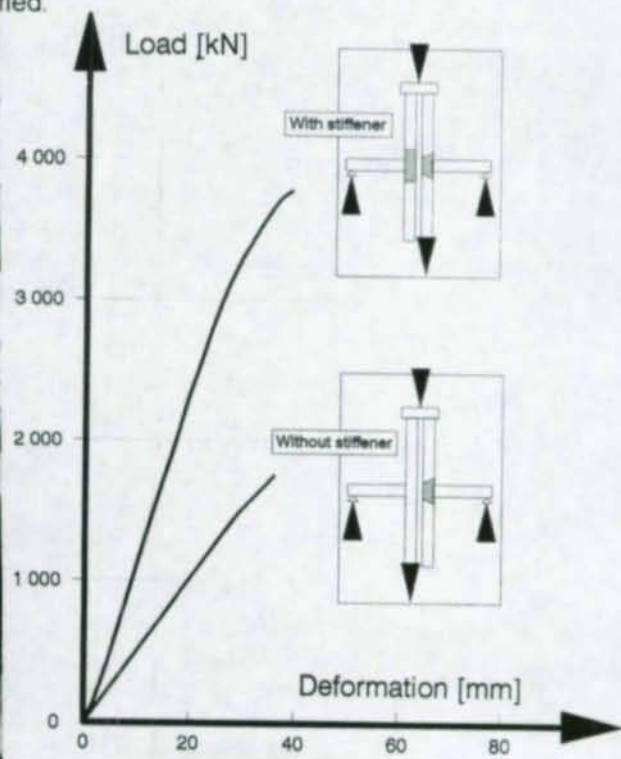


Fig. 11 Comparison of the deformation of the T-joints  
a) without stiffener  
b) with stiffener

After this test, the unstiffened joint was stiffened by welding 20 mm thick rectangular plates. Then the test has been continued. With a load of 3920 kN, a crack in the weld occurred unexpectedly on the additionally stiffened joint. This position has been reinforced again by two 30 mm thick transverse stiffeners and the test has been continued. With a load of 4560 kN, the test has been interrupted, since there were big deformations on the joint area and buckling occurred in the lamellated plates. When achieving the ultimate load, big lateral deformations occurred in the whole joint. The deformation behaviour of the unstiffened and stiffened joint can be taken from Fig. 11.

## 7 FINAL CONCLUSIONS

The Quenching and Self-Tempering (QST) process has resulted in the creation of a new generation of beams with high yield strengths (up to 460 MPa) and excellent toughness properties down to very low temperatures. HISTAR beams are weldable without preheating and offer important advantages in terms of weight savings and fabrication costs, compared to conventionally produced grades. This new development contributes to improve the market position of steel structures in competition with other materials and will help to increase its share in general construction.

To get better fatigue life or resistance against crack initiation, some tests will be done with mis-matched weldments and/or with a modified welding sequence.

## 8 REFERENCES

- (1) "HISTAR Rolled Beams: Product Description", ARBED-Recherches Document, Luxembourg, 1991
- (2) de la Hamette, J.; Panunzi, C.; Rasquin, M.; Becker, F.; Dengler, J.-M.; Wilmotte, S.: QST (HISTAR) Beams a New Generation of High Performance Products", Proceedings of the 3rd Mechanical Working and Steel Processing Conference, Volume XXVII, Cincinnati, OH, 1990, published by ISS of AIME, 1991, pp. 53-59
- (3) Defourny J.M.; D'Hayer, R.; Leroy, V.: "A Metallurgical Approach of the Parameters Affecting the Fracture Behaviour of Base Metal and Welded Components", Doc. IIW-IX-1607-90/X-1206-90
- (4) Dengler, J.M.; Becker, F.; Henrion, R.: "HISTAR: A New Generation of High-Strength Beams with Excellent Weldability", Proceedings of the International Conference on Processing, Microstructure and Properties of Microalloyed and Other Modern High-Strength Low Alloy Steels", Pittsburgh, PA, June 3-6, 1991
- (5) "HISTAR 355 TZ OS: Weldability Evaluation in Accordance with API RP 2Z", ARBED-Recherches Document, Luxembourg, 1992
- (6) Mang, F.; Bucak, Ö.; Klingler, J.; Becker, F.; Henrion, R.; Stammel, A.: "Geschweißte Stumpfstoße an gewalzten H-Trägern", Technica 2/1989
- (7) Becker, F.; Henrion, R.; Stammel, L.; Mang, F.; Bucak, Ö.: "Recherche sur le Comportement en Fatigue de Poutrelles Soudées Bout à Bout", La Revue de Métallurgie - CIT, März 1990
- (8) Wippel, H.; Meier, D.: Investigations into the Design of Haunches for Cube-Cross Main Supporting Frameworks of the ZKM-Karlsruhe (Untersuchungen zur Ausbildung der Rahmenecken bei den würfel-überspannenden Haupttragwerken des ZKM-Karlsruhe, Report, Ingenieurgruppe Bauen, Hübschstr. 21, Karlsruhe
- (9) NN. Tests on specimens (lamellated joints) made of St E 460 (HISTAR), Versuche an Probekörpern (lamellierte Rahmenknoten) aus St E 460 (HISTAR), Test report no. 92-1567, 15.06.92 Research Centre for Steel, Timber and Masonry (unpublished)

# THE STATIC STRENGTH AND BEHAVIOUR OF UNIPLANAR AND MULTIPLANAR CONNECTIONS BETWEEN I-BEAMS AND RHS COLUMNS

L.H. Lu <sup>1</sup>  
J. Wardenier <sup>2</sup>

## Abstract

In this paper, the results of the research work on the static behaviour of semi-rigid connections are presented. The considered connections include uniplanar and multiplanar connections between plates and RHS columns loaded by compression, where a pair of the plates represent the flanges of the I-beams, uniplanar and multiplanar I-beam to RHS column connections loaded by compression or in-plane bending moments. This paper shows the influence of the most important geometrical parameters which determine the connection strength and the influence of the multiplanar loading. Based on analytical models and numerical results, strength formulae for these connections loaded by compression or in-plane bending moments are given.

## 1. INTRODUCTION

Welded connections between I-section beams and RHS columns are attractive for use in offshore deck structures and industrial buildings. However, insufficient information is available for such connections. The existing design formulae, as given by CIDECT design guide (Packer et al, 1992), are based on limited test data for axially tension loaded uniplanar plate to RHS column connections. No multiplanar geometrical and loading effects have been taken into account. This may result in conservative or unsafe strengths for design depending on the geometry and load case. To fill this gap, an extensive experimental and numerical research is being carried out in this project to investigate the static behaviour of these connections and finally to establish

---

<sup>1</sup> Research Engineer, Delft University of Technology, Faculty of Civil Engineering, Steel Structures, Stevinweg 1, 2628 CN Delft, The Netherlands

<sup>2</sup> Professor, Delft University of Technology, Faculty of Civil Engineering, Steel Structures, Stevinweg 1, 2628 CN Delft, The Netherlands

design formulae for such connections.

Experiments have been carried out on multiplanar connections between plates or I-beams and RHS columns in the framework of ECSC project 7210-SA/611 at Delft University of Technology and TNO Building and Construction Research. The connections are multiplanar plate to RHS column connections loaded with compression on the plates and multiplanar I-beam to RHS column connections loaded with axial compression or in-plane bending moments on the I-beams. The composite action of concrete filling of the RHS column and the influence of a steel or a steel-concrete floor has also been investigated as well as the influence of multiplanar loading.

Extensive parametric studies have been carried out using finite element analyses, based on the numerical models which have been calibrated against the performed experiments. A wide range of the most important geometrical parameters of the connections, such as  $\beta$  ( $\beta = b_1/b_0$ ),  $2\gamma$  ( $2\gamma = b_0/t_0$ ),  $\eta$  ( $\eta = h_1/b_0$ ) etc. and the different load cases have been considered. To investigate the multiplanar load effects, each multiplanar connection has been analysed with five load ratios ( $J = -1, -0.5, 0, 0.5, 1$ ), see figure 3.

Further, for each type of connection and loading, analytical models have been developed based on the yield line model. Combining the numerical results and analytical models, strength formulae have been derived. These strength formulae have been based on the ultimate strength or on a defined deformation or rotation limit if the deformation or rotation exceeds a practical value.

## 2. EXPERIMENTAL RESEARCH

The experimental research programme is shown in table 1. Two  $\beta$  values ( $\beta = 0.4, 0.6$ ) and one  $2\gamma$  ( $2\gamma = 30$ ) have been considered. The measured mechanical properties and the actual dimensions of all connection members have been reported by Lu (Lu et al, 1992). A total of twenty tests have been carried out, including 8 multiplanar plate to RHS column connections, 4 multiplanar connections with two levels of plates (I-beam flanges only) and RHS columns loaded with axial compression, 4 multiplanar connections between I-beams and RHS columns loaded by in-plane bending moments with or without a steel floor and 4 bolted multiplanar I-beam to RHS column connections with a composite floor. The influence of the concrete infill in the RHS columns has also been investigated (1R2 and 1R4, 2R2 and 2R4, 4R2 and 4R4). Three load cases ( $J = 0, 1, -1$ ) have been considered to study the multiplanar load effects.

From the experiments it has been found that failure of the connections is mainly related to the chord face yielding. For the axially loaded connections considered, an increase of the  $\beta$  value results in an increase of the stiffness and non-dimensional static strength of the connections. The initial stiffness and strength of the connection can be increased significantly by the structural action of the steel

floor or composite floor or by concrete filling of the RHS columns. Further, a positive load ratio causes an increase of the initial stiffness and the strength compared to that of the connections with  $J = 0$ . A negative load ratio leads to a significant decrease of the initial stiffness and the strength of the connections.

### 3. NUMERICAL RESEARCH

#### 3.1 Calibration Of The Numerical Models

The results of the experiments of series 1 to 3 have been used for calibration of the numerical models. These experiments have been simulated using finite element analyses. Pre- and post processing have been performed by using program IDEAS on SUN SPARC Workstations. The finite element analyses have been carried out with program MARC. The following aspects have been considered in the numerical models:

- Element types
- Modelling of the connections
- Modelling of the welds
- Modelling of the material properties
- Boundary conditions
- Modelling of the concrete filling in the columns

The details of the numerical simulations have been presented by Lu et al (Lu et al, 1993a, 1993b, 1994a). As an example shown in figure 2, a good agreement has been obtained between the numerical results and the experimental results. The finite element analyses are therefore a practical approach for the evaluation and extension of the design procedures for these semi-rigid connections.

#### 3.2 Parameter Studies

To provide more insight into the geometrical and load effects and to establish the design formulae for connections with RHS columns, first, parameter studies have been carried out on welded connections with steel members only.

##### 3.2.1 Research Programme

The numerical research programme is summarized in table 2 to table 4. It includes:

- 18 uniplanar and 12 multiplanar connections between plates and RHS columns loaded by compression
- 15 uniplanar and 11 multiplanar connections between I-beams and RHS columns loaded by compression or in-plane bending moments.

For all connections, the width of the RHS column is  $b_0 = 300$  mm. Six  $\beta$  values ( $\beta = 0.18, 0.3, 0.5, 0.73, 0.87, 0.93$ ), three  $2\gamma$  values ( $2\gamma = 15.8, 25.0, 37.5$ ) and seven  $\eta$  values ( $\eta = 0.3, 0.6, 0.9, 1.0, 1.5, 2.0, 2.5$ ) have been selected. For multiplanar connections, only connections with  $\beta \leq 0.73$  have been investigated, due to the way of the numerical modelling. In addition, to determine the individual influence of the  $\eta$  values on the compression loaded I-beam to RHS column

connections, extra calculations have been performed on uniplanar connections with  $2\gamma = 25$  with six  $\eta$  values, as shown in table 4. To check the multiplanar loading effects on multiplanar connections, each multiplanar connection has been analyzed with five load ratios, namely  $J = -1, -0.5, 0, 0.5, 1$ .

### 3.2.2 Numerical Modelling

The numerical modelling has been done in the same way as used for the calibrations with the experiments (Lu et al, 1993a, 1993b). A typical finite element mesh is shown in figure 1 for multiplanar connections between I-beams and RHS columns. Eight noded thick shell elements (MARC element type 22) have been used for connection modelling. It should be mentioned that throughout the numerical parameter study, butt welds are considered which are stronger than the parent material being connected. Since the nominal size of the fillet part of butt welds is relative small, no weld elements have been modelled in the numerical models. However, the actual weld sizes are general larger than the nominal sizes, which may lead to an increase of the actual connection strength.

In the numerical modelling, steel grade Fe510 with a yield stress of  $355 \text{ N/mm}^2$  is used for all RHS columns. In order to avoid beam failure before connection failure, a steel grade of StE 690 with a yield stress of  $690 \text{ N/mm}^2$  is taken for all I-beams.

During the numerical analyses, displacement control has been used for  $J = 0$  and  $+1$ . For  $J = -1, -0.5$  and  $+0.5$ , load control is used so that a fixed load ratio applied on the connections can be maintained even after plastic deformation.

### 3.2.3 Results Of The FE Analyses

From the post-processing of the numerical modelling, it is found that for the connections with  $\beta < 0.9$ , failure of the connection is caused by chord face yielding, while for connections with  $\beta \geq 0.9$ , chord side wall failure occurs. Typical moment - rotation diagrams for in-plane bending loaded connections are given in figure 3, showing the connection behaviour with  $\beta = 0.5$ ,  $2\gamma = 25.0$  and  $\eta = 1.0$  under five different load ratios. There is almost no difference between the uniplanar connection and the multiplanar connection for a load ratio  $J = 0$ . But a positive load ratio increases the stiffness and the strength of the connections and a negative load ratio causes a decrease of the stiffness and strength of the connections compared to those with  $J = 0$ .

### 3.2.4 Ultimate Deformation Limit

As shown in figure 2, the strength of the connection still increases after large deformations of the connections. No peak loads are obtained. This phenomenon is also obtained for other types of tubular joints. A decision has to be made which strength will be considered as the "ultimate strength" of the connection. A ultimate deformation criterion is thus needed to determine the strength of the connection.

To solve this problem, different types of tubular joints under different loading cases have been studied by Lu et al. Since failure of the connection is mainly related to

plastification of the chord face around the intersection, a local indentation  $3\%b_0$  ( $d_0$ ) of the chord face at the intersection has been chosen as the ultimate deformation limit. This deformation limit is consistent with the experiments where a peak load is found and has been checked for different types of connections with RHS or CHS as chord member. It has been shown that it is an appropriate choice for all tubular connections (Lu et al, 1994b). For bending loaded I-beam to RHS column connections, this deformation limit is chosen at the intersection of the compression flange. However, this deformation limit gives a very large rotation limit for connections with small  $\eta$  ratios. Therefore, for connections with  $\eta \leq 0.6$  the strength is limited at a rotation of 0.1 rad.

#### 4. STRENGTH FORMULAE

The connection strength at a deformation limit of  $3\%b_0$  has been reported by Lu (Lu and Wardenier, 1995a,b,c). To establish strength formulae, analytical models based on the plasticity theory have been used for different types of connections under different load cases. However, especially due to the deformation limit criteria used, the numerically determined connection strengths are in the most cases lower than those according to analytical models, especially for connections with small  $\beta$  values. Thus a modified factor is needed if the yield line model is taken as a basis. For this reason, regression analyses have been carried out using the results of parametric studies to develop the connection strength formulae (Lu and Wardenier, 1995a,b,c). The derived strength formulae are given in table 5 and plotted in figures 4 to 6.

#### 5. LIST OF SYMBOLS

- $b_0$  : width of the RHS columns  
 $b_1$  : width of the plates or the flanges of an I-beam  
 $h_1$  : height of the I-beams  
 $h_m$  :  $h_m = h_1 - t_1$   
 $t_0$  : wall thickness of the RHS columns  
 $t_1$  : thickness of the plates or the flanges of an I-beam  
 $f_{y0}$  : yield stress of the RHS columns  
 $f_{y1}$  : yield stress of the plates or I-beams  
 $f(J)$  : multiplanar load effect function  
 $F_1, F_2$  : vertical loads applied at the ends of the I-beams  
 $J$  : load ratio on multiplanar connections  $J = F_2/F_1$  or  $N_2/N_1$   
 $M_{u,xb}$  : connection strength at a deformation limit of  $3\%b_0$  for uniplanar I-beam to RHS column connection loaded by in-plane bending moments  
 $M_{u,xxb}$  : connection strength at a deformation limit of  $3\%b_0$  for multiplanar I-beam to RHS column connection under in-plane bending moments  
 $N_1, N_2$  : axial compression applied on the plates and I-beams

- $N_{u,xb}$  : connection strength at a deformation limit of  $3\%b_0$  for uniplanar I-beam to RHS column connection loaded by compression  
 $N_{u,xxb}$  : connection strength at a deformation limit of  $3\%b_0$  for multiplanar I-beam to RHS column connection loaded by compression  
 $N_{u,xp}$  : connection strength at a deformation limit of  $3\%b_0$  for uniplanar plate to RHS column connection loaded by compression  
 $N_{u,xxp}$  : connection strength at a deformation limit of  $3\%b_0$  for multiplanar plate to RHS column connection loaded by compression  
 $\beta$  : width ratio between I-beam's flange and RHS column  $b_1/b_0$   
 $2\gamma$  : width to thickness ratio of RHS column  $b_0/t_0$   
 $\eta$  : I-beam depth to RHS column width ratio  $h_1/b_0$   
 $\tau$  : thickness ratio of I-beam's flange and RHS column  $t_1/t_0$   
 RHS : rectangular hollow section  
 CIDECT : Comité International pour le Développement et l'Étude de la Construction Tubulaire  
 ECSC : European Coal and Steel Community

## 6. REFERENCES

- Lu, L.H., Puthli, R.S., Wardenier, J. (1992), "The Static Strength of Multiplanar Connections between I-beams and Rectangular Hollow Section Columns", Stevin report 6.93.17/A1/11.10, TU Delft, The Netherlands.  
 Lu, L.H., Puthli, R.S., Wardenier, J. (1993a), "The Static Behaviour of Semi-Rigid Multiplanar Connections between I-beams and Rectangular Hollow Section Columns", Proc. Third International Offshore and Polar Engineering Conference (ISOPE-93), 1993, Singapore.  
 Lu, L.H., Puthli, R.S., Wardenier, J. (1993b), "Semi-Rigid Connections between Plates and Rectangular Hollow Section Columns", Proc. Tubular Structures V, E&FN SPON, 1993, Nottingham, U.K.  
 Lu, L.H., Puthli, R.S., Wardenier, J. (1994a), "The Static Behaviour of Connections between I-Beams and Composite RHS Columns", Proc. SOSC-94 Beijing Special Offshore Symposium, 1994, Beijing, China  
 Lu, L.H., Winkel, G.D. de, Yu, Y., Wardenier, J. (1994b), "Deformation Limit for the Ultimate Strength of Hollow Section Joints", Proc. The Sixth International Symposium on Tubular Structures, 1994, Melbourne, Australia.  
 Lu, L.H., Wardenier, J. (1995a), "Parametric Study on the Static Strength of Uniplanar and Multiplanar Plate to RHS column Connections", Proc. The 5th International Offshore and Polar Engineering Conference, 1995, The Hague, The Netherlands.  
 Lu, L.H., Wardenier, J. (1995b), "The Static Strength of Uniplanar and Multiplanar Connections between I-beams and RHS Columns Loaded by In-Plane Bending Moments", Proc. The Third International Conference on Steel and Aluminium Structures, 1995, Istanbul, Turkey  
 Lu, L.H., Wardenier, J. (1995c), "The Static Strength of Uniplanar and Multiplanar I-beam to RHS column Connections Loaded by Axial Compression", Proc. the 14th International Conference on Offshore Mechanics and Arctic Engineering,

1995, Copenhagen, Denmark.

Packer, J.A., Wardenier, J., Kurobane, Y., Dutta, D., Yeomans, N. (1992), "Design Guide for Rectangular Hollow Section (RHS) Joints under Predominantly Static Loading", Verlag TÜV Rheinland GmbH, Köln.

Table 1 Experimental research programme for multiplanar plate or I-beam to RHS column connections loaded by compression or in-plane bending moments

series	I						
		1R1 $\beta=0.4$	1R2 $\beta=0.4$	1R3 $\beta=0.57$	1R4 $\beta=0.57$		
		1R5 $\beta=0.4$	1R6 $\beta=0.4$	1R7 $\beta=0.57$	1R8 $\beta=0.57$		
		II					
			2R1 $\beta=0.4$	2R2 $\beta=0.4$	2R3 $\beta=0.57$	2R4 $\beta=0.57$	
			III				
				3R1 $\beta=0.4$	3R2 $\beta=0.4$	3R3 $\beta=0.4$	3R4 $\beta=0.4$
	IV						
		4R1 $\beta=0.4$		4R2 $\beta=0.4$	4R3 $\beta=0.4$	4R4 $\beta=0.4$	

Table 2 Uniplanar and multiplanar plate to RHS column connections loaded with compression

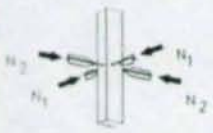
		$2\gamma$		
	$\beta$	15.8	25.0	37.5
	0.18 *	xp13 *	xp14 *	xp15 *
	0.30 *	xp1 *	xp2 *	xp3 *
	0.50 *	xp4 *	xp5 *	xp6 *
	0.73 *	xp7 *	xp8 *	xp9 *
	0.87	xp16	xp17	xp18
	0.93	xp10	xp11	xp12

Table 3 Uniplanar and multiplanar I-beams to RHS column connections loaded by compression or in-plane bending moments

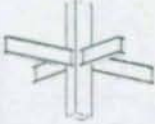
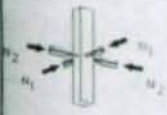
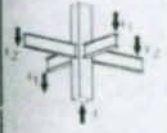
	$\beta$	$2\gamma$			$\eta$
		15.8	25.0	37.5	
	0.18	xb13 *	xb14 *	xb15 *	0.3
	0.30	xb1 *	xb2 *	xb3 *	0.6
	0.50	xb4 *	xb5 *	xb6 *	1.0
	0.73	xb7 *	xb8 *	xb9 *	2.0
	0.87			xb18	0.8
	0.93	xb10	xb11	xb12	0.9

Table 4 The influence of  $\eta$  for axially loaded uniplanar I-beams to RHS column connections

	$\eta=0.3$	$\eta=0.6$	$\eta=1.0$	$\eta=1.5$	$\eta=2.0$	$\eta=2.5$
$\beta=0.18$	xb14a	xb14a-e2	xb14a-e3	xb14a-e4	xb14a-e5	
$\beta=0.50$	xb5a-e1	xb5a-e2	xb5a	xb5a-e4	xb5a-e5	xb5a-e6
$\beta=0.73$	xb8a-e1	xb8a-e2	xb8a-e3		xb8a	xb8a-e6
$\beta=0.93$	xb11a-e1	xb11a-e2		xb11a-e4	xb11a-e5	xb11a-e6

Remark : connection with \* means for both uniplanar and multiplanar

Table 5 Strength formulae for plate to RHS column connections and I-beam to RHS column connections

	Uniplanar connection	Multiplanar connection
	Chord face yielding : $\frac{N_{u,xp}}{f_{y0}t_0} = (0.5 + 0.7\beta) + \frac{4}{\sqrt{1-0.9\beta}}$ Chord side wall failure : $N_{u,xp} = 2(t_1 + 5t_0) f_{y0}t_0$	$N_{u,xxp} = f(J) N_{u,xp}$ $f(J) = 1 \quad J \geq 0$ $f(J) = 1 + J(0.2 + 0.2\beta) \quad J < 0$
	Chord face yielding : $N_{u,xb} = f(\beta, \eta) N_{u,xp}$ For $\eta < 0.5$ : $f(\beta, \eta) = 1 + \frac{\eta}{0.5} (f(\beta, \eta=0.5) - 1)$ For $\eta \geq 0.5$ : $f(\beta, \eta) = \left( \frac{1.25}{1-0.9\beta} + \frac{\eta}{(0.8+2.4\beta)\sqrt{1-0.9\beta}} \right) (1 - (0.9\beta)^2)^*$ Chord side wall failure : $N_{u,xb} = 4(t_1 + 5t_0) f_{y0}t_0 \quad \text{for } h_1 \geq 2t_1 + 5t_0$ $N_{u,xb} = 2(h_1 + 5t_0) f_{y0}t_0 \quad \text{for } h_1 < 2t_1 + 5t_0$	$N_{u,xxb} = f(J) N_{u,xb}$ $f(J) = 1 \quad J \geq 0$ $f(J) = 1 + 0.37J \quad J < 0$
	$M_{u,xb} = N_{u,xp} \cdot h_m$	$M_{u,xxb} = f(J) M_{u,xb}$ $f(J) = 1 \quad J \geq 0$ $f(J) = 1 + J(0.95\beta - 0.6\beta^2) \quad J < 0$

\* This needs further analysis (simplification)

# The Static Strength and Behaviour of Multiplanar I-Beam to Tubular Column Connections loaded with In-plane Bending Moments.

G.D.de Winkel<sup>1</sup>

J. Wardenier<sup>2</sup>

## Abstract

This paper describes recent experimental and numerical research on the behaviour and static strength of multiplanar connections between I-section beams and circular hollow section columns loaded with in-plane bending moments.

Five different ratios between the bending moments on the in-plane and out-of-plane beams are investigated. A parameter investigation has been carried out which covers the most important geometrical parameters. These connections are analyzed using both geometrical and material non-linear finite element analyses. Parametric formulae are made based upon analytical models. The parameters in the formulae are modified with regression analyses, using the finite element results. A good agreement is found between the strength as predicted by the formula and the finite element results.

## 1. TABLE OF SYMBOLS

$\beta$	-	flange width to tubular column diameter ratio
$\eta$	-	beam height to column diameter ratio
$\phi$	-	beam rotation at column face
$2\gamma$	-	wall thickness to tubular column diameter ratio
COV	-	covariance of the errors
$d_0$	-	column diameter
DOF	-	degrees of freedom
$f_{y0}$	-	yield stress of the column material

---

<sup>1</sup> Research engineer, Delft University of Technology, Stevinweg 1, Delft, The Netherlands

<sup>2</sup> Professor, Delft University of Technology, Stevinweg 1, Delft, The Netherlands

- $f_{y1}$  - yield stress of the beam material
- $h_1$  - beam height
- $h_m$  - distance between the mid-planes of the flanges of the beam
- $F$  - F statistic, which gives the overall significance
- $J$  - the ratio between the load on the in-plane and out-of-plane beams
- $M_p$  - full plastic moment (ring model)
- $M_u$  - bending moment in the beam at the column face at the rotation limit or the maximum bending moment in case a maximum moment is found at an rotation that is smaller than the rotation limit.
- $N_u$  - axial load at the deformation limit or the maximum axial load in case a maximum is found at an rotation that is smaller than the rotation limit.
- $r^2$  - correlation coefficient
- $R_1 \dots R_8$  - regression constants
- $t_0$  - wall thickness of the column
- $t_f$  - beam flange thickness

## 2. INTRODUCTION

Semi-rigid connections between I-section beams and circular hollow sections columns can be fabricated in a cost effective manner, if stiffening plates are absent. For design, currently only formulae are available for uniplanar I-beam to CHS column connections (CIDECT, 1993 and AIJ, 1990). These formulae cannot directly be used for multiplanar connections, since there are both geometrical multiplanar effects as well as multiplanar loading effects.

Multiplanar in-plane bending moments on multiplanar I-section to circular hollow section columns may have a considerable influence on the strength and stiffness of the connections (de Winkel, et al 1993b).

This paper gives an overview of recent experimental and numerical research on multiplanar I-beam to tubular column connections. Since this research relates to plate to CHS column connections, also the recent experimental and numerical research on these type of connections is given.

In this paper 24 multiplanar I beam to circular column connections are studied loaded with five different combinations of in-plane bending loading on the in-plane and out-of-plane beams. For the plate to CHS column connections 15 connections are analyzed.

For the finite element calculations both geometrical and material non-linearities are taken into account. The finite element models have been calibrated with experiments.

In previous research (de Winkel, et al, 1994a, 1994b) a regression model has been built on the bases of Togo's ring model (Togo, 1967). With non-linear regression analyses, the regression model has been calibrated with the results of the finite element programs.

### 3. RESEARCH PROGRAMME

#### 3.1. Experimental work

##### 3.1.1. Introduction

Experimental tests have been carried out in the framework of ECSC programme "Semi-rigid I-beam to Tubular Column Connections" (Verheul, et al 1994). Relevant for this paper are 8 tests on plate to CHS column connections loaded with axial loading, 4 tests on I-beam to CHS column connections loaded with in-plane bending moments, and 4 tests on bolted I-beam to CHS column connections comprising a composite steel-concrete floor, loaded with in-plane bending moments. Table 1 shows an overview of the research programme.

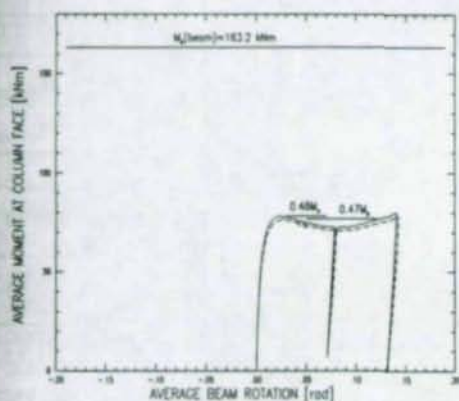


Fig. 1 Experimental M- $\phi$  diagramme for test 3C4

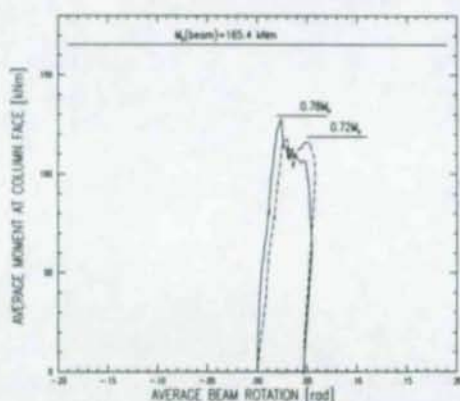
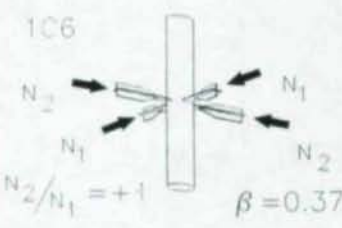
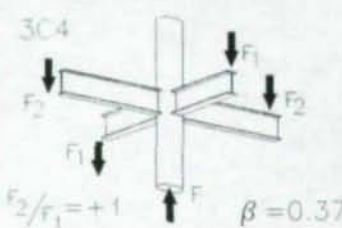
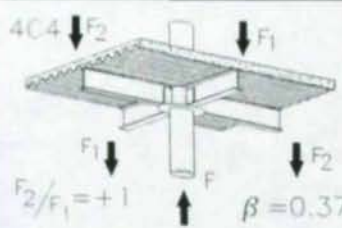


Fig. 2 Experimental M- $\phi$  diagramme for test 4C3

##### 3.1.2. Results experimental work

Table 1 shows the main results of the experimental work. Typical load-deformation curves are shown in Figures 1 and 2. For all experimental tests peak loads were found. As can be seen in Figure 1, a considerable deformation capacity can be achieved. Failure of the connections without concrete infill of the columns and without composite floor is caused by chord face yielding. For test 1C2, where the column has a concrete infill and the test specimen was loaded with a tensile load, a small deformation capacity was found. This specimen failed by punching shear. The failure mode of the specimens with a composite steel-concrete floor failed by progressive failure of the reinforcement bars (see Figure 2). The reinforcement of the floor was a matrix  $\Phi 6-150$  (cold formed) and additional reinforcement at the connection  $8-\Phi 8$  (hot formed). Due to the limited deformation capacity of the cold formed matrix the deformation capacity of these tested composite connections is also limited. At fabrication a hot formed matrix  $\Phi 6-150$  could not be delivered in time. The experimental results are reported in detail by Verheul et al. (1994).

Table 1 Overview experimental test results and comparison with FE results

	TEST	$\beta$	Concrete infill in column	$\frac{N_2}{N_1}$	$N_1$ in Compr. or Tens.	$N_{u,expt}$	$\frac{N_{u,num}}{N_{u,expt}}$
						[kN]	
	1C1	.37	no	0	C	245.3	1.05
	1C2	.37	yes	0	T	510.8	1.06
	1C3	.52	no	0	C	325.0	1.08
	1C4	.52	yes	0	C	670.8	1.12
	1C5	.37	no	-1	C	175.6	1.08
	1C6	.37	no	+1	C	300.8	1.05
	1C7	.52	no	-1	C	220.1	1.07
	1C8	.52	no	+1	C	499.9	1.00
	TEST	$\beta$		$\frac{M_2}{M_1}$		$M_{u,expt}$	$\frac{M_{u,num}}{M_{u,expt}}$
						[kNm]	
	3C1	.37	no	0	ipb	82.5	0.99
	3C2	.37	+ steel floor	0	ipb	87.6	0.98
	3C3	.37	no	-1	ipb	54.1	1.12
	3C4	.37	no	+1	ipb	79.0	1.01
	4C1	.37	no	0	ipb	161.7	N/A
	4C2	.37	yes	0	ipb	178.5	N/A
	4C3	.37	no	+1	ipb	117.8	N/A
	4C4	.37	yes	+1	ipb	133.3	N/A

### 3.2. Numerical work

#### 3.2.1. Introduction

The numerical work consists of two parts. Firstly, finite element models were made using actual measured geometrical and material properties to simulate the experimental tests. These models are calibrated with the experimental tests. Secondly, finite element models are made similar to the calibrated models, but now with nominal dimensions. These models were used for parameter investigations. The

finite element models are generated with the pre- and post processor program SDRC I-DEAS. A typical finite element mesh is shown in Figure 3. For the finite element models parabolic thick shell elements are used with four integration points at Gauss locations in 7 layers across the thickness. For the finite element analyses, including geometrical and numerical non-linearities, the general purpose finite element program MARC K5.2 is used. More details about the modelling are given by de Winkel, et al (1993a, 1993b, 1994a, 1994b).

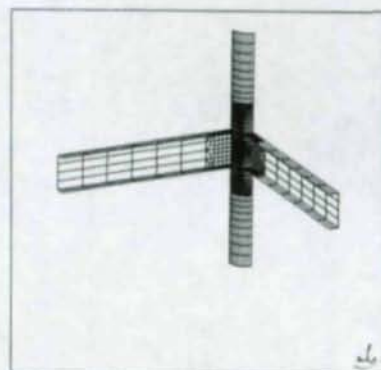


Fig. 3 Typical finite element mesh for a multiplanar XXP4 connection (xxp4-38)

Table 2 Geometrical and material characteristics of the I-beam to CHS column connections

model	$\beta$	$2\gamma$	$\eta$	$r$	$f_{y1}$ [MPa]
xxp4-02	0.25	15	0.50	0.3375	3550
xxp4-04	0.25	30	0.50	0.6750	690
xxp4-06	0.25	45	0.50	1.0125	355
xxp4-07	0.40	15	0.80	0.3600	3550
xxp4-08	0.40	15	0.80	0.5400	3550
xxp4-09	0.40	30	0.80	0.7200	355
xxp4-10	0.40	30	0.80	1.0800	355
xxp4-11	0.40	45	0.80	1.0800	355
xxp4-14	0.65	15	1.30	0.8775	690
xxp4-20	0.25	15	0.25	0.3375	3550
xxp4-22	0.25	30	0.25	0.6750	690
xxp4-24	0.25	45	0.25	1.0125	355
xxp4-25	0.40	15	0.40	0.3600	3550
xxp4-26	0.40	15	0.40	0.5400	3550
xxp4-28	0.40	30	0.40	1.0800	355
xxp4-32	0.65	15	0.65	0.8775	690
xxp4-34	0.65	30	0.65	1.7550	355
xxp4-36	0.65	45	0.65	2.6325	355
xxp4-38	0.55	15	1.10	0.7425	690
xxp4-40	0.55	30	1.10	1.4850	355
xxp4-42	0.55	45	1.10	2.2275	355
xxp4-44	0.55	15	0.55	0.7425	690
xxp4-46	0.55	30	0.55	1.4850	355
xxp4-48	0.55	45	0.55	2.2275	355

Table 3 Geometrical and material characteristics of the plate to CHS column connections

model	$\beta$	$2\gamma$	$r$	$f_{y1}$ [Mpa]
xxp1-02	0.25	15	0.3375	3550
xxp1-04	0.25	30	0.6750	690
xxp1-06	0.25	45	1.0125	690
xxp1-08	0.40	15	0.5400	3550
xxp1-10	0.40	30	1.0800	690
xxp1-12	0.40	45	1.5200	690
xxp1-14	0.65	15	0.8775	690
xxp1-34	0.65	30	1.7550	690
xxp1-36	0.65	45	2.6325	690
xxp1-38	0.55	15	0.7425	690
xxp1-40	0.55	30	1.4850	690
xxp1-42	0.55	45	2.2275	690
xxp1-50	0.60	15	0.8100	690
xxp1-52	0.60	30	1.6100	690
xxp1-54	0.60	45	2.4300	690

Note:

\*: In cases where beam failure would be critical, a higher steel grade for the I-beam was used, to avoid local buckling in the compression flanges. The steel grades used for this purpose is a steel grade with  $f_y = 690 \text{ N/mm}^2$  or an artificial elasto-plastic steel grade with  $f_y = 3550 \text{ N/mm}^2$ . For the columns  $f_{y0} = 355 \text{ N/mm}^2$  and  $d_0 = 300$

mm for all models.

### 3.2.2. Calibration

In general, a good agreement is found between the experimental and the finite element results. The calibration of the finite element models is reported by de Winkel, et al (1993a, 1993b) and summarized in Table 1.

### 3.2.3. Parameter investigation

In the finite element models, to simulate the I-beam to CHS columns connections loaded with in-plane bending, four different  $\beta$  ratios, two different  $\eta$  ratios, three  $2\gamma$  ratios and two  $r$  ratios are used. Combining these parameters gives 48 finite element models. From these models 24 are selected for analyses. The geometrical parameters of the models are listed in Table 2. The column length is taken as six times the column diameter  $d_0$  plus the beam height  $h_1$ . The beam length is five times the beam height. These lengths are sufficient to minimize boundary and load introduction effects. The thicknesses of the flanges are taken either 6% or 9% of the flange width. Only for a few connections the thickness of the flanges is varied. The thickness of the web is 0.6 times the flange thickness.

Similarly, these geometrical parameters are chosen for the plate to CHS column connections (see Table 3).

Each of the models is used to investigate five different load cases, namely  $N_2/N_1$ , respectively  $M_2/M_1 = -1., -0.5, 0, +0.5$  and  $+1.0$ . For the finite element analyses, displacement control is used for  $N_2/N_1$ , respectively  $M_2/M_1 = 0$ , and  $+1.0$ , and load control for the other load cases. Displacement control saves a lot of computer time. However, to preserve a fixed ratio between the bending moments or axial loads on the in-plane and on the out-of-plane beams, only load control can be used.

### 3.2.4. Results and observations

The results of the finite element analyses are listed in Tables 4 and 5. The bending moments and beam rotations are taken at the column face. It is found that negative load ratios always cause a reduction in connection strength, in comparison with the case with unloaded out-of-plane beams. Positive load ratios cause in general an increase in connection strength. In general, this increase is relatively small. For larger  $\beta$  ratios and smaller  $2\gamma$  ratios a stronger multiplanar loading effect is found. In cases without a peak load the maximum load is taken at a deformation limit equal to an indentation of  $3\%d_0$ , which is equivalent to a rotation of  $.06/\eta$  (see also Lu et al. 1994).

## 3.3. Analytical models and results regression analyses

Analytical yield line models for connections between tubular columns and plates or I-beams cannot easily be made. A more simple model, also based on plasticity theory, has been derived for connections between tubular members by Togo

Table 4 Results finite element analyses I-beam to tubular columns loaded with in-plane bending moments

name	$\beta$	$2\gamma$	$\eta$	$r$	$M_u/(t_0^2 f_{y0} h_m)$ for load ratio J				
					-1.	-0.5	0.	0.5	1.0
xhp4-02	0.25	15.	0.50	0.3375	4.256	4.904	5.307	5.414	5.334
xhp4-04	0.25	30.	0.50	0.6750	5.687	6.310	6.497	6.566	6.192
xhp4-06	0.25	45.	0.50	1.0125	6.535	6.668	6.694	6.690	6.495
xhp4-07	0.40	15.	0.80	0.3600	4.654	5.802	7.011	7.705	7.792
xhp4-08	0.40	15.	0.80	0.5400	4.711	5.876	7.121	7.832	7.942
xhp4-09	0.40	30.	0.80	0.7200	6.493	7.669	8.337	8.629	8.141
xhp4-10	0.40	30.	0.80	1.0800	6.660	7.894	8.658	9.003	8.494
xhp4-11	0.40	45.	0.80	1.0800	8.309	9.510	9.921	10.095	9.477
xhp4-14	0.65	15.	1.30	0.8775	5.659	8.043	10.470	12.779	13.499
xhp4-20	0.25	15.	0.25	0.3375	4.369	4.760	4.868	4.884	4.908
xhp4-22	0.25	30.	0.25	0.6750	5.807	6.104	6.133	6.150	6.100
xhp4-24	0.25	45.	0.25	1.0125	6.900	0.455	0.474	0.464	0.353
xhp4-25	0.40	15.	0.40	0.3600	5.309	6.257	6.961	7.155	7.032
xhp4-26	0.40	15.	0.40	0.5400	5.073	5.875	7.082	6.474	7.133
xhp4-28	0.40	30.	0.40	1.0800	7.318	8.335	8.871	9.041	8.391
xhp4-32	0.65	15.	0.65	0.8775	6.966	0.000	10.647	11.594	11.513
xhp4-34	0.65	30.	0.65	1.7550	10.228	12.690	15.279	17.576	18.935
xhp4-36	0.65	45.	0.65	2.6325	13.430	16.626	19.687	22.798	25.641
xhp4-38	0.55	15.	1.10	0.7425	5.198	6.630	8.455	10.022	10.566
xhp4-40	0.55	30.	1.10	1.4850	7.632	9.627	11.754	13.431	13.691
xhp4-42	0.55	45.	1.10	2.2275	9.603	12.228	14.500	16.135	15.924
xhp4-44	0.55	15.	0.55	0.7425	5.971	7.322	8.674	9.352	9.294
xhp4-46	0.55	30.	0.55	1.4850	8.669	10.521	12.172	13.226	12.761
xhp4-48	0.55	45.	0.55	2.2275	11.064	13.415	15.226	15.973	14.951

Table 5 Results finite element analyses plate to tubular column connections, loaded with axial compression loads.

name	$\beta$	$2\gamma$	$r$	$N_u/(t_0^2 f_{y0})$ for load ratio J				
				-1.0	-0.5	0.	0.5	1.0
xhp1-02	0.25	15	0.3375	3.53	4.21	4.72	4.95	5.10
xhp1-04	0.25	30	0.6750	4.16	4.75	5.15	5.47	5.62
xhp1-06	0.25	45	1.0125	4.44	4.98	5.39	5.78	6.06
xhp1-08	0.40	15	0.5400	4.22	5.20	6.32	7.01	7.50
xhp1-10	0.40	30	1.0800	5.10	6.23	7.29	8.13	8.41
xhp1-12	0.40	45	1.6200	5.57	6.80	7.90	8.87	9.37
xhp1-14	0.65	15	0.8775	7.80	9.54	11.66	-	-
xhp1-34	0.65	30	1.7550	8.32	10.24	12.90	16.14	21.49
xhp1-36	0.65	45	2.6325	9.51	11.58	14.46	18.22	28.51
xhp1-38	0.55	15	0.7425	4.98	6.19	7.77	9.08	10.03
xhp1-40	0.55	30	1.4850	6.35	7.86	9.93	12.20	14.20
xhp1-42	0.55	45	2.2275	6.88	8.54	10.92	13.64	15.85
xhp1-50	0.60	15	0.8100	5.45	6.76	8.50	10.03	11.11
xhp1-52	0.60	30	1.6100	6.94	8.55	10.80	13.50	16.75
xhp1-54	0.60	45	2.4300	7.55	9.29	11.77	15.00	19.43

(1967), Mäkeläinen et al (1988), Paál (1987), Van der Vegte (1995) and others. In the literature, this model is known as "ring model". The connection is represented by a two dimensional model in the shape of a ring. The connection characteristics in axial direction of the column are not included in the model, but are defined by a function representing the effective length of the ring. This effective length cannot theoretically be derived, but must be determined, using experimental or finite element analyses results. The 2-dimensional model, with no qualities in axial direction, implies that the beam or brace type, e.g. I-beam, plate or tubular member, has no influence on the definition of the model. The ring model can only be used for axial loaded connections. However, in-plane bending can be simulated by using two ring models at a distance equal to the I-beam height. The exact solution of the ring model for axial loaded X-joints was derived for multiplanar load cases by de Winkel et al. (1994a, 1994b). Based upon the ring model approach, the formula for I-beam to CHS column connections, loaded with in-plane bending moments is derived and shown in Eq. 1. In Eq. 1,  $h_m$  is the distance between the mid-planes of the top and bottom flanges of a I-beam.

$$\frac{M_u d_0}{t_0^2 f_y h_m} = \frac{R_1 \gamma^{R_2 (\beta - R_3 \beta^2)}}{(\sqrt{1-\beta^2} - \beta) + \sqrt{(\sqrt{1-\beta^2} - \beta)^2 + \frac{2}{\gamma^{R_4}}}} \quad (1)$$

Similarly, the formula for plate-to-CHS column connections is derived:

$$\frac{N_u d_0}{t_0^2 f_y} = \frac{R_1 \gamma^{R_2 (\beta - R_3 \beta^2)}}{(\sqrt{1-\beta^2} - \beta) + \sqrt{(\sqrt{1-\beta^2} - \beta)^2 + \frac{2}{\gamma^{R_4}}}} \quad (2)$$

The multiplanar loading effects can be described with the following formula:

$$\frac{N(J)}{N(J=0)} \quad \text{or} \quad \frac{M(J)}{M(J=0)} = 1 + J(R_5 \beta + R_6 \beta^2) + J^2 (R_7 \beta + R_8 \beta^2) \quad (3)$$

For the regression analyses the ultimate loads from the finite element analyses are used.

The results of the regression analyses are listed in Table 6 to 9 and shown in Figure 7. As shown in these Tables, there is a good agreement between the finite element results and the calibrated regression formula.

Table 6 Results of the regression analyses for in-plane bending with load ratio  $J=0$

$R_1$	$R_2$	$R_3$	$R_4$	$r^2$	COV	F	DOF
5.16	1.28	1.64	1.0	0.99	0.037	581	21

Table 7 Results of the regression analyses for multiplanar in-plane bending

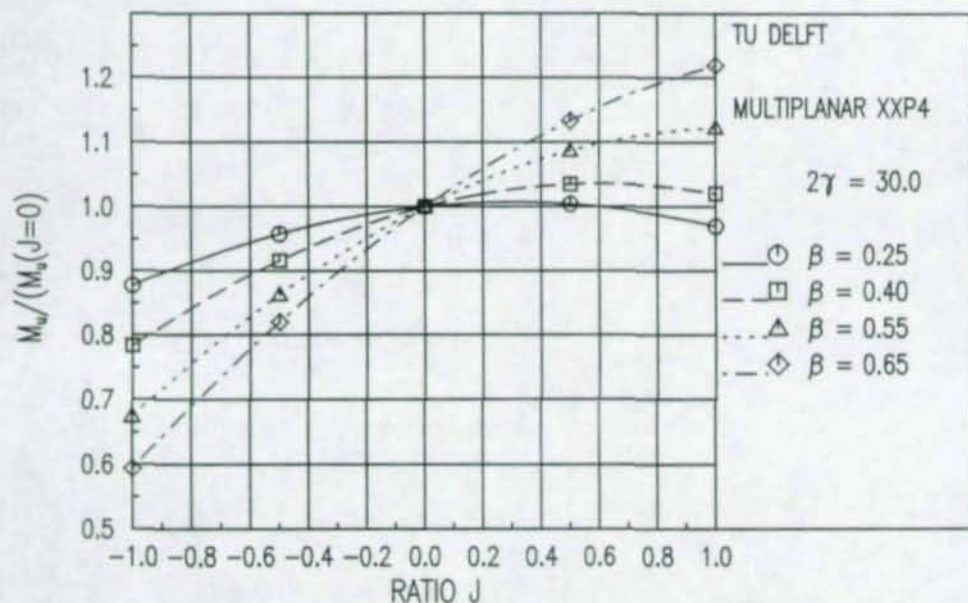
$R_5$	$R_6$	$R_7$	$R_8$	$r^2$	COV	F	DOF
0.	.74	-.41	$-R_7$	.88	0.056	422	117

Table 8 Results of the regression analyses for axial loading with load ratio  $J=0$ 

$R_1$	$R_2$	$R_3$	$R_4$	$r^2$	COV	F	DOF
6.01	0.66	1.0	1.0	.99	.03	734	11

Table 9 Results of the regression analyses for multiplanar axial loading

$R_5$	$R_6$	$R_7$	$R_8$	$r^2$	COV	F	DOF
0.46	$R_5$	$-R_5$	1.	.94	0.047	1051	68

Fig.4 Results regression analyses multiplanar in-plane bending for  $2\gamma = 30$

#### 4. CONCLUSIONS

- Both I-beam to CHS column connections loaded with in-plane bending moments and plate to CHS column connections loaded with axial loading show similar behaviour:
  - \* Larger  $\beta$  ratios and larger  $2\gamma$  ratios give a larger non-dimensionalized strength.
  - \* Negative load ratios can give a considerable reduction in connection strength in comparison with uniplanar loaded connections.
  - \* In general, positive load ratios give higher strengths in comparison with uniplanar loaded connections. For axial loading is this effect stronger than for in-plane bending.
  - \* Both connection types show large deformation capacity.
  - \* Concrete filled columns increase the connection strength, but results in a considerable decrease in deformation capacity.
- The derived formulae based on the ring model approach for multiplanar connections between I-section beams and tubular columns, loaded with multiplanar in-plane bending and for the connections between plate to CHS column connections loaded with axial load show a good agreement with the finite element results.

#### REFERENCES

- AIJ (1990), "Recommendations for the design and fabrication of tubular structures in steel", Architectural Institute of Japan, Japan (in Japanese).
- Lu, L.H., Winkel, G.D. de, Wardenier, J. and Yu, Y. (1994), "Ultimate Deformation Limits for Tubular Joints", Proc. Sixth International Symposium on Tubular Structures, Melbourne, Australia.
- Mäkeläinen P.K., Puthli R.S., Bijlaard F.S.K., Strength (1988), "Stiffness and Non-Linear Behaviour of Simple (Multi-Braced) Welded Tubular Joints." T.N.O. Report BI-87-72/63.6.1098.
- Paul, J.C. (1987), "The Static Strength of Tubular Multiplanar Double T-Joints", Thesis report, RKER.88.076, KSEPL, Rijswijk, The Netherlands.
- Togo, T. (1967), "Experimental Study on Mechanical Behaviour of Tubular Joints", Doctoral Dissertation, Osaka University, Japan (in Japanese).
- Vegte, G.J. van der (1995), "The Static Strength of Uniplanar and Multiplanar Tubular T- and X-Joints", Doctoral Dissertation, Delft University of Technology, The Netherlands.
- Verheul, A., Frater, G.S., Rink, H.D., Lu, L.H., Winkel, G.D. de, Puthli, R.S., Wardenier, J., Koning, C.H.M. de, Foeken, R.J. van (1994), "Semi-rigid Connections between I-beams and Tubular Columns. Draft Final Report 7210-SA/611 (F6.6/90).", Delft Univ. of Technology Stevin Lab. Steelstructures., Delft, The Netherlands.
- Wardenier, J., Kurobane, Y., Packer, J.A., Dutta, D. Yeomans, N. (1991), "Design Guide for Circular Hollow Section (CHS) joints under

- predominantly static loading", CIDECT, Köln, Germany.
- Winkel, G.D. de, Rink, H.D., Puthli, R.S., Wardenier, J. (1993a), The Behaviour and Static Strength of Plate to Circular Column Connections under Multiplanar Axial Loadings, Proceedings of the Fifth Int. Symposium Nottingham UK 25-27 August 1993, Tubular Structures V p. 703-711, England, Nottingham.
- Winkel, G.D. de, Rink, H.D., Puthli, R.S., Wardenier, J. (1993b), The Behaviour and the Static Strength of Unstiffened I-Beam Circular Column Connections Under Multiplanar In-Plane Bending Moments., Proceedings ISOPE Third International Offshore and Polar Engineering Conference, Vol. IV, Singapore 6-11, June 1993., Singapore, p. 167/174.
- Winkel, G.D. de, Rink, H.D., Puthli, R.S., Wardenier, J. (1994a), "The Static Strength of Uniplanar and Multiplanar I-Beam to Tubular Column Connections Loaded with In-plane Bending Moments", Proc. Fourth (1994) International Offshore and Polar Engineering Conference (ISOPE) in Osaka, Japan.
- Winkel, G.D. de, and Wardenier, J. (1994b), Parametric Study on the static Behaviour of I-beam to Tubular Column Connections under In-plane Bending Moments., Proceedings Sixth Int. Symp. Melbourne Australia 14-16 dec.1994. Tubular Structures VI p. 317-324., Australia, Melbourne.

Technical Papers on

**DESIGN METHODS**

## DESIGN METHODS FOR TRUSS AND BRACING CONNECTIONS

W. A. Thornton<sup>1</sup>

### Abstract

A recently developed method for the design of orthogonal bracing connections is presented and then generalized to non-orthogonal connections such as occur in trusses. The method has been checked against existing physical tests and found to be safe. The method produces cost effective designs.

### 1. INTRODUCTION - THE UNIFORM FORCE METHOD

Bracing connections constitute an area in which there has been much disagreement concerning a proper method of design. Beginning about 15 years ago, the American Institute of Steel Construction began to address this problem with a research program at the University of Arizona. This program resulted in published work by Richard (1986) which contained figures similar to Fig. 1. In this figure, the resultant forces on the gusset edges for a wide variety of gusset edge support conditions are seen to fall within the envelopes shown. The edge resultants appear to intersect with the line of action of the brace at a point on this line on the other side of the working point (WP) from the gusset. Note that no couples were required in Fig. 1. This information from Richard is the genesis of the author's development of what has come to be called the Uniform Force Method (Thornton 1991, 1992 and AISC 1992, 1994). The method is shown in Fig. 2. This figure shows a force distribution which captures the essence of the distributions given "fuzzily" in Fig. 1. In other words, a force structure is imposed on Richard's data. In order to test the efficacy of this structure, the data of six full scale tests were filtered through it. The tests were performed by Chakrabarti and Bjorhovde, (1983, 1985) and Gross and Cheok (1988, 1990). Typical test specimens are shown in Figs. 3 and 4. The limit states considered in the filtering process are given in Tables 1 and 2. Table 3 shows the results. For the Chakrabarti/Bjorhovde tests, excellent agreement is achieved. The ratio of test capacity to predicted capacity is close to but slightly larger than unity as is desired. The agreement for the Gross/Cheok tests is not as good, but the method is clearly conservative. The reason for the poorer agreement in this second series of tests is due to frame action. The tests include it but the Uniform Force Method

<sup>1</sup> Chief Engineer, Cives Steel Company, Roswell, Georgia, U.S.A.

does not. Perhaps frame action can be included in some future design method, but for the present, the data available indicate that its neglect is conservative.

## 2. GENERALIZATION TO NON-ORTHOGONAL CONNECTIONS

The Uniform Force Method (UFM) can be applied to trusses as well as to bracing connections. After all, a vertical bracing system is just a truss. But bracing systems generally involve orthogonal members whereas trusses, especially roof trusses, often have a sloping top chord. In order to handle this situation, the UFM has been generalized as shown in Fig. 5 to include non-orthogonal members. As before,  $\alpha$  and  $\beta$  locate the centroids of the gusset edge connections and must satisfy the constraint shown in the box on Fig. 5. This can always be arranged when designing a connection, but in checking a given connection designed by some other method, the constraint may not be satisfied. The result is gusset edge couples which must be considered in the design.

## 3. AN EXAMPLE

The design example is shown in Fig. 6, which also shows the final design.

The geometry of Fig. 6 is arrived at by trial and error. First, the brace to gusset connection is designed and this establishes the minimum size of gusset. Normally, the gusset is squared off as shown by the broken lines in Fig. 6, which gives about 16 rows of bolts in the gusset to truss vertical connection. The gusset to top chord connection is pretty well constrained by geometry to be about 70 inches long plus about  $13\frac{1}{2}$  inches for the cutout. Starting from the broken line configuration of Fig. 6, the UFM forces are calculated from the formulas of Fig. 5 and the design is checked. Although the gusset to top chord connection cannot be reduced in length because of geometry, the gusset to truss vertical is subject to no such restraint. Therefore, the number of rows of bolts in the gusset to truss vertical is sequentially reduced until failure occurs. The last achieved successful design is the final design as shown in Fig. 6.

The calculations for Fig. 6 are performed in the following manner. The given data are:

$$P = 611 \text{ kips}$$

$$e_B = 7 \text{ in.}$$

$$e_C = 7 \text{ in.}$$

$$\gamma = 17.7^\circ$$

$$\theta = 36.7^\circ$$

The relationship between  $\alpha$  and  $\beta$  is

$$\alpha - \beta (.9527 \times .7454 - .3040) = 7(.7454 - .3191) - 7/.9527$$

$$\alpha - .4061 \beta = 4.3634$$

This relationship must be satisfied for there to be no couples on the gusset edges. For the configuration of Fig. 6, with 7 rows of bolts in the gusset to truss vertical connection (which is considered the gusset to beam connection of Fig. 5)  $\alpha = 18.0$  inches. Then,

$$\beta = (18 + 4.3634)/.4061 = 55.1 \text{ in.}$$

From Fig. 6, the centroid of the gusset to top chord (which is the gusset to column connection of Fig. 5) is  $\bar{\beta} = 13.5 + 70/2 = 48.5$  in. Since  $\bar{\beta} \neq \beta$ , there will be a couple on this edge unless the gusset geometry is adjusted to make  $\bar{\beta} = \beta = 55.1$ . In this case, we will leave the gusset geometry unchanged and work with the couple on gusset to top chord interface.

Rather than choosing  $\alpha = 18.0$  in., we could have chosen  $\beta = 48.5$  and solved for  $\bar{\alpha} \neq \alpha$ . In this case, a couple will be required on the gusset to truss vertical interface unless gusset geometry is changed to make  $\bar{\alpha} = \alpha$ .

Of the two possible choices, the first is the better one because the rigidity of the gusset to top chord interface is much greater than that of the gusset to truss vertical interface. This is so because the gusset is direct welded to the center of the top chord flange and is backed up by the chord web, whereas the gusset to truss vertical involves a flexible end plate and the bending flexibility of the truss vertical flange. Thus, any couple required to put the gusset in equilibrium will tend to migrate to the stiffer gusset to top chord interface.

With  $\alpha = 18.0$ ,  $\beta = 55.1$ ,

$$r = [(18.0 + 7 \times .3191 + 55.1 \times .3040 + 7/.9527)^2 + (7 + 55.1 \times .9527)^2]^{1/2} = 74.2 \text{ in.}$$

and from the equations of Fig. 1

$$V_c = 432 \text{ kips}$$

$$H_c = 198 \text{ kips}$$

$$V_B = 57.7 \text{ kips}$$

$$H_B = 167 \text{ kips}$$

For subsequent calculations, it is necessary to convert the gusset to top chord forces to normal and tangential forces as follows: The tangential or shearing component is

$$T_c = V_c \cos \gamma + H_c \sin \gamma = (\beta + e_c \tan \gamma) \frac{P}{r}$$

The normal or axial component is

$$N_c = H_c \cos \gamma - V_c \sin \gamma = \frac{e_c P}{r}$$

The couple on the gusset to top chord interface is then

$$M_c = N_c (\beta - \bar{\beta})$$

Thus

$$T_c = (55.1 + 7 \times 3191) \frac{611}{74.2} = 472^k$$

$$N_c = 7 \times \frac{611}{74.2} = 57.7^k$$

$$M_c = 57.7 \times (55.1 - 48.5) = 381^k\text{-in.}$$

Each of the connection interfaces, i.e. gusset to top chord, gusset to truss vertical, and truss vertical to top chord, can now be designed, because all of the interface forces are known. The limit states to be considered for each interface are similar to those shown in Table 2. Space does not permit the detailed calculations for these limit states to be shown here, but the interested reader can find the complete calculations for this problem in Thornton (1993) or for similar problems in AISC (1992) and AISC (1994). Fig. 6 shows the completed design.

#### REFERENCES

1. American Institute of Steel Construction, 1992, **Manual of Steel Construction, Vol. II, Connections**, ASD 9th Ed/LRFD 1st Ed, pages 7-105 through 7-170.
2. American Institute of Steel Construction, 1994, **Manual of Steel Construction, Vol. II, Connections**, LRFD 2nd Ed., pages 11-17 through 11-48.
3. Bjorhovde, Reidar, and Chakrabarti, S.K., 1985, "Tests of Full Size Gusset Plate Connections," **Journal of Structural Engineering, ASCE**, Vol. 111, No. 3, March, pp. 667-684.
4. Chakrabarti, Sekhar, K., and Bjorhovde, Reidar, "Tests of Gusset Plate Connections," 1983, Department of Civil Engineering and Engineering Mechanics, University of Arizona, Tucson.
5. Gross, John, and Cheek, Geraldine, 1988, "Experimental Study of Gusseted Connections for Laterally Braced Steel Buildings," National Institute of Standards and Technology Report, NISTIR 89-3849, Gaithersburg, Maryland, November.
6. Gross, John L., "Experimental Study of Gusseted Connections," 1990, **AISC Engineering Journal**, 3rd Quarter, Vol. 7, No. 3, pp. 89-97.

7. Richard, Ralph M., 1986, "Analysis of Large Bracing Connection Designs for Heavy Construction," Proceedings of the AISC National Engineering Conference, Nashville, TN, June, pp. 31-1 through 31-24.
8. Thornton, W.A., 1991, "On the Analysis and Design of Bracing Connections," Proceedings of the AISC National Steel Construction Conference, Washington, D.C., June, pp. 26-1 through 26-33.
9. Thornton, W.A., 1992, "Design for Cost Efficient Fabrication and Construction," **Constructional Steel Design - An International Guide**, Edited by Dowling, Harding, and Bjorhovde, Elsevier Applied Science, London and New York, pp. 845-854.
10. Thornton, W.A., 1993, "Application of the Uniform Force Method to Non-Orthogonal Trusses," in Design of Steel Buildings, a short course offered by Georgia Institute of Technology, Atlanta, Georgia, October 14-15, Section 3, pp. 70-85. (Available from the author.)

Table 1, Limit State Identification for Bracing Connections

<u>Limit State Type</u>	<u>Limit State Number</u>
Bolt Shear Fracture	1
Bolt Shear/Tension Fracture	2
Whitmore Yield	3
Whitmore Buckling	4
Tearout Fracture	5
Bearing	6
Gross Section Yield	7
Net Section Fracture	8
Fillet Weld Fracture	9
Beam Web Yield (beyond k distance)	10
Bending (including Prying Action) Yield	11
Bending (including Prying Action) Fracture	12

Table 2, Limit States Considered for Each Interface of Bracing Connections

<u>Connection Interface</u>	<u>Connection Element</u>	<u>Limit States</u>
Brace to Gusset (A)	Bolts to Gusset	1
	Gusset	3,4,5,6
	Bolts to Brace	1
	Brace	5,6,7,8
	Splice plates or WT's	5,6,7,8
Gusset to Beam (B)	Gusset	7
	Fillet Weld	9
	Beam Web	10
Gusset to Column (C)	Bolts to Gusset	1
	Fillet Weld to Gusset	9
	Gusset	6,7,8
	Bolts to Column	2
	Clip Angles	6, 7, 8, 11, 12
	Column	6, 11, 12
Beam to Column (D)	Bolts to Beam Web	1
	Fillet Weld to Beam Web	9
	Beam Web	6, 7, 8
	Bolts to Column	2
	Clip Angles	6,7,8,11,12
	Column	6,11,12

<sup>(1)</sup> See Fig. 3 for Interface Identification

Table 3 Comparison of Uniform Force Method Predicted Results with Test Results

Test Specimen	Predicted Results					Test Results		Test Capacity + Predicted Capacity	
	Brace to Gusset A (kips)	Gusset to Beam B (kips)	Gusset to Column C (kips)	Beam to Column D (kips)	Predicted Capacity (kips)	Predicted Failure Interface	Test Capacity (Kips)		Test Failure Interface
Chakrabarti/Bjorhovde 30°	142 (3,5) <sup>(1)</sup>	184 (7)	216 (5)	152 (12)	142 (3,5)	A (3,5)	143	A (5)	1.01
Chakrabarti/Bjorhovde 45°	142 (3,5)	182 (7)	164 (5)	210 (12)	142 (3,5)	A (3,5)	148	A (5)	1.04
Chakrabarti/Bjorhovde 60°	142 (3,5)	169 (7)	155 (5)	342 (12)	142 (3,5)	A (3,5)	158	C (5)	1.11
Gross/Cheek No. 1	73 (4)	212 (7)	67 (12)	149 (9)	67 (12)	C (12)	116	A (4)	1.73
Gross/Cheek No. 2	78 (4)	77 (7)	143 (7)	NL <sup>(2)</sup>	77 (7)	B (7)	138	A (4)	1.79
Gross/Cheek No. 3	84 (4)	94 (7)	171 (7)	NL <sup>(2)</sup>	84 (4)	A (4)	125	A (5)	1.49

(1) Limit state number from Table 1, typical

(2) NL = No Limit: this part of connection does not carry any of brace load P.

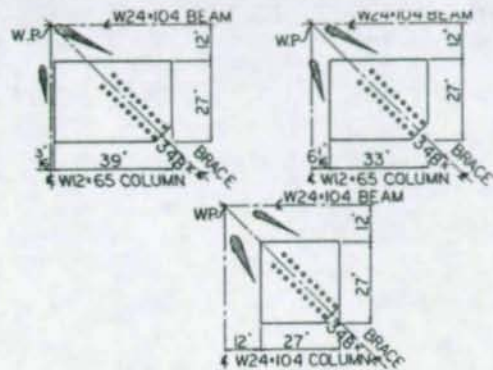


FIG. 1 GUSSET EDGE FORCE RESULTANT ENVELOPES  
45° WORKING POINT MODELS  
(Adapted From Richard, 1986)

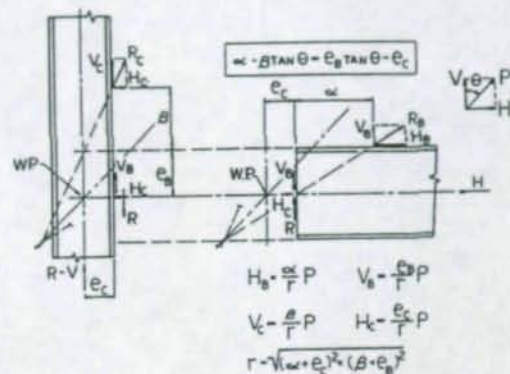


FIG. 2B FORCE DISTRIBUTIONS FOR THE  
UNIFORM FORCE METHOD

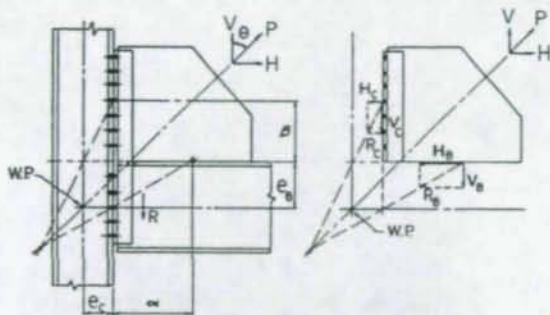


FIG. 2A THE UNIFORM FORCE METHOD

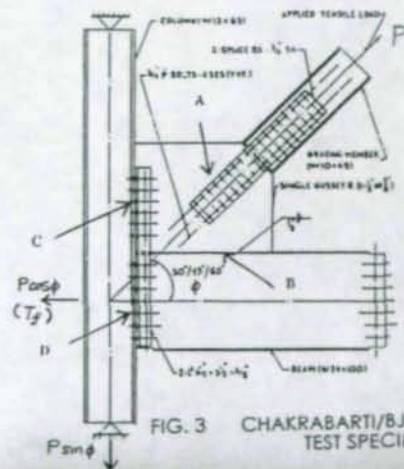


FIG. 3 CHAKRABARTI/BJORHOVDE  
TEST SPECIMEN

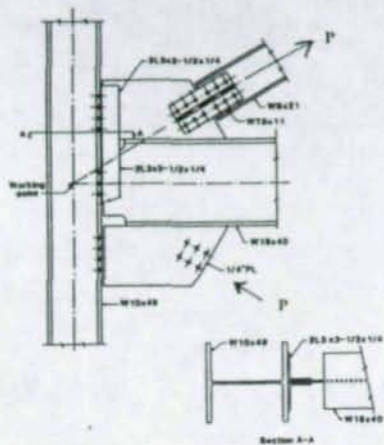


FIG. 4  
GROSS/CHEEK  
TEST SPECIMEN NO. 1

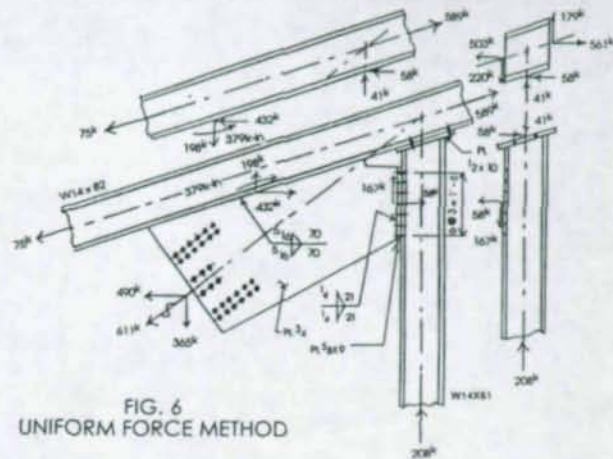


FIG. 6  
UNIFORM FORCE METHOD

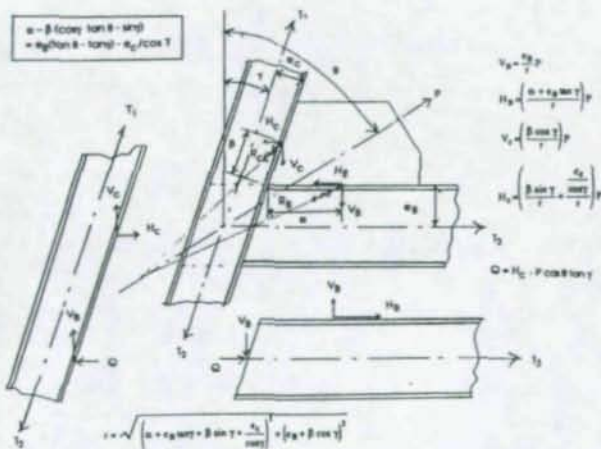


FIG. 5 GENERALIZED UNIFORM FORCE METHOD

## STEEL MOMENT CONNECTIONS ACCORDING TO EUROCODE 3

### Simple design aids for rigid and semi-rigid joints

by J.P. JASPART

on behalf of the RA 351 SPRINT Partners.

#### Abstract

In this paper, simplified design procedures for structural joints in building frames are presented. These ones can be used either to obtain the mechanical properties of a given joint or to select a joint so as to comply with expected mechanical properties. They have been prepared so to be in full agreement with the new revised Annex J of Eurocode 3 (*Revised Annex J, 1994*) in the frame of the european RA 351 SPRINT project involving CRIF (J. JANSSE as Coordinator) and the University of Liège (R. MAQUOI, J.P. JASPART) in Belgium, CTICM (B. CHABROLIN, Y. RYAN, A. SOUA) and ENSAIS Strasbourg (A. COLSON) in France, the University of Trento (R. ZANDONINI, O. BURSI) in Italy and LABEIN Bilbao (W. AZPIAZU) in Spain.

### 1. INTRODUCTION

The design of a building frame for economy requires a good knowledge of the response of the constitutive structural joints in terms of flexural stiffness and resistance. In this respect, the freedom for the designer to select the most convenient joint for design, fabrication or erection is quite important. Such a freedom is offered by the new revised Annex J of Eurocode 3 on "Joints in Building Frames".

Through the so-called "component method" [(JASPART and MAQUOI, 1994) and (JASPART et al, 1995)], Annex J allows the designer to cover a large range of usual structural joints. The understanding of the "component method" philosophy and of its application requires anyway some time and efforts from the designer; it has therefore been felt that simplified design guidelines should be prepared so to allow him to profit directly and in an easy way from the advantages linked to the new design concepts on joints.

The opportunity to develop such simplified tools has been given to the above-mentioned SPRINT partners who prepared these two last years a set of design guidelines, a free copy of which has been made available to each of the Workshop participants.

## 2. THE SPRINT DOCUMENT

The SPRINT documents contains the six following chapters:

- Chapter 1 : Simple design model for joint stiffness and resistance calculation
- Chapter 2 : Stiffness and resistance calculation for beam-to-column joints with extended end plate connections
- Chapter 3 : Stiffness and resistance calculation for beam-to-column joints with flush end plate connections
  - a) End plate height smaller than beam depth
  - b) End plate height larger than beam depth
- Chapter 4 : Stiffness and resistance calculations for beam splices with flush end plate connections
  - a) End plate height smaller than beam depth
  - b) End plate height larger than beam depth
- Chapter 5 : Stiffness and resistance calculation for beam-to-column joints with flange cleated connections
- Chapter 6 : Global analysis of frames with semi-rigid joints.

The first part of Chapter 1 gives general indications about the semi-rigid behaviour of the joints, their modelling for frame analysis, their characterization through the component method, the idealization of their characteristic  $M-\phi$  curves and their classification, in terms of stiffness, as pinned, semi-rigid and rigid.

The second part of Chapter 1 gives guidelines on how to use the design tools for joints described in Chapters 2 to 5.

How to perform the global structural analysis of a frame, the constitutive joints of which have been classified as semi-rigid is explained in a simple way in Chapter 6. In this chapter, the designer's attention is turned to elastic methods of global analysis which are of first interest in daily design practice.

### 3. THE DESIGN TOOLS FOR JOINTS

For design purposes, design aids are detailed in chapters 2 to 5. Chapter 2 is partly reproduced, as an example, at the end of the present paper. Each of these chapters is devoted to a specific type of joint. It is composed of two parts:

- a. a calculation procedure, presented in the format of design sheets;
- b. design tables.

The calculation procedure is aimed at assisting the designer who is willing to take account of all the capacities of the semi-rigidity, without having to go through the more complex approach of Annex J of Eurocode 3.

For a specific joint, a first design sheet is devoted to the useful mechanical and geometrical characteristics of the joint under consideration. In the following sheets, the calculation procedure gives the expressions of both stiffness and resistance for all the components of the joint. How to derive the global properties of the whole joint, i.e. its nominal stiffness and its design moment resistance, is summarized at the end of the design sheet. Additional design considerations are given in Chapter 1.

Of course the shear resistance of the joint is of major importance for the design. It is not given in the design sheets for sake of clarity. Relevant information in this respect is however provided in Chapter 1 (as well as information on weld design).

The second part of each of the chapters 2 to 5 consists in design tables, which can be used in a straightforward manner as an alternative to the design sheets. These design tables are established for standard combinations of connected shapes and provide the designer with the values of:

- the initial stiffness  $S_{j,ini}$  and the reduced stiffness  $S_{j,inf}/2$  to be possibly used for elastic design;
- the design moment  $M_{Rd}$  and the shear resistance  $V_{Rd}$  of the joint ;
- the component of the joint which is governing the moment resistance ;
- the reference lengths in case of a braced ( $L_{bb}$ ) or unbraced ( $L_{bu}$ ) structural system.

The knowledge of the "governing component", and of its ductility, allows to determine the level of rotation capacity for the joint while the reference length allows to classify the joint as pinned, semi-rigid or rigid. Reference lengths are boundaries to which the actual beam span (beam to which the considered joint is attached) has to be compared. Too such reference lengths exist for each joint:

- one to distinguish between a rigid and a semi-rigid joint ;
- one to distinguish between a semi-rigid and a pinned joint.

The design tables have been obtained from the expressions given in the design sheets

but by taking some options which generally give conservative results. There are however some extreme situations where the use of the design tables cannot be furthermore recommended. These situations are mostly related to the stress state - shear and direct stresses - which exists in the column web panel and is controlled by factors  $\xi$  and  $\eta$ . Some comments regarding the physical meaning and the values of  $\xi$  and  $\eta$ , recommended for the use of design sheets or adopted implicitly in the design tables, are given in Chapter 1.

In the design tables, the following information is provided to the designer for what concerns the classification:

- a number followed by the label R: the number is the reference length, the label R means that the reference length is the upper boundary between rigid and semi-rigid;
- a label P followed by a number: the number is the reference length, the label P means that the reference length is the lower boundary between pinned and semi-rigid.

In the case of non reasonable values for the reference length, only an ad-hoc indication P, R or S is given (S for semi-rigid).

#### 4. THE DIFFERENT WAYS TO USE THE DESIGN TOOLS

The SPRINT design sheets and tables can be used in isolation or in combination so to assist effeciently the designer in different situations which can result from the design procedure he has decided to follow. Some examples are discussed hereafter.

- The predesign and the design of the frame is based on the assumption that the constitutive joints are rigid or pinned. At the end of the design procedure, the joints have to be designed so to resist the internal forces resulting from the structural analysis and to fulfil the stiffness requirements (pinned or rigid). In such a case, the tables can be used to select an approximate joint.
- To get rigid joints, transverse stiffeners are traditionnally welded on the columns, at the level of the beam flanges. In the tables, it is seen that several unstiffened joints (mainly joints with extended end plates) may be considered as rigid for frame analysis. In this respect, the tables allow the designer to profit from a substantial economy on the joint fabrication (no stiffeners) without altering at all the design procedure he is used to apply (rigid design).
- When predesigning a frame, economical benefit from the semi-rigid design may be achieved more easily by selecting, through the use of the design tables, the

most convenient joint for fabrication and erection as well as the corresponding structural properties.

- For joints, components of which are different from these listed in the tables, a combined use of the design sheets and tables can strongly reduce the amount of calculations to be done to characterize the response of the joints.

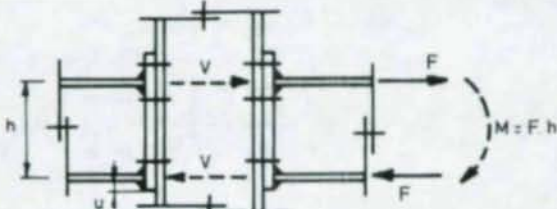
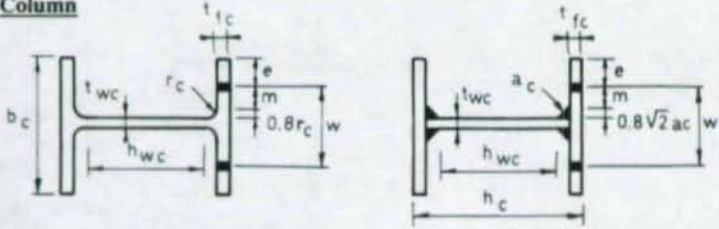
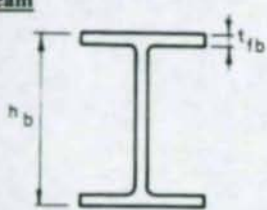
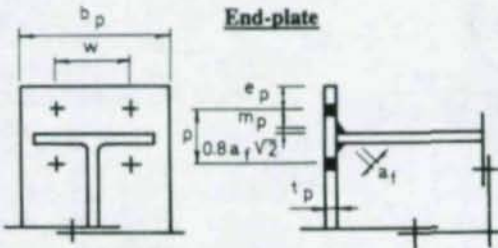
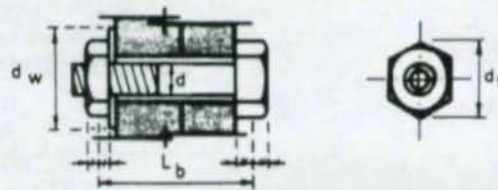
## 5. CONCLUSIONS

To achieve an economical design of the frames and of the constitutive joints - as it is now possible through the new possibilities offered by Eurocode 3 - the designers require design tools adopted to their search of efficiency and profitability. The RA 351 SPRINT has performed a step in this direction by establishing design tables and design sheets for commonly used types of beam-to column joints and beam splices. These design aids allow the designer to select the well known fully rigid joints or fully pinned joints or to select semi-rigid joints which generally give a significant benefit by simplifying joint details thereby reducing shop and erection costs.

## 6. REFERENCES

1. EUROCODE 3, ENV-1993-1-1, *Revised Annex J*, Design of Steel Structures, European Committee for Standardization, Document CEN/TC250/SC3-N419E, Brussels, June 1994.
2. JASPART, J.P. and MAQUOI, R., *Prediction of the semi-rigid and partial strength properties of structural joints*, Proceedings of the SSRC Technical Annual Session, Lehigh, U.S.A., June 20, 1994, pp. 177-192.
3. JASPART, J.P., STEENHUIS, M. and WEYNAND, K., *The stiffness model of revised Annex J of Eurocode 3*, Proceedings of the Third International Workshop on Connections in Steel Structures, Trento, Italy, May 28-31, 1995.

## Chapter 2. 1. Calculation procedure.

<i>Mechanical characteristics</i>		
	<u>Yield stresses</u>	<u>Ultimate stresses</u>
Beam web	$f_{ywb}$	-
Beam flange	$f_{yfb}$	-
Column web	$f_{ywc}$	-
Column flange	$f_{yc}$	$f_{ultc}$
End-plate	$f_{yp}$	$f_{up}$
Bolts	-	$f_{ub}$
If hot-rolled profiles : $f_{ywc} = f_{yc}$ and $f_{ywb} = f_{yfb}$		
<i>Geometrical characteristics</i>		
<u>Joint</u>		
<u>Column</u>	 <p style="text-align: right;"> <math>s = r_c</math>  for a rolled section  <math>s = \sqrt{2} a_c</math>  for a welded section </p> <p> <math>A_w = A_c - 2 b_c t_{fc} + (t_{wc} + 2 r_c) t_{fc}</math>  with <math>A_c =</math> column section area </p> <p> <math>A_w = (h - 2 t_{fc}) t_{wc}</math> </p>	
<u>Beam</u>		
	 <p style="text-align: center;"><u>End-plate</u></p>	
<u>Bolts</u>	<p> <math>d_w</math> : see figure or = <math>d_f</math> if no washer  <math>A_b</math> : resistance area of the bolts </p> 	

	<b>STIFFNESS</b>	<b>RESISTANCE</b>
<b>Column web panel in shear</b>	$k_1 = \frac{0,385 A_v}{\xi h}$	$F_{Rd,1} = \frac{V_{wc,Rd}}{\xi} \quad \text{with} \quad V_{wc,Rd} = \frac{0,9 A_v f_{yw}}{\sqrt{3} \gamma_{M0}}$
	<p><math>\xi = 1</math> for one-sided joint configurations;  <math>0</math> for double sided joint configurations symmetrically loaded;  <math>1</math> for double-sided configurations non-symmetrically loaded with balanced moments;  <math>2</math> for double-sided joint configurations non-symmetrically loaded with unbalanced moments.</p> <p>For other values, see 1.2.2.1 in chapter 1.</p>	
<b>Column web in compression</b>	$k_2 = \frac{0,7 b_{eff,wc,z} t_{wc}}{h_{wc}}$	$F_{Rd,2} = \eta \rho_c b_{eff,wc,z} t_{wc} f_{yw} / \gamma_{M0}$ <p>with <math>\eta = \min [1,0 ; 1,25 - 0,5 \frac{\sigma_n}{f_{yw}}]</math> (*)</p> $\rho_c = \sqrt{\frac{1}{1 + 1,3(\xi b_{eff,wc,z} t_{wc} / A)^2}}$ <p><math>\sigma_n</math> : normal stresses in the column web at the root of the fillet radius</p>
	$b_{eff,wc,z} = t_{fb} + a_f \sqrt{2} + t_p + \min(u ; a_f \sqrt{2} + t_p) + 5(t_{fc} + s)$ <p>(*) see 1.2.2.2 in chapter 1.</p>	
<b>Beam flange in compression</b>	$k_3 = \infty$	$F_{Rd,3} = M_{c,Rd} / (h_b - t_{fb})$ <p><math>M_{c,Rd}</math> : beam design moment resistance</p>
<b>Bolts in tension</b>	$k_4 = 3,2 \frac{A_1}{L_b}$	$F_{Rd,4} = 4 B_{t,Rd} \quad \text{with} \quad B_{t,Rd} = F_{t,Rd}$ $F_{t,Rd} = \frac{0,9 f_{ub} A_1}{\gamma_{M0}}$
<b>Column web in tension</b>	$k_5 = \frac{0,7 b_{eff,wc,t} t_{wc}}{h_{wc}}$	$F_{Rd,5} = \rho_t b_{eff,wc,t} t_{wc} f_{yw} / \gamma_{M0}$ <p>with <math>\rho_t = \sqrt{\frac{1}{1 + 1,3(\xi b_{eff,wc,t} t_{wc} / A)^2}}</math></p> $b_{eff,wc,t} = \min [4m ; 8m + 2,5e ; p + 4m + 1,25e]$

Column flange in bending	$k_6 = \frac{0,85 l_{eff,c} t_c^3}{m^3}$	$F_{Rd6} = \min [ F_{c,Rd61} ; F_{c,Rd62} ]$ $F_{c,Rd61} = \frac{(8n - 2e_w) l_{eff,c} m_{pl,c}}{2mn - e_w(m+n)}$ $F_{c,Rd62} = \frac{2 l_{eff,c} m_{pl,c} + 4 B_{t,Rd} n}{m+n}$ $n = \min [ e ; 1,25m ; (b_p - w)/2 ]$ $e_w = d_w / 4$ $m_{pl,c} = 0,25 t_c^2 f_{yc} / \gamma_{M0}$ $l_{eff,c} = b_{eff,c}$
End-plate in bending	$k_7 = \frac{0,85 l_{eff,p} t_p^3}{m_p^3}$	$F_{Rd7} = \min [ F_{ep,Rd71} ; F_{ep,Rd72} ]$ $F_{ep,Rd71} = \frac{(8n_p - 2e_w) l_{eff,p} m_{pl,p}}{2m_p n_p - e_w(m_p + n_p)}$ $F_{ep,Rd72} = \frac{2 l_{eff,p} m_{pl,p} + 4 B_{t,Rd} n_p}{m_p + n_p}$ $n_p = \min [ e_p ; 1,25m_p ]$ $m_{pl,p} = 0,25 t_p^2 f_{yp} / \gamma_{M0}$ $l_{eff,p} = \min [ 4\pi m_p ; 8m_p + 2,5e_p ; w + 4m_p + 1,25e_p ; b_p ]$
<b>JOINT</b>	<p>Initial stiffness :</p> $S_{joint,init} = E h^2 / \sum_{i=1}^7 1/k_i$ <p>Nominal stiffness :</p> $S_{joint} = S_{joint,init} / 2$	$F_{Rd} = \min [ F_{Rd,i} ]$ <p>Plastic design moment resistance :</p> $M_{Rd} = F_{Rd} h$ <p>Elastic moment resistance :</p> $\frac{2}{3} M_{Rd}$

## Chapter 2. 2. Design table.

S235	Column	Beam	bolts hr8.8																			failure mode	Reference length(m)	
				End-plate S235 (mm)			Connection detail (mm)						Welds (mm)		Rotational stiffness (kNm/rad)		Resistance			Code	L <sub>bb</sub>		L <sub>bu</sub>	
				t <sub>p</sub>	h <sub>p</sub>	h <sub>p</sub>	e <sub>p</sub>	p	p <sub>p</sub>	e <sub>p1</sub>	u <sub>1</sub>	w	w <sub>1</sub>	u	a <sub>w</sub>	a <sub>f</sub>	Stal	S <sub>bd</sub> /2	M <sub>Rd</sub>					2/3M <sub>Rd</sub>
HEB140	IPE220	M16	15	130	300	35	80	130	55	35	70	30	10	3	5	11604	5802	27.2	18.1	157	CWC	4.0-R	S	
	IPE240	M16	15	130	320	35	80	150	55	35	70	30	10	4	5	13212	6606	29.7	19.8	157	CWC	4.9-R	S	
	IPE270	M16	15	134	350	35	85	170	60	35	70	32	10	4	6	15968	7984	33.7	22.5	157	CWC	6.1-R	S	
HEB160	IPE220	M16	15	130	300	35	80	130	55	35	70	30	10	3	5	13993	6997	35.7	23.8	157	CWC	3.3-R	S	
	M20	20	160	320	45	100	110	65	45	90	35	10	3	5	14344	7172	36.2	24.1	245	CWC	3.2-R	S		
	IPE240	M16	15	130	320	35	80	150	55	35	70	30	10	4	5	16008	8004	39.0	26.0	157	CWC	4.1-R	S	
	M20	20	160	340	45	100	130	65	45	90	35	10	4	5	16392	8196	39.6	26.4	245	CWC	4.0-R	S		
	IPE270	M16	15	134	350	35	85	170	60	35	70	32	10	4	6	19520	9760	44.3	29.5	157	CWC	5.0-R	S	
	M20	20	160	370	45	105	150	70	45	90	35	10	4	6	19834	9917	44.9	29.9	245	CWC	4.9-R	S		
	IPE300	M16	15	150	380	35	85	200	60	35	70	40	10	4	6	23030	11515	49.4	32.9	157	CWC	6.1-R	S	
	M20	20	160	400	45	105	180	70	45	90	35	10	4	6	23189	11594	50.1	33.4	245	CWC	6.1-R	S		
	IPE330	M16	15	160	410	35	85	230	60	35	70	45	10	4	6	26543	13271	54.5	36.3	157	CWC	7.4-R	S	
	M20	20	160	430	45	105	210	70	45	90	35	10	4	6	26607	13304	55.3	36.8	245	CWC	7.4-R	S		
HEB180	IPE220	M16	15	130	300	35	80	130	55	35	70	30	10	3	5	14691	7346	39.9	26.6	157	CWC	3.2-R	S	
	M20	20	160	320	45	100	110	65	45	90	35	10	3	5	15299	7649	40.5	27.0	245	CWC	3.0-R	S		
	IPE240	M16	15	130	320	35	80	150	55	35	70	30	10	4	5	16868	8434	43.7	29.1	157	CWC	3.9-R	S	
	M20	20	160	340	45	100	130	65	45	90	35	10	4	5	17538	8769	44.3	29.5	245	CWC	3.7-R	S		
	IPE270	M16	15	134	350	35	85	170	60	35	70	32	10	4	6	20691	10345	49.5	33.0	157	CWC	4.7-R	S	
	M20	20	160	370	45	105	150	70	45	90	35	10	4	6	21322	10661	50.2	33.5	245	CWC	4.6-R	S		
	IPE300	M16	15	150	380	35	85	200	60	35	70	40	10	4	6	24534	12267	55.2	36.8	157	CWC	5.7-R	S	
	M20	20	160	400	45	105	180	70	45	90	35	10	4	6	25024	12512	56.0	37.4	245	CWC	5.6-R	S		
	M24	20	180	410	50	115	170	75	50	100	40	10	4	6	24667	12334	56.0	37.4	352	CWC	5.7-R	S		

## STRENGTH OF MOMENT END-PLATE CONNECTIONS WITH MULTIPLE BOLT ROWS AT THE BEAM TENSION FLANGE

Thomas M. Murray<sup>1</sup>

Jeffrey T. Borgsmiller<sup>2</sup>

### Abstract

A design method for the multiple row, eight bolts at the tension flange, moment end-plate connection is presented. The method uses yield-line theory to determine plate size and the modified Kennedy method, which includes prying force effects, to determine bolt size. Ten full-scale test results were used to verify the method.

### 1. INTRODUCTION

In North America, moment end-plate connections are used primarily in pre-engineered metal buildings. To reduce inventory costs, manufacturers currently attempt to stock a minimum number of bolt diameters. The required strength for a connection is then obtained by increasing the number of bolt rows at the tension flange from the usual one or two to as many as six, rather than by the more traditional method of increasing the bolt diameter. This increase in bolt rows significantly effects the complexity of the design procedure. In the following sections, a design procedure for the eight bolt at the tension flange, extended, unstiffened, moment end-plate connection shown in Figure 1 is presented. Yield-line analysis is used to determine end-plate strength and the so called "modified Kennedy method" is used to estimate bolt forces including prying effects. The procedure is verified using data from ten tests.

---

<sup>1</sup>Montague-Betts Professor of Structural Steel Design, Department of Civil Engineering, Virginia Polytechnic Institute and State University, Blacksburg, VA 24061.

<sup>2</sup>Design Engineer, J. Mueller International, 400 N. Michigan Avenue, Suite 1500, Chicago, IL 60611.

## 2. CONNECTION STRENGTH

### 2.1 End-Plate Strength

The end-plate strength is determined using classical yield-line analysis. Morrison *et al* (1986) showed that two yield-line mechanisms must be evaluated for the end-plate configuration shown in Figure 1. The yield-line patterns of these mechanisms differ in the location of a single pair of yield lines within the depth of the beam near the beam tension flange. The equations for required plate thickness,  $t_p$ , for each mechanism are as follows:

*Mechanism I:*

$$t_p = \left[ \frac{M_u / F_{py}}{\frac{b_f}{2} \left( \frac{1}{2} + \frac{h}{p_{f,o}} + \frac{h-p_t}{p_{f,i}} + \frac{h-p_{t3}}{u} \right) + 2(p_{f,i} + p_{b1,3} + u) \left( \frac{h-p_t}{g} \right)} \right]^{1/2} \quad (1)$$

$$u = \frac{1}{2} \sqrt{b_f g \left( \frac{h-p_{t3}}{h-p_t} \right)} \quad (2)$$

*Mechanism II:*

$$t_p = \left[ \frac{M_u / F_{py}}{\frac{b_f}{2} \left( \frac{1}{2} + \frac{h}{p_{f,o}} + \frac{h-p_t}{p_{f,i}} + \frac{h-p_{t3}}{u} \right) + \frac{2}{g} (p_{f,i} + p_{b1,3}) (h-t_f) + \frac{2u}{g} (h-p_{t3}) + \frac{g}{2}} \right]^{1/2} \quad (3)$$

$$u = \frac{1}{2} \sqrt{b_f g} \quad (4)$$

The parameter,  $u$ , is found by taking the derivative of the internal work expressions with respect to  $u$  and setting equal to zero.

### 2.2 Bolt Strength

Yield-line theory predicts a moment capacity for end-plate connections which is controlled by yielding of the plate. It does not predict the connection capacity based on bolt rupture. Because both the plate and the bolts are essential to the connection performance, it is necessary to analyze the capacity of the connection based on bolt forces including prying action. Experimental tests have shown that prying action in the bolts arises when the end-plate deforms out of its original flat state. As shown in Figure 2, contact points are made when the plate deforms, giving rise to the points of application of prying forces. A simplified form of a method introduced by Kennedy *et al.* (1981) has been adopted for predicting the connection strength for the limit state of bolt rupture which includes prying action.

The primary assumption in the Kennedy method is that, as the end-plate deforms out of its original state, it displays one of three stages of behavior depending on the thickness of the plate and the magnitude of the applied load. The three stages of plate behavior are thick, intermediate, and thin. Each stage of plate behavior has a corresponding equation for calculating the prying force which is incorporated into the bolt force calculation. Once the stage of plate behavior is determined, the prying force, and hence, the bolt force can be calculated. The moment at which bolt failure occurs,  $M_{u,bolt}$ , is designated as the moment at which one of the bolts first reaches its proof load. The bolt proof load,  $P_t$ , is calculated by multiplying the bolt cross-sectional area,  $A_b$ , with the nominal tensile strength of the bolt,  $F_{yb}$ .

The modified Kennedy method has been proven to be quite accurate for predicting bolt forces with prying action in end-plate connections at any stage of loading (Murray 1988). However, extensive calculations and iterations are involved. When considering the ultimate strength of the connection, these calculations can be reduced considerably.

After reviewing the results of previously conducted connection tests, two rational assumptions were devised to simplify the bolt force calculations in the Kennedy method. The first assumption considers bolt yielding. It was evident that, in most of the tests, the connection continued carrying load beyond the point at which the first bolt reached its proof load,  $M_{u,bolt}$  (Figure 3). Because the proof load of a bolt designates the point at which yielding commences, and because of the ductile nature of steel, it can be assumed that bolts that have reached their proof load can continue yielding without rupture until the other bolts reach their proof load as well. This assumption is justified by the notable yield plateau on bolt stress-strain graphs obtained by Abel and Murray (1992). The second assumption is a conservative one, and states that when a bolt reaches its proof load, the plate behaves as a "thin" plate and the maximum possible prying force,  $Q_{max}$ , is incorporated into the bolt analysis.

When calculating the connection strength using the simplified approach, all load-carrying bolt forces are set equal to their proof load,  $P_t$ , then the maximum possible prying force for a given end-plate configuration,  $Q_{max}$ , is calculated, and the two are incorporated into the analysis of the connection strength for the limit state of bolt rupture. If a bolt does not carry any load, its force is always equal to the minimum pretension force,  $T_b$ , specified. A "load-carrying bolt" is one that has been experimentally proven to carry load in an end-plate connection. For instance bolts  $B_1$ ,  $B_2$ , and  $B_4$  in Figure 3 show an increase in bolt load as the applied moment increases, whereas  $B_3$  stays at approximately the pretension force throughout the entire test. The load-carrying bolts in this hypothetical test are therefore  $B_1$ ,  $B_2$ , and  $B_4$ .

Using the above assumptions, the predicted ultimate moment capacity,  $M_q$ , of the connection for the limit state of bolt rupture including prying action in any end-plate configuration is calculated by:

$$M_q = \max \left\{ \begin{array}{l} \sum_{i=1}^{N_i} 2(P_t - Q_{\max})_i d + \sum_{j=1}^{N_j} 2(T_b)_j d \\ \sum_{n=1}^N 2(T_b)_n d \end{array} \right. \quad (5)$$

where  $N_i$  = the number of load-carrying bolt rows,  $N_j$  = the number of non-load-carrying bolt rows,  $N$  = the total number of bolt rows,  $d$  = the distance from the respective bolt row to the compression flange centerline, and the subscript  $q$  signifies that prying action is included. It is noted that the general expression for  $M_q$  is not always algebraically correct for all end-plate configurations when summing the moments. Much depends on the assumed location of the maximum prying force,  $Q_{\max}$ . Because of the fact that it is impossible to pinpoint the exact location of the prying force, and in keeping the design of all end-plate configurations unified, Equation 5 has been adopted to predict the ultimate strength of the connection when controlled by bolt force. The maximum possible prying force for an end-plate configuration,  $Q_{\max}$ , is calculated using (Kennedy 1981):

$$Q_{\max} = \frac{w' t_p^2}{4a} \sqrt{F_{py}^2 - 3 \left( \frac{F'}{w' t_p} \right)^2} \quad (6)$$

and  $F'$  is:

$$F' = \frac{t_p^2 F_{py} (0.85 b_f / 2 + 0.80 w') + \pi d_b^3 F_{yb} / 8}{4 p_f} \quad (7)$$

Kennedy *et al.* (1981) caution that, if the quantity under the radical in Equation 6 is negative, the end-plate will fail locally in shear before prying forces can be developed, and the connection is inadequate for the applied load. Also, the distance "a" is dependent on whether  $Q_{\max}$  is being calculated for an interior bolt or an exterior bolt. For interior bolt calculation from (Hendrick *et al.* 1984)

$$a_i = 3.682 (t_p / d_b)^3 - 0.085 \quad (8)$$

When calculating  $Q_{\max}$  for an outer bolt,  $a$  is the minimum of:

$$a_o = \min \left\{ \begin{array}{l} 3.682 (t_p / d_b)^3 - 0.085 \\ p_{\text{ext}} - p_{f,o} \end{array} \right. \quad (9)$$

where  $p_{\text{ext}}$  = the distance from the outer face of the beam tension flange to the edge of the end-plate extension, and  $p_{f,o}$  = the outer pitch distance between the outer face of the beam tension flange and the centerline of the exterior bolt line.

To verify the above for the multiple row end-plate configuration shown in Figure 1, ten full-scale tests were evaluated. The bolt force versus applied moment plots

of six of the ten tests indicate that all of the bolts carry a portion of the applied load except for the middle row of interior bolts. In one test, the bolt force of the middle row of interior bolts was not plotted against the applied moment, as the appropriate data was "not available" (Morrison *et al.*, 1986). The deformed shape of the end-plate in most tests is as shown in Figure 2. It was therefore concluded that the load-carrying bolt rows are the exterior, first interior, and far interior lines of bolts. The moment capacity of the connection controlled by bolt rupture is then obtained from expanding Equation (5):

$$M_Q = \max \begin{cases} 2(P_t - Q_{\max,o})(d_1) + 2(P_t - Q_{\max,i})(d_2 + d_4) + 2(T_b)d_3 \\ 2(P_t - Q_{\max,o})(d_1) + 2(T_b)(d_2 + d_3 + d_4) \\ 2(P_t - Q_{\max,i})(d_2 + d_4) + 2(T_b)(d_1 + d_3) \\ 2(T_b)(d_1 + d_2 + d_3 + d_4) \end{cases} \quad (10)$$

where  $Q_{\max,o}$  and  $Q_{\max,i}$  are calculated from Equation 6. Two different values of  $F'$  are used in the prying force calculations.  $F'_i$  is used in calculating  $Q_{\max,i}$  with the inner pitch distance,  $p_{r,i}$ , and  $F'_o$  is used in calculating  $Q_{\max,o}$  with the outer pitch distance,  $p_{r,o}$ . Both  $F'_i$  and  $F'_o$  are calculated from Equation 7. The values  $a_i$  and  $a_o$  are calculated from Equations 8 and 9, respectively. The  $d_i$  distances are measured from the centerline of the compression flange to the centerline of the respective bolts.

### 3. Comparison of Experimental Results and Predictions

To compare the experimental results to the predicted strength of the connections, it was necessary to determine the experimental failure load of each test. Depending on the shape of the applied moment versus end-plate separation plot from the experimental tests, one of two different failure loads was identified,  $M_u$  or  $M_y$ . Applied moment versus end-plate separation plots came as a result of placing measuring devices on the end-plates at or near the beam tension flange during the test procedure. These plots are an indication as to whether or not the end-plate yields. If the plot has a nearly horizontal yield plateau, such as Plot A in Figure 4, the failure load of the specimen is taken as the maximum applied load in the test,  $M_u$ . From a design standpoint, this is acceptable since the maximum applied load in the test closely correlates to the point at which the connection yields. A connection displaying this behavior is in relatively little danger of experiencing excessive deformations under service loads. Plot B in Figure 4 shows a curve with no distinct yield point and a sloped yield plateau. Connections displaying this type of applied moment versus end-plate separation behavior would experience large deformations under working loads if the design failure load were assumed to be the maximum applied moment in the test. Therefore, the failure load is determined to be near the point at which the connection yields,  $M_y$ . This experimental yield moment is established by dividing the applied moment versus end-plate separation plot into two linear segments which intersect at the yield moment.

The maximum applied moment,  $M_u$ , and experimental yield moment,  $M_y$ , for each of the ten tests were determined and are shown in Table 1. It was necessary to establish a numerical threshold for distinguishing which value,  $M_u$  or  $M_y$ , to use for the experimental failure load,  $M_{fail}$ . In some cases, it was difficult to determine whether some of the applied moment versus plate separation plots displayed the behavior of Plot A or Plot B in Figure 4. This threshold was empirically established through the ratio of  $M_y$  to  $M_u$ , and is expressed as follows:

$$M_{fail} = M_y \quad \text{if } M_y/M_u < 0.75 \quad (11)$$

$$M_{fail} = M_u \quad \text{if } M_y/M_u > 0.75 \quad (12)$$

It should be noted that this threshold is an approximate one, and that if the  $M_y/M_u$  ratio is approximately equal to 0.75,  $\pm 0.02$ , either value,  $M_y$  or  $M_u$ , can be taken as the experimental failure load. The values corresponding to the appropriate experimental failure load of each test are shown shaded in Table 1.

Once the connection strength predictions for the end-plate yield and bolt rupture limit states are calculated, a final, controlling connection strength prediction,  $M_{pred}$ , is chosen. To do so, an important assumption is necessary: the end-plate must sufficiently yield for prying action to occur in the bolts. If the end-plate does not substantially deform out of its original state, there can be no points of application for prying forces. This concept was originally introduced by Kennedy *et al.* (1981), as they presented the three stages of plate behavior caused by increasing load. The circumstance initiating the different stages of plate behavior is the formation of plastic hinges, or end-plate yielding.

The outcome of this assumption is the concept of a "prying action threshold." Until this threshold is reached, the plate behaves as a thick plate, and no prying action takes place in the bolts. Beyond the threshold, maximum prying action occurs in the bolts due to the sufficient deformation of the plate. The prying action threshold is taken as 90% of the full strength of the plate as determined by yield-line analysis, or  $0.90M_{pl}$ . Thorough review of the past experimental data has led to the conclusion that the plate begins deforming out of its original state at approximately 80% of the full strength of the plate, or  $0.80M_{pl}$ . However, to assume maximum prying action in the bolts at the point at which yielding in the plates commences would be unreasonably conservative. Therefore, it was assumed that the plate has deformed sufficiently at 90% of the plate strength to warrant the use of maximum prying action in the bolts. The predicted strength of the connection is controlled by the following guidelines: (1) if applied moment  $< 0.90M_{pl}$ , then thick plate behavior exists, or (2) if applied moment  $> 0.90M_{pl}$ , then thin plate behavior exists.

If the plate behaves as a thick plate, no prying action is considered in the bolts. Calculation of the connection strength for the limit state of bolt rupture with no prying action,  $M_{np}$ , follows the same philosophy outlined above, except  $Q_{max}$  is set equal to zero and all of the bolts in the connection are assumed to carry load. The connection strength for the limit state of bolt rupture with no prying action is therefore calculated from a revised version of Equation 5:

$$M_{np} = \sum_{i=1}^N 2(P_t)_i d_i \quad (13)$$

where  $N$  = the number of bolt rows,  $d_i$  = the distance from the respective bolt row to the compression flange centerline, and "np" signifies that no prying action is included.

Once  $M_{np}$ ,  $M_q$ , and  $M_{pl}$  are known, the controlling prediction of the connection strength,  $M_{pred}$ , can be determined. As mentioned earlier, the prying action threshold is 90% of the plate strength, or  $0.90M_{pl}$ . If the strength for the limit state of bolt rupture with no prying action,  $M_{np}$ , is less than the prying action threshold, the connection will fail by bolt rupture before the plate can yield and before prying action can take place in the bolts ("thick" plate failure). If the strength for the limit state of bolt rupture with no prying action,  $M_{np}$ , is greater than the prying action threshold, prying action takes place in the bolts, because the plate yields before the bolts rupture. If the strength for the limit state of bolt rupture with prying action,  $M_q$ , is less than the strength of the plate,  $M_{pl}$ , the connection will fail by means of bolt rupture with prying action before the plate can fully yield. However, if  $M_q$  is greater than  $M_{pl}$ , the connection will fail by plate yielding. In summary:

$$M_{pred} = M_{np} \quad \text{if } M_{np} < 0.90M_{pl} \quad (14)$$

$$M_{pred} = M_q \quad \text{if } 0.90M_{pl} \leq M_{np} \text{ and } M_q \leq M_{pl} \quad (15)$$

$$M_{pred} = M_{pl} \quad \text{if } M_{pl} < M_q \quad (16)$$

The predicted and experimental results for ten multiple row moment end-plate connection tests are listed in Table 1. Included in the table are  $M_q$ ,  $M_{pl}$ ,  $0.90M_{pl}$ ,  $M_{np}$ ,  $M_{pred}$ ,  $M_y$ , and  $M_u$ . Note that in the cases where  $M_{pl} < M_q$ , it was not necessary to calculate either  $0.90M_{pl}$  or  $M_{np}$  as the connection strength was controlled by  $M_{pl}$ , thus the dashes in the columns containing  $0.90M_{pl}$  and  $M_{np}$ . Also in the table are design ratios, comparing  $M_{pred}$  to  $M_y$  and  $M_u$ . A design ratio smaller than 1.0 is conservative, and a design ratio larger than 1.0 is unconservative. The shaded values are the ratios corresponding to the applicable failure load, determined by the  $M_y$  to  $M_u$  ratio as described above. If  $M_y/M_u < 0.75$ , the applicable design ratio is  $M_{pred}/M_y$ ; if  $M_y/M_u > 0.75$ , the applicable design ratio is  $M_{pred}/M_u$ .

Design ratios for the ten tests ranged from 0.87 to 1.39, indicating scatter in these results. However, aside from the value equal to 1.39, the other nine test design ratios vary from 0.87 to 1.10. The test that produced a design ratio of 1.39 was conducted by SEI (1984), who said, "the yield-line prediction of the failure load [is] not close since the failure was due to large bolt forces and the full strength of the plate was not reached." This confusing statement would lead to the conclusion that bolt prying action can occur prior to plate bending. However, due to the overwhelming evidence against this statement, it can be concluded that, with the exception of the one test, the simplified procedure accurately predicts the failure load of multiple row extended end-plate configurations.

#### 4.0 Conclusions

A simplified design procedure for eight bolts at the tension flange, extended, unstiffened end-plate moment connections presented appears to accurately predict the failure moment as determined from ten full-scale tests.

#### 5.0 References

Abel, M. S. and T. M. Murray (1992b), "Analytical and Experimental Investigation of the Extended Unstiffened Moment End-Plate Connection with Four Bolts at the Beam Tension Flange," Research Report CE/VPI-ST-93/08, Department of Civil Engineering, Virginia Polytechnic Institute and State University, Blacksburg, VA, December 1992, Revised October 1994.

Borgsmiller, J. T., E. A. Sumner and T. M. Murray (1995), "Tests of Extended Moment End-Plate Connections Having Large Inner Pitch Distances," Research Report CE/VPI-ST-95/01, Department of Civil Engineering, Virginia Polytechnic Institute and State University, Blacksburg, VA, March 1995.

Hendrick, D., A. R. Kukreti and T. M. Murray (1984), "Analytical and Experimental Investigation of Stiffened Flush End-Plate Connections with Four Bolts at the Tension Flange," Research Report FSEL/MBMA 84-02, Fears Structural Engineering Laboratory, University of Oklahoma, Norman, OK, September 1984.

Kennedy, N. A., S. Vinnakota and A. N. Sherbourne (1981), "The Split-Tee Analogy in Bolted Splices and Beam-Column Connections," *Joints in Structural Steelwork*, John Wiley & Sons, London-Toronto, 1981, pp. 2.138-2.157.

Morrison, S. J., A. Astaneh-Asl and T. M. Murray (1986), "Analytical and Experimental Investigation of the Multiple Row Extended Moment End-Plate Connection with Eight Bolts at the Beam Tension Flange," Research Report FSEL/MBMA 86-01, Fears Structural Engineering Laboratory, University of Oklahoma, Norman, OK, May 1986.

Murray, T. M., (1988), "Recent Developments for the Design of Moment End-Plate Connections," *Journal of Construction Steel Research*, 10, pp. 133-162.

Rodkey, R. W. and T. M. Murray (1993), "Eight-Bolt Extended Unstiffened End-Plate Connection Test," Research Report CE/VPI-ST-93/10, Department of Civil Engineering, Virginia Polytechnic Institute and State University, Blacksburg, VA, December 1993.

SEI (1984), "Multiple Row, Extended End-Plate Connection Tests," Research Report, Structural Engineers, Inc., Norman, OK, December 1984.

Table 1. Predicted and Experimental Results

Test <sup>(1)</sup>		Moments (k-ft) <sup>(7)</sup>							Design ratios <sup>(6)</sup>		
		$M_q$	$M_{pl}$	$0.90 M_{pl}$	$M_{np}$	$M_{pred}^{(2)}$	$M_y^{(3)}$	$M_u^{(4)}$	$M_y/M_u^{(5)}$	$M_{pred}/M_y$	$M_{pred}/M_u$
Borgsmiller <i>et al.</i> (1995)	1-3/4-64	2081.7	1810.4	--	--	1810.4	1870	1870	1.00	0.97	0.97
Morrison <i>et al.</i> (1986)	3/4-3/8-30	505.5	258.9	--	--	258.9	270	404.9	0.67	0.96	0.64
Morrison <i>et al.</i> (1986)	1-1/2-30	900.5	325.6	--	--	325.6	300	425.1	0.71	1.09	0.77
Morrison <i>et al.</i> (1986)	7/8-7/16-46	1114.5	570.0	--	--	570.0	520	866.1	0.60	1.10	0.66
Morrison <i>et al.</i> (1986)	1 1/8-5/8-46	1727.4	966.7	--	--	966.7	975	975.1	1.00	0.99	0.99
Morrison <i>et al.</i> (1986)	1 1/4-5/8-62	2697.8	1166.5	--	--	1166.5	1200	1635	0.73	0.97	0.71
Morrison <i>et al.</i> (1986)	1 1/2-3/4-62	3846.0	1601.6	--	--	1601.6	1600	2329.6	0.69	1.00	0.69
Rodkey and Murray (1993)	3/4-5/8-33 1/4	600.0	760.1	684.1	783.7	600.0	690	692.5	1.00	0.87	0.87
SEI (1984)	3/4-1/2-62	1089.7	923.2	--	--	923.2	750	929	0.81	1.23	0.99
SEI (1984)	1-3/4-62	2050.7	1896.3	--	--	1896.3	1250	1364	0.92	1.52	1.39

<sup>1</sup>—Test designation:  $d_b$  -  $t_p$  -  $h$  all in inches

<sup>2</sup>—If  $M_{tp} < 0.90M_{pl}$ ,  $M_{pred} = M_{tp}$ ; If  $0.90 M_{pl} < M_{np}$  and  $M_q < M_{pl}$ ,  $M_{pred} = M_q$ ; If  $M_{pl} < M_q$ ,  $M_{pred} = M_{pl}$

<sup>3</sup>— $M_y$  was determined from the plot of applied moment vs. end-plate separation via two intersecting lines.

<sup>4</sup>— $M_u$  = the maximum applied moment in the test.

<sup>5</sup>—If  $M_y/M_u < 0.75$  (+/- 0.02) use  $M_{pred}/M_y$  ratio, if  $M_y/M_u > 0.75$  (+/- 0.02) use  $M_{pred}/M_u$  ratio. Values to be used are shown shaded.

<sup>6</sup>—If Design ratio > 1.0, prediction is unconservative; if Design ratio < 1.0, prediction is conservative

<sup>7</sup>—1 kips-ft = 0.738 kn-m.

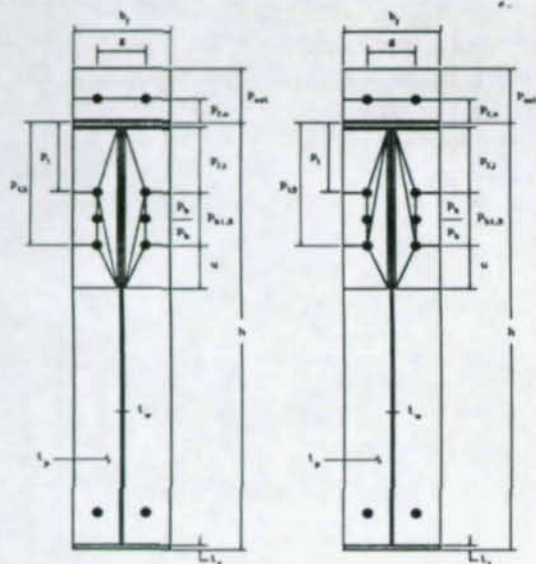


Figure 1. End-Plate Configuration and Yield-Line Patterns

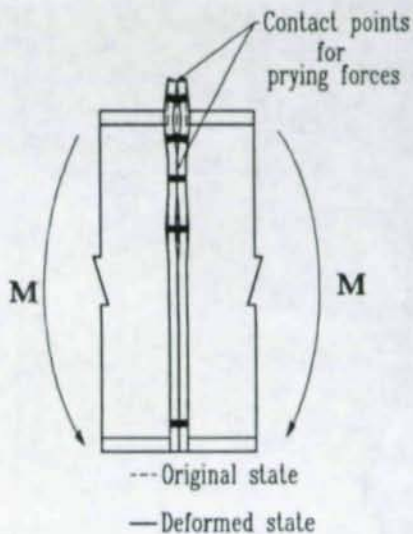


Figure 2. Contact Points for Prying Forces

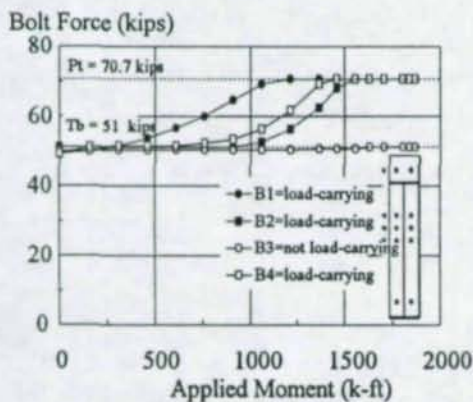


Figure 3. Sample Applied Moment vs. Bolt Force Plots

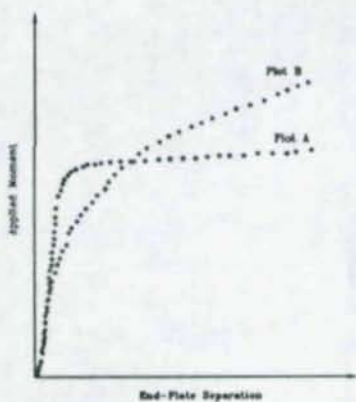


Figure 4. Applied Moment vs. End-Plate Separation Plots

## STIFFENED SEATED CONNECTIONS ON COLUMN WEBS

Duane S. Ellifritt<sup>1</sup>

Thomas Sputo<sup>2</sup>

Andrew S. Miller<sup>3</sup>

### ABSTRACT

In multistory braced frame construction, the connection of choice for simple connections between beams and column webs is the seated connection. This connection lends itself to ease of erection because of its greater tolerance when compared to framing angles. The strength and stability of the column web supporting these connections is a factor questioned by many engineers. Research has been undertaken to study the behavior of this connection. Fifty-three connections were tested. Limit states of column web yielding, weld shear, stiffener buckling, and beam-column failure were noted.

### 1. INTRODUCTION

In multistory braced frames, simple connections of beam to column web are often made by beam seats for ease of erection. In more heavily loaded connections, a stiffened seat, is frequently used to support the beam reaction. The design of such seats is an area where little guidance is available because of the lack of research. Elastic design procedures for stiffened seats generally consider first yield as the limit state. Because the column web is a highly indeterminate system with a high shape factor, the range of additional load between first yield and ultimate inelastic failure is large. If plastic analysis is used, some of the inconsistencies of the elastic method are removed. The most significant advantage of plastic analysis, is the additional strength derived from the redistribution of stresses due to yielding.

---

<sup>1</sup> Professor of Structural Design, University of Florida, 345 Weil Hall, Gainesville, FL, USA

<sup>2</sup> Chief Engineer, Sputo Engineering, Gainesville, FL, USA

<sup>3</sup> Former Graduate Student, University of Florida, USA

## 2. YIELD LINE ANALYSIS

Abolitz and Warner (1965) have calculated the yield line collapse mechanism for a T-shaped seat, considering the flange to web connection as fixed and hinged. The fixed situation is shown in Figure 1. The ultimate load may be calculated as

$$P_u = k L m / e \quad (1)$$

where:

$P_u$  = Ultimate applied load

$k$  = Yield line factor

=  $A [ C(D) + E + G ]$

$A = 2 / [2T-B]$

$C = 2 + [0.866T/L]$

$D = [(T-B)(3T+B)]^{1/2}$

$E = T(T-B)/2L$

$G = 4L + 3.464T$

$L$  = Stiffener length

$m$  = Moment capacity of a unit width of plate

=  $1/4 t_w^2 F$

$t_w$  = Column web thickness

$e$  = Load eccentricity

$T$  = Clear distance between column web fillets

$F$  = Limiting stress

$B$  = Seat width

## 3. PHASE ONE TESTS

In Phase One tests were performed on 16 welded stiffened seated connections on column webs, with column web aspect ratios in excess of the mean aspect ratio of standard rolled wide-flange shapes. Connections were loaded through a reaction beam. Each connection was tested both with and without an applied column axial load, for a total of 32 tests.

All failure modes were that of weak axis inelastic beam-column failure. Whitewash applied to the test columns showed visually the beginnings of the formation of the yield line mechanisms. Because the test column flanges were torsionally weak, compared to those of sections usually used as columns, a large degree of out of plane rotation of the flanges was noted. This flange rotation tended to relieve the stresses in the column web and thereby prevented the yield line mechanism from proceeding to completion.

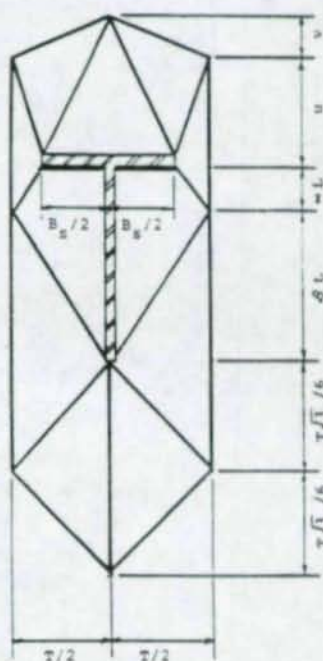


Figure 1. Yield Line Pattern

#### 4. PHASE TWO TESTS

In Phase Two, tests were performed on 16 welded stiffened seated connections, 15 to column webs, and one to a column flange as a baseline test. The column sections tested were W250x49 (W10x33), W310x60 (W12x40), and W360x91 (W14x61). These sections were chosen as representative of normal column sections with relatively high web slenderness ratios ( $T/t_w$ ). The connection chosen had a stiffener length of 203 mm (8 in.), a seat width of 165 mm (6.5 in.), and an outstanding leg of 152 mm (6 in.). The erection bolts were 22 mm (7/8 in.) A-325 bolts, placed 76 mm (3 in.) out from the column face.

The reaction beam was a welded girder of 480 mPa (70 ksi) steel. The flange plates were 152 mm (6 in.) by 19 mm (3/4 in.) and the web plate was 356 mm (14 in.) by 13 mm (1/2 in.).

Failure loads for all 16 tests are shown in Table 1. The initial series of three tests had the beam connected to the seat by the erection bolts, but without an erection angle being attached to the top flange of the beam. The mode of failure for these connections was weld shear as shown in Figure 2.

The second series of tests again had the beam bolted to the seat, but a L102x102x6.4 (L4x4x1/4) erection angle was welded along the angle toes to the

Table 1. Phase Two Test Results

Section			$P_{FAIL}$		$P_{ULT}$		$P_{FAIL}/P_{ULT}$
W250x49	(W10X33)	NA	652	(146.6)	327	(73.6)	1.99
W310x60	(W12X40)	NA	451	(101.5)	327	(73.6)	1.38
W360x91	(W14X61)	NA	468	(105.3)	327	(73.6)	1.43
W250x49	(W10X33)	TA	425	(95.5)	327	(73.6)	1.30
W310x60	(W12X40)	TA	358	(80.5)	327	(73.6)	1.09
W360x91	(W14X61)	TA	535	(120.3)	327	(73.6)	1.63
W250x49	(W10X33)	TA-R	495	(111.3)	327	(73.6)	1.51
W310x60	(W12X40)	TA-R	498	(112.0)	327	(73.6)	1.52
W250x49	(W10X33)	TA-WAA	371	(83.4)	509	(114.4)	0.73
W310x60	(W12X40)	TA-WAA	378	(85.0)	509	(114.4)	0.74
W360x91	(W14X61)	TA-WAA	401	(90.2)	509	(114.4)	0.79
W250x49	(W10X33)	TA-R-W	201	(45.1)	327	(73.6)	0.61
W310x60	(W12X40)	TA-R-W	227	(51.1)	327	(73.6)	0.69
W360x91	(W14X61)	TA-R-W	201	(45.1)	327	(73.6)	0.61
W360x91	(w14X61)	TA-FLA	258	(57.9)	246	55.2	1.05

NA = No erection angle installed

TA = Top angle installed

R = Weld return of 13 mm (1/2 in.) on seat

WAA = Weld across both top and bottom of seat

W = Beam welded to seat in addition to erection bolts

FLA = Connection attached to flange rather than web

$P_{FAIL}$  = Test failure load, kN (kips)

$P_{ULT}$  = Unfactored ultimate design load, kN (kips)

Note: 1. All welds are 6.4 mm (1/4 in.) E70 fillet welds except for W360x91 (W14x61) TA-FLA, which was 4.8 mm (3/16 in.) fillet.

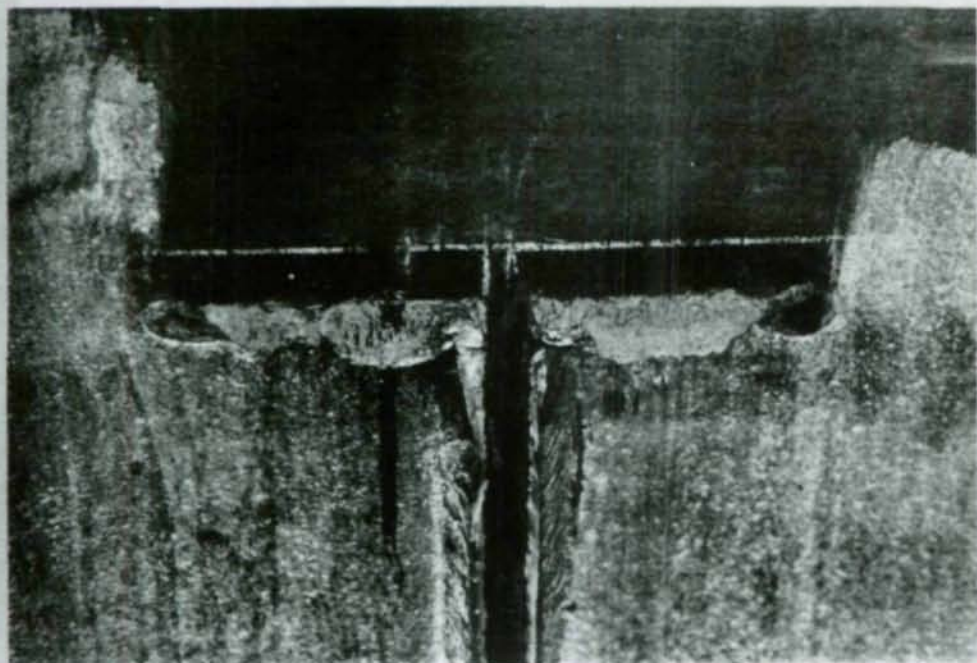


Figure 2. Shear Failure of Welds

top flange of the beam and column web, as is recommended in the Manual of Steel Construction (1993). Again, the mode of failure for these connections was weld shear. Large rotations of the column web were evident during the testing. These large rotations, which exceeded the end rotation of the beam, are a cause of beam web crippling and yielding. Figure 3 shows the amount of rotation of the seat during a test.

It was noted from the initial six tests that the weld failure began at the corners of the seat nearest the column flange. It was assumed that this was because of a stress concentration due to a shear lag effect. This effect would be caused by the force in the seat plate and weld "migrating" towards the stiffer column flanges. Based on this observation, some specimens had a weld return of 13 mm (1/2 in.) placed around the corner of the seat plate.

The third series of tests had the beam again bolted to the seat, and a top angle installed, but with the addition of the weld returns. The mode of failure for this series of tests was again weld shear, but at a higher load than the second series, indicating that the return did, in fact, help with this stress concentration due to shear lag. Test W14X61 TA-R had strain gages installed on the seat, which confirmed the stress gradient in the seat, with a high concentration at the corners of the seat.

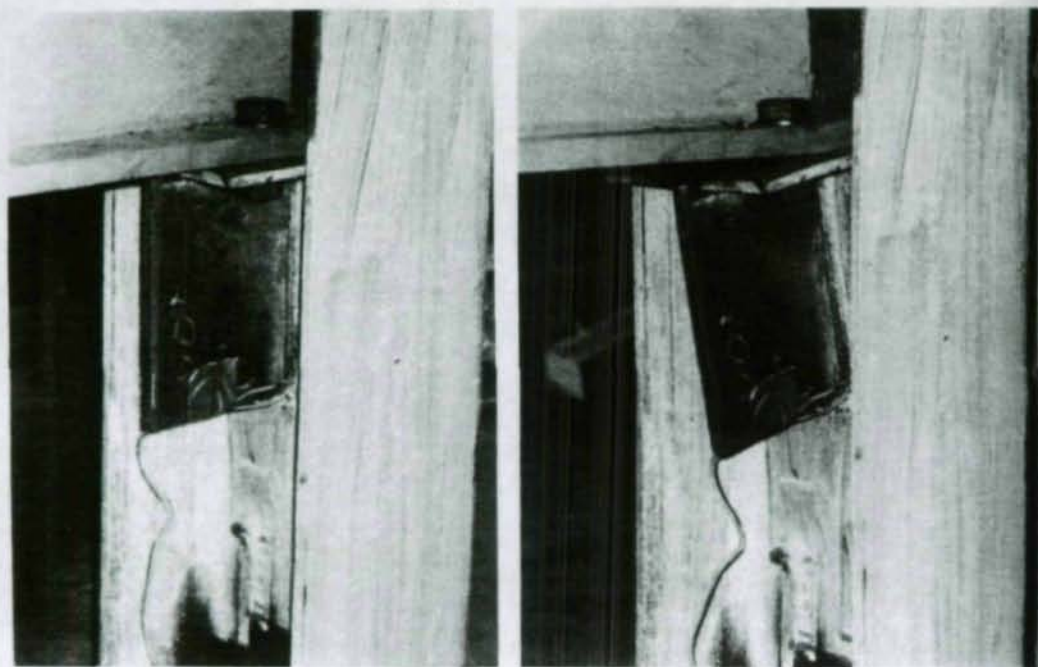


Figure 3. Rotation of Seat and Web Under Load

In the previous nine tests, the weld failed before the yield line mechanism could proceed to failure. Evidence of the mechanism beginning to develop was shown by the flaked whitewash in the regions where yielding was predicted to develop. The fourth series of tests had the weld on the seat carried fully around the seat, hoping to provide enough weld strength to allow the yield line mechanism to fully develop to failure. The mode of failure for this series of tests was tearing of the column web at a greatly reduced load. The column web was too thin to fully develop the welds and it tore prematurely, at a load below that predicted by the weld strength or yield line criteria.

The fifth series of tests had the beams bolted and welded to the seat with 51 mm (2 in.) of 3.2 mm (1/8 in.) fillet weld. As with previous tests, a welded top angle was installed. The failure loads with the beam welded to the seat were lower than those with only erection bolts installed. It was probably because the welds increased the effective eccentricity on the connection welds to the column, thereby increasing the stress in the welds, causing premature failure.

The last test was a seat welded to the flange of a W360x91 (W14x61) column with 4.8 mm (3/16 in.) E7013 fillet welds. The beam was bolted to the seat, and a welded top angle was installed. This connection failed at a load slightly higher than predicted by the present design method, thereby verifying it and providing a good baseline by which to judge the web connections.

A connection should be judged satisfactory if  $P_{FAE}/P_{ULT}$  is greater than 1.0. Looking at Table 1, the first three series of tests meet this criteria. While the weld return did increase the strength of the connection, it is judged not necessary because connections without the weld return performed satisfactorily when compared to those with weld returns, and could in fact, cause erection clearance problems.

The fourth and fifth series of tests did not meet this criteria. Therefore, welding all around the seat is seen to be counterproductive. Welding the beam to the seat, should also not be done. This welding is seen to be redundant, since the erection bolts must be installed initially to properly place the beam.

## 5. CONNECTION LIMIT STATE CRITERIA

Laboratory testing indicates that two modes of failure need to be considered: connection weld strength and web yielding. Additionally, web crippling and web yielding of the supported beam must be considered.

### 5.1 Weld Strength

The load tables in both the LRFD and ASD Manual of Steel Construction [4,5] are based on weld stress with the load located at an eccentricity of 0.8 times the *outstanding leg of the connection*. How is the eccentricity affected by the location of the connection? When the connection is on a column flange, the connection will be less prone to rotate than the beam, thereby increasing the effective eccentricity. Because of this, the assumption of 0.8 W is probably reasonable and safe. But when the connection is on the web, the web may rotate more than the beam, thereby decreasing the eccentricity, reducing to some extent the theoretical weld stress. Since the allowable load for weld stress is a combination of shear and tension due to eccentricity, varying the eccentricity does not make a drastic difference in the allowable capacity.

But as noted in test W14X61 TA-R, the stress in the seat plate is decidedly non-uniform, due to the previously discussed shear lag effect. Therefore, the weld stress at the outside corners of the seat plate is magnified, where initial failure begins. These two actions of shear lag and decreased effective eccentricity tend to counterbalance themselves, rendering the existing weld tables somewhat conservative.

### 5.2 Column Web Yielding

The yield line model used by Abolitz and Warner 1965, when properly modified, provides a convenient solution. The actual eccentricity of the load is the most sensitive variable in this method. The allowable load from a yield line analysis of the web is based only on the applied moment on the web, and is therefore directly related to the eccentricity of the load.

Because of previously noted reduction in eccentricity of the load, the design eccentricity should be considered as the distance from the column web face to the center of the bearing area of the beam. The beam bearing area for the beam end should be considered to be between the end of the beam and the center of the seat erection bolts. This assumption is based on the observed fact that the eccentricity of load in all test specimens moved toward the column face and rapidly decreased to approximately this value.

It is important to consider what stress value to use in the yield line analysis. It has been noted by many researchers that the ultimate capacity of a plate is far in excess of the yield strength. Packer and Bruno (1986) have suggested the following effective yield stress, which seems reasonable:

$$F^* = F_y + 2/3(F_u - F_y) \quad (2)$$

This value considers the contribution of strain hardening to the ultimate strength, as caused by the extensive rotations of the web along the observed yield line pattern.

## 6. PHASE III TESTS

After reviewing the results of Phases I and II, the AISC Research Committee felt there were a few other variables that needed to be explored. Six more tests were conducted, some with the seat extending beyond the stiffener and one with a much longer stiffener than had previously been tested. Since one of the concerns was excessive seat rotation in the web, it was felt that a longer stiffener would reduce this rotation. However, in the test, the stiffener buckled at around 3/4 of the ultimate load (See Figure 4). A list of the Phase III test specimens is shown in Table 2. All seats were attached to W14x61 columns. An additional effort in Phase III was to strain gage the web of the loading beam to see if some knowledge could be obtained about the migration of the resultant load point, or eccentricity.

The results of these tests are shown in Table 3. It was found that the test specimens had been over-welded. Instead of the 6.4 mm (1/4 in.) welds specified on the drawings, the actual welds were actually 7.9 mm (5/16 in.) to 9.5 mm (3/8 in.) in size. The calculated capacities in Table 3 reflect the actual weld size.

## CONCLUSIONS

It is evident from laboratory testing of stiffened seat connections on column webs that the existing design criteria for stiffened seat connections to column flanges needs to be expanded to consider column web bending capacity and beam-column action to ensure proper performance. However, the AISC procedure for calculating the capacity of a stiffened seat attached to the flange of a standard rolled W-shape can with a few minor exceptions, be safely used when the seat is

attached to the web. This has been added to the tables in the 1993 LRFD Manual, Volume II. If a "beam" type section is being used as a column, one must check the web using an analysis similar to the yield line analysis presented herein.

It should be noted that the laboratory studies demonstrated that the column web possesses capacity in excess of that predicted from any previous analytical study. This is due to membrane stresses induced in the web due to large deflections, and increased material strength due to strain hardening.

### ACKNOWLEDGMENTS

Funding for this study was provided by the American Institute of Steel Construction.

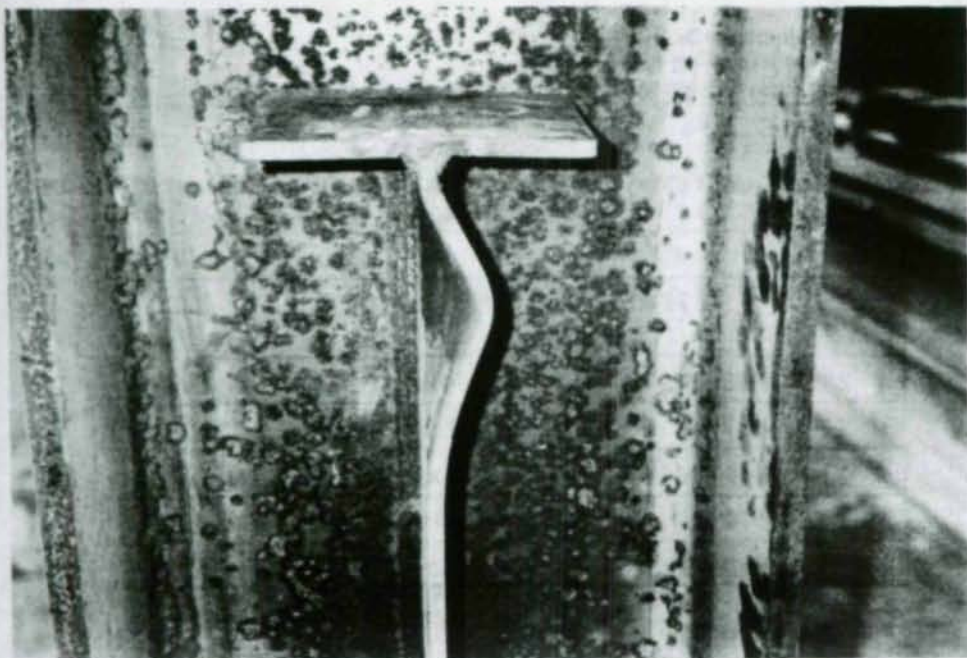
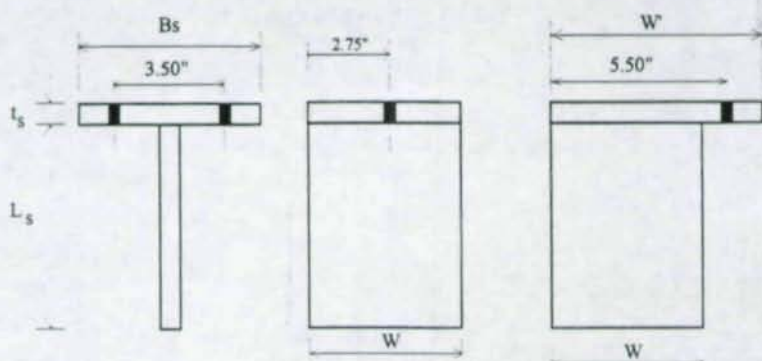


Figure 4. Stiffener Buckling

Table 2. Seat Dimensions for Phase Three Tests



Test	$t_s$ mm. (in.)	$L_s$ mm. (in.)	$W'$ mm. (in.)
1	9.5 (3/8)	203 (8)	W
2	9.5 (3/8)	406 (16)	W
3	9.5 (3/8)	203 (8)	178 (7)
4	12.7 (1/2)	203 (8)	178 (7)
5	19.0 (3/4)	203 (8)	178 (7)
6	9.5 (3/8)	203 (8)	W

All columns are W14x61  
 All stiffeners are 3/8"  
 W is 102 mm (4 in.) for all tests  
 $B_s$  is 152 mm (6 in.) for all tests

Table 3. Phase Three Test Results Compared with AISC Calculated Values

Test	$P_{Test}^*$	$P_{Calc.}$	$P_{Test}/P_{Calc.}$
1	592 kN (133.1 <sup>k</sup> )**	456 kN (102.6 <sup>k</sup> )	1.30
2	788 kN (177.2 <sup>k</sup> )*	1344 kN (302.2 <sup>k</sup> )	0.59
3	657 kN (147.6 <sup>k</sup> )	289 kN (65.0 <sup>k</sup> )	2.27
4	661 kN (148.7 <sup>k</sup> )	289 kN (65.0 <sup>k</sup> )	2.29
5	812 kN (182.5 <sup>k</sup> )	289 kN (65.0 <sup>k</sup> )	2.81
6	742 kN (166.9 <sup>k</sup> )	456 kN (102.6 <sup>k</sup> )	1.63

\* Stiffener buckled at 578 kN (130<sup>k</sup>)

\*\* No top angle used.

$P_{Test}$  = Failure load from tests.

$P_{Calc.}$  = Calculated weld failure load according to AISC procedure.  
 actual values with 3/8 in. x 5/16 in. welds:

## REFERENCES

1. Abolitz, A.L. and Warner, M.E., Bending under seated connections. *Engineering Journal*, 1965, Vol.2, No.1.
2. American Institute of Steel Construction, *Manual of Steel Construction, Load and Resistance Factor Design*, First Edition, Chicago, IL., 1986.
3. American Society of Civil Engineers, *Plastic Design in Steel*, New York, 1971.
4. Hoptay, J.M. and Ainso, H., An experimental look at bracket loaded webs. *Engineering Journal*, 1981, Vol.18, No.1.
5. Hopper, B.E., Batson, G.B. and Ainso, H., Bracket loaded webs with low slenderness ratios. *Engineering Journal*, 1985, Vol.22, No.1.
6. Packer, J.A. and Bruno, T., Behavior of bolted flange-plate connections in rectangular hollow tension members." Proceedings of the 10th Australasian Conference on Mechanics of Structures and Materials., 1986.
7. Ellifritt, D.S., and Sputo, T., "Stiffened Beam Seats on Wide-Flange Column Webs," Proceedings, 3rd International Conference on Steel Structures, Singapore, 1991.

## PARTIAL FIXITY FROM SIMPLE BEAM CONNECTIONS

Socrates A. Ioannides, Ph.D., S.E.<sup>1</sup>

### Abstract

The minimum connection stiffness required to produce a desirable reduction (say 20%) in the simple beam deflection is presented. New methodology, "the Visual Semi-rigorous Curve Fitting", is described and utilized to formulate and solve the problem. It is shown that for most "standard shear connections" this amount of reduction is achievable. Three different predictors for estimating the minimum connection stiffness required to produce this reduction are presented and their limitations explained.

### 1. INTRODUCTION

Serviceability design often controls the selection of steel beam sizes. In calculating deflections for simply supported beams (with standard shear connections at the ends) the rotational stiffness of the connections is usually ignored. Rigorous inclusion of semi-rigid connections in the analysis requires advanced computer software and Moment-Rotation properties which are usually not available to the average designer. Is there a simple way of accounting for partial fixity of these types of connections (Fig. 1) to approximate the resulting simple beam deflections? This question formed the basis for this study.

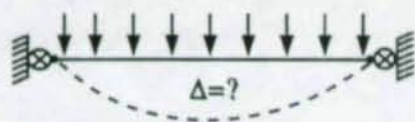
More than a decade ago, a fellow engineer (Ruddy 1984) suggested that he could design steel beams without referring to a steel manual for section properties. He used the following equation for allowable stress design:

$$Wt = M * 5.2 / d \quad (1)$$

---

<sup>1</sup> President, Structural Affiliates International, Inc.  
2424 Hillsboro Road, Nashville TN 37212; Tel (615) 269-0069

where:  $M$  = Moment in Kip.Ft  
 $d$  = Depth of beam in inches  
 $Wt$  = Weight of section in Lbs/Ft.



Is There a Simple Way to Approximate the Deflection of Simply Supported Beams, Taking Partial Fixity into Account?

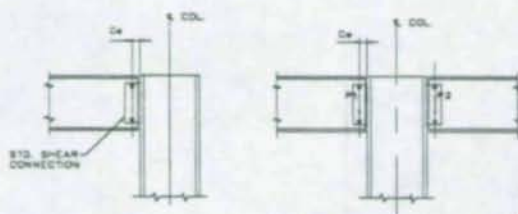


Figure 1: Partial Fixity of Simple Beam

This apparent oversimplification of the design process intrigued the writer and led to a computer program to evaluate its accuracy at that time. Impressed with the closeness of this approximation the writer has utilized this formula for preliminary designs ever since. Figure 2 shows a plot of the actual divided by the predicted moment capacity of all the sections in the AISC (1989) database.

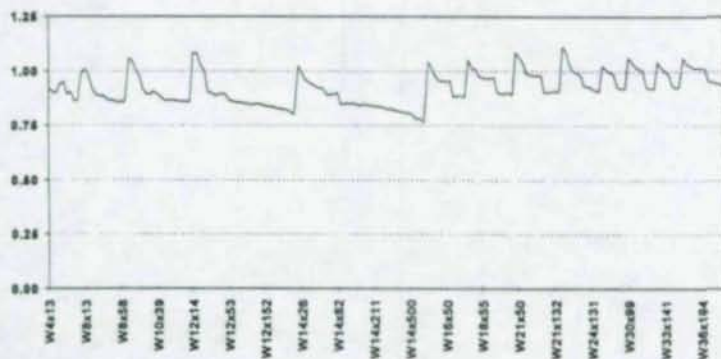


Figure 2: Calculated / Predicted Capacity ( $Wt = M \cdot 5.2 / d$ )

Armed with more appropriate computer tools such as spread sheets and charting / graph routines the writer developed a technique for generating such approximations for various aspects of the design of steel structures. This technique, coined "Visual Semi-rigorous Curve Fitting" was first presented by the author at the 1995 ASCE Structures Congress (Ioannides 1995) and will again be briefly explained throughout this paper.

The original question has been reformulated to the following:

**"What are the minimum connection properties that would produce at least 20% reduction in the simple beam deflection?"**

The goals for this effort were thus defined as follows:

- Develop a simple predictor expression (similar to  $Wt = M \cdot 5.2 / d$ ) for the minimum connection stiffness required to produce a 20% reduction in the simple beam deflection.
- Utilize simple Visual Semi-Rigorous Curve-Fitting.

## 2. BACKGROUND AND DEVELOPMENT

A method for predicting the amount of deflection reduction when semirigid connections with known stiffness are utilized has been developed by Geschwindner (1991). The resulting equation is:

$$\frac{D_{-m}}{D} = \frac{4}{5 \cdot (2u + 1)} \quad (2)$$

Where:	n	=	Connection Stiffness
	u	=	(EI/L) / n
	D	=	Simple Beam Deflection
	D <sub>m</sub>	=	Reduction of Simple Beam Deflection

The variation of  $D_{-m}/D$  with respect to the stiffness ratio (u) is graphically depicted in Figure 3.

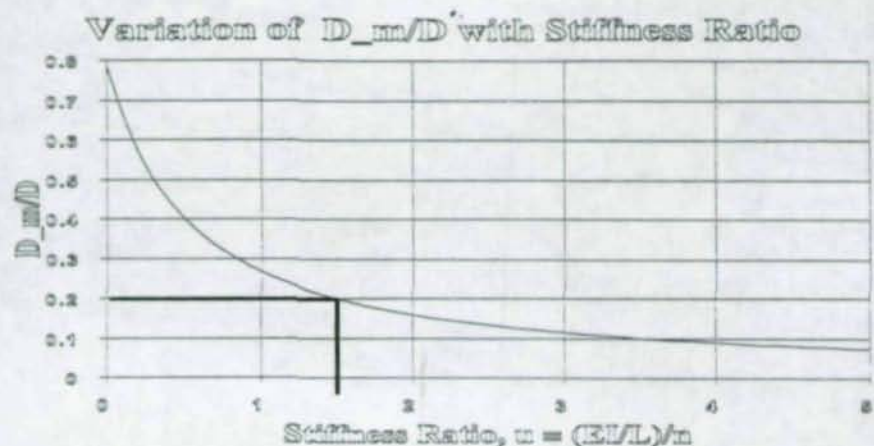


Figure 3: Variation of Reduced Deflection Ratio with Stiffness ratio

The end rotation of a simply supported beam under uniformly distributed load is given by the following equation:

$$\theta_s = \frac{WL^2}{24EI} \text{ or } \frac{ML}{3EI} \quad (3)$$

Assume  $L/d = 800/f_y$  (AISC max.) then

$$L = \frac{800d}{f_y} \quad (4)$$

Also,  $M = S f_b$  and  $I = S \cdot \frac{d}{2}$  (5)

Further, assume the allowable bending stress is:

$$f_b = 0.6 \cdot f_y \quad (6)$$

Substituting equations (4), (5) and (6) into equation (3)

$$\theta_s = \frac{S \cdot (0.6 f_y) \cdot \frac{800d}{f_y}}{3 \cdot 29000 \cdot S \cdot \frac{d}{2}} = 0.011 \text{ rad} \quad (7)$$

In the forgoing development all symbols represent the standard AISC definitions.

A typical moment-rotation curve is shown in Figure 4 superimposed with the beam line which shows the simple beam rotation of 0.011 radians and a fixed moment of  $WL/12$ . The connection stiffness "n" is defined as the secant stiffness of the moment-rotation curve at the intercept with the beam line. For further development, assume that the rotation at this point ( $\vartheta_c$ ) is approximately equal to 0.01 radians.

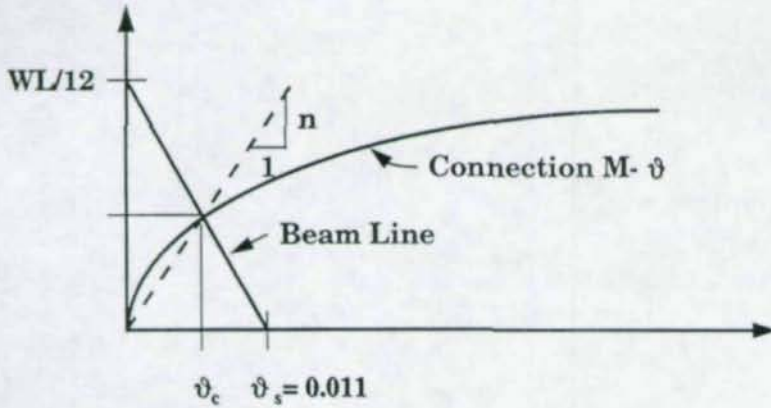


Figure 4: Typical Moment-Rotation Curve

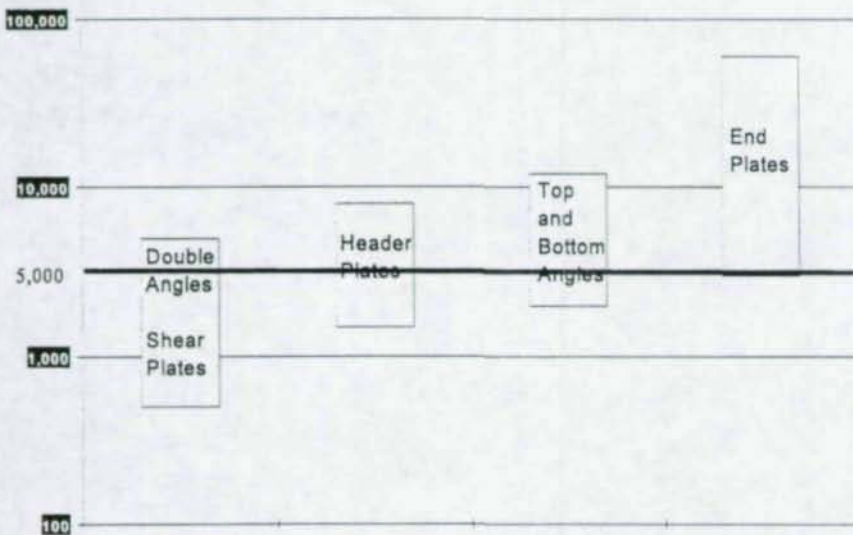


Figure 5. Typical Connection Stiffness (K.Ft./rad) @ 0.01 rad)

Non-availability of moment-rotation curves still remains the major hurdle in the utilization of semi-rigid connections by designers. Ioannides (1978) presented results for end plate connections and Goverdhan (1983) presented a compilation of all available tests at that time as well as simple predictor equations for different types of connections. These connections varied from the most flexible (double angles) to the most rigid (end plates). A visual scan of the reported results resulted in the range of stiffness at a rotation of 0.01 radians indicated in Figure 5. As may be seen it is not difficult to achieve a stiffness of 5,000 K.Ft./rad. by almost any type of connection. Does this minimum stiffness produce 20% reduction in the simple beam deflection?

### 3. PROCEDURE

#### 3.1. Visual Semi-rigorous Curve Fitting

This method (Ioannides, 1995) is a simple curve fitting technique that relies on visually matching the exact results from a design procedure to a predictor equation. The X-axis of the chart is composed of the sizes of the sections in the data base. The Y-axis represents the calculated values. Components of the predictor equation are selected by comparing the resulting shape of the exact solution to the shape of certain properties of the sections included in the data base, such as weight, depth, flange width etc. The property whose shape most closely matches the exact solution is first included in the predictor.

The exact solution is then divided by the predictor and a new curve plotted. By visually observing the resulting shape, different powers of the selected property may also be investigated in an attempt to arrive at as straight a line as possible, with a slope of zero. The procedure is then repeated by including other section properties until the desired accuracy is achieved. Once a "straight line with zero slope" is achieved, a final numerical correction factor is included in the predictor such that the exact/predictor capacities values are always less than unity.

In choosing properties to be included in the predictor equation an attempt is made to utilize readily remembered properties such as the weight per foot, depth, flange width, etc. Also, simplification of the resulting equation (easily remembered) is usually favored over more accurate complex expressions.

### 3.2. Application to this Problem

The above described method was used to develop simplified predictor equations for the minimum connection stiffness required to produce 20% reduction in the simple beam deflection. The following assumptions were made:

- $f_y = 36$  Ksi
- $L = 22.2d$  ( $800d/f_y$ )
- $n = 1000$  to  $100,000$

For all sections in the AISC database, and for the range of stiffness "n" defined above, the stiffness ratio "u" is calculated.  $D_m/D$  is then calculated and the results are plotted (Fig. 6).

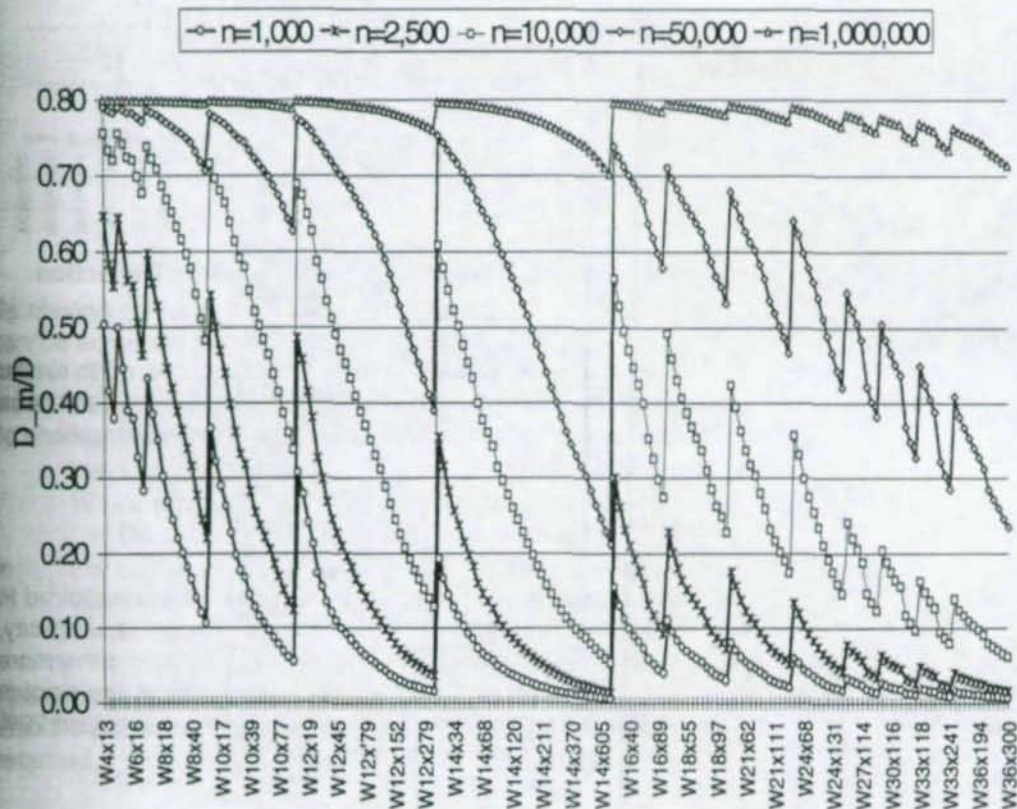


Figure 6:  $D_m/D$  variation with "n"

The value of "n" producing 20% reduction in simple beam deflection is also calculated and plotted (Fig. 7).

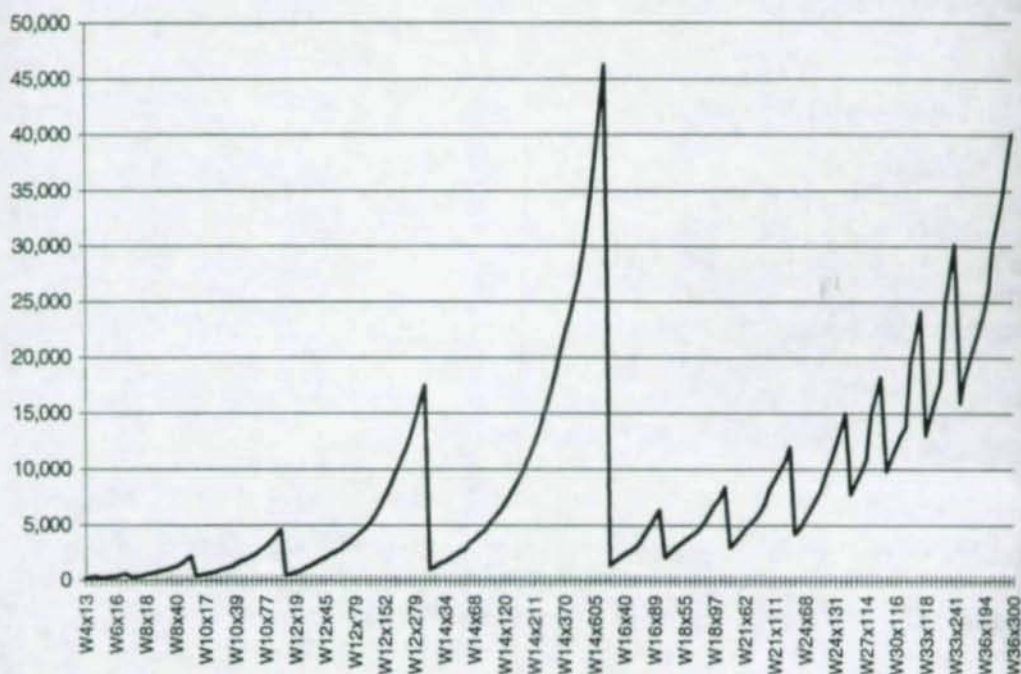


Figure 7: Value of "n" Producing 20% Reduction in Simple Beam Deflection

The shape of the resulting curve in Figure 7 is visually examined and compared to similar curves plotted for the different properties of the database sections (these have not been included here for brevity). The final predictor equation, chosen after several iterations of the Visual Semi-rigorous Curve Fitting algorithm, is:

$$n = 3 \cdot Wt \cdot d \quad (8)$$

Figure 8 shows the comparison of predicted vs. actual connection stiffness required to produce 20% reduction in the simple span moment. As may be seen, despite its simplicity, the predictor approximates the exact results to within approximately 20%. Furthermore since the independent variables are the weight per foot and the depth of the section (parameters always known), the minimum connection stiffness required to produce 20% reduction in the simple beam deflection can easily be calculated.

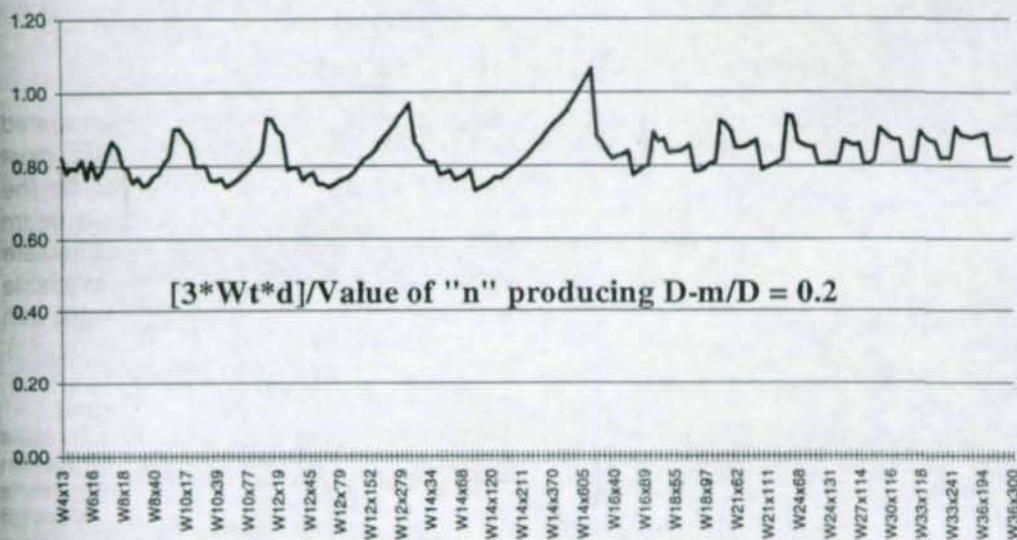


Figure 8: Predicted Vs Calculated "n"

#### 4. RESULTS

By observing Figure 6 it can be deduced that 20% reduction in the simple beam deflection can be achieved for the following conditions:

- For all sections in the database if connection stiffness "n" is greater than 50,000 K.Ft./rad. Although this is a very simple predictor it is too restrictive. Furthermore, the shapes that require the highest connection stiffness are the heaviest of the W14's (usually column shapes) and the heaviest of the W36's.
- For sections that weigh 70 Lbs./Ft. or less "n" must be at least 3,000 K.Ft./rad. As may be seen from Figure 5, this is the average stiffness of the most flexible type of shear connection.

The two predictors above may be used where applicable. If more accuracy is required, then the predictor equation (Equation 8) may be used to calculate the minimum stiffness required.

## 5. CONCLUSIONS

The "Visual Semi-rigorous Curve Fitting" technique has been explained and demonstrated for the specific problem at hand. Three different predictors (from the simplest, most restrictive to the still simple, but more encompassing) have been presented for the minimum connection stiffness required to produce 20% reduction in the simple beam deflection. The methodology and development presented can be utilized to reformulate the problem for any reduction in the simple beam deflection. Use of readily available computer software, in conjunction with this methodology and engineering judgement, can produce simple solutions to difficult engineering problems.

## 6. REFERENCES

- AISC (1989). American Institute of Steel Construction Manual of Steel Construction Allowable Stress Design, 9th ed.
- Geschwindner, L. F. (1991). "A Simplified Look at Partially Restrained Beams." Engineering Journal of American Institute of Steel Construction, Inc. vol. 28, p. 73-78.
- Goverdhan, A. V. (1983). "A Collection of Experimental Moment-Rotation Curves and Evaluation of Prediction Equations for Semi-Rigid Connections." Ph.D. Dissertation, Vanderbilt University, Nashville, Tennessee, 1983.
- Ioannides, S. A. (1978). "Column Flange Behavior in Bolted End Plate Moment Connections." Ph.D. Dissertation, Vanderbilt University, Nashville, Tennessee, 1978.
- Ioannides, S. A. (1995). "Minimum Eccentricity for Simple Columns?" Proceedings American Society of Civil Engineers Structural Division, Structures Congress XIII, vol. 1, pp. 349-352.
- Ruddy, J. (1984). Unpublished personal communication.

ESTIMATES OF DUCTILITY REQUIREMENTS  
FOR  
SIMPLE SHEAR CONNECTIONS

W. A. Thornton<sup>1</sup>

Abstract

Simple Shear Connections must often be designed to accommodate some axial forces in addition to shear. These axial forces can be code required tying or robustness forces, or actual calculated forces. These axial forces tend to make shear connections less flexible to simple beam end rotation. This paper develops formulas which can be used to determine if this reduced flexibility will lead to progressive fracture of the connection.

**I. INTRODUCTION**

As its name implies, a simple shear connection is intended to transfer shear load out of a beam while allowing the beam end to rotate without significant restraint. The most common simple shear connections are the double clip, Fig. 1, the shear end plate, Fig. 2, and the tee, Fig. 3. This paper will deal with the ductility requirements for these connections.

**2. GENERAL**

Under shear load, these connections are flexible regarding simple beam end rotation because there is an element of the connection which while remaining stiff in shear has little restraint to motion perpendicular to its plane. This is an angle leg for the double clips, a plate for the shear end plate, and the tee flange for the tee connection. There are shown in Figs. 1-3 where the thickness  $t$  and the leg width  $b$  are the fundamental variables. When these connections are subjected to axial loads, either calculated or from code required "robustness", considerations, the important limit states are angle leg bending and prying action. These tend to require the thickness  $t$  to increase or the leg width  $b$  decrease, or both, and these requirements compromise the connection's ability to remain flexible to simple beam end rotation. This lack of connection flexibility causes a tensile load on the upper bolts (field bolts for the double clips and shear end plate, shop bolts for the tee) or the upper part of the welds. This tensile load could lead to fracture of the bolts or welds and to a progressive failure of the connection and the resulting collapse of the beam. To the author's knowledge, there has never been a reported failure of this type, but is perceived to be possible.

---

<sup>1</sup> Chief Engineer, Cives Steel Company, Roswell, Georgia, U.S.A.

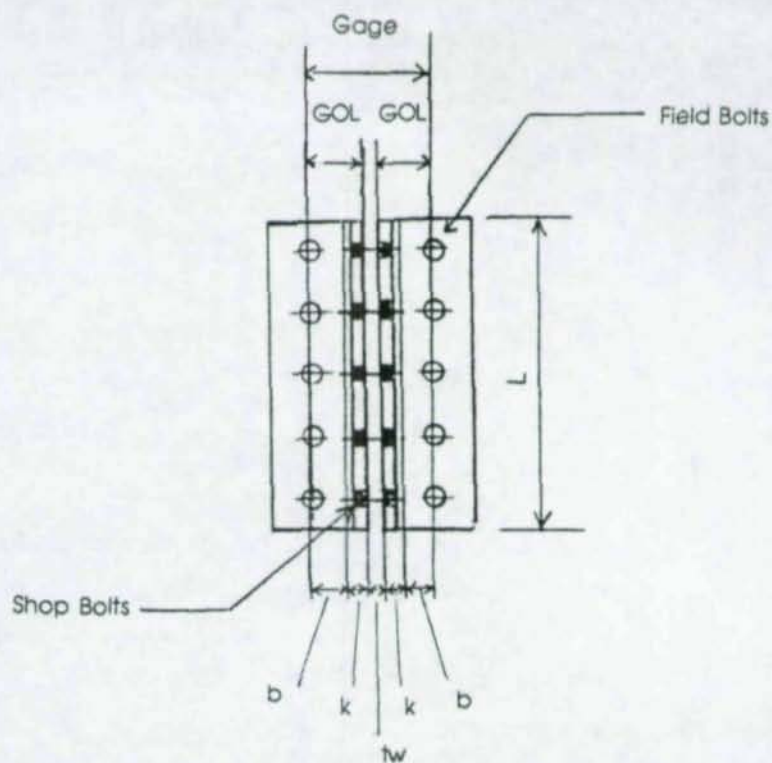


**Fig.1. Geometry of double angles (shop bolted down).**

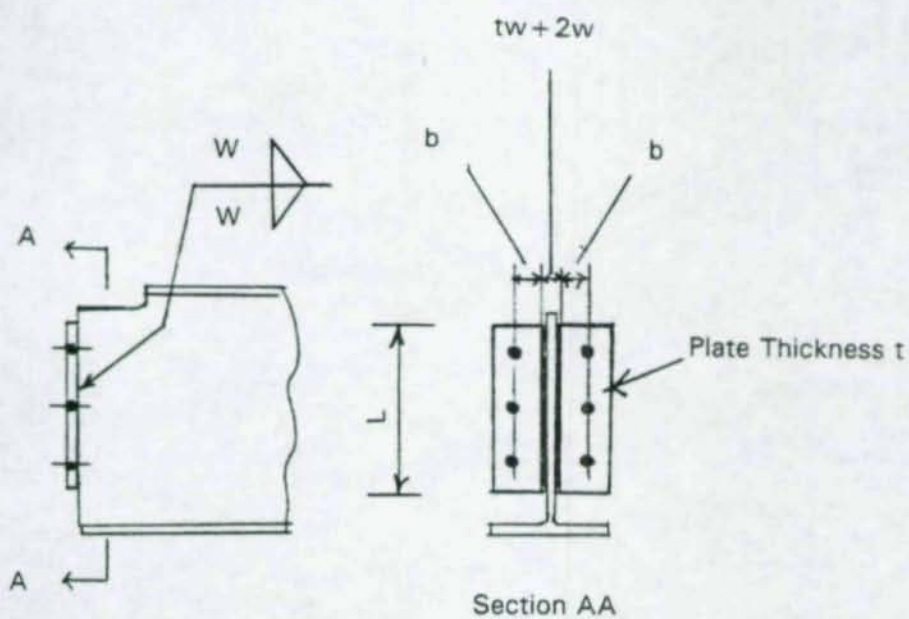


**Fig.2. Shear end plate connection.**

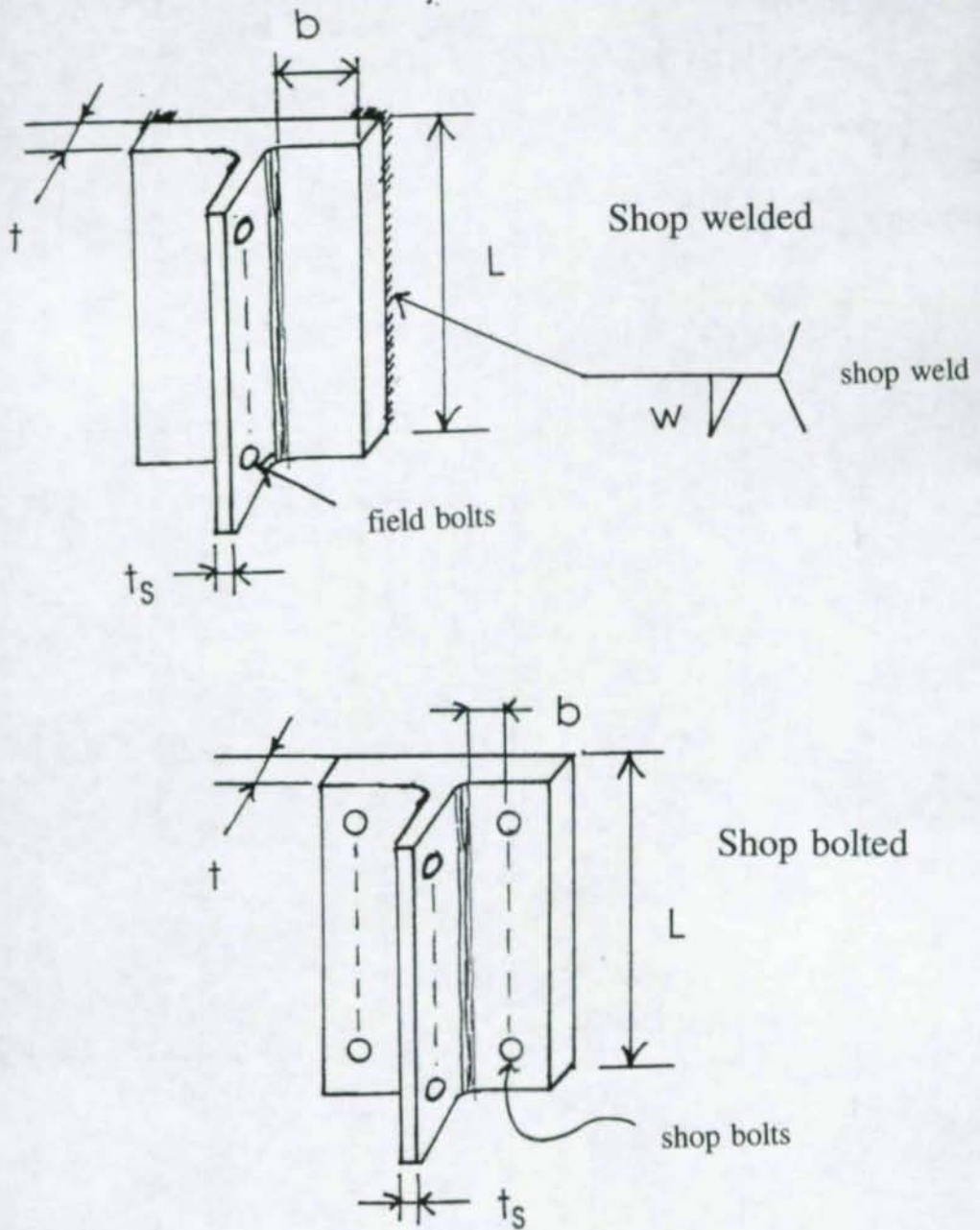


Fig.3. Tee shear connections.

## 3. THEORY

As the beam end rotates under gravity loads a moment will be induced by the stiffness of the angle leg, end plate, or tee flange. Based on yield line theory, a formula for the maximum possible moment that can be induced by the connection has been given by Thornton (1995) as

$$M = \frac{1}{2} F_y \frac{L^2 t^2}{b} \left( \frac{b^2}{L^2} + 2 \right) \quad 1$$

where  $F_y$  is the material yield strength and the remaining parameters are defined in Figs. 1 - 3. Data are available to test the efficacy of this formula from Lewitt, Chesson, and Munse (1969) for double angles and from Astaneh and Nader (1988, 1989) for tees. Table 1 compares the moment calculated from Eq. 1 with the experimental moments obtained by Lewitt, et al, at a simple beam end rotation  $\phi$  of 0.03 radian. This rotation is chosen as the maximum a beam end connection need be subjected to because it exceeds the beam end rotation for most beams when a plastic hinge forms at the center. Table 1 shows that Eq. 1 provides an excellent estimate for the beam end moment induced by the connection. Eq. 1 provides a fairly tight upper bound to the experimental results, and so provides a safe estimate of the maximum connection induced moment. Table 2 compares the moment of Eq. 1 with the experimental moments for tee connections obtained by Astaneh and Nader. Here, the experimental moments are given for rotations of 0.03 radian and 0.07 radian (except test No. 4, which is given at 0.06 radian). Except for test No. 1, Eq. 1 is seen to overestimate the induced moment at 0.03 radian. Eq. 1 also generally over-estimates the moment at the very large rotation of 0.07 radian. Thus it can be said that Eq. 1 is not a tight upper bound to the experimental data, and therefore will yield very safe estimates for the maximum connection induced couple.

Using Eq. 1, the following requirements can be derived (Thornton, 1995) for the minimum weld and bolt sizes to resist progressive failure by fracture:

For the bolts subjected to tension due to connection rigidity

$$d_{\min} \geq \sqrt{\frac{5p}{2\pi}} \frac{F_y}{F_{ut}} t \sqrt{\frac{\eta^2 + 2}{b}} \quad 2$$

and for the welds

$$w_{\min} \geq \frac{5\sqrt{3}}{8} \frac{F_y}{F_{\text{exx}}} \frac{t^2}{b} (\eta^2 + 2) \quad 3$$

In the above expressions

$d_{\min}$  = min. bolt diameter

$F_y$  = material yield strength

$F_{ut}$  = bolt tensile strength adjusted to gross area

**Table 1 Theoretical and Experimental Connection Couples  
(Bolted and Riveted Double Angles)**

Specimen	Angle Properties					$\frac{V}{k/in.}$ Eq. 1	Theoretical M (Eq. 2) k-in.	Experimental M (Lewitt, Chesson, & Munse) @0.03 Radian k-in.
	$E_v$ ksi.	$\frac{t}{in.}$	$L$ in.	$b^{(1)}$ in.	$\frac{r}{b/L}$			
FK-3	39.3	0.354	8 <sup>1/2</sup>	1.771	0.2084	2.841	205	170
FK-4AB	39.3	0.354	11 <sup>1/2</sup>	1.708	0.1486	2.915	385	330
FK-4P	39.3	0.354	11 <sup>1/2</sup>	1.708	0.1486	2.915	385	330
WK-4	39.3	0.354	11 <sup>1/2</sup>	1.708	0.1486	2.915	385	320
FK-4AB-M	41.6	0.375	11 <sup>1/2</sup>	1.6875	0.1467	3.504	463	370
FB-4	38.8	0.371	11 <sup>1/2</sup>	1.8165	0.1580	2.9767	394	330
FB-4A	38.8	0.371	11 <sup>1/2</sup>	1.8165	0.1580	2.9767	394	330 <sup>(2)</sup>
FK-5	38.8	0.443	14 <sup>1/2</sup>	1.6195	0.1117	4.4872	943	810
WB-10AB	40.1	0.440	29 <sup>1/2</sup>	1.7475	0.0592	4.4503	3873	3,500 <sup>(2,3)</sup>

<sup>(1)</sup>  $b = (5^{1/2} \cdot t_w(\text{beam})) / 2 \cdot k$

<sup>(2)</sup> Slip between clip angles and beam web not included

<sup>(3)</sup> Extrapolated from Fig. B35 of Lewitt, Chesson and Munse

$F_{\text{exx}}$  = weld tensile strength

$\eta = b/L$

$p$  = bolt pitch

$L$  = length of connection (see Figs. 1 -3 )

$b$  = bending length (see Figs. 1-3)

$w_{\text{min}}$  = min. weld leg size

$t$  = thickness of angle leg, tee flange, or load plate.

Note that Eqs. 2 and 3 are valid in all unit systems and for both allowable stress design (ASD) and ultimate strength or limit states design (LRFD).

#### 4. APPLICATIONS

In US customary units, Eqs. 2 and 3 become, for ASTM A36 connection material, A325 bolts, E70 electrodes, and  $p = 3$  inches:

$$d_{\text{min}} \geq 0.978t \sqrt{\frac{\eta^2 + 2}{b}} \quad 4$$

$$w_{\text{min}} \geq 0.557 \frac{t^2}{b} (\eta^2 + 2) \quad 5$$

##### 4.1 Double Angles

Eq. 4 can be used to develop Table 3 which gives minimum angle thicknesses and bolt diameters. Table 3 can be seen to validate a long standing (since 1970) American Institute of Steel Construction (AISC 1970, 1994) recommendation that for double clip angle framing connections, the angle thickness should not exceed 5/8 inch for the usual gages and bolt sizes.

##### 4.2 Tee and Shear End Plate Connections

Tables similar to Table 3 for double angles can be developed for these connections.

#### 5. Conclusion

Formulas have been presented which can be used to determine if a simple shear connection is sufficiently flexible to preclude over loading the less ductile elements of the connections, i.e., the field bolts of Figs. 1 and 2, and the shop bolts or shop welds of Fig. 3. It was noted above that these formulas are valid for all design methods. It should also be recognized that these formulas provide a test criterion against which a connection can be checked for ductility. They do not provide a design of a connection for specific applied loads. Connection design would be performed in the usual manner for specified shears and axial forces.

**Table 2 Theoretical and Experimental Values of Connection Couple (Shop Welded WT)**

Test No.	Section	L in.	t in.	$b_f$ in.	$k_f$ in.	$b^{(1)}$ in.	Theoretical M	Experimental M	
							(Eq. 2) $F_y = 44.77$ k-in.	(Astaneh & Nader) @ $\theta = .03$ @ $\theta = .07$ k-in. k-in.	
1	WT4x7.5	8.5	0.315	4.00	1/2	1.5	217	180 <sup>(4)</sup>	223
2	WT7x19	14.5	0.515	6.77	5/8	2.76	921	300 <sup>(4)</sup>	533
3	WT7x19	8.5	0.515	6.77	5/8	2.76	327	110 <sup>(4)</sup>	218
4	WT4x7.5	14.5	0.315	4.00	1/2	1.5	626	370 <sup>(4)</sup>	413 <sup>(5)</sup>
5	WT4x20	14.5	0.56	8.07	5/8	3.4	890	250 <sup>(4)</sup>	479 <sup>(5)</sup>
6	WT4x20	8.5	0.56	8.07	5/8	3.41	321	50 <sup>(4)</sup>	227
7	WT7x19 <sup>(2)</sup>	14.5	0.515	6.77	1/2 <sup>(3)</sup>	2.89	881	290 <sup>(4)</sup>	683
8	WT4x20 <sup>(2)</sup>	8.5	0.56	8.07	1/2 <sup>(3)</sup>	3.53	312	30 <sup>(4)</sup>	228
9	WT4x20 <sup>(2)</sup>	14.5	0.56	8.07	1/2 <sup>(3)</sup>	3.53	861	440 <sup>(4)</sup>	748

<sup>(1)</sup>  $b = b_f/2 - k_f$

<sup>(2)</sup> With stem replaced with 1/2 A36 plate, 1/4 fillet welds

<sup>(3)</sup>  $k_f = 1/4 + 1/4 = 1/2$

<sup>(4)</sup> Estimated from Fig. 4.5 of Astaneh & Nader (1988) or Fig. 11 of Astaneh & Nader (1989).

<sup>(5)</sup> 47.9 in original. Data assumed corrupt.

<sup>(6)</sup> Value is for 0.06 radian.

**Table 3**

Estimated Minimum Angle Gages (GOL) for A36 Angles and A325 Bolts for Rotational Flexibility

ANGLE THICKNESS (in.)	Minimum Gage of Angle (GOL) <sup>a</sup>		
	$\frac{3}{4}$ in. dia. bolt (in.)	$\frac{7}{8}$ in. dia. bolt (in.)	1 in. dia. bolt (in.)
$\frac{3}{8}$	$1\frac{3}{8}$	$1\frac{1}{4}$	$1\frac{1}{8}$
$\frac{1}{2}$	$1\frac{7}{8}$	$1\frac{5}{8}$	$1\frac{1}{2}$
$\frac{5}{8}$	$2\frac{1}{2}$	$2\frac{1}{8}$	$1\frac{7}{8}$
$\frac{3}{4}$	$3\frac{1}{4}$	$2\frac{11}{16}$	$2\frac{5}{16}$
1	6	$4\frac{5}{16}$	$3\frac{1}{2}$

<sup>a</sup> Driving clearances may control minimum GOL. GOL is defined in Fig. 1.

## REFERENCES

1. Astaneh, A., and Nader, M. N. (1988), "Behavior and Design of Steel Tee Framing Shear Connections," Department of Civil Engineering, University of California, Berkeley, Report to Sponsor, AISC, July.
2. Astaneh, A., and Nader, M.N., (1989) "Design of Tee Framing Shear Connections, **AISC Engineering Journal**, 1st Quarter, Vol. 26, No. 1, pp. 9-20.
3. American Institute of Steel Construction, AISC, 1970, **Manual of Steel Construction**, Seventh Ed., p. 4-12.
4. American Institute of Steel Construction AISC (1994), **Manual of Steel Construction, LRFD**, 2nd Ed., Vol. II, Connections, p 9-12.
5. Lewitt, C.S., Chesson, E., Jr., and Munse, W. H., (1969), "Restraint Characteristics of Flexible Riveted and Bolted Beam to Column Connections," University of Illinois Engineering Experiment Station Bulletin 500, Vol. 66, No. 63, Jan.
6. Thornton, W.A. (1995), "A Rational Approach to Design of Tee Shear Connections," **AISC Engineering Journal**, Vol. 32, No. 2 (2nd Qtr.), AISC, Chicago, IL, USA.

## PLASTIC DESIGN OF SEMI-RIGID FRAMES

Roberto T. Leon<sup>1</sup>

Jerod J. Hoffman<sup>2</sup>

### Abstract

Checks for ultimate strength of frames with partially restrained connections require that the non-linear connection characteristics and the P- $\Delta$  effects be appropriately modelled. This complexity is unwarranted for preliminary design but few alternatives exist. In this paper an alternate approach, utilizing a second-order plastic analysis method called the mechanism curve (Horne and Morris, 1982), is described. This approach results in a simple and reliable estimation of the collapse capacity of the frame. It was found that this ultimate capacity seldom controls since limitations of drift at service loads results in *strong, stiff structures that provide an adequate safety margin against stability failures.*

### 1. INTRODUCTION

In the U.S.A. the widespread use of frames with partially restrained (PR) connections has always been hampered by the perceived complexity of the analyses required and by the onerous provisions imposed on the design engineer by current codes (AISC, 1994). Amongst the latter are the general requirements that the engineer demonstrate both that the connection is capable of providing some minimum proportion of fixed end restraint and that the non-linear moment-rotation ( $M-\theta$ ) characteristics of the connection be taken into account in the analysis. Even if the designer were able to surmount these obstacles, he/she often finds that the remaining, more prescriptive clauses of the specifications do not provide any guidance on how to handle the effects of PR connections on issues such as stability or serviceability calculations. The net result is that in the United States, almost fifty years after their introduction into the specifications, only a handful of design firms have developed the in-house capability to analyze and design PR frames.

---

<sup>1</sup> Professor, School of Civil and Environmental Engineering, Georgia Institute of Technology, Atlanta, GA 30332.

<sup>2</sup> Structural Engineer, Meyer, Borgman and Johnson, Inc., Minneapolis, MN.

However, there are powerful economic incentives and inherent structural behavior advantages for promoting the use of PR frames. In both braced and unbraced frames, PR connections can lead to substantial savings in the gravity load systems and to improved serviceability behavior (Leon, 1994). In unbraced frames subjected to seismic loads, the contribution of partially restrained, partial strength (PR/PS) connections can result in increases in ductility and energy dissipation as well as lower design forces due to period shifts (Nader and Astaneh, 1992; Leon and Shin, 1994). Perhaps the strongest endorsement for PR frames stems from their role as a backup structural system in many of the rigid frames damaged during the 1994 Northridge earthquake (Bertero et al., 1994). It is clear from preliminary assessments that many of the so-called shear connections present in these structures behaved as PR ones due to the influence of the floor slabs. These PR connections were able to dissipate energy and control drift even after a large number of fully rigid (FR) connections had failed. The role of PR/PS connections in seismic design is bound to increase as our understanding of these failures improves since the need to limit the strength and ductility demand on columns seems clear.

The design of PR braced frames is straight forward (Leon and Ammerman, 1990). The design of PR unbraced frames, on the other hand, presents very challenging obstacles, ranging from the level of analysis required to the detailing of the connections themselves. Recently the authors have proposed a two-level design approach for PR unbraced frames (Hoffman, 1994). The first level, to be used for all serviceability checks and for ultimate strength under wind loads, involves analysis utilizing linear springs with a reduced secant stiffness. The second level, to be used for ultimate strength checks under seismic loads, involves a preliminary plastic analysis approach followed by a more exact final analysis. The latter can range from a push-over analysis for simple, regular structures to a complete inelastic, second-order analysis for critical, irregular structures.

The reader should recognize that under the new, unified seismic design provisions that will be enforced in the U.S. by 1998 (ASCE, 1993; NEHRP, 1994) vast parts of the U.S. will require a minimum level of seismic design and detailing even for buildings whose overall design is controlled by wind or other lateral forces. Thus PR frames can make significant inroads into practice if design methodologies are available to structural engineers once these provisions are enforced. This paper will discuss one such methodology, a two-level approach for design of PR/PS frames. The first level will be discussed briefly in the next section, but the paper will concentrate on the plastic designs aspects of the second level. In keeping with the senior author's biases, the approach assumes the use of unbraced frames, unshored composite construction, and design at ultimate governed by seismic loading.

## 2. PRELIMINARY DESIGN

In the context of this paper, the purpose of a preliminary design is to provide a complete set of beam, girder, column and connection sizes from which a more rigorous analysis and design of the frame can proceed. For the case of regular frames (equal bays and equal story heights) the preliminary design procedure proposed here will result in element

sizes very close to optimal and thus minimize design iterations.

In the preliminary design the size of the steel beams and girders will be fixed by the strength required during construction since unshored erection is assumed. These sections will provide more than ample capacity to resist the design live loads once the composite action and continuity provided by the connections are achieved. In fact for many of the beams and girders only partial composite action will be required. However, it is recommended that enough studs for full composite action be provided in all girders and that no less than 50% composite action be used in the beams in order to reduce hysteretic degradation under cyclic loads.

The column sizes and stiffness of the connections will be dictated by the need to limit the drift under wind loads. Although no specific limits are given by American codes, most designers assume a maximum story drift of 0.25% ( $h/400$ ) for preliminary design purposes. For the case of PR frames, the story drift can be computed as:

$$\Delta = \frac{V_i h_i^2}{12 E} \left( \frac{1}{\sum K_{g,i}} + \frac{1}{\sum K_{c,i}} + \frac{12 E}{\sum K_{conn,i}} \right) \quad (1)$$

where,  $V_i$  is the story shear for story  $i$ ,  $h_i$  is the story height for story  $i$ ,  $E$  is the modulus of elasticity,  $K_{g,i}$  is the product of  $I_g/L_g$  for each girder at level  $i$ ,  $K_{c,i}$  is the product of  $I_c/h$  for each column at level  $i$ ,  $K_{conn,i}$  is the stiffness for each connection at level  $i$ ,  $L_g$  is the bay length, and  $I_c$  and  $I_g$  are the inertias of the columns and girders respectively.

This formula is a straight forward modification of the one commonly used for rigid unbraced frames. Previous studies have shown that for composite girders under lateral loads an equivalent girder stiffness ( $I_{g,eq}$ ) can be used instead of  $I_{g,i}$  in Equation (1). This equivalent stiffness can be approximated by:

$$I_{g,eq} = 0.6 I_{pos} + 0.4 I_{neg} \quad (2)$$

where  $I_{neg}$  is the inertia of the steel beam plus slab steel and  $I_{pos}$  is the inertia of the composite section. Values of  $I_{neg}$  and  $I_{pos}$  for common sections can be found tabulated in many design manuals. In general it should be assumed in calculating  $I_{neg}$  that the effective width of the slab is only about 2 m (80 in.) since it is difficult to activate bars farther away at low levels of drift.

Equation (1) indicates that the additional flexibility provided by the connections in a PR frame needs to be compensated by engaging more frames in resisting the lateral loads. In fact, in PR frames the intention should be that all frames in the structure participate in resisting lateral loads since the additional redundancy and lack of leaner columns results in a safer system. The only alternative, if the same number of frames is used in a PR frame as in the prototype FR one, is to use larger girders and/or columns to compensate for the additional connection flexibility. From the structural and economic standpoint this alternative is unreasonable.

Activating all the frames in the system is not as uneconomical as it would seem at a first look for two reasons. First, the composite connections envisioned for use as PR/PS ones only require some additional slab steel and do not necessitate any special detailing or quality control as fully welded FR connections would (Leon, 1994). Thus the total cost of the PR connections is probably lower than that of a few, expensive FR ones. Second, the composite action of the floor system significantly increases the stiffness of the girders, resulting in a decrease of the lateral drift.

For preliminary design it is recommended that the three components of deflection (beam, columns, and connections) contribute similar amounts to the overall drift. However, since the girder sizes have already been determined by the construction loads, their contribution to drift (the first term in parenthesis in Equation (1)) can be calculated. If the girders' contribution to the story drift is less than  $\Delta/3$ , the difference should be split between columns and connections. If the girder drift contribution is more than  $\Delta/3$ , then their size should be increased so that the drift components are balanced. From Equation (1) and assuming that the columns will take a certain proportion of the total  $\Delta$  and knowing the story height, the required column size can be calculated easily.

The remaining portion of  $\Delta$  has to be taken by the connections. It is assumed that a  $M-\theta$  relationship for the PR/PS connections is available (Leon, 1994). It is recommended that the connection stiffness be calculated as the secant stiffness at a nominal rotation of 0.002 radians. This is a conservative assumption since actual rotations of the connections at service loads seldom exceed 0.0015 radians. From this connection stiffness and the variables in the  $M-\theta$  equations the detailing of the connections can proceed.

### 3. PLASTIC ANALYSIS

Once the preliminary sizes for a frame have been established and drift criteria at service level satisfied, it is necessary to determine the ultimate strength of the frame. The ultimate strength is generally controlled by a set of equivalent lateral loads that simulate the seismic or wind action actions. If the wind forces govern, then an analysis for the factored loads utilizing linear springs as described above should be carried out. The connection rotations should be carefully checked to insure that they have not exceeded the rotations assumed in computing the secant stiffness. In addition a minimum level of seismic detailing should be provided depending on the importance of the structure and the PGA specified for the site. For composite PR frames governed by seismic actions, the elastic seismic forces are reduced by a factor ( $R$ ) equal to 6 while the elastic drifts are increased by 5.5 to account for inelastic action and damping (NEHRP, 1994).

For the ultimate strength case it is necessary to account in the analysis for the non-linearity of the connections and the second-order effects (stability). The latter are perceived as particularly important for PR frames because of the additional flexibility

provided at the connections. The analysis required is not trivial since even for the equivalent lateral loads used in preliminary design a non-linear analysis program that accounts for leaner column effects would be required. Even if a program were available and it contained advanced pre- and post-processors, the checking of the input and output is time consuming and only gross errors are usually spotted. In addition, any redesign would require substantial additional design time.

In order to bypass the complications described above, it was decided that a second-order plastic analysis approach should be explored. Plastic analysis can easily account for semi-rigid connections if care is exercised in estimating the deflections at collapse (Neal, 1956). From a first-order plastic analysis the collapse load factor ( $\lambda_p$ ) for a PR/PS frame assuming a sidesway mechanism (Fig. 1) is given by:

$$\lambda_p = \frac{\sum M_{hinges}}{\sum P_i H_i} \quad (3)$$

where,

$$\begin{aligned} \sum M_{hinges} = & (N+1) M_{p,col} + ((N-1) * S) (M_{p,conn}^+ + M_{p,conn}^-)_{inte} \\ & + (S) (M_{p,conn}^+ + M_{p,conn}^-)_{exte} \end{aligned} \quad (4)$$

and  $N$  is the number of bays,  $S$  is the number of stories,  $P_i$  and  $H_i$  are the concentrated lateral loads and heights at each story, the superscripts "+" and "-" refer to the capacity in positive and negative bending, and the subscripts "inte" and "exte" refer to the exterior and interior connections.

The second-order effects need to be included, since the rigid-plastic collapse load factor is likely to substantially overestimate the actual collapse load (Fig. 2(a)). After investigating several possibilities, the mechanism curve method proposed by Horne and Morris was selected (Horne and Morris, 1973, 1982).

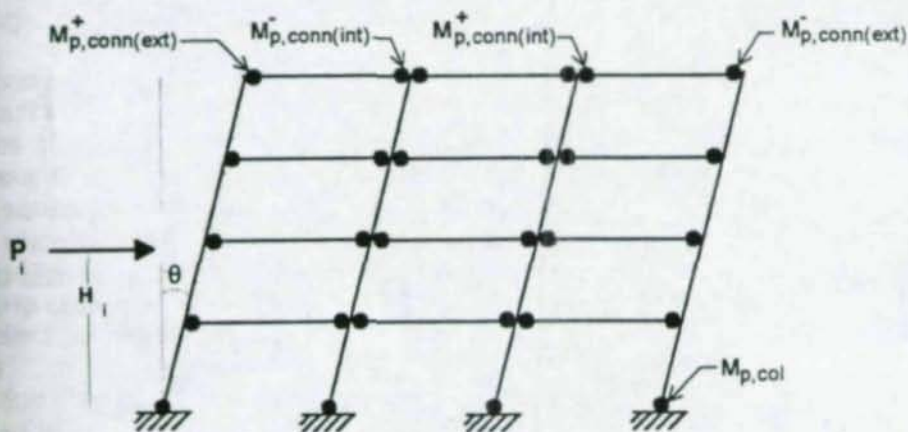


Figure 1 - Sidesway mechanism.

In this method the influence of the axial loads (Fig. 2(b)) results in a collapse load factor  $\lambda_k$  which is a function of the rigid plastic collapse load ( $\lambda_p$ ) and the ratio of the lateral displacement at collapse ( $\Delta_k$ ) to the displacement at a load factor of one ( $\Delta_w$ ). From Fig. 2(a), this ratio ( $S_p$ ) is given by:

$$\frac{\Delta_k}{\Delta_w} = \frac{\Delta_k}{\Delta_e} + \frac{\Delta_e}{\Delta_w} = S_p \lambda_p \quad (5)$$

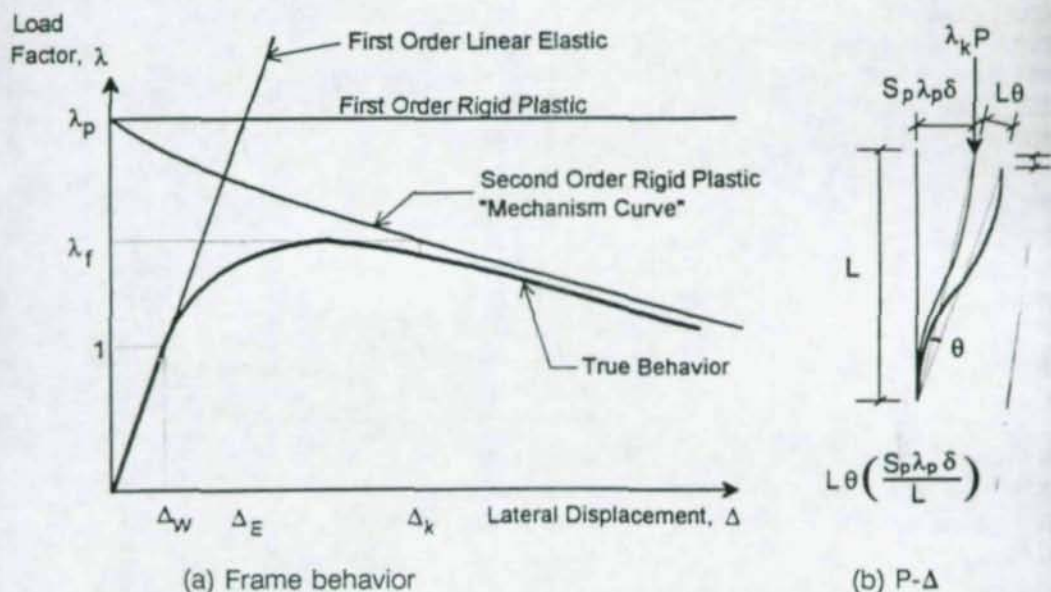


Figure 2 - Mechanism-curve method.

For proportional loading this leads to a collapse load factor,  $\lambda_k$ , equal to (Horne and Morris, 1982):

$$\lambda_k = \frac{\lambda_p}{1 + S_p \lambda_p^2 \left( \frac{\sum P \theta \delta}{\sum M_p \phi} \right)} \quad (6)$$

where the variables are as defined as before and in Fig. 2(b). The terms  $\theta/\phi$  in the denominator disappear when the member rotations ( $\theta$ ) are equal to the plastic hinge rotations ( $\phi$ ). For non-proportional loading, where the gravity loads are held at a load factor of 1 while the lateral loads are increased until collapse, the collapse load factor becomes (Hoffman, 1994):

$$\lambda_k = \lambda_p - S_p \lambda_p^2 \left( \frac{\sum P \theta \delta}{\sum M_p \phi} \right) \quad (7)$$

In essence, Equations (6) and (7) correspond to the mechanism curve shown in Fig. 2(a).

The most difficult part of this procedure is the determination of  $S_p$ . For rigid frames, a value of  $S_p = 2.5$  has been proposed (Horne and Morris, 1973) although the studies on which that value was based showed considerable scatter. For this study a frame database originally developed by Leon and Forcier for PR frames was used (Leon and Forcier, 1992). The database contained 27 basic three-bay frames with 4, 6 and 8 stories, three different story heights, and three ratios of beam length to column height. The behavior of these frames was tracked with a non-linear analysis program that modelled both the non-linear moment-rotation curves and the second-order effects. The analyses were carried out for both proportional and non-proportional loading. Based on these analyses, a series of  $S_p$  values based on story height and number of stories were computed (Table 1).

Number of Stories	Story Height (ft)	Proportional Loading	Nonproportional Loading
4	12	8	10.8
	14	7.2	9.4
	16	5.4	6.5
6	12	5.9	7.4
	14	4.5	5.8
	16	3.9	4.6
8	12	3.6	4.3
	14	2.8	3.9
	16	2	1.7

Table 1 - Values of  $S_p$  (Hoffman, 1994).

Fig. 3 shows the percent deviation between collapse load factors given by Equations (6) and (7) using the  $S_p$  given in Table 1 and the exact value of  $\lambda_k$  for the twenty-seven frames for the non-proportional loading case. This and similar scatter diagrams indicate that for preliminary design purposes the values in Table 1 are more than accurate enough.

Calibration studies have shown that the frames in the database used were stiffer than those that would result from the design procedure described in Section 2. Thus the values of  $S_p$  given in Table 1 will overestimate the second-order effects and be very conservative in most cases. The values shown in Table 1 are being revised downwards in a second phase of this study. Preliminary results indicate that the values in Table 1 should be reduced by about 2/3 to be consistent with the design procedure proposed here. These studies also show that frames with  $\lambda_k$  of 1.5 to 2.0 for the proportional loading case and 2.5 to 3.5 for the non-proportional loading case usually resulted in excellent performance.

The final step in this investigation was to insure that a sidesway mechanism such as that shown in Fig. 1 actually controlled over any beam or combined ones. Attempts at deriving exact expressions for all collapse mechanisms proved fruitless given the number

of variables involved. An extensive numerical investigation was therefore carried out using a prototype six-story, three-bay frame (Hoffman, 1994). The variables involved included four load levels (moderate wind, high winds, low seismic, high seismic), the loading sequence (proportional and non-proportional), the ratios of lateral-to-gravity and dead-to-live loads, the ratio of beam and column strength to connection strength, and the ratio of composite to non-composite beam strength.

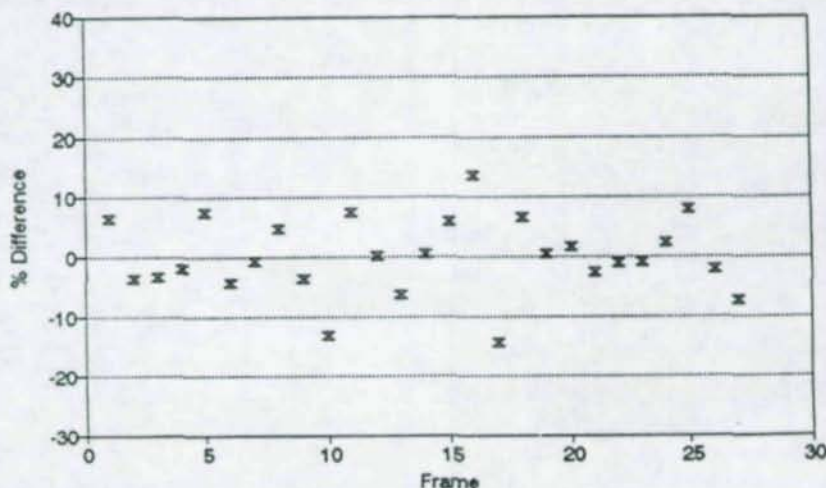


Figure 3 - Accuracy of proposed method (non-proportional).

Figure 4 shows a typical result of these studies for the case of proportional loading. The story heights for this case are 4.3 m, the bay lengths are 9.6 m, the dead load is 4 kN/m<sup>2</sup>, the ratio of LL to DL is 0.75, the ratio of composite to non-composite beam strength (a variable labelled  $\alpha$ ) is 1.9, and the ratio of the connection strength to the steel beam  $M_p$  (labelled  $\beta$ ) is 0.75. For these frames it was also assumed that three beams frame into each girder. This variable needs to be set so that collapse mechanisms associated with gravity loads and combined mechanisms can be studied.

In Fig. 4 the values of the load factor ( $\lambda_k$ ) are plotted as a function of the ratio of lateral-to-gravity load for the different possible mechanisms: sway (Sway-RP = rigid plastic; and Sway-SO = second order), combinations (Comb1-RP = rigid plastic with hinges at a connection and at the third point of the girder; Comb2 = rigid plastic with hinges at a connection and at midspan; and Comb-SO = governing combination for second-order effects) and beam mechanism (Beam).

The influence of second order effects on the sway mechanism is clear, since the Sway-SO case governs for ratios of lateral-to-gravity loads greater than about 0.05, while the Sway-RP case never governs. Care should be taken in interpreting these graphs since the large difference between  $\lambda_k$  (Sway-SO) and  $\lambda_p$  (Sway-RP) arises because of the difference in initial gravity load. Fig. 5 illustrates this difference schematically: for low ratios of lateral-to-gravity loads the shaded area, which corresponds to the work done by

the P- $\Delta$  effects, is very large because the gravity loads dominate (Fig. 5(a)). Since the Sway-RP case does not account for the second order effects, the resulting first-order collapse load factor is unduly large with respect to  $\lambda_k$  for low values of lateral-to-gravity loads. As the ratio of lateral to gravity loads increases, the role of the gravity loads decreases (Fig. 5(b)) and the difference between  $\lambda_p$  and  $\lambda_k$  decreases.

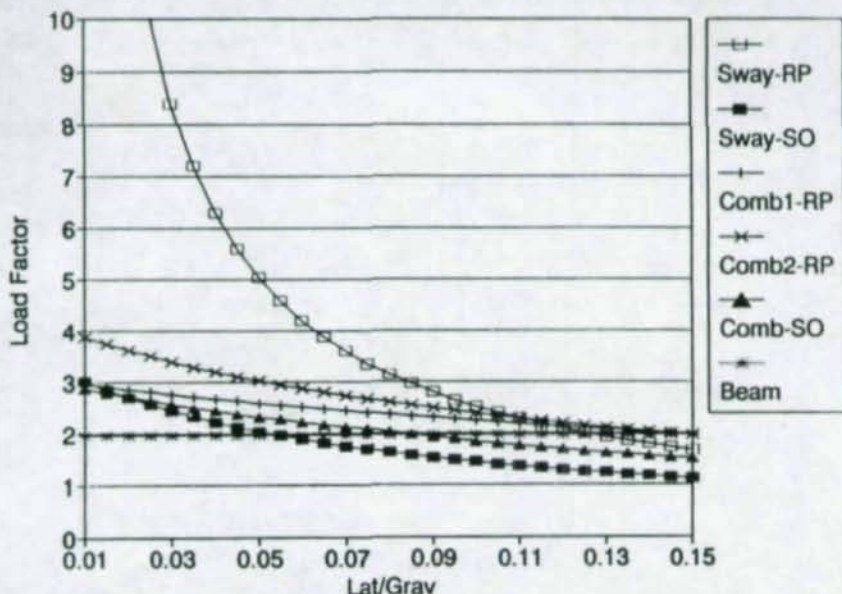


Figure 4 - Collapse load factors for proportional loading.

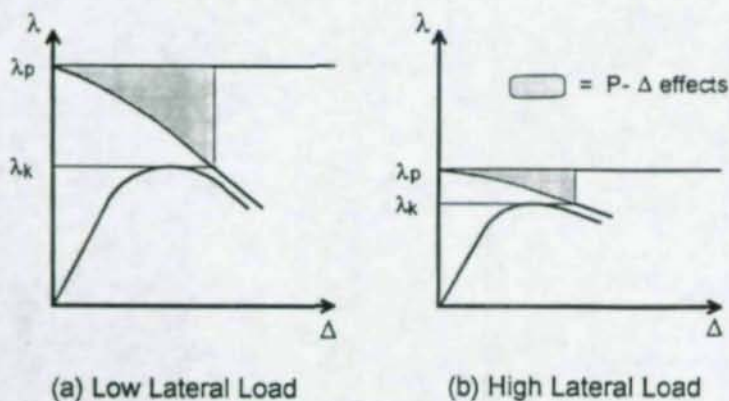


Figure 5 - Effect of P- $\Delta$  on  $\lambda_k$ .

For the four loading cases considered the ratio of lateral-to-gravity load ranged from about 0.04 for the moderate wind (suburban setting with winds of 130 kph) and low

earthquake (PGA of 0.1g on good soil) to about 0.14 for the high wind (open terrain with winds of 200 kph) and high seismic cases (PGA of 0.4g with good soils). As can be seen from Fig. 4, the combined mechanisms never govern and are relatively insensitive to variations in lateral-to-gravity load ratios. On the other hand, beam mechanisms control if the ratio of lateral-to-gravity load is less than about 0.05. Thus beam mechanisms should be checked carefully if proportional loading is considered the governing case and low lateral loads are present.

Figure 6 shows a plot similar to that of Fig. 4 except that it corresponds to the non-proportional load case. The beam mechanism is missing from this graph because the gravity loads were held constant and thus no beam mechanisms could form. As expected and in sharp contrast to the results shown in Fig. 4, all mechanisms show large increases in the collapse load factor as the initial ratio of lateral-to-gravity loads decreases.

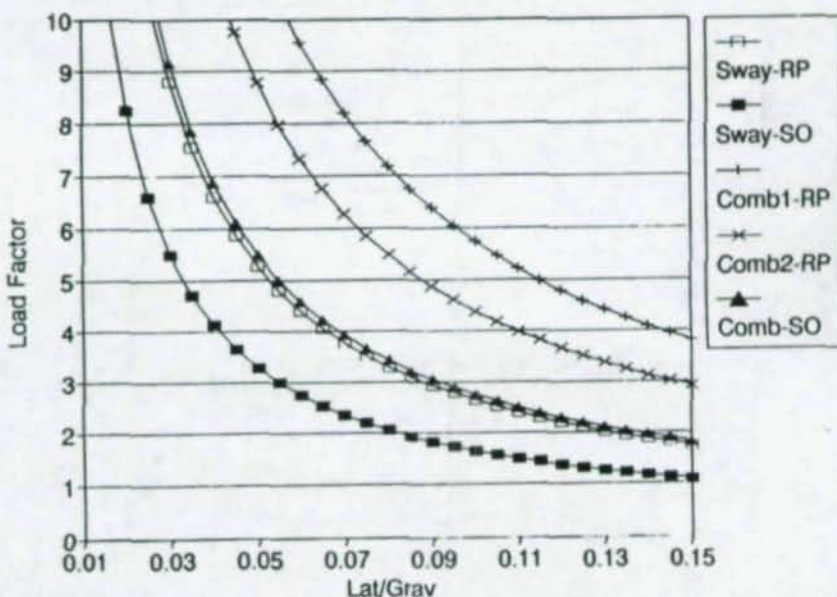


Figure 6 - Collapse load factors for non-proportional loading.

In both Figs. 4 and 6 the sway mechanism postulated in developing the preliminary design approach governs. This is not always the case. Fig. 7 shows a plot of what the maximum ratios of composite to non-composite beam strength ( $\alpha$ ) would be required for a combined mechanism to govern for various ratios of dead-to-live loads. These are plotted for two levels of connection strength ( $\beta = 0.8$  and  $1.0$ , where  $\beta$  is the ratio between the connection strength and the plastic capacity of the steel section alone). This figure shows that the amount of interaction, which is reflected directly in  $\alpha$ , would have to be very small for the combined mechanisms to govern. For LL/DL ratios greater than 1.9, a beam mechanism would govern. Extensive studies similar to those shown in Fig. 7 indicate that for all practical cases a sidesway mechanism will govern.

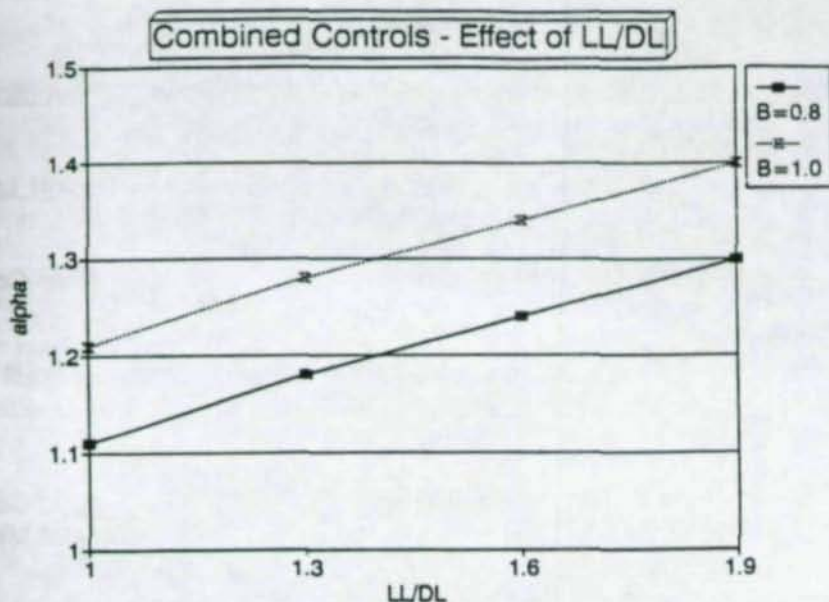


Figure 7 - Limits for which combined mechanisms govern.

#### 4. CONCLUSIONS

The second-order plastic analysis method proposed here provides a quick and conservative approach for determining the ultimate strength of regular PR frames. This method is a straight forward extension of the work by Horne and Morris (Horne and Morris, 1973). Its value lies in showing that the load factor at collapse far exceeds the accepted minimum values for frames designed according to a particular design procedure. Thus the design of the overall frame is driven by the elastic analysis at the service level. Since many of the commercially available software already incorporates linear spring elements at the ends of the beams, this brings PR design within the grasp of most engineers. It is suggested that PR frame preliminary design be a stiffness-based design, and the ultimate strength checked by the mechanism method proposed here.

#### 5. ACKNOWLEDGEMENTS

This work was made possible by a generous grant from the American Institute of Steel Construction and the support of the Graduate School at the University of Minnesota where both authors worked when this work was carried out.

## 6. REFERENCES

- American Institute of Steel Construction, 1994. Manual of Steel Construction, Load Resistance Factor Design, Second Edition, AISC, Chicago.
- American Society of Civil Engineers, 1993. ASCE 7-93: Minimum Design Loads for Buildings and Other Structures, ASCE, New York.
- Ammerman, D.J., and Leon R.T., 1990. "Unbraced Frames With Semi-Rigid Composite Connections," AISC Engineering Journal, 1st Quarter, pp. 12-21.
- Bertero, V.V., Anderson, J.C., and Krawinkler, H, 1994. "Performance of Steel Building Structures during the Northridge Earthquake." UCB/EERC-94/09, Earthquake Engineering Research Institute, U. of California at Berkeley, 169 pp.
- Hoffman, J.J., 1994. "Design Procedures and Analysis Tools for Semi-Rigid Composite Members and Frames." M.S. Thesis, Graduate School, The University of Minnesota, Minneapolis, MN.
- Horne, M.R., and Morris, L.J., 1973. "Optimum Design of Multi-storey Rigid Frames," in Optimum Structural Design - Theory and Application, R.H. Gallagher and O.C. Zienkiewicz (eds.), John Wiley and Sons, New York, NY.
- Horne, M.R., and Morris, L.J., 1982. Plastic Design of Low-Rise Frames, The MIT Press, Cambridge, MA.
- Leon, R.T., and Ammerman, D.J., 1990. "Semi-Rigid Composite Connections for Gravity Loads," AISC Engineering Journal, 1st Quarter, pp. 1-11.
- Leon, R.T., and Forcier, G.P., 1992. "Parametric Study of Composite Frames," Proc. of the 2nd Intl. Workshop on Connections in Steel Structures (R. Bjorhovde and A. Colson, eds.), AISC, Chicago, 1992, pp. 152-159.
- Leon, R.T., 1994. "Composite Semi-Rigid Construction," AISC Engineering Journal, 2nd Quarter, pp. 57-67.
- Leon, R.T., and Shin, K. J., 1994. "Seismic Performance of Semi-Rigid Composite Frames," Proc. of the 5USNCEE, Vol. 1, EERI, Oakland, pp. 243-252.
- Nader, M.N., and Astaneh, A., 1992. "Seismic Design Concepts for Semi-Rigid Frames," Structures Congress 92: Compact Papers, ASCE, New York, pp. 971-974.
- Neal, J.G., 1956. The Plastic Methods of Structural Analysis, Chapman & Hall, London.
- NEHRP, 1994. "NEHRP Recommended Provisions for the Development of Seismic Regulations for New Buildings," Building Seismic Safety Council, Washington, D.C.

## EUROCODE 4 AND DESIGN OF COMPOSITE JOINTS

David Anderson<sup>1</sup>

### Abstract

As a Prestandard, Eurocode 4 gives little guidance on the design of composite joints. The reasons for this are explained. The likely form of provisions in the forthcoming Euronorm is described and background studies currently in progress are summarised.

### 1. INTRODUCTION

In codes for steel structures the treatment of connections has often been limited to little more than a list of strengths for welds and fasteners. For many designers, ENV 1993-1-1 Eurocode 3 (1992) is unusual in providing a detailed method for moment-resisting beam-to-column joints. This was originally restricted to fully-welded connections or those made by end plates. Following preparation of a revised Annex J for Eurocode 3 (to be published 1995), the scope now includes joints with flange cleats.

For several reasons the drafting of the Eurocodes has proved to be a lengthy task. For composite structures, provisions should ideally be harmonised with those for concrete structures and structural steelwork. For this reason, ENV 1994-1-1 Eurocode 4 (1992) includes a short section, clause 4.10, applicable to composite connections in braced frames for buildings. A composite connection is defined in clause 1.4.2 as 'a connection between a composite member and any other member in which reinforcement is intended to contribute to the resistance of the connection'.

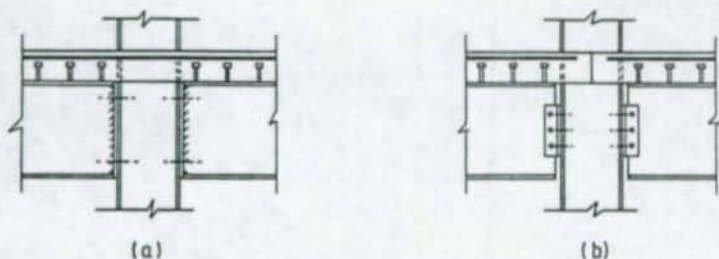


Fig. 1. (a) Moment-resisting composite joint and (b) "simple" joint.

1. Reader, Department of Engineering, University of Warwick, Coventry, UK

An example of a moment-resisting composite joint is shown in Fig. 1(a). Those in which the reinforcement is not continuous (Fig. 1(b)), or where only a brittle welded mesh is provided, were, by implication, to be designed as steelwork connections to Eurocode 3.

No attempt was made in ENV 1994-1-1 to provide a complete set of design rules for composite connections. Their behaviour had been the subject of extensive research in the second half of the 1980s (Zandonini, 1989; Leon and Zandonini, 1992), which continues at the present time. However, the conclusions were judged to be not sufficiently well-established for inclusion in an international code. Reference was made instead to the possibility of using the detailed rules of Eurocode 3 for steel components of composite connections.

In Eurocode 3, the provisions for connections are accompanied by a classification system related to rotational stiffness and moment resistance. This in turn is related to classification of the framing system as simple, continuous or semi-continuous. Elastic, rigid-plastic and elastic-plastic methods of global analysis can be used for continuous or semi-continuous systems. At the time of drafting ENV 1994-1-1, the determination of the stiffness of composite connections was regarded as even more problematical than that of moment resistance. Eurocode 4 permits substantial redistribution of moment to be made to elastic bending moments, but the influence of connection flexibility on redistribution had not been quantified. For these reasons, ENV 1994-1-1 does not provide application rules for frames with semi-rigid connections. Rigid-plastic analysis of frames with partial-strength connections is however included, provided that it has been demonstrated that the proposed connections have sufficient rotation capacity. This capacity was not quantified.

The Eurocodes are being published initially as 'Prestandards' (ENVs) for 'provisional application'. After two years, the members of CEN (i.e. national standards bodies) are requested to submit comments, particularly concerning whether the Prestandard can be converted into a European Standard (EN). This enquiry has now taken place for the first parts of Eurocodes 2, 3 and 4. It is likely that CEN will authorise conversion of these codes to EN status, provided there are some technical revisions to the provisions of the Prestandards. For Eurocode 4, this provides the opportunity to include detailed rules for composite joints, based on the revised Annex J of Eurocode 3. This paper explains how these provisions are being developed, and indicates the likely scope and contents of the new clauses.

## 2. CONVERSION OF EUROCODE 4 TO EN-STATUS

At the time of Eurocode 4's approval as a Prestandard, it was recognised that its provisions should be developed during the period of provisional application. This task was to be undertaken by Technical Committee 11 of the European Convention for Constructional Steelwork (ECCS-TC11). A Monitoring Group was also established under the auspices of CEN Technical Committee 250 : Sub-committee 4, to act as a focus for enquiries and comments on Eurocode 4 during this period. A further development was the establishment of Project C1 on Semi-rigid Behaviour, as part of the programme for European Cooperation in the Field of Scientific and Technical Research (COST-C1).

These three groups all have interests in composite connections, and a joint COST-C1/ECCS-TC11 Drafting Group was established in 1994. The aims of the Group are:

- (i) to use present knowledge to prepare state-of-the-art documents on the design of composite connections,
- (ii) to prepare a draft annex for inclusion in the EN version of Eurocode 4 : Part 1.1.

Following a 'Declaration of Intent' by CEN TC250 concerning availability of EN-Eurocodes for building structures, the technical work required for conversion of Eurocode 4 is scheduled to be completed by the end of 1996. This work has to be carried out in a manner which will satisfy the national standard bodies that constitute the members of CEN. In guidelines for conversion, it is stated that those working must "quickly achieve what is practicable" and must "avoid repeated attempts to incorporate last-minute research results". The EN-Eurocodes should not "prevent innovative or alternative designs which satisfy the established Principles" but "Application Rules [for] novel forms of construction may be excluded". Such forms "will require additional consideration by the designer" (Lazenby, 1994). The guidelines reinforce the understanding that the periods of provisional application of the Prestandards are to enable experience to be gained from use of the Eurocodes, so that they can be finalised in the light of such practical experience. The guidelines and the timetable for conversion influence the scope of the proposed annex on composite joints.

### 3. SCOPE OF PROPOSED DESIGN DOCUMENTS FOR COMPOSITE JOINTS

#### 3.1 Annex for EN 1994-4-1

For the EN-version of Eurocode 4, it is being assumed that only those design assumptions given in Table 4.8 of the Prestandard need be covered by detailed rules. This avoids the need during conversion to extend the clauses dealing with global analysis and the buckling lengths of columns.

No application rules will be given for elastic global analysis of frames with semi-rigid joints; nor for unbraced non-sway frames. These types remain within the scope of the code as "innovative designs" which satisfy the Principles but which "require additional consideration by the designer".

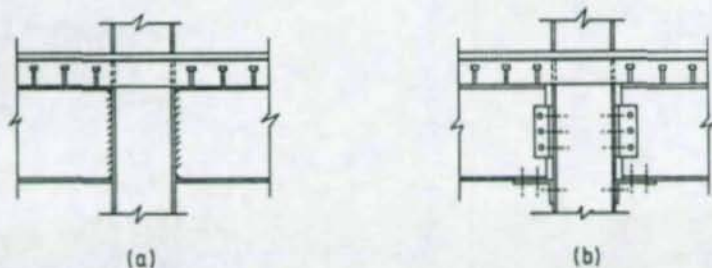


Fig.2. (a) Fully-welded and (b) flange-clip composite joints.

Table 1 Design assumptions in ENV 1994-1-1 (Table 4.8)

Type of Framing	Method of Global Analysis for Ultimate Limit States	Types of Connections
Simple	Statically-determinate	Nominally pinned, steel
Continuous	Elastic	Rigid, steel Nominally pinned Rigid, composite
	Rigid-plastic	Full-strength, steel Nominally pinned Full-strength, composite
Semi-continuous	Rigid-plastic	As for continuous framing, and: Partial-strength, steel Partial-strength, composite

The scope of the proposed annex is therefore intended to be as follows:

- (i) It applies only to joints in braced frames.
- (ii) It treats composite versions of the types of steelwork joint included in the revised Annex J of Eurocode 3. In addition to the end-plate connection shown in Fig. 1(a), it will therefore include fully-welded joints (Fig. 2(a)).
- (iii) Composite action permits simpler joints in which tensile forces are resisted solely by the slab reinforcement, compressive force being transmitted by a flange cleat (Fig. 2(b)), or a contact plate (Fig. 3). These should also be treated, because of their potential for economy in fabrication.
- (iv) Account should be taken of concrete encasement to steel column sections.
- (v) The rules should enable the design moment resistance of the joint to be calculated.
- (vi) The rules should permit calculation of the stiffness of the joint, for use in serviceability calculations and in classification of joints.
- (vii) As an alternative to calculation, classification by stiffness should be possible by "deemed to satisfy" provisions.
- (viii) Adequate rotation capacity is ensured by "deemed to satisfy" provisions, rather than by detailed calculation.
- (ix) The scope includes internal joints with unbalanced moment and external joints.
- (x) Guidance is given on types of joint suitable for simple framing.

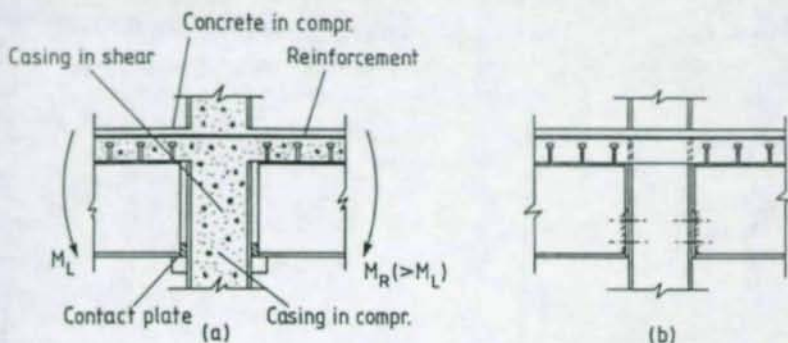


Fig.3 (a) Contact-plate and (b) partial-depth end plate composite joints

### 3.2 COST-C1 Document

COST is a scientific programme and provides a suitable means for a state-of-the-art report on composite joints, aimed at the academic and research community, national committees concerned with codes and also the more enquiring practitioners. The document will therefore explain the principles for design adopted in the Eurocode annex, and the derivation of the design rules. These would be related to observed behaviour and calibrated against test results. The report will therefore be in part a background document on the annex, although the scope will be wider. For example, the use of the finite element method will be addressed, as will calculation methods for rotation capacity.

### 3.3 ECCS-TC11 Document

The second publication is aimed specifically at the needs of designers. It will give guidance on the application of composite joints in practice, including their influence on frame behaviour and member design, information relevant to preliminary design, summary of design formulae, flow diagrams for calculation procedures, tables of properties for defined joints and worked examples. Although also related to the Eurocode annex, its scope will be wider, including for example elastic global analysis for the ultimate limit state, and further simplifications such as use of rigidity factors and span: depth ratios to avoid detailed calculation checks.

## 4. BACKGROUND STUDIES

### 4.1 Properties of Basic Components

In the revised Annex J for Eurocode 3, the design moment-rotation characteristic is determined from the properties of the joint's basic components, which include, for example, the column web panel in shear and the end plate in bending.

For each component, rules are given to determine design resistance and elastic stiffness. Relationships between the properties of the basic components and the structural properties of the overall joint are given for design moment resistance and rotational stiffness.

For composite joints additional basic components can be identified:

- concrete encasement to the column web panel in shear
- concrete encasement to the column web in compression
- longitudinal slab reinforcement in tension
- slab concrete in compression
- contact plate in compression.

These components are shown in Fig. 3. Furthermore, unless the global analysis accounts for partial interaction in the beam, appropriate allowance should be made for the additional flexibility due to deformation of the shear connection.

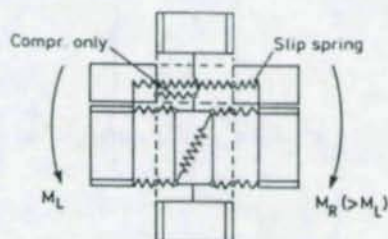


Fig.4. Spring model.

To determine the properties of the additional components, use is being made of a sophisticated spring model (Tschemmerneegg et al, 1994, 1995), shown in Fig. 4. So far this has been applied to the column web in compression, when connection between the column flange and the beam section is either by welding (Fig. 2(a)) or by a contact plate (Fig. 3(a)) (Tschemmerneegg and Huber, 1995). For the stiffness coefficient there is a substantial difference between the two forms of connection; much greater flexibility is shown when the load is applied to the column section by the contact plate, due to the more localised action in this case. A stiffness coefficient has also been determined for concrete encasement to the column web in compression, and resistance formulae for both steel and concrete components.

Further studies are in progress on the column panel zone when subject to shear and on the tension zone.

#### 4.2 Influence of Slip of the Shear Connection on Composite Joint Behaviour

From comparisons between spring models and tests, several authors (e.g. Anderson and Najafi, 1994) have concluded that appropriate account should be taken of slip at the steel-concrete interface, in order to model experimental behaviour. In order to investigate further, limited numerical studies have been performed (Aribert 1994), using a finite element approach (Aribert et al, 1993). The shear connectors were taken to be cold-formed angles (Hilti connectors). Conclusions are:

- (i) For this type of connector, the contribution of slip to the moment-rotation ( $M-\phi$ ) response of the joint was significant even for degrees of shear connection of the order of 1.3.
- (ii) For these ductile connectors, the precise arrangement of the connection (uniform distribution or non-uniform) had negligible influence on the  $M-\phi$  response.
- (iii) Comparisons of the behaviour of a cantilever loaded at the tip and a beam subject to uniformly distributed loading showed that the  $M-\phi$  response of the joint is virtually unchanged, although approaching ultimate moment the distributions of slip in corresponding regions do differ if the degree of shear connection is high.
- (iv) For a high degree of shear connection, a steep gradient of slip was observed in the region very close to the joint, at values of moment of approximately  $0.67M_{Rd}$  and  $1.0M_{Rd}$ .

These conclusions confirm the significance of slip but also permit the same joint response to be assumed independent of the precise nature of the member and the distribution of the shear connectors.

#### 4.3 Addition of $M-\phi$ Response in Composite Joints

Comparisons with tests on end-plate connections show that it is often possible to determine the response of a composite joint by combining the action of the rebars and shear connectors with the  $M-\phi$  response of the complete steelwork connection (Anderson and Najafi, 1994; Aribert, 1995). The spring model of Fig. 4 (Tschemmernegg et al, 1994, 1995) is to be used to determine what conditions (if any) are required to ensure appropriate accuracy from this simplified approach.

#### 4.4 Required Rotation Capacity

Rotation capacity at joints is needed to permit the redistribution of moment assumed by the Eurocode rules for global analysis. The limits to redistribution are dependent on the local-buckling classification of the beam section in hogging bending and, for plastic analysis, on simple rules which avoid excessive demands for rotation capacity at midspan. Calculation of required rotation capacity is thereby avoided.

Studies of recent research on required rotation capacity are now in progress though, because numerical values are needed to ensure that composite joints designed by the proposed annex are sufficiently ductile (Xiao, 1995; Couchman, 1994; Li, 1994).

#### 4.5 Available Rotation Capacity

Full-scale cruciform tests on composite joints with end plates (Fig. 1(a)) have shown that fracture of welded mesh and, more importantly, reinforcing bars is a possible failure mode (Anderson and Najafi, 1994; Aribert and Lachal, 1992; Aribert et al, 1994; Xiao, 1994). Substantial local deformation occurs in the tension region of the steelwork connection, due to bending of the column flange and the end plate. This leads to fracture of the mesh (if present) and later fracture of the rebars in the region of the slab above the steelwork connection, accompanied by a wide crack across the slab, at the face of the column.

A simple calculation model has been proposed (Xiao, 1994) for the rotation  $\phi_u$  at the peak of the  $M-\phi$  curve (Fig. 5) based on an assumed strain in the rebars, in the zone of the connection, of 0.5%. Tests show though that substantial further rotation may occur before fracture occurs, albeit with some reduction in moment resistance (Anderson and Najafi, 1994). Numerical simulations to determine rotation capacity can also be employed (Ren and Crisinel, 1994).

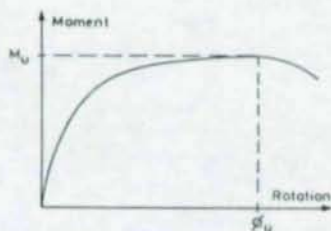


Fig 5. Rotation at maximum moment

The tests quoted above have used relatively small diameter reinforcing bars (Aribert and Lachal, 8mm; Xiao 10mm and 12mm; Anderson and Najafi, 12mm), spread across the effective breadth of the slab. Although of small diameter, the bar sizes used by Najafi and Xiao conformed to current UK requirements for plastic design of continuous composite beams, those used by Najafi showing an elongation at fracture of approximately 17%.

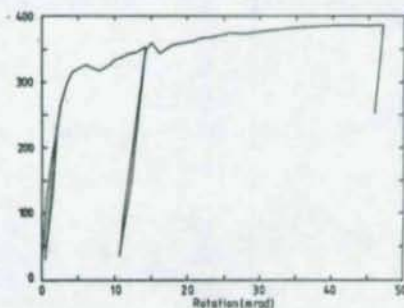


Fig.6. Ductile composite joint.

Further tests have recently been carried out using a minimum of four 16mm bars, in conjunction with steel beam sections up to 530mm deep (Brown, 1995). These have shown

much improved ductility (Fig. 6) even though failure was still eventually by fracture. These bars conform to the Eurocode requirement that for plastic global analysis only reinforcement of 'high ductility', as defined by Eurocode 2, is used (Beeby and Narayanan, 1995). Elongation at fracture was approximately 25%. For the proposed Eurocode annex, studies are therefore in progress to develop detailing rules for composite joints to ensure ductility which matches the required capacity.

To ensure an adequate margin of safety against loss of ductility, two possible approaches are:

- (i) to apply a factor (or factors) when comparing required capacity against that available. A minimum factor of two has been suggested (Kemp and Dekker, 1991). The resulting comparison could be used when developing detailing rules to provide adequate ductility;
- (ii) to rely on the reduced rotation capacity required at a joint when, as usually occurs, the moment resistance achieved in practice exceeds the design value.

Choice of approach is still under discussion.

## 5. OUTLINE OF THE PROPOSED ANNEX

### 5.1 Scope

The annex will contain design methods for moment-resisting composite beam-to-column joints in braced frames, for buildings subject to predominantly static loading. Nominally-pinned joints are to be designed in accordance with Eurocode 3. In addition to the types of moment-resisting connections now covered by Eurocode 3, Eurocode 4 is to treat bolted connections with partial depth end plates or contact plates (Fig. 3). The design methods are principally for major axis connections, but they can also be applied to connections to the web of a column's steel section provided no transfer of bending moment into the column is assumed in analysis.

### 5.2 Basic Components of a Joint

The component approach adopted in the revised Annex J of Eurocode 3 is to be extended to composite joints, as explained in 4.1 above. The need to consider the action of the slab in compression arises because the slab bears against the column when unbalanced loading occurs. In practice account will usually be taken of deformation of the shear connection in the joint model. However, as this deformation could be taken account of in a partial interaction analysis of the beam, shear connectors are not listed as 'basic' joint components.

### 5.3 Classification

Classification by strength compares the resistance of the joint with that of the adjacent beam section in hogging bending.

Comparison of tests with classification by the Prestandard showed that joints with 12mm thick flush end plates, connected to cantilevers with full shear connection, were rigid (Anderson and Najafi, 1994). The classification limits for rigid and semi-rigid joints given in the revised Annex J of Eurocode 3 are to be adopted for Eurocode. The limits are related to the initial stiffness of the joint,  $S_{j,ini}$ , relative to that of the connected beam,  $EI_b/L_b$  (Fig. 7). For composite construction, the stiffness of the beam is to be the uncracked value. Deemed to satisfy rules are to be developed.

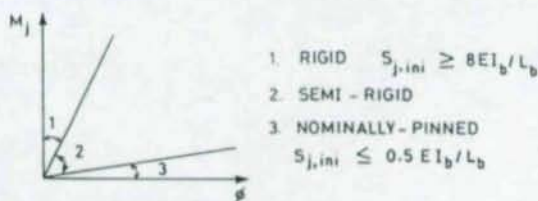


Fig.7. Classification by stiffness

No explicit reference is made in the formal classification system to ductility, but recent research to quantify required rotation capacity, referenced in 4.5 above, could lead to classification for this characteristic as well, in subsequent revisions of the Eurocodes.

### 5.4 Simplified Modelling

As in Eurocode 3, a single sided joint configuration may be modelled as a single joint, and a double-sided configuration as two separate but interacting joints (Fig. 8). The interaction is determined by the relative values of moment on each side, expressed as a transformation parameter. This influences the contribution of the column web, in shear and compression, to the resistance of each joint, and the joint stiffness due to the web panel in shear.

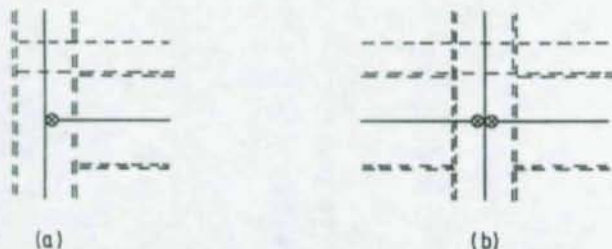


Fig.8. Modelling of (a) single-sided and (b) double-sided configurations

## 5.5 Resistance

The moment resistance of the joint may depend on resistance of the slab within the region of the joint, the tension zone of the steelwork connection (if any), the compression zone of the steelwork connection and the shear zone of the column web.

The effective resistance of each zone depends in turn on the resistance of the components within that zone. For example, although the resistance provided by the slab depends primarily on the tensile resistance of the reinforcement, this may be limited by the strength of the concrete bearing against the column if unbalanced loading occurs.

## 5.6 Stiffness

This is to be determined from the stiffness of the joint's components. As an alternative it is intended where appropriate to treat the stiffness (and resistance) of the steelwork components as single quantities, as described in 4.3 above.

## 5.7 Rotation Capacity

This is required when plastic global analysis is used, if joints are partial-strength or have a design resistance only slightly above that of the adjacent member. Deemed-to-satisfy provisions are seen as the most appropriate approach in view of the limited time available for technical work during conversion.

## 5.8 Detailing

Particular care is needed when unbalanced loading occurs. The proposed rules mainly concern:

- (i) the need for reinforcement to resist transverse tension in the slab due to compressive action between the slab and the column (Fig. 3(a)), and
- (ii) adequate anchorage of tensile reinforcement in single-sided joints.

## 6. CONCLUSIONS

Eurocode 4 as a Prestandard gave very limited guidance for design of composite connections; methods to predict properties were judged to be insufficiently well-established.

During the period of provisional application, research has continued and it is widely accepted that design rules can now be formulated. Those proposed for Eurocode 4 as a Euronorm are based on the component approach of the revised Annex J for Eurocode 3. For composite

joints additional components are necessary because of the actions of the slab and because composite action permits additional types of connection.

At present the proposed design rules are being drafted as modifications and additions to those given in the revised Annex J for Eurocode 3. This reduces the size of the code, but raises questions of ease of use. Once drafting is complete, the presentation may need to be revised to secure a sensible balance between repetition of material and the need to cross-refer to Eurocode 3.

To assist in introducing the Eurocode, a background document and a design guide are also being prepared, under the auspices of the COST-C1 project and ECCS Technical Committee 11, respectively.

## 7. ACKNOWLEDGEMENTS

The author acknowledges with thanks the work of other members of the COST-C1/ECCS-TC11 Group on Composite Connections, namely J.-M. Aribert (Rennes), J.-P. Jaspart (Liège), H.-J. Kronenberger (Kaiserslautern), F. Tschemmernegg (Innsbruck), J.W.B. Stark (Delft) and Y. Xiao (Southampton, formerly Nottingham).

## 8. REFERENCES

1. Anderson D. and Najafi A.A. Performance of composite connections: major axis end plate joints. *J. Construct. Steel Research* 31, (1994) 31-57.
2. Aribert J.M. and Lachal A., Experimental investigation of composite connection and global interpretation. *Proceedings of the First State of the Art Workshop, COST-C1 Semi-rigid Behaviour of Civil Engineering Structural Connections*, ed. Colson A., Strasbourg (1992), 158-169.
3. Aribert J.M., Ragneau E. and Xu H., Développement d'un élément fini de poutre mixte acier-béton intégrant les phénomènes de glissement et de semi-continuité avec éventuellement voilement local. *Construction Métallique*. No. 2 (1993).
4. Aribert J.M., Partial investigation of the influence of slip of the shear connection on composite joint behaviour. Working paper, COST-C1/ECCS-TC11 Group on Composite Connections (1994).
5. Aribert J.M., Lachal A., Muzeau J.P. and Racher P., Recent tests on steel and composite connections in France. COST-C1 Workshop, Prague (1994).
6. Beeby A.W. and Narayanan R.S., *Designers' Handbook to Eurocode 2*. Thomas Telford, London (1995).

7. Brown N.D. Ph.D Thesis, University of Warwick, UK. (To be submitted 1995).
8. Couchman G., Design of continuous composite beams allowing for rotation capacity. Ph.D Thesis, EPFL, Switzerland (1994).
9. ENV 1993-1-1, *Eurocode 3: Design of Steel Structures Part 1.1: General Rules and Rules for Buildings*. CEN, Brussels (1992).
10. *Eurocode 3 : Design of Steel Structures Part 1.1 : General Rules and Rules for Buildings, Revised Annex J : Joints in Building Frames*. CEN, Brussels. (To be published 1995).
11. ENV 1994-1-1 *Eurocode 4 : Design of Composite Steel and Concrete Structures Part 1.1: General Rules and Rules for Buildings*. CEN, Brussels (1992).
12. Kemp A.R. and Dekker N.W., Available rotation capacity in steel and composite beams. *The Structural Engineer* **69** (1991) 88-97.
13. Lazenby D.W., Guidelines for content of structural Eurocodes (Future ENV, and conversions to EN). Working paper N169, CEN Technical Committee 250 (1994).
14. Leon R.T. and Zandonini, R., Composite Connections. In *Constructional Steel Design : an International Guide*, ed. Dowling P.J., Harding J.E. and Bjorhovde R., Elsevier Applied Science Publishers (1992), 501-522.
15. Li T.Q., The analysis and ductility requirements of semi-rigid composite frames. Ph.D Thesis, University of Nottingham, UK. (1994).
16. Ren P. and Crisinel, M., Effect of reinforced concrete slab on the moment-rotation behaviour of standard steel beam-to-column joints : experimental study and numerical analysis. COST-C1 Workshop, Prague (1994).
17. Tschemmernegg F., Brugger R., Hittenberger R., Wiesholzer J., Huter M., Schaur B.C., Badran M.Z., Nachgiebigkeit von Verbundkonstruktionen. *Stahlbau*, **63** (1994) No. 12 and **64** (1995) No. 1.
18. Tschemmernegg F. and Huber G., Compression region in the panel zone of a composite joint. Working Paper T2, COST-C1/ECCS TC11 Group on Composite Connections (1995).
19. Xiao Y., Behaviour of composite connections in steel and concrete. Ph.D Thesis, University of Nottingham, UK (1994).
20. Xiao Y., Available and required rotation capacities for composite beams and frames. Working Paper, COST-C1/ECCS TC11 Group on Composite Connections (1995).
21. Zandonini R., Semi-rigid composite joints. In *Structural Connections : Stability and Strength*, ed. Narayanan R., Elsevier Applied Science Publishers (1989), 63-120.

# MECHANICAL MODELING OF SEMI-RIGID JOINTS FOR THE ANALYSIS OF FRAMED STEEL AND COMPOSITE STRUCTURES

F. Tschemmernegg<sup>1</sup>

G. Queiroz<sup>2</sup>

## Abstract

Some mechanical models of semi-rigid joints are analyzed, taking into account the behaviour of the joint with actual dimensions. A new model is described which can be used with available software for the analysis of framed steel structures.

## 1. INTRODUCTION

Semi-rigid connection is a type of moment connection for which the initial angle between the connected members, at the intersection of their axes, changes with the connection moment (Fig. 1). The joint is an infinite small point.

Based on this concept, the first mechanical model used to represent a semi-rigid connection consisted of a rotational spring placed between the end of the beam axis and the column axis as used in EC3 Annex J (Fig. 2).

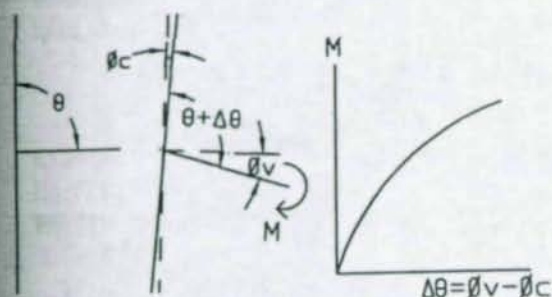


Fig.1 - Semi-rigid connection

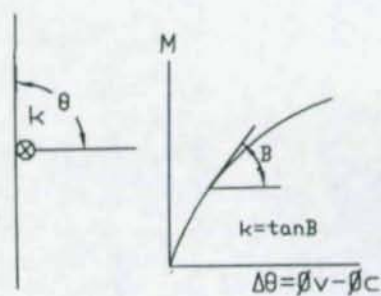


Fig. 2 - Rotational spring

<sup>1</sup> o. Univ. Prof. Dipl. Ing. Dr. techn. Ferdinand Tschemmernegg  
Institute of Steel and Timber construction; University of Innsbruck, A-6020 Innsbruck, Technikerstraße 13

<sup>2</sup> M.sc. Gilson Queiroz,  
Universidade Federal de Minas Gerais, Av. do Contorno, 842 - 2 andare 30110-060 - Belo Horizonte

Due to local deformations which arise when column web stiffeners are absent and due to bending and shear deformations of the column zone between the upper and lower beam flanges (joint zone), the more general concept of semi-rigid joint was introduced (Tschemmerneegg et al., 1987). It is assumed that the joint has a finite size ( $h_j, b_j$ ).

It was shown (Tschemmerneegg et al., 1987) that it is not possible to represent the connection deformations, the joint zone bending and shear deformations with a single rotational spring for each beam. In fact, each connection takes the moment applied by the corresponding beam, but the joint zone takes over the resultant of the two beam moments (Fig. 3).

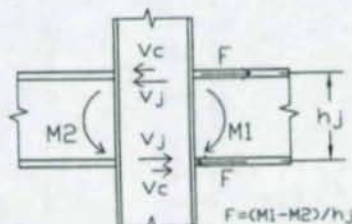


Fig. 3 - Joint forces

It was also shown that for taking into account the deformations of the column in the joint zone the mechanical model of the joint must hold the actual joint dimensions.

The basic deformation modes of the joint will be described in the next section.

## 2. JOINT DEFORMATION MODES

Fig. 4 shows a two-beam-joint with bolted end-plate connections; it will be supposed that  $M_1 > M_2$ . Points  $A, A_m, A_s$  as well as points  $E, E_m, E_s$  are located on the end plate, while points  $B, B_m, B_s$  as well as points  $D, D_m, D_s$  are located on the column. Before deformation takes place, points  $A, A_m, A_s$  coincide with  $B, B_m, B_s$  and points  $E, E_m, E_s$  coincide with  $D, D_m, D_s$ . The position of those points will be determined according to:

- deformation caused by pure bending;
- deformation caused by pure shear;
- local deformation of the connection and the column regions opposite to the beam flanges.

The static system shown in Fig. 5 will be used as a reference. The shear forces and the bending moments in the column, taking into account the beam height  $h_j$ , are also shown.

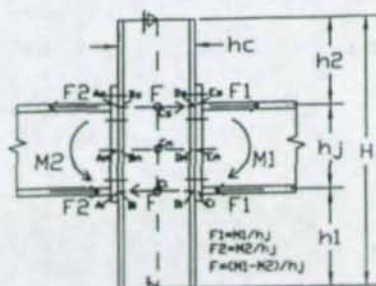


Fig. 4 - Initial geometry of a two-beam-joint

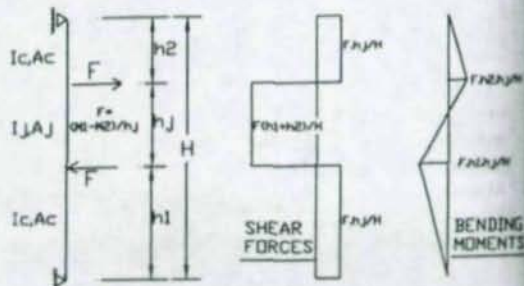


Fig. 5 - Reference static system

## 2.1 Deformation caused by pure bending

The deformed column axis is shown in Fig. 6, with the new positions  $C_1'$ ,  $C_m'$ ,  $C_2'$  of the points  $C_1$ ,  $C_m$ ,  $C_2$ . Because the cross sections remain at right angles to the axis, the new positions  $B_1'$ ,  $B_m'$ ,  $B_2'$ ,  $D_1'$ ,  $D_m'$ ,  $D_2'$  of the points  $B_1$ ,  $B_2$  etc. are easily to determine, as shown in Fig. 6.

The average rotation of the joint zone is given by:

$$\Phi_m = (\delta s + \delta i) / h_j \quad (1)$$

In the elastic domain (Brugger, 1993):

$$\Phi_m = (M_1 - M_2)(h_1^3 + h_2^3) / (3H^2 E I_c) + (M_1 - M_2) h_j (h_1^2 + h_2^2 - h_1 h_2) / (3H^2 E I_j) \quad (2)$$

The second part on the right side corresponds to the joint zone deformation and the first part to the deformation of the remaining parts of the column.

$E$  = elastic module

$I_j$  = cross section inertia moment of the joint zone

$I_c$  = cross section inertia moment of the remaining parts of the column

The other terms in Eqs. (1) and (2) are shown in Figs. 4, 5 and 6.

Particular situations

a) - If  $h_j \ll H$  and/or  $I_j \gg I_c$ , the joint zone deformation would have little influence on the average joint rotation and the axis portion  $C_1 - C_2$  would remain nearly straight, with the left and right beam axes tangent to  $B_m' - D_m'$  at  $B_m'$  and  $D_m'$ , acc. Fig. 7a. The vertical displacement  $\delta v$  of the points  $B_m'$  and  $D_m'$  amounts:

$$\delta v = (\Phi_m) h_c / 2 \quad (3)$$

b) - Using the traditional rigid joint model (Fig. 7b), we would get the joint rotation (setting  $h_j = 0$  in equ. (2)):

$$\Phi_m = (M_1 - M_2)(h_1^3 + h_2^3) / (3H^2 E I_c) \quad (4)$$

Example - for  $h_j = 0,1H$ ,  $h_1 = h_2 = 0,45H$ ,  $h_1' = h_2' = 0,5H$  and  $I_j = I_c$  (Fig. 8):

Eq. (2)  $\Phi_m = 0,0675(M_1 - M_2)H / (E I_c)$

Eq. (4)  $\Phi_m = 0,0833(M_1 - M_2)H / (E I_c)$  (23% larger)

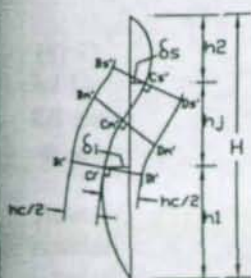


Fig. 6 - Deformation caused by pure bending

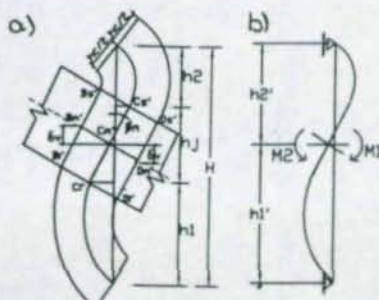


Fig. 7 - Particular situations

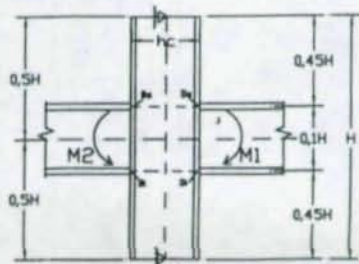


Fig. 8 - Example

## Notes

I) For the same example, with a bending stress of  $200\text{N/mm}^2$  at the column points  $B_1, B_m, D_1, D_m$ ,  $h_c=h_j$  and  $E=210000\text{N/mm}^2$ , we would get:

$$\Phi_m = 0,0029 \text{ (Eq. (2))} \quad \Phi_m = 0,0035 \text{ (Eq. (3))}$$

II) For  $I_j \gg I_c$  the difference between the two results would be still bigger.

It can be seen that the traditional rigid joint model is not appropriate to represent the deformation caused by pure bending.

## 2.2 Deformation caused by pure shear

The deformed column axis is shown in Fig. 9, with the new positions  $C_1', C_m', C_s'$  of the points  $C_1, C_m, C_s$ . The axis segments  $I-C_1', C_1'-C_s'$  and  $C_s'-S$  remain straight after the deformation.

Rotation of the joint zone:

$$\Phi = (\delta_s + \delta_i) / h_j \quad (5)$$

In the elastic domain (Brugger, 1993):

$$\Phi = (M_1 - M_2)(h_1 + h_2) / (H^2 G A_s) + (M_1 - M_2)(h_1 + h_2)^2 / (h_j H^2 G A_{sj}) \quad (6)$$

The second part on the right side corresponds to the joint zone deformation and the first part to the deformation of the remaining parts of the column.

$G$  = shear module

$A_{sj}$  = cross section shear area of the joint zone

$A_s$  = cross section shear area of the remaining parts of the column

The other terms in Eqs. (5) and (6) are shown in Figs. 4, 5 and 9.

The shear distortion of the joint zone amounts (Fig. 4 and 5):

$$\gamma = \tau / G = \Phi(h_1 + h_2) / (H G A_{sj}) = (M_1 - M_2)(h_1 + h_2) / (h_j H G A_{sj}) \quad (7)$$

The cross section rotation of the joint zone amounts (Fig. 9):

$$\alpha = \Phi - \gamma \quad (8)$$

With the cross section rotation, the new positions  $B_1', B_m', B_s', D_1', D_m', D_s'$  of the points  $B_1, B_m$  etc. are determined, as shown in Fig. 9. The left and right beam axes undergo a rotation  $\Phi$  at points  $B_m'$  and  $D_m'$  (Fig. 9).

### Particular situations

a)-If  $A_{sj} = A_s$  then, in the joint zone,  $\gamma = \Phi$  and  $\alpha = 0$ , i.e., the cross sections would remain horizontal.

- b)-If  $As_j \gg As$  then the shear distortion in the joint zone would be very small and  $\Phi$  would be given by the first part of the right side of Eq. (6).
- c)-Using the traditional rigid joint model (Fig. 10), the column axis would remain straight for the whole length and all the column cross sections (as well as the beam axes) would undergo a rotation of:  $\gamma = (M_1 - M_2)/(HG.A_s)$  (9)

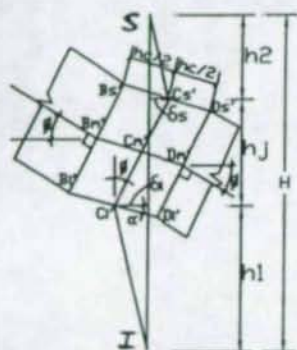


Fig. 9 - Deformation caused by pure shear

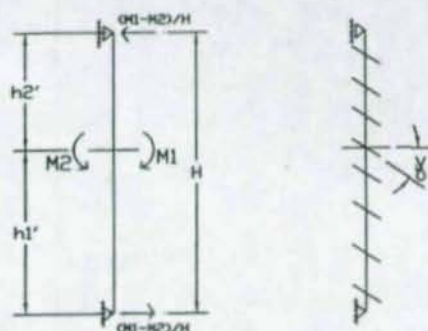


Fig. 10 - Traditional rigid joint model

Example - for the same situation shown in Fig. 8, we would get the following beam axis rotations:

I)-For  $As_j = As$

$$\text{Eq. (7)} \quad \Phi = \gamma = 9(M_1 - M_2)/(HG.A_s)$$

$$\text{Eq. (9)} \quad \Phi = \gamma = (M_1 - M_2)/(HG.A_s) \quad (9 \text{ times smaller})$$

Note - For a resultant moment  $(M_1 - M_2)$  corresponding to a shear stress of  $126 \text{ N/mm}^2$  in the joint zone ( $14 \text{ N/mm}^2$  in the remaining parts of the column) and  $G = 80800 \text{ N/mm}^2$ :

$$\Phi = 0,0015 \quad (\text{Eq. (7)}) \quad \Phi = 0,00017 \quad (\text{Eq. (8)})$$

II)-For  $As_j \gg As$

$$\text{Eq. (6)} \quad \Phi = 0,9(M_1 - M_2)/(HG.A_s)$$

$$\text{Eq. (8)} \quad \Phi = \gamma = (M_1 - M_2)/(HG.A_s) \quad (11\% \text{ larger})$$

It can be seen that the traditional rigid joint model is also not appropriate to represent the deformation caused by pure shear.

### 2.3 Local deformations of the connection and the column regions opposite to the beam flanges

Three different types of moment connections are shown in Fig. 11:

- welded connection - stiffened column (Fig. 11a)
- welded connection - non stiffened column (Fig. 11b)
- end plate bolted connection - non stiffened column (Fig. 11c)

For the situation shown in Fig. 11a, the stiffeners help to keep the segment lengths  $B_1-C_1$  and  $C_1-D_1$  (compressed by the beams) practically unchanged as well as the segment lengths  $B_2-C_2$  and  $C_2-D_2$  (tensioned by the beams). However, for the situation shown in Fig. 11b, the segments  $B_1-C_1$  and  $C_1-D_1$  will be shortened, the segments  $B_2-C_2$  and  $C_2-D_2$  will be stretched by the beam flange forces, due to column web horizontal deformation and column flange bending (Fig. 12a). For the bolted connection shown in Fig. 11c, not only the column web and flanges but also the end-plate and the bolts contribute to the local deformations (Fig. 12b).

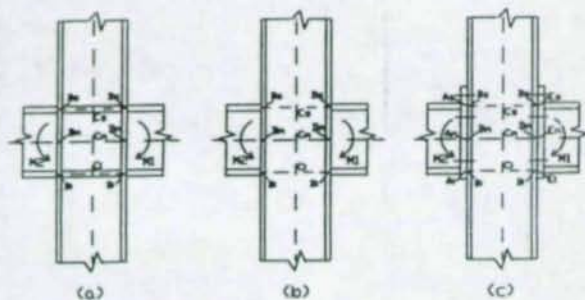


Fig. 11 - Three different types of moment connections

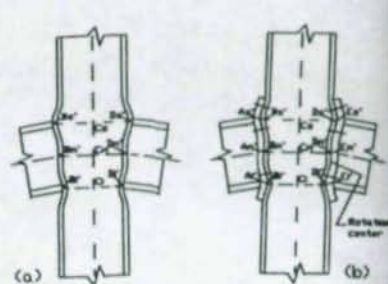


Fig 12 - Local deformations

It can be seen in Figs. 12a and 12b that the local deformations cause a rotation of the left and the right beam axes, and that the positions of the points  $B_m$  and  $D_m$  are not affected by the deformations. If the tensioned and the compressed regions of the joint have the same local rigidity, then the left and the right beams will rotate about points  $B_m$  and  $D_m$ , respectively; if this does not happen, then the rotation center will be displaced, as shown in Fig. 12b, where the tensioned region was supposed to be more flexible than the compressed region.

### 3. ANALYSIS OF SOME EXISTING SEMI-RIGID JOINT MECHANICAL MODELS

#### 3.1 Non-displaced rotational spring model - (EC3 part 1.1)

This model (Fig. 13), with appropriate springs, can represent the local deformations of the connection and of the column regions opposite to the beam flanges, except for the position of the rotation center of the beam axes. Because of the same reasons already mentioned for the traditional rigid joint model (sections 2.1 and 2.2), and also because of the resultant moment on the joint zone (as explained in section 1), it can not represent the bending and shear deformations of the joint zone. However, there is an iterative procedure (EC3 part 1.1) to take into account the influence of the joint zone shear deformation on the rotation of the beam axes. Two transformation parameters  $\beta_1$  (for one spring) and  $\beta_2$  (for the other spring) are used to correct the spring stiffnesses after each analysis step. Parameters  $\beta_1$  and  $\beta_2$  depend on the beam moments  $M_1$  and  $M_2$  and on the column shear forces above and below the joint zone. Although it is possible to get the beam rotations due to the joint zone shear with this procedure, it does not allow for the column axis deformation within the joint zone and, because of this, can not detect the interaction between column axial force and bending/shear deformation of the joint zone.

### 3.2 Displaced rotational spring model

This model is similar to the previous one, but the springs are placed on the positions corresponding to the column faces (Fig. 14). The cross section inertia moment and shear area of the auxiliary members  $B_m-C_m$  and  $C_m-D_m$  should be infinite. The rotation center of the beam axes is correct if the upper and lower local flexibilities included in the spring are the same. As for the previous model, it is not possible to represent the joint zone deformations with this model.

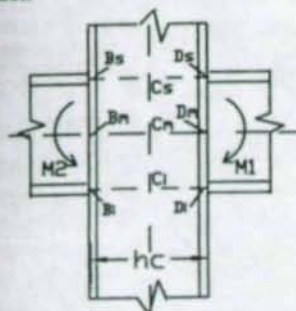


Fig. 13 - Non-displaced rotational spring model

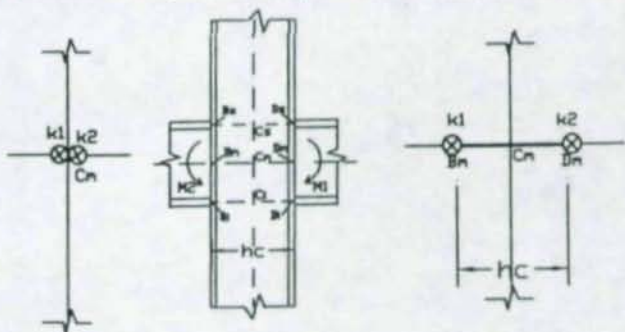


Fig. 14 - Displaced rotational spring model

### 3.3 Model with rotational springs on the beam and column axes for non-linear computer programs (Tschemmerneegg et al., 1994)

This model has rotational springs placed on the positions corresponding to the column faces, to represent the local deformations of the connection and of the column regions opposite to the beam flanges (Fig. 17). It further has rotational springs placed on the positions corresponding to the upper and lower limits of the joint zone, to represent the shear deformation of the joint zone. The cross section inertia moment and shear area of the auxiliary members  $B_m-C_m$ ,  $C_m-D_m$ ,  $C_1-C_m$  and  $C_m-C_2$  should be set infinite. An additional condition must be imposed on the stiffness matrix to get the correct bending deformation between points  $C_1$  and  $C_2$ . Alternatively, an additional member with the cross section inertia moment of the joint zone (with zero shear area) could be used between the point immediately above  $C_1$  and the point immediately below  $C_2$ . This model represents very closely all the types of deformation described in sections 2.1, 2.2 and 2.3. However, because the segment  $B_m-D_m$  remains always perpendicular to the segment  $C_1-C_2$ , the vertical displacements of the points  $B_m$  and  $D_m$ , corresponding to shear deformation of the joint zone, are not correct (see section 2.2). With this model it is not possible to take into account different local flexibilities for the upper and lower regions of the connection (or of the column), as for end plate bolted connections. The mentioned disadvantages are, in general, of minor importance. There are much available information on semi-rigid behavior using this model, including non linear analysis.

As described in (Tschemmerneegg et al., 1994) this model can be extended for composite joints by introducing additional springs: redirection spring, load introduction spring, slip-spring for the slab (Fig. 15, 16).

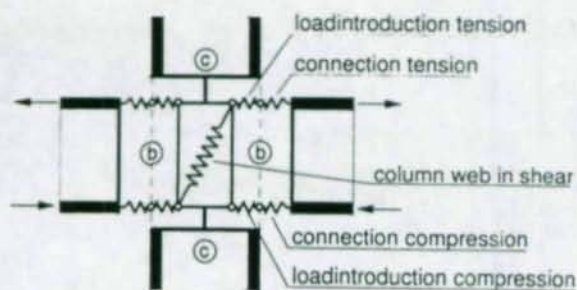


Fig. 15 - General model for steel joints

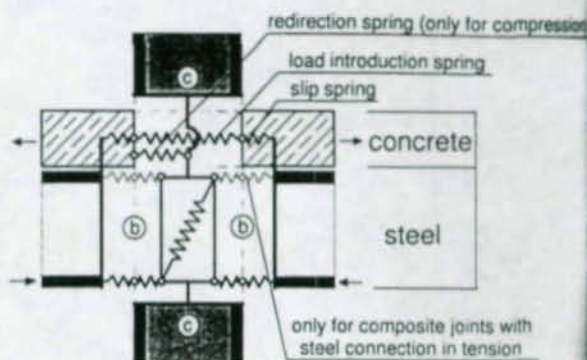


Fig. 16 General model for composite joints

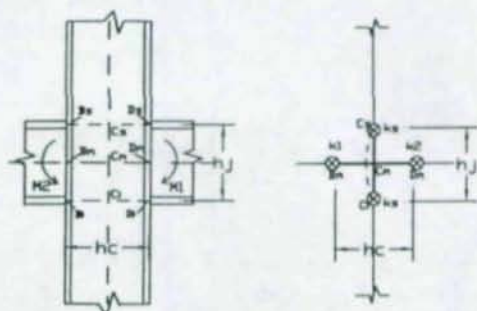


Fig. 17 - Model with rotational springs on the beam and column axes

#### 4. A NEW PROPOSAL FOR SEMI-RIGID JOINT MECHANICAL MODELING

The general behavior of a semi-rigid joint was first described by Tschemmerneegg (Tschemmerneegg et al., 1987). The model used in (Tschemmerneegg et al., 1987) to explain the behavior is shown in Fig. 15.

The mechanical model proposed below for semi-rigid joints (Fig. 18) was based on the general model shown in Fig. 15 and on the deformation modes described in sections 2.1, 2.2 and 2.3. It can be used with available software for the analysis of framed structures. This proposal was already presented in (Queiroz, 1992).

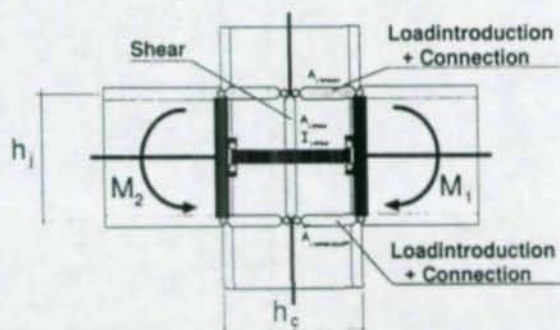


Fig. 18 - A new proposal for semi-rigid joint mechanical modeling

With this model, the bending and shear deformations of the joint zone are obtained simply by defining the correct cross section inertia moment and shear area for the members  $C_1-C_m$  and  $C_m-C_1$  (Fig. 18b). For the members  $B_1-B_m$ ,  $B_m-B_1$ ,  $D_1-D_m$ ,  $D_m-D_1$ , and also for the members  $B_m-C_m$ ,  $C_m-D_m$ , the cross section inertia moment and shear area should be infinite. The axial flexibility of the members  $B_1-C_1$  and  $C_1-D_1$  must correspond to the sum of local flexibilities of the connection and of the column, on the regions opposite to the lower flanges of the left and the right beams, respectively. The same is valid for members  $B_1-C_1$  and  $C_1-D_1$ , but with the upper instead of the lower flanges of the beams. The members  $B_m-C_m$  and  $C_m-D_m$  must transmit only the beam shear forces to the column (the left and right beam bending moments and axial forces are transmitted by  $B_1-C_1/B_1-C_1$  and by  $C_1-D_1/C_1-D_1$ , respectively); to provide for this, the link between members  $B_m-C_m$  and  $B_1-B_m$ , at  $B_m$ , and the link between members  $C_m-D_m$  and  $D_1-D_m$ , at  $D_m$ , only transmit a vertical force (Fig. 17c).

This model represents very accurately all the deformation modes described in sections 2.1, 2.2 and 2.3, including the correct position of the rotation center of the beams for shear deformation of the joint zone as well as for different local flexibilities of the connection (or of the column) on the upper and lower regions.

## 5. TRANSFORMATION PROBLEMS BETWEEN FINITE AND INFINITE JOINT-MODELS

The simplification of a realistic joint-model with finite dimensions to a joint-model with an infinite small joint-area at one hand leads to a very simply input for the frame-analysis, at the other hand the simplified joint-model is not able to represent the joint-behaviour exactly due to the flexibility of the extended beam and column, not in existence in the real joint. So the simplification causes the necessity of a 'joint-transformation' (Tschernegg, Huber, 1995) increasing the stiffness of the realistic joint-model when displacing the springs into the center of the joint to compensate the weakness of the beam and column extended into the joint-area. Unfortunately the simplified joint-model limits the stiffness of the joint with the bending-stiffness of the extended beam and column, a stiffer connection as it occurs for composite joints cannot be represented by the simplified joint-model. So when using the simplified joint-model one has to be conscious of the limiting boundary-conditions.

As the proposed joint-transformation-formulae are based on the assumption of a constant bending moment in the extended beam and column the errors of the simplified joint-model can be reduced significantly but not fully compensated. Parameter-studies for the transformation of the loadintroduction-spring have shown that in the worst case the overestimation of the beam-deflection can be reduced from 17% to 11% when using the joint-transformation and the underestimation of the fixing moments can be improved from 7% to 3%. So a further increase of stiffness would help to improve the results for the global frame-analysis, however the increasing-factor cannot be fixed but depends on the moment-distribution in the extended beam and column and therefore on the frame-system and the loading situation.

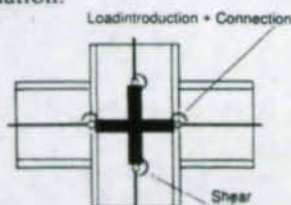


Fig. 19 - Finite joint-model

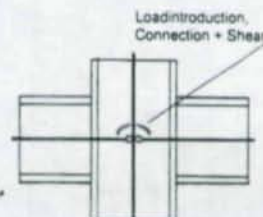


Fig. 20 - Infinite joint-model (EC3, EC4)

## 6. EXPERIMENTAL DATA

All the mechanical models only work if the force/displacement relations can be determined for each model component. These relations can be linear (at the beginning of the loading) or non linear and they are always obtained from tests. References (EC3 part 1.1), (Tschemmerneegg et al., 1994), (Klein, 1985), (Humer, 1987) and (Braun, 1987) contain much information about this subject.

## 7. CONCLUSIONS

The semi-rigid joint behavior was discussed and some mechanical models were presented that allow to analyze framed steel structures taking into account that behaviour. It was shown that the point model can not represent accurately the joint deformations, even if the joint is considered rigid. A new proposal for mechanical modeling of semi-rigid joints was presented that fits very accurately the joint deformation modes. Although only elastic behavior has been considered in this paper, the general concepts are also valid for inelastic behavior, with the appropriate force/displacement relations of the model components. The model described in section 3.3 and the new proposal described in section 4 work well for the interaction between column axial force and bending/shear deformation of the joint zone, when a non linear analysis is performed. There is no model that can represent the interaction between column axial force and local deformations of the connection or of the column region opposite to the beam flanges; however, tests have shown that this type of interaction is not important for rolled profiles (Lener, 1988).

When using a simplified joint-model with an infinite small joint area the stiffness of the rotational springs has to be increasing according the joint-transformation. The very simple joint-transformation-formula brings a significant improvement for the global analysis, however the real joint-behaviour can only be represented by a joint-model with finite dimensions.

## LIST OF REFERENCES

- BRAUN Ch. - Das Momenten-Rotationsverhalten von geschweissten, steifenlosen Rahmenknoten bei Querkraftbeanspruchung - Doctarate thesis, Innsbruck University, Austria, 1987
- BRUGGER R. - Zur Schubtragfähigkeit von Verbundknoten - Doctarate thesis, Innsbruck University, Austria, 1993
- EUROCODE 3 : Part 1.1 - Revised Annex J : Joints in Building Frames - Draft, ENV 1993-1-1
- HUMER Ch. - Das Momenten-Rotationsverhalten von steifenlosen Rahmenknoten mit Kopfplattenanschlüssen - Doctarate thesis, Innsbruck University, Austria, 1987
- KLEIN H. - Das elastisch-plastische Last-Verformungsverhalten M-n steifenloser, geschweisster Knoten für die Berechnung von Stahlrahmen mit HE-B Stützen - Doctarate thesis, Innsbruck University, Austria, 1985
- LENER G. - Berechnung räumlicher Stahlrahmen mit nichtlinearem Knotenverhalten unter Berücksichtigung der Normalkraftsinteraktion - Doctarate thesis, Innsbruck University, Austria, 1988
- QUEIROZ G. - Estudo do Comportamento e Sistematização do Projeto de Ligacões Rígidas entre Perfis I com Almas Coplanares - M. Sc. dissertation, UFMG Eng. School, Brasil, 1992
- TSCHEMMERNEGG F., BRUGGER R., HITTENBERGER R., WIESHOLZER J., HUTER M., SCHAUR B.C. und BADRAN M.Z. - Semi-Rigid Composite Joints - Der Stahlbau, Dec. 1994 and Jan. 1995
- TSCHEMMERNEGG F., TAUTSCHNIG A., KLEIN H., BRAUN Ch. und HUMER Ch. - Zur Nachgiebigkeit von Rahmenknoten - Stahlbau, 10/1987, pp.299-306
- TSCHEMMERNEGG F., HUBER G. - Joint-transformation and influence for the global analysis - Technical Paper T6 - COST C1/ECCS TC11 - Drafting group for Composite Connections, May 1995

## PROPOSAL OF THE STIFFNESS DESIGN MODEL OF THE COLUMN BASES

František Wald<sup>1</sup>

Zdeněk Sokol<sup>2</sup>

Martin Steenhuis<sup>3</sup>

### Abstract

The connection between the steel column footing and the concrete foundation has a rotational rigidity significant for the overall frame analysis. This rigidity could be taken into account to predict the horizontal drift of the frame in serviceability limit state. A proposal of the stiffness design model compatible with stiffness prediction according to Eurocode 3, Annex J is presented in the paper. The model is based on the component method. Three patterns of the base plate internal forces distribution represent different collapse modes based on axial force – total bearing capacity ratio. The prediction model is compared to experimental observations. A parametric study of the main parameters of the model is included.

### 1. INTRODUCTION

In the structural frames, the column base joints have a high restraining capacity. However, their semi-rigid behaviour is seldom introduced into the frame analysis because of absence of simple and reliable stiffness models. The full scale frame experiments, in situ measurements and numerical studies document the high rigidity of the column base joints. The frame finite element analysis and the application of ultimate limit state enable the introduction of the advantages of column base stiffness, Eurocode 3, cl. 5.2.3.3, into the design procedure.

---

<sup>1</sup> Assoc. Prof., Czech Technical University, Thákurova 7, 166 29 Praha 6, Czech Republic.

<sup>2</sup> Grad. Res. Asst., Czech Technical University, Thákurova 7, 166 29 Praha 6, Czech Republic.

<sup>3</sup> Research Assistant, TNO, Lange Kleiweg 5, Rijswijk, P.O. Box 49, 2600 AA Delft, The Netherlands.

The small number of tests concerning the column base rotational stiffness has resulted in development of only a few prediction models for specific purpose. The elastic – plastic model of rotational stiffness prediction was published by Salmon *et al* (1957). The model of cyclic behaviour for the seismic design was derived from the Japanese experiments (Akiyama, 1985; Nakashima *et al*, 1991). The Penserini – Colson's model based on component damages predicts the cyclic behaviour very accurately (Penserini and Colson, 1991). The stiffness and soil interaction of the column bases with bolts inside the column cross section (pinned column base joints) were studied by Melchers, (1992).

The presented model is derived to be compatible with stress design published in Eurocode 3, Annex L, and with the beam to column connection stiffness prediction, Annex J. The development of this model was preceded by derivation of complex analytical models for unstiffened base plate with bolts outside the column (Sokol *et al*, 1995; Ermopoulos and Stamopoulos, 1995) and for base plates with bolts inside the column of H cross-section (Wald and Sokol, 1995). These models were compared to the tests summarised in the COBADAT database and to tests made at CTU (Wald *et al*, 1994). The presented model enables to calculate a moment–axial force–rotation curve for constant axial force. This represents typical loading in buildings, when the joint is firstly loaded by vertical force from dead and live loads (remaining constant) and secondly by changeable horizontal wind load.

## 2. STIFFNESS OF THE COMPONENTS

The stiffness of each component is calculated separately compatible to Eurocode 3, Annex J. The relevant stiffness coefficients  $k_i$  are taken into calculation of the stiffness.

### 2.1. The Base Plate in Tension

The stiffness coefficient of the base plate  $k_B$  is calculated from an equation for plate in bending as

$$k_B = 0,425 \frac{L_{eff,1} t^3}{m^3} \quad (2.1)$$

when there is no prying, or

$$k_B = 0,85 \frac{L_{eff,1} t^3}{m^3} \quad (2.2)$$

when prying occurs (Jaspart *et al*, 1995). In the above formulas,  $t$  is the plate thickness and  $L_{eff,1}$  is the effective length taken from Eurocode 3, Annex J, Tab. 3.3.3

(circular and other patterns). The prying occurs only for thin plates and short bolt elongation length (Wald et al, 1994), i.e. when

$$t \leq 3 \sqrt{\frac{6em^2 A_b}{(L_{bf} + L_{be}) L_{eff}}} \quad (2.3)$$

When the prying occurs the plate could also collapse in Mode 2 with effective length  $L_{eff,2}$  (other patterns only).

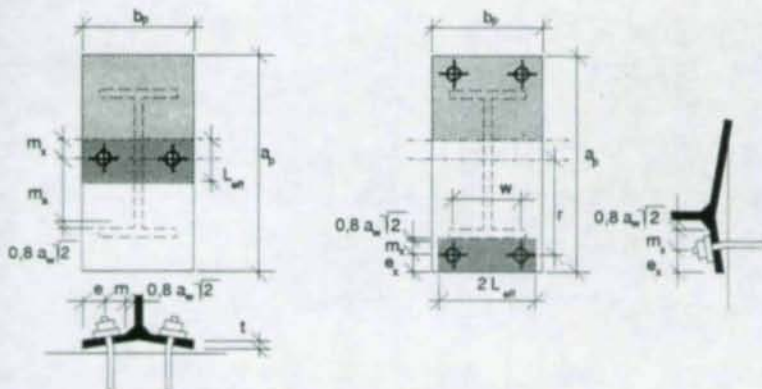


Fig. 1 Calculation of the base plate T-stub effective length.

## 2.2 The Anchor Bolts

The stiffness coefficient of one bolt row in tension should be taken as

$$k_s = 2,0 \frac{A_s}{L_b} \quad (2.4)$$

$$L_b = L_{bf} + L_{be} \quad (2.5)$$

where  $A_s$  is the stress area of one bolt and the elongation length of the bolt  $L_b$  is calculated from the free bolt length  $L_{bf}$  and from the part of the bolt embedded in the concrete  $L_{be}$ , see Fig. 2. The free bolt length  $L_{bf}$  may be taken as the total grip length (thickness of the material and washer) plus the grout thickness plus half the height of the nut. The embedded part of the bolt  $L_{be}$  contributing to bolt extension could be estimated as 8 times the bolt diameter  $d$  for long bolts (Salmon et al, 1957; Sato, 1987). The effective bolt length  $L_{be}$  could be predicted for short headed bolts (Furche, 1994; Wald and Sokol, 1995) or for the other types of anchoring (Eligehausen, 1991). The coefficient 2.0 is used for long bolts without prying (see Eq. 2.3). The coefficient 1,6 should be used for short bolts, as in Eurocode 3 (Jaspart et al, 1995).

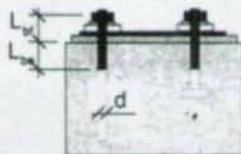


Fig. 2 Elongation length of embedded and headed bolts.

### 2.3. The Base Plate in Compression

The flexible base plate loaded in compression is in the calculation represented by effective rigid plate. The effective area taken into calculation for stiffness prediction is simplified to rectangular area, see Fig. 3. The use of effective area assures compatibility between the stress design in Annex L and the stiffness calculation in Annex J. The calculation of the effective width  $c$  was fully adopted from Annex L:

$$c = t \sqrt{\frac{f_{yD}}{3 f_c \gamma_{M0}}} \quad (2.6)$$

In the formula  $f_{yD}$  is yield strength of base plate material and  $f_c$  is the concrete bearing strength and  $\gamma_{M0}$  is partial safety factor.

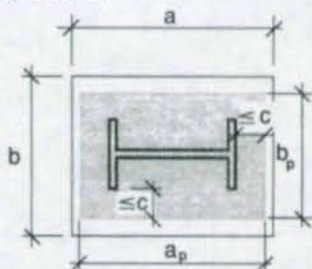


Fig. 3 The effective area for stiffness calculations.

### 2.4. The Concrete Block

A new stiffness coefficient for concrete in compression is introduced into the calculations as

$$k_{10} = 0,5 \frac{a_p b_p E_c}{h E} \quad (2.7)$$

where  $a_p$  and  $b_p$  are the effective dimensions of the base plate,  $E$  and  $E_c$  are the modules of elasticity of steel and concrete respectively and  $h$  is height of the concrete block.

## 3. The Stiffness Calculation

### 3.1. The Stress Distribution

An elastic plastic stress distribution in concrete has been assumed. The concrete bearing stress  $f_j$  is given by

$$f_j = \frac{2}{3} k_j f_{cd} \quad (3.1)$$

where  $k_j$  is the concentration factor and  $f_{cd}$  is the concrete cylinder strength (Eurocode 3, Annex L).

The maximum force acting in the tension part of the joint is derived from resistance of the equivalent T-stub. The following formulas cover different failure modes: complete yielding of the base plate (Eq. 3.2), bolt failure with yield of the base plate (Eq. 3.3) and bolt failure (Eq. 3.4). The effective stress of the tension part  $f_t$  is taken as the smallest value from

$$f_t = \frac{2 L_{\text{eff}} t^2 f_{yp}}{m A_s} \quad (3.2)$$

$$f_t = \frac{L_{\text{eff}} t^2 f_{yp}}{(m+n) A_s} \quad \text{in case of prying only, (Eq. 2.3), } n = \min(e; 1,25 m) \quad (3.3)$$

$$f_t = f_{yb} \quad (3.4)$$

It is necessary to input the corresponding values into the equations, i.e. the distances  $m$  and  $e$  for bolts inside the column or  $m_x$  and  $e_x$  for bolts outside the column cross section, see Fig. 1.

It is possible to distinguish between three basic modes of collapse depending on the bearing stress distribution under the base plate with respect to the tension part, see Fig. 4.

The concrete bearing stress  $f_j$  is never reached, when the column base joint is loaded by low axial force (compared to the ultimate bearing capacity). The collapse occurs either by yielding of the bolts or by developing plastic mechanism in the base plate (pattern 1). When medium axial force is applied, the concrete bearing stress  $f_j$  and the effective stress of the tension part  $f_t$  are reached at the collapse (pattern 2). For high axial force only collapse of the concrete occurs (pattern 3).

The boundaries between these three modes will be calculated. The axial force representing the boundary between low and medium forces is calculated as

$$N_{1,2} = \frac{a_p b_p^2 f_j^2 (2r + a_p) \frac{1}{k_{10}}}{4 \left( a_p b_p f_j \frac{1}{k_{10}} + 4 A_s f_t \left( \frac{1}{k_s} + \frac{1}{k_b} \right) \right)} - 2 A_s f_t \quad (3.5)$$

and the boundary between medium and high forces is given by

$$N_{2,3} = \frac{(2r + a_p) b_p f_j - 2 A_s f_t}{2} \leq a_p b_p f_j \quad (3.6)$$

where  $r$  is the lever arm of the bolt row from the centre line of the base plate, see Fig. 1.

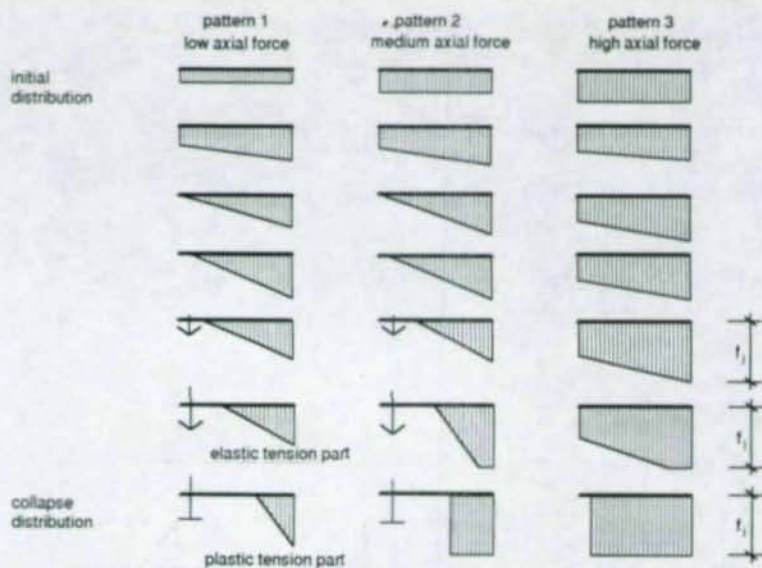


Fig. 4 The internal force distribution for three patterns of the base plate joint in initial and collapse stages.

### 3.2. The Rotational Stiffness

The rotational stiffness of the joint may be calculated by

$$S_i = \frac{E z^2}{\mu \sum_i \frac{1}{k_i}} \quad (3.7)$$

where  $k_i$  is the stiffness coefficient for component  $i$  and  $z$  is the lever arm, see Tab. 1 and Fig. 5.

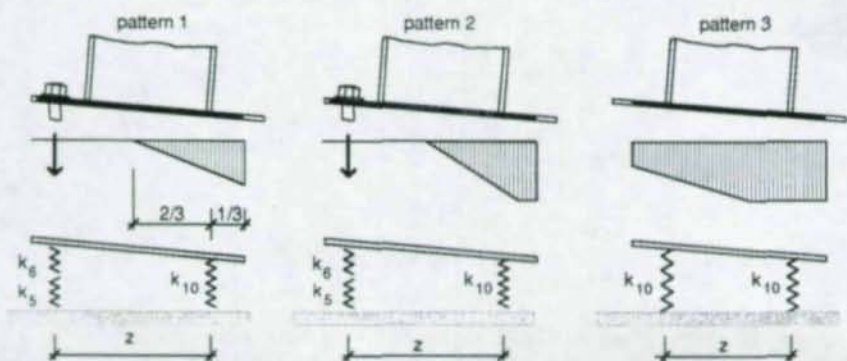


Fig. 5 The mechanical simulation of the components deformability.

The ratio between the rotational stiffness with respect to moment can be calculated as

$$\mu = \frac{S_{i, int}}{S_i} = \left( \kappa \frac{M_{Sd}}{M_{Rd}} \right)^\xi \geq 1 \tag{3.8}$$

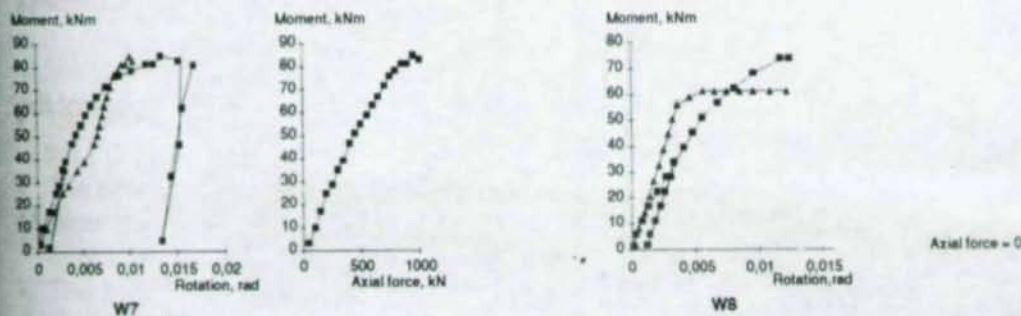
where  $\xi$  is the shape parameter of the curve. The coefficient  $\kappa$  introduces the beginning of non-linear part of the curve and varies from 1,1 to 1,5, see Tab. 1.

Tab. 1 Values to be considered in stiffness calculation for different patterns.

	Stiffness coefficients $k_i$ to be considered	$\kappa$	$\xi$	$z$
pattern 1 low axial force $N \leq N_{1,2}$	$k_5, k_6, k_{10}$	1,1	6	$\frac{M_{sd} + Nr}{N + 2 A_s f_y}$ but $M_{sd} \geq \frac{M_{Rd}}{\kappa}$
pattern 2 medium axial force $N_{1,2} < N < N_{2,3}$				linear transition between patterns 1 and 3
pattern 3 high axial force $N_{2,3} \leq N$	$k_{10}, k_{10}$	1,5	8	$\frac{a_p}{\sqrt{3}}$

#### 4. COMPARISON OF THE MODEL TO EXPERIMENTS

All the test specimens have the same geometry, see Fig. 7, and material properties. They were loaded by axial and horizontal forces increasing proportionally (experiments W7, W10, W12) or by bending moment only (experiment W8), see Fig. 6 (Wald et al, 1994). Because the model is derived for constant axial force, the curves were calculated point by point for corresponding axial forces and eccentricities.



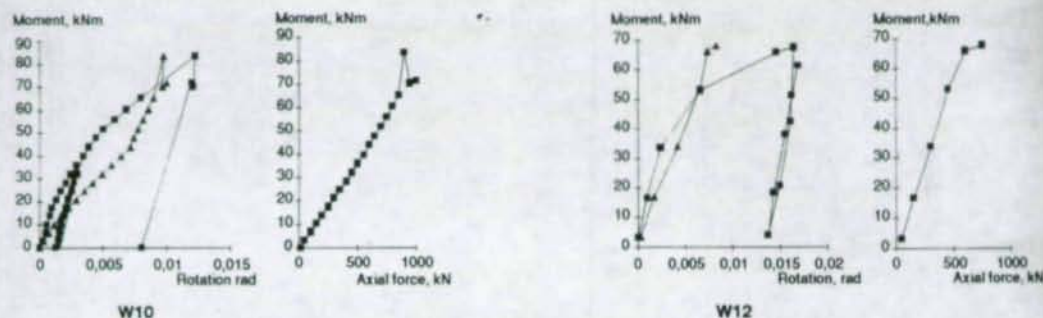


Fig. 6 Experimental and analytical moment-rotation curves; ■ experiments, Δ prediction.

## 5. PARAMETRICAL STUDY

The bolt elongation length (Fig. 7) and diameter, the base plate thickness (Fig. 8) and the quality of concrete (Fig. 9) are the parameters which have the most significant influence on the behaviour of the joint. The history of the loading (Fig. 6) and the axial force / bearing capacity ratio (Fig. 10) should be considered as other parameters influencing the rotation and the moment capacity of the connection. The sensitivity to these parameters is shown on the following pictures.

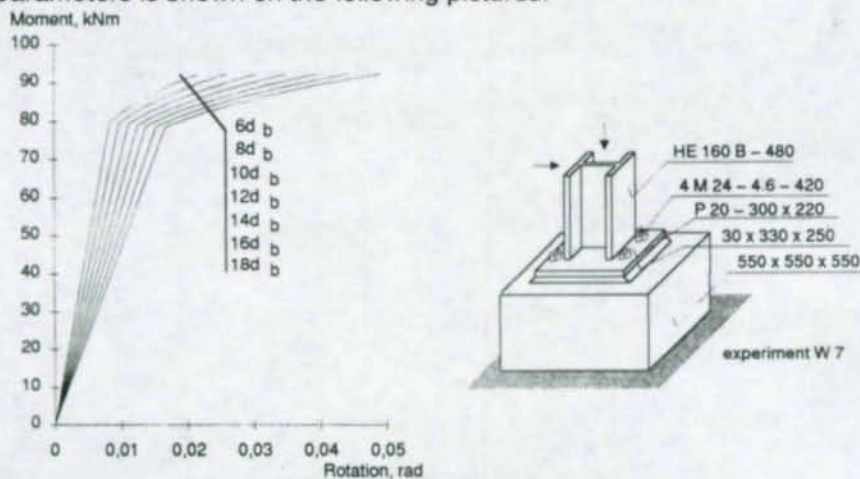


Fig. 7 The influence of the bolt embedded length  $L_{be}$  on base plate joint stiffness (experiment W 7, constant axial force 700 kN).

The Young's modulus of concrete was calculated for the prediction of influence of the concrete quality from the equation

$$E_c = 9500 \sqrt[3]{(f_{cd} + 8)} \quad (5.1)$$

where the concrete cylinder strength  $f_{cd}$  should be input in MPa.

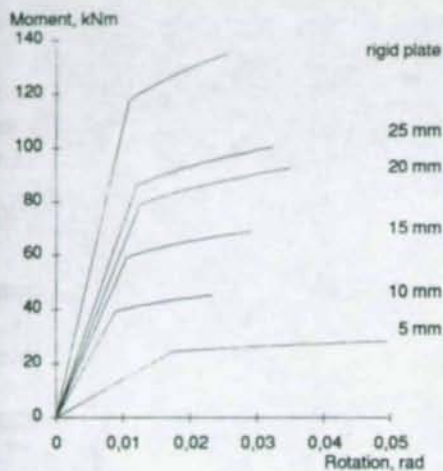


Fig. 8 The influence of the base plate thickness on base plate joint stiffness (experiment W 7, constant axial force 700 kN).

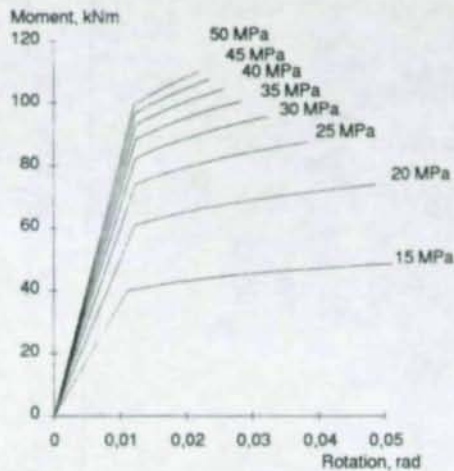


Fig. 9 The influence of the concrete quality on base plate joint stiffness (experiment W 7, constant axial force 700 kN).

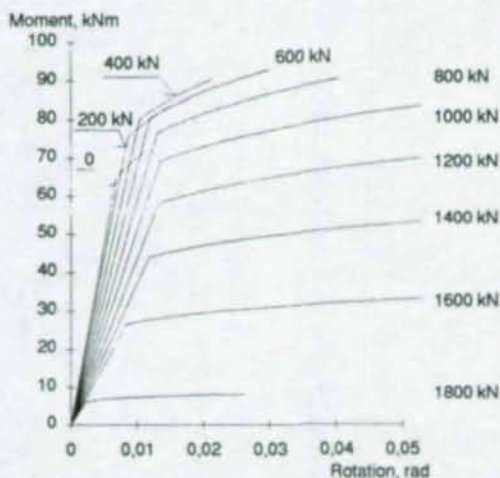


Fig. 10 The influence of the axial force on base plate joint stiffness (experiment W 7).

## 6. CONCLUSIONS

- The presented stiffness model complements the strength prediction according to the Eurocode 3, Annex L.
- The presented design model predicts the stiffness behaviour with a good level of accuracy. The model is build up on principles of stiffness prediction published in Eurocode 3, Annex J.
- The model is evaluated based on a limited number of experiments. Wider test observations could therefore lead to further changes in the model parameters.

### Acknowledgement

The research has been conducted at the Department of Steel Structures as a part of the research project "Column-Base Strength and Rigidity Modelling" which has been supported by the PECO grant No. 143 E6 / 92 and by the Czech government grant COST C1.

### References

- Eurocode 3, ENV 1993-1-1, (1992): *Design of Steel Structures*, European Pre-norm, Commission of the European Communities, Brussels, Aug.
- Akiyama H., (1985): *Seismic Design of Steel Column for Architecture*, in Japanese, Gibodokupan, Tokyo.
- Eligehausen R., (1991): *CEB Design Concept for Fastenings to Concrete*, CEB 91/09/20, p.42.
- Ermopoulos J.Ch., Stamopoulos, G.N., (1995): *Moment-rotation curves for semi-rigid column bases*, in *Steel Structures - Eurosteel 95*, Kounadis ed., Balkema, Rotterdam, pp. 211 - 217.
- Furche J., (1994): *Zum Trag - und Verschiebungsverhalten von Kopfbolzen bei zentrischem Zug*, IWG 2, Universität Stuttgart, Stuttgart, p. 182.
- Jaspart J.P., Steenhuis M., Weynand K., (1995): *The Stiffness Model of revised Annex J of Eurocode 3*, Third International Workshop on Connections in Steel Structures, Trento, in printing.
- Melchers R. E., (1992): *Column-Base Response Under Applied Moment*, Journal of Construct. Steel Research, No. 23, pp. 127-143.
- Nakashima S., Suzuki T., Igarashi S., (1989): *Mechanical Characteristics of Exposed Type Steel Column Bases*, in International Conference Bolted and Special Structural Connections, Vol. 2., Moscow, May, pp. 148-152.
- Penserini P., Colson A., (1991): *Modelling of Column-Base Connections*, in Czechoslovakian XVI. International Conference, April, Ostrava, pp. 95-99.
- Salmon C. G., Schenker L., Johnston G. J., (1957): *Moment - Rotation Characteristics of Column Anchorage*, Transaction ASCE, Vol. 122, No. 5, pp. 132-154.
- Sato K., (1987): *A Research on the Aseismic Behaviour of Steel Column Base for Evaluating its Strength Capacity and Fixity*, Pacific Structural Steel Conference, August, Auckland, New Zealand.
- Sokol Z., Wald F., Dunai L., Steenhuis M., (1994): *The Column-Base Stiffness Prediction*, in *Semi-Rigid Behaviour of Civil Engineering Structural Connections*, Second State of the Art Workshop, Brussels, pp. 259-270.
- Stockwell F. W. Jr., (1975): *Preliminary Base Plate Selection*, Engineering Journal AISC, Vol. 21, No. 3, pp. 92-99.
- Wald F., Šimek I., Sokol Z., Seifert J., (1994): *The Column-Base Stiffness Tests*, in *Semi-Rigid Behaviour of Civil Engineering Structural Connections*, Second State of the Art Workshop, Brussels, 1994, pp. 273-282.
- Wald F., Sokol Z., Pultar M., (1994): *Effective Bearing Area under the Flexible Base Plate*, in *New Requirements for Structures and their Reliability*, Prague, CTU, pp. 175 - 181.
- Wald F., Sokol Z., (1995): *Design Approach of the Column Base Plate Resistance of Components in Tension*, in ČVUT FSV report, p. 3, Prague, in printing.
- Wald F., Sokol Z., (1995): *The Simple column - base stiffness modelling*, in *Steel Structures - Eurosteel 95*, Kounadis ed., Balkema, Rotterdam, pp. 277 - 286.

Technical Papers on

**MODELLING OF CONNECTIONS**

## Modelling Composite Connection Response

B Ahmed<sup>1</sup>

T Q Li<sup>2</sup>

D A Nethercot<sup>3</sup>

### Abstract

A finite element model to simulate the structural behaviour of composite flush endplate beam to column connections is described. This model has been validated against test results and compared with a simplified calculation method; both checks demonstrate its accuracy. Parametric studies using the model to investigate variations in: reinforcement ratio, degree of shear connection and shear-span/moment ratio are presented.

### 1 INTRODUCTION

Numerous recent studies have demonstrated the potential for using composite action in beam to column connections as a way of developing the semi-continuous framing that is a permitted alternative for design in the Structural Eurocodes. Understanding of the detailed aspects of the connection behaviour has, thus far, largely relied on test evidence and the subsequent development of behavioural models. Because of the large number of variables and potential failure modes associated with composite connections, such an approach is unlikely ever to be able to thoroughly examine all aspects of the problem.

It is therefore natural to explore the possibility of using alternative numerical approaches. Of these, the finite element method, which has previously been used successfully to model several

---

<sup>1</sup>Research Student, Department of Civil Engineering, University of Nottingham, University Park, Nottingham NG7 2RD, UK

<sup>2</sup>Research Assistant, Department of Civil Engineering, University of Nottingham, University Park, Nottingham NG7 2RD, UK

<sup>3</sup>Professor and Head, Department of Civil Engineering, University of Nottingham, University Park, Nottingham NG7 2RD, UK

different forms of bare steelwork connection, was selected as the most promising. Although some initial work in this area has been undertaken (Leon and Lin, 1986 and Puhali *et al.*, 1990), an accepted approach to the finite element modelling of composite connections has yet to be developed.

This paper reports an on-going study using a standard nonlinear finite element package - ABAQUS. The first task has been to develop a finite element model that faithfully represents all aspects of the physical behaviour of composite endplate connections that have been observed in physical tests. Validation of the modelling has been assisted by the availability of a comprehensive database of all known composite connection test results, especially the very detailed test histories that were produced in the series conducted in the University of Nottingham (Li, 1994).

## 2 FINITE ELEMENT MODELLING

The key components in a composite connection are: reinforcement in the slab, shear studs in the slab, the concrete slab itself, the steel beam, the steel column, the fittings (endplate, fin plate, cleats *etc.*), the bolts connecting the beam and the column.

When loaded, the concrete part is active in taking tensile force in the initial linear region only, after which tensile cracks form and the slab merely serves to transfer tensile force to the reinforcement with the help of the shear studs. The reinforcement and the upper row of bolts take the tensile force, while the beam bottom flange together with part of the beam web transfers the compressive force to the column flange through the endplate or fin plate. In the case of a flush endplate joint, the upper part of the endplate separates from the column flange, whilst the beam web and the bottom flange in the compression region remain in firm contact and transfers the compressive force directly to the column. As the joint approaches its ultimate load capacity, its resistance may be controlled by any or a combination of: fracture of reinforcement, failure of shear studs, excessive deformation of column flange, local buckling of column web, buckling of beam flange, buckling of beam web, bolt failure, twisting of fin plate *etc.*

For successful numerical modelling of any composite connection the following items must be properly represented: reinforcement, shear studs (considering slip between the slab and the beam and also the percentage of shear interaction provided), steel beam and column (including buckling and plasticity), bolts (including slip), separation and closure at the interface of the endplate and the column flange and load introduction. ABAQUS (Hibbitt *et al.*, 1994), which is a general purpose finite element software, was selected for this purpose; it is capable of conducting finite element analyses considering both geometric and material non-linearity and also includes interface elements and constraint conditions.

## 2.1 Finite element modelling of a bare steel joint

### 2.1.1 Test set-up

Before modelling the composite joint, a simpler bare steel flush endplate joint was modelled. The joint (SJS1) had been tested (Li, 1994) in the University of Nottingham. It comprised a 254x102 UB 25 steel beam, 203x203 UC 46 steel column, 280x130x10 mm endplate and four M20 bolts (bolt hole diameter 22 mm). The bolt holes were positioned 175 mm centre to centre vertically and 70 mm centre to centre horizontally. The column length was 1800 mm, and it was restrained at the top and bottom. SJS1 was a cruciform joint, with load applied 1473 mm from the column face through load cells. The material properties obtained from coupon tests are shown in Fig 1 and the test rig and specimen set-up is shown in Fig 2. The specimen failed at a load of 42.63 kN.

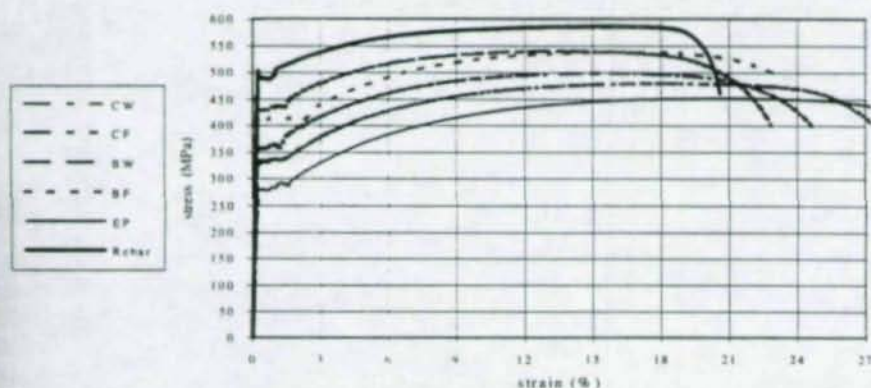


Fig 1 Typical stress-strain curves of steel specimens

Note: CW is column web, CF is column flange, BW is beam web, BF is beam flange  
EP is endplate and Rebar is reinforcement

### 2.1.2 Finite element mesh

The finite element mesh, obtained after some trials, is shown in Fig 3. Since the joint was symmetrical, only one side was modelled so as to reduce the problem size. The beam, column and the endplate were modelled using four node shell elements with six degrees of freedom per node. Interface elements, capable of transferring any compression when in contact and allowing no tensile force to be transferred during separation, were used to model contact between the endplate and the column flange. At the column flange and the endplate, holes were specified to represent the bolt holes. Bolts were modelled by joint elements and load displacement curves of the bolts were used to obtain the required characteristics. These were

derived from a combination of finite element analysis of bolt and plate contact and elastic analysis. The resulting properties are shown in Fig 4.

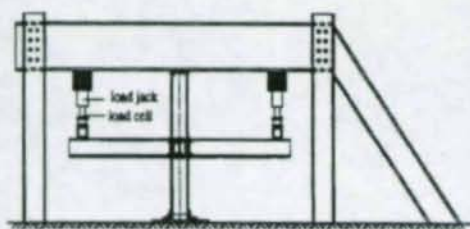


Fig 2 Test rig and specimen (SJS1) set-up

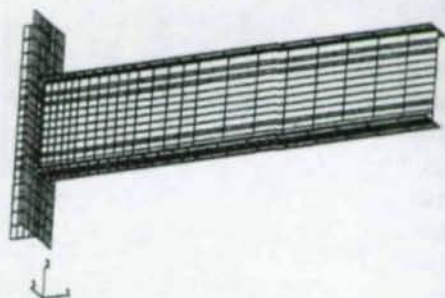


Fig 3 FE mesh layout for the bare steel joint SJS1

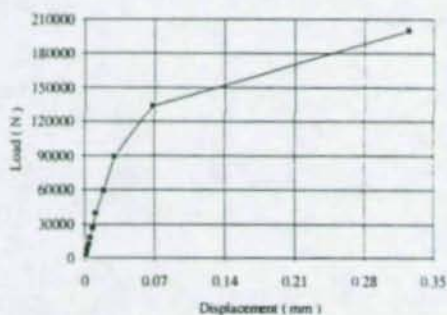


Fig 4a Load-shear deformation curve for bolt

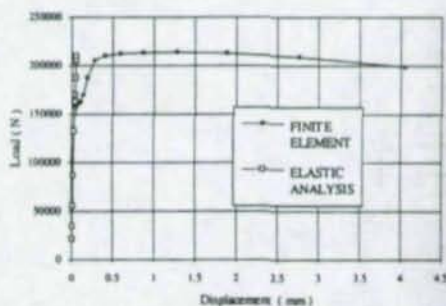


Fig 4b Load-axial deformation curve for bolt

### 2.1.3 Boundary conditions

Since advantage was taken of symmetry, appropriate boundary conditions were required to address the problem correctly. The nodes of the column web centreline were restrained from movement along the direction of the beam axis (Fig 3), and from rotation about both the centreline itself and the line perpendicular to the plane of the column web. Nodes at the bottom of the column were restrained from any movement in the three directions, while for the nodes at the top of the column only vertical movement was allowed. In the test load was applied through load cells; in the FE model load was applied directly to the nodes of the beam web. To overcome the problem of local yielding, this was divided equally between ten nodes.

### 2.1.4 Comparison of test and finite element results

The moment-rotation curves obtained from the test and from the finite element analysis are shown in Fig 5; they are very close to each other. The displaced shapes of the joint observed in the test and given by analysis are shown in Figs 6 and 7 respectively. As noted in the test, column web Von-Mises stresses exceeded the yield stress of the material.

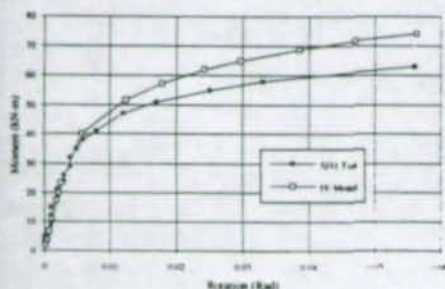


Fig 5 Comparison of moment-rotation curves for SJS1

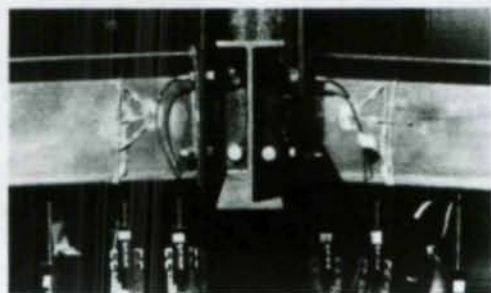


Fig 6 Displaced shape of the joint after test (SJS1)

### 2.2.1 FE modelling of a composite connection

Test CJS1 (Li, 1994) was selected for verification purposes. The reason was that joints SJS1 and CJS1 had the same beam, column, endplate, bolt detail and test set-up; the only difference was the inclusion of the reinforced concrete slab and the shear studs. The early FE studies (Li et al., 1991) had indicated that the concrete model in ABAQUS did not work well when applied to composite connections. A similar experience was faced by the authors. When the concrete slab started to crack the solution did not proceed, whereas in the test, the load was taken by the reinforcement after cracking of the slab and the ultimate load is much higher than the cracking load. To solve this problem, bearing in mind that the role of the concrete is to transfer the tensile force to the reinforcement with the help of the shear studs, concrete was ignored in the model and multi point constraints were used in the stud sections. Studs were modelled by beam elements and the reinforcement by truss elements. At the stud and reinforcement connection joint elements were used to model the slip between the slab and beam and to model the degree of shear interaction. The load-deformation curve for these joint elements is shown in Fig 8.

### 2.2.2 Comparison of test and FE results

The ultimate load capacity of the joint was 122 kN, the test being stopped at a rotation of 48 mrad. The FE analysis gave a load capacity of 124 kN and an ultimate rotation of 79 mrad. The moment-rotation curves from the test and the FE analysis are shown in Fig 9. Comparison

of horizontal strains in the beam web are given in Fig 10 and rebar strains are compared in Fig 11. Figs 9 to 11 show each of these measures of the experiment and the analysis to be very close. It was therefore concluded that the model could be used to study further the behaviour of composite joints.

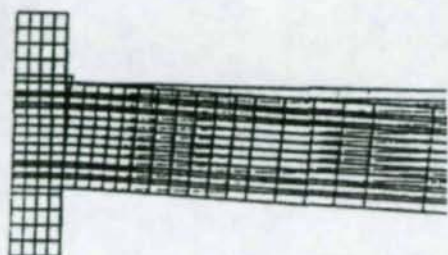


Fig 7 Displaced shape of the joint from analysis (SJS1)

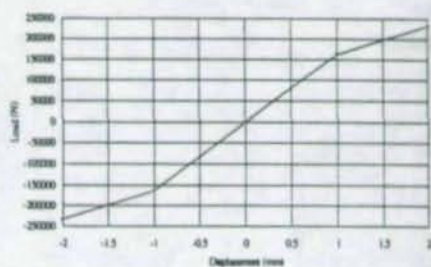


Fig 8 Load-deformation curve used for shear stud

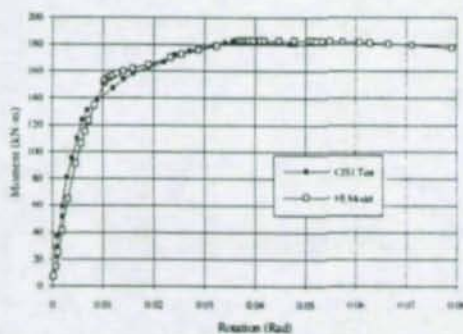


Fig 9 Comparison of moment rotation curves for CJS1

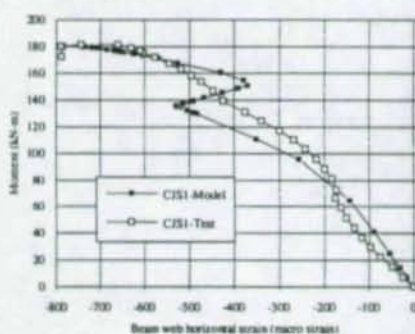


Fig 10 Comparison of beam web horizontal strain for CJS1

### 3 STUDY FOR REINFORCEMENT RATIO

After the successful modelling of CJS1, some studies were carried out to check the effect of varying the reinforcement ratio. These also served as a check on whether the reinforcement had been correctly introduced. If so, then reinforcement areas between a bare steel joint i.e. 0 mm<sup>2</sup> and 767 mm<sup>2</sup> should produce load carrying capacities and moment-rotation curves which would lie between the two already obtained. Reinforcement areas of 767, 637, 425 and 212 mm<sup>2</sup> were used for the analyses, with other parameters kept constant. Using a test base design model (Li, 1994) the moment capacities for these reinforcement areas were calculated

by taking the material strength as either the yield strength (calculated result-A in Table 1) or the ultimate strength (calculated result-B in Table 1) as obtained from Li's supplementary tests. The results of the design calculation and the FE analyses are shown in Table 1, from which it appears that the design model is most appropriately used with the ultimate material strengths. Fig 12 shows the comparison of moment-rotation curves for various reinforcement areas, including the bare steel joint. Both the load carrying capacities and the moment-rotation curves appear reasonable. The ultimate moment capacity is consistent with the design model. The variation of the initial stiffness and the ultimate moment capacity with the changes to the reinforcement area are shown in Figs 13 and 14.

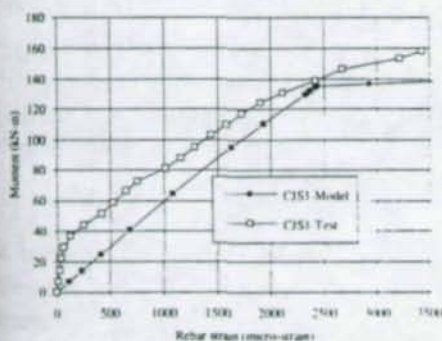


Fig 11 Comparison of reinforcement strain for CJS1

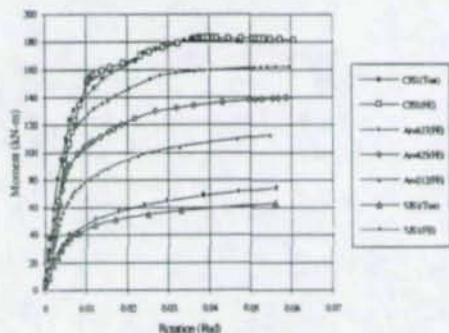


Fig 12 Effect of reinforcement area on composite joint moment capacity

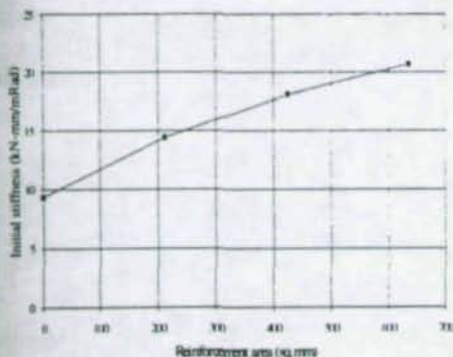


Fig 13 Variation of Joint initial stiffness with reinforcement area

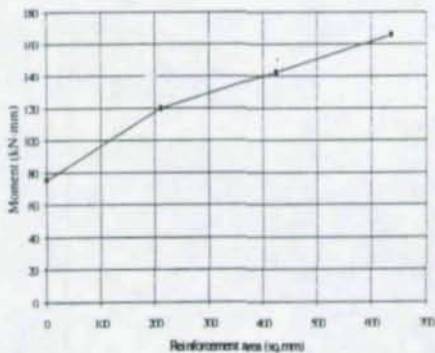


Fig 14 Variation of ultimate moment capacity with reinforcement area

Table 1 Comparison of calculated moments for variation of reinforcement ratio

Reinforcement area mm <sup>2</sup>	Calculated moment-A kN·m	Calculated moment-B kN·m	FE moment kN·m	Test moment kN·m
767	146	183	183	181
637	129	164	163	-----
425	98	129	142	-----
212	70	92	119	-----
0	30	59	74	62

Note: Material properties used for calculations

1) Calculation-A (material strength is taken as the yield strength obtained from the tests)  
Column: 350 N/mm<sup>2</sup>, Beam: 420 N/mm<sup>2</sup>, Endplate: 350 N/mm<sup>2</sup>, reinforcement: 450 N/mm<sup>2</sup>

2) Calculation-B (material strength is taken as the ultimate strength obtained from the tests)  
Column: 480 N/mm<sup>2</sup>, Beam: 530 N/mm<sup>2</sup>, Endplate: 450 N/mm<sup>2</sup>, reinforcement: 600 N/mm<sup>2</sup>

#### 4 STUDY ON SHEAR INTERACTION

From the above it is clear that the reinforcement acts in the model in the same way as it behaves in a test. The test CJS1 with 300% interaction had more studs than required to develop the full tensile capacity of the reinforcement. Stud capacity was varied to investigate its effect on the moment carrying capacity. Analyses were made for 300%, 100% and 4% shear interaction (by changing the stud capacity, not the spacing). Results of the FE analyses are shown in Fig 15. As expected 300% and 100% shear interaction gave little difference in the overall behaviour, whilst the 4% shear interaction model behaved almost as the bare steel joint, thus confirming that the shear studs were modelled properly.

#### 5 STUDY ON SHEAR SPAN/MOMENT RATIO

Tests CJS1, CJS4, CJS5 conducted in the University of Nottingham (Li, 1994) had shown that varying the shear force had little effect on the moment capacities of flush endplate composite connections. These three tests used identical specimens, the only difference was the position of the applied load. In CJS1 the load was applied 1473 mm away from the column face, reduced to 1023 mm for CJS4 and 573 mm for CJS5. Moment capacities were 181.5 kN·m, 177.5 kN·m and 197.5 kN·m respectively. From the results it would appear that there is actually no interaction between shear and moment at these levels of shear loading, since the small observed difference could easily have been due to slight variations in material properties. To

verify this, the FE model of CJS1 was used, the only change being in the position of the load. In the model load was applied at 1473 mm, 1049 mm and 579 mm from the column face for CJS1, CJS4, CJS5 models respectively, this small change in position being accepted so as to keep the original mesh unchanged.

The moment rotation curves for CJS4 and CJS5 are compared in Figs 16 and 17. In Fig 18, the FE results for all three different positions of load are plotted. The moment-rotation curves are almost identical for the three models. This confirms the finding (Li, 1994) that there is no significant effect of shear/moment ratio on the connection moment capacity for the flush endplate joint with symmetric loading. It can be concluded that as long as the tensile and compressive forces can be supported by the associated components, then the position of the applied load has negligible effect on the moment-rotation curve.

## 6 CONCLUSIONS

A numerical model using the general purpose finite element software ABAQUS to simulate the response of semi-rigid composite connections has been described. Tests carried out in the University of Nottingham were used to verify the model. One flush endplate bare steel joint test result and three flush endplate composite joint test results were used. In addition, the method of introducing the reinforcement in a simplified way was checked by comparing results from the finite element analysis with those given by a test-based design method. The developed model can address the important joint characteristics of: variation of reinforcement area, position of application of load, degree of shear interaction, changes in material properties, interface separation and closure, slip between slab (reinforcement) and beam top flange and bolts in a realistic fashion. The modelling work is still undergoing in Nottingham University and more studies will be conducted on the above parameters as well as on the column loading.

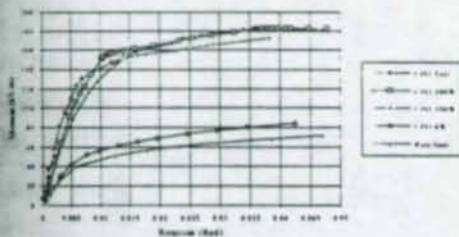


Fig15 Effect of shear interaction on moment rotation Values

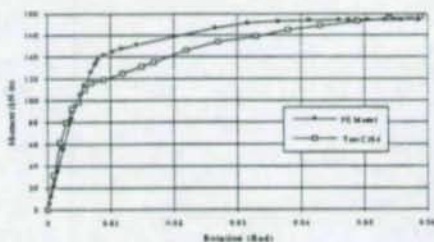


Figure 16 Comparison of moment rotation curves for test CJS4

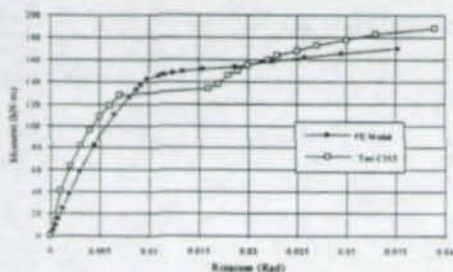


Fig 17 Comparison of moment rotation curves for test CJS5

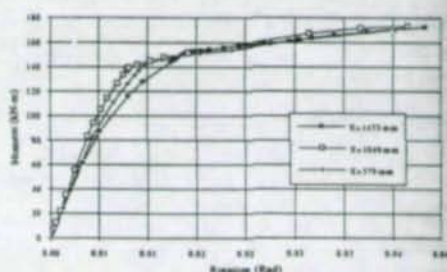


Fig 18 Comparison of moment rotation curves for different shear/moment ratio

## 7 ACKNOWLEDGEMENTS

The work presented in this paper is a part of the research project that is now in progress for a higher degree sponsored by the Commonwealth Scholarship Commission. The initial work on finite element modelling and the test results used for validation purposes formed part of an EPSRC investigation.

## References

- ABAQUS user manual, Version 5.3.1, Hibbitt, Karlsson & Sorensen, inc. (1994) 35 Angle Street, Providence, Rhode Island 02906, USA
- Li, T.Q. (1994) *The Analysis and Ductility Requirements of Semi-Rigid Composite Frames*, Ph.D thesis, University of Nottingham
- Li, T.Q., Nethercot, D.A., Choo, B.S. (1991), *Continuity Effects in Composite Frames*, Progress report No.2 to SERC, SR92006, University of Nottingham
- Leon, R. and Lin, J. (1986) *Towards the Development of an Analytical Model for Composite Semi-Rigid Connections*. Report to AISC, Struct.Eng.Rep.No.86-06, University of Minnesota, Minneapolis, p.83
- Puhali, R., Smotlak, I. and Zandonini, R. (1990) *Semi-Rigid Composite Action: Experimental Analysis and a Suitable Model*, Journal of Constructional Steel Research, Vol.15, pp121-151

## MOMENT - ROTATION MODEL OF STEEL-TO-CONCRETE END-PLATE CONNECTIONS

László Dunai <sup>1</sup>

Sándor Ádány <sup>2</sup>

Yuhshi Fukumoto <sup>3</sup>

### Abstract

In this paper a prediction model is introduced for the moment-rotation behaviour of end-plate type steel-to-concrete connections under combined axial force and bending moment. The developed model predicts the global response of the connection from the local behaviour of the "tension" and "compression" zones. The load-deformation relationships of the zones are analyzed by two nonlinear 2D FEM models. The calculated moment-rotation curves are presented and compared to the experimental results and to a simplified analytical method. It is concluded that the proposed method provides good prediction for the initial range of the moment-rotation relationship but underestimates the ultimate moment capacity.

### 1. INTRODUCTION

Steel-to-concrete mixed connections are connecting steel, concrete, reinforced concrete and composite structural elements. End-plate type mixed connections are applied in steel beam-to-reinforced concrete or composite column joints (Wakabayashi, 1994) and steel or composite column bases (Lescouarch and Colson, 1992). Research have been doing on the application of steel-to-concrete end-plate connections in beam-to-beam joints of composite bridges (Ohtani et. al. 1994).

---

<sup>1</sup> Asst. Professor, Department of Steel Structures, Technical University of Budapest, H-1521 Budapest, P.B. 91, Hungary

<sup>2</sup> Ph.D. Student, Department of Steel Structures, Technical University of Budapest, H-1521 Budapest, P.B. 91, Hungary

<sup>3</sup> Professor, Department of Civil Engineering, Osaka University, 2-1 Yamada-Oka, Suita, Osaka 565, Japan

Previous studies on end-plate type mixed connections concentrate mainly on the strength of column base-plate connections. Formulas for full strength design are derived assuming reinforced concrete cross-section and equivalent rigid plate approach (Eurocode 3, 1991, Wald, 1993). Although the applied hypotheses are not correct in general (Penserini and Colson, 1989), the methods provide acceptable prediction for the ultimate strength in the design practice. Connections that are designed in this way are considered as "rigid". From the available test results it can be seen, however, that the nominally fixed mixed connections exhibit semi-rigid nature, the rotational stiffness depends on the axial force, and its deterioration is significant under cyclic loading (Akiyama, 1985, Penserini, 1991, Astaneh *et al.*, 1992, Wald, 1993, Dunai *et al.*, 1994). Different level of models are developed to analyze the phenomena and to predict the moment-rotation ( $M-\theta$ ) relationship (Penserini, 1991, Melchers, 1992, Fléjou, 1993, Wald, 1993, Sokol *et al.* 1994, Iványi and Balogh, 1994).

In the current research a fundamental experimental program is completed on the rigidity of general steel-to-concrete end-plate connections. Specimens with typical structural details are designed mostly to exhibit the phenomena rather than to represent practical connections. On the basis of experimental findings a model is developed to predict the moment-rotation behaviour under combined axial force and bending moment. The developed model is an extended component model which predicts the moment-rotation response from the local behaviour of the "tension" and "compression" zones of the connection. The load-deformation relationships of the zones are analyzed by nonlinear 2D FEM models. This paper has a focus on the details of the proposed model. The application is demonstrated by the calculated  $M-\theta$  curves which are compared to the results of the experimental study (Dunai *et al.*, 1994) and of a simplified analytical method (Sokol *et al.* 1994).

## 2. EXPERIMENTAL PROGRAM

Figure 1 shows the three test specimens, which are designed to demonstrate the behavioural aspects of the typical structural arrangements of end-plate type mixed connections.

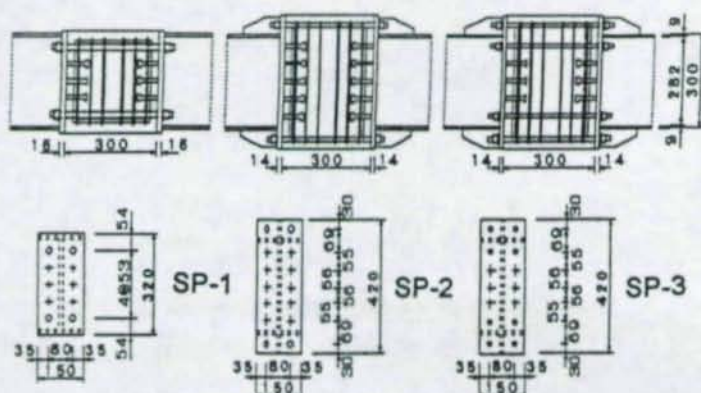


Fig. 1 Test specimens.

SP-1 and SP-2 are designed as partial strength connections, while SP-3 as a full strength connection. The symmetrical steel-concrete-steel connection detail is placed in the center of a steel beam. The steel beam, containing the mixed connection is loaded by cyclic bending moment in a four-point-bending arrangement in a combination of constant axial compressive force. The end-plate deformation of the connection is measured by relative displacement measurement devices between the pertinent edge points of the two end-plates, as illustrated in Fig. 2. Further details of the experimental study can be found in (Dunai et al., 1994).

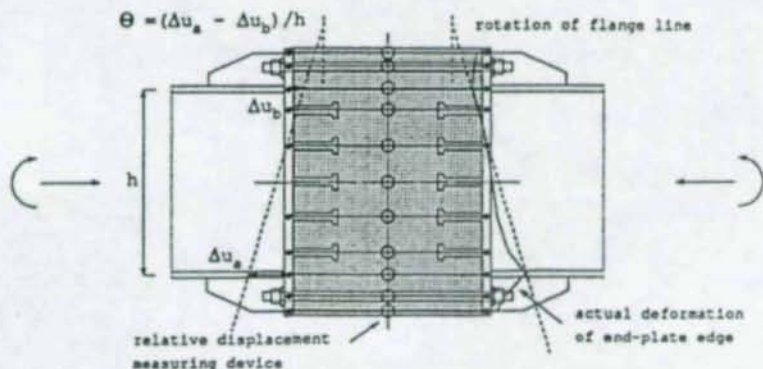


Fig. 2 Measuring and interpretation of rotation.

The measured positive and negative envelopes of axial force-moment-rotation and relative displacement relationships of specimen SP-1 are illustrated in Fig. 3 (a), (b), and (c), respectively. These results demonstrate the behaviour of the tension and compression zones and their influence in the global response. On the basis of this experiences a prediction model is introduced.

### 3. MOMENT - ROTATION MODEL

#### 3.1 General

In the previous analytical studies of column base-plate connections three modelling levels are applied:

- (a) equivalent reinforced concrete (RC) cross-section model,
- (b) component model,
- (c) 3D FEM model.

The (a) level model is simple to use, however, it is difficult to take into consideration the local plate bending deformation (Sokol et al. 1994). By the derivation of equivalent cross-section the model provides good prediction for the strength of the connection. The application of (b) level model is relatively easy, the accuracy, however, is very much dependent on the derivation of the individual components behaviour, especially if the interaction between the components is significant (Melchers 1992). The (c) level model provides the best prediction of the real behaviour, but its application arises a lot of numerical difficulties and significant computational efforts (Iványi and Balogh 1994).

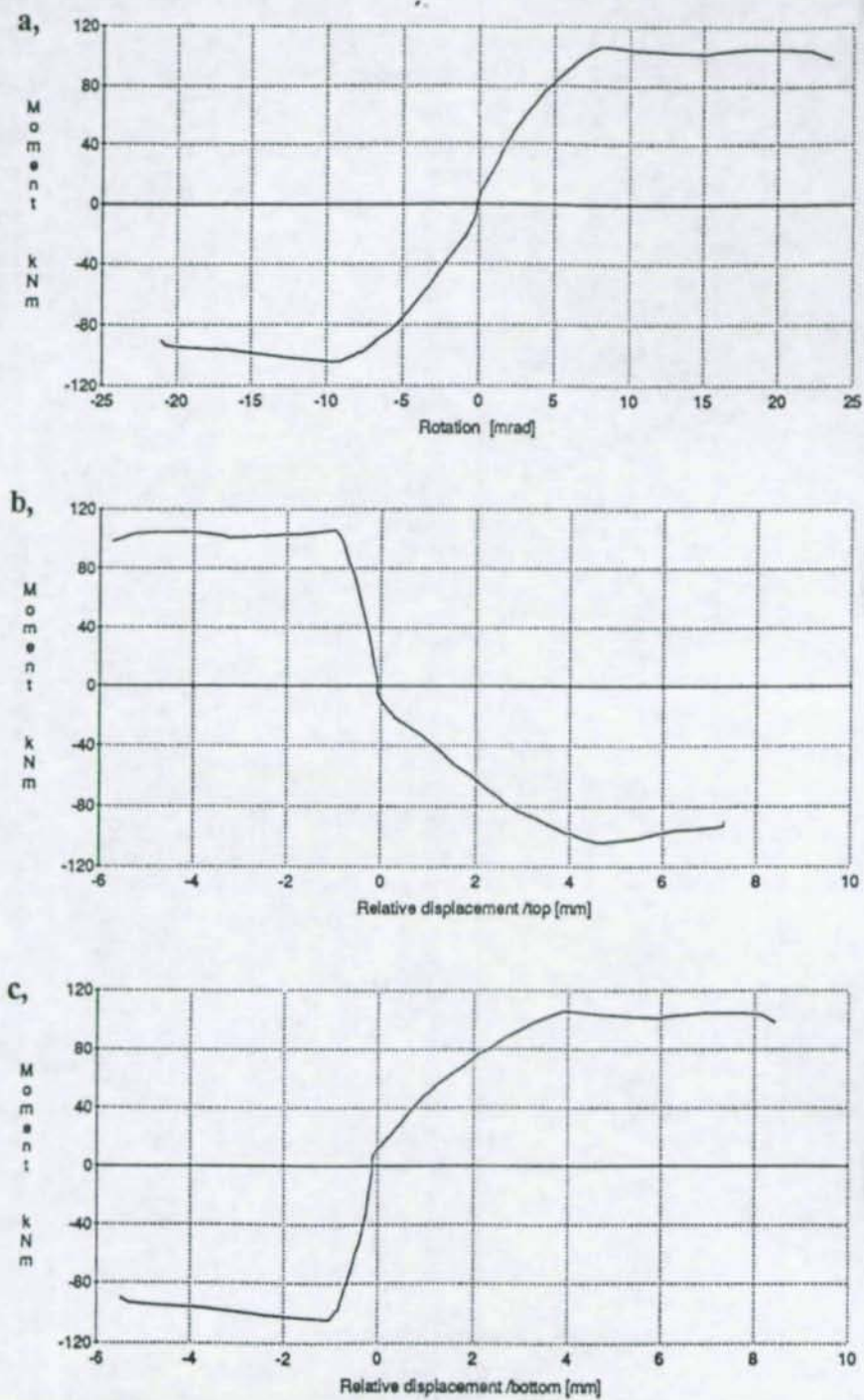


Fig. 3 SP-1: P-M- $\theta$ , P-M- $\Delta_{u_a}$ , and P-M- $\Delta_{u_b}$  envelope curves.

The proposed  $M-\theta$  model is a modified (b) level model, as shown in Fig. 4. It is assumed that the interaction in the local behaviour of the compression and tension zones of the connection can be neglected. Accordingly the two zones can be handled and analyzed separately, as shown on Fig. 4(a), and (b). The zone models are loaded by the beam flanges and the pertinent deformation in the center of the flanges are determined. The nonlinear load-deformation relationships of the zone models are the springs' characteristics of the two-spring-connection model of Fig. 4(c). The rotation response under combined axial force and bending moment can be determined according to the equilibrium conditions of the rigid bar supported by the springs.

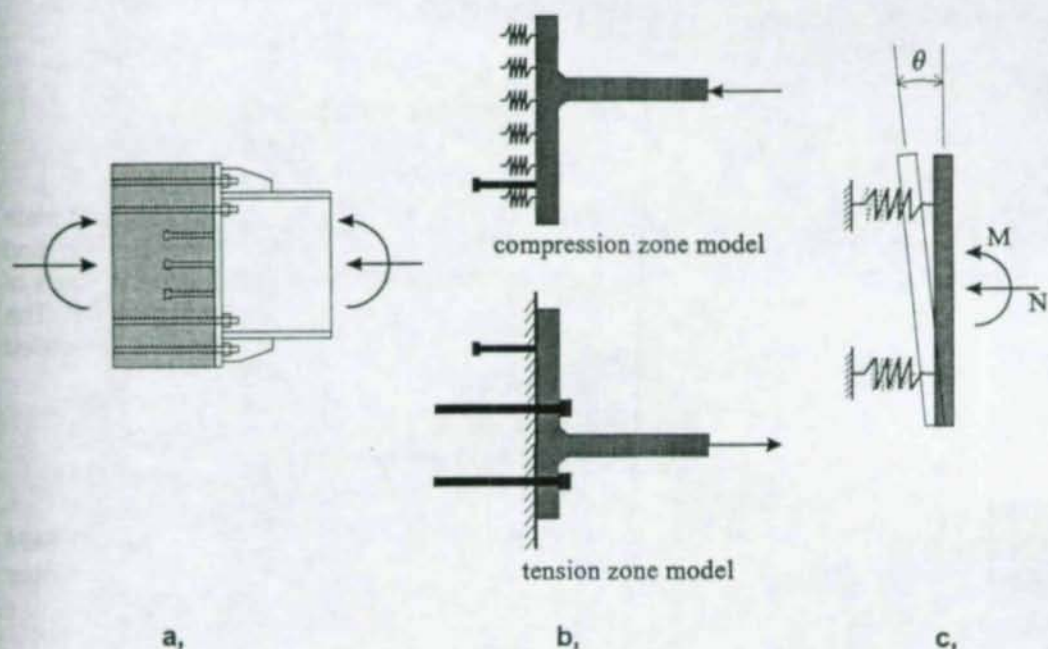


Fig. 4 Derivation of the  $M-\theta$  model.

### 3.2 Tension and Compression Zone Models

The load-deformation behaviour of the tension and compression zones are analyzed by nonlinear plane stress FEM models of the bolted and studed segments in Fig. 4(b). The characteristics of the zone models can be summarized as follows:

- the 3D geometry of the bolted/studed segment is transformed to the plane stress model by the equivalent thickness procedure (Dunai 1992),
- the concrete support is assumed to be rigid in the tension zone model,
- the concrete support is modelled by a nonlinear one direction Winkler-type bedding in the compression zone model in which equivalent elastic modulus is used,
- the constitutive model of the steel components and concrete bedding is a multi-surface Mroz model; the material properties are derived from material tests,
- prescribed displacement of the flange component is applied as kinematic loading; the resulting tension/compression force and the pertinent out-of-plate deformation in the axis of the flange gives the characteristic curve of the zone.

### 3.3 Two - Spring - Connection Model

In the connection model it is assumed that a rigid bar connects the cross points of the plate and flange centerlines which are supported by nonlinear springs, as shown in Fig. 4(c). The characteristics of the springs are the pertinent load-deformation curves of the tension and compression zones. The connection model is analyzed by a simplified load increment procedure. The external axial force and moment are applied in small steps and the rotation response of the bar is determined according to the equilibrium condition.

## 4. NUMERICAL STUDIES

### 4.1 General

The proposed model is applied for the analysis of the three steel-to-concrete end-plate connections described in Section 2. In the first step of the study the tension and compression zones are analyzed by the model detailed in Section 3.2. On the basis of these results the moment-rotation behaviour is obtained by the two-spring-model. The results are compared to the experimental curves and to the results of a simplified analysis of Sokol *et al.*, 1994.

### 4.2 Load - Deformation Curves of Tension and Compression Zones

The tension and compression zones of the three specimens are analyzed by 2D FEM models of 700-1000 degrees of freedom and 20-30 load increments. The nonlinear behaviour is illustrated in Fig. 5 for SP-1 by the load-deformation relationships.

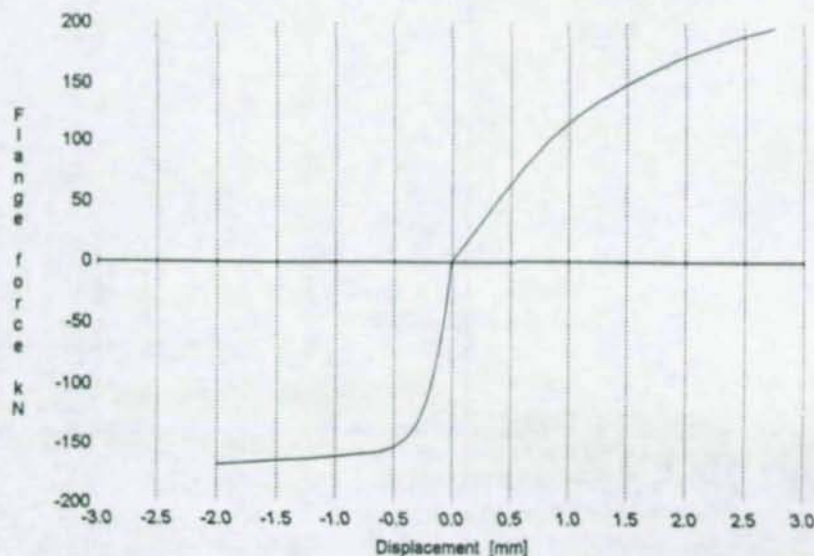
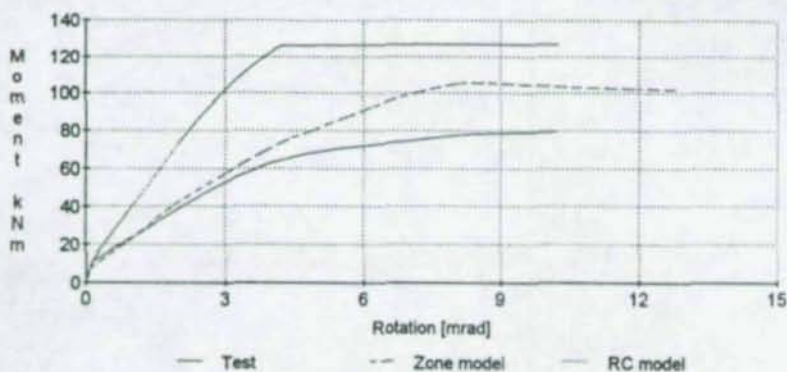


Fig. 5 SP-1: Load-deformation curves of tension and compression zones.

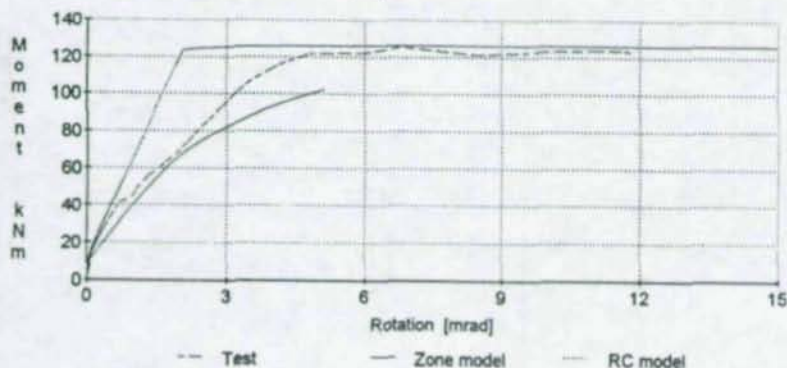
### 4.3 Axial Force - Moment - Rotation Curves

The three specimens are analyzed by combined constant axial force ( $P=103.5$  kN) and bending moment. The experimental and analytical results are described together in Fig. 6(a), (b), and (c), for SP-1, SP-2, and SP-3, respectively.

(a) SP-1



(b) SP-2



(c) SP-3

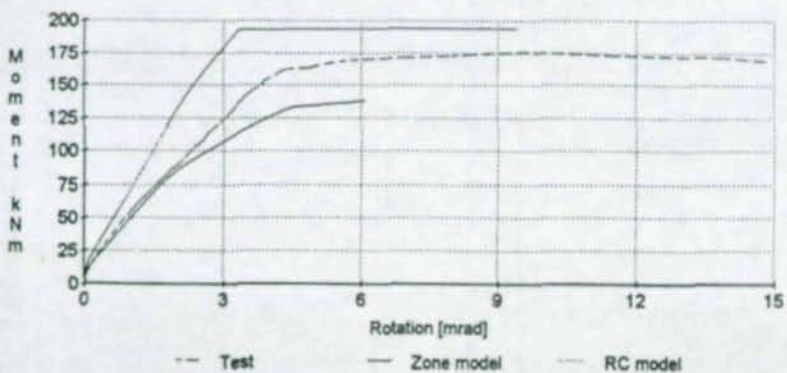


Fig. 6 Experimental and analytical axial force - moment - rotation curves.

By comparison of the obtained results it can be seen that the proposed model gives very good prediction for the initial range of the axial force - moment - rotation relationship. The strength of the connections, however, is underestimated by about 20-25%. It is because the two-dimensional behaviour of the concrete in the compression zone model is not considered (one-dimensional concrete springs are installed in the bedding). If the 2D effect is taken into account - e.g. by a simplified way - the strength prediction can be improved.

The results of the equivalent RC model of Sokol *et. al.* (1994) are also shown in Fig. 5. The model significantly overestimates the stiffness and the strength since the local plate deformation is neglected.

## 5. CONCLUSION

On the basis of experimental results an M- $\Theta$  model is proposed for the analysis of steel-to-concrete end-plate connections. It is an extended component model in which the global behaviour is derived from the pertinent connection zones' behaviour. On the experiences of its application the following conclusions can be drawn:

- The model requires advanced nonlinear 2D FEM analysis on the zone model level; this solution, however, can not be compared in difficulties to a global 3D analysis of the whole connection.
- The model gives very good prediction for the initial range of the moment-rotation behaviour; it can be applied to predict the rotational stiffness and the nominal elastic limit of the connection.
- The model significantly underestimates the ultimate moment; this feature of the model can be improved by the consideration of the 2D effect in the behaviour of concrete bedding of compression zone model.
- A possible application of the model is to combine the results of the zone model analysis by the results of equivalent RC model.

## 6. REFERENCES

- Akiyama, H. (1985), "Seismic Resistant Design of Steel Frame Column Bases", Gihodoshuppan, Tokyo.
- Astaneh, A., Bergsma, G., and Shen, J. H. (1992), "Behavior and Design of Base Plates for Gravity, Wind and Seismic Loads", Proc. of National Steel Construction Conference, American Institute of Steel Constructions.
- Dunai, L. (1992), "Modelling of Cyclic Behaviour of Steel Semi-Rigid Connection," First State-of-the-Art Workshop on Semi-Rigid Behaviour of Civil Engineering Structural Connections: COST C1, Proceedings, Brussels, 394-405.

Dunai, L., Ohtani, Y., and Fukumoto, Y. (1994), "Experimental Study of Steel-to-Concrete End-Plate Connections under Combined Thrust and Bending", Technology Reports of Osaka University, Vol. 44, No. 2197, pp. 309-320.

Eurocode 3 (1991), Design Rules for Steel Structures, Part 1. General Rules and Rules for Buildings. European Norm, Commission of the European Communities, Brussels.

Fléjou, J-L. (1993), "Comportement dynamique des structures de génie civil avec liaisons semi-rigides", Thèse the Doctorat, Université Paris VI.

Iványi, M., Balogh J. (1994), "Numerical Study of a Column Base Connection," Second State-of-the-Art Workshop on Semi-Rigid Behaviour of Civil Engineering Structural Connections: COST C1, Proceedings, Brussels.

Lescouarch, Y. and Colson, A. (1992), "Column Bases", in Proceedings of the First World Conference on Constructional Steel Design, An International Guide, eds. Dowling, P., Harding, J. E., and Bjorhovde, R., Elsevier Applied Science, Acapulco, Mexico, 240-249.

Melchers, R. E. (1992), "Column Base Response under Applied Moment", J. Construct. Steel Research 23, 127-143.

Ohtani, Y., Satoh, T., Fukumoto, Y., Matsui, S., Nanjo, A. (1994), "Performance of Connection in Continuous System of Simple Composite Girders", Proceedings of the 4th ASCCS International Conference, Bratislava, Slovakia, pp. 438-441.

Penserini, P. and Colson A. (1989), "Ultimate Limit Strength of Column Base Connections", J. Construct. Steel Research 14, 301-320.

Penserini, P. (1991), "Modélisation de la liaison structure métallique-fondation", Thèse the Doctorat, Université Paris VI.

Sokol, Z., Wald, F., Dunai, L., Steenhuis, M. (1994), "The Column-Base Stiffness Prediction," Second State-of-the-Art Workshop on Semi-Rigid Behaviour of Civil Engineering Structural Connections: COST C1, Proceedings, Brussels.

Wakabayashi, M. (1994), "Recent Development and Research in Composite and Mixed Building Structures in Japan", Proceedings of the 4th ASCCS International Conference, Bratislava, Slovakia, pp. 237-242.

Wald, F. (1993), "Column Base Connections; a Comprehensive State-of-the-Art Review", COST C1 Project, CIPE 3510 PL 20 143, Technical University of Prague, Prague.

## SOME BASIC PRINCIPLES FOR SEMI-RIGID CONCEPT

André COLSON<sup>1</sup>

### Abstract

The context of the dissemination of the semi-rigid concept is discussed. Obtaining moment-rotation curves from a reasonable process is presented as one of the key parameter. Aside the experimental way several mechanical or physical models have been developed during the last fifteen years. Now it appears that finite element method, used at various scales, is able to bring satisfying results as far as computing costs are dropping down. Various scales means various levels of geometrical description and meshing : local, semi-local as the so-called components method, or global. The interest and the potential capabilities of each description are discussed as well as the questions that have to be solved.

### 1. INTRODUCTION

Most of the present regulation codes regarding constructional steelwork allow for the semi-rigid concept as model for connection behavior. Numerous examples have shown the interest of such a modelization in terms of economy but also in terms of safety in the case of seismic action. Nevertheless during the last years it appeared some reluctance from the designers to use this concept. In the author opinion there are mainly two origins for this reluctance : i) the content of the background engineering education in the field of structural analysis and ii) the lack of available material for day to day practise in terms of  $M - \phi$  curves. Moreover one can think that there is a link between these two problems because if more material would be available, the task of the educational staff would be easier.

---

<sup>1</sup> Professor of civil engineering, Director, Ecole Nationale Supérieure des Arts et Industries de Strasbourg, 24, bld de la Victoire, F 67084 Strasbourg Cedex

i) the content of the background education in structural analysis. Semi-rigid design is probably taught at advanced level, when taught ... !!, so it appears as research subject and not as basic and elementary component of structural behavior. Of course at basic level, with junior students, it is not possible to go deeply within semi-rigid design but, at least, the connection behavior has to be pointed out, in terms of  $M - \phi$  curves, as the members behavior is exhibited in terms of moment - curvature curves. In order to convince our colleagues, teachers of structural analysis, to teach the essential background, it has to be widely accepted that semi-rigid behavior is the main and most common feature of connection in civil engineering structures, whatever the material. Starting from this consideration semi-rigid concept is an inevitable item of education and should not be missed. It is the purpose of the COST C1 european project to gather all the knowledge regarding connections behavior in concrete, timber, steel and composite structures in order to elaborate the essential "corpus".

ii) the available material in terms of  $M - \phi$  curves : despite the numerous experimental and analytical studies that have been performed during the last fifteen years there is not a general agreement on the way to get the  $M - \phi$  curves. Of course the experimental results are certainly the most reliable but not convenient for the day to day practise in the design office for several reasons :

- they are not available in a ready for use format (ultimate limit state and serviceability limit state characteristics, ... etc).

- they are not gathered within a well agreed handbook.

- they do not give by the same time the internal distribution forces which are necessary for the detailing design.

- generally the very specific case the designer is studying does not exist ... !!

- and most of all design from testing is not a current practise excepted some experimental checking, generally at reduced scale, at the end of the design process.

So, in the designer mind a calculation procedure, as simple as possible i.e. presented in tables or spread sheets format, is the only rational way to proceed in the design office. To prepare such a material, research and development has to be done above, to investigate all connection types. During the last fifteen years several mechanical or physical models have been developed, as well as numerical simulations with finite element method. These last one were not very successful due to the lack of specific elements including contact problem, lack of fit description, microcracks propagation ... etc and due to the very large number of degrees of freedom inducing high calculation costs. So the mechanical and physical models were more attractive. Unfortunately these models include always some curve fitting parameter which need to be identify from experimental results. Briefly they are not able to give the entire  $M - \phi$  curve from the sole geometrical and mechanical data of the connection. Furthermore the meaning of some parameters can not be explained in an engineering fashion.

Nevertheless such models have allowed the comparison of various approaches and the development of the basic knowledge on connection behavior.

Since one or two years most of the finite element method software packages offer the *relevant elements that are needed for connection modeling* : Evolutive contact elements, friction elements, damage model for concrete including strain-softening ... etc. By the same time automatic meshing is available in the case of complex geometry (CHS joints with double K configuration for example) and the computing costs are strongly decreasing while the computer capabilities are strongly increasing. It is therefore reasonable to undertake connection modeling through finite element method. Three level of geometrical description, i.e. three scales of geometrical modeling, have to be considered.

- local modeling (LEVEL 1). In that case each element (fastener, plate, angle) is meshed with all the necessary refinement, including contact zone, to take care of all the phenomena that take place inside the connection.

- global modeling (LEVEL 3). The whole joint is considered as a single element with one, two or three degrees of freedom (as a spring for example). This case requires a form of analytical model, or can be combined with experimental results or with a result coming from the local modeling approach.

- semi-local (or semi-global) modeling (LEVEL 2). The "meshing" is such that an element is only a part of the connection ; T-stub, web panel, anchorage bolt for example which can contains several pieces like bolts, plate, web, surrounding concrete. The word "Components method" often used in combination with hand calculation is dedicated to this approach (Jaspart & Maquoi 1994). From a mechanical point of view the word "meso-mechanics" could be used by comparison with "micro-mechanics" (LEVEL 1) and "macro-mechanics" (LEVEL 3).

These three levels of modeling can be used in combination, according to the degree of refinement which is required.

As a remark it has to be kept in mind that the level of accuracy of the  $M - \phi$  curves is not clearly defined at the moment, more especially in comparison with the level of accuracy of the moment curvature curves of the bars (Mebarki et al 1995).

## 2. LOCAL MODELING (LEVEL 1)

All the connection area is meshed with the more appropriated type of element (plate, shell, brick, contact element) including specific element for simulating pretensionning of the bolts. The boundary conditions (forces and displacements) allow the link to the adjacent bars. Generally the connection area is isolated from the whole structure.

Nevertheless the whole structure, containing several bars and several connections can be meshed and analyzed in a global calculation. Of course this is not very realistic in terms of computational time.

Such calculations have been made recently for end plate connections (Bursi & Leonelli 1994 : figure 1), CHS joints or column bases connections (Sedlacek et al. 1994) (Lee & Wilmshurst 1995 : figure 2).

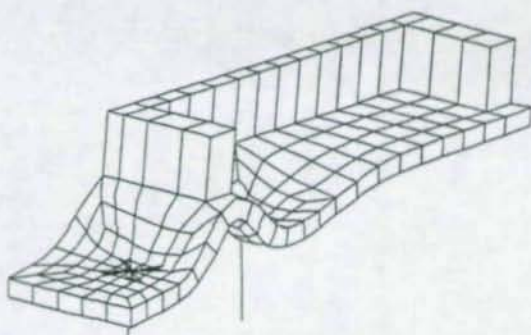


Figure 1. Finite element mesh for end plate connection

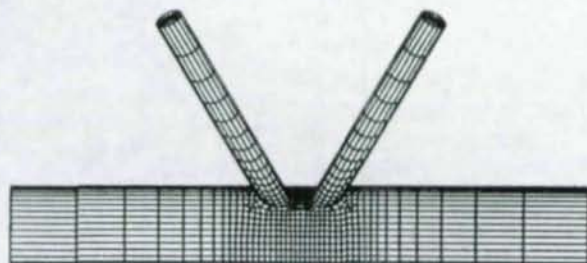


Figure 2. Finite element mesh for CHS-K joint

The specific connections "ingredients" (evolutive contact area, bolt pretensioning ...) can be introduced along with relevant constitutive laws (plasticity, strain-hardening) for the material properties. Therefore the results in terms of  $M - \phi$  curves are quite satisfactory even if some phenomena like residual stresses, initial lack of fit ... are not taken into account.

We can expect, in a near future, the same results for composite connections since it has been demonstrated that 3 D calculations are fully relevant for reinforced concrete connections including longitudinal and transversal reinforcement (La Borderie & Merabet 1994). (figures 3, 4 and 5). Damage theory including strain - softening branch and relevant bond conditions between concrete and reinforcements are used.

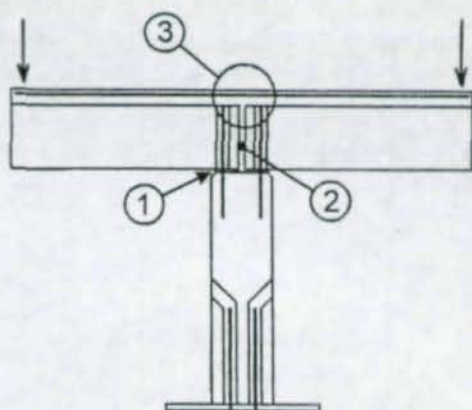


Figure 3. Experimental device for precast reinforced concrete connection

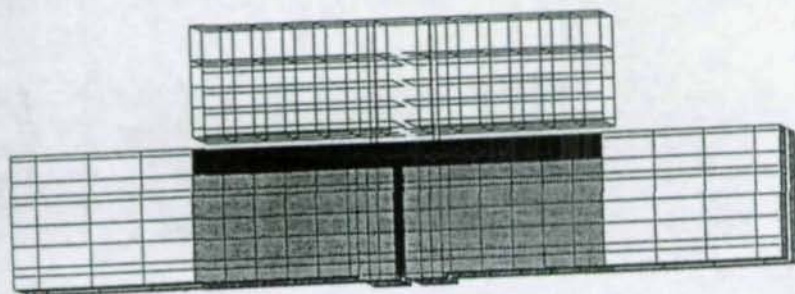


Figure 4. Finite element mesh for concrete and reinforcement (above)

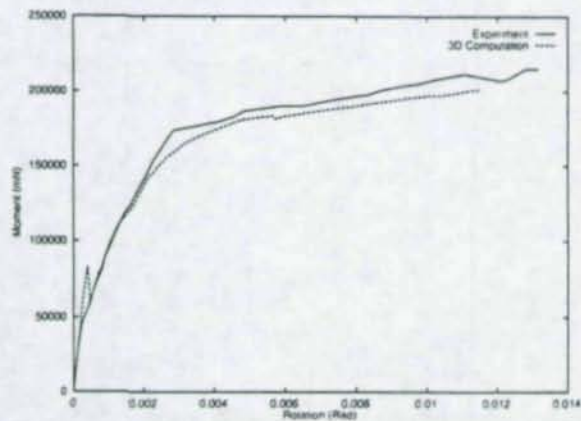


Figure 5. Computational result and experimental result

Therefore it appears that finite element methods are now able to take into account a lot of mechanical and physical phenomena which strongly influence the connection behavior.

### 3. GLOBAL MODELING (LEVEL 3)

The connection area is modeled with a unique element in the sense of figure 6 as it is now well agreed. For most cases this element is a "one degree of freedom element": the rotation. However it could be interesting, or necessary, to have several degrees of freedom for this single element in the following situations:

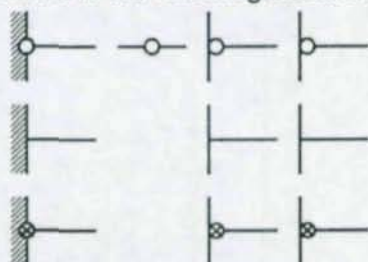


Figure 6.

- i: In the case of three dimensional structures (Deierlein 1991). Two degrees of rotation within two different planes, at least.
- ii: In the case of column base connections for which the normal force-bending moment interaction requires translation and rotation displacements associated with the forces (Penserini 1992).
- iii: In the case of dynamic loading (seismic) where inertia effects induce shear force-bending moment interaction into the connection (Fléjou 1992). Two degrees of freedom are therefore necessary: translation and rotation associated with shear force and bending moment.

The situations i and iii are somewhat specific and will not be discussed in this paper. The situation ii is on the stage of undergoing research. It seems relevant to exhibit different  $M - \phi$  curves depending on constant values of the normal force, i.e the normal force is considered as an external parameter (one  $M - \phi$  curve for one normal force value).

For all other cases a "one degree of freedom element" is relevant. Therefore the global modeling allows for the whole frame analysis. Most of the present software packages taking semi-rigid effects into account are based on this modeling, as well as the recommendations or the requirements included in the regulation codes (EUROCODE 3 for example). The necessary  $M - \phi$  curve can be got through various ways:

- Experimental results
- Any form of analytical model
- Any available simplified model
- Numerical simulation at level 1 (local modeling)
- Result of level 2 analysis like components method.

The two last approaches will be certainly, in a near future, the most commonly used because computing facilities are in progress from one hand and they are now presented in an engineering fashion on the other hand.

Nevertheless from the conceptual point of view, the analytical models, expressed directly in forces-displacements format, have several advantages. They allow for :

- the utilization of the language and the parameters of whole frame analysis methods
- the possibility to introduce directly some specific effects (clearance, variation of slope, strain-hardening ...)
- efficient parametric studies to look at the influence of the connection behavior on the response of the whole structure
- the introduction of several degrees of freedom in the connection (rotations, displacements)
- the presentation of the "connection deformability concept" for educational purpose.

In the author opinion such analytical model allow to take very finely into account some random phenomena at the material level such as residual stresses for example. This is the purpose of the last proposed model (Fléjou 1992). In fact most of the characteristics of the global behavior (non linearity) are due to local effects (plasticity, strain-hardening, damage ...) which are very well known in mechanics theory at local level. Because it is impossible to describe finely each phenomenon for each fastener or element it is proposed to transfer at the global level of the connection the concepts, and the "formalism" which are used generally at local level (elasticity, strain hardening, damage for concrete ...). Only one extra parameter is necessary to take friction into account (named flow in the model).

This model is relevant for all civil engineering materials (steel, composite, reinforced concrete, timber). Of course some numerical values are strongly material dependant. The general format is given in figure 7.

Material	Associated phenomenon	State Variables		Associated Variables	
		Observable	Internal		
		$\rightarrow D$		$\rightarrow F$	
Steel	Elasticity, kinematical hardening		$\rightarrow D^e$	$\rightarrow F$	Elasticity
Concrete	Elasticity, damage		$\rightarrow D^{an}$	$\rightarrow -F$	Non Elasticity
Wood	Elasticity, damage		$\alpha$	$\rightarrow -F^k$	Kinematic hardening
Assembly (Slip, friction)	Flow			$\rightarrow K$	Flow of connection
		$\rightarrow d$		$\rightarrow -y$	Damage

Figure 7.

In this paper the model is presented in a 2D format which is the more relevant for a written description. All the degrees of freedom are possible. It is a multi-surfaces model (figure 8).

- the limit surface which represents the maximum strength of the connection
- the initial elastic surface, which can move for kinematical hardening modeling
- the loading surface growing accordingly to the displacement of the elastic surface.

The size of the limit surface can decrease if damage appears (in concrete).

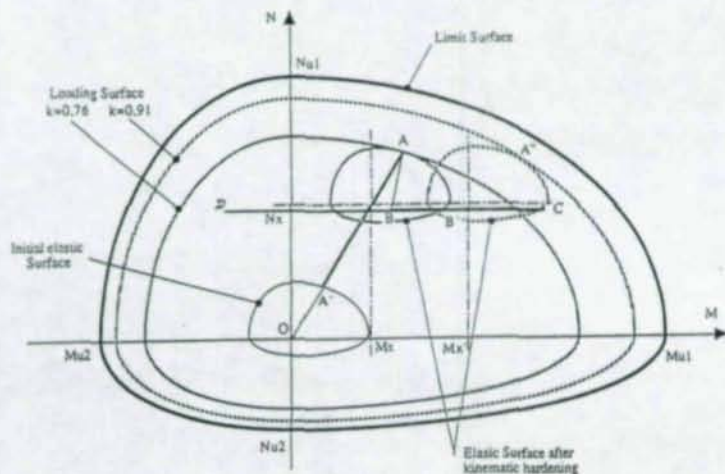


Figure 8.

Such a model is able to describe monotonic and cyclic loading, including "pinching effect" (Figure 9). Of course it requires some numerical parameters, which have not a direct physical meaning but which are probably "constant" for a given family of connections (bolted connections, welded connections, composite ...).

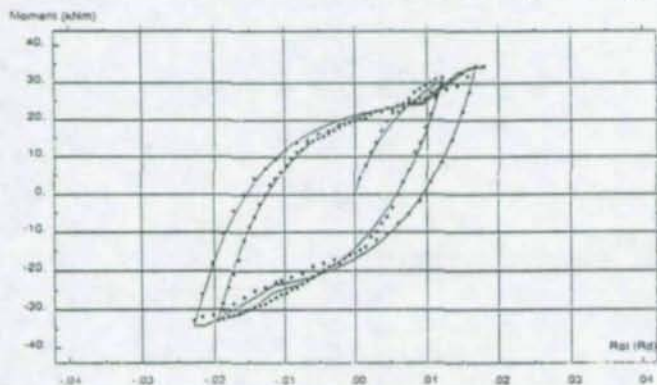


Figure 9.

#### 4. SEMI-LOCAL MODELING (LEVEL 2)

Semi-local or "semi global" modeling have been used from time to time in several areas of mechanics. In the field of semi-rigid design it appears now as the most convenient approach from the engineering point of view. In Europe, and more especially for Eurocode 3 dissemination, it is called "components method" (Jaspart & Maquoi 1994). The connection is divided into typical "sub mechanisms" and not necessary elementary mechanism, for which the mechanical behavior is not directly dependant on the lay out of the whole connection. The T-stub approach is a form of component method. Of course the whole connection has to be divided into a finite number of components (this is the reason for which it is a form of finite element method) and the behavior of each component has to be known before to make "the assembly" to go up to the whole behavior. The assembly is done following the well known "serial model" or "parallel model" or both. This approach is quite relevant for constructional steelwork in case of end plate connections and angle connections and can be extended to other connection types.

The individual behavior of each component can be obtained itself from a local modeling (Dunai 1992) or a global modeling (Penserini 1992). In most of the cases the "assembly calculation" to get the whole connection behavior can be made by hand because there is more or less three to six components. Nevertheless some checking regarding "compatibility equations" in terms of force or in terms of displacement have to be done. For example in the simple case of column base connection subjected to pure bending, if the designer decides to take two components : the anchor bolt mechanism and the compression zone mechanism (figure 10), he has to check either

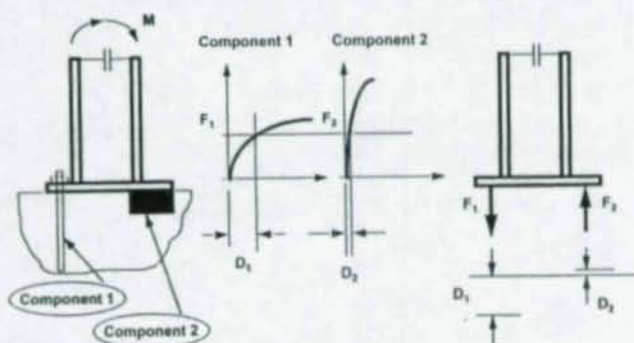


Figure 10.

equilibrium or displacement condition. Generally the equilibrium equation is chosen as first condition because of its engineering meaning and the displacement condition appears of second importance. However in the author opinion the displacement condition has to be examined too (and perhaps more or less satisfied) in order to avoid non physical solution. In the specific case of the chosen column base, because the behavior of the anchor bolt is quite different of the behavior of the compression zone, the equilibrium equation leads to a vertical displacement of the column base which is not compatible with the initial kinematic scheme.

One can think that these compatibility checkings do not lead to actual difficulties and can be solved, if necessary, with appropriate engineering hypothesis.

## 5. CONCLUSION

The finite element method, used at all the available levels (local, semi-local, global and sometimes in combination) is now able to give the necessary material to get the  $M - \phi$  curves. Of course a data-bank containing the numerical simulations could allow some economy by avoiding repeated calculations. The analytical models, expressed in a global manner will be probably dedicated and limited to educational purpose.

## 6. REFERENCES

- . Bursi, O., Leonelli, L. "A finite element model for the rotational behavior of end plate connection". COST C1 workshop proceedings. Prague 28-30 October 1994
- . Déierlein, G. "An inelastic analysis and design system for steel frames with partially restrained connections". Second international workshop proceedings : Connections in steel structures. Pittsburgh 1991
- . Dunaĭ, L. "Modeling of cyclic behavior of steel semi-rigid connections". Proceedings of the COST C1 workshop. Strasbourg 28-30 October 1992
- . Fléjou, J.L., Colson, A. "A general model for cyclic response of structural civil engineering connections". Proceedings of the COST C1 workshop. Strasbourg 28-30 October 1992
- . Jaspert, J.P., Maquoi, R. "Prediction of the semi-rigid and partial strength properties of structural joints". SSRC technical annual session proceedings. Lehigh 20 June 1994
- . La Borderie, C., Merabet, O. "Modeling the behavior of reinforced concrete connections : availability of different approaches and scales". Proceedings of the COST C1 workshop. Prague 28-30 October 1994
- . Lee, M., Wilmshurst, S. "Numerical modeling of CHS joints with multiplanar double K-configuration". Journal of constructional steel research. Vol 32. N° 3. 1995
- . Penserini, P., Colson, A. "Modeling of column base connections". Proceedings of the COST C1 workshop. Strasbourg 28-30 October 1992
- . Sedlacek, G., Weynand, K., Byung-Seung Kong, Saal, H., Klinkenberg, A., Bode, H., Kronenberger, H. "Research work done in Germany in the field of semi-rigid connections". COST C1 workshop proceedings. Prague 28-30 October 1994

## BEHAVIOUR AND MODELING OF TOP & SEAT AND TOP & SEAT AND WEB ANGLE CONNECTIONS

Antonello De Luca<sup>1</sup>

### Abstract

In this paper a review of the research activities carried out by the Author and other co-researchers in the field of behaviour and modeling of semirigid angle connections is presented. In particular, starting from the behaviour of a single component: the angle, the monotonic behaviour firstly and then the cyclic performance of Top & Seat Web angle connections are analyzed with specific reference to the problems of modeling.

The mechanical models developed, which are always verified against experimental evidence, are then reviewed with some criticism in order to evidence their pitfalls and to investigate on the real potentials of modeling and on the need of stating the ranges of applicability defined from experimental indications.

A brief comment on the recently drafted extensive provision of the Eurocode 3 on semirigid connections, with specific reference to these connections is given at the end of the paper.

### 1. INTRODUCTION

Semirigidity has attracted the major efforts of research in the field of steel structures in the last decades. This concept, already familiar to the earlier designers of the "Empire State Building", who used to say that "Connections are smart enough to know what to take", has produced efforts in the fields of testing of connections, modelling of entire semirigid structures and finally implementation into codes and/or provisions. Most of these efforts are devoted to classification of fixed, hinged and "in between the two" connections. After all these activities we can't really draw a line on this subject, but we can simply say that connections represent a dominant part of the steel structure and their behaviour can't be easily predicted, experimentation remaining a major reference. We could say that since any connection can be considered semirigid, it is better to more appropriately speak simply in terms of connections.

---

<sup>1</sup>Professor, Università di Reggio Calabria, 89100 Reggio Calabria, ITALY

It is believed that a moment of reflection is now needed also in view of the fact that provisions are coming out [1,2] for the use of semirigid connection in order to allow for a more extensive use in the design practice. Within this philosophy, and considering that it is not plausible to review the activities of the different Authors, in this paper only the research carried out from the Author and other co-researchers in last years is reviewed with specific reference to a particular type of connection.

After early studies devoted to the investigation of frames characterized by semirigid behaviour [3,4,5,6], the attention has been concentrated to the behaviour of connections. In particular the analysis of the experimental behaviour has allowed to develop a mechanical model which has been verified against the experimental evidence both in the monotonic and cyclic range. For this purpose research has been carried out in co-operation with major laboratories and researchers in the field of steel structures i.e. University of California at Berkeley and University of Trento.

In the following sections firstly the behaviour of a single component: the angle is analyzed under axial pull-push conditions. The monotonic behaviour and then the cyclic performance of Top & Seat Web angle connections are consequently examined in order to develop a mechanical model capable of predicting the response without the introduction of any curve fitting parameter. Finally this model, in an oversimplified version, is analyzed from the point of view of the sensitivity of its main parameters. This critical review also allows to draw some considerations on the recently drafted Annex J of the Eurocode 3 which refers to a similar model for these connections.

## 2. AXIAL PULL-PUSH BEHAVIOUR AND MODELING OF ANGLES

From a mechanical point of view a Top & Seat angle connection is built up by the coupling of different components which all contribute to the stiffness and strength of the connection. Among all these components the angles represent the prominent parts due to flexural bending of the outstanding leg (Figure 1).

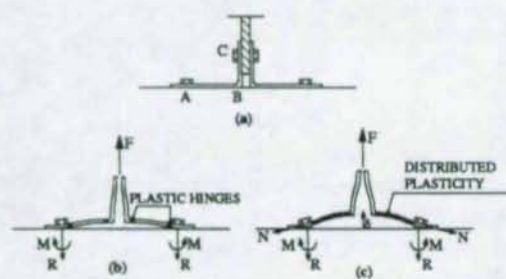


Figure 1: Axial behaviour of angles subjected to axial pull-push [7]

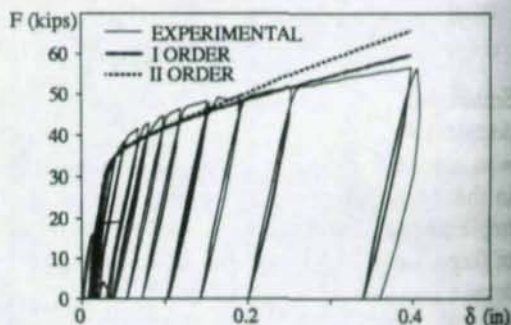


Figure 2: Comparison between experimental behaviour and numerical modeling [8]

The axial force displacement behaviour of double angles is therefore significant either for the repercussions on the analysis of Top & Seat connections under bending conditions and of deep truss girders in which the top and bottom chords are often connected through angles which are subjected to axial pull-push conditions.

The monotonic behaviour of angles subjected to axial pull-push has been investigated by De Stefano and Astaneh in [7] where the experiments were carried out by appropriate loading conditions accounting for the shear effect. The comparison between the experimental response and the numerical model is provided in figure 2 where the simulation have been carried out also by taking into account second order effects.

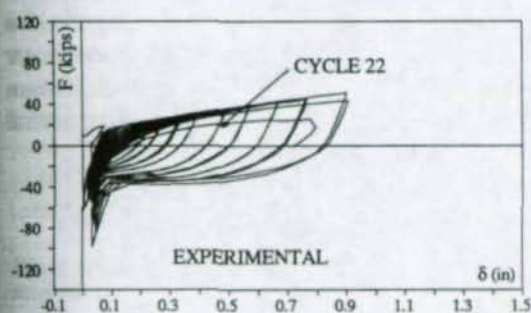


Figure 3: Experimental response of angles subjected to cyclic axial pull-push [8]

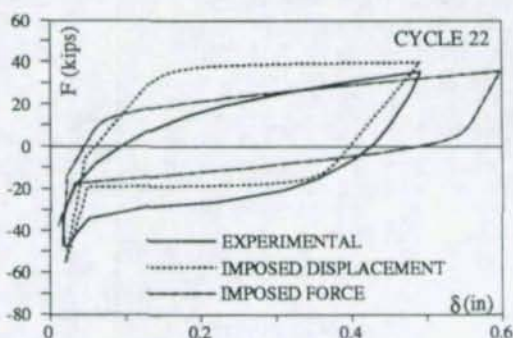


Figure 4: Comparison between experimental and numerical modeling [8]

The same mechanical model has been extended in [8] to the case of cyclic loading. The comparison between the experimental response (figure 3) and the mechanical model (figure 4) has proved the capability of the model, which makes use of a gap element, to account for the non linear behaviour (sudden stiffening) arising from touching of the leg-to-leg angle to the column flange.

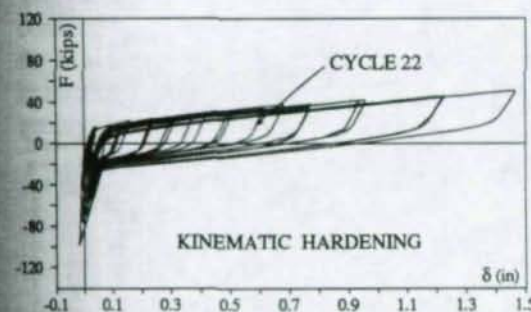


Figure 5: Simulation by means of kinematic hardening [8]

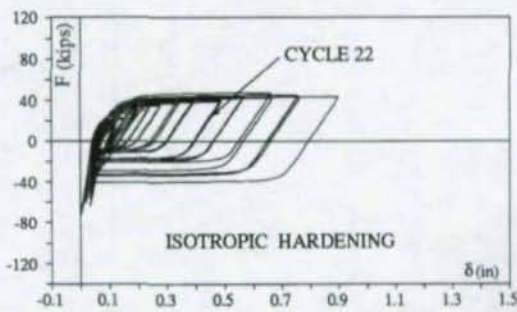


Figure 6: Simulation by means of isotropic hardening [8]

In figures 5 and 6 is demonstrated the differences in simulation when adopting a Kinematic or Hardening type hypothesis. Both the simulated curves are obtained by imposing the force and looking for the displacement.

### 3. MONOTONIC & CYCLIC BEHAVIOUR AND MODELING OF WEB ANGLE AND TOP & SEAT CONNECTIONS CONNECTIONS

#### 3.1 Web Angle Connections

The appropriate coupling of different springs, each of them being representative of the behaviour of an angle subjected to axial pull-push conditions, by means of the mechanical model explained in the previous section has allowed [9, 10, 11] to develop a complete mechanical model for the simulation of web angle connections. The slicing of the web angle into strips and the geometrical parameters, to be used for the definition of each nonlinear spring, are given in figure 7. The web angle connection is then simulated by appropriate coupling of these springs, following the idea presented in [12, 13] by means of the model provided in figure 8. In order to simulate the nonlinear response an incremental algorithm has been set up based on compatibility and equilibrium equations. The algorithm imposes an incremental rotation and looks for the position of the neutral axis which allows then to express the moment from the equilibrium equations.

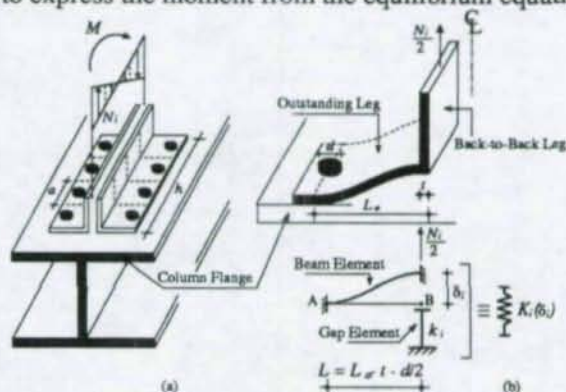


Figure 7: Definition of the geometrical properties of the model of web angle connection [11]

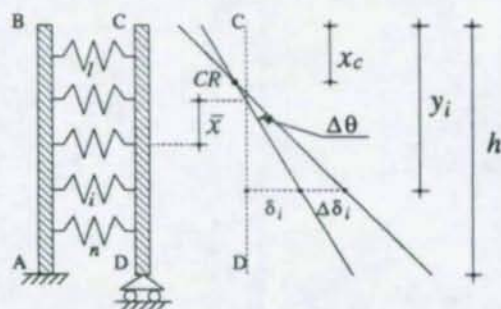


Figure 8: Model and numerical procedure for simulation of nonlinear response [11]

The same procedure has allowed to simulate, in the same manner, also the cyclic response of the connection. It should be underlined that, practically all the existing models [14 to 21] are referred

to the monotonic behaviour and introduce some curve fitting parameters differently from the model herein presented which adopts as parameters only the stress-strain relations and the geometrical properties underlined previously.

A mechanical approach is followed in [22] and in [23] the cyclic response is considered. A more complete overview of the existing models is provided in the extensive state of art given in [24].

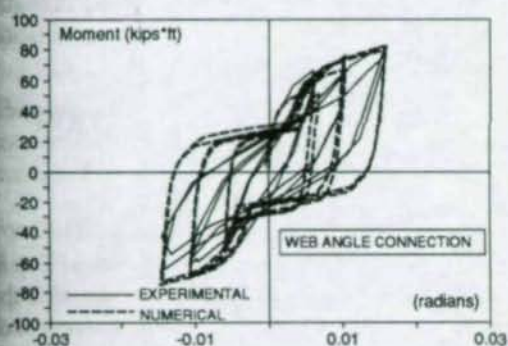


Figure 9: Comparison between experimental and numerical response [11]

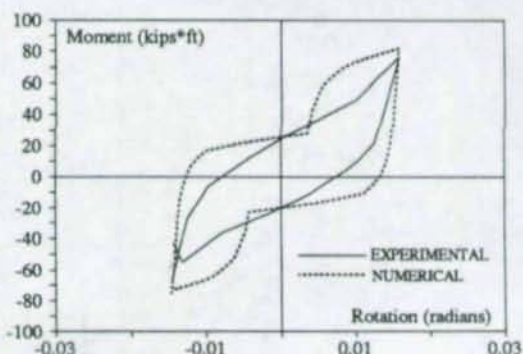


Figure 10: Close up view of comparison between experimental and numerical response [11]

The comparison between the experimental results provided in [25] and the numerical prediction is reported in figure 9. From this figure it is evident that the model is capable of providing a pinching of the hysteresis loops even though no slippage has been introduced. This fact derives from the opening and closing of gaps which are well simulated by the model. The comparison between experiments and simulation is better evidenced by figure 10 in which a single cycle is extracted from simulation.

### 3.2 Top & Seat Angle Connections

The mechanical model presented previously has been extended to the case of Top & Seat connections in [26, 27]. In particular in [26] it has been demonstrated the potential of the model for simulating the cyclic behaviour of Top & Seat and Top & Seat Web angle connections by indicating how to derive the spring properties of the Top & Seat cleats (figure 11) from the geometrical data of the connection.

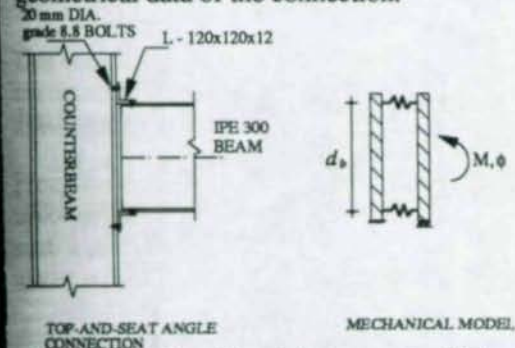


Figure 11: Modeling of Top & Seat connection [26]

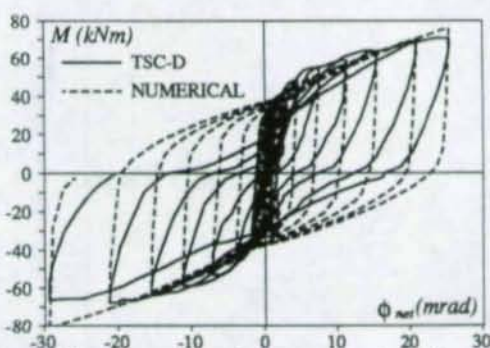


Figure 12: Comparison between experimental and numerical response of Top & Seat connection [27]

In [27] the model has been verified against experimental tests carried out at the University of Trento [28] on Top & Seat among other connections. In [27] it has been also evidenced the need of avoiding potential slippages in the connection by adopting a *slip capacity design* which consists in taking the plastic shear withstandable from the outstanding legs smaller than the slip force. Since the experimental tests in this case measured also the slippages, the simulation of the net rotations of connections was carried out. The comparison between the experimental tests and the numerical simulation (figure 12) shows the perfect prediction in terms of stiffness and strength. It should be also noted that in this case, due to the absence of web angle connections, the simulation does not provide any pinching in the hysteresis loops.

#### 4. CONSIDERATIONS FOR DESIGN USE AND CODE IMPLEMENTATION

##### 4.1 Premise

In this paper a review of the activities carried out in last years in the field of modeling of Top & Seat connections in the monotonic and cyclic range has been made. The comparison with the experimental results has confirmed the good prediction achievable by this model. A moment of reflection though is needed in order to investigate on the potentials of providing such a model, or a simplified version, to professional for predicting any type of experimental behaviour of such connections.

It is also important to make this considerations since a new and very extensive provision [2] has been recently set up. This provision includes all types of semirigid connections by providing methods for computation of stiffness and strength. In the following a brief review of the Eurocode 3 approach is provided, firstly and then a sensitivity analysis is suggested.

##### 4.2 Eurocode 3 approach and simplified approach

The approach followed within Annex J of the Eurocode 3 refers to a mechanical model which simulates the connection by a series of different component each being representative of an elastic spring, characterized by a specific stiffness. The appropriate coupling of these springs, which, for the case of Top & Seat connections, results in the model of figure 13, provides the global stiffness of the connection.

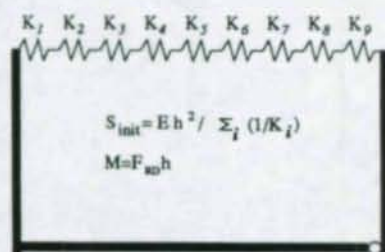


Figure 13: Eurocode 3 model

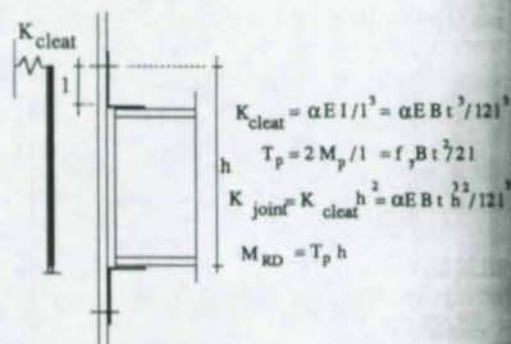


Figure 14: Simplified model for sensitivity analysis

The simplified model, as shown in figure 14, provides the following expressions for connection stiffness and strength:

$$K = \frac{aEBt^3}{12L^3} H^2$$

$$M = \frac{f_y B t^2}{2L} H$$

The parameters characterizing stiffness and strength are therefore: flange cleat length  $L$ , global connection height  $H$ , flange cleat effective width  $B$ , flange cleat boundary conditions  $a$  and yield strength  $f_y$ . It should be also taken into account the hardening ratio  $S_{lim}/S_h$ .

For all of the previous parameters different values have been suggested by different authors and actually each of them depends by several facts which cannot always be predicted. For this reason a prediction has been made for the same test reported in figure 15 by assuming, in one case all the minimum values for each parameter and in the other case all the maximum values. In this manner it is possible to define a range of variation and to somehow define a sensitivity of the model to the variation of parameters.

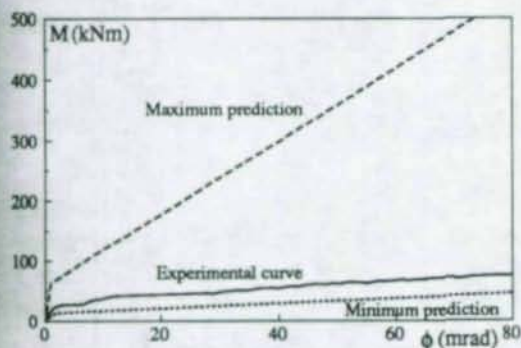


Figure 16: Ranges provided by sensitivity analysis and comparison with experimental curve up to rupture

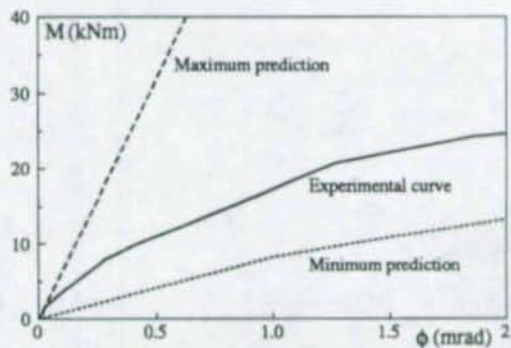


Figure 17: Ranges provided by sensitivity analysis and comparison with experimental curve in the elastic range

This comparison is made in figures 16 and 17 where the experimental curve is compared to the maximum and minimum predictions. The two figures are provided in different scales for allowing to evidence the ultimate response and the elastic response.

From this figure it is evident that the two results differ substantially but the experimental curve is comprised between the two bounds both in terms of stiffness and strength. This means that such a procedure, with further improvements deriving from a more extensive comparison and aimed at restricting the range of variation, could be advised in design and implemented into codes.

For what concerns the global connection strength the different failure mechanisms are identified, the minimum value of failure capacity being the strength of the connection. Such a "component model" does not provide any information on the ultimate deformation capacity.

Due to the good agreement achieved with the mechanical model presented extensively in this paper, which is more complicated, but which only adopts as unique component of behaviour the outstanding leg of the angle in bending it has been thought that an oversimplified version of the Eurocode 3 would result in a more "friendly use" tool to be proposed to designers. This model is provided in figure 14.

A comparison between experimental behaviour and this simplified proposal together with the more refined model previously discussed is given figure 15.

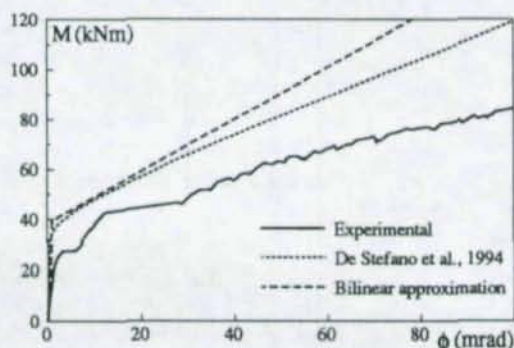


Figura 15: Comparison between experimental curve, refined model [11] prediction and simplified approach

An extensive application of the Eurocode 3 has been made in [29] where all the data concerning Top & Seat connection and included into two data banks [30,31] respectively set up in Europe and United States have been considered for carrying out the comparison between Eurocode 3 and experimental behaviour. In [29] it has been also demonstrated that even within the application of Eurocode 3 the only component affecting the connection behaviour is the cleat in bending.

### 4.3 Sensitivity analysis

It is believed that it is not possible to set the parameters of any model in a unique way and to expect to foresee the real experimental behaviour of the connection. It should be advised instead to provide a range of variation of the parameters governing the behaviour and therefore to provide a range of variations in predicted stiffness and strength.

For this purpose, and considering that the angle in bending has demonstrated to affect the connection response, such a simplified approach could be used also to provide the different bound of prediction.

A more extensive sensitivity analysis of this type has been carried out in [32] where all the experimental data comprised in [30, 31] have been considered. The result found in [32] confirms the need for considering two different bounds representing maximum and minimum prediction.

## 5. CONCLUSIVE REMARKS

The activity carried out in last years for modeling the monotonic and cyclic behaviour of Top & Seat and Top & Seat and Web angle connections has provided very promising tools for the analysis of the behaviour of these connections since the comparison with the experimental behaviour was always very satisfactory.

If a prediction method should be advised to professionals and implemented into codes it should be provided in a simplified form such as the one herein suggested.

In any case it seems necessary to provide, for specific type of connections the range of applicability of the models suggested and always to advise for the use of two bound both for strength and stiffness.

**Acknowledgments** This research was partially sponsored by MURST (Ministry of University and of Scientific and Technological Research).

## REFERENCES

- 1 CEN (1994) - Eurocode 3 - Design of steel structures. Part. 1.1: A2 General rules and rules for buildings.
- 2 CEN (1994) - Eurocode 3, Part. 1.1 - Joints in Building Frames (Revised Annex J). draft July 94.
- 3 Cosenza, E., De Luca, A. and Faella, C. 1988. Approximate methods for computing the elastic critical load of semirigid sway frames. *Proceedings, Structural Stability Research Council, Annual Technical Session, Minneapolis.*
- 4 Cosenza, E., De Luca, A. and Faella, C. 1988. The concept of "frame slenderness" for the definition of "frame stability curves". *Proceedings, Structural Stability Research Council, Annual Technical Session, Minneapolis.*
- 5 Cosenza, E., De Luca, A. and Faella, C. 1989. "Elastic buckling of semirigid sway frames." Chap.8 In *Structural Connections: Stability and Strength*, edited by R. Narayanan, Elsevier Applied Publishers.
- 6 Cosenza, E., De Luca, A. and Faella, C. 1989. "Inelastic buckling of semirigid sway frames." Chap.9 In *Structural Connections: Stability and Strength*, edited by R. Narayanan, Elsevier Applied Publishers.
- 7 De Stefano, M. And Astanteh, A. (1991). "Axial force-displacement behavior of steel double angles", *J. Construct. Steel Research*, Elsevier Applied Science Publishers, 20(3), 161-181
- 8 De Stefano, M., Astanteh, A., De Luca, A. And Ho, I. (1991). "Behavior and modeling of double angle connections subjected to axial loads", *Proceedings, Structural Stability Research Council Annual Technical Session, Chicago*, 323-334.
- 9 De Stefano, M., De Luca, A., Astanteh, A. 1992. Prediction of double angle connections cyclic moment-rotation behaviour by a mechanical model. *Proceedings, Structural Stability Research Council, Annual Technical Session, Pittsburgh.*
- 10 De Stefano, M., De Luca, A. 1992. A mechanical model for simulating the cyclic flexural response of double angle connections. *Proceedings, COST C1 Workshop, Strasbourg.*
- 11 De Stefano, M., De Luca, A. and Astanteh, A. (1994) Modeling of cyclic moment-rotation response of double-angle connections. *Journal of Structural Engineering*, ASCE, Vol. 120, No. 1.
- 12 Wales, M.W. And Rossow, E.C. (1983). "Coupled moment-axial force behavior in bolted joints", *J. Struct. Engrg.*, ASCE, 109(5), 1250-1266.

- 13 Driscoll, G.C. (1987). "Elastic-plastic analysis of top-and-seat-angle connections", *J. Construct. Steel Research*, Elsevier Applied Science Publishers, 8(Special Issue on Joint Flexibility in Steel Frames), 119-136
- 14 Lothers, J.E. (1951). "Elastic restraint equations for semi-rigid connections", *Transactions*, ASCE, 1, 480-502.
- 15 Frye, M.J. And Morris, G.A. (1975). "Analysis of flexibly connected steel frames", *Canad. J. Civ. Engrg.*, 2(3), 280-291
- 16 Richard, R.M. and Abbott, B.J. (1975). "Versatile elastic-plastic stress-strain formula", *J. Eng. Mech. Div.*, ASCE, 101(EM4), 511-515.
- 17 Richard, R.M., Hsia, W.K. and Chmielowiec, M. (1987). "Moment rotation curves for double framing angles", *Proceedings, Materials and Members Behavior, Session at ASCE Structures Congress '87, Orlando, Florida*, 107-119.
- 18 Atiogbe, E. and Morris, G. (1991) Moment-rotation functions for steel connections. *J. Struct. Engrg.*, ASCE, 117(6), 1703-1718.
- 19 Azizinamini, A., Bradburn, J.H. and Radziminski, J.B. (1987) Initial stiffness of semi-rigid steel beam-to-column connections. *J. Construct. Steel Res.*, 8, 71-90.
- 20 Kishi, N. And Chen, W.F.(1990). "Moment-rotation relations of semirigid connections with angles", *J. Struct. Engrg.*, ASCE, 116(7), 1813-1834.
- 21 Azizinamini, A., Bradburn, J.H. And Radziminski, J.B. (1987). "Initial stiffness of semi-rigid steel beam-to-column connections", *J. Construct. Steel Research* (Special Issue on Joint Flexibility in Steel Frames), Elsevier Applied Science Publishers, 8, 71-90
- 22 Jaspert, J.P. (1991) Study of semirigidity of beam-to-column joints and of its influence on the strength and stability of steel frames (in French), Ph.D. Thesis, University of Liege, Dept. of Applied Sciences, Belgium.
- 23 Shen, J.H. and Astaneh, A. (1993). "Behavior and hysteresis model of steel semi-rigid connections with bolted angles", *Report UCB/EERC-93*, Earthquake Engrg. Res. Center, University of California, Berkeley.
- 24 Nethercot, D.A. And Zandonini, R. (1989). "Methods of prediction of joint behaviour: beam-to-column connections", Chap.2 in *Structural Connections: Stability and Strength*, ed. by R. Narayanan, Elsevier Applied Science Publishers, 23-62.
- 25 Astaneh, A., Nader, M. and Malik, L. (1989) Cyclic behaviour of double angle connections, *J. Struct. Engrg.*, ASCE, 115(5), 1101-1118.
- 26 De Stefano, M. And De Luca, A. (1992). "Mechanical models for semirigid connections", *Proceedings, First World Conference on Constructional Steel Design, Acapulco*, 276-279.
- 27 Bernuzzi, C., De Stefano, M., D'Amore, E., De Luca, A., Zandonini, R. 1994. Moment rotation behaviour of Top and Seat Angle connections, *Proceedings STESSA 94*.
- 28 Bernuzzi, C. (1992) Cyclic response of semi-rigid steel joints. *Proceedings, First State of the Art Workshop - Semi-Rigid Behaviour of Civil Engineering Structural Connections, COST-C1, Strasbourg, France*.
- 29 De Luca, A., De Martino, A., Pucinotti, R., Puma, G., (Semirigid ?) Top & Seat angle Connections: Review of Experimental Data and Comparison with Eurocode 3, *Proceedings, CTA, Riva del Garda*, 1995.
- 30 K. Weinand, "SERICON-Databank on joints in building frames", *Proceeding of the 1st COST C1 Workshop, Strasbourg*, 28-30 October
- 31 N. Kishi, W.F. Chen, "Database of Steel Beam-to-Column Connections", *Structural Engineering Report, No. CE-STR-86-26*, School of Civil Engineering, Purdue University, 1986
- 32 De Luca, A., De Martino, A., Pucinotti, R., Puma, G., (Semirigid ?) Top & Seat Angle Connections: Critical Review of Eurocode 3 Approach, *Proceedings, CTA, Riva del Garda*, 1995.

Technical Papers on

**FRAME BEHAVIOUR**

## CHARACTERISTIC SEMI-RIGID CONNECTION RELATIONSHIPS FOR FRAME ANALYSIS AND DESIGN

Donald W. White<sup>1</sup>

Wai-Fah Chen<sup>2</sup>

### Abstract

Normalized moment-rotation relationships, representing different families of connections, are needed to facilitate the design of frames with semi-rigid connections. This paper takes stock of some efforts to define and use normalized moment-rotation curves based on mechanistic models of the connection components. The goal is to illustrate one approach to how analytical equations for design analysis can be developed and applied. To focus attention on the overall framework of the problem, only the simple case of a top and seat angle connection (no web angles) is considered.

### 1. INTRODUCTION

Although the direct consideration of connection moment-rotation characteristics in steel frame design has received substantial research attention during the last two decades, only a few engineering firms in the United States have actively applied this knowledge in design practice. One reason for this is the lack of firm recommendations for characteristic connection relations that can be utilized in the design process. Although there are large databases of test data (Chen and Kishi, 1989; Nethercot, 1987), the tests that have been catalogued are only a sparse sampling of the actual combinations of design parameters that can occur in the field. This paper takes the position that the best approach to facilitate the design of frames with semi-rigid connections is the establishment of "standard" mechanistic equations, which characterize the effects of all the primary behavioral parameters for a given type of connection. Much recent progress has been made by various researchers throughout the world in developing such equations (Colson, 1995).

This paper utilizes mechanistic equations developed by Kishi and Chen (1990) for top and seat angle connections (without web angles) to elucidate some of the issues associated with development and application of such equations for design of semi-rigid frames. The next section reviews a specific  $M-\theta$  equation used successfully by Kishi and Chen as well as by many others. Section 3 then outlines the basics of a suggested approach to semi-rigid frame design, and emphasizes certain attributes of and

<sup>1</sup> Associate Professor, School of Civil Engineering, Purdue University, West Lafayette, IN

<sup>2</sup> Professor, School of Civil Engineering, Purdue University, West Lafayette, IN

requirements for potential characteristic connection relationships. Sections 4 and 5 outline mechanistic and empirical procedures used by Kishi and Chen to define the parameters of the selected  $M-\theta$ , equation. Section 6 then presents equations for these parameters in a form useful for connection classification and design application. The paper closes with key observations and conclusions in Sections 7 and 8.

## 2. MOMENT-ROTATION EQUATIONS

A four-parameter equation, first proposed by Richard and Abbott (1975), has proven to be quite versatile for representing a wide range of connection responses. This equation may be expressed in the form

$$M = \frac{R_i \theta_r}{\left[ 1 + \left( \frac{\theta_r}{\theta_o} \right)^n \right]^{1/n}} + R_{kp} \theta_r \quad (1)$$

where:

$M$  = connection moment

$M_u$  = connection ultimate moment capacity

$R_i = R_{ki} - R_{kp}$

$R_{ki}$  = initial connection stiffness

$R_{kp}$  = connection strain-hardening stiffness

$\theta_r$  = connection rotation

$\theta_o = \text{reference rotation} = M_u / R_{ki}$

$n$  = shape parameter.

The tangent stiffness is equal to  $R_{ki}$  if the connection is unloaded. Kishi and Chen (1990) have adopted this model in research aimed at mechanistic prediction of the connection  $M-\theta_r$  behavior, with the exception that they assume  $R_{kp} = 0$ . With  $R_{kp}$  set to zero, the  $M-\theta_r$  relationship has the shape shown in Fig. 1. It can be observed that for larger values of the power term  $n$ , the transition from the initial stiffness,  $R_{ki}$ , to the final curve of maximum moment,  $M_u$ , is more abrupt. As  $n$  approaches infinity, the model becomes a bilinear elastic-plastic curve that has initial connection stiffness,  $R_{ki}$ , and ultimate moment capacity,  $M_u$ . For  $n < 1$ , the connection curve deviates rapidly from the initial stiffness, and approaches  $M_u$  in a very gradual fashion.

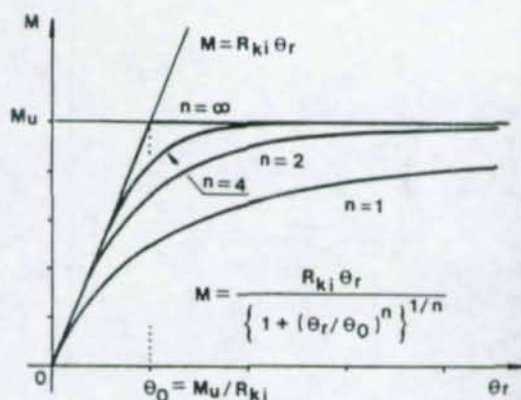


Figure 1. Moment-Rotation Equation with  $R_{kp} = 0$ .

A principal merit of Eq. (1) is that it allows the engineer to execute a nonlinear structural analysis efficiently and accurately. This is because the connection moment and stiffness can be determined directly for a given  $\theta_r$  without iteration. Also, as demonstrated by Kishi and Chen (1990) for angle connections, the parameters  $M_u$  and  $R_{ki}$  can be developed analytically in terms of basic geometrical parameters. Alternate equations that consider other types of connections and additional behavioral attributes not addressed by the Kishi and Chen model are outlined in (Jaspart, 1992). Given the

analytical values for  $M_u$  and  $R_{ki}$ , Kishi, et al. (1993) have proposed equations for the shape parameter  $n$  based on a least-squares fit to available test data for several angle connection types.

### 3. DESIGN APPROACH

In semi-rigid frame design, there is no avoiding the fact that the both the members and the connections must be considered as "primary elements" in designing the frame to support the gravity and lateral loads in a safe and serviceable manner. Consideration of the connections and how their details affect the frame performance significantly increases the number of design parameters to be controlled. This increase is one of the key benefits of semi-rigid connections in structural steel framing. Clearly, the ability to control the frame performance far exceeds that available with rigid framed design. However, generalizations need to be made to focus the design process. The authors suggest the use of either a target ratio of the connection to beam stiffness,  $R_{ki}/(EI/d)$ , or a target ratio of the connection to beam ultimate moment capacity  $M_u/M_p$ , as a convenient starting point for design. These ratios are based on the connection classification system proposed by Bjorhovde et al. (1990). The term  $d$  is the beam depth, and  $(EI/d)$  is representative of the beam stiffness. This term may be converted to possibly a more precise relative stiffness by multiplying by  $L/d$ , where  $L$  is the individual beam length, and used with charts such as that suggested by Gerstle (1988). Of course, the precise relative stiffness effect depends on how the individual beams are loaded.

It is desired to be able to determine a set of dimensional parameters for a given connection type that will provide the target strength and/or stiffness ratios. These relations can be derived based on mechanistic analysis of the connection components. For a given connection type, parametric equations can be expressed for  $R_{ki}/(EI/d)$ ,  $M_u/M_p$ , and the ratio of the strength to stiffness,  $(M_u/M_p)/(R_{ki}/(EI/d))$ . Generally, there are many connection parameters that affect these ratios, and thus, there is no one single characteristic  $M-\theta$  curve for a given connection type (e.g., the ratio of the strength to stiffness can vary for a specific connection type by changing the connection dimensional parameters). For design calculations, the engineer may be interested in the actual characteristic  $M-\theta$  curve, or in a secant stiffness and the associated connection design strength that may be derived from this curve.

### 4. MECHANISTIC MODELS - TOP AND SEAT ANGLE CONNECTIONS

#### Initial Connection Stiffness

Based on the experimental observations reported in (Hechtman and Johnson, 1947; Altman et al., 1982; Azizinamini et al., 1985), the top and seat angle connection type is assumed to behave as follows:

1. The center of rotation for the connection is at the edge of the angle leg attached to the compression flange of the beam, and is located at the end of the beam
2. The top angle acts as a cantilever beam that has a fixed support at edge of the fastener-hole closest to beam flange, and in the leg attached to the column face
3. The bending rigidity of the angle leg at the center of rotation is small and can be neglected.

The kinematics of the connection behavior (applicable for both the stiffness and strength calculations) are illustrated in Fig. 2. The cantilever model of the top angle for determining the initial connection stiffness is shown in Fig. 3. Based on this model, the connection initial stiffness (including the shear deformability of the angle leg as a short beam) can be expressed as

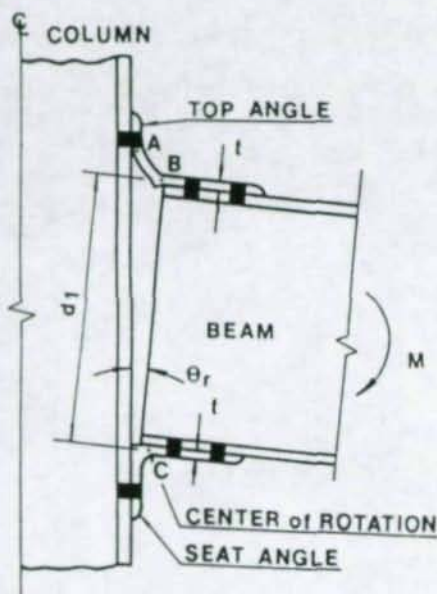


Figure 2. Kinematic assumptions.

$$R_{ki} = \frac{3EI_o \frac{l}{t}}{\frac{g_l}{t} \left[ \left( \frac{g_l}{t} \right)^2 + 0.78 \right]} \left( 1 + \frac{d}{t} \right)^2 \quad (2)$$

where  $I_o = \frac{t^3}{12}$ . The parameters  $l$  and  $d$  (not shown in the figure) are respectively the width of the connection angles and the total depth of the beam cross-section. Therefore, it can be observed that  $\frac{R_{ki}}{I_o}$  is a function of  $\frac{d}{t}$ ,  $\frac{l}{t}$ , and  $\frac{g_l}{t}$ :

$$\frac{R_{ki}}{I_o} = \frac{R_{ki}}{I_o} \left( \frac{d}{t}, \frac{l}{t}, \frac{g_l}{t} \right) \quad (3)$$

#### Ultimate Connection Moment Capacity

The ultimate moment capacity of the connection is derived using the work equation for the assumed mechanism shown in Fig. 4 in conjunction with Drucker's yield criterion (Drucker, 1956) for flexure-shear interaction. A yield line is assumed to form both in the top angle as shown, and in the bottom angle at the center of rotation of the connection. The resulting equation for the connection ultimate moment can be written as

$$M_u = \frac{l}{t} \left[ 1 + \frac{V_p}{V_o} \left( 1 + \frac{g_2}{t} + 2 \left\{ \frac{k}{t} + \frac{d}{t} \right\} \right) \right] M_o t \quad (4)$$

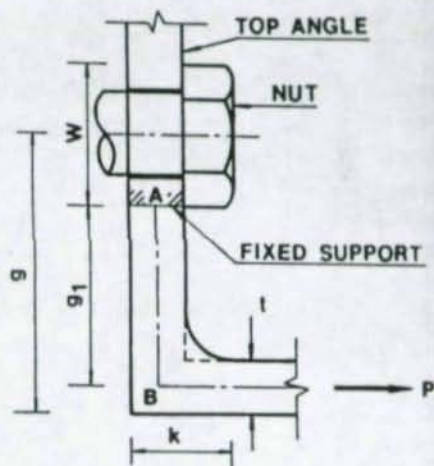


Figure 3. Cantilever model of top angle for calculation of initial stiffness.

if it is assumed that both angles have equal thickness, where  $M_o = \frac{F_y t^2}{4}$  and  $V_o = \frac{F_y t}{2}$  are the plastic moment capacity per unit width and the plastic shear capacity of the angle legs in the absence of any interaction effects. The yield criterion is expressed solely in terms of the actual plastic shear strength,  $V_p$ , as

$$\left(\frac{V_p}{V_o}\right)^2 + \frac{g_2}{t} \left(\frac{V_p}{V_o}\right) - 1 = 0 \quad (5)$$

For specific value of  $\frac{g_2}{t}$ , Eq. (5) may be solved

iteratively for  $\frac{V_p}{V_o}$ , and then this ratio may be

substituted into Eq. (4) for determining the connection ultimate moment capacity,  $M_u$ . It can be seen that  $\frac{M_u}{M_o t}$  is a function of  $\frac{l}{t}$ ,  $\frac{g_2}{t}$ ,  $\frac{k}{t}$ , and  $\frac{d}{t}$ ,

that is:

$$\frac{M_u}{M_o t} = \frac{M_u}{M_o t} \left( \frac{l}{t}, \frac{g_2}{t}, \frac{k}{t}, \frac{d}{t} \right) \quad (6)$$

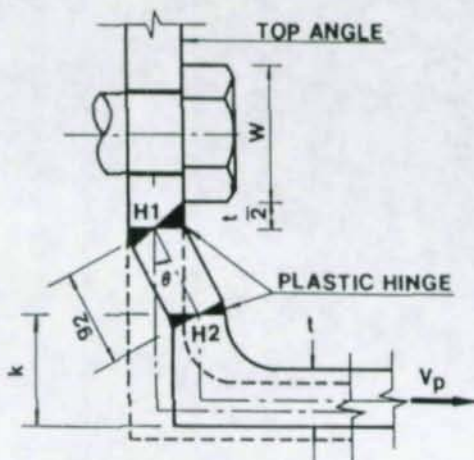


Figure 4. Mechanism of top angle at ultimate condition.

## 5. SHAPE PARAMETER BASED ON REFERENCE ROTATION

Kishi and Chen propose that once the connection initial stiffness  $R_{ei}$ , and ultimate moment capacity  $M_u$ , are evaluated for a given connection type (using the model outlined in Section 4), the shape parameter  $n$  should be determined such that the connection model given by Eq. (1) can best fit the experimental data. Kishi et al. (1993) performed statistical analyses of test data to develop formulas for the  $n$  values of several types of angle connections. For top and seat angle connections,

$$n = 2.003 \log_{10} \theta_o + 6.070 \geq 0.302 \quad (7)$$

The correlation of Eq. (7) with the test data studied by Kishi et al. is shown in Fig. 5.

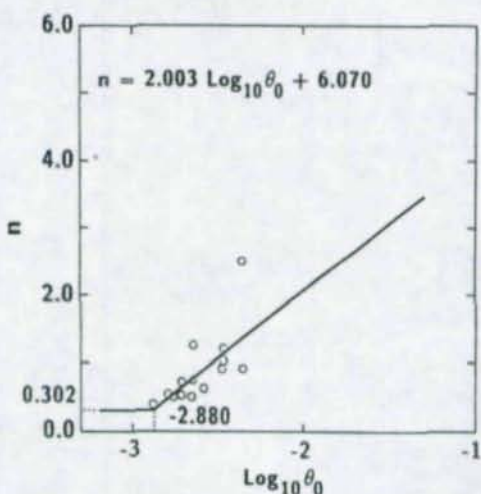


Figure 5. Comparison of the empirical equation for  $n$  with experimental test data (Kishi et al., 1993).

### 6. NORMALIZED CHARACTERISTIC EQUATIONS FOR DESIGN ANALYSIS

Based on the models for the top and seat angle connection discussed in Section 4, and writing the beam stiffness parameter as

$$\frac{EI}{d} = \frac{E}{d} \left( 2b_f t_f \left( \frac{d-t_f}{2} \right)^2 + \frac{d^3 t_w}{12} \right) = \frac{E b_f t_f d}{2} \left( 1 - \frac{l}{b_f d} + \frac{l d t_w}{6 b_f t_f} \right) \quad (8)$$

(where  $b_f$  is the beam flange width,  $t_f$  is the beam flange thickness, and  $t_w$  is the beam web thickness) the relative connection to beam stiffness can be expressed as

$$\frac{R_{ki}}{EI/d} = \frac{\frac{l}{b_f} \frac{b_f}{2t_f} \frac{d}{b_f} \left[ \frac{\frac{t}{t_f}}{2 \frac{b_f d}{2t_f b_f}} + 1 \right]^2}{\frac{g_l}{t} \left[ \left( \frac{g_l}{t} \right)^2 + 0.78 \right] \left( 1 - \frac{l}{b_f d} + \frac{l d t_w}{6 b_f t_f} \right)} \quad (9)$$

Therefore, the functional relationship between  $\frac{R_{ki}}{EI/d}$  and the various nondimensional parameters is

$$\frac{R_{ki}}{EI/d} = \frac{R_{ki}}{EI/d} \left( \frac{l}{b_f}, \frac{t}{t_f}, \frac{g_l}{t}, \frac{d}{b_f}, \frac{b_f}{2t_f}, \frac{t_w}{t_f} \right) \quad (10)$$

Similarly, by writing the plastic moment capacity of the beam as

$$M_p = b_f t_f F_y (d-t_f) + F_y t_w \frac{d^2}{4} = b_f t_f F_y d \left( 1 + \frac{l t_w d}{4 t_f b_f} - \frac{l}{2 \frac{b_f d}{2t_f b_f}} \right) \quad (11)$$

the ratio of the connection ultimate moment to the beam capacity can be expressed as

$$\frac{M_u}{M_p} = \frac{\frac{l}{b_f} \left( \frac{t}{t_f} \right)^2}{2 \frac{b_f d}{2t_f b_f} \left( 4 + \frac{t_w d}{t_f b_f} - \frac{2}{\frac{b_f d}{2t_f b_f}} \right)} \left[ 1 + \frac{V_p}{V_o} \left( 1 + \frac{g_l}{t} + 2 \frac{k}{t} + 4 \frac{b_f d / b_f}{2t_f t / t_f} \right) \right] \quad (12)$$

Therefore,  $\frac{M_u}{M_p}$  has the following functional dependency:

$$\frac{M_u}{M_p} = \frac{M_u}{M_p} \left( \frac{l}{b_f}, \frac{t}{t_f}, \frac{g_2}{t}, \frac{k}{t}, \frac{d}{b_f}, \frac{t_w}{2t_f}, \frac{t_w}{t_f} \right) \quad (13)$$

Finally, based on Eqs. (9) and (12), it can be seen that that ratio of the stiffness to strength is of the following functional relationship:

$$\frac{R_{ks}/(EI/d)}{M_u/M_p} = \frac{R_{ks}/(EI/d)}{M_u/M_p} \left( \frac{t}{t_f}, \frac{g_1}{t}, \frac{g_2}{t}, \frac{k}{t}, \frac{d}{b_f}, \frac{t_w}{2t_f}, \frac{t_w}{t_f} \right) \quad (14)$$

Example plots of Eq. (12) are demonstrated for several combinations of parameters in Figs. 6 through 8, plots of the inverse of Eq. (9) are illustrated in Figs. 9 through 11, and Figs. 12 and 13 show the relationship between stiffness and strength (Eq. (14)). It can be observed that the strength ratio varies significantly based on the ratio  $t/t_f$ , whereas the stiffness ratio does not exhibit much variation relative to this parameter. Both the stiffness and the strength ratios, and the ratio of stiffness to strength, vary significantly with the gage parameters  $g_1/t$  and  $g_2/t$ , and with several parameters that are section properties of the beam ( $b_f/2t_f$  and  $d/b_f$ ). The relationships are not sensitive to  $t_w/t_f$  and  $k/t$ . The plots have all been produced with  $t_w/t_f = 0.66$ , which is a median value for rolled W sections of Groups 1 through 3 (AISC, 1994), and with  $k/t = 1.5$ . Also, all the plots are based on  $l/b_f = 1$ . The equations illustrated in the plots can be used directly for design, and/or simpler relationships characteristic of top and seat angle connections might be developed by synthesizing these curves into "average" curves for certain restricted or target ranges of the significant parameters.

## 7. PITFALLS

A major advantage of mechanistic equations is that they can capture significant parametric effects that might be overlooked by "brute force" statistical analysis of experimental data. However, a pitfall is that the equations are only as correct as the models on which they are based. The Kishi and Chen model is based on several assumptions that must be satisfied for its correct use. These assumptions include:

- Column web and flange deformations due to introduction of the load from the angles are negligible (or are included elsewhere in the analysis model).
- Column panel zone shear deformations are negligible (or included elsewhere).
- Connection slippage in the attachment to the beam does not occur, and beam flange deformations and yielding due to introduction of the load from the angles is negligible (or included elsewhere).
- The beam idealization of the top angle leg is valid (probably not the case as  $g_2$  approaches zero).
- Membrane effects due to deformation of the top angle leg are negligible.
- A sufficient number of fully-pretensioned bolts is provided such that: (a) the strength and stiffness of the bolts in tension do not influence the connection behavior, (b) the bolts are able to hold a fixed point in the outstanding top angle leg as shown in Fig. 3, and (c) the bolts are able to hold the top yield line in the outstanding top angle leg at the location shown in Fig. 4.
- The gap between the end of the beam and the column face is small (in some cases in which the beam is slightly under-length, the bottom yield line in the top angle can form in the leg attached to the beam rather than at the position shown in Fig. 4).

Jaspart (1992) discusses a number of these assumptions and has outlined how a some of the additional effects may be modeled, at the expense of some additional complexity of the resulting equations. It should be noted that the effects of variations associated with the last two assumptions in the above list can be considered approximately by studying the effects of varying  $g_1/t$  and  $g_2/t$  in Figs. 6-13.

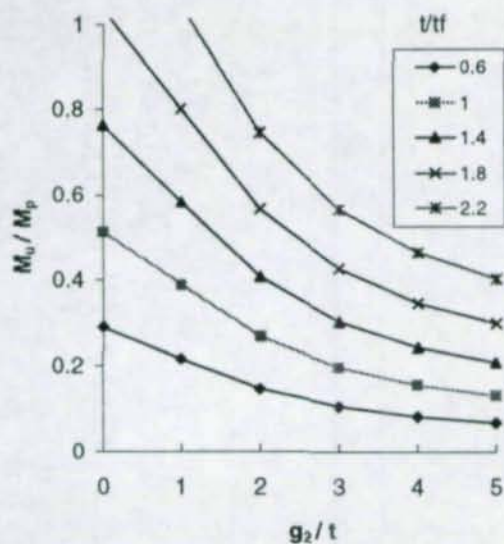


Figure 6.  $M_u / M_p$  for  $b_f / 2t_f = 7$ ,  $d / b_f = 1$ .

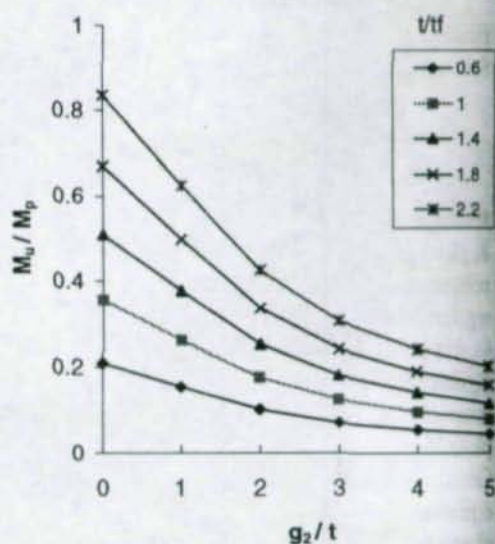


Figure 7.  $M_u / M_p$  for  $b_f / 2t_f = 7$ ,  $d / b_f = 3$ .

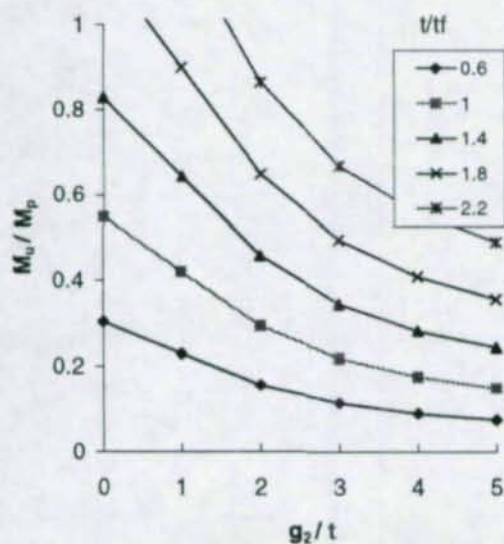


Figure 8.  $M_u / M_p$  for  $b_f / 2t_f = 5$ ,  $d / b_f = 1$ .

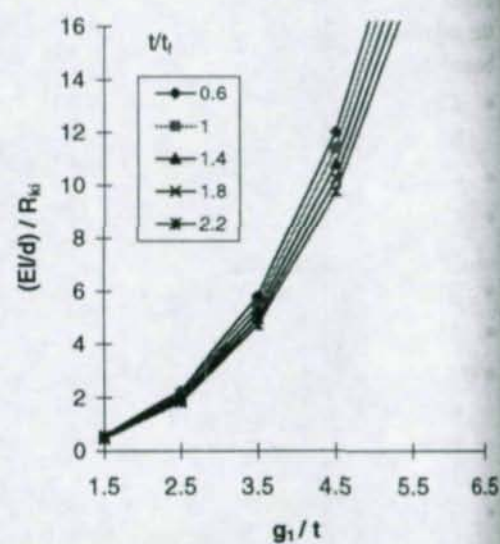


Figure 9.  $(EI/d) / R_{kl}$  for  $b_f / 2t_f = 7$ ,  $d / b_f = 1$ .

Figure 5 shows that  $n$  should be less than one for the best least square fit of the model outlined in Sections 2 and 4 to the available experimental data. This indicates that the connection stiffness reduces from  $R_{ki}$  very rapidly, and that the connection response does not reach  $M_u$  until large rotations. While this may be true for certain connections, it is expected that larger values of  $n$  would be obtained if

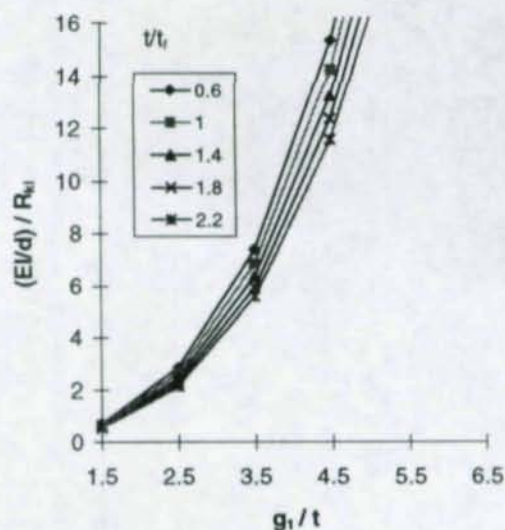
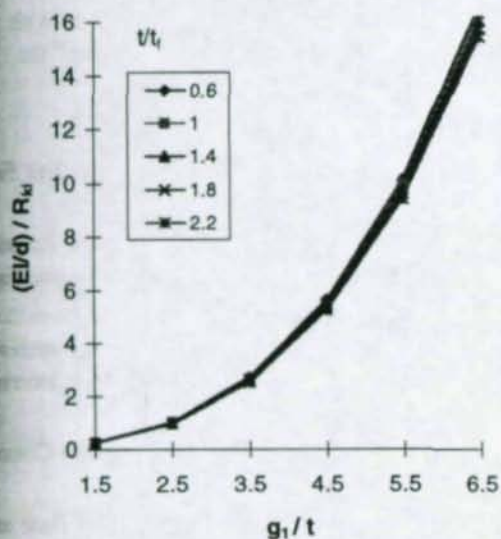


Figure 10.  $(EI/d) / R_{ki}$  for  $b_f/2t_f = 7$ ,  $d/b_f = 3$ . Figure 11.  $(EI/d) / R_{ki}$  for  $b_f/2t_f = 5$ ,  $d/b_f = 1$ .

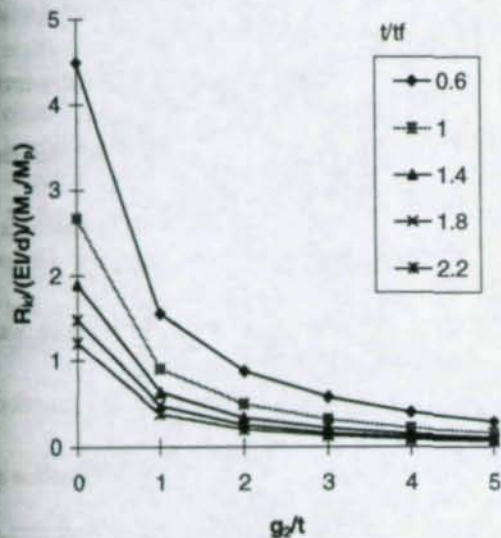


Figure 12.  $R_{ki} / (EI/d) / (M_u / M_p)$  for  $b_f/2t_f = 5$ ,  $d/b_f = 1$ .

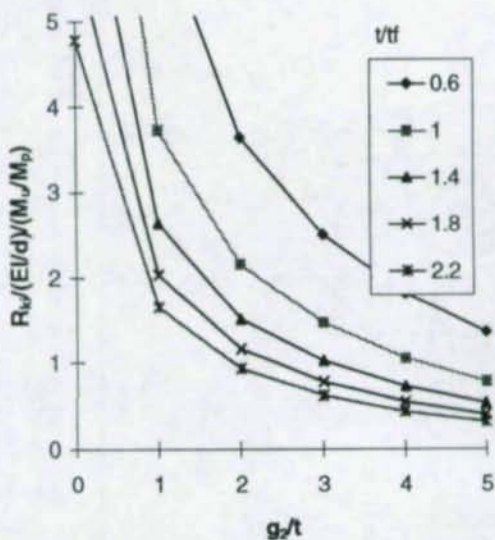


Figure 13.  $R_{ki} / (EI/d) / (M_u / M_p)$  for  $b_f/2t_f = 7$ ,  $d/b_f = 3$ .

additional effects such as those suggested by Jaspert are included in the models for  $R_{ki}$  and  $M_x$ , and if a non-zero  $R_{kp}$  relation is developed and utilized. Non-zero  $R_{kp}$  equations may be derived from mechanistic models such as (Lay, 1966).

## 8. CONCLUSIONS

The promise and the pitfalls of using mechanistic models to develop characteristic moment-rotation relationships for analysis and design of frames with semi-rigid connections has been discussed. With coordinated industry efforts, approaches similar to those described can be used to "standardize" the connection moment-rotation curves that may be used for design.

## REFERENCES

- AISC (1994). *Manual of Steel Construction, Load and Resistance Factor Design*, 2nd Ed. American Institute of Steel Construction, Chicago, IL.
- Altman, W.G., Azizinamini, A., Bradburn, J.H. and Radziminski, J.B. (1982). *Moment-Rotation Characteristics of Semi-Rigid Steel Beam-to-Column Connections*, Department of Civil Engineering, University of South Carolina, Columbia, SC.
- Azizinamini, A., Bradburn, J.H., and Radziminski, J.B. (1985). *Static and Cyclic Behavior of Semi-Rigid Steel Beam-Column Connections*, Structural Research Studies, Department of Civil Engineering, University of South Carolina, Columbia, SC.
- Bjorhovde, R., Colson, A., and Brozzetti, J. (1990). "Classification System for Beam-to-Column Connections," *Journal of Structural Engineering*, ASCE, 116(11), 3059-3076.
- Chen, W.F. and Kishi, N. (1989). "Semi-Rigid Steel Beam-to-Column Connections: Data Base and Modeling," *Journal of Structural Engineering*, ASCE, 115(1), 105-119.
- Colson, A. (1995). "Some Basic Principles for Semi-Rigid Concept," *Preliminary Proceedings*, Third International Workshop on Connections in Steel Structures, Trento.
- Drucker, D.C. (1956). "The Effect of Shear on the Plastic Bending of Beams," *Journal of Applied Mechanics*, ASME, 23(4), 509-514.
- Gerstle, K.H. (1988). "Effect of Connections on Frames," *Journal of Constructional Steel Research*, 10, 241-267.
- Hechtman, R.A. and Johnson, B.G. (1947). *Riveted Semi-Rigid Beam-to-Column Building Connections*, Progress Report No. 1, AISC Research at Lehigh University, Bethlehem, PA.
- Jaspert, J.-P. and Maquoi, R. (1992). "Plastic Capacity of End-Plate and Flange Cleated Connections - Prediction and Design Rules," *Connections in Steel Structures II: Behavior, Strength, and Design*, Proceedings of Second International Workshop, Pittsburgh, PA, 225-235.
- Kishi, N. and Chen, W.F. (1990). "Moment-Rotation Relations of Semi-Rigid Connections with Angles," *Journal of Structural Engineering*, ASCE, 116(7), 1813-1834.
- Kishi, N., Chen, W.F., Goto, Y. and Matsuoka, K.G. (1993). "Design Aid of Semi-Rigid Connections for Frame Analysis," *Engineering Journal*, AISC, 30(3), 90-107.
- Lay, M.G. (1966). "A New Approach to Inelastic Structural Design," *Proceedings of the Institution of Civil Engineers*, pp. 1-24.
- Nethercot, D.A. (1987) *Steel Beam to Column Connections - A Review of Test Data*, CIRIA, RP 339, London.
- Richard, R.M. and Abbott, B.J., "Versatile Elastic-Plastic Stress-Strain Formula," *Journal of the Engineering Mechanics Division*, ASCE, 101(4), 511-515.

**LARGE-SCALE TESTS ON STEEL FRAMES WITH  
SEMI-RIGID CONNECTIONS.  
EFFECT OF BEAM-COLUMN CONNECTIONS AND COLUMN-BASES**

IVÁNYI, Miklós<sup>1</sup>

Abstract

Experimental investigations of full scale frames are shown with regard to the effect of beam-column connections and column bases.

This work was supported by PECO-COST C1 "Semi-rigid behaviour" project.

**1. INTRODUCTION**

A great number of tests have been performed on isolated semi-rigid connections and flexibly connected subframes. Tests on full-scale three-dimensional frames are somewhat less numerous. However, experimental data on full-scale frame behaviour is important. Firstly it enables the effect of column continuity through a loading level to be investigated - a parameter not present in many subframe tests - and secondly; it confirms whether the experimentally observed performance of isolated joints and subframes is indeed representative of their behaviour when they form part of an extensive frame. This latter point is of particular importance if the extensive work on isolated specimens is to be incorporated into universally accepted methods of semi-rigid and partial strength frame design.

The frame tests, presented in this contribution, were carried out in the large structures testing hall of the Building Research Laboratory, Department of Steel Structures, Technical University of Budapest.

---

<sup>1</sup>Prof. Dr., Department of Steel Structures, Technical University of Budapest, Budapest, P.O. Box. 91. H-1521, Hungary

## 2. GENERAL ARRANGEMENT OF THE EXPERIMENTAL TESTS

### 2.1. Test program and description of test frames

The test programme included tests of three complete frames:

- |              |  |
|--------------|--|
| Frame COST 2 | proportional loading process<br>[ horizontal load ratio: $R=1$ ]       |
| Frame COST 3 | variable repeated loading process<br>[ horizontal load ratio: $R=0$ ]  |
| Frame COST 4 | variable repeated loading process<br>[ horizontal load ratio: $R=-1$ ] |

$$\text{where } R = \frac{H_{max}}{H_{min}}$$

The test frames were partially two-storey and partially two-bay ones. In the first storey the frames had two bays, and the larger one was continued in the second storey. The frames were built up from European hot-rolled sections (Fig. 1).

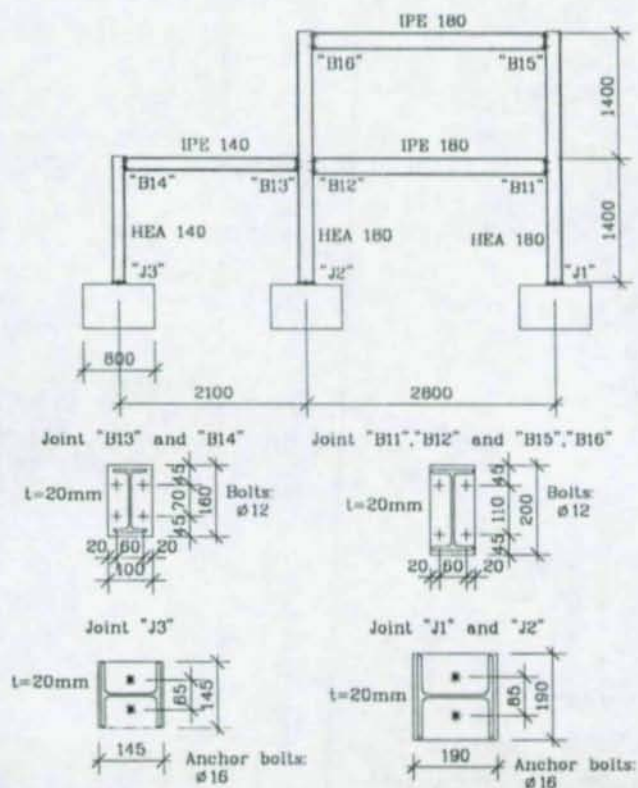


Fig.1 Overall view of test frames

Typical flush end plate connections have been used between the main members of the frame. There were a number of reasons for selecting this particular type of connections.

Firstly, cleated connections are very often susceptible to bolt slip at relatively low moment levels. Once bolt slip has occurred, the precise moment - rotation characteristics of the connection are usually irreversibly changed. The flush end plate connection however is not affected by bolt slip to the same degree and therefore, exhibits similar moment - rotation behaviour under repeated moderated loading. Using such a connection, small levels of load could be applied to the frame without irreversibly deforming either the connections or the frame members. This was an important facility which allowed the loading devices and load control system to be fully commissioned prior to carrying out a test to failure.

The test frames were supported by separated rigid concrete blocks, which were connected to the testing floor. The connections of columns to the "separated" concrete blocks were realized as "hinged" bolted connections between the base plate and the concrete block.

Concrete blocks were poured into a steel formwork. The formwork contained four tubes for those bolts, which were used later to connect the concrete blocks to the testing floor. Concrete blocks are reinforced, main dimensions of the blocks and the amount and form of reinforcing bars was adopted from the similar blocks of the tests of PENSERINI and COLSON 1989.

Anchor bolts were jointed to the reinforcement of the blocks before concreting. Between the top of the blocks and the bottom of baseplates, according to the usual practice, app. 1cm thick cement layer were used.

## 2.2 Loading system

Test frame COST 2 was loaded by combined (vertical and horizontal) loads (Fig. 2).

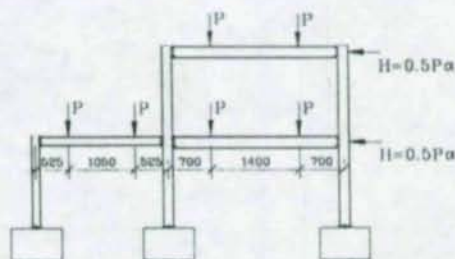


Fig. 2 Loading arrangement

Vertical loads were applied to the upper flanges of beams, this way webs and lower flanges were not restrained laterally. Loading was exerted by means of hydraulic jacks.

To make horizontal displacements (sideways) unrestricted, jacks were fastened not directly to the floor slab, but through a so-called gravity load simulator (HALÁSZ-IVÁNYI 1979). This latter consisted of three elements: two "rigid" bars and one "rigid" triangle. The two bars had pin-joints at both ends, resulting in a one-degree-of-freedom mechanism. Hydraulic jacks

joined the third corner of the rigid triangles. This mechanism produced a vertical load acting in the intersection of the two bar axes.

The simulators were designed and manufactured in the Building Research Laboratory, Department of Steel Structures, Technical University of Budapest.

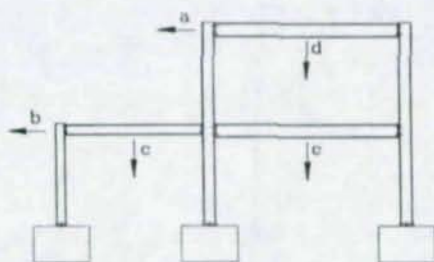


*Fig. 3 Measured displacements*

Horizontal loads were applied at the levels of beams and they were exerted by hydraulic jacks driven by the same oil-pressure circuit as the vertical ones, thus achieving a constant ratio of vertical loads, namely this value was 0.5, when proportional loading process was used. For the cyclic loading process the horizontal loads were driven by the different oil-pressure circuit.

The original structure consists of frames and a "perpendicular" system of purlins, side-rails and wind bracing. The effect of this latter system was simulated by a "back-ground" construction, located at three meter distance behind the test frames and connecting rods at the top of columns and the middle of beams.

### 2.3. Measuring techniques

Forces were measured by means of a pressure transducer built in the oil circuit of the hydraulic system. The intensities of the forces were calculated from the pressure and the effective cross sectional area of the jacks.

Main important horizontal and vertical displacements of the frames were measured on the beam levels (a and b in Fig. 3) and in the midspans of the beams (c, d and e) by inductive transducers.

Strains were measured by means of strain gages. Altogether 16 cross sections of the frame elements were chosen and one cross section contained four strain gages on the four edges of the section.

Relative rotations at joints were measured in similar sections as strain, their distribution and notation are given in Fig. 4.

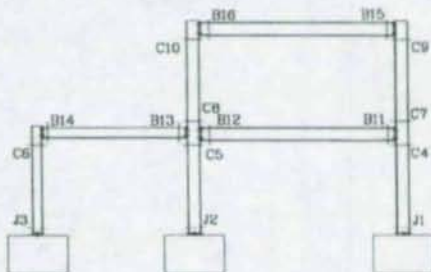


Fig. 4 Cross sections with relative rotation measuring scales

For this purpose two simple scales were inserted in every section in a known distance (app. 200 mm) from each other, they were hinged connected and always kept the vertical direction because of gravity. Measurements were made by geodetic devices and from the measured differences the rotation was calculated.

After inducing the appropriate loading level, a five-ten minute delay was kept and after that the measurements took place. Such a delay is necessary to let the deformations to develop.

### 3. SOME RESULTS OF THE EXPERIMENTS

#### 3.1. Frame under proportional loading

For frame COST 2 the load - displacement curves are presented in Fig. 5. Notation of displacements can be seen in Fig. 3. The load axis contains the total load produced by the hydraulic system (that is  $7xP$ ).

Load - relative rotation and displacement curves at column bases of Fig. 4 are drawn in Fig. 6. The further load - relative rotation curves of other sections in Fig. 4 are given in Fig. 7. The curves are giving both the load - rotation characteristics of the different sections and the differences between the neighbouring sections. These differences in case of columns (as between 4 and 7 or between 5 and 8) are not remarkable, while on two sides of a beam-to-column connection (as between 4 and 11 or between 5 and 13, etc.) they are nonnegligible.

The loading was increased step by step. After the load level No. 6 an unloading took place. At this stage the whole structure, its connections were elastic, only the column bases showed some changes. On the compression zone there were some cracks in the cement layer, while on the tension side there was a gap. During this unloading process the rigidity of the structure caused some further cracks on the opposite side of the cement layer.

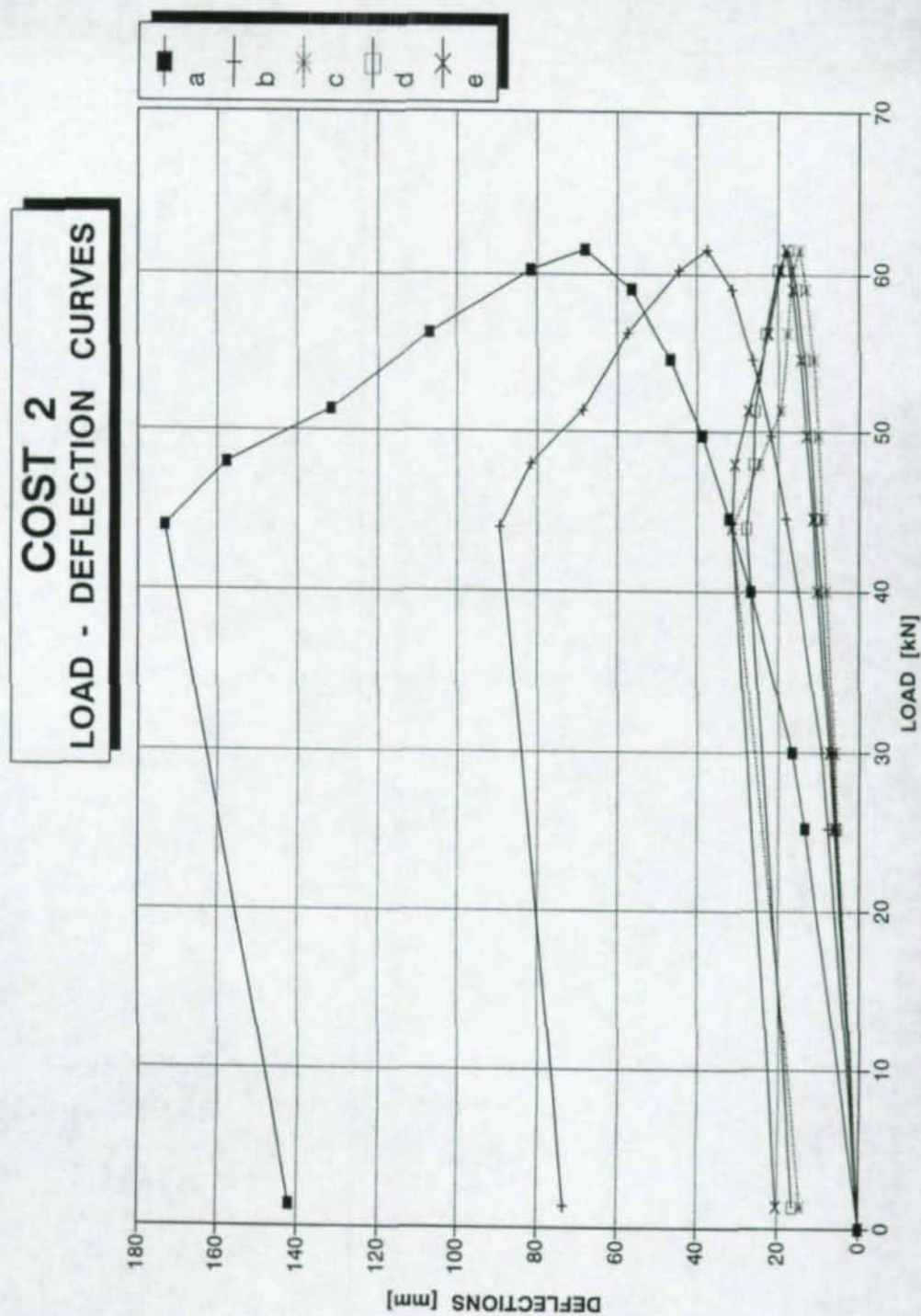


Fig. 5 Load - displacements curves

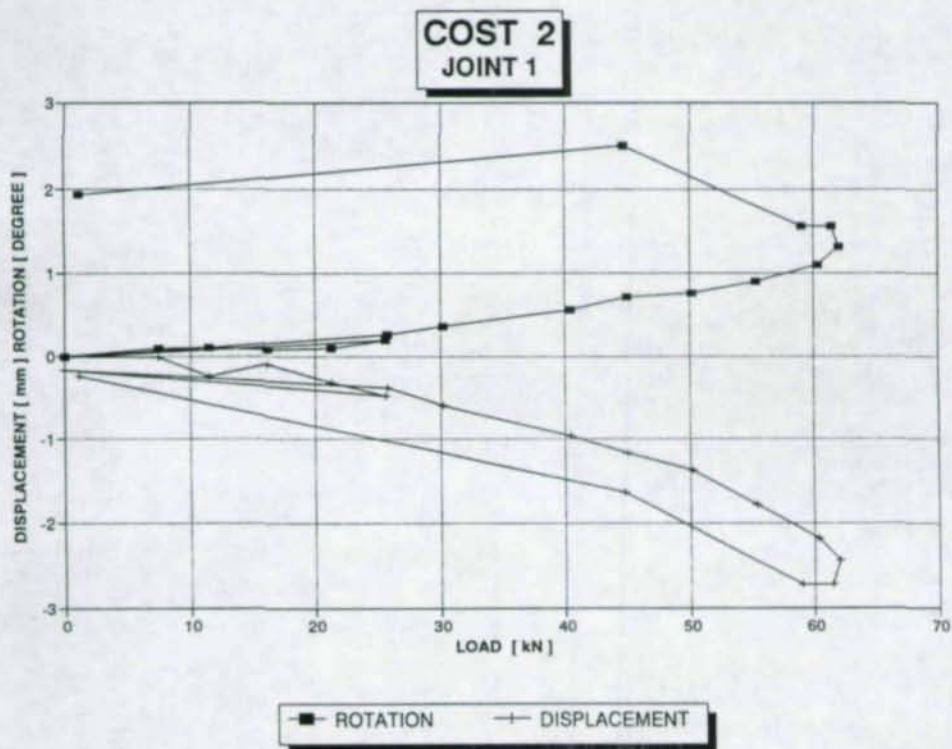


Fig. 6 Load - relative rotation and displacement curves at column base

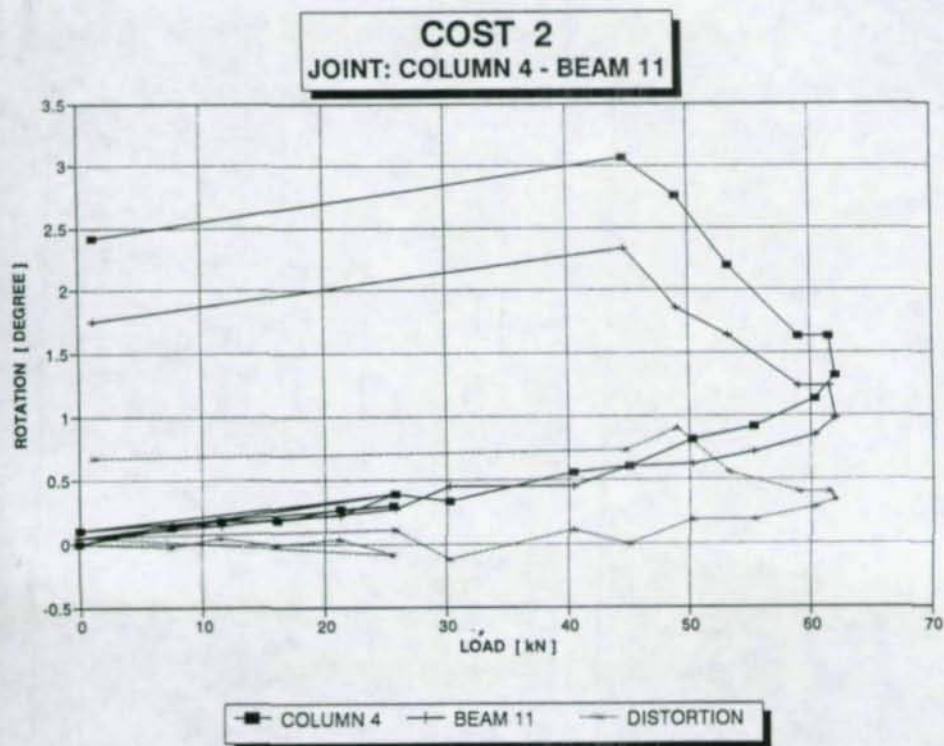
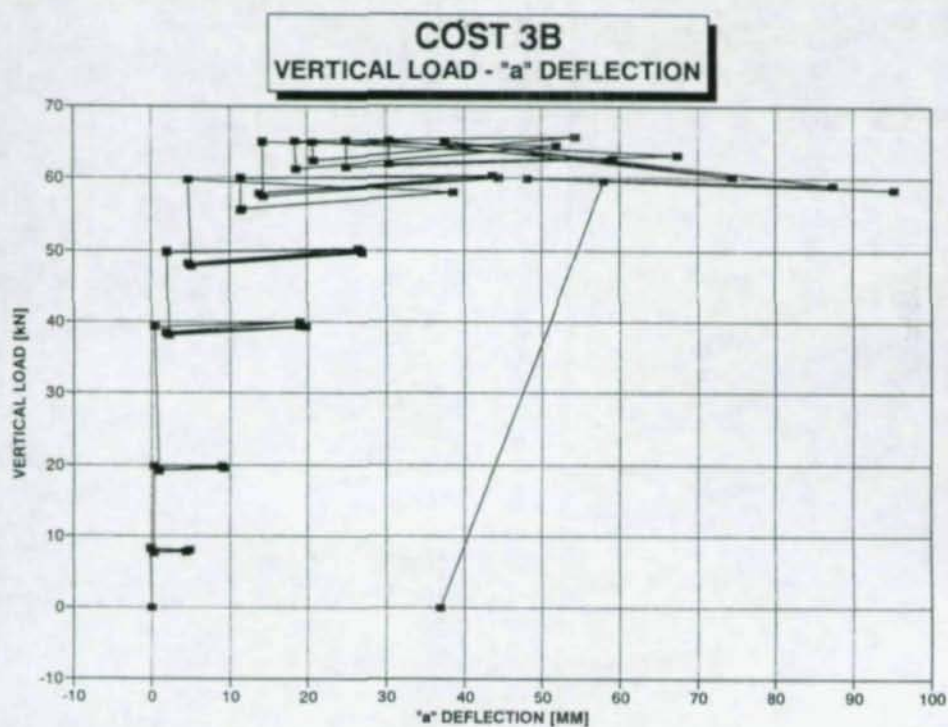
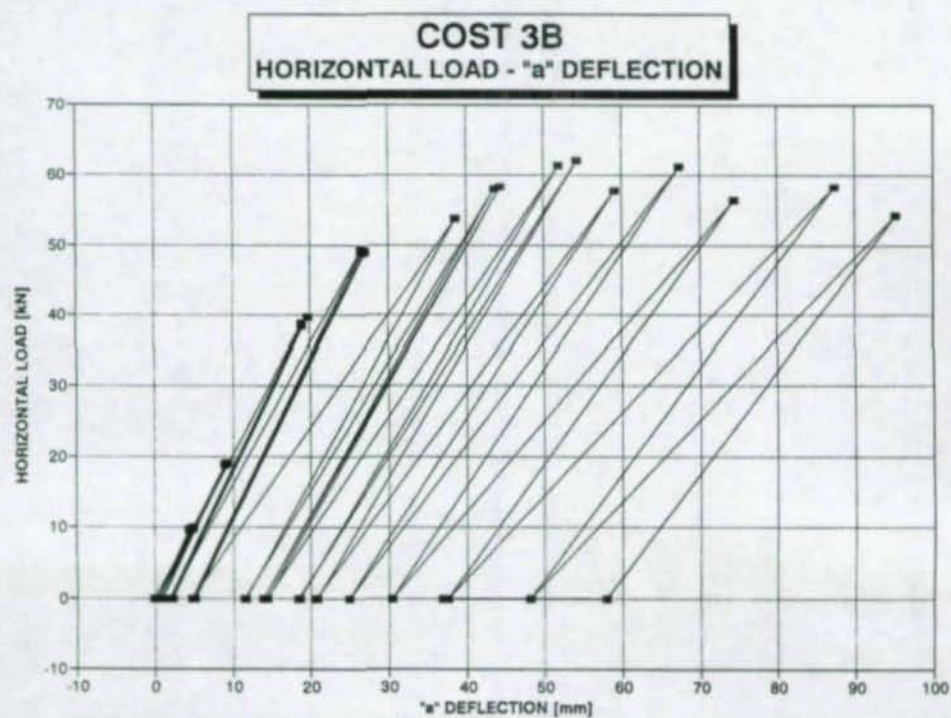


Fig. 7 Load - displacement curves



*Fig. 8 Vertical load - deflection*



*Fig. 9 Horizontal load - deflection*

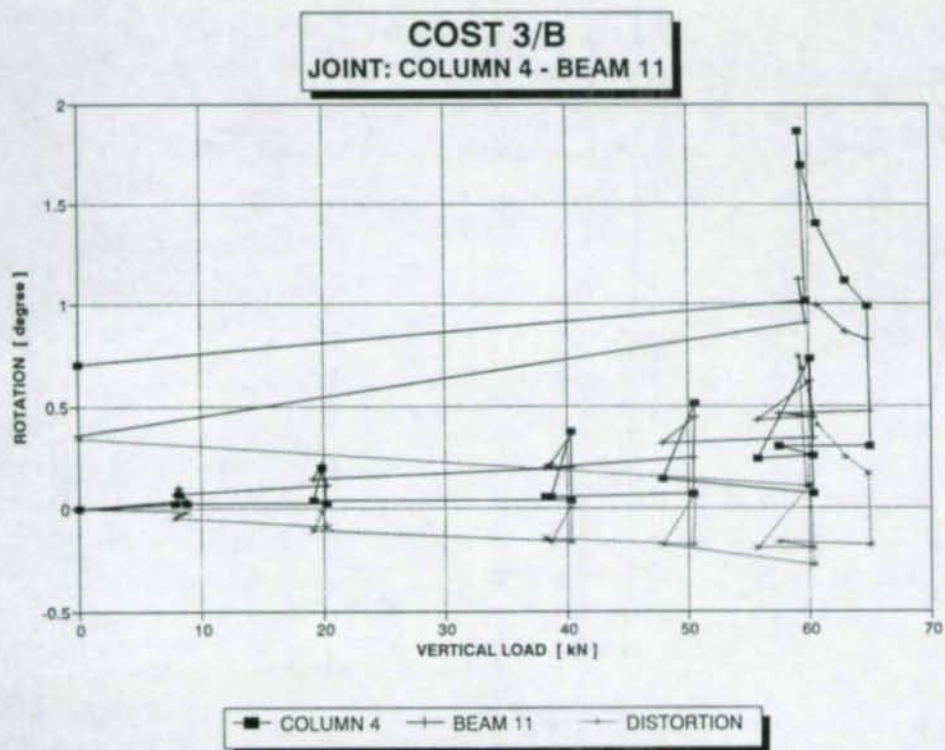


*Fig. 10 Vertical load - rotation curves*

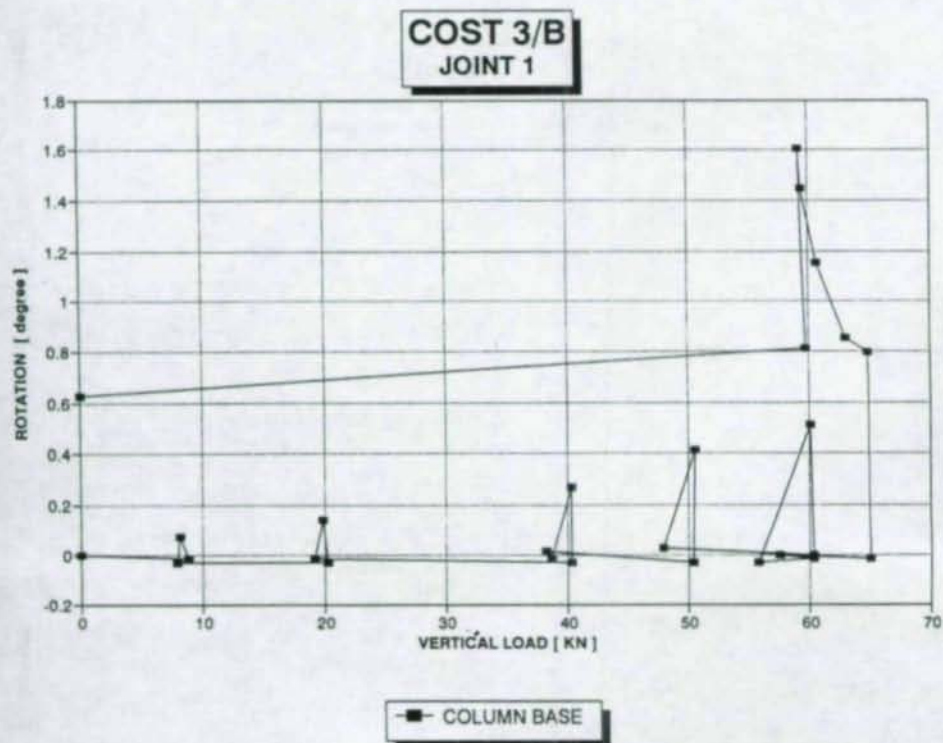


*Fig. 11 Vertical load - rotation curve*

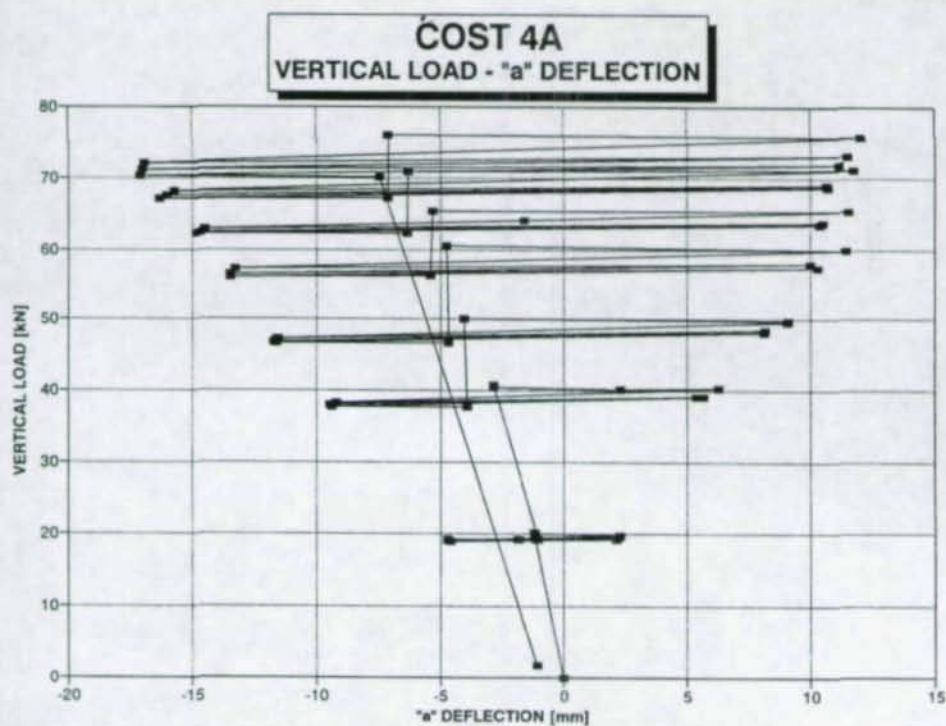


*Fig. 12 Vertical load - deflection curve*

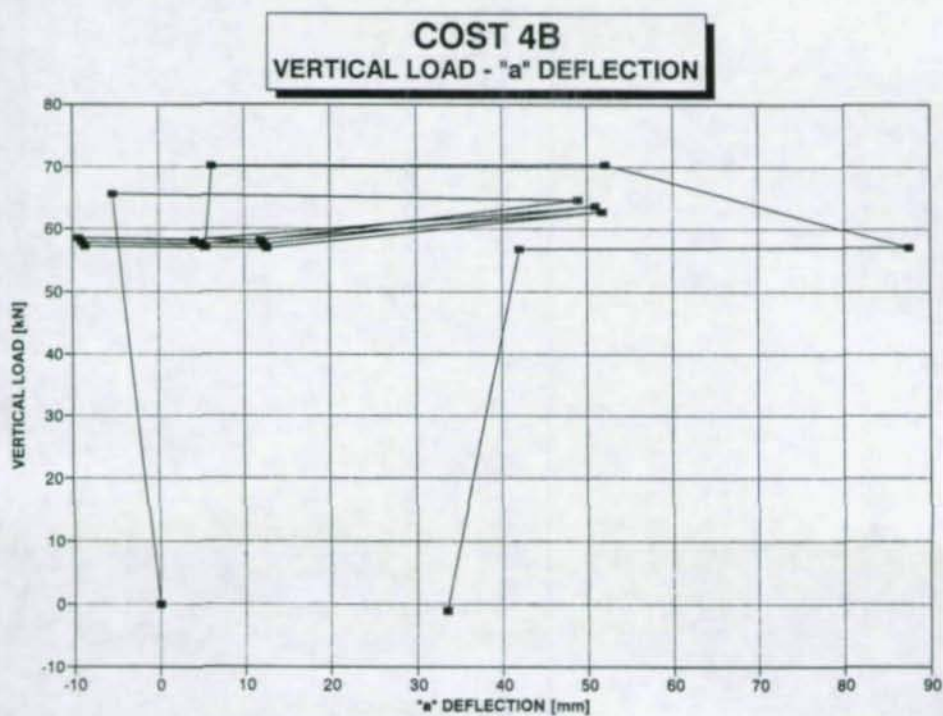


*Fig. 13 Vertical load - deflection curve*

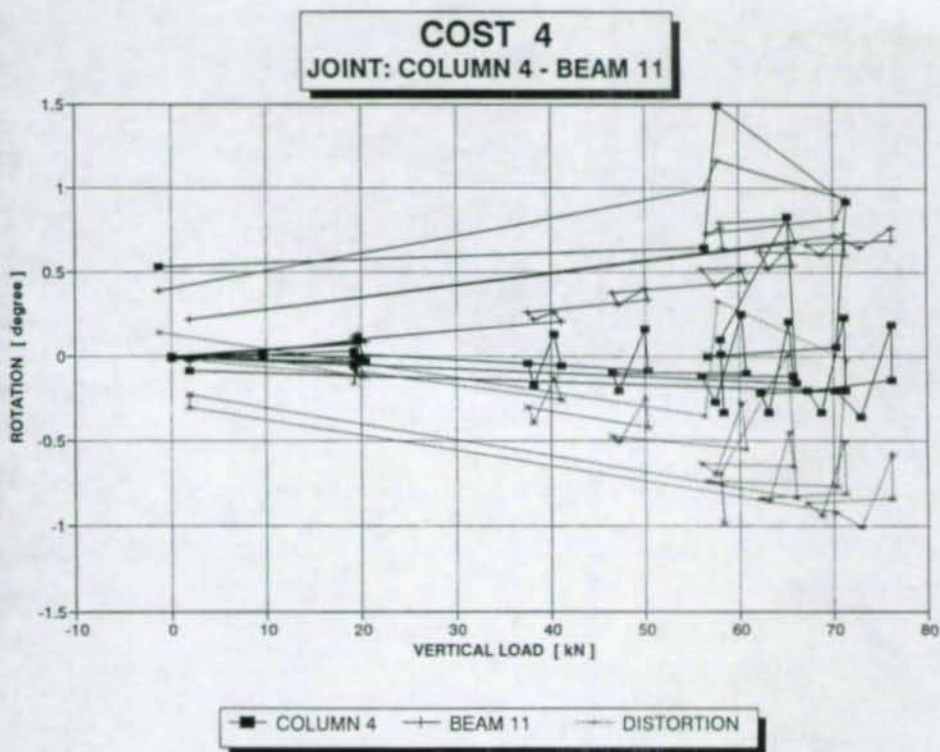


*Fig. 14 Vertical load - rotation curves*

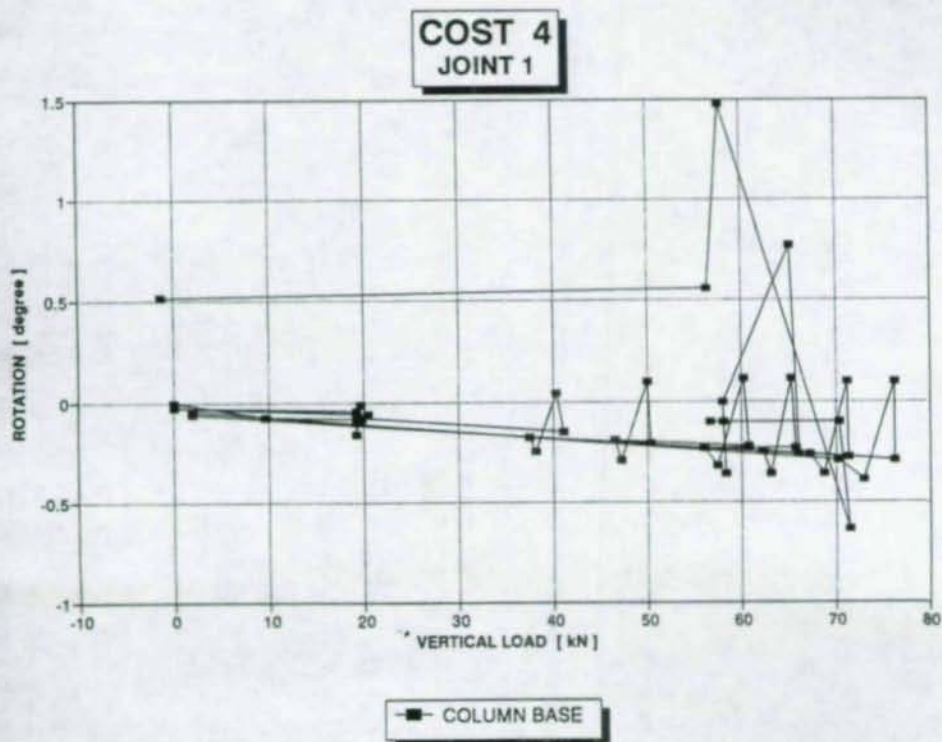


*Fig. 15 Vertical load - rotation curve*

### 3.2. Frames under variable repeated load

For frame COST 3B ( $\alpha=1$ ) the vertical load  $P$  - "a" deflection curve is presented in Fig. 8. Notation of "a" deflection can be seen in Fig. 3. The total vertical load produced by the hydraulic system is  $6xP$ .

The total horizontal load  $Px\alpha$  - "a" deflection curve is presented in Fig. 9.

Load-relative rotation curves of Joint: C4 - B11 are given in Fig. 10, and load-relative rotation of Joint 1 at column bases are drawn in Fig. 11.

At load level ( $P=65.1$  kN), substantial horizontal deflection was observed, at the Joint B12 a bolt was cracked.

For frame COST 4A ( $\alpha=0.16$ ) the vertical load  $P$  - "a" deflection curve is presented in Fig. 12.

For frame COST 4B ( $\alpha=1$ ) the vertical load  $P$  - "a" deflection curve is presented in Fig. 13.

Total load relative rotation curves of Joint: C4 - B11 are given in Fig. 14, and load relative rotation of Joint 1 at column bases are drawn in Fig. 15.

At load level ( $P=71$  kN), substantial horizontal deflection was observed, at the Joint B12 two bolts were cracked.

## 4. CONCLUSIONS

As part of an extensive experimental study into the behaviour of semi-rigid connections, three full-scale, three-dimensional multi-storey frames have been tested. This paper presents a brief overview of the features of the experimental set-up and briefly explains how the complexities arising from the three-dimensional nature of the tests were addressed.

In the course of this experimental study

- full scale tests were carried out
- in a complex way.

The quality of the collected experimental data has justified the effort which was expended in addressing the experimental complexities.

## REFERENCES

- PENSERINI P - COLSON A., 1989., Ultimate limit strength of column-base connections, *Journal of Constructional Steel Research*, 14, pp. 301-320.
- HALÁSZ O. - IVÁNYI M., 1979., Tests with simple elastic-plastic frames, *Periodica Polytechnica, Civil Engineering*, Vol. 23. No. 3-4. pp. 151-182.

# INFLUENCE OF STRUCTURAL FRAME BEHAVIOUR ON JOINT DESIGN

Stephane GUISSSE ( 1 )

Jean-Pierre JASPART ( 2 )

## Abstract

Joints between H or I hot-rolled sections are subjected to internal forces induced by the connected members. The interaction between these forces can lead to a substantial reduction of the joint design resistance. Annex J of Eurocode 3 has been recently revised and, on the basis of theoretical models developed in Liege, the design rules for web panels have been modified to take those effects into account. Those new rules have been recently compared in Liege with new numerical simulations and experimental tests.

The aim of this paper is first to present briefly the modifications introduced in the Annex J of Eurocode 3 and related to the interaction of internal forces, and then to show the main conclusions that can actually be drawn from the comparisons with new numerical simulations and experimental tests.

## 1. INTRODUCTION

The department M.S.M. of the University of Liege is studying since several years at the semi-rigid response of structural joints and building frames. Since two years, a three years COST project funded by the Walloon Region of Belgium has started; it is aimed at investigating some different specific topics, related to the semi-rigid concept. The present paper concerns one of them.

It is well known that the joint behaviour has a major influence on the frame response. On the opposite side, the interaction between the forces acting in the connected members influences, generally in a negative way, the joint design resistance.

---

(1) Assistant, Department MSM, University of Liège, Quai Banning 6, 4000 LIEGE, BELGIUM

(2) Research Associate, Dr, Idem.

Annex J of Eurocode 3 (CEN / TC 250, 1994) has been recently revised to take those effects into account by means of some different reduction factors. One of the aims of the COST research project is to check again and possibly improve the expression of these last ones.

## 2. EFFECTS OF INTERNAL FORCES ON JOINT DESIGN RESISTANCE

### 2.1. WEB PANEL DESIGN RESISTANCE

In a strong axis joint between H or I hot-rolled sections, the collapse of the column web panel can result from two different modes: shear yielding or local yielding under the tension or compression forces carried over from the beam to the column by the connection (also called *load-introduction collapse*). For slender webs, a third mode (web buckling or web crippling) can also be observed.

For a given joint, the collapse mode of the web panel depends on its external loading; this is illustrated in figure 1 where the ratio  $\eta$  between the left and right loads,  $P_l$  and  $P_r$ , varies from 0 to 1. Figure 1 corresponds to a joint with a web of low slenderness, so, not likely to buckle.

The ratio  $\eta$  is the one between the two bending moments induced by the beams on each side of the column. When it is close to *zero*, the web panel is subjected to high shear forces what leads to a shear collapse. A ratio close from *one* means that the joint is symmetrically loaded; in this case, the collapse can only result from load-introduction yielding (web buckling or crippling is also possible for more slender webs)

In the joint web panel, three kinds of stresses are acting together:

- shear stresses  $\tau$ ;
- longitudinal stresses  $\sigma_n$  due to normal force and bending moment in the column;
- transverse stresses  $\sigma_t$  due to load-introduction (local effect).

The interactions between these stresses have different effects on the joint resistance:

- longitudinal stresses  $\sigma_n$  decrease the shear resistance;
- shear stresses  $\tau$  decrease the load-introduction resistance;
- longitudinal stresses  $\sigma_n$  may decrease the load-introduction resistance (compression zone).

If the last kind of interactions is known for several years, the two first ones were not taken into account by the rules of the old version of Eurocode 3 Annex J (Eurocode 3, 1992). They have been pointed out by JASPART (Jaspart, 1991). The unsafe

character of the previous Annex J, compared to the JASPART model, is represented by the hachured zone of figure 1.

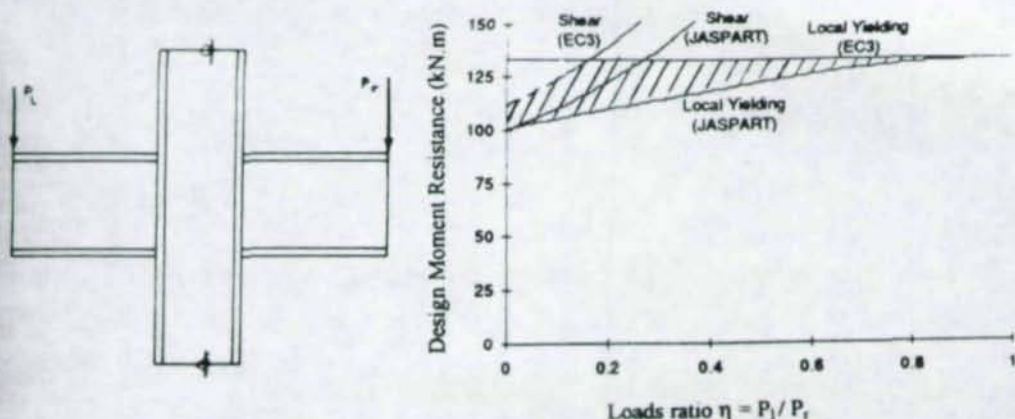


figure 1 - Variation of web panel resistance according to the external loading

Annex J has been recently completely revised: the rules concerning the web panel design resistance have been modified according to JASPART's proposals (Jaspart, 1991). The first modification concerns the shear resistance,  $V_{wc,Rd}$ . The influence of the longitudinal stresses  $\sigma_n$  has been simply taken into account with a constant reduction factor equal to 0,9:

$$V_{wc,Rd} = 0,9 \frac{A_{v,c} \cdot f_{ywc}}{\gamma_{m0} \cdot \sqrt{3}} \quad (1)$$

$A_{v,c}$  is the shear area of the profile,  $f_{ywc}$  the yield stress and  $\gamma_{m0}$  the partial safety factor. The second modification consists in a reduction of the design resistance  $F_{wc,Rd}$  of the column web in tension or compression (equation 2), due to the possible presence of shear stresses, by means of a reduction factor  $\rho$ :

$$F_{wc,Rd} = \rho \frac{f_{ywc} \cdot t_{wc} \cdot b_{eff}}{\gamma_{m0}} \quad (2)$$

$$\text{with } \rho = \begin{cases} \rho_1 = \frac{1}{\sqrt{1 + 1,3 \cdot \left(\frac{b_{eff} \cdot t_{wc}}{A_{v,c}}\right)^2}} & \text{if } \eta = 0 \\ \rho_1 + (1 - \rho_1) \cdot 2 \cdot \eta & \text{if } 0 < \eta < 0,5 \\ 1 & \text{if } 0,5 \leq \eta \leq 1 \end{cases} \quad (3)$$

$t_{wc}$  is the web thickness and  $b_{eff}$  is the effective yielding length. This last parameter depends on the connection details. Equation (3), represented by two lines, is a simplification of the initial JASPART's proposal. The difference between the two approaches is illustrated in figure 2.

The effect of the longitudinal stresses  $\sigma_n$  on the resistance of the column web in compression is taken into account by means of an other reduction factor,  $k_{wc}$  (equation 4), that was already existing in the old Annex J (Zoetemeijer, 1975) :

$$k_{wc} = 1,25 - 0,5 \frac{\sigma_{n,Ed}}{f_{ywc}} \leq 1 \quad (4)$$

$\sigma_{n,Ed}$  is the normal stress in the column web, at the root of the fillet or of the weld, due to longitudinal force and bending moment. The minimum value of  $k_{wc}$  is 0,75 (when  $\sigma_{n,Ed}$  is equal to  $f_{ywc}$ ).  $k_{wc}$  covers the possible buckling of the web panel under the combined action of the  $\sigma_t$  and  $\sigma_n$  compression stresses.

Finally, the last modification introduced in Annex J concerning web panel is the extension of the design rules to slender webs ( $\bar{\lambda} > 0,673$ ) by limiting the design resistance, given in equation 2 to the buckling resistance value of the web:

$$F_{wc,Rd} = \rho \frac{f_{ywc} \cdot t_{wc} \cdot b_{eff}}{\gamma_{m0}} \quad \text{if } \bar{\lambda} \leq 0,673$$

$$F_{wc,Rd} = \rho \frac{f_{ywc} \cdot t_{wc} \cdot b_{eff}}{\gamma_{m0}} \cdot \left[ \frac{1}{\bar{\lambda}} \cdot \left( 1 - \frac{0,22}{\bar{\lambda}} \right) \right] \quad \text{if } \bar{\lambda} > 0,673 \quad (5)$$

$$\text{with } \bar{\lambda} = 0,93 \sqrt{\frac{b_{eff} \cdot d_c \cdot f_{ywc}}{E \cdot t_{wc}^2}}$$

$d_c$  is the clear depth of the column web,  $E$  the Young modulus and the other parameters are given here above.

Equations 1 to 5 are discussed in the present paper on the basis of comparisons with numerical simulations (section 3) and experimental tests (section 5).

## 2.2. COLUMN FLANGE DESIGN RESISTANCE IN BOLTED JOINTS.

In bolted joints (with flush or extended endplates, flange cleats), the column flange is subjected to transverse forces. The design resistance of this component, given in Annex J of Eurocode 3 - it was already in the old Annex J -, is reduced because of possible high longitudinal stresses  $\sigma_{com,Ed}$  ( $> 180$  MPa) in the column flange by means of a reduction factor  $k_{fc}$  (Zoetemeijer, 1975) equal to :

$$k_{fc} = \frac{2 \cdot f_{y,fc} - 180 - \sigma_{com,Ed}}{2 \cdot f_{y,fc} - 360} \leq 1 \quad (6)$$

$f_{y,fc}$  is the yield stress of the column flange.

### 3. NUMERICAL SIMULATIONS

A large set of numerical simulations have been performed in Liege with the non linear finite element program FINELG (Finelg, 1994). This software is developed in Liege since several years. It is able to simulate the behaviour of structures until collapse and to take into account various phenomena such as non linear mechanical properties, second order effects, residual stresses, initial imperfections...

The welded joints have been modelled with shell elements (figure 2). These numerical 3D simulations, based on the geometry of experimental tests performed some years ago in INNSBRUCK (Klein, 1985), provide very interesting informations such as strains and stresses anywhere in the joint, or global behaviour curves which allow direct comparisons with the theoretical models of JASPART and Eurocode 3 revised Annex J.

More than hundred simulations of welded joints have been performed in order to

investigate the effect of the following parameters: dimensions of the joint (three different geometries have been considered), loading, steel grade, effect of strain-hardening and effect of the initial imperfection of the column web.

But the two main parameters of this parametrical study were the loading factors  $\eta$  (figure 1) and the ratio  $\beta$  between the normal force in the column and its squash load.

Figure 3 illustrates the evolution of the joint design resistance versus the loading ratio  $\eta$ . The graph has an extremum at about  $\eta=0.7$  and its shape is different from both the theoretical prediction of the new Annex J, and the analytical model developed by JASPART. Despite these differences, the agreement between the models and the numerical simulations can be considered as good.

The effect of a normal force in the column on the joint behaviour (represented by the value of  $\beta$ , see above) has also been considered for some joint configurations, either symmetrically loaded ( $\eta=1$ ) or just loaded on one side ( $\eta=0$ ). Generally, the agreement between equation (4), though as very simple, and the numerical simulations is good. However, some joint configurations lead to a higher difference

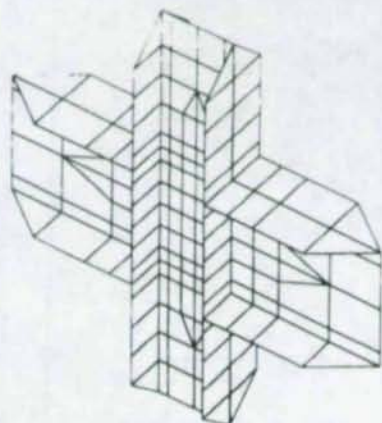


figure 2 - Discretisation of welded joints.

between the numerical results and the theoretical rules. In particular, the steel grade seems to have a great influence on the normal force effect: figure 4 shows that more the steel resistance is high, more the Eurocode rule is accurate.

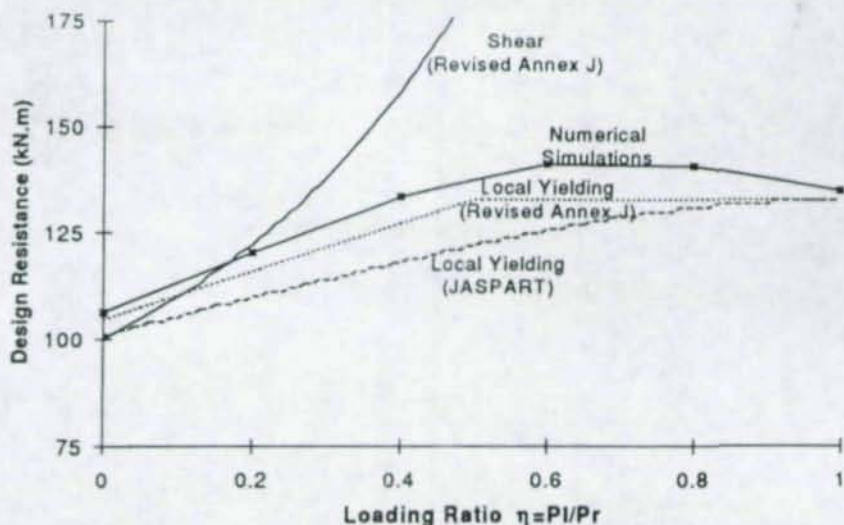


figure 3 - Variation of the joint resistance with the loading ratio  $\eta$ .

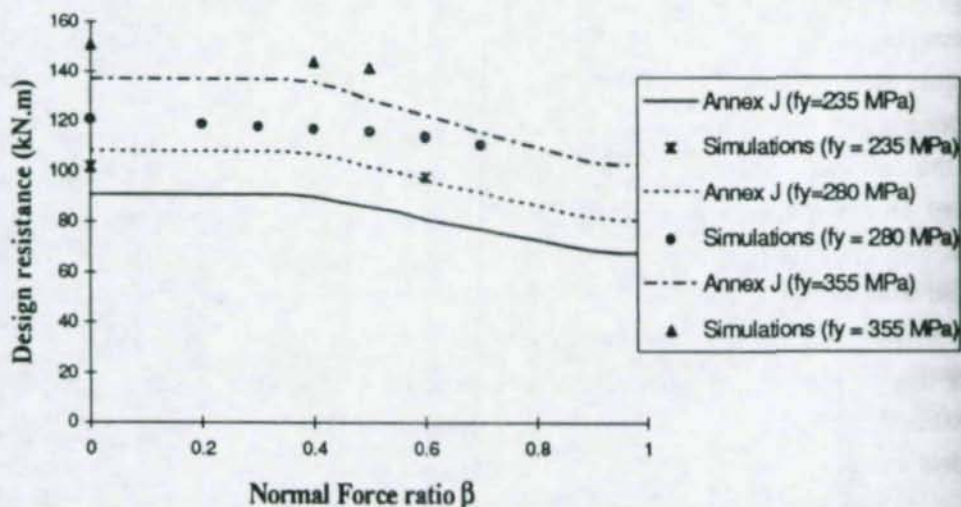


figure 4 - Example of the variation of the joint resistance with the normal force in the column and the steel grade. Cruciform joint ( $\eta=1$ ).

#### 4. NEW THEORETICAL MODEL

In order to understand the shape of the curve got by the numerical simulations in figure 3, a new theoretical model has been developed, inspired by ROBERTS and JOHANSSON theories (Roberts, 1991): the column flange connected to the beam is considered as a rigid-plastic beam lying on a rigid-plastic support (the column web). The new model reproduces precisely the results of the numerical simulations. The comparison of the model with the experimental results is actually in progress. It will be presented in a next paper.

#### 5. EXPERIMENTAL TESTS

Recently, 24 experimental tests on joints have been performed at the University of Liege. 16 of them were welded joints while the others were bolted ones, with flush endplates. The results of tests on bolted joints are not reported in this paper.

Two different welded joint configurations (same beams, same columns) have been tested experimentally. The first one is dedicated to the study of the shear stresses effect. Its generic name is « WS » (as Welded and Shear). It is represented in figure 5. The second is aimed at testing the effect of the normal force in the column; it is called WN (as Normal force). For the first one, the only parameter is the ratio  $\eta$  between the forces applied on the left and right beams.

Experimental tests provide a lot of different informations. In particular, figure 6 shows the complete  $M-\phi$  curves for six of the eight WS tests. The joint design resistance is different from the ultimate one: the first one is calculated by neglecting the strain-hardening in the joint. If the ultimate resistance can be identified as « the top » of the  $M-\phi$  curve, the design one is much more difficult to determine precisely. The procedure used in this paper is derived from the stiffness model of the revised Annex J (see related paper in these proceedings): the design resistance is identified as the intersection point between the actual  $M-\phi$  curve and a straight line characterised by a slope equal to the third of the initial stiffness of the curves. This last value is almost

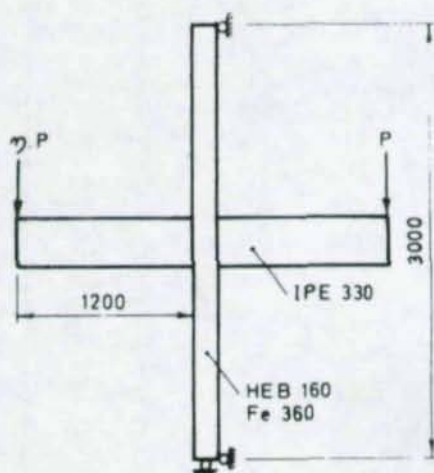


figure 5 - Example of test configuration.

the same for each test (see figure 6). The number contained in the test name is equal to ten times the ratio  $\eta$  between the left and right forces. For example, WS2 is a test characterised by a ratio  $\eta$  of 0,2.

Moment (kN.m)

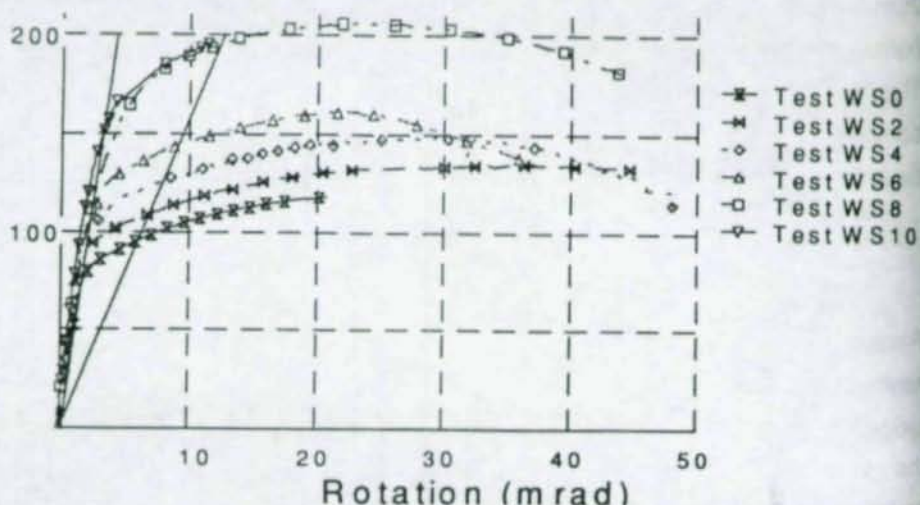


figure 6 - Results of WS tests ( $M-\phi$  curves).

Figure 7 gives a comparison between the experimental design resistance for the WS tests, derived as described here above, and the prediction according Eurocode 3.

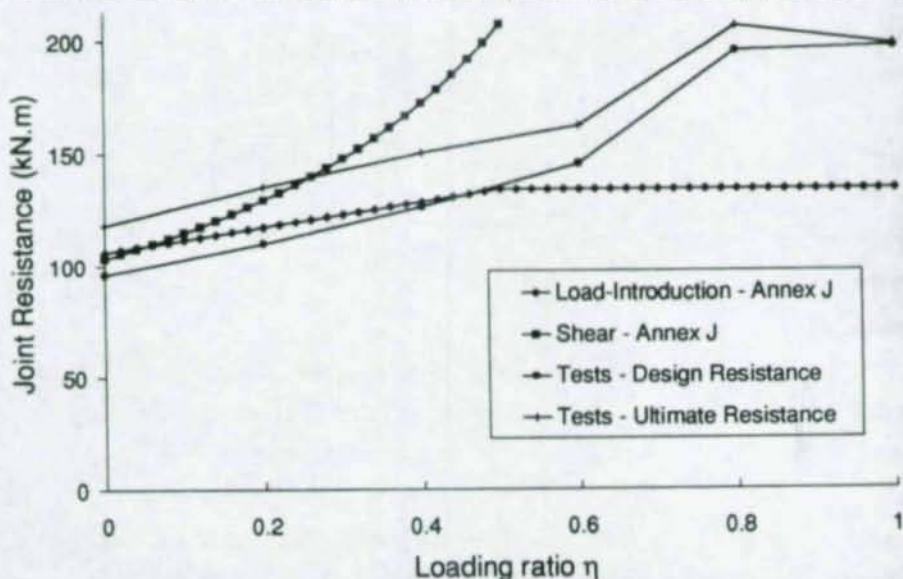


figure 7 - Comparison between WS tests results and Annex J of Eurocode 3.

The shape of the variation of the design resistance with the loading ratio is almost the same than the one observed for the numerical simulations (figure 3). The

theoretical values have been calculated on the basis of the actual yield stresses, of dimensions measured in laboratory and of a partial safety factor equal to 1.

While the theoretical predictions can be considered as very good for small and intermediate values of  $\eta$ , they seem to be too safe for the symmetrically loaded joints. Such a difference between tests and Annex J rules have never been observed before; some investigations are actually in progress to explain this difference.

On an other hand, the design resistances of WS8 and WS10 tests are almost equal to the ultimate ones. This can be explained by the fact that the column web buckles as soon as it has been crushed.

For WN tests, the length of the column is smaller to avoid any buckling problem, due to the high compression force. The tests are realised in two steps: first, the normal force is progressively applied to the column until the nominal value; after, the loads on the beams are increased until the joint collapse while the normal force in the column is kept constant.

Figure 8 shows a comparison between the results of the WN tests and the Annex J rules (equation 4). Four of the 8 tests, called WN S, were symmetrically loaded whilst the other ones were completely unbalanced ( $\eta=0$ ). For one of these four last tests, some experimental problems have been observed; so, it is not reported here.

The number contained in the test name is here relative to ten times the nominal ratio  $\beta$ , between the normal force in the column and its squash load. For example, the test WN5 S is a test characterised by a ratio  $\beta$  of almost 0,5 and symmetrically loaded.

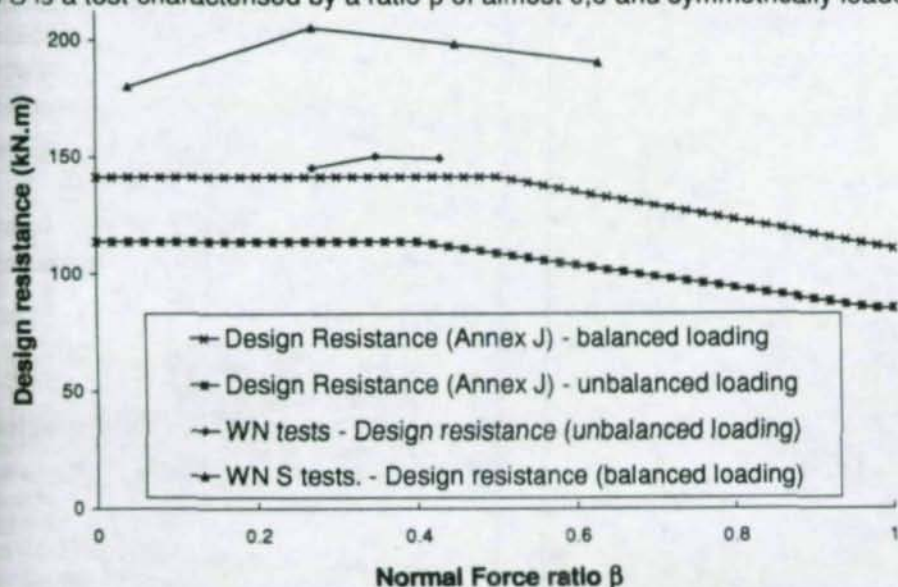


figure 8 - Comparison between results of WN tests and Eurocode 3 Annex J.

The normal force in the column seems to have no effect on the joint resistance despite the substantial value of the normal force applied. This one is limited by the

buckling of the column, as well for the tests than in the reality. The rules of the Eurocode 3 revised Annex J are conservative, especially for the symmetrically loaded joints. With regard to both the results of the numerical simulations (figure 4) and of the experimental results (figure 6), equation (4) can be considered as overconservative.

## 6. CONCLUSIONS

Considering either the results of numerical simulations or the experimental tests, the modifications of the design rules of annex J of Eurocode 3 appear to be really pertinent, tough as too safe in some circumstances.

Anyway, the effect of stress interactions, pointed out by JASPART a few years ago, is confirmed by the two different approaches.

Further improvements are actually in progress.

## 7. REFERENCES

- CEN / TC 250, 1994, New Revised Annex J of Eurocode 3 : Part 1.1, CEN document N419 E.
- EUROCODE 3, 1992, Design of Steel Structures, Part 1.1 : General Rules for Buildings, European Prestandard, ENV 1993-1-1, February 1992.
- FINELG, 1994, Non Linear Finite Element Analysis Program, Version 6.2, User's Manual, Department MSM, University of Liège, BEG Design Office.
- JASPART, 1991, Etude de la semi-rigidité des noeuds poutre-colonne et son influence sur la résistance et la stabilité des ossatures en acier, Ph.D. Thesis, Department MSM, University of Liège.
- KLEIN, 1985, Das elastisch-plastische Last-Verformung verhalten Mb- $\theta$  steifenloser, geschweißter Knoten für die Berechnung von Stahlrahmen mit HEB-Stützen. Dr Dissertation, Univ. Innsbruck.
- ROBERTS - ROCKEY, 1979, A mechanism solution for predicting the collapse loads of slender plate girder when subjected to in-plane patch loading. Proc. Instn Civ. Engrs Part 2, pp 155-175.
- ZOETEMEIJER, 1975, Influence of normal-, bending- and shear stresses in the web of European rolled sections. Report N° 6-75-18, Stevin Laboratory, Delft University of Technology.

# RELIABILITY OF STEEL STRUCTURES WITH SEMI-RIGID CONNECTIONS

A. Sellier<sup>1</sup>

A. Mébarki<sup>2</sup>

A. Colson<sup>3</sup>

R. Bjorhovde<sup>4</sup>

## Abstract

The paper presents a reliability assessment of a beam supported by two semi-rigid (Type PR) connections. The beam and the connections were designed in accordance with Eurocode 3, using beam cross sections satisfying the criteria for classes 1,2,3 and 4 (corresponding to US criteria for plastic design (PD), compact, compact, non compact and slender). Mechanical and cross sectional properties have been treated as random variables, as have the ultimate moment capacity, the initial stiffness, and the coefficient defining the shape of the  $M-\phi$  curve for the connections. Dead and live load are also random variables. Structural reliability is expressed in terms of probabilities of failure and reliability indices. The results of sensitivity studies for the structure are presented, including means and variances of the connections features.

## 1. STRUCTURAL RELIABILITY ASSESSMENT

### 1.1 Evaluation of the probability of failure and reliability index

Figure 1 defines the random structural parameters and the random operating space, in which the subspace  $D_f$  is the failure domain shown in Fig 2.

<sup>1</sup> Assistant Professor, Laboratoire de Mécanique et Technologie (LMT), Ecole Normale Supérieure de Cachan /CNRS /Université Paris 6, France

<sup>2</sup> Associate Professor, Laboratoire de Mécanique et Technologie (LMT), ENS Cachan/CNRS/Université Paris 6, Cachan, France

<sup>3</sup> Professor and Director, Ecole Nationale Supérieure des Arts et Industries de Strasbourg, Strasbourg, France

<sup>4</sup> Professor and Chairman, Departement of Civil and Environmental Engineering, University of Pittsburgh, Pittsburgh, Pennsylvania, USA

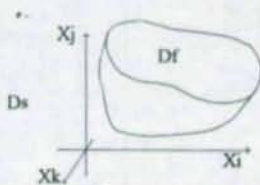
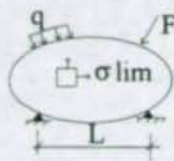


Figure 1- Structural parameters      Figure 2- Operating space and the failure domain  $D_f$

The probability of failure  $P_f$  is defined as follows:

$$P_f = P(q > q_{lim}(s_{lim}, L, F)) = P(X \in D_f) = P(E(X) \leq 0) \quad (1)$$

where  $E(\cdot)$  defines the limit state function associated with the ultimate limit state under study. The failure indicator is defined by:

$$\begin{cases} 1_{D_f}(X) = 1 & \text{si } E(X) \leq 0 \\ 1_{D_f}(X) = 0 & \text{si } E(X) > 0 \end{cases} \quad (2)$$

so that the failure probability appears as the probability that the random vector  $X$  (random structural parameters) belongs to the failure domain  $D_f$ :

$$P_f = \int_{R^n} 1_{D_f}(x) f_X(x) dx \quad (3)$$

where  $f_X(x)$  is the probability density function of the random vector  $X$ . As the probability of failure for ultimate limit states is very small ( $10^{-6}$  to  $10^{-4}$ ), an adequate and efficient method which is based on a combination of the conditioning techniques and importance sampling requiring Monte Carlo simulations, has been used (Sellier and Mebarki, 1993).

This method requires two steps, as follows:

1 The first step transforms, through the Rosenblatt transformation, the basic random variables,  $X$ , into standardized and independent gaussian variables denoted  $U$ . In this standardized operating  $U$ -space, the reliability index  $\beta$  is also the euclidian distance  $OP^*$  where  $O$  is the origin of the  $U$ -space and  $P^*$  is the nearest point on the limit state surface to the origin  $O$ , as illustrated in Fig. 3.

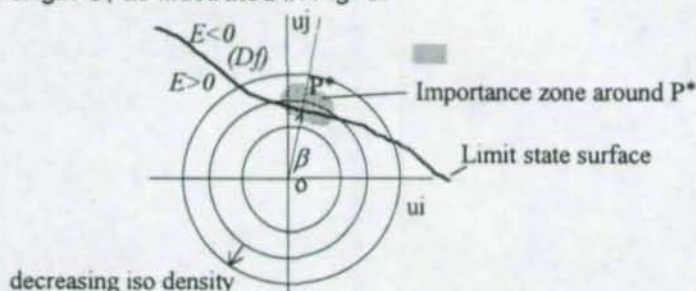


Figure 3- Design point  $P^*$  in the standardized  $U$ -space

$$\begin{cases} OP^* = \min(\|U\|) = \beta \\ \text{with : } E(H^{-1}(U)) = 0 \end{cases} \quad (4)$$

Mazzolani et al (1993) have demonstrated that the importance zone, on Pf, is a restricted area located around the design point P\*.

2 The Monte Carlo simulations are performed with an importance sampling around P\*.

The importance and conditioned sampling requires then the evaluation of two terms in order to reduce the number of required simulations (Mazzolani et al, 1993).

$$\begin{aligned} pf &= p1 \times p2 \text{ (conditioning)} \\ \text{with: } p1 &= p(u \in H(Df) / u \in B_n^c(\beta)) \\ \text{Denoting: } \hat{u} &= (u \in B_n^c(\beta)), \quad p1 = p(\hat{u} \in H(Df)) \end{aligned} \quad (5)$$

$B_n^c$  is the complementary subspace to the hypersphere centred on O and tangent to Df at P\*, as indicated in Fig. 3.

P2 is the conditioning probability. It is determined analytically, thus reducing the required number of simulations. The importance sampling is in fact used to evaluate P1. The probability density function,  $f_{\hat{u}}(\hat{u})$ , used for the importance sampling around P\* is different from the initial probability density function  $f_u(\hat{u})$ :

$$\begin{aligned} p1 &= \int_{R^*} 1_{(\hat{u} \in H(Df))} f_u(\hat{u}) d\hat{u} \\ p1 &= \int_{R^*} (1_{(\hat{u} \in H(Df))} \frac{f_{\hat{u}}(\hat{u})}{f_u(\hat{u})}) f_u(\hat{u}) d\hat{u} \end{aligned} \quad (6)$$

$f_{\hat{u}}(\hat{u})$  depends on P\* coordinates.

P1 is determined numerically, for a total number Nsim of simulations

$$\hat{p}1 = \frac{1}{n\text{sim}} \sum_{i=1}^{n\text{sim}} 1_{(\hat{u}_i \in H(Df))} \frac{f_{\hat{u}}(\hat{u}_i)}{f_u(\hat{u}_i)} \quad (7)$$

$$p2 = p(\tilde{u} \in B_n^c(\beta)) \quad (8)$$

where  $1_{(\hat{u}_i \in H(Df))} \frac{f_{\hat{u}}(\hat{u}_i)}{f_u(\hat{u}_i)}$  = failure indicator, P2 is calculated analytically. The failure probability is then  $Pf = \hat{p}1 \times p2$ , [4]. Once the design point P\* is located, the probability of failure is calculated with a reduced number of additional simulations, i.e. less than 100 simulations even for small values of the probabilities of the order ( $10^{-6}$  to  $10^{-4}$ ).

## 1.2 Structure under Study

The structure under study, is shown in Fig. 4. It has been designed for a bending moment equal to  $pl^2/16$ . The steel beam is an IPE 270 (W 10.26).

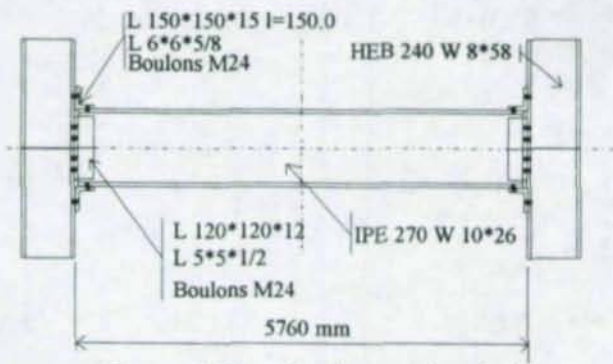


Figure 4- The structure under study

The mean values and the standard deviations adopted for the distributions of the applied loads are derived from the characteristic values. For this purpose, the characteristic values are in accordance with ISO 2394, which requires two conditions:

- 1 The occurrence probability of the characteristic value,  $Q_k$ , for a reference period equal to 50 years, should not exceed 25%. It is usually taken as 15%
- 2- The occurrence probability of  $(1.4 Q_k)$  should not exceed 1.25%, for the same reference period.

The first condition leads to the definition of a return period, for  $Q_k$ , of 307 years:

$$T = -50 / \ln(1 - 0.15) = -nt / \ln(1 - pnt) = 307 \text{ years}$$

$$p(q > q_k) = 0.15$$

$$p(q > 1.4 * q_k) = 0.0125$$

These two conditions give, for a type 1 extreme distribution:

$$F_x(x) = P(X < x) = \exp(-\exp(-\frac{x-u}{\alpha}))$$

with

$$\bar{x} = u + 0.5772\alpha$$

$$\bar{\bar{x}} = 1.2825\alpha$$

The coefficient of variation becomes 24%, which is usually adopted for live loads. It seems, too large for the dead loads, for which a coefficient of variation of 10% is used. The probability of exceedance of the characteristic value is usually equal to 5%. A gaussian distribution is generally adopted leading to:

$$x_k = \bar{x}(1 + 1.645 \times 0.1)$$

## 1.3 Limit states under study

For the beam, four cross-sectional types of limit states are considered, in accordance with internationally accepted criteria (AISC, 1986,1994, CSA, 1989, Eurocode 3, 1992). For ease of reference, the eurocode provisions are used here, as follows:

- Class 1** The same designation is used in the Canadian code (CSA, 1989); the American code refers to this as a *plastic design shape (PD)* (AISC, 1986,1994). The cross section is capable of reaching the full plastic moment and to rotate plastically a significant amount (6 to 8 times the rotation when the plastic moment is first reached). Local buckling does not occur until the large rotation has taken place.
- Class 2** The same designation is used in the Canadian code (CSA, 1989); the American code refers to this as a *compact shape* (AISC, 1986,1994). The cross section is capable of reaching the full plastic moment and to rotate plastically an amount of at least 3 times the rotation when the plastic moment is first reached before local buckling occurs.
- Class 3** The same designation is used in the Canadian code (CSA, 1989); the American code refers to this as a *non compact shape* (AISC, 1986, 1994). The cross section is capable of reaching the yield moment, inelastic rotations are small.
- Class 4** The same designation is used in the Canadian code (CSA, 1989); The American code refers to this as a *slender shape* (AISC, 1986, 1994). The cross section fails in elastic local buckling.

The ultimate states and ultimate curvatures for each class are illustrated in Fig 5.

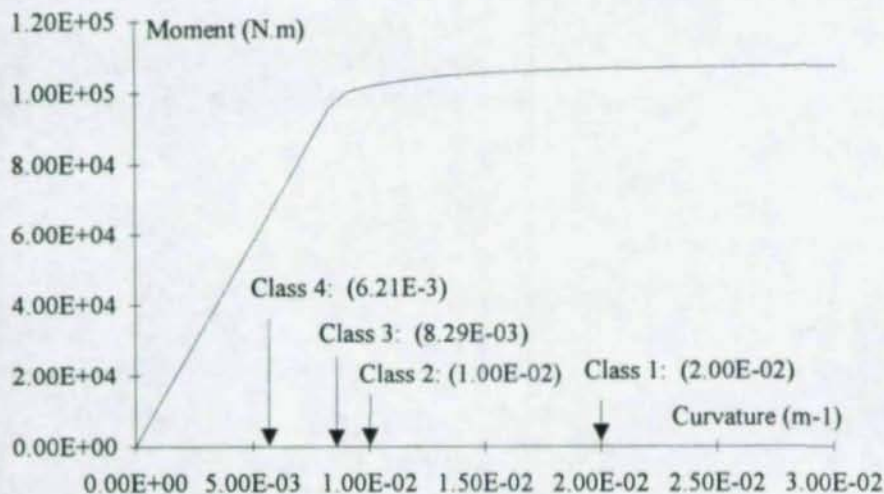


Figure 5 Behaviour of the Beam Adopted to Define the Various Limit States

Figure 6 shows the moment rotation behaviour of a semi rigid connection compared to the EC3-defined beam diagram. Non-dimensional moments and rotations are used, with:

$$\bar{m} = M / M_p = \text{non dimensional moment}$$

$$\bar{\phi} = (Elb\phi) / (LbMp) = \text{non-dimensional rotation}$$

where  $M$  is the connection moment,  $M_p$  is the fully plastic moment,  $Elb$  is the bending stiffness of the beam cross section,  $\phi$  is the actual rotation, and  $Lb$  is the beam span.

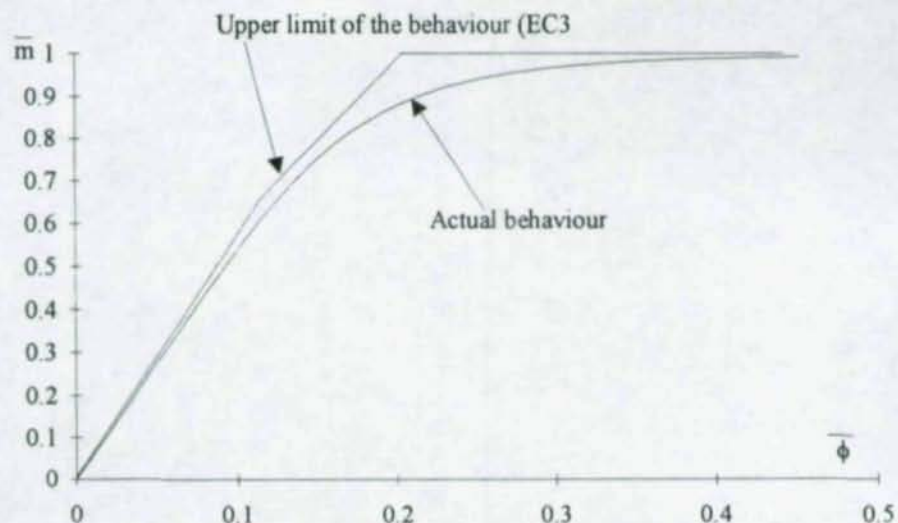


Figure 6- Semi-rigid Connections Behaviour

The mean value of the plastic moment is set equal to 0.101 MN.m, this corresponds to the ultimate curvature for a class 2 section. The semi-rigid connections are in accordance with the definition suggested by Eurocode 3 while their actual behaviour is located below those suggested by EC3. The connections and the beam correspond to an unbraced structure requiring a reduced value of the connection rigidity. The mean values of the connection characteristics are indicated in Table 1.

Table 1- Connections Characteristics

	Class 1	Class 2	Class 3	Class 4
Ultimate bending moment (N.m)	112000.	112000.	101000.	75500.
Initial rigidity (Nm/rd)	1.1E+07	1.1E+07.	1.1e+07	1.1E+07
Curvature (m <sup>-1</sup> )	4.	4.	4.	4.

Mean values of the moment-rotation curves for classes 1 through 4 are shown in Fig 7, along with the elastic beam lines for beams of classes 2 though 4.

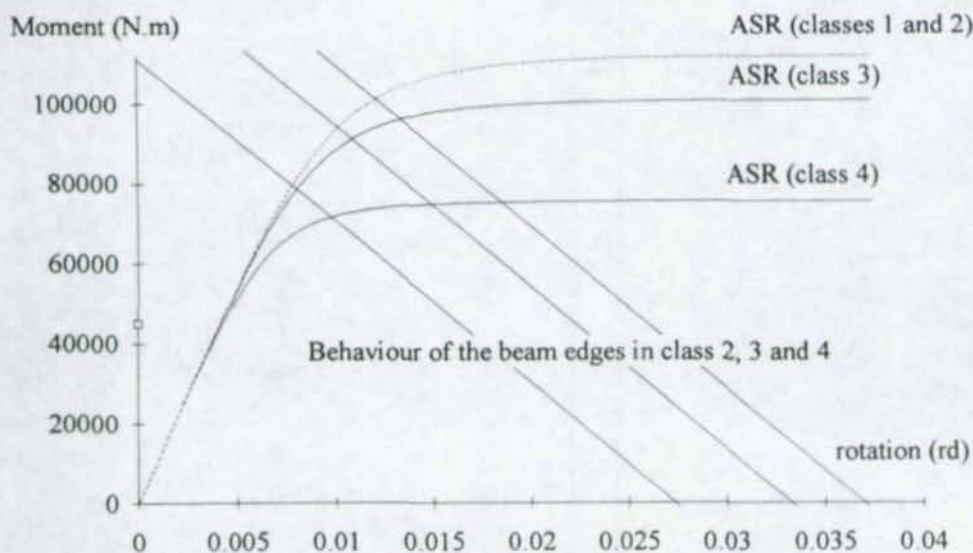


Figure 7- Mean properties of beams and semi-rigid connections.

The basic random variables are indicated in Fig 8. It is emphasized that the properties of the connections at each end of the beam in general are different.

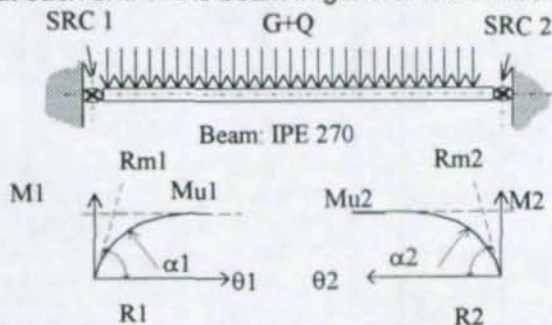


Figure 8- Basic Random Variables for the Semi-Rigid Connections

The two connections for the beam are designated SRC1 and SRC2. Their characteristic properties are:

SRC1 ultimate bending capacity =  $Mu1$   
 initial Stiffness =  $R1$   
 Non linear M-f curve coefficient =  $\alpha1$

SRC2 ultimate bending capacity =  $Mu2$   
 initial Stiffness =  $R2$   
 Non linear M-f curve coefficient =  $\alpha2$

The Dead load is given by the term G and live load is Q.

The coefficient of variations related to the SRC parameters have been reported by Bjorhovde *et al* (1988, 1992); their values are given in Table 2.

Table 2- Coefficient of Variation of Connection Parameters

Variable	Coefficient of variation
Ultimate moment capacity	18%
Initial stiffness	25%
Coefficient $\alpha$	15%

The design values of the loads and the load combinations are shown in Table 3.

Table 3- Design values of the loads and their combinations

Limit state	Gk (N/m)	Qk (N/m)	1.35Gk+1.5Qk (N/m)
Class 1	17543	17543	50000
Class 2	15690	15690	44690
Class 3	14209	14209	40498
Class 4	11023	11023	31416

The structural parameters values, corresponding to the various limit states under study, are given in Table 4.

Table 4- Structural parameters for the 4 limit states

	Random variable	Distribution	Class 1		Class 2		Class 3		Class 4	
			$\mu$	$\sigma$	$\mu$	$\sigma$	$\mu$	$\sigma$	$\mu$	$\sigma$
SRC 1	Mu1 (N.m)	Gaussian	112 000	20 160	112 000	20 160	101 000	18 180	75 500	13 590
	Rm1 (N.m/rd)	Gaussian	1.1 E7	2.75 E6						
	$\alpha_1$	Gaussian	4	0.6	4	0.6	4	0.6	4	0.6
SRC 2	Mu2 (N.m)	Gaussian	112 000	20 160	112 000	20 160	101 000	18 180	75 500	13 590
	Rm2 (N.m/rd)	Gaussian	1.1 E7	2.75 E6						
	$\alpha_2$	Gaussian	4	0.6	4	0.6	4	0.6	4	0.6
Loads	G (N)	Gaussian	15 034	1 503	13 479	1 348	12 207	1 221	9 470	947
	Q (N)	E1Max	14 108	3 508	12 649	3 145	11 455	2 848	8 886	2 209

where  $m$  = mean value and  $s$  = standard deviation.

#### 1.4 Reliability and Reliability index evaluation

The most likely mode of failure and the corresponding probability of occurrence (i.e the probability of failure) have been determined through the computational facility of the computer program STAT, in combination with the non linear finite element program EFICOS (Fléjou, 1994). Figure 9 gives a symbolic illustration of the procedure.

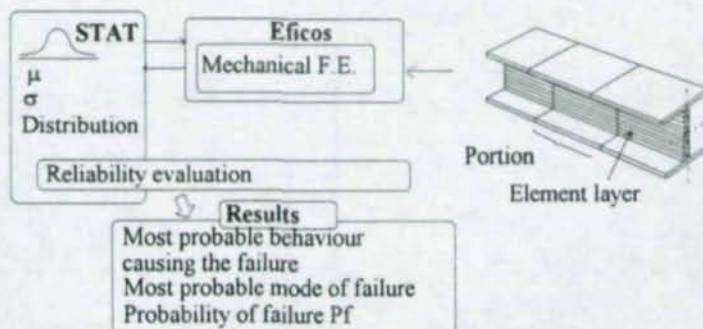


Figure 9- Computational Process for Reliability Assessment

## 2. RESULTS AND SENSITIVITY ANALYSIS

### 2.1 Limit state for the beam of Class 1

#### 2.1.1 Limit state surface

Fig.10 illustrates the limit state surface in the U-space where  $U_{(G+Q)}$  corresponds to the loads,  $U_{R_m}$  corresponds to the connections stiffness, and  $U_a$  addresses the coefficient  $a$  that defines the shape of the M-f curve for the semi rigid connection. The failure domain  $D_f$  is located above the limit state surface and the safety domain  $D_s$  is below. The origin  $O$  of the U-space corresponds to the mean values of the random variables ( $G$ ,  $Q$ ,  $R_m$ ,  $a$ ) and belongs to the safety domain.

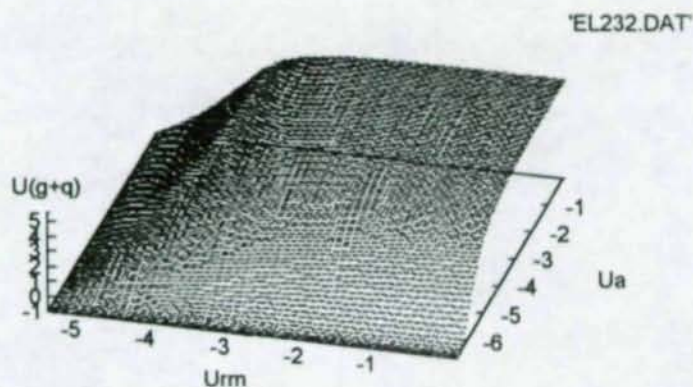


Figure 10- Shape of the Limit State Surface in the Standardized U-space

Fig

#### 2.1.2 Results Obtained with the Reference Data

The design point  $P^*$ , the reliability index and the probability of failure that are obtained are indicated in Table 5. The probability of failure obtained by Monte Carlo Simulations is given in Fig. 11.

Table 5- The design point coordinates and the probability of failure

SRC 1			SRC 2			Loads		$\beta$	Pf
$\mu_1$ (N.m)	$R_{m1}$ (N.m/rd)	$\alpha_1$	$\mu_2$ (N.m)	$R_{m2}$ (N.m/rd)	$\alpha_2$	G (N)	Q (N)		
112 000	3200	4	88 300	1.1 E7	4	15 800	19 000	4.58	0.8 E-5
$\sim \mu_{u1}$	$\sim R_{m1}$	$\sim \alpha_1$	$\sim \mu_{u2}$	$\sim R_{m2}$	$\sim \alpha_2$	$\sim \mu_G$	$\sim \mu_Q$		

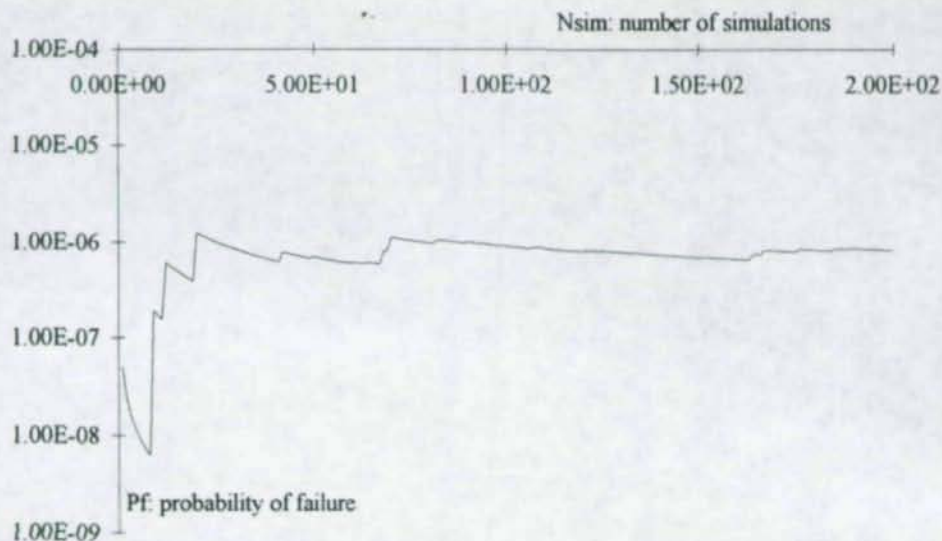


Figure 11- Probability of Failure vs. Number of Monte Carlo Simulations

The results show that the mode of failure corresponds to non symmetric behaviour of the two connections when:

- the rigidity of SRC 1 is small
- the plastic capacity of SRC 2 is small
- the loads take on values that are higher than the mean values.

The "optimal" design, from a reliability point of view, therefore requires lower values for the connections (rigidity and moment capacity), but higher values for the loads.

### 2.1.3 Sensitivity analysis

The reliability sensitivity to connection rigidity, its mean value or its standard deviation values has been evaluated, giving:

- the effect of the mean value, while the standard deviation remains constant, in Table 6
- the effect of the standard deviation, while the mean value remains constant, in Table 7.

The results indicate that:

- the mode of failure is non symmetric, regarding the behaviour of the connection, when the mean value of the rigidity is important. This is due to the fact that the failure corresponds to a small value of both the moment capacity and the rigidity.

Table 6- Reliability sensitivity to the mean value of the connections rigidity

$m_{Rm1} = m_{Rm2}$ (N.m/rd)	$\mu_{u1}$ (N.m)	$R_{m1}$ (N.m/rd)	$\alpha_1$	$\mu_{u2}$ (N.m)	$R_{m2}$ (N.m/rd)	$\alpha_2$	G (N)	Q (N)	$\beta$	Pf
2.8 E7	113 000	3 240	4	74 600	2.8 E7	4	15 600	17 700	4.57	0.6 E-5
	$\sim \mu_{u1}$	$\sim R_{m1}$	$\sim \alpha_1$	$\sim \mu_{u2}$	$\sim R_{m2}$	$\sim \alpha_2$	$> \mu_G$	$> \mu_Q$		
3.5 E8	111 000	1 E6	4	109 000	0.96 E6	3.99	16 500	18 200	4.41	0.5 E-5
	$\sim \mu_{u1}$	$\sim R_{m1}$	$\sim \alpha_1$	$\sim \mu_{u2}$	$\sim R_{m2}$	$\sim \alpha_2$	$> \mu_G$	$> \mu_Q$		
2.8 E6	111 000	1 E6	4	113 000	1.01 E6	3.99	16 700	18 200	4.04	0.26 E-4
	$\sim \mu_{u1}$	$\sim R_{m1}$	$\sim \alpha_1$	$\sim \mu_{u2}$	$\sim R_{m2}$	$\sim \alpha_2$	$> \mu_G$	$> \mu_Q$		
2.2 E6	113 000	94 400	4	113 000	853 000	4	16 100	17 600	2.96	0.15 E-2
	$\sim \mu_{u1}$	$\sim R_{m1}$	$\sim \alpha_1$	$\sim \mu_{u2}$	$\sim R_{m2}$	$\sim \alpha_2$	$> \mu_G$	$> \mu_Q$		
1.1 E6	113 000	918 000	3.99	113 000	908 000	4	16 200	17 700	1.71	0.44 E-1
	$\sim \mu_{u1}$	$\sim R_{m1}$	$\sim \alpha_1$	$\sim \mu_{u2}$	$\sim R_{m2}$	$\sim \alpha_2$	$> \mu_G$	$> \mu_Q$		

Table 7- Reliability sensitivity to the coefficient of variation of the connections rigidity

$\frac{R_{m1}}{m_{Rm1}} = \frac{R_{m2}}{m_{Rm2}}$ (N.m/rd)	$\mu_{u1}$ (N.m)	$R_{m1}$ (N.m/rd)	$\alpha_1$	$\mu_{u2}$ (N.m)	$R_{m2}$ (N.m/rd)	$\alpha_2$	G (N)	Q (N)	$\beta$	Pf
10%	55 700	1.1 E7	4	55 500	1.1 E7	4	17 800	19 500	4.87	0.4 E-6
	$\sim \mu_{u1}$	$\sim R_{m1}$	$\sim \alpha_1$	$\sim \mu_{u2}$	$\sim R_{m2}$	$\sim \alpha_2$	$> \mu_G$	$> \mu_Q$		
15%	55 700	1.1 E7	4	55 500	1.1 E7	4	17 800	19 500	4.87	0.4 E-6
	$\sim \mu_{u1}$	$\sim R_{m1}$	$\sim \alpha_1$	$\sim \mu_{u2}$	$\sim R_{m2}$	$\sim \alpha_2$	$> \mu_G$	$> \mu_Q$		
20%	55 500	1.1 E7	4	55 700	1.1 E7	4	17 800	19 500	4.87	0.4 E-6
	$\sim \mu_{u1}$	$\sim R_{m1}$	$\sim \alpha_1$	$\sim \mu_{u2}$	$\sim R_{m2}$	$\sim \alpha_2$	$> \mu_G$	$> \mu_Q$		
31%	112 000	1 380	4	91 400	1.1 E7	4	16 000	19 200	3.95	0.4 E-4
	$\sim \mu_{u1}$	$\sim R_{m1}$	$\sim \alpha_1$	$\sim \mu_{u2}$	$\sim R_{m2}$	$\sim \alpha_2$	$> \mu_G$	$> \mu_Q$		
38%	109 000	3 000	4	92 600	1.1 E7	4	16 000	19 200	3.52	0.2 E-3
	$\sim \mu_{u1}$	$\sim R_{m1}$	$\sim \alpha_1$	$\sim \mu_{u2}$	$\sim R_{m2}$	$\sim \alpha_2$	$> \mu_G$	$> \mu_Q$		
50%	112 000	1 580	4	83 300	1.1 E7	4	16 100	18 100	2.92	1.76 E-2
	$\sim \mu_{u1}$	$\sim R_{m1}$	$\sim \alpha_1$	$\sim \mu_{u2}$	$\sim R_{m2}$	$\sim \alpha_2$	$> \mu_G$	$> \mu_Q$		

- the mode of failure becomes symmetric, regarding the behaviour of the connections, when the mean value of the rigidity decreases. The failure depends mainly on the connection rigidity. Actually, the beams have small rotation capacity producing then small bending moments. The beam fails, whereas the connections are still in the linear part of their behaviour. This causes a low carrying capacity of the structure, leading to small values of the reliability. This is shown in Fig. 12, where the coefficient of variation of the connections rigidity is set equal to 25%.

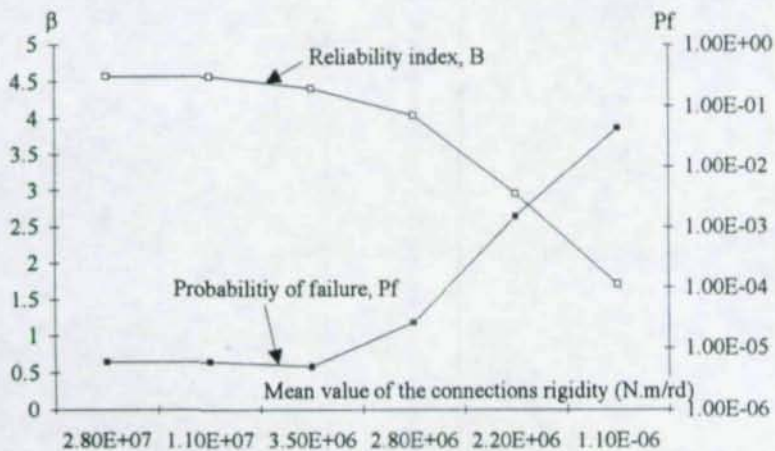


Figure 12- Reliability Sensitivity to the Mean Value of the Connections Rigidity

The safety level appears independent of the connections rigidity while the rigidity remains larger than  $3.5 E6$ , leading to a non symmetric mode of failure. However, if the rigidity is smaller than  $3.5 E6$ , the mode of failure becomes symmetric regarding the two connections, in turn giving a small structural reliability.

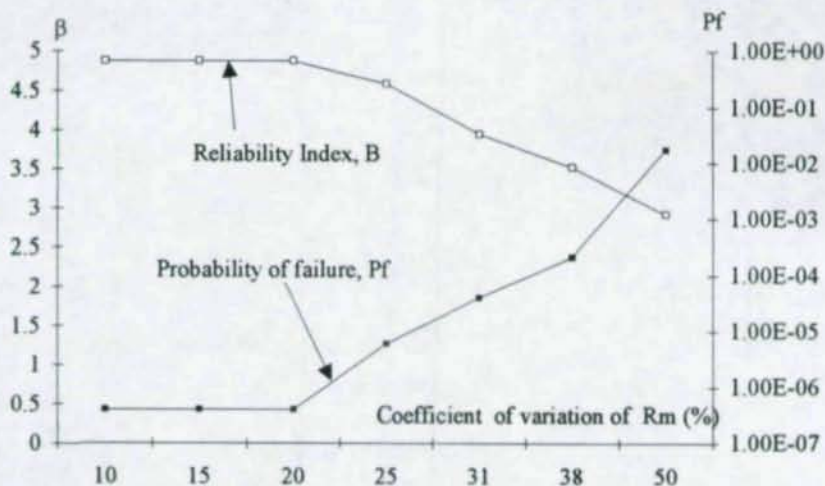
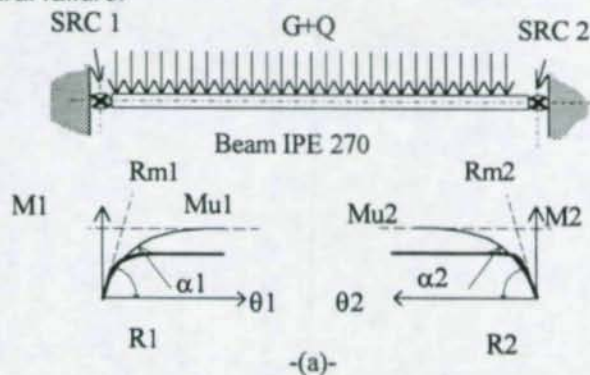


Figure 13- Reliability Sensitivity to the Coefficient of Variation of Connection Rigidity

These results show that the mode of failure is symmetric with respect to the connection behaviour, as long as the coefficient of variation of the rigidity is smaller than 20%. The failure then depend mainly on the ultimate behaviour of the connections. Actually, Fig. 13 shows that the reliability remains almost constant while this coefficient of variation remains smaller to 20%.

Figure 14 illustrates the three main combinations of the connections behaviours that lead to the structural failure.



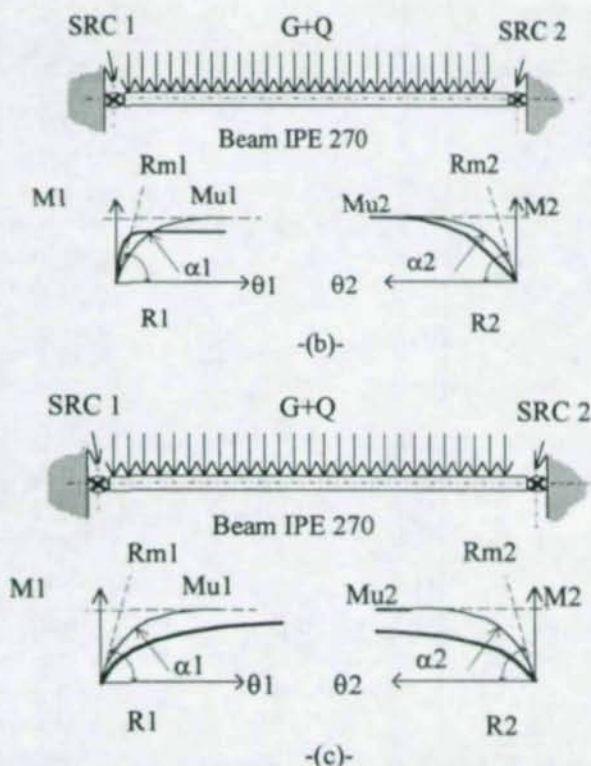


Figure 14- Connections Behaviours Corresponding to the Failure Mode of the Structure  
 (a)- Symmetric mode with small values of the moment capacity  
 (b)- Non symmetric mode with small moment capacity or small rigidity  
 (c)- Non symmetric mode with small values of the connection rigidity

Two primary conclusions can be drawn on the basis of the results presented here:

- For class 1 shapes, the connection stiffness has a relatively small influence on the structural safety, as long as the coefficient of variation of the stiffness is smaller than approximately 20 percent. The shaded area in fig 15 may be representative of acceptable behaviour when performing elasto-plastic analysis.
- The mode of failure becomes non-symmetric for connection stiffness coefficients of variation larger than 20 percent. The most probable mode of failure reflect different connections at the beam ends. An "optimal" solution may be to have one connection with small stiffness and the other connection with small moment capacity.

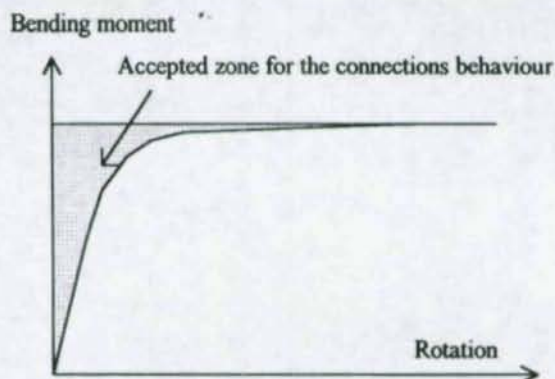


Figure 13- Accepted zone for the connections behaviour

## 2.2 Limit state for beams of class 2

### 2.2.1 Results obtained with the reference data

The design point  $P^*$ , the reliability index and the probability of failure that were obtained are indicated in Table 8. The results correspond to a coefficient of variation of the connection rigidity of 25%. As stated for class 1 beams, the mode of failure is also non symmetric

Table 8- Design point coordinates and the probability of failure

SRC 1			SRC 2			Loads		$\beta$	Pf
$Mu_1$ (N.m)	$Rm_1$ (N.m/rd)	$\alpha_1$	$Mu_2$ (N.m)	$Rm_2$ (N.m/rd)	$\alpha_2$	G (N)	Q (N)		
112 000	1.09 E4	4	68 100	1.1 E7	4	14 800	16 100	4.83	1.49 E-6
$\sim \mu_{Mu1}$	$\sim \mu_{Rm1}$	$\sim \mu_{\alpha1}$	$\sim \mu_{Mu2}$	$\sim \mu_{Rm2}$	$\sim \mu_{\alpha2}$	$> \mu_G$	$> \mu_Q$		

### 2.2.2 Sensitivity analysis

The results of the sensitivity analysis with respect to connection stiffness coefficients of variation from 10 to 45 percent are illustrated in Table 9 and Fig 16.

Table 9- Reliability Sensitivity to Connection Stiffness Coefficient of variation

$\frac{s_{Rm1}/m_{Rm1}}{s_{Rm2}/m_{Rm2}}$ (N.m/rd)	$Mu_1$ (N.m)	$Rm_1$ (N.m/rd)	$\alpha_1$	$Mu_2$ (N.m)	$Rm_2$ (N.m/rd)	$\alpha_2$	G (N)	Q (N)	$\beta$	Pf
10%	46 400	1.1 E7	4	46 700	1.1 E7	4	16 100	17 500	5.43	2.7 E-6
	$\sim \mu_{Mu1}$	$\sim \mu_{Rm1}$	$\sim \mu_{\alpha1}$	$\sim \mu_{Mu2}$	$\sim \mu_{Rm2}$	$\sim \mu_{\alpha2}$	$> \mu_G$	$> \mu_Q$		
35%	112 000	1 E4	4	72 100	1.1 E7	4	15 500	15 900	3.94	1.2 E-5
	$\sim \mu_{Mu1}$	$\sim \mu_{Rm1}$	$\sim \mu_{\alpha1}$	$\sim \mu_{Mu2}$	$\sim \mu_{Rm2}$	$\sim \mu_{\alpha2}$	$> \mu_G$	$> \mu_Q$		
45%	112 000	984 000	4	112 000	958 000	4	13 800	14 100	2.9	1.3 E-3
	$\sim \mu_{Mu1}$	$\sim \mu_{Rm1}$	$\sim \mu_{\alpha1}$	$\sim \mu_{Mu2}$	$\sim \mu_{Rm2}$	$\sim \mu_{\alpha2}$	$> \mu_G$	$> \mu_Q$		

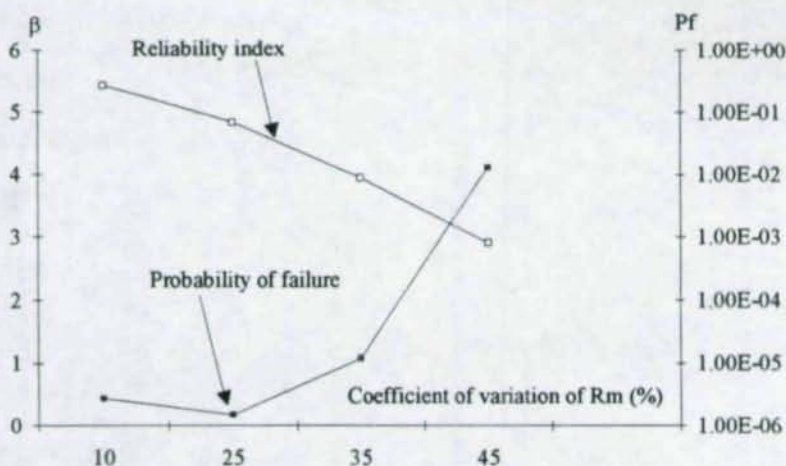


Figure 14- Reliability Sensitivity to the Coefficient of Variation of the Connections Rigidity

The results show that the reliability decreases when the coefficient of variation of the connection rigidity increases. The mode of failure is symmetric for either small (10%) or large (45%) values of the coefficient of variation. For this latter case, the failure is due to very small values of the connection rigidity. However, the failure mode is symmetric for medium values (35%) of this coefficient.

### 2.3 Limit state for the beams of class 3

#### 2.3.1 Results Obtained with Data from references

The design point  $P^*$ , the reliability index and the probability of failure that were obtained are indicated in Table 10. The results correspond to a coefficient of variation of the connection rigidity of 25%. As stated for class 1 or 2 beams, the mode of failure is also non symmetric

Table 10- Design Point Coordinates and Probability of Failure

SRC 1			SRC 2			Loads		$\beta$	Pf
$Mu_1$ (N.m)	$Rm_1$ (N.m/rd)	$\alpha_1$	$Mu_2$ (N.m)	$Rm_2$ (N.m/rd)	$\alpha_2$	G (N)	Q (N)		
101 000	1.02 E4	4	76 700	1.1 E7	4	14 000	16 700	4.46	2.9 E-5
$\sim \mu_{Mu1}$	$< \mu_{Rm1}$	$\sim \mu_{\alpha1}$	$< \mu_{Mu2}$	$\sim \mu_{Rm2}$	$\sim \mu_{\alpha2}$	$> \mu_G$	$> \mu_Q$		

#### 2.3.2 Sensitivity analysis

The results of the sensitivity analysis with respect to connection stiffness coefficients of variation from 10 to 45 percent are illustrated in Table 11..

Table 11- Reliability Sensitivity to Connections Stiffness Coefficient of Variation

$\frac{Rm_1}{Rm_2} = \frac{mRm_1}{mRm_2}$ (N.m/rd)	$Mu_1$ (N.m)	$Rm_1$ (N.m/rd)	$\alpha_1$	$Mu_2$ (N.m)	$Rm_2$ (N.m/rd)	$\alpha_2$	G (N)	Q (N)	$\beta$	Pf
10%	38 700	1.01 E4	4	38 500	1.1 E7	4	14 700	16 100	5.73	8.4 E-7
	$< \mu_{Mu1}$	$\sim \mu_{Rm1}$	$\sim \mu_{\alpha1}$	$< \mu_{Mu2}$	$\sim \mu_{Rm2}$	$\sim \mu_{\alpha2}$	$> \mu_G$	$> \mu_Q$		
15%	38 400	1.10 E4	4	38 500	1.1 E7	4	14 700	16 000	5.73	8.3 E-7
	$< \mu_{Mu1}$	$\sim \mu_{Rm1}$	$\sim \mu_{\alpha1}$	$< \mu_{Mu2}$	$\sim \mu_{Rm2}$	$\sim \mu_{\alpha2}$	$> \mu_G$	$> \mu_Q$		
35%	101 000	8.5 E5	4	101 000	8.5 E5	4	12 600	13 300	3.78	2.32 E-5
	$\sim \mu_{Mu1}$	$< \mu_{Rm1}$	$\sim \mu_{\alpha1}$	$\sim \mu_{Mu2}$	$< \mu_{Rm2}$	$\sim \mu_{\alpha2}$	$> \mu_G$	$> \mu_Q$		
45%	101 000	7.6 E5	4	101 000	6.9 E5	4	12 400	12 900	2.96	4.4 E-4
	$\sim \mu_{Mu1}$	$< \mu_{Rm1}$	$\sim \mu_{\alpha1}$	$\sim \mu_{Mu2}$	$< \mu_{Rm2}$	$\sim \mu_{\alpha2}$	$> \mu_G$	$> \mu_Q$		

The results show that the reliability decreases when the coefficient of variation of the connection rigidity increases. The mode of failure is symmetric for either small (<15%) or large (45%) values of the coefficient of variation. For this latter case, the failure is due to very small values of the rigidity. However, the failure mode is symmetric for medium values (25 to 35%) of this coefficient.

## 2.4 Limit state for the beams of class 4

### 2.4.1 Results Obtained with Data from References

The design point P\*, the reliability index and the probability of failure are indicated in Table 12. The results correspond to a coefficient of variation of the connection rigidity of 25%. As stated for class 1, 2, 3 beams, the mode of failure is also non symmetric

Table 12- Design point Coordinates and Probability of Failure

SRC 1			SRC 2			Loads		$\beta$	Pf
$Mu_1$ (N.m)	$Rm_1$ (N.m/rd)	$\alpha_1$	$Mu_2$ (N.m)	$Rm_2$ (N.m/rd)	$\alpha_2$	G (N)	Q (N)		
75 500	1 E4	4	58 700	1.1 E7	4	10 600	11 200	4.5	1 E-6
$\sim \mu_{Mu1}$	$< \mu_{Rm1}$	$\sim \mu_{\alpha1}$	$< \mu_{Mu2}$	$\sim \mu_{Rm2}$	$\sim \mu_{\alpha2}$	$> \mu_G$	$> \mu_Q$		

### 2.4.2 Sensitivity analysis

The results of the sensitivity analysis with respect to connection stiffness coefficient of variation from 10 to 45 percent are illustrated in table 13.

Table 13- Reliability Sensitivity to Connection Stiffness Coefficient of Variation

$\frac{Rm_1}{Rm_2} = \frac{mRm_1}{mRm_2}$ (N.m/rd)	$Mu_1$ (N.m)	$Rm_1$ (N.m/rd)	$\alpha_1$	$Mu_2$ (N.m)	$Rm_2$ (N.m/rd)	$\alpha_2$	G (N)	Q (N)	$\beta$	Pf
10%	36400	1.10e4	4	35500	1.1e7	4	11200	12200	4.87	8.3e-7
	$< \mu_{Mu1}$	$\sim \mu_{Rm1}$	$\sim \mu_{\alpha1}$	$< \mu_{Mu2}$	$\sim \mu_{Rm2}$	$\sim \mu_{\alpha2}$	$> \mu_G$	$> \mu_Q$		
15%	36700	1.10e4	4	36600	1.1e7	4	11200	12200	4.87	8.3e-7
	$< \mu_{Mu1}$	$\sim \mu_{Rm1}$	$\sim \mu_{\alpha1}$	$< \mu_{Mu2}$	$\sim \mu_{Rm2}$	$\sim \mu_{\alpha2}$	$> \mu_G$	$> \mu_Q$		
35%	75600	1 e3	4	58700	1.1e7	4	10900	10800	3.58	4.8e-5
	$\sim \mu_{Mu1}$	$< \mu_{Rm1}$	$\sim \mu_{\alpha1}$	$< \mu_{Mu2}$	$\sim \mu_{Rm2}$	$\sim \mu_{\alpha2}$	$> \mu_G$	$> \mu_Q$		
45%	75600	1.01e3	4	62100	1.1e7	3.99	10500	11600	3.06	2.4e-4
	$\sim \mu_{Mu1}$	$< \mu_{Rm1}$	$\sim \mu_{\alpha1}$	$< \mu_{Mu2}$	$\sim \mu_{Rm2}$	$\sim \mu_{\alpha2}$	$> \mu_G$	$> \mu_Q$		

The conclusions that can be drawn are similar to those concerning the beams of classes 1, 2 and 3. The three modes of failure also depend on the coefficient of variation of the connections stiffness.

### 3. SUMMARY AND CONCLUSIONS

The results of this study show that the variability of the rigidity of the connections has significant influence on the behaviour and mode of failure of the structure, as follows:

1. Symmetric failure modes govern the behaviour when the connections have low ultimate moment capacity, and coefficient of variation of the connection stiffness that are less than 20 percent.
2. Non symmetric modes of failure govern when the coefficient of variation lies within the medium range of values, i.e. from 20 to 30 percent.
3. Symmetric modes of failure govern when the coefficient of variation is larger than 30 percent.

These conclusions are valid for all classes of beams.

For small values of the coefficient of variation of the connection stiffness, failure normally occurs as a result of low ultimate moment capacity of the connection. In these cases it appears that the reliability is independent of the behaviour of the connection. The results obtained in this study indicate that such response characteristics will govern when the connection stiffness coefficient of variation is less than approximately 20 percent.

### 4. REFERENCE

- American Institute of steel Construction (AISC) (1994), "Load and resistance Factor Design Specification for the design, Fabrication and erection of Structural Steel for Buildings", AISC, Chicago, Illinois, December. (First Edition published 1986)
- Bjorhovde, R., Colson, A. (1988), "Connections in steel Structures: Behaviour, Strength and Design", Elsevier Applied Science Publishers, London, England.
- Bjorhovde, R., Colson, A. Haaijer, G. and Stark, J.W.B (1992) "Connection in steel Structures II: Behaviour, Strength and Design", American Institute of Steel Construction, Chicago, Illinois.
- Canadian Standards Association (CSA) (1989) " Steel Structures for Buildings - Limit States Design", CSA Standard No. S16-89, CSA, Rexdale, Ontario, Canada.
- Commission of the European Communities (EC) (1992), "Eurocode 3; Design of steel Structures", EC, Brussels, Belgium, June.

European Convention for Constructional Steelworks (ECCS), "Calcul d'ossatures et Assemblages: Considérations Economiques", Construction métallique, Vol.31, No 1, CTICM ST Rémy les Chevreuses (Paris), France.

Rauscher and Kurt.H.Gerstle (1992) "Reliability of rotational behaviour of framing connections" Engineering journal / American institute of steel construction-First quarter /1992 (pp218-224).

Mazzolani, F.,Mele, E.,Piluso, V. (1993) "Statistical characterisation of constructional steels for structural ductility control" Costruzioni Metalliche n°2-1993.

Fléjou, J.L.(1994); "Etude des structures métalliques à assemblages semi-rigides";Thèse de doctorat de l'Université Paris VI, LMT Cachan.

Sellier, A. Mebarki, A.(1993) "Evaluation de la probabilité d'occurrence d'un événement rare, sensibilisation aux risques liés aux effets d'échelle."; *Annales des Ponts et Chaussées*, 3° trimestre.

R.Bjorovde,J.Brozetti,A.Colson (1987) ;"Connection in steel structure, Behaviour, strength & design" Elsiver Applied Science, Proceedings of the Workshop on connection , Laboratoire de mécanique et technologie,Ecole Normale supérieure de cachan, France, 25-27 May 1987.

Goyet, J.Rémy, B. (1988),"Fiabilité des structure,Méthodologie d'ensemble et application aux structures à barres" ; CTICM n°4.

Sellier, A.Mébarki, A.(1994),"Fast Monte Carlo Simulations and Safety Index Checking", ASCE Structures Congress XII, Atlanta, ;pp 260-265, April 24-28 .

## EVALUATION ON STATIC AND DYNAMIC STRUCTURAL COEFFICIENT OF STEEL FRAMES WITH SEMI-RIGID JOINTS VIA NUMERICAL SIMULATIONS

Dan Dubina<sup>1</sup>

Daniel Grecea<sup>2</sup>

Raul Zaharia<sup>3</sup>

### Abstract

This paper summarises the results of some numerical simulations concerning the response of steel frames with semi-rigid joints and different moment-rotation models, under static and seismic loads. It focuses on the influence of EC3 Annex J and JJ  $M-\phi$  curve on the stability and dynamic behaviour of steel structures. A simplified computation model dedicated to analyse steel frames with semi-rigid joints via a bi-linear  $M-\phi$  curve is presented in the last part of the paper.

### 1. INTRODUCTION

In a previous paper presented at STESSA'94 Conference (Dubina et al., 1994) the authors have parametrically analysed the influence of rotational stiffenes in bi-linear  $M-\phi$  model on the response of steel frames with semi-rigid joints. This study was developed on the four sway frames having the main geometrical and structural parameters shown in Figure 1.

The results of static and dynamic analysis are summarised in Table 1 and 2, respectively. Both ROBOT and PEP-micro computer codes were used for elastic-plastic static analysis respectively; the input data have been adapted for a bi-linear  $M-\phi$  characteristic curve of semi-rigid joints.

---

<sup>1</sup> Professor, T.U. Timisoara, Stadion 1, RO-1900 Timisoara, Romania

<sup>2</sup> Lecturer, T.U. Timisoara, Stadion 1, RO-1900 Timisoara, Romania

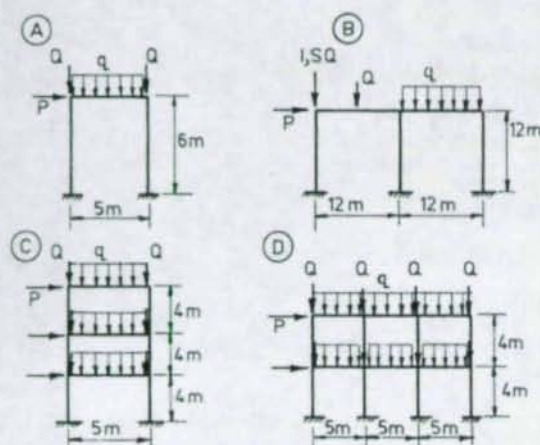
<sup>3</sup> Assistant, T.U. Timisoara, Stadion 1, RO-1900 Timisoara, Romania

## Member Cross-Sections

Frame	A	B	C	D
Member				
Column	HE160B	HE160B	HE200B	HE160A
Beam	IPE200	IPE300	IPE300	IPE300

## Initial out of plane

A	B	C	D
1/200	1/219	1/273	1/276



## Semi-rigid joints characteristics

Frame	A	B	C	D
$M_{Rd}$	47.1	72.0	103.0	54.5
(KNm)	31.4	70.0	100.0	37.0
$S_j$	12962.0	26101.0	32861.0	16974.0
(KNm/rad)	8641.2	22100.0	17420.0	9459.0

## Loading characteristics

Frame	Load	Static and Dynamic		
		P (N)	Q (N)	q (N/mm)
A		6.E3	108000.	12.363
B		3.E3	36000.	4.05
C		1.E4	207.684	41.537
D		5.E3	205.89	41.178

Fig.1. Calibration frames used for the parametrical study

Table 1. Characteristic load multiplier for static analysis

Frame	$M_{Rd}$ (KNm)	$S_{sec}$			$S/2$			$S_j$			Rigid		
		$\lambda_{cr}$	$\lambda_p$	$\lambda_u$									
A	47.0	6.504	1.924	2.037	6.884	1.833	2.036	7.337	1.736	2.039	7.699	1.665	2.042
	31.4		1.418	1.855		1.344	1.855		1.233	1.859		1.141	1.863
B	72.0	8.677	1.778	2.758	8.841	1.585	2.757	9.011	1.385	2.756	9.161	1.209	2.756
	70.0		1.765	2.735		1.611	2.734		1.383	2.734		1.176	2.733
C	10.3	10.66	1.254	1.545	12.21	1.135	1.542	14.43	1.017	4.553	17.08	0.913	1.533
	10.0		1.404	1.554		1.135	1.531		1.090	1.53		0.887	1.537
D	54.5	5.71	1.259	1.464	6.056	1.034	1.461	6.433	0.778	1.452	6.804	0.538	1.403
	37.0		1.121	1.35		0.947	1.346		0.671	1.341		0.366	1.307

In table 1 the following notation were used :  $\lambda_{cr}$  - the elastic critical multiplier;  $\lambda_p$  - the first plastic hinge multiplier;  $\lambda_u$  - the ultimate elastic-plastic multiplier.

DRAIN 2D computer code was used for dynamic analysis. The semi-rigid joint behaviour was modelled by the semi-rigid element implemented in DRAIN-2D following a bi-linear  $M-\phi$  curve;

a 5% degradation was assumed after  $M_{Rd}$  attainment. The March 4, 1977 Bucharest earthquake accelerogram, component N-S, was used to simulate the seismic response.

Table 2. Results of dynamic analysis

Frame	Joint	Accelerogram multiplier		Displacement (mm)		Structural coefficient
		$\lambda_p$	$\lambda_u$	$D_p$	$D_u$	
A	rigid	0.13	0.26	82	139	3.40
	semi-rigid	0.15	0.40	86	143	4.65
B	rigid	0.89	1.30	387	460	3.10
	semi-rigid	0.60	1.40	235	509	4.20
C	rigid	0.12	0.66	89	447	2.40
	semi-rigid	0.04	0.50	68	381	30.80
D	rigid	0.06	0.20	44	122	3.50
	semi-rigid	0.03	0.27	25	133	9.00

In table 2  $\lambda_p$  is the first plastic hinge accelerogram multiplier,  $\lambda_u$  is the plastic mechanism multiplier,  $D_p$  and  $D_u$  are the corresponding horizontal displacement and  $q = \lambda_{max}/\lambda_p$ .

On the basis of this study the following concluding remarks have been outlined:

#### Static analysis.

The rigid frames, characterised by  $\lambda_{cr} = \alpha_{cr} \geq 10$  are more sensitive with the decreasing of rotational stiffness of the joint, so that they require a finer modelling of  $M-\phi$  curve.

First plastic hinge multiplier,  $\lambda_p$  is really influenced by rotational stiffness value in the bi-linear  $M-\phi$  model, while the ultimate multiplier is not influenced. Thus the configuration of failure plastic mechanism generally remains the same, only the appearance moment of first plastic hinge being modified. As a consequence, for the same structure, using different  $M-\phi$  bi-linear curves, depending of rotational stiffness, different  $\lambda_p-\lambda_u$  intervals are resulting.

#### Dynamic analysis.

Displacement of semi-rigid joint frames are with about 15-35% larger than the rigid joint ones, so they have greater eigenperiods and, consequently, smaller response factors and smaller design seismic loads.

The q factor is greater in semi-rigid joint frames, which also means a smaller design seismic load.

The failure mechanism can become a global mechanism in frames with semi-rigid joints, while for the structure of rigid joints depending on the ratio of the joint ultimate moment versus plastic moment of the beam,  $M_{Rd}/M_{pl,b}$ , partial floor mechanism may occur.

The  $M-\phi$  model, corresponding to revised Annex J of EUROCODE 3 (JJ) (1993) is different from the previous model in Annex J. The difference is consisting in both values of rotational stiffness and ultimate moment of the joint. In these circumstances starting from the results and concluding remarks summarised above, we have estimated that it would be very interesting and useful to analyse the influence of J and JJ moment-rotation models on the static and dynamic response of the ECCS calibration frames. Both three and bi-linear  $M-\phi$  curves, that are provided by EUROCODE 3, are used to evaluate the static response; only the bi-linear curve was used in the dynamic analysis. In last part of this paper, a simplified model, based on the bi-linear  $M-\phi$  curve, is proposed for elastic-plastic FEM analysis of steel frames with semi-rigid joints.

## 2. INFLUENCE OF ANNEX J AND REVISED ANNEX J MOMENT-ROTATION CURVES ON THE STATIC AND DYNAMIC RESPONSE OF STEEL FRAMES WITH SEMI-RIGID JOINTS

### 2.1 Analysed Structures

The same four frames shown in Figure 1 have been analysed, but the type of member cross-sections, the load values and the joint characteristic were changed. IPE 360 in beams and HEB 200 in columns were used in all frames. The load values for both static and dynamic analysis are presented in table 3.

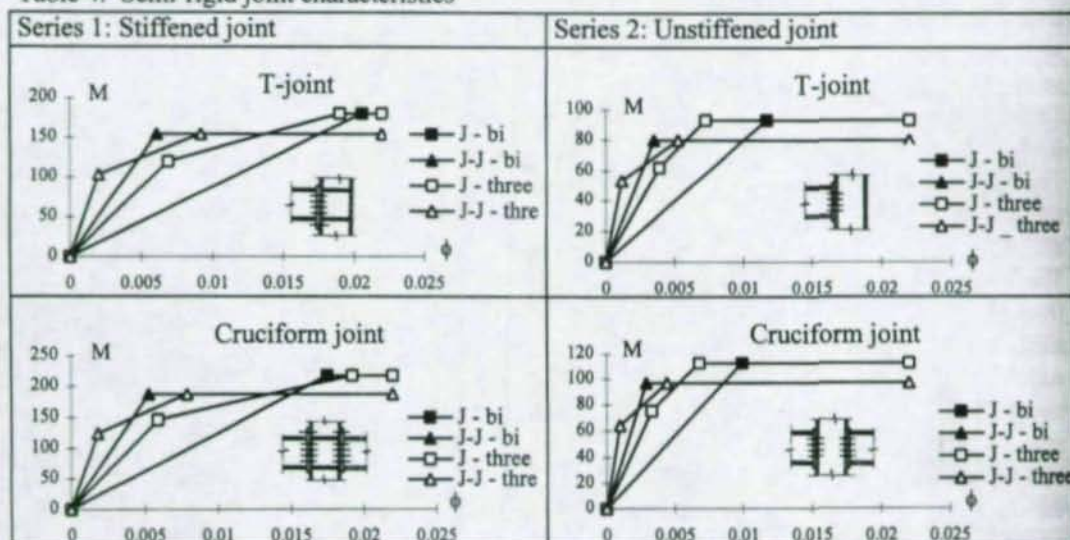
Table 3. Load values

Frame	Load case	Static			Dynamic		
		P (N)	Q (N)	q (N/mm)	P (N)	Q (N)	q (N/mm)
A		1.8E4	3.24E5	37.089	6000	1.08E5	12.363
B		0.9E4	0.72E5	12.150	3000	0.24E5	4.050
C		1.5E4	3.12E2	62.305	10000	2.08E5	41.537
D		0.75E4	3.09E2	61.767	5000	2.06E5	41.178

The same earthquake accelerogram of Bucharest from 4<sup>th</sup> of March 1977, component N-S was used for seismic analysis.

Two types of semi-rigid joints, with stiffened and unstiffened web column, were used. Table 4 contains the characteristics M- $\phi$  curves for both T and cruciform joints.

Table 4. Semi-rigid joint characteristics



## 2.2. Results of Static Response

The results of static analysis are related to characteristic load multipliers, time-history of plastic hinge appearance and characteristic curves of the behaviour of the frames in terms of horizontal displacements and beam deflections. These results are presented in tables 5 to 7 on bottom.

Table 5. Characteristic load-multipliers

M- $\phi$	Joint series 1				Joint series 2			
	J-three	JJ-three	J-bi	JJ-bi	J-three	JJ-three	J-bi	JJ-bi
$\lambda$								
	A				A			
$\lambda_{cr}$	5.88	6.6	5.08	6.2	5.8	6.6	5	6.2
$\lambda_{\eta}$	1.678	1.633	1.624	1.667	1.621	1.417	1.613	1.409
$\lambda_{\gamma}$	1.779	1.81	1.684	1.793	1.664	1.687	1.613	1.664
	B				B			
$\lambda_{cr}$	6.346	6.629	5.931	6.431	6.281	6.671	5.949	6.452
$\lambda_{\eta}$	1.575	1.368	1.536	1.336	0.914	0.724	1.166	0.712
$\lambda_{\gamma}$	1.796	1.736	1.796	1.736	1.494	1.442	1.493	1.442
	C				C			
$\lambda_{cr}$	8.567	11.077	6.533	9.649	8.355	10.891	6.315	9.422
$\lambda_{\eta}$	1.625	1.735	1.516	1.679	1.411	1.088	1.501	1.125
$\lambda_{\gamma}$	1.961	1.91	1.961	1.913	1.633	1.564	1.627	1.564
	D				D			
$\lambda_{cr}$	11.474	13.005	9.795	12.202	11.258	12.935	9.488	12.031
$\lambda_{\eta}$	1.824	1.886	1.665	1.6	1.333	1.011	1.632	1.006
$\lambda_{\gamma}$	2.15	2.05	2.167	2.053	1.728	1.653	1.728	1.655

Table 6. Time-history of plastic hinge appearance

Joint series 1				Joint series 2			
Frame A							
J-three	J-bi	JJ-three	JJ-bi	J-three	J-bi	JJ-three	JJ-bi
Frame B							
J-three	J-bi	JJ-three	JJ-bi	J-three	J-bi	JJ-three	JJ-bi

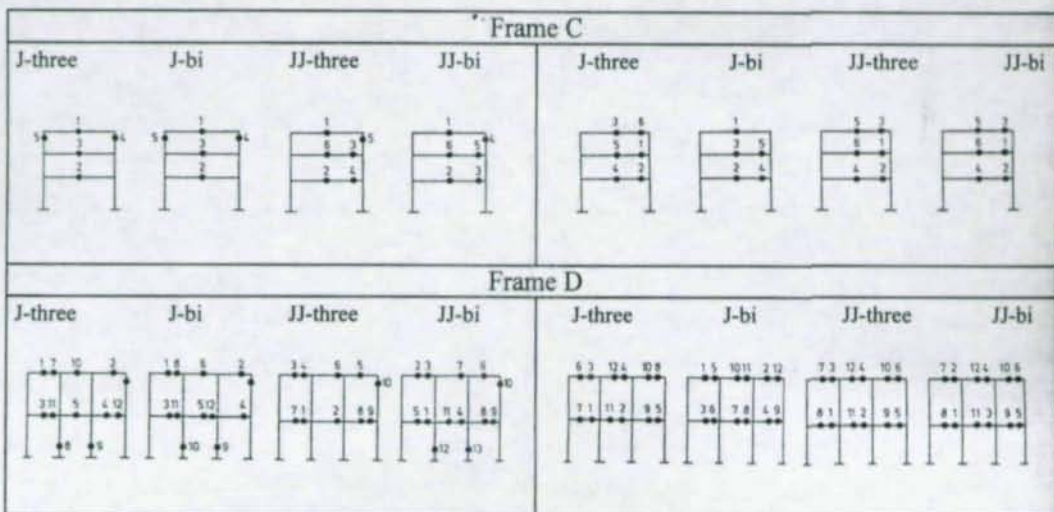
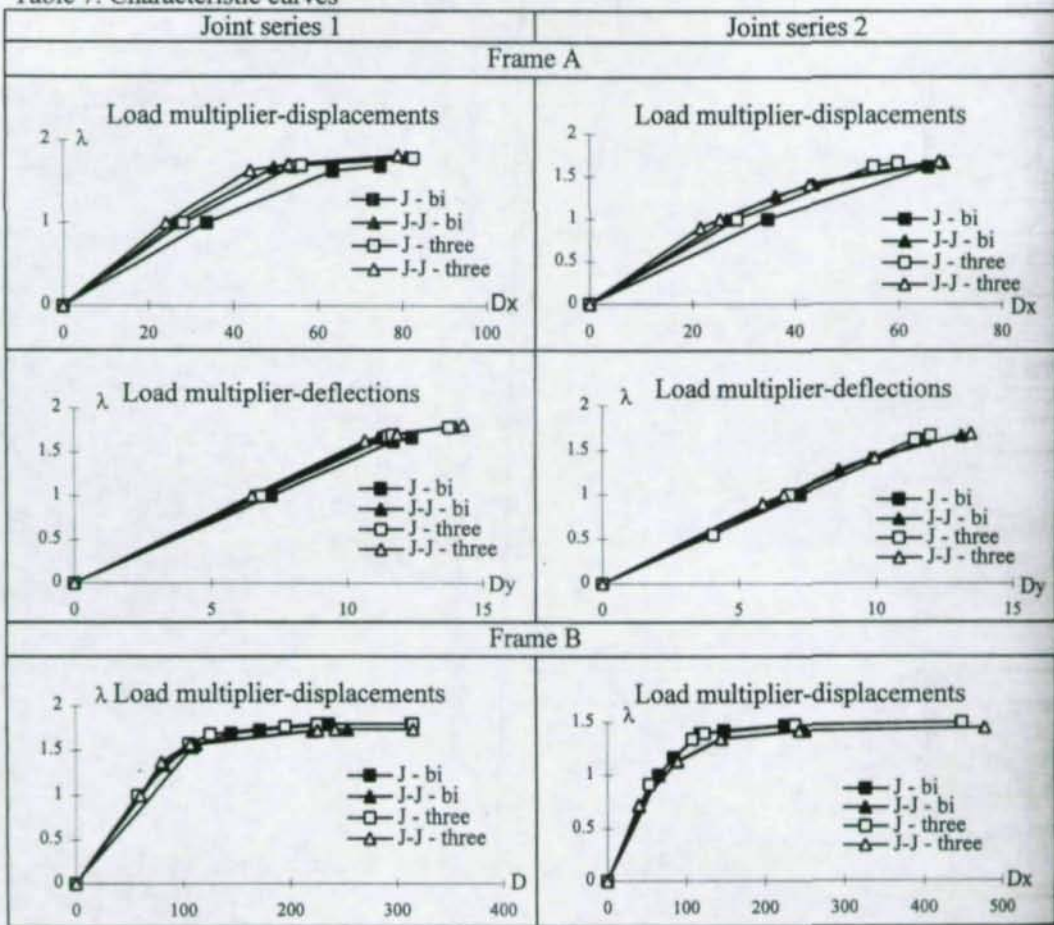
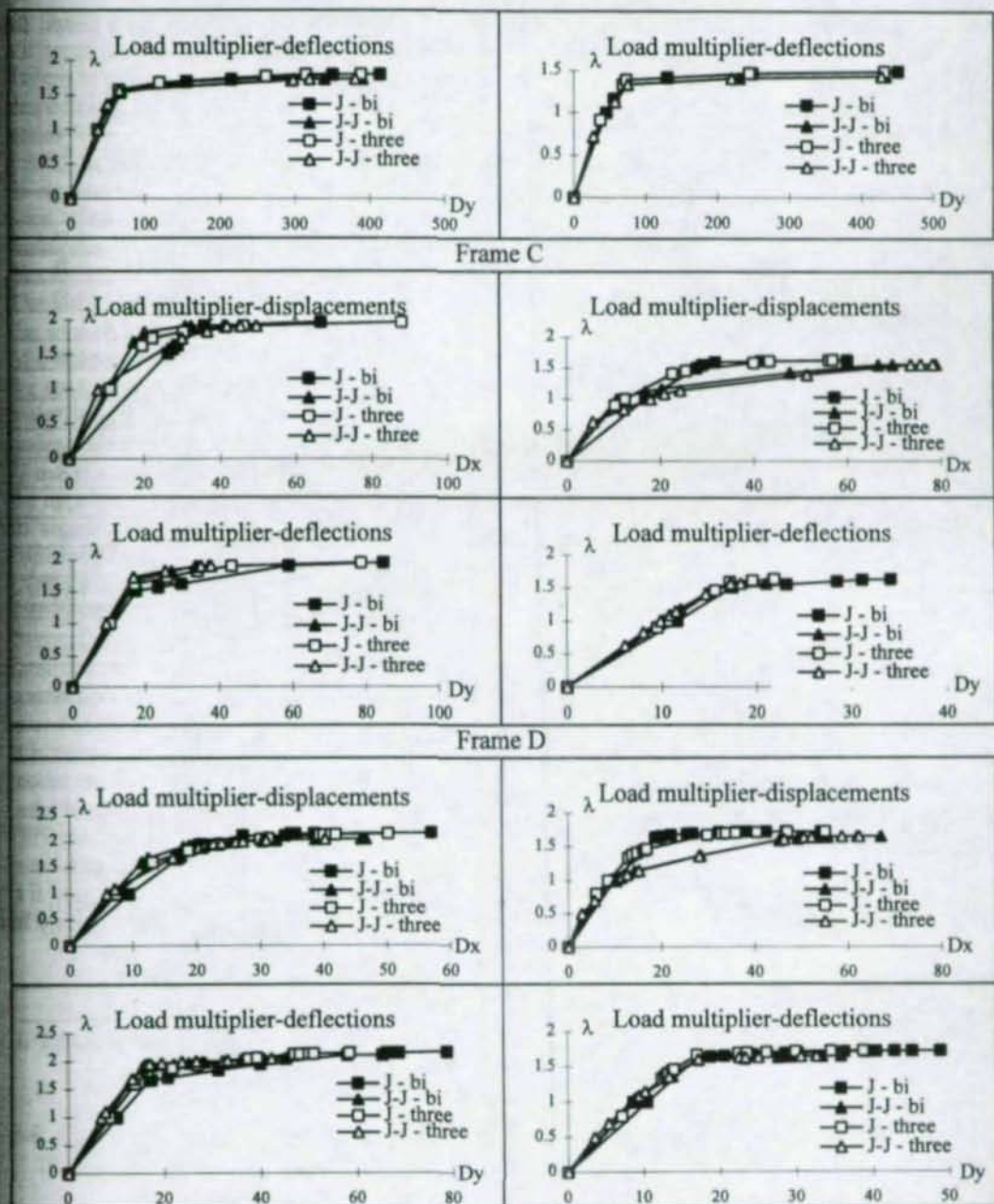


Table 7. Characteristic curves





### 2.3. Results of seismic response

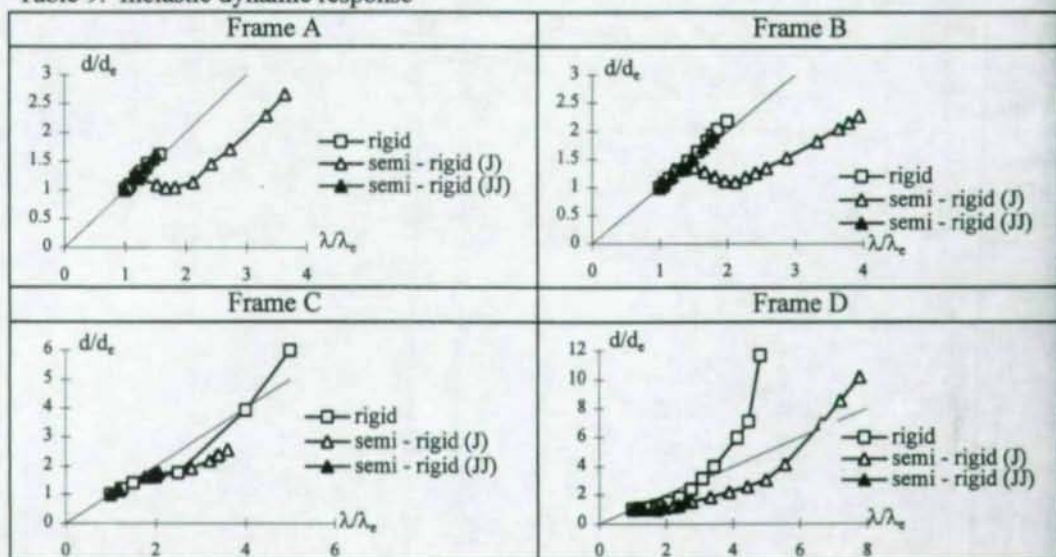
Only the semi-rigid joint series 1 (stiffened column web) was analysed in order to evaluate the seismic response of four forms. In table 8 and 9 are summarised the main results of seismic

response obtained both for also given J and JJ bi-linear M- $\phi$  curves of semi-rigid joints; for comparison those corresponding to rigid ones.

Table 8. Results of seismic analysis

Type	$\lambda_p$	$D_{p,max}$ (m)	$D_{p,min}$ (m)	$\lambda_m$	$D_{u,max}$ (m)	$D_{u,min}$ (m)	q
A							
R	0.51	0.074	-.078	0.64	0.070	-.101	1.25
SR-J	0.33	0.099	-.081	0.90	0.169	-.201	2.73
SR-JJ	0.41	0.087	-.079	0.62	0.084	-.128	1.51
B							
R	0.70	0.305	-.245	1.30	0.303	-.499	1.86
SR-J	0.66	0.329	-.256	2.60	0.749	-.562	3.94
SR-JJ	0.67	0.319	-.245	1.20	0.342	-.467	1.79
C							
R	0.20	0.098	-.049	0.30	0.137	-.085	1.5
SR-J	0.25	0.200	-.100	0.84	0.472	-.066	3.36
SR-JJ	0.17	0.134	-.053	0.34	0.236	-.102	2.0
D							
R	0.29	0.051	-.056	0.44	0.056	-.084	1.52
SR-J	0.18	0.081	-.067	0.46	0.112	-.155	2.56
SR-JJ	0.23	0.070	-.063	0.45	0.079	-.116	1.96

Table 9. Inelastic dynamic response



## 2.4. Conclusions

Related to J and JJ moment-rotation curves, the changes in rotational joint stiffness influence the critical multiplier  $\lambda_{cr}$ , which is sensibly greater in case of Annex JJ, especially for structures A,

C, D (22 - 48%; see table 5). The level of the plastic multipliers  $\lambda_p$  is evidently influenced by different joint ultimate moments  $M_{Rd,J}$  and  $M_{Rd,JJ}$ . Looking in the same table it results that the failure multiplier  $\lambda_u$  is not major influenced by the different values of the initial stiffness  $S_0$ , respectively by the different  $M-\phi$  models in Annex J and JJ. Concerning the two different joint series it is evident that for the second series, corresponding to the more flexible and weaker joints, the plastic hinges appear earlier in connections.

In case of two different  $M-\phi$  models, if for the stiffer one the first plastic hinge appears in the joint, than for the second one (more flexible), the same hinge results for a greater loading multiplier  $\lambda_p$ . This apparent paradox can be explained by the moment redistribution due to the fact the joint moment is relaxed.

The sway-displacements are in accordance with  $M-\phi$  models. For the bi-linear JJ  $M-\phi$  model in the serviceability limit state ( $\lambda=1$ ) the displacements are smaller than those corresponding to J  $M-\phi$  model: the difference is from 11% for D1 structure to 39% for C2. Taking into account that for such frames, the serviceability limit state corresponding to sway displacements may be the main design criteria, the revised J model must be carefully analysed because it could lead to underevaluated results. Significant differences for beam deflections, corresponding to the J and JJ models can be observed for the bi-linear  $M-\phi$  curves, especially for C and D structures. After the appearance of the beam plastic hinges the J  $M-\phi$  model leads to greater beam deflections.

In seismic response the interval  $\lambda_p-\lambda_u$  is larger in the case of J model. The related values corresponding to the rigid joints frames are closed to the semi-rigid ones if JJ  $M-\phi$  model is used.

Displacements corresponding to plastic mechanism are greater for the semi-rigid joint frames than for the rigid joints ones: 15% to 50% for JJ model and 100-350% for J model are obtained.

Generally, the time-history of yielding mechanism is the same for each type of structure.

In structures with semi-rigid JJ model connections, due to the smaller ultimate moment of the connection, plastic hinges occur also in connections. So, a local mechanism with plastic hinges in connection and beam-end occurs, generating large rotations and the structure collapse.

It is very clear that using the JJ  $M-\phi$  model structures become less ductile than in the case the J model is used. From this point of view, the two models have to be very seriously analysed in order to establish which of them is the correct one.

Different results obtained with J and JJ models are in fact produced by different values of rotational stiffness and plastic resistance of the joint  $M-\phi$  curve. Consequently, we appreciate that it is very important to develop the comparison between the two models, in order to decide which of them is closer to the actual behaviour of the semi-rigid joint.

### 3. PROPOSAL FOR A SIMPLIFIED APPROACH

#### 3.1. Generals

In a paper presented by Maquoi & Jaspert (1992) several FEM computer codes that are implementing the *separate modelling* of connection and sheared web panel or *concentrated modelling* of the joint (including both connection and web panel deformations) have been compared by means of two sway steel frames with semi-rigid joints. Those codes are based either on the plastic hinge or plastic zone theory. Excepting the detailed conclusions outlined by the authors of the study from above, it must be observed that the numerical results obtained with

those computer codes are relatively closed, at least from practical point of view. However for design practice the use of such sophisticated non-linear computation tools is not useful because they are too complex both for designer and the real needs of structural analysis. That is the reason why other researches in the field are proposing for the design analysis of steel frames with semi-rigid joints the use of a *concentrated bi-linear M- $\phi$  model* instead of the non-linear M- $\phi$  model (Maquoi & Jaspart, 1994). Otherwise the bi-linear model is included in EUROCODE 3 provisions. The problem is that even the bi-linear model is accepted, this is generally used by means of the same sophisticated computer codes as the non-linear one.

In these circumstances, the authors of this paper are trying to propose a very simple and versatile model capable to introduce the semi-rigid bi-linear behaviour of semi-rigid joints in the elastic-plastic analysis of steel building frames.

### 3.2. Simplified Model for the Bi-linear Elastic-Plastic Behaviour of Semi-rigid Joints

An equivalent beam element can be used to simulate the bilinear behaviour of the joint. The beam will simulate the M- $\phi$  bilinear behaviour of the joint by means of its own elastic-plastic moment-rotation relationship as is shown in Figure 2. The M- $\phi$  model of the beam element behaviour is derived from the idealised curve of the material (Prandtl model). The moment corresponding to the yield plateau is the joint plastic capacity; the rotational stiffness may be the secant stiffness as EC 3 (1992) recommends, or it can be assumed to be equal to  $S_0/2$  for the unbraced frames, respectively to  $S_0/3$  for the braced frames ( $S_0$  is the initial rotational stiffness of the joint).

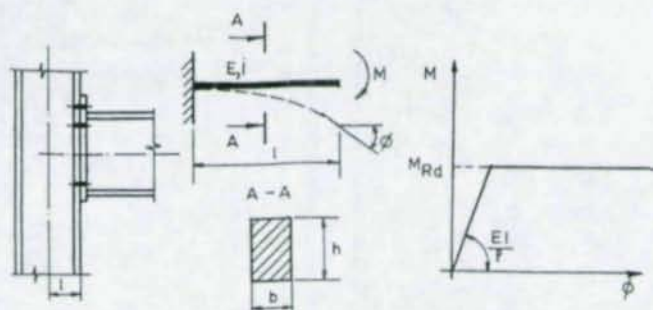


Fig.2. Simplified model

The equivalent geometrical characteristic of the beam element are obtained as follows (Fig. 2):

$$I = S_j l / E$$

$$W_{pl} = M_{Rd} / f_y$$

where:  $S_j$  - rotational stiffness of the joint;  $M_{Rd}$  - plastic moment of the joint;  $W_{pl}$  - full plastic modulus of the beam cross-section;  $I$  - second order moment of the beam cross section area.

Assuming a rectangular cross-section, the depth and the width result:

$$h = 3 I / W_{pl}$$

$$b = 4 W_{pl} / h^2$$

In the case of a rectangle cross section beam element, these relations overestimate the cross-section area, but it is not significant in the static analysis because the frame beams are working mainly in bending.

### 3.3. Numerical Comparison

In order to validate the proposal model, a comparative numerical study was developed on the four frame analysed in Chapter 2. The first series of semi-rigid joints were used modelled by means of revised Annex J bi-linear  $M-\phi$  curves (see Table 4) have been used.

From static analysis of frames A, B, C, D the following characteristic load multipliers values are resulting (Table 10).

Table 10. Comparative values of load multipliers

Frame	A		B		C		D	
	SRM	SM	SRM	SM	SRM	SM	SRM	SM
$\lambda$								
$\lambda_{cr}$	6.2	6.32	6.431	6.51	9.649	10.34	12.202	12.9
$\lambda_{cp}$	1.667	1.66	1.336	1.238	1.679	1.71	1.899	1.637
$\lambda_{cl}$	1.793	1.803	1.736	1.734	1.913	1.913	2.053	1.768

In table 10 the values related to SRM columns are obtained with PEP-micro computer code with a non-linear semi-rigid joint model described by means of a Ramberg-Osgood type moment-rotation relation, that was configured for a bi-linear  $M-\phi$  curve, while the SM values are obtained with the same program, but, this time, in stead of semi-rigid joint model was used the elastic-plastic element presented in §§ 3.2.

Figure 3 shows the characteristic curves related to load-maximum horizontal displacement change. Figure 4 shows the results corresponding to load-maximum beam deflection change.

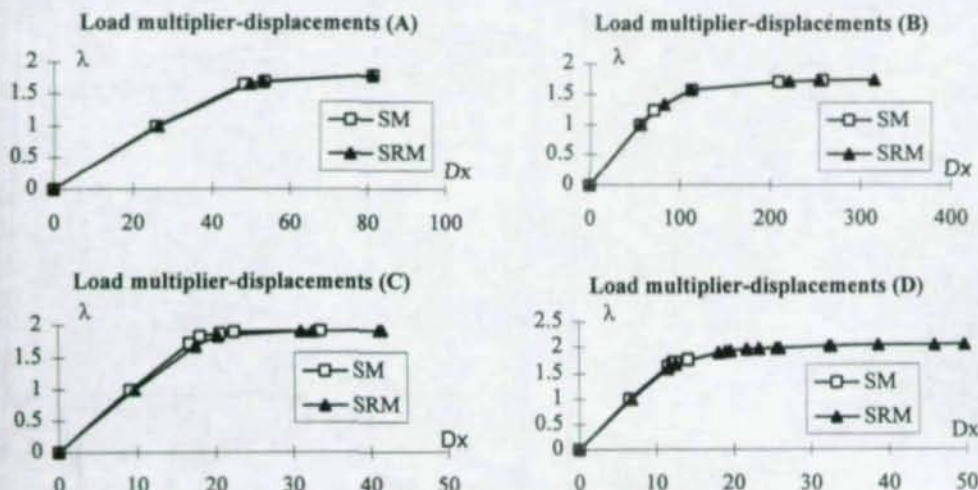


Fig.3. Load-displacements diagrams

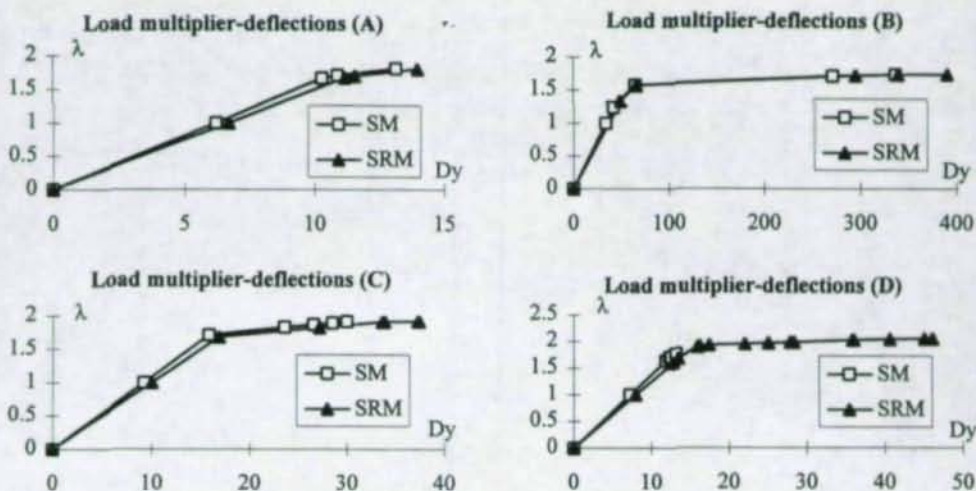


Fig.4. Load - deflections diagrams

### 3.4. Conclusions

A good correlation may be observed in the case of characteristic load multipliers and displacements for  $\lambda=1$  related to SRM and SM models. The only significant difference occurs over plastic range in magnitude of ultimate plastic factor in the case of frame D. However using the authors' model the results are on the safe side in each case.

To conclude, if a bilinear  $M-\phi$  model is accepted for the semi-rigid joint behaviour, the main advantage of this proposal consists in the fact that any non-linear elastic-plastic computer code, or even an elastic first order one, may be used to analyse steel frames with semi-rigid connections.

### References

- Dubina, D. & Grecea, D. & Zaharia, R. *Numerical simulation concerning the response of steel frames with semi-rigid joints under static and seismic loads*. Proc. of STESSA'94 Conf. Timisoara, June 26-28, 1994.
- ENV 1993-1-1. EUROCODE 3: Design of steel structures. Part 1.1: General rules and rules for buildings. CEN, February 1992, Annex J and Revised Annex J.
- Maquoi, R. & Jaspart, J.P., *Modelling of Beam-to-column Joints for the Design of Steel Building Frames* Constructional Steel Design: World Developments, Elsevier Appl. Sc. 1992, 196-205.
- Maquoi, R. & Jaspart, J.P., *Influence of the non-linear and bi-linear modellings of beam-to-column joints on the structural response of braced and unbraced steel building frames*, 4<sup>th</sup> Int. Colloquium on Structural Stability, Istanbul, Turkey, Sept. 16-20, 1991, pp. 133-151.

Technical Papers on

**CYCLIC RESPONSE**

## SEISMIC LOADING OF MOMENT END-PLATE CONNECTIONS: SOME PRELIMINARY RESULTS

Thomas M. Murray<sup>1</sup>

Ronald L. Meng<sup>2</sup>

### Abstract

Fractures in welded steel connections have been discovered in numerous building structures with moment-resisting frame connections due to the Northridge, California, earthquake of 1994. A possible alternative to on-site welded moment connections is the moment end-plate. Conventional designs, as well as shimmed end-plates, are being tested and analyzed for their adequacy under seismic induced cyclic loading. For the conventional designs, required end-plate thicknesses are determined from yield-line analysis and bolt size is determined using an analysis procedure which includes prying forces. Prying forces do not need to be considered for the designs with shims. From preliminary results, it appears that the extended moment end-plate, when properly designed, may be an acceptable alternative to the welded moment-resisting connection.

### 1. INTRODUCTION

Subsequent to the January 17, 1994, Northridge, California earthquake, numerous fractures in beam-to-column welds in steel moment resisting frames were reported. Damage was found in many buildings in the earthquake area with the cause attributed to unexpected high stress concentrations in the beam flange-to column flange connections. The primary cause of the fractures was probably due to the welding methods and techniques used. One obvious and possible solution to prevent future cracks and weld failure is to eliminate beam flange-to-column welds

---

<sup>1</sup>Montague-Betts Professor of Structural Steel Design, Department of Civil Engineering, Virginia Polytechnic Institute and State University, Blacksburg, VA 24061.

<sup>2</sup>Research Assistant, Department of Civil Engineering, Virginia Polytechnic Institute and State University, Blacksburg, VA 24061.

entirely as in a moment end-plate connection. Moment end-plate connections eliminate the field welding problems, but do require tension bolts which introduce the necessity to predict prying forces and the resulting uncertainty of the strength of the connection under seismic loading. Connection failure can be precluded by designing the connection for a strength greater than the beam strength and properly accounting for prying forces in the bolts. Although field inspection is still required, bolt tightening inspection is much less demanding than full penetration weld inspection.

Extensive research on the cyclic behavior of welded moment connections has been completed; very limited research has been conducted using cyclic loading of moment end-plate connections. Tsai and Popov (1990) conducted three tests to determine the cyclic behavior of unstiffened, four-bolt at the tension flange, moment end-plate connections. They experienced premature inner bolt failure in the first test of a conventionally designed connection, e.g. one where prying forces are ignored. The end-plate of the specimen was then reinforced with a vertical stiffener between the extended portion of the end-plate and the beam tension flange and stronger bolts installed. The connection was then retested and excellent behavior was found under large cyclic loads. A second specimen with larger diameter bolts and a slightly thicker end-plate was also tested with good results. Recommendations for increasing the strength of connecting bolts, over that used when prying forces are ignored, were made. Ghobarah *et al* (1990, 1992) conducted several cyclic loading tests to examine the behavior of both stiffened and unstiffened, extended end-plate connections. Both beam and column sections were included in the test setups. For some tests, the columns were axially loaded. Column flange and end-plate stiffeners, as well as, end-plate thickness were varied. In general, they found that end-plate connections were able to dissipate energy from cyclic loading without loss of strength. However, stiffness of the joint was reduced due mostly to bolt pretension losses. Murray *et al* (1992) also reported a loss in pretension bolt forces due to repeated loadings. Eleven end-plate moment connections were subjected to cyclic loading representing expected wind loading in the range of 33% to 100% of the connection allowable design moment. Six different end-plate configurations were tested, all with "snug-tightened" bolts. Typically, the residual bolt forces decreased as the number of loading cycles increased, with a rapid decrease during the first few loading cycles and then asymptotically approaching a lower bound.

Thus, completed research indicates that end-plate moment connections can be designed with sufficient strength to develop the beam plastic moment capacity and required beam inelastic rotation capacity. However, uncertainty of prying forces and reduced pretension due to repeated loadings remains a major concern. The prying force problem can possibly be eliminated with the use of shims between the end-plate and column as shown in Figure 1(b). With the shims placed as shown, the force in the tension bolts theoretically will not change until separation occurs at the shim location. Thus, the connection is in effect load tested at the time of bolt installation. The use of shims eliminates the uncertainty of any prying forces as none theoretically exist.

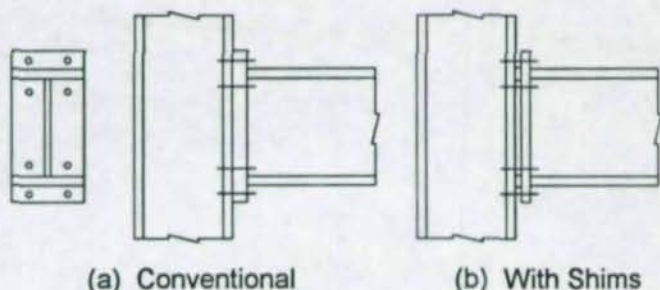


Figure 1. End-Plate Configurations

The authors are currently in the initial phase of a research project to study the behavior of large-capacity moment end-plate connections subject to cyclic loading. It is planned to experimentally study the behavior of three moment end-plate configurations connected to unstiffened columns using both A325 and A490 bolts. Results from the first three tests of four-bolt at the tension flange, extended unstiffened connections are presented here. Two tests were conducted without shims and one test with shims. All three tests were conducted using A325 bolts.

## 2. TEST SPECIMEN DESIGN

Test specimen design included the determination of end-plate thickness, bolt diameter and a column section with sufficient flange thickness to resist the plastic moment capacity of the selected test beam, W18x35 (W460x52). For the tests without shims, the end-plate thickness was determined using yield-line analysis. Simple bending concepts were used to determine the required end-plate thickness for the test with shims. The bolt diameter for both types of tests was determined using the "modified Kennedy" method which includes estimated bolt prying forces. Column flange strength was checked using previously published techniques.

### 2.1 Determination of End-Plate Thickness

The yield-line mechanism shown in Figure 2 was used to determine the required end-plate thickness for the specimens tested without shims (Srouji *et al*, 1983; Abel and Murray, 1992). The external work was taken as

$$W_e = M_U \theta = M_U (1/h) \quad (1)$$

where  $M_U$  is the ultimate beam moment at the end-plate and  $\theta$  is the virtual rotation of the connection, equal to  $1/h$ , where  $h$  is the total depth of the beam section. The internal work stored in the yield-line mechanism is then:

$$W_i = \frac{4m_p}{h} \left[ \left( \frac{b_f}{2} \left( \frac{1}{p_f} + \frac{1}{s} \right) + (p_f + s) \left( \frac{2}{g} \right) \right) (h - t_f - p_f) + \frac{b_f}{2} \left( \frac{h}{p_f} + \frac{1}{2} \right) \right] \quad (2)$$

where the geometric parameters are shown in Figure 2 and

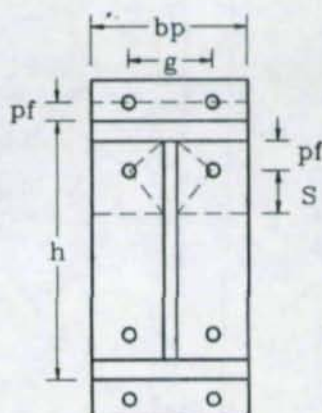


Figure 2. Yield-Line Mechanism

$$m_p = F_{py} t_p^2/4 \quad (3)$$

where  $F_{py}$  is the yield stress of the end-plate material and  $t_p$  is the end-plate thickness. The required end-plate thickness is found by equating Equations (1) and (2) and solving for  $t_p$ :

$$t_p = \left[ \frac{M_u / F_{py}}{\left( \frac{b_f}{2} \left( \frac{1}{p_f} + \frac{1}{s} \right) + (p_f + s) \left( \frac{2}{g} \right) \right) (h - t_f - p_f) + \frac{b_f}{2} \left( \frac{h}{p_f} + \frac{1}{2} \right)} \right]^{1/2} \quad (4)$$

The unknown dimension,  $s$ , in Figure 2 is found by differentiating the internal work expression with respect to  $s$  and equating to zero, resulting in

$$s = \sqrt{b_f g} / 2 \quad (5)$$

The end-plate thickness for the test with shims was determined assuming the required plate bending moment is equal to the effect of the pretensioned bolt forces acting on the end of a cantilever of length  $p_f$ . Equating this moment to the plate plastic moment strength,  $F_{py} b_p t_p^2/4$ , the required end-plate thickness is

$$t_p = \sqrt{8B_t p_f / (F_{py} b_p)} \quad (6)$$

where  $B_t$  is the specified bolt pretension force.

## 2.2 Determination of Bolt Diameter

Kennedy *et al* (1981) proposed a method for predicting bolt forces with prying action in split-tee connections. The Kennedy split-tee analogy consists of a flange bolted to a rigid support with two bolts. The total force at a bolt,  $B$ , is then one-half of the

applied force,  $2F$ , plus the prying force per bolt,  $Q$ . The basic assumption in the Kennedy method is that the plate goes through three stages of behavior as the applied load increases. At the lower levels of applied load, plastic hinges have not developed in the split-tee flange plate and the behavior is termed thick plate behavior. The prying force,  $Q$ , at this stage is assumed to be zero. As the applied load increases, two plastic hinges form at the intersections of the plate centerline and each web face. This yielding marks the "thick plate limit" and indicates the initiation of the second stage or intermediate plate behavior. The prying force at this stage is somewhere between zero and the maximum value. As more load is applied, two additional plastic hinges form at the centerline of the plate and each bolt line. The formation of this second set of plastic hinges marks the "thin plate limit" and indicates the initiation of the third stage or thin plate behavior. The prying force at this stage is at a maximum constant value. Once the status of the plate behavior has been determined, the bolt force is calculated by summing the portion of the applied flange force assigned to the bolt with the appropriate prying force, e.g.  $B = F + Q$ .

Srouji *et al* (1983) and Abel and Murray (1992) modified the Kennedy procedure for the four bolt, end-plate connection. These results are also reported by Murray (1988) and will not be repeated here for lack of space.

Since prying force theoretically does not exist in the connections with shims, the bolt force is simply the pretension forces,  $B_t$ , or  $F$ , whichever is greater.

### 2.3 Determination of Required Column Flange Strength

The required column flange strength was determined using the procedures developed for monotonically loaded moment end-plate connections by Hendrick and Murray (1984) and Curtis and Murray (1989) and summarized in Murray (1990).

## 3.0 TEST SETUP AND INSTRUMENTATION

The physical test setup for the evaluation of the connections is a cantilevered beam connected to a column section as shown in Figure 3. The test setup is in a horizontal plane. Axial loads are not applied to the column or beam. Instrumentation includes displacement transducers to measure beam end deflections, instrumented calipers to measure end-plate and column flange deformations and instrumented bolts to measure bolt forces. To instrument a bolt, a 2 mm hole is first drilled in the head of the bolt to a depth so that a "bolt" strain gage can be installed below the head of the bolt but above the threaded portion of the shank. After insertion of the strain gage, an epoxy is injected into the hole which, on curing, forms a tight bond between the gage and bolt material. The final step is to calibrate the bolt using a tensile test machine.

Quasi-static loading is applied to the end of the cantilever using a hydraulic actuator. The loading history prescribed by ATC-24 "Guidelines for Cyclic Seismic Testing of Components of Steel Structures" (Guidelines 1992) is used for the tests. The loading history consists of two load steps below beam yield, one load step at

yield, and then necessary load steps in excess of yielding until fracture of the connection or severe deterioration of strength is achieved. Each load step consists of three cycles; a cycle consists of two sequential excursions, one in the positive and one in the negative bending direction. The cycles below yield are load controlled and those above yield are displacement controlled. Displacement step increments above yield are equal to the deflection of the beam at yield.

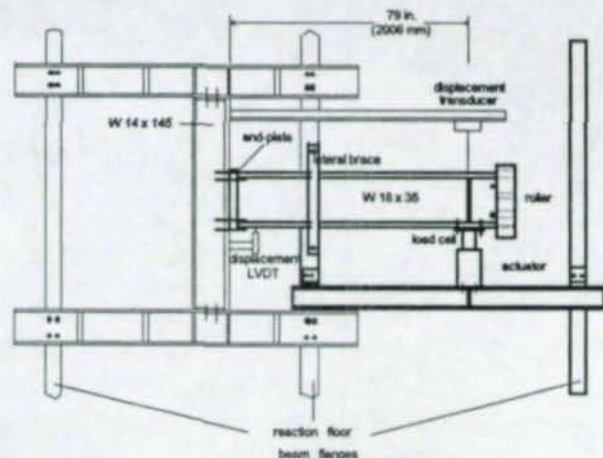


Figure 3. Test Setup

#### 4.0 RESULTS

Table 1 shows the end-plate and bolt dimensions and measured yield stresses for the material used in the three tests. For each test, the end-plate was welded, using full penetration welds, to a W18x35 (W460x52), A36 steel, beam section and bolted to the flange of a W14x145 (W360x216), A36 steel, column section.

Table 1  
Test Specimen End-Plate Dimensions and Material Properties

Test No.	$b_p$ in. (mm)	$t_p$ in. (mm)	$g$ in. (mm)	$p_f$ in. (mm)	$d_b$ in. (mm)	$F_y$ ksi (N/mm <sup>2</sup> )	$F_u$ ksi (N/mm <sup>2</sup> )
1	7.0 (178)	1.0 (25)	4.5 (114)	1.5 (38)	1.0 (25)	40.2 (277)	62.2 (429)
2	7.0 (178)	1.0 (25)	4.5 (114)	1.5 (38)	1.0 (25)	40.2 (277)	62.2 (429)
3	7.0 (178)	1.5 (38)	4.5 (114)	1.5 (38)	1.0 (25)	35.1 (242)	67.2 (463)

For Test 1, a shim was not used and the bolts were tightened, as determined from the instrumented bolts, to the prescribed pretension force in the AISC LRFD Specification (Load 1993). The applied load versus deflection and beam moment

rotation histories from the test are shown in Figure 4(a). Figure 5(a) shows the corresponding exterior and interior bolt force versus applied load history. Local buckling of the beam flange, 9 in. - 11 in. (229 mm - 279 mm) from the face of the end-plate occurred toward the end of the 16th cycle. Neither the end-plate, welds, bolts or column flange showed any distress during the test. The hysteresis loops shown in Figure 4(a) are robust and significantly wider than those reported for fully welded connections. As seen in Figure 5(a), there was a substantial loss of bolt forces. However, these losses did not effect the strength of the connection.

Test 2 was identical to Test 1, except that the bolts were tightened using the turn-of-nut method (Load 1993). This tightening method resulted in larger strains in the bolts on completion of tightening. Figures 4(b) and 5(b) show results corresponding to those for Test 1. Again, failure was local buckling of the beam flanges without end-plate, weld, bolt or column flange distress. The bolt forces decreased as in Test 1, but not as significantly.

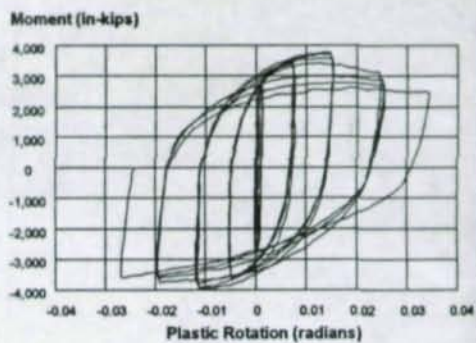
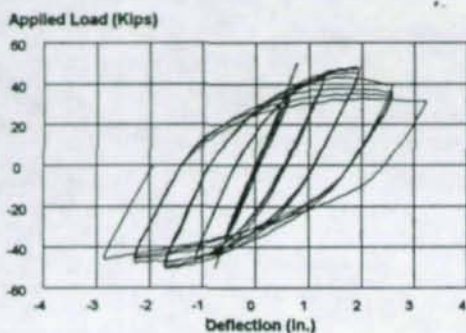
Test 3 was conducted with 0.50 in. (13 mm) thick shims placed as shown in Figure 1(b). The bolts were tightened to the minimum pretension level as measured by the instrumented bolts. Failure was by local buckling of the beam flange without end-plate, weld, bolt or column flange distress. Figures 4(c) and 5(c) show the load-displacement and bolt force-load histories. Again, the hysteresis loop is wide. Bolt forces decreased unexpectedly, possibly because of yielding of the shim plates.

## 5.0 CONCLUSIONS

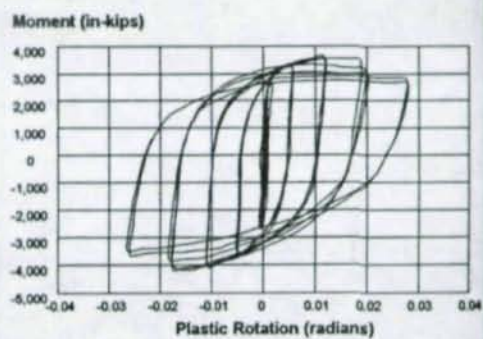
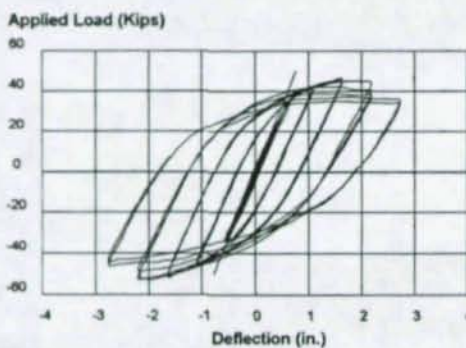
Properly designed end-plate connections appear to be viable connections for frames designed for seismic loading. The end-plate connection tests reported here show that the strength and energy dissipation capability, necessary to resist large seismic loadings, are available.

## 6.0 ACKNOWLEDGMENT

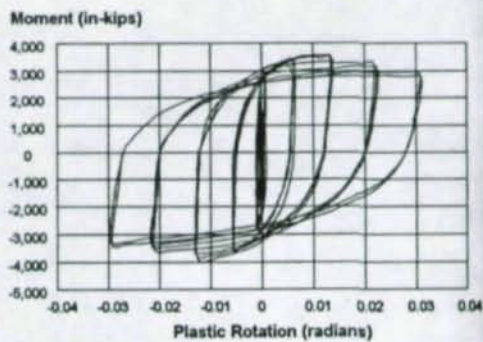
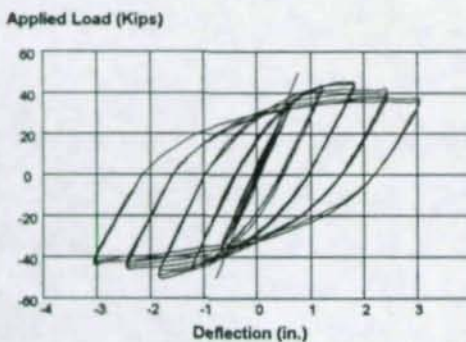
This research was funded in part by the National Science Foundation, Arlington, Virginia, Grant No. CMS-9416171.



(a) Test #1

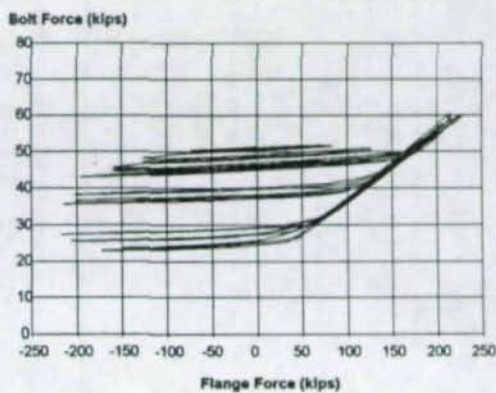
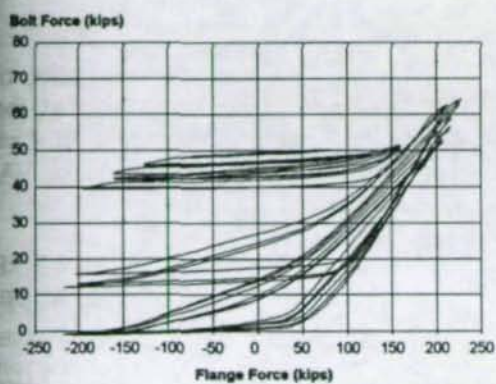


(b) Test #2

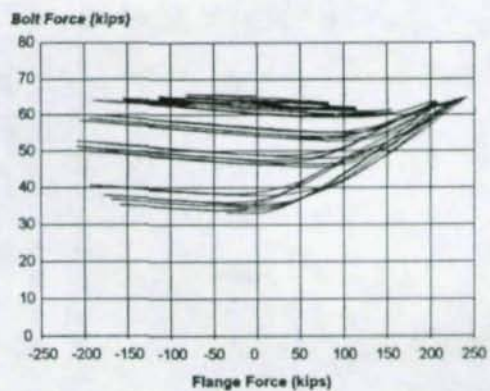
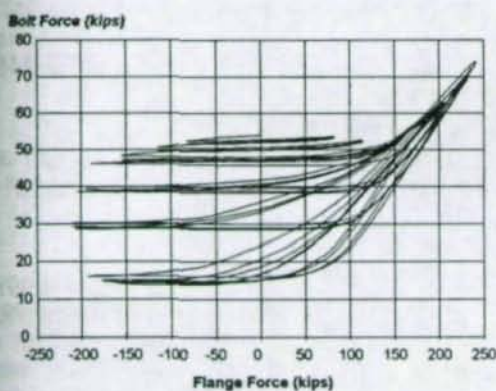


(c) Test #3

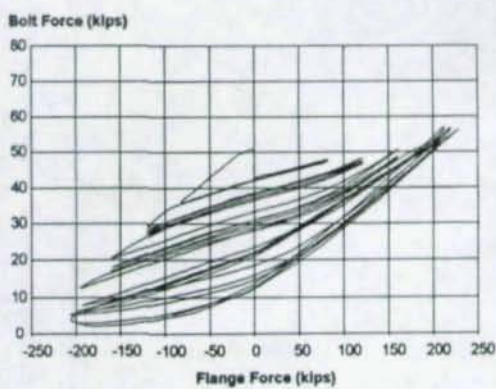
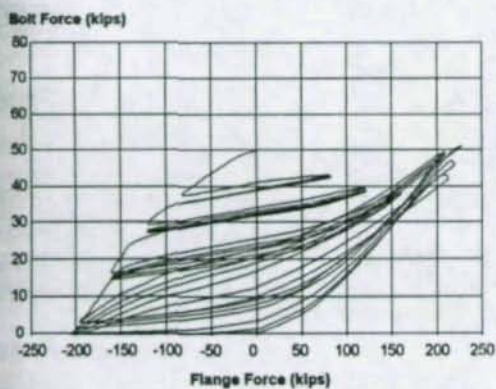
Figure 4. Load Deflection and Beam Rotation Histories



(a) Test #1 Inner and Outer Bolt Forces



(b) Test #2 Inner and Outer Bolt Forces



(c) Test #3 Inner and Outer Bolt Forces

Figure 5. Bolt Force Histories

## 7.0 REFERENCES

- Abel, M. S. and T. M. Murray (1992), "Analytical and Experimental Investigation of the Extended Unstiffened Moment End-Plate Connection with Four Bolts at the Beam Tension Flange," Research Report CEVPI-ST-93/08, Department of Civil Engineering, Virginia Polytechnic Institute and State University, Blacksburg, VA, December (Revised October 1994).
- Curtis, L. E. and T. M. Murray (1989), "Column Flange Strength at Moment End-Plate Connections," *Engineering Journal*, 26, (2) (2nd Qtr), AISC, Chicago, IL, pp. 16-19.
- Ghobarah, A., Osman, A. and Korol, R. M. (1990), "Behavior of Extended End-Plate Connections under Cyclic Loading," *Engineering Structures*, Vol. 12(1), pp. 15-27.
- Ghobarah, A., Korol, R. M. and Osman, A. (1992), "Cyclic Behavior of Extended End-Plate Joints," *Journal of Structural Engineering*, Vol. 118(5), pp. 1333-1353.
- "Guidelines for Cyclic Seismic Testing of Components of Steel Structures (ATC-24)" (1992), Applied Technology Council, Redwood City, CA.
- Hendrick, R. A. and T. M. Murray (1984), "Column Web Compression Strength at End-Plate Connections," *Engineering Journal*, 21, (3), AISC, Chicago, IL, pp. 161-169.
- Kennedy, N. A., S. Vinnakota and A. N. Sherbourne (1981), "The Split-Tee Analogy in Bolted Splices and Beam-Column Connections," *Joints in Structural Steelwork*, John Wiley & Sons, London-Toronto, pp. 2.138-2.157.
- "Load and Resistance Factor Design Specification for Structural Steel Buildings" (1993), AISC, Chicago, IL.
- Murray, T. M., "Extended End-Plate Moment Connections," (1990), *Steel Design Guide Series*, 4, AISC, Chicago, IL.
- Murray, T. M., (1988), "Recent Developments for the Design of Moment End-Plate Connections," *Journal of Construction Steel Research*, 10, pp. 133-162.
- Murray, T. M., Kline, D. P. and Rojiani, K. B. (1992), "Use of Snug-Tightened Bolts in End-Plate Connections," *Connections in Steel Structures II: Behavior, Strength and Design, Proceedings of the Second International Workshop*, Pittsburgh, Pennsylvania, pp. 27-34.
- Srouji, R., A. R. Kukreti and T. M. Murray (1983), "Yield-Line Analysis of End-Plate Connections with Bolt Force Predictions," Research Report FSEL/MBMA 83-05, Fears Structural Engineering Laboratory, University of Oklahoma, Norman, OK, December.
- Tsai, K. C. and Popov, E. (1990), "Cyclic Behavior of End-Plate Moment Connection," *Journal of Structural Engineering*, 116 (11), pp. 2917-2930.

# LOW CYCLE FATIGUE TESTING OF SEMI-RIGID BEAM-TO-COLUMN CONNECTIONS

Luis Calado<sup>1</sup>

Carlo Castiglioni<sup>2</sup>

## Abstract

A research was carried out to investigate the cyclic behaviour of beam-to-column connections. Three different typologies were tested, which represent frequent applications in steel construction. The specimens were submitted, in a multi-specimen testing program, to constant amplitude displacement histories, in order to develop a cumulative damage model. Such a model is based on the Ballo-Castiglioni hypothesis and Miner's rule, and lead to the assessment of possible classes of fatigue resistance for the examined typologies of beam-to-column connections. Based on the experimental results of this and previous research programs carried out by the authors, a general failure criterium is proposed for steel components under low-cycle fatigue.

## 1. INTRODUCTION

For constructions in seismic regions, steel structures in general offer a large advantage with respect to r.c. structures, due to reduced dead load, and thus reduced inertial forces. Furthermore, the material ductility is satisfactory. However, evidence of structural collapses has been reported in occasion of recent earthquake events (Northridge 1994, Kobe 1995) and a significant population of steel structures suffered extended damage, in buildings, bridges, and viaducts.

Following the Northridge Earthquake of January 17, 1994 several cases have been reported (Bertero et al., 1994) of steel frame buildings which did not collapse, yet exhibited significant structural damage. Local failures of steel structural members or their connections, or both, took place. Such failures, however, did not result in severe overall deformations, thus remaining hidden behind undamaged architectural panels. A variety of local collapses was observed, among which the recurrent case was identified in the failure of welded beam-to-column joints in moment resisting space frames. Investigations have been carried out about the nature and the causes of the observed failures and have shown that several topics pose unsolved problems, thus providing subjects of primary importance for research programs.

Recent analyses have shown that well proportioned semi-rigid connections designed to allow active participation in non-linear deformation may enhance the dynamic performance of steel frames in low and medium rise buildings and reduce the ductility demand on other members under severe ground motions.

---

<sup>1</sup> Associate Professor, Civil Engineering Department, Technical University of Lisbon

<sup>2</sup> Associate Professor, Department of Structural Engineering, Politecnico of Milan

For these reasons, recently, several research programs have been conducted to investigate the cyclic behaviour of semi-rigid connections. Among them the tests performed by Ballio et al. (1987) on flange plated connections, flange and web cleated connections, extended-end-plate connections and welded connections is pointed out. Astaneh et al. (1989) investigated the behaviour of steel double angle framing connections under severe cyclic loading of earthquakes. The experimental research that Bernuzzi et al. (1992) have conducted was on top-and-seat angle and flush-end-plate connections under cyclic loading.

In addition to these and other experimental research programs, a number of numerical models were also developed by various authors. Most of these models are empirical, and need experimental results for the calibration of the various parameters assumed as governing the behaviour of the connection.

This paper presents preliminar results of a research program on low-cycle fatigue of semi-rigid beam-to-column connections. After identifying a limited number of structural steel details, they were realised and tested under low cycle fatigue. The aim of the research is to try to establish classes of (low cycle) fatigue resistance for connections, similar to those existing for structural details under high cycle fatigue (EC3 - Design of steel structures, 1992).

## 2. EXPERIMENTAL PROGRAM

### 2.1 Test Set up

The experimental set-up used for the tests on the semi-rigid steel connections is shown in Figure 1. It was designed in order to simulate the conditions of beam-to-column connections within the frame structure. It consists mainly in a foundation, a supporting girder, a reaction wall, a power jackscrew and a lateral frame.



Figure 1 - Test set-up.

The power jackscrew, which displays a 1000 kN capacity and a 400 mm stroke, is attached to a specific frame, designed to accommodate the screw backward movement, which has been prestressed against the reaction wall. The specimen was connected to the supporting girder through two steel elements. Due to the characteristics of the test set-up the column lies horizontally, while the beam is vertical. The supporting girder was fastened to the reaction wall and to the foundation by prestressed bars. The forces  $F$  are measured in a load cell located between the power jackscrew and the specimen, while the top displacement  $v$ , is evaluated at the level of the applied force. An automatic testing technique was developed to allow computerised control of the power jackscrew, the displacement and all the transducers used to monitor the specimen.

## 2.2 Specimen Set up

The specimen consisted of a beam attached to a column by means of different details. Three typologies of connections were selected which represent frequent solutions adopted in steel construction for beam-to-column connections: web and flanges cleats - BCC1 type, (Fig. 2a), extended end plate - BCC2 type, (Fig. 2b) and flange plates with web cleats - BCC3 type, (Fig. 2c). For each typology three specimens were realised and tested, according to a multi-specimen testing program.

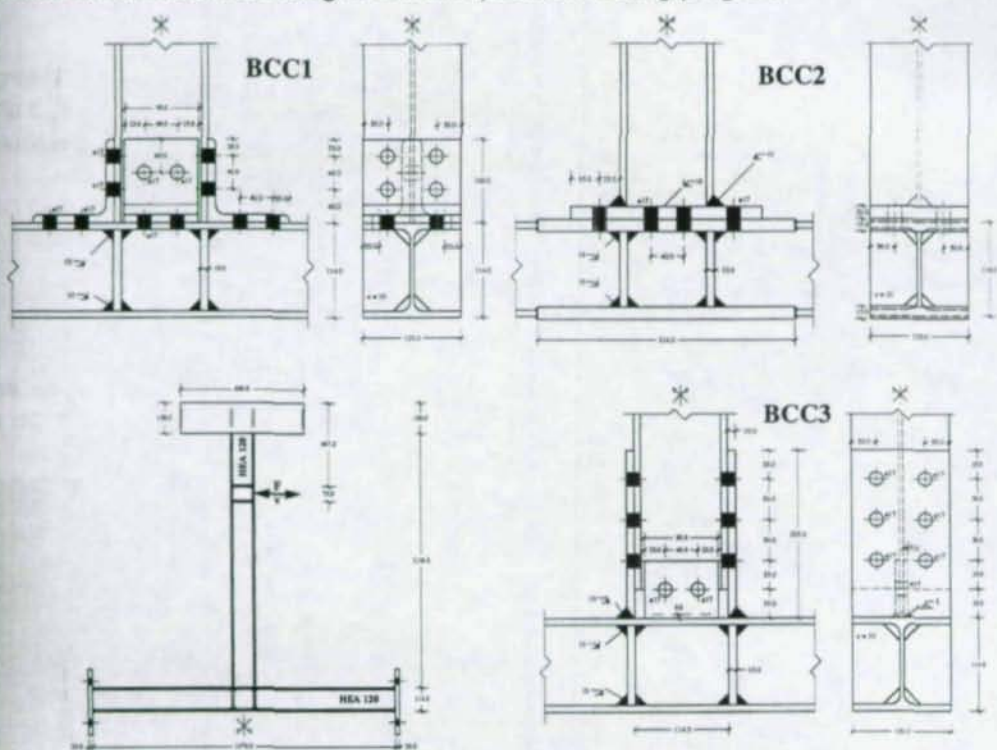


Figure 2 - Typologies of connections considered in this research.

The profile used for columns and beams in all specimens was a HEA120 in Fe360. For the web and flanges cleats specimens 100x100x10 angles in Fe360 were adopted. The bolts used were M16 grade 8.8 and all welds were full penetration butt welds. Specimens were instrumented with electrical displacement transducers. They measure the displacement of the specimen supporting plates, the vertical displacement of the joint and the relative and absolute rotation of the cross-section and joint.

### 2.3 Loading History Adopted

The choice of a testing history associated to a testing program depends on the purpose of the experiment, type of test specimen and type of anticipated failure mode. In general, a *single-specimen testing program* is adopted. The recommended loading history to be applied in such a testing program (such as those proposed by ECCS (1986) and ATC (1992)) consists of stepwise increasing deformation cycles; the cycles are usually symmetric in peak deformations.

However, as it is also clearly stated in ATC Guidelines (1992), a *multi-specimen testing program* is needed if a cumulative damage model is to be developed for the purpose of assessing the performance of a component under arbitrary loading histories. In particular a cumulative damage model may be adopted to evaluate the cumulative effect of inelastic cycles on a limit state of acceptable behaviour.

A cumulative damage model is generally based on a damage hypothesis and may include several structural performance parameters that must be determined experimentally. For these reasons testing program utilising this cumulative damage model requires at least three constant amplitude loading tests on identical test specimens. For each test, a new specimen must be used, since each specimen is to be tested to failure. The deformation amplitudes for the three tests should be selected so that they cover the range of interest for performance assessment.

In the present study, the following amplitudes of displacement cycles were considered  $\Delta v/v_y = 6, 8$  and  $12$  for BCC1 type,  $\Delta v/v_y = 6, 7$  and  $8$  for BCC2 type and  $\Delta v/v_y = 6, 8$  and  $10$  for BCC3 type, where  $\Delta v$  is the imposed displacement at the top of the specimen, while  $v_y$  is the yield displacement.

## 3. EXPERIMENTAL RESULTS

Hysteresis loops in a load-displacement diagram ( $F-v$ ) and the failure mode are presented in Figure 3, 4 and 5. Some observations on the behaviour of each type of connections during the cyclic test until the collapse are made.

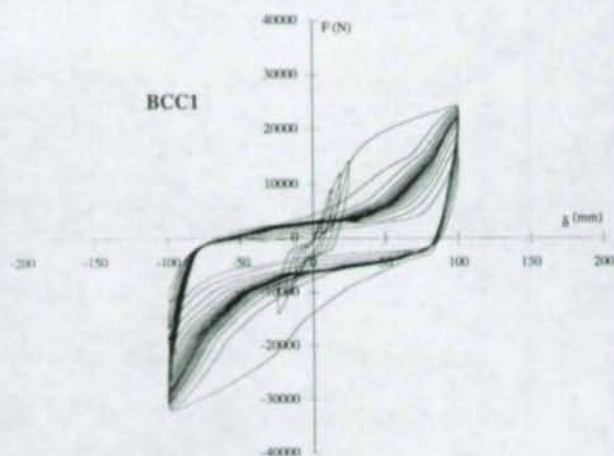


Figure 3 - Experimental hysteresis loops and the failure mode of a web and flanges cleats connection.

*Web and flanges cleats connections - BCC1 type:* the behaviour of this type of connection is characterised by large bolt slippage. The increment of plastic deformations in both legs of the angles in the flange connections was observed during the test. Slip occurred mainly in the vertical plane between the beam flange and the vertical angle leg due to the ovalization of the holes in the flange of the beam and in the vertical leg of the angle. For all specimens of this type the failure was due to a horizontal crack that started in the middle of each vertical leg of the angles when they were in tension. These cracks propagated with increasing the number of cycles until complete failure of the angle.

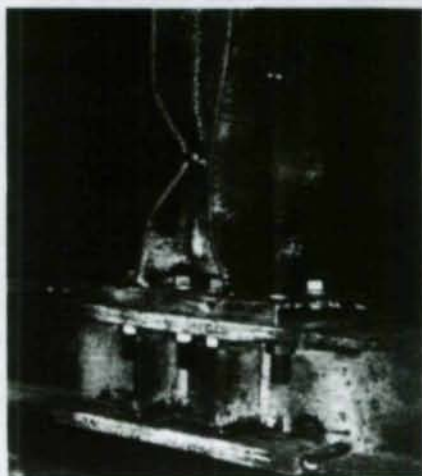
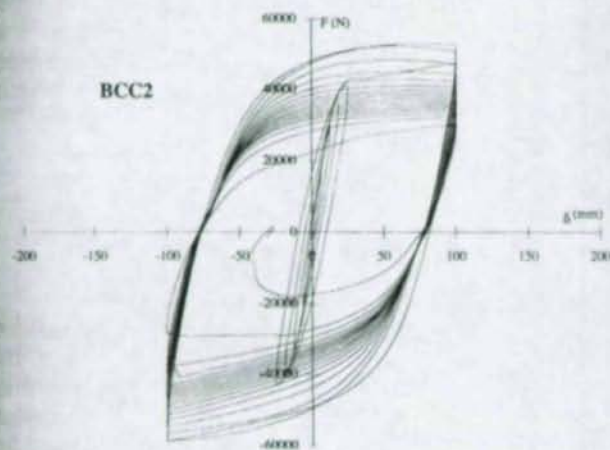


Figure 4 - Experimental hysteresis loops and the failure mode of an extended end plate connection.

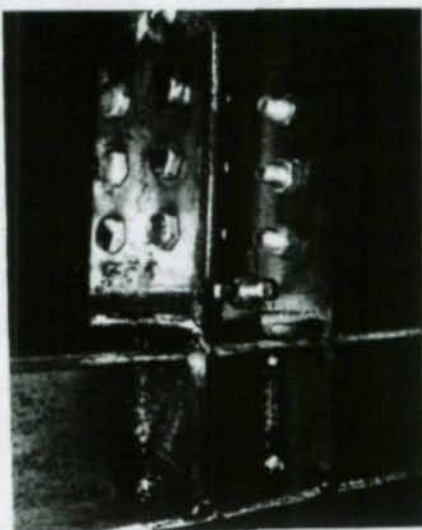
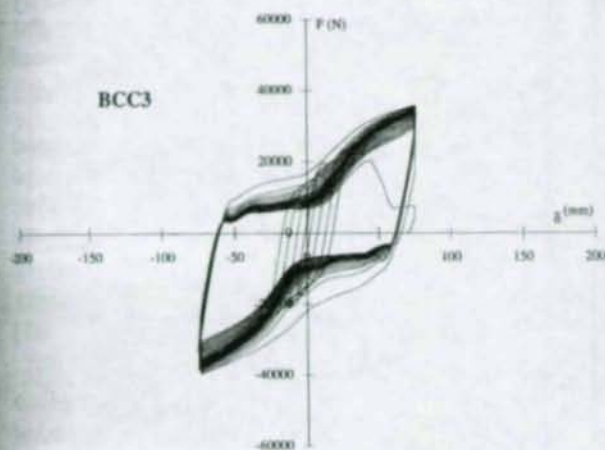


Figure 5 - Experimental hysteresis loops and the failure of a flange plates with web cleats connection.

*Extended end plate connections - BCC2 type:* the connections of this type are characterised by regular hysteresis loops, without any slippage and with a regular deterioration of the absorbed energy and the maximum force at the end of each cycle. For the three specimen a plastic hinge took place in the beam. The local buckling of the flanges and web of the beam induce large plastic deformations in these zones. The effect of the bending and the tension of these zone induce the development of cracks which started for the three specimens in the flange of the beam. The cracks grow with

the increase of the number of the cycles until they reach all the section of the flange and part of the section of the web cause the failure of the specimen. At the end of each test an axial shortening of the specimen was observed due to the occurrence of a highly localised deformations of the specimens.

*Flange plates with web cleats connections - BCC3 type:* this type of connection has a behaviour between the BCC1 type, and the BCC2 type. They exhibit slippage between flange plates and the flange of the beam due to the ovalization of the holes, but this phenomena has lower importance when compared with web and flanges cleats connections. The flange plate had a similar behaviour as the angles in BCC1 type under bending deformation but the vertical separation between the beam and the column is avoid. In all specimens the failure was due to the crack in the vertical plates that connect the flange of the beam with the flange of the column. No shear deformation was observed in all bolts.

#### 4. FAILURE CRITERIUM

It is particularly interesting to formulate some failure criteria based on the achievement of a given level of deterioration of the mechanical properties of the material. In fact, by means of such a collapse criterium, the limit state at which a structural component is considered out-of-service, can be a-priori defined. Such a situation, of course, may not coincide with actual collapse of the component. However, in order to be applied in standard design procedures, such a collapse criterium must allow an assessment of the failure conditions as close to reality as possible, and always on the safe side.

Some authors (Calado and Azevedo, 1989) proposed to adopt as unified failure criterium the reduction of the energy dissipated in a cycle to 50% of that dissipated by a structural component made of an elastic perfectly plastic material, cycled under the same amplitude. That criterium was formulated based on a number of numerical simulations of the cyclic behaviour of steel members (Ballio and Calado, 1986).

Based on the experimental results obtained during extensive testing programs carried out on beams, beam-columns, welded connections (Castiglioni, 1995, Ballio and Castiglioni, 1994) and on beam-to-column connections (Calado and Ferreira, 1994) the following failure criterium can be formulated having a general validity for structural steel components under variable amplitude loading:

$$\eta_f / \eta_0 \leq \alpha \quad (1)$$

where  $\eta_f$  represents the ratio between the real absorbed energy at the last cycle before collapse ( $E_{cf}$ ) and the energy that might be absorbed in the same cycle if the structural member had an elasto-plastic behaviour ( $E_{cppf}$ ), while  $\eta_0$  represents the ratio between the real absorbed energy in the first cycle in plastic range ( $E_{c0}$ ) and the energy that might be absorbed in the same cycle if the structural member had an elasto-plastic behaviour ( $E_{cpp0}$ ).

In the case of constant amplitude displacement,  $E_{cppf}$  is equal to  $E_{cpp0}$ , and equation (1) may be rewritten as follows:

$$E_{cf} / E_{c0} \leq \alpha \quad (2)$$

In equations 1 and 2  $\alpha$  is a parameter which value should be determined by fitting the experimental results. Based on the results obtained in a multi-specimen tests program for beam-to-column connections under different levels of constant amplitudes it is proposed for  $\alpha$  a constant value equal to 0.50. This means that the failure of the connection took place when the ratio between the real absorbed energy and the real absorbed energy in the first cycle in plastic range is less or equal to 0.50. The value leads to consistent results also in the case of beams and beam-columns made by HEA220 and IPE300 profiles. Other types of profiles are presently under investigation.

The proposed value of  $\alpha$  can be adopted for a safe assessment of the damage cumulated in the beam-to-column connections. Hence, this value is not to be considered as the best fit of experimental results, but can be regarded as possible reference value in damage assessment procedures.

## 5. CUMULATIVE DAMAGE ASSESSMENT

From tests carried out it was noticed (Ballio and Chen, 1993) that, in good agreement with other previous studies (Coffin, 1954, Mason, 1954), for all structural components (beams, beam columns, welded joints, beam-to-column connections), the relationships which best fitted the experimental results in terms of cycle amplitude  $\Delta v$  (normalised on the yield displacement  $v_y$ ) and number of cycles to failure  $N_f$ , were exponential functions of the type  $N_f = a (\Delta v/v_y)^b$ , with  $a$  and  $b$  constant parameters to be defined and calibrated on the experimental test results. If the cycle amplitude  $\Delta v$  can be correlated to the stress range in the component  $\Delta\sigma$ , this kind of relationships become similar to the Wöhler S-N lines [Wöhler, 1860] usually adopted in high-cycle fatigue design.

Starting from these considerations, Ballio and Castiglioni (1994) recently proposed an approach to unify the design and damage assessment procedures for steel structures under low and/or high cycle fatigue.

According to Ballio and Castiglioni (1994), if the material can be regarded as an elastic perfectly plastic one (as in the case of steel), it can conventionally be assumed that strains are proportional to the generalised displacement component  $s$ , and it can be stated that:

$$\frac{\Delta\epsilon}{\epsilon_y} = \frac{\Delta s}{s_y} \quad (3)$$

This equation defines the nominal strain range in a particular way, taking into account the local reduction of stiffness at plastic hinge location by an equivalent uniform reduction of stiffness along the total beam length, and can be re-written as follows:

$$\Delta\sigma^* = E = E \frac{\Delta s}{s_y} \epsilon_y = \frac{\Delta s}{s_y} \sigma(F_y) \quad (4)$$

$\Delta\sigma^*$  is an effective stress range, associated to the real strain range  $\Delta\varepsilon$  in an ideal member made of an indefinitely linear elastic material and, in the case of high cycle fatigue (i.e. under cycles in the elastic range) coincides with the actual stress range  $\Delta\sigma$ .

Once determined the number of cycles to failure  $N_f$ , test data can be re-processed to plot in a log-log scale  $N_f$  vs.  $\Delta\sigma^*$  given by eq. (4). The domain  $\log(\Delta\sigma^* = E\Delta\varepsilon)$  vs.  $\log N$  is the usual domain for the Wöhler (S-N) curves adopted by various International Codes and Standards for (high cycle) fatigue design of steel structures. In practice, by adopting the S-N curves of EC3, which can be mathematically expressed in the form:

$$N_f \Delta\sigma^3 = K \quad (5)$$

(where  $K$  is a constant value depending on the fatigue strength category of the detail), and by substituting in eq. (5) to  $\Delta\sigma$  the expression of  $\Delta\sigma^*$  given in eq. (4), the relationship between  $N_f$  and the generalised displacement amplitude  $\Delta s$  becomes:

$$N_f \left[ \frac{\Delta s}{s_y} \sigma(F_y) \right]^3 = K \quad (6)$$

By comparing this expression to the Manson (1954) Coffin (1954) one (7):

$$N_f [\Delta s_p]^c = C^{-1} \quad (7)$$

it can be concluded that the two expressions are similar; the only difference is that in equation (6) the total cycle amplitude  $\Delta s$  is adopted while Manson and Coffin consider the excursion in the plastic range  $\Delta s_p$ .

The two expressions (6) and (7) coincide for  $C=1/K$ ,  $c=3$  and  $\Delta s_p = \frac{\Delta s}{s_y} \sigma(F_y)$ .

By considering equation (6) and adopting Miner's rule, the proposed damage model becomes:

$$D = \frac{1}{K} \sum_i^L n_i \left( \frac{\Delta s_i}{s_y} \sigma(F_y) \right)^3 \quad (8)$$

where  $n_i$  is the number of occurrences of cycles having an amplitude  $\Delta s_i$ , and the summation is extended to the number  $L$  of different cycle amplitudes  $\Delta s_i$  to be considered.

## 6. CONCLUSIONS

If an equivalent stress range  $\Delta\sigma^* = E \Delta\varepsilon$  is considered, associated with the actual strain range in an ideal indefinitely elastic material, the S-N lines given by Codes for high cycle fatigue can be adopted for interpreting the low cycle fatigue behaviour of beam-to-column connections, as shown in Figure 6 with regard the experimental results described in previous section 3.

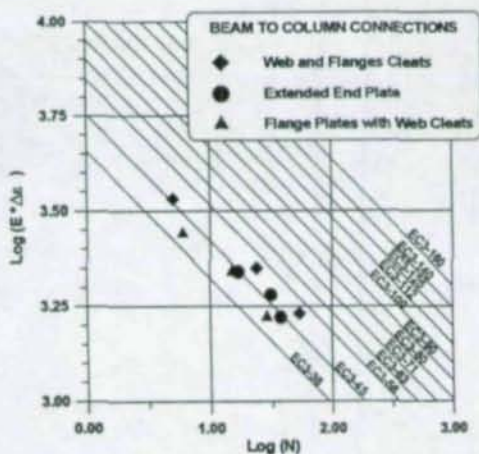


Figure 6 - Fatigue strength of beam-to-column connections.

Miner's rule can be adopted, together with the previously defined S-N curves and with a cycle counting method (e.g. Rainflow) to define a unified collapse criterion, valid for both high and low cycle fatigue.

The main issue became, in this case, the assessment of fatigue strength category of various typologies of the connections, i. e., of the appropriate S-N curve to be associated with each type of detail. This can be done either by means extensive experimental research or by numerical modelling. Such models should, however, be calibrated on tests results.

In any case a reliable failure criterium must be defined, allowing conservative definition of the number of cycles to failure, i. e. of the conditions corresponding to specimen collapse.

A possible failure criterium having a general validity and giving consisting results for a number of structural components has been proposed in this paper. The validity of such criterium must however to be furtherly investigated and extended to other structural details.

## 7. ACKNOWLEDGMENTS

This experimental work was sponsored by the JNICT - Junta Nacional de Investigação Científica e Tecnológica through the research programme PBIC/C/CEG/1344/92 - Ligações em Estruturas Metálicas. The authors wish to thank the collaboration of Ing.s João Ferreira and Alberto Drei for their contribution in this research program. The execution of the experimental tests had the participation and dedication of Ing. Raúl Malho.

## 8. REFERENCES

Bertero V., Anderson J., Krawinkler H., "Performance of steel buildings structures during the Northridge earthquake", Rept. UCB/EERC-94/09, August 1994.

Ballio G., Castiglioni C.A., "Seismic behaviour of steel sections", *Journal of Constructional Steel Research*, 1994, n.29, pp.21-54.

Astaneh, A. Nader, M. N. and Malik, L., "Cyclic behaviour of double angle connections", *ASCE, Journal of Structural Engineering*, 1989, vol. 115, n.5.

ECCS, Technical Committee 1 - Structural Safety and Loadings, Technical Working Group 1.3 - Seismic Design, 1986, Recommended testing procedure for assessing the behaviour of structural steel elements under cyclic loads.

Ballio, G. Calado, L. De Martino, A. Faella, C. and Mazzolani, F. M. "Cyclic behaviour of steel beam-to-column joints: experimental research", 1987, *Costruzioni Metalliche* n.2.

Bernuzzi, C. Zandonini, R. and Zanon, P. "Semi-rigid steel connections under cyclic loads", 1992, *First World Conference on Constructional Steel Design*. Acapulco.

ATC - Applied Technology Council, "Guidelines for cyclic seismic testing of components of steel structures", ATC 24, 1992.

Eurocode 3: Design of Steel Structures-Part 1-1: General rules and rules for buildings, ENV1993-1-1, February 1992.

Wöhler A., "Zeitschrift für Bauwesen", vol.10, 1860.

Ballio G., Chen Y., "An experimental research on beam to column joints: exterior connections", *Proc. C.T.A., Viareggio*, 1993, pp. 110-120.

Calado L., Ferreira J., "Cyclic behaviour of steel beam to column connections: an experimental research", *Proc. Int. Workshop on Behaviour of Steel Str. in Seismic Areas, Timisoara*, 26-6/1-7, 1994.

Ballio G., Castiglioni C.A. "An approach to the seismic design of steel structures based on cumulative damage criteria", *Earthquake Engineering & Structural Dynamics*, Vol. 23, n.9, 1994, pp. 969-986.

Castiglioni C.A., "Seismic behaviour of steel beam-column members", *SSRC Proc. ATS&M, Kansas City*, March 1995.

Castiglioni C.A., "Seismic damage assessment of steel members and joints", *SSRC Proc. ATS&M, Kansas City*, March 1995.

Calado, L and Azevedo, J., "A model for predicting failure of structural steel elements", *Journal of constructional steel research*, n<sup>o</sup> 14, 1989.

Ballio, G. and Calado, L., "Steel bent sections under cyclic loads. Experimental and numerical approaches", *Costruzioni Metalliche*, n<sup>o</sup> 1, 1986.

Coffin, L. F., "A study of the effects of cyclic thermal stresses on a ductile method", *trans. ASME*, 76, 1954.

Mason, S., "Behaviour of material under conditions of thermal stress", *Heat transfer Symposium*, NACA TN 2933, 1954.

## DEVELOPMENT OF INTERIM RECOMMENDATIONS FOR IMPROVED WELDED MOMENT CONNECTIONS IN RESPONSE TO THE NORTHRIDGE EARTHQUAKE

Michael D. Engelhardt<sup>1</sup>  
Thomas A. Sabol<sup>2</sup>  
Riyad S. Aboutaha<sup>3</sup>  
Karl H. Frank<sup>4</sup>

### Abstract

A short term research and testing program was conducted in response to damage observed at a large number of welded steel moment connections following the 1994 Northridge Earthquake. The test program investigated several changes to joint welding and design procedures intended to improve earthquake response of steel moment frame connections. Sixteen very large scale beam-to-column connections were tested under cyclic load. The most successful connections tested in this program were those in which the beam flanges were reinforced with cover plates or vertical ribs. The test results showed that reinforcing the connection to reduce stress at the beam flange groove welds, combined with reasonable care in welding can significantly enhance joint performance.

### 1. STEEL MOMENT CONNECTION DAMAGE

Following the January 17, 1994 Northridge Earthquake, significant damage was observed at beam-to-column moment connections in steel moment resisting frames. More than 100 modern steel buildings suffered moment connection damage. This damage was observed primarily at the conventional welded flange-bolted web type moment connection detail widely used in west coast U.S. practice for the past 25 years. A variety of different types of fractures were observed

---

<sup>1</sup>Assoc. Prof. of Civil Eng., Univ. of Texas at Austin, Austin, Texas 78712

<sup>2</sup>President, Englekirk & Sabol, Inc., PO Box 77-D, Los Angeles, Calif., 90007

<sup>3</sup>Asst. Prof. of Civil Eng., Georgia Inst. of Tech., Atlanta, Georgia 30332

<sup>4</sup>Prof. of Civil Eng., Univ. of Texas at Austin, Austin, Texas 78712

at these connections, including fractures at the beam flange groove welds, and fractures in the columns within the joint region, typically initiating at the beam flange groove weld. Fractures occurring at or initiating at the beam bottom flange groove weld appear to have occurred far more frequently than at the beam top flange.

None of the connection damage resulted in collapse of a steel moment frame building nor did it result in loss of life. This damage, however, is contrary to the design intent of an earthquake resistant steel moment frame, and may represent a more serious safety concern for ground motions that differ in intensity, duration, or frequency content from that experienced in Northridge. The causes of the observed connection damage have been the subject of considerable debate. It appears, however, that a number of factors related to welding, joint design, and steel material properties played a role in the damage. More detailed descriptions of damage and discussions of contributing causes are available elsewhere (AISC 1994b, Bertero *et al.* 1994, SAC 1994a, SAC 1994b, SAC 1994c, SAC 1995). In addition to its poor performance in the Northridge Earthquake, the conventional welded flange-bolted web connection detail has also shown a history of poor performance in laboratory tests (Engelhardt and Husain 1993).

## 2. TEST PROGRAM

Within approximately three months following the Northridge Earthquake, a short term intensive testing program was initiated under the guidance of the AISC Task Committee on the Northridge Earthquake. This test program was intended to generate some immediate data on the effectiveness of various measures intended to improve connection performance under earthquake loading. This program was directed towards steel moment frames that were under design or construction at the time of the earthquake, and that were in need of immediate guidance. Thus, the objective of the test program was to develop interim guidelines for the design and construction of improved steel moment connections, *in the shortest possible time*. The test program emphasized connection details for new construction, and was not intended to investigate repair procedures for damaged joints. This paper provides a brief overview of the test program. More complete details are available elsewhere (AISC 1994a).

Tests were conducted on single cantilever type test specimens, as shown in Figure 1. Slowly applied cyclic loads were applied at the tip of the cantilever. Beam tip displacement was increased until connection failure occurred, or until the limits of the testing apparatus were reached. Test specimen performance was judged primarily based on the level of inelastic deformation achieved in the beam prior to connection failure. All test specimens were constructed of W36x150 beams of ASTM A36 steel, and either W14x455 or W14x426 columns of ASTM A572 Gr. 50 steel. These member sizes resulted in joints with very strong panel zones, so that inelastic action at the joint was forced into the beam.

A number of different connection details were investigated in the test program. The connections incorporated what were intended to be improvements both in welding and in connection design.

In order to guide the test program, AISC organized an advisory group representing a broad range of expertise, including researchers, structural engineers, fabricators, erectors, steel mill representatives, welding specialists, and welding inspection and NDT personnel. Based on the advise of this group, improved connection design details and welding procedures were developed.

For each connection investigated in this test program, two replicates were constructed by two different structural steel fabricators in order to gain some confidence in the repeatability of results. A total of sixteen specimens were tested. Highlights for several of these tests are discussed below.

The first connection detail investigated was the conventional welded flange - bolted web detail, designed in accordance with the seismic detailing provisions of the 1991 Uniform Building Code (Uniform 1991), the governing code in the western U.S. The detail for this specimen, designated as Specimen 1, is shown in Figure 2. Although the conventional connection detail was used, several improvements were incorporated in the welding, including removal of backup bars and weld tabs, and close attention to welding workmanship. Welding was accomplished by the self shielded flux cored arc welding (FCAW) process, as it was for all specimens in this test program. The electrode used for the beam flange groove welds for Specimen 1 was classified as E70T-4, typical of past field welding practice for this connection. This electrode is characterized by very high deposition rates, but can result in weld metal with rather low toughness and ductility. The purpose of this specimen was to determine if the conventional connection detail, when provided with very good welding workmanship, was likely to provide satisfactory performance.

Both replicates of Specimen 1 showed poor performance, developing only very limited ductility in the beam prior to connection failure. The load-deflection response at the tip of the beam for one of the two replicates of this detail (designated as Specimen 1A) is shown in Figure 3. Failure of both replicates occurred by sudden fracture at the beam flange groove welds, with the fractures occurring near the weld column interface. No welding workmanship defects were visible on the fracture surfaces.

The second connection detail investigated in this test program was an all-welded connection. It was similar to the first detail, except that the beam web, rather than being bolted, was welded directly to the column flange. As with the previous detail, the E70T-4 electrode was used for the beam flange groove welds. Past test programs have typically shown better performance from all-welded connections, as compared to welded flange-bolted web details (Popov and Stephen 1972, Tsai and Popov 1988). This better performance has been attributed to the improved ability of the welded web connection to transfer bending moment at the connection, thereby reducing stress on the beam flange welds. Unfortunately, both replicates of this connection detail showed poor performance, with fractures occurring at the beam flange groove welds early in the inelastic loading history for the specimens. As above, no significant workmanship defects were identified on the fracture surfaces.

These first four test specimens showed unsatisfactory performance, despite very good welding workmanship, removal of back up bars, and removal of weld tabs. These results suggest that

the poor performance of these connections in the Northridge Earthquake likely cannot be attributed solely to poor welding workmanship. This observation does not necessarily indicate that workmanship was not a significant issue in the Northridge connection damage. It does indicate, however, that there are factors other than workmanship that significantly affect connection performance. The poor performance of the first four specimens does not necessarily warrant condemnation of these connection details. These details may have shown better performance if, for example, a different welding electrode or welding process had been chosen. Unfortunately, there was no opportunity to investigate this hypothesis as part of this test program. The effects of varying weld metal properties, and most notably weld metal toughness, is being investigated in a new test program currently underway by the authors.

The majority of the remaining connection details tested in this program were classified as reinforced connections. The beam flanges were reinforced with cover plates or with vertical "ribs". An example of a connection reinforced with vertical ribs, designated as Specimen 6, is shown in Figure 4. An example of a connection reinforced with cover plates, designated as Specimen 8, is shown in Figure 6.

The intent of these reinforced connections was to significantly reduce the stress on the beam flange groove welds and surrounding base metal regions, and to move the location of the beam plastic hinge away from the face of the column. The design goal adopted for the reinforced connection was that the region of the connection at the face of the column should remain essentially elastic under the maximum bending moments and shear forces developed by the fully yielded and strain hardened beams. For the various reinforcement configurations tested, the section modulus of the reinforced cross-section was on the order of 1.6 to 2.0 times the section modulus of the unreinforced beam cross-section. In addition to reinforcing the flanges, different FCAW electrodes were used for some of these specimens, and continuity plates were added for some of the specimens.

Eight of the ten reinforced connections showed excellent performance, developing very large inelastic deformations in the beam without connection failure. The beam tip load versus deflection response for a connection reinforced with ribs (Specimen 6B) is shown in Figure 5. The response for a connection reinforced with cover plates (Specimen 8A) is shown in Figure 7. These connections performed as intended. The beam plastic hinge formed at the end of the reinforcement, away from the face of the column, while the region of the connection near the face of the column remained essentially elastic. The connections were capable of developing the full flexural strength and ductility of the beams.

Two of the connections reinforced with cover plates showed poor performance, experiencing brittle failures at low levels of beam ductility. One cover plated specimen failed by a sudden fracture at the top flange/cover plate weld to the column. This fracture occurred near the weld-column interface, and showed no visible workmanship defects. Inspection data for this specimen suggested that some of the welding parameters (voltage, electrical stickout, etc.) were likely beyond the range specified in the Welding Procedure Specification. Studies of this failure suggest that the improper choice of welding parameters lead to weld metal with unusually low toughness. The replicate of this specimen, with the same connection design and welding electrode, but for which the Welding Procedure Specification was followed, showed excellent

performance. *The Structural Welding Code - Steel*, AWS D1.1-94 (AWS 1994) requires that welding be executed in accordance with a written and approved Welding Procedure Specification. These test results emphasize the importance of this requirement. They also suggest a relationship between weld metal toughness and overall connection performance.

A second cover plated specimen failed by a sudden fracture within the column flange material at the beam's bottom flange connection, pulling out a portion of the column flange material. The fracture surface suggested a possible problem with through-thickness properties of the column flange. This test specimen indicated that even with a reinforced connection and careful welding practices, material properties may represent a "weak link" for this type of connection.

### 3. CONCLUSIONS

The results of this test program suggest that improved welding workmanship, by itself, may not be adequate to assure satisfactory performance of the conventional welded flange - bolted web connection detail under inelastic cyclic loading. The results also indicate that a large improvement in cyclic loading performance is possible at steel moment frame joints by the use of a reinforced connection combined with careful attention to welding.

Based on the limited evidence provided by these tests, definitive guidelines for the design and construction of welded steel moment connections are not possible. However, based on their judgement and interpretation of the available data, the writers recommend the use of reinforced connections as an interim measure until additional data becomes available. Sizing reinforcement so that the section modulus of the reinforced cross-section at the face of the column is on the order of 1.5 to 2 times the section modulus of the unreinforced beam cross-section appears reasonable. Items likely to be beneficial for welding include: removal of backup bars and weld tabs, use of electrodes that provide high toughness weld metal, careful inspection at the time of welding, including the rigorous enforcement of Welding Procedure Specifications, and thorough ultrasonic inspection.

It should be noted that even with a reinforced connection and careful attention to welding, the test results indicate poor performance may still be possible due to potential weaknesses in the column flange through-thickness properties. Nonetheless, while perhaps not guaranteeing success 100 percent of the time, the use of reinforced connections is expected to provide a much higher level of performance and structural safety, as compared to pre-Northridge practices. It is also clear from these tests that a large number of welding, design, and materials related factors significantly affect connection performance. A long term research effort will be needed to fully resolve all the issues raised by the Northridge Earthquake.

### Acknowledgements

The primary funding for this work was provided by the American Institute of Steel Construction, Inc., and by the J. Paul Getty Trust. Additional funding or donation of materials or services were provided by PDM Strocal, Inc., The Herrick Corporation, The Lincoln Electric Company, Twining Laboratories of Southern California, British Steel Inc., Nucor-Yamato Steel Co., TradeArbed Steel, Gayle Manufacturing, Dr. P.V. Banavalker, and the National Science Foundation Young Investigator Award (Grant BCS-9358186).

Many individuals provided advice or other services to this project, including Ed Beck, Omer Blodgett, Al Collin, Robert Englekirk, Mike Engstrom, Roger Ferch, J.C. Gerardy, Nestor Iwankiw, Fred Long, Jim Malley, Hank Martin, Duane Miller, Lowell Napper, Clarkson Pinkham, Tom Pike, Egor Popov, Jeff Post, Tim Potyraj, Bob Pyle, Rob Ryan, Mark Saunders, Alan Shiosaki, Bill Shindler, Tim Wharton, Nabih Yousef, and Joseph Yura. The writers are especially grateful to the late Geerhard Haaijer of AISC for providing leadership and guidance for this test program. The opinions expressed in this paper are those of the writers and do not necessarily reflect the views of the sponsors or of the individuals listed above.

### References

- American Institute of Steel Construction, Inc. (1994a). *Northridge Steel Update I*.
- American Institute of Steel Construction, Inc. (1994b). *Proceedings of the AISC Special Task Committee on the Northridge Earthquake Meeting, March 14-15, 1994*.
- Bertero, V.V., Anderson, J.C., Krawinkler, H. (1994). "Performance of Steel Building Structures During the Northridge Earthquake," *Report No. UCB/EERC-94/09*, Earthquake Engineering Research Center, University of California at Berkeley.
- Engelhardt, M.D. and Husain, A.S. (1993). "Cyclic Loading Performance of Welded Flange-Bolted Web Connections," *Journal of Structural Engineering*, ASCE, Vol. 119, No. 12.
- Popov, E.P and Stephen, R.M. (1972). "Cyclic Loading of Full Size Steel Connections," *Bulletin No. 21*, American Iron and Steel Institute, Washington, D.C.
- SAC Joint Venture. (1994a). *Invitational Workshop on Steel Seismic Issues, September 8-9, 1994*. Report No. SAC 94-01.
- SAC Joint Venture. (1994b). *Steel Moment Frame Connection - Advisory No. 1*.
- SAC Joint Venture. (1994c). *Steel Moment Frame Connection - Advisory No. 2*.

SAC Joint Venture. (1995). *Steel Moment Frame Connection - Advisory No. 3*. Report No. SAC 95-01.

*Structural Welding Code - Steel*, American Welding Society, Miami, Fla., 1994.

Tsai, K.C. and Popov, E.P. (1988). "Steel Beam-Column Joints in Seismic Moment Resisting Frames," *Report No. UCB/ERC-88/19*, Earthquake Engineering Research Center, University of California at Berkeley.

*Uniform Building Code*, International Conference of Building Officials, Whittier, California, 1991.

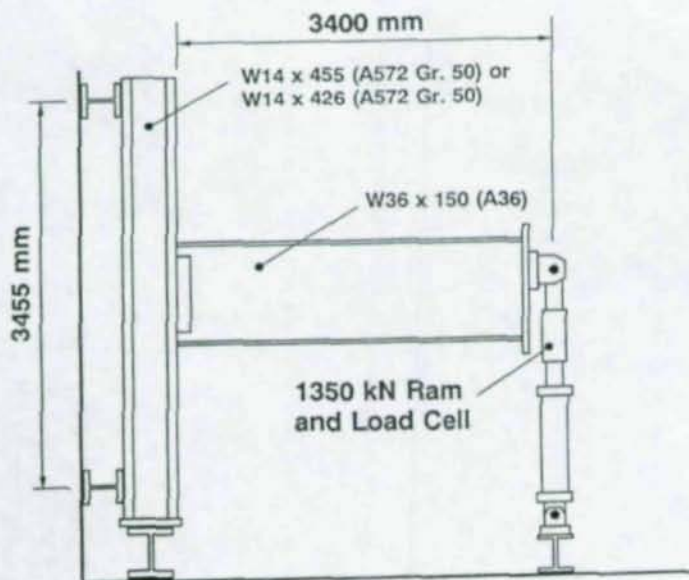


FIGURE 1 - TEST SETUP

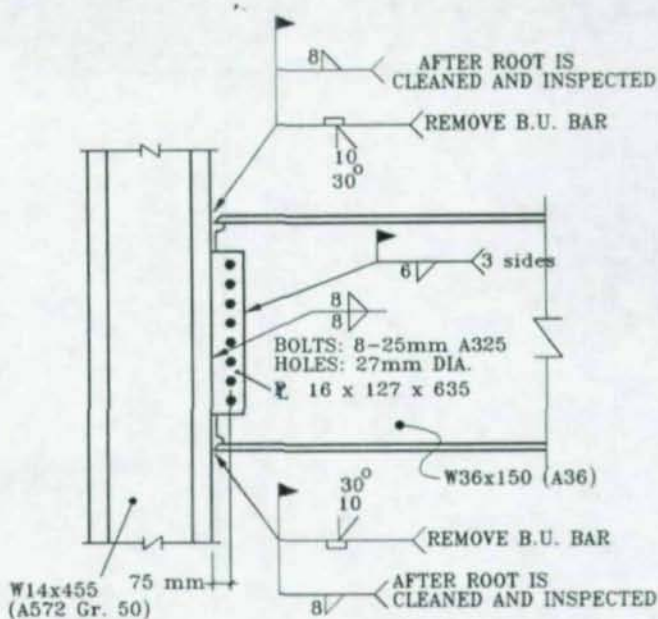


FIGURE 2 - SPECIMEN 1 CONNECTION DETAIL

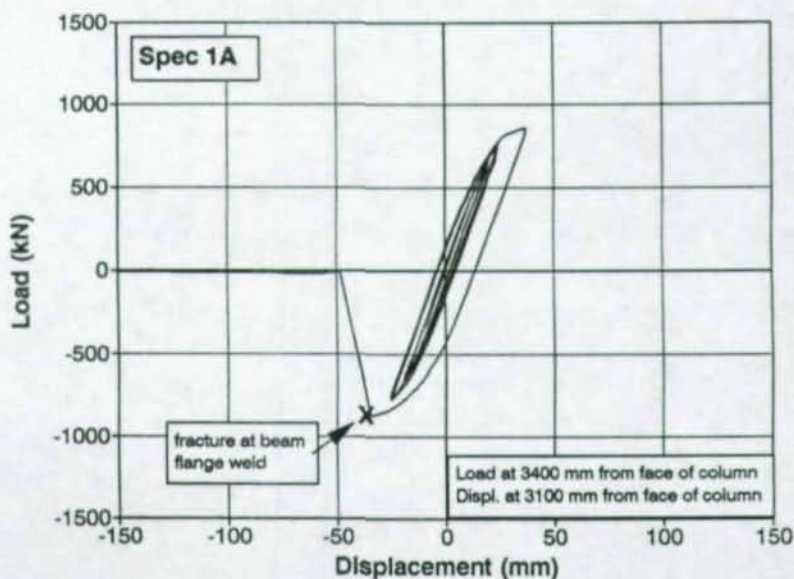


FIGURE 3 - HYSTERETIC RESPONSE FOR SPECIMEN 1A



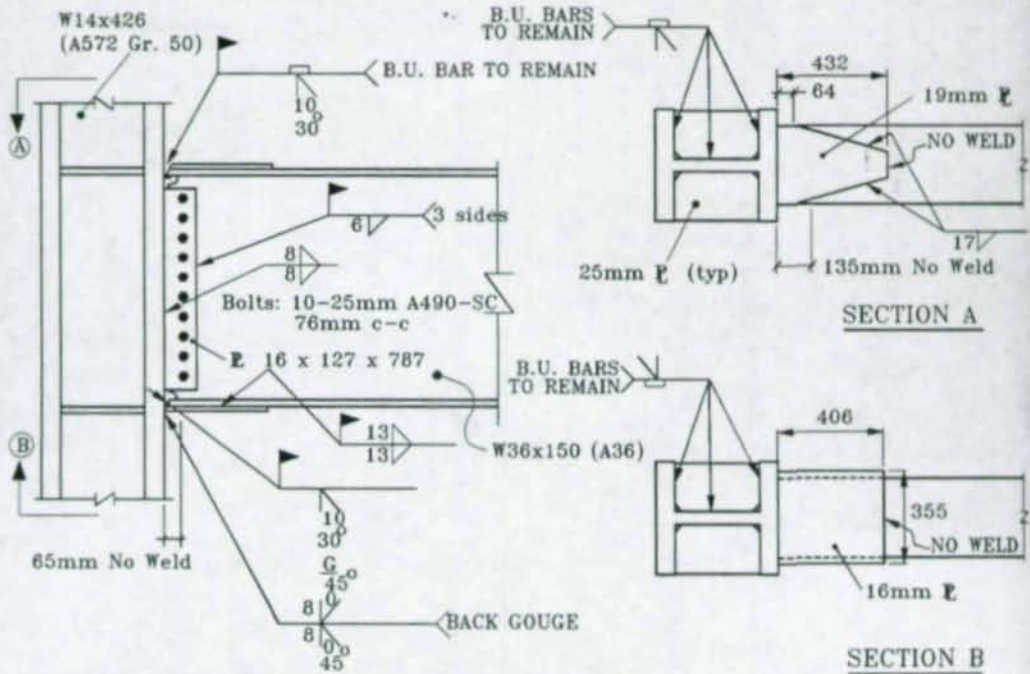


FIGURE 6 - SPECIMEN 8 CONNECTION DETAIL

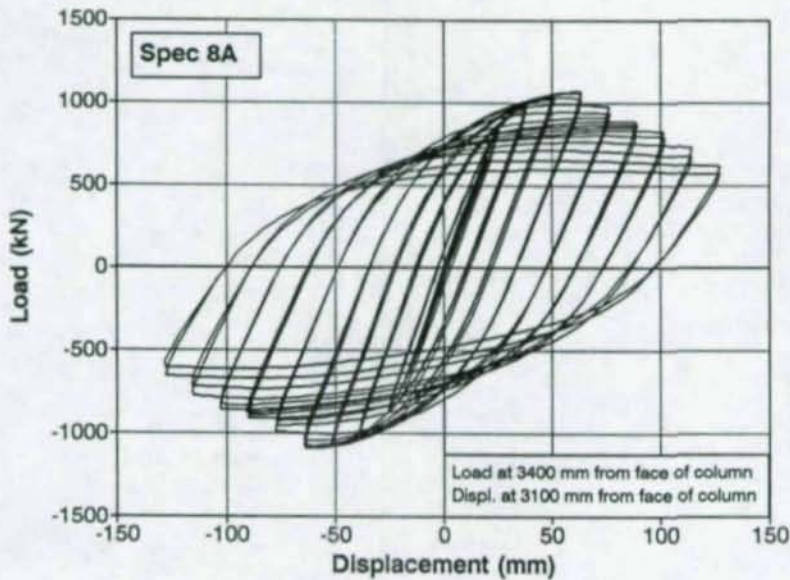


FIGURE 7 - HYSTERETIC RESPONSE FOR SPECIMEN 8A

# POST-EARTHQUAKE STABILITY OF STEEL MOMENT FRAMES WITH DAMAGED CONNECTIONS

Abolhassan Astaneh-Asl<sup>1</sup>

## Abstract

The objective of this study was to study seismic safety of welded steel moment frames damaged during the 1994 Northridge earthquake. A 4-story, a 14-story and a 27-story buildings in Los Angeles were studied. Inelastic 2-D models of the undamaged and damaged frames representing the three buildings were subjected to various intensities of several past earthquake records. The results indicated that seismic behavior of the damaged frames was somewhat similar to the behavior of steel semi-rigid frames. The cracks in the bottom flange welds did not cause the study-frames to be more susceptible to collapse than the same frames before the damage. No tendency to collapse due to  $P-\Delta$  effects was detected in the three study-frames subjected to various intensities of the earthquake records that were used.

## 1. INTRODUCTION

### 1.1. Background

During the January 17, 1994 Northridge earthquake the welded joints of more than 100 steel moment frame buildings in Los Angeles cracked. The cracks in the welded rigid

---

<sup>1</sup>Professor, Department of Civil and Environmental Engineering, 781 Davis Hall, University of California, Berkeley, CA, 94720, USA.

connections were mostly in the full-penetration welds or the heat-affected zone of the bottom flange of the girders. However, to lesser extent, cracks were also found in the top flange welds, column flanges, column webs and the panel zones. A few shear connections have also been cracked. In many cases, the damaged buildings did not exhibit visible out-of-plumbness or damage to their non-structural elements. A few weeks after the quake, this study of seismic safety of the damaged welded steel moment frames was initiated. The highlights of the study are summarized here. More information can be found in (Astaneh-Asl et al., 1995).

### **1.2. Objectives of the Study**

The main objective of the study was to investigate life-safety aspects of the welded steel moment frames damaged in Los Angeles by the 1994 Northridge earthquake. More specifically, the objective was to develop information on the question of: is there a safety concern in case the damaged steel moment frame buildings are shaken by another earthquake or by a sizable aftershock of the Northridge earthquake before appropriate repairs or retrofits are done?

## **2. RESEARCH**

### **2.1. Methodology**

To achieve the objectives and considering the public concern for the safety of the damaged steel structures, the research team conducted case studies and investigated seismic safety of three modern buildings that were damaged. The buildings were a 4-story, a 14 story and a 27 story welded steel moment frame buildings in Los Angeles. The frames are shown in Figure 1. Table 1 provides major properties of the three buildings. The structures were designed according to the modern seismic codes and are representative of the current design practices in California.

The study consisted of building inelastic computer models of one critical frame from each of the three buildings and subjecting the models to various intensities of

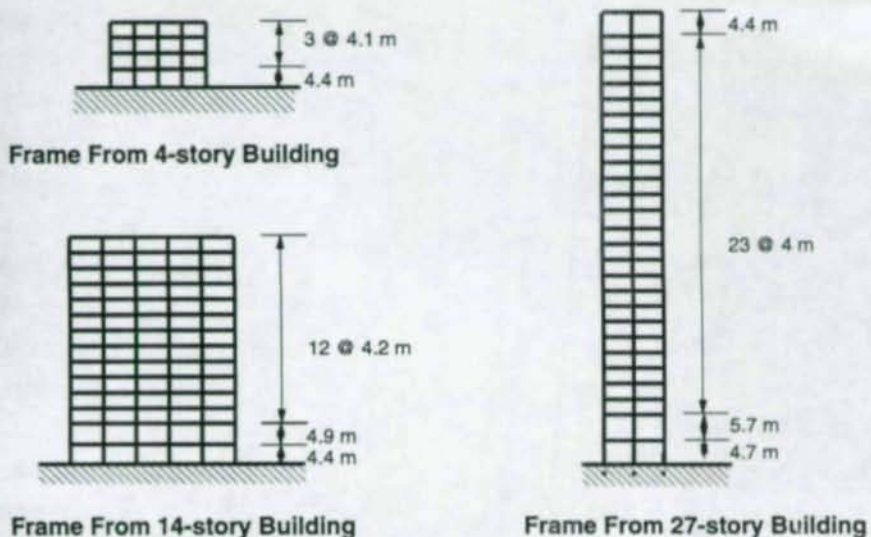


Figure 1. Frames from Three Case Study Buildings

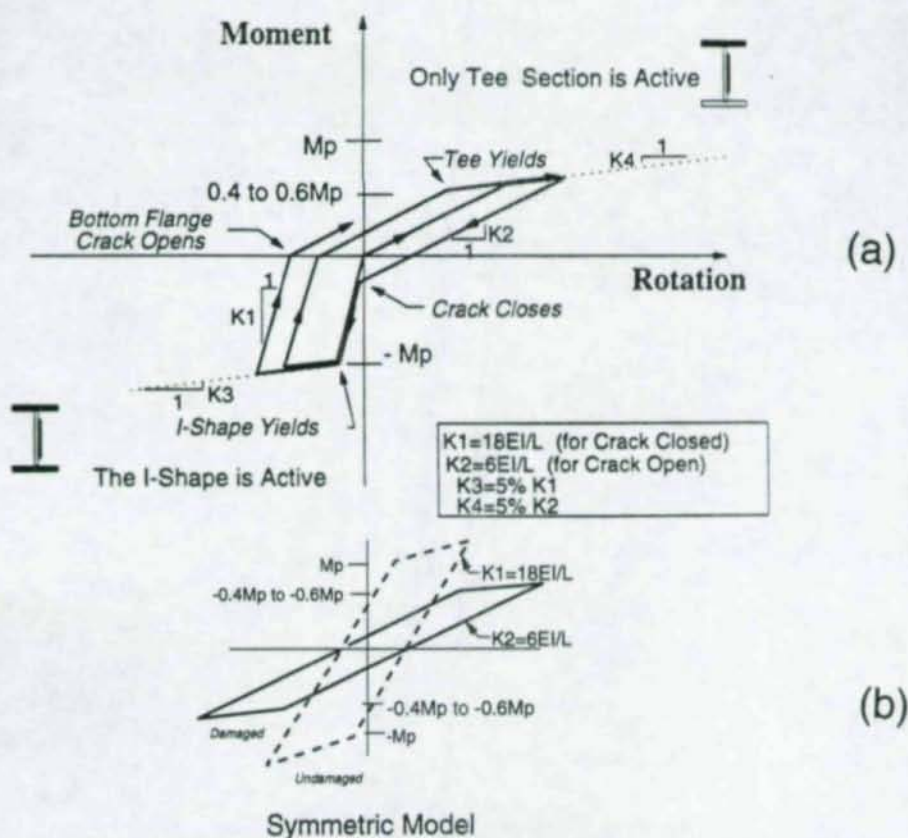


Figure 2. Model of Damaged Connections

acceleration time history records. The acceleration time history records of the 1940 El-Centro, 1952 Taft, 1978 Miyagi-ken-Oki, and the 1994 Northridge-Newhall earthquakes were used. Whenever the vertical component was available, the horizontal and vertical components of the earthquake were applied simultaneously. In selecting the past earthquake records for these studies the records representing pulse type near fault earthquakes, long duration earthquakes as well as long distance earthquakes were included. The results presented in this paper are only for various intensities of Northridge earthquake records. The responses of the frames to El-Centro, Miyagi-ken-Oki and Taft records were in general similar to Northridge results.

## **2.2. Modeling of the Undamaged and Damaged Frames**

One rigid frame from each of the three buildings was selected to represent the structure. Then, two models were developed for each frame: one undamaged and one heavily damaged model. The undamaged frames represented the structures before the earthquake. In the damaged structure, the frame was modeled with the bottom weld in all of its connections cracked. A recently released survey of the damage in 59 buildings in Los Angeles (Youssef et al., 1995) indicates that, on the average, only about 20% of the connections in surveyed buildings had cracked. The assumption of all bottom flange welds cracked was a conservative assumption to represent the possibility that during future larger earthquakes more connections can develop cracks.

The girders and columns in both damaged and undamaged frames were modeled to have a bi-linear cyclic moment-rotation behavior. The cracked connections were modeled as semi-rigid as explained in the following section.

## **2.3. A Proposed Model to Represent Cracked Welded Connections**

The analysis program DRAIN-2DX used in these studies could only accept symmetric, bi-linear moment-rotation models for the connections. The actual behavior of the connections with one flange crack is unsymmetric. To overcome this limitation and still to obtain meaningful results, the unsymmetric moment-rotation behavior of the cracked connections was converted to their equivalent symmetric moment-rotation curves. At the time of these studies, February through July of 1994, no test data was available on the actual cyclic behavior of the cracked connections of welded steel moment frames. Therefore, by using the available information on cyclic behavior of steel semi-rigid

connections (Nader, and Astaneh-Asl, 1992), and by considering mechanics of the cyclic behavior of the welded connections before and after crack, the model shown in Figure 2(a) was developed and proposed by the author.

Recently, four cyclic tests of actual cracked connection specimens, taken from a damaged building in Los Angeles, have been conducted (Anderson and Xiao, 1995). The results of these tests, although very limited in numbers, are very close to the proposed model and confirm the above assumptions. To be fit for DRAIN-2DX program, the model in Figure 2(a) was then converted to the symmetric model of hysteretic behavior shown in Figure 2(b).

In developing the cyclic model of the moment-rotation behavior, it was assumed that the connection with bottom flange cracked can develop full strength of the girder if applied moment is negative (i.e. the weld crack is closed and is in compression) and the connection can develop 40-60% of the girder plastic moment capacity when moment is positive (i.e. the weld crack in the bottom flange is open). The value of 40-60% moment capacity for the cracked connections was established by calculating  $M_p$  of the Tee cross section that is left after the bottom flange is cracked, see Figure 2(a).

### 3. RESULTS

#### 3.1 Behavior of Undamaged and Damaged Frames From the 4-Story Building

Figure 3 shows time histories of roof drift for the actual record of the 1994 Northridge earthquake obtained from a California Strong Motion Instrumentation Program (CSMIP) station located about 1.5 km from this 4-story building. The studies indicate that the base shear and roof drift responses of the damaged frame is less than the undamaged rigid frame. The exception is the first peak at about 4 seconds into the earthquake when damaged frame indicates a drift of about 3.5%. Up to the Point "A" in Figure 3, the drift responses of both frames are almost identical. However, after the first peak the response of damaged (semi-rigid) frame is much less than the undamaged (rigid)

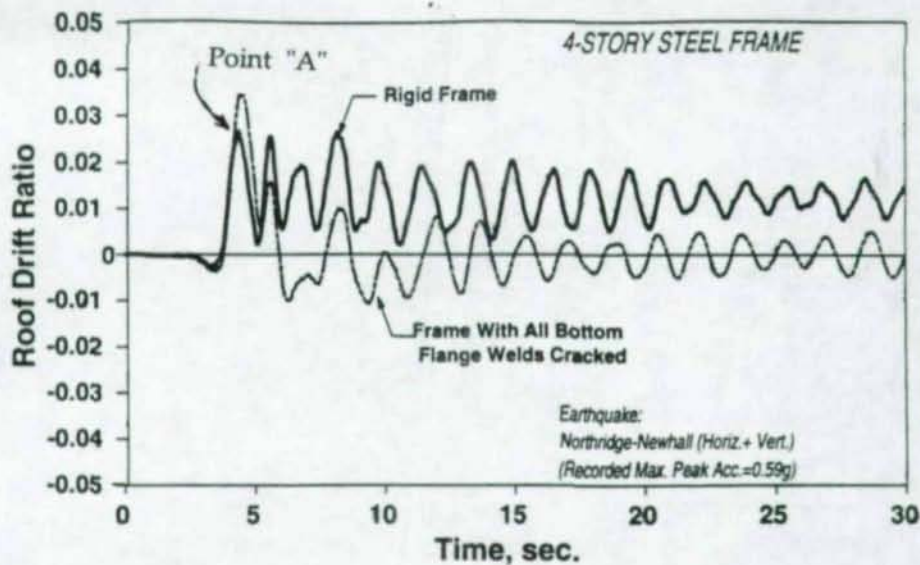


Figure 3. Drift Responses of Frames from 4-Story Building

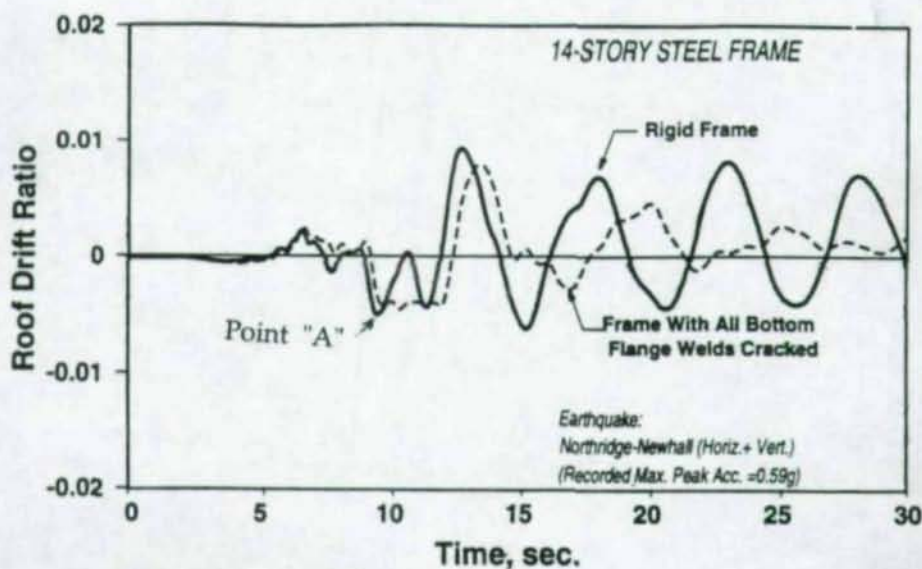


Figure 4. Drift Responses of Frames from 14-Story Building

frame. Also, notice that the undamaged frame shows a permanent drift (out-of-plumbness) of more than 1%.

During the Northridge earthquake, in the case of this 4-story building, probably at Point "A" in Figure 3, the connections have been cracked. After the frames were damaged at the time of about 4 seconds into the quake, the structure has become a semi-rigid structure and has responded according to the substantially smaller "dashed" line response in Figure 3. This can be an explanation why the observed damage to the non-structural elements of this building was relatively minor and the out-of-plumbness after the quake was only about 5 cm (less than 0.3% drift) at the roof level.

### **3.2 Behavior of Undamaged and Damaged Frames From the 14-Story Building**

Figure 4 shows time histories of roof drift of the 14-story structure, when subjected to the same Northridge-Newhall earthquake record used for the 4-story building. However, it should be mentioned that the 14-story building is located about 30 km from the station that recorded the Northridge-Newhall ground motion. The results indicate that for this building, subjected to Northridge-Newhall records, the roof drift and base shear of the damaged semi-rigid frame is smaller than the roof drift of the undamaged but rigid frame throughout the response.

The undamaged rigid frame develops a maximum peak roof drift of about 1.3% while maximum peak roof drift of damaged semi-rigid frame is about 1.1%. Up to the Point A in Figure 4, the responses of both frames to Northridge-Newhall record are very close. However, after the first peak at Point A in Figure 4, the response of the damaged (semi-rigid) frame is less than the response of the undamaged (rigid) frame. This behavior is very similar to the behavior of 4-story building presented earlier.

### **3.3 Behavior of Undamaged and Damaged Frames From the 27-Story Building**

As mentioned earlier, the study-frames were subjected to ever-increasing maximum peak acceleration levels of the records from Northridge-Newhall, El-Centro, Taft and Miyagi-ken-Oki earthquakes. In this section, the results of undamaged and damaged frame models of the 27-story building subjected to scaled-up Northridge-Newhall records with 1.5g maximum peak acceleration are presented.

Figure 5 shows the results of dynamic response of the 27-story structure, (see Table 1) before it was damaged and after it is assumed that all bottom flange welds have been cracked.

The results indicate that the roof drift of the undamaged and damaged frame models are very similar during the earthquake. After ground shaking has stopped at the time of 15 seconds, the response of the damaged frame (semi-rigid) is less than the undamaged (rigid) structure. Similar to previous cases, this indicates that after the frame is damaged, the response is "slowed down". The maximum value of roof drift for both undamaged and damaged frames subjected to Scaled-up Newhall record with 1.5g MPA was about 2%

The fact that the roof drift of the damaged (semi-rigid) frame is less than the roof drift in undamaged (rigid) frame might appear to be contrary to the belief of some structural engineers who feel that after the structure is damaged, it is more flexible and weaker, therefore, it will develop larger drifts. This feeling might be correct for static loading and might have stemmed from the code based equivalent static load design concept. However, the available data on seismic response of steel structures do not support this simplistic and somewhat erroneous view of the actual complex dynamic behavior of steel structures.

Figure 6 shows the time history of axial load in one of the exterior columns of the first floor of the 27-story Undamaged and damaged frames. The undamaged (rigid) frame developed large tension during many cycles even after the earthquake had stopped. The damaged frame developed relatively small tension and only during the earthquake. Similar phenomenon was also noted when the frames were subjected to smaller intensities and other earthquakes.

The large value of axial forces in the columns of these moment frames was in part related to the inclusion of the vertical component of the ground motion. Often dynamic analysis is done by only applying the horizontal components of the acceleration records. However, these and other studies (Astaneh-Asl, et al., 1994) have indicated that in many structures including buildings and bridges relatively large vertical inertia forces can be developed.

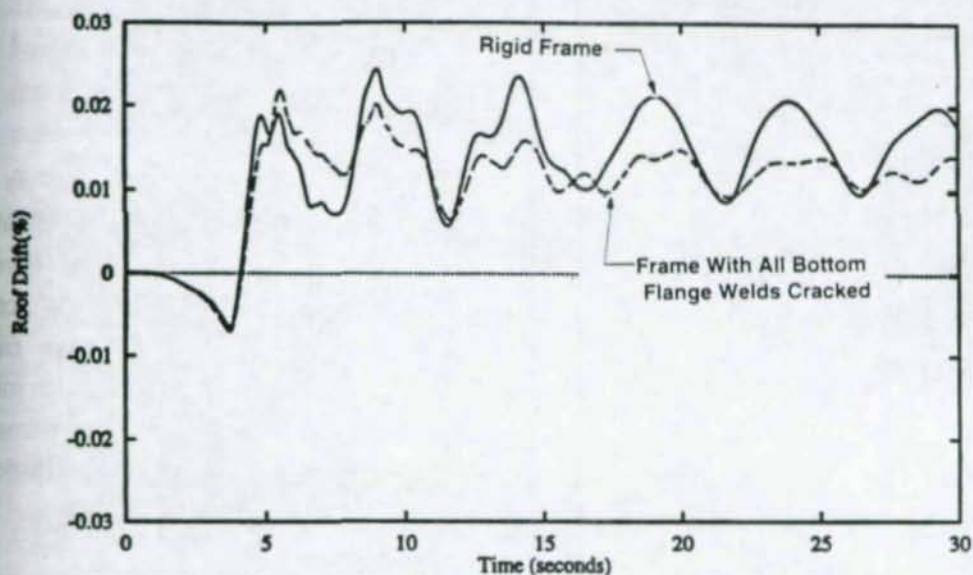


Figure 5. Drift Responses of Frames from 27-Story Building

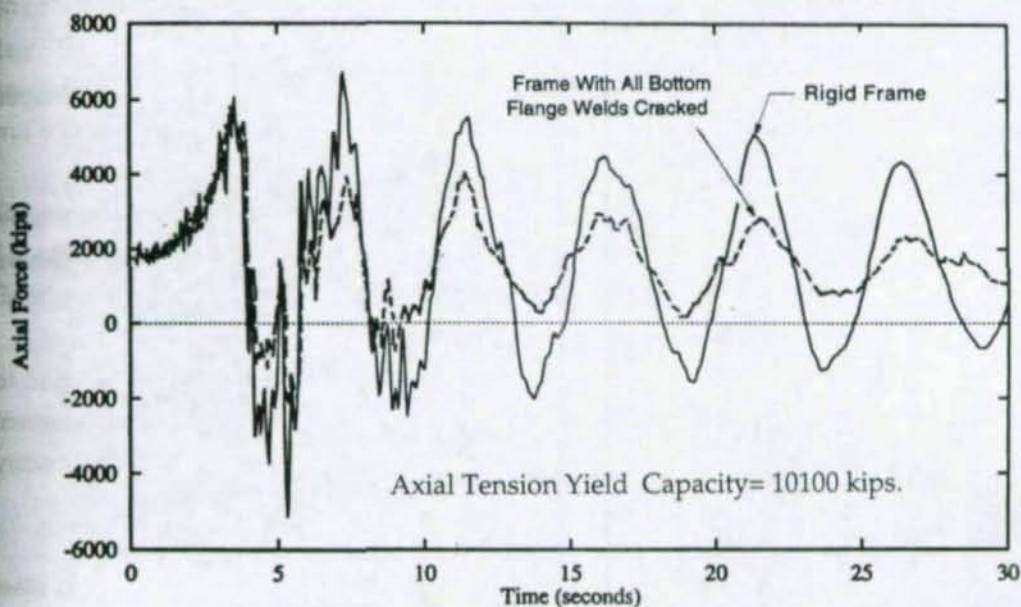


Figure 6. Axial Loads in the First Floor Columns of 26-Story Building

#### 4. CONCLUSIONS

The study reported here was a relatively limited study conducted in 1994 as an emergency investigation to the seismic safety of the damaged buildings in Los Angeles. No generalized conclusions should be drawn from the results reported herein. However, the study resulted in better and more realistic understanding of the actual behavior of steel moment frames before and after their connections have been damaged. In this new field of "Seismic Safety of Damaged Steel Structures" much more work is needed to establish what type of steel structure with what level of damage should be considered seismically safe and what type should be declared hazardous and be evacuated.

Some of the findings of this study related to seismic safety of steel moment frames are:

1. The seismic behavior of damaged steel welded moment frames was found to be somewhat similar to the behavior of steel semi-rigid frames.
2. Almost in all case studies done as part of this project, the response of damaged (semi-rigid) frames was less than the undamaged (rigid) frame.
3. The fact that due to cracks in the weld, lateral strength and stiffness of a steel frame is reduced does not necessarily mean that the structure cannot survive similar or stronger earthquakes.
4. The concept of equivalent static lateral load (code approach) cannot be used to understand the complex seismic behavior of damaged (semi-rigid) steel moment frames. Particularly with regard to the drift values, realistic inelastic time history analyses are necessary.
5. In any analysis of structures, particularly in dynamic analyses of semi-rigid steel structures, the connection models should be as realistic as possible. The model developed in 1994 for this study appears to have closely predicted the results of the cyclic tests of damaged connections conducted in 1995.

6. The technology of computer analysis has advanced significantly in recent years. However, the art and science of predicting connection behavior and establishing rational ground motions have not been advanced as much. As a result, using powerful computer analyses programs to analyze unrealistic structural models subjected to fictitious base excitations will not provide meaningful results. Much research work remains to be done in the field of seismic behavior and modeling of steel connections.

## 5. ACKNOWLEDGMENTS

The research summarized here was conducted at the Department of Civil and Environmental Engineering, University of California, Berkeley. Other than the author, the research team included Professor Jie-Hua Shen of Illinois Institute of Technology, Kurt M. McMullin, Doctoral Student at UC-Berkeley, Professor Djavad Modjtahedi of Sharif University in Tehran and Enzo D' Amore of the University of Reggio Calabria in Italy. The opinions expressed in this paper are solely those of the author and do not necessarily represent the views of the University of California, Berkeley or agencies and individuals whose name appear in this paper.

The project was in part supported by a Grant-in-Aid from the American Institute of Steel Construction. The interest and support of Nestor Iwankiw and particularly the late Dr. Geerhard Haaijer of the AISC are sincerely appreciated.

## 6. REFERENCES

- Anderson, J. and Xiao, Y., (1995), "Cyclic Testing of the AAA Connection Specimens", *Progress Report*, Dept. of Civil Engineering, University of Southern California.

Astaneh-Asl, A., Bolt, B., McMullin, K. M., Donikian, R., Modjtahedi, D. and Cho, S. W., (1994), "Performance of Steel Bridges during the 1994 Northridge Earthquake," *Report No. UCB/CE-Steel -94/01*, Department of Civil and Environmental Engineering, University of California at Berkeley.

A. Astaneh-Asl, (1995), "Seismic Design of Bolted Steel Moment-Resisting Frames" *Steel Tips, July 1995 Issue*, Structural Steel Educational Council, Moraga, CA.

Astaneh-Asl, A., Shen, J.H., McMullin, L.M., Modjtahedi, D. and D'Amore, E. (1995), "Seismic Safety of Damaged Welded Steel Moment Frames", *Report No. UCB/CE-Steel -95/01*, Dept. of Civil and Environmental Engineering, University of California, Berkeley.

Nader, M. N., and Astaneh-Asl, A., (1992) , "Seismic Behavior and Design of Semi-rigid Steel Frames", *Report No. UCB/EERC-92/06*, University of California, Berkeley.

Youssef, N. F. G., Bonowitz, D. and Gross J. L., (1950) " A Survey of Steel Moment-Resisting Frame Buildings Affected by the 1994 Northridge Earthquake", *Report No. NISTIR 5625*, National Institute of Standards and Technology, Washington, D.C.

Table 1. Information on Three Buildings, the Subjects of This Study  
(Source: Youssef et al, 1995)

Building ID	Dist. to Epicenter	No. of Stories	Typical Floor Area	Framing System	Design code/ Year built	Connects. Inspected	No. of Connects. Damaged
EQE1	15 km	4	2300(m <sup>2</sup> )	Partial Frame	UBC-88/ 1992	112	4 BG, 16 BC, 8 S, 6 CW
NYA577	15 km	14	3500(m <sup>2</sup> )	Perim. Frame	Unknown/ 1981	29	2 TW, 19 BW
ESI4	15 km	27	1500m <sup>2</sup> )	Partial Frame	UBC-85/ 1991	20	5 TW, 6 BW

Notes:

BG: Bottom girder flange, BC: Column flange near bottom flange of girder,

S: Shear connection, CW: Column web or doubler plate,

TW: Top flange weld of the girder, BW: Bottom flange weld of the girder,

Technical Papers on

**DESIGN STANDARDS**

## SERVICEABILITY LIMIT STATE FOR COLD-FORMED STEEL BOLTED CONNECTIONS

Roger A. LaBoube<sup>1</sup>

Wei-Wen Yu<sup>2</sup>

Jeffrey L. Carril<sup>3</sup>

### Abstract

Experimental studies were performed to investigate the tensile capacity, bearing capacity and the interaction of tension and bearing capacities of flat sheet cold-formed steel bolted connections. The influence of bolt hole deformation was also investigated. In the experimental investigation, single shear flat sheet connections were investigated for single bolt and multiple bolt configurations. The intent of this investigation was to compare the current design equations for the nominal bearing and tensile capacities and to develop appropriate serviceability design criteria. The focus of this paper is the development of a serviceability limit for the nominal bearing capacity of cold-formed steel flat sheet connections.

### 1. INTRODUCTION

In the United States, the design of cold-formed steel bolted connections is governed by the Specification for the Design of Cold-Formed Steel Structural Members (Specification, 1986). Development of the Specification, is based primarily on research on the behavior of bolted connections conducted at Cornell University, University of Missouri-Rolla (UMR), and University of Wyoming. This research studied only bolted connections in flat sheets.

The Specification's design provisions for the bearing capacity of a bolted connection are based on the ultimate bearing capacity between the connected parts and the bolts.

---

<sup>1</sup>Assoc. Prof., Dept. of Civil Eng., University of Missouri-Rolla, Rolla, MO, USA

<sup>2</sup>Curators Prof. Emeritus, Dept. of Civil Eng., University of Missouri-Rolla

<sup>3</sup>Formerly Res. Asst., Dept. of Civil Eng., University of Missouri-Rolla, Rolla, MO,

To reach the ultimate bearing capacity, large deformations commonly occur around the bolt hole. Therefore, if the deformation around the hole is a critical design consideration, the Specification provision may be unconservative.

When connecting thicker plates, research (Frank and Yura, 1981) has demonstrated that hole elongation, or ovalization, greater than 6.35 mm (0.25 in.) will be present when the ultimate bearing capacity is achieved. Therefore, both strength and serviceability limit states are addressed in the Load and Resistance Factor Design Specification for Structural Steel Buildings (Load, 1993).

The purpose of the UMR investigation was to study the tensile capacity, bearing capacity, and the interaction of tensile and bearing capacities of connected flat sheets in bolted connections, and to develop appropriate strength and serviceability design recommendations. This paper will summarize the serviceability study.

## 2. SCOPE OF INVESTIGATION

The UMR investigation consisted of a review of pertinent literature, an analysis of available test data, an experimental study of bolted connections using flat steel sheets, and an analysis of the experimental results.

The analytical study of available test data consisted of a comparison between tested failure load and predicted failure load, where the predicted load was computed by the United States, Canadian, and European design guidelines (Carril *et al.*, 1994).

The experimental phase of this investigation explored the bearing and tensile strength behavior of thin steel sheets connected by bolts. Particular emphasis was placed on defining the influence of hole deformation on load capacity of a connection.

## 3. UMR EXPERIMENTAL INVESTIGATION

To evaluate the effect of hole deformation on the load capacity of bolted connections, experimental work was conducted to investigate further the bearing strength and tensile strength of bolted connections made of thin flat sheets. The test specimens were designed such that joint failure would occur due to bearing, fracture in the net section, or a combination of bearing and fracture in the net section. The specimens were designed for the following parameters: (1) nominal sheet thickness: 1.02 mm (0.04 in.), 1.78 mm (0.07 in.) and 3.05 mm (0.12 in.); (2) ratios of  $d/s$ : 0.12, 0.15 and 0.31; (3) 12.7 mm (1/2 in.) diameter A325T bolts; (4) bolt pattern configurations, as shown in Figure 1; and (5) with and without washers. All tests were single shear

connections and were performed using the 26.7 kN (120,000 lb.) Tinius Olsen Universal Testing machine located in the Engineering Research Laboratory of the University of Missouri-Rolla.

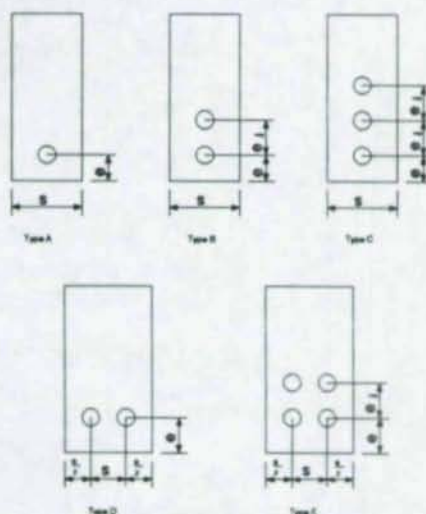


Figure 1. Geometry of test specimens

### 3.1 Mechanical Properties Of Steel Sheets

Tensile coupon tests were conducted to obtain the mechanical properties of the steel sheets. Table 1 shows the measured thicknesses and mechanical properties of the test specimens used in the investigation. The mechanical properties were determined by standard coupon tests following ASTM A370 procedures.

Table 1 - Material Properties

Thickness (in.)	$F_y$ (ksi)	$F_u$ (ksi)	% Elongation
0.040	35.80	55.84	50
0.070	32.06	52.47	50
0.120	36.61	53.02	44

Note:  $F_y$  and  $F_u$  values are the average of two tests  
 1 in. = 25.4 mm; 1 ksi = 6.9 N/mm<sup>2</sup>

### 3.2 Preparation Of Test Assemblies

One hundred and two test assemblies were fabricated for this investigation. This allowed for the testing of three identical tests of the thirty-four different bolted connections. Each assembly consisted of two identical flat sheet test specimens, bolted together (Fig. 2). Figure 1 shows the various types of specimens tested.

The purpose of fabricating three identical test assemblies of the thirty-four different bolted connections was to provide consistent results in identical bolted connection tests. Initially all three identical test assemblies were tested. As the testing program proceeded, it became apparent that if the first and second tests gave consistent results, the third test was not providing any additional useful information. Therefore, in order to provide for a more efficient testing program, if the first and second tests gave consistent results, the third test was not be conducted. Of the 102 test assemblies fabricated, it was only necessary to test seventy-five assemblies. Carril *et al.* (1994) lists the dimensions and mechanical properties of the seventy-five tests that were conducted.

All tests used 13.7 mm (1/2 in.) diameter A325T bolts with 14.29 mm (9/16 in.) diameter punched bolt holes. Washers were used on some of the assemblies, but since it is more common in practice not to use washers under the head and nut of a bolted connection, the majority of the tests did not include washers. Of the seventy-five assemblies tested, twenty-five were tested with washers.

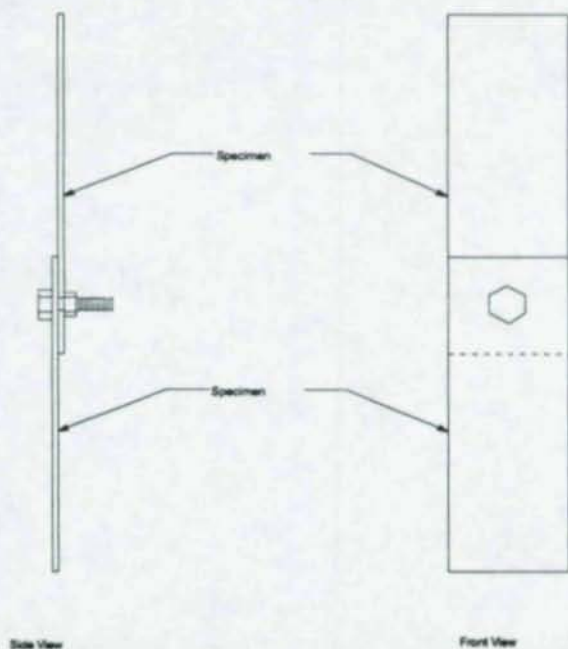


Figure 2. Typical test assembly

## 4. TESTING OF CONNECTION ASSEMBLIES

### 4.1 Attachment of Test Assembly to Testing Machine

Because most of the test specimens that were used were too wide to be gripped by the testing machine, specially designed grip plates were connected to each end of the test assembly to transmit the applied loads. The specimens were connected to the grip plates using 12.7 mm (1/2 in.) diameter A325T bolts.

### 4.2 Installation of Bolts

Two identical test specimens, that is sheets, were bolted together to form a test assembly. The bolts were snugged tight to simulate the bolt tightening procedure in practice. To insure the approximate same bolt tightness between test assemblies, the same individual tightened the bolts for all test assemblies.

Slippage between the two identical flat sheet test specimens was acceptable, but slippage between the test specimens and the grip plates was not. Therefore, the ends of the specimens, which were to be attached to the grip plates, were roughened using sandpaper. The test assembly was bolted to the grip plates using 12.7 mm (1/2 in.) diameter A325T bolts with washers. These bolts were tightened to achieve a tightness much greater than snug, to aid in preventing slippage between the test specimens and the grip plates.

### 4.3 Measurement of Load and Elongation

The elongation of the bolted connections was measured using a LVDT attached to the test assembly as shown in Fig. 3. A detail of the attachment is shown in Fig. 4. The applied load and elongation readings of the connection were recorded at one second intervals, using a computer data acquisition system. Typical load deflection curves are presented by Carril et al. (1994).

## 5. DEVELOPMENT OF DEFORMATION OR SERVICEABILITY LIMIT

A detailed presentation of the connection test results are summarized by Carril et al. (1994). The following discussion will focus on the serviceability limit state study.

The results of the tests which failed in bearing or any combination that included

bearing were considered for the serviceability limit state evaluation. The results of the test assemblies whose failure mode included bearing are listed in Tables 2.

The intent of this investigation was to develop an equation for the nominal bearing capacity,  $P_n$ , of a bolted connection that would limit the amount of deformation around a bolt to an acceptable limit. For consistency with the AISC Specification (Load, 1993), a deformation limit of 6.35 mm (0.25 in.) was selected as an acceptable limit. To be consistent with existing design expressions, it was desired to have an equation in the form of:

$$P_n = cdtF_u \quad (\text{Eq. 1})$$

where  $c$  = constant recognizing serviceability limit;  $d$  = nominal bolt diameter;  $t$

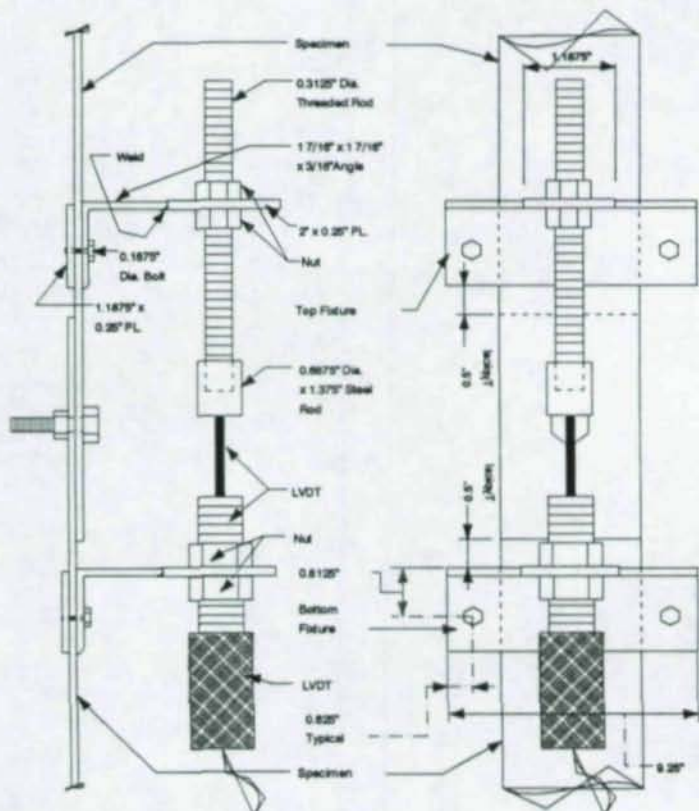


Figure 3. Detail of LVDT attachment

= thickness of the thinnest connected sheet; and  $F_u$  = tensile strength of connected part.

The constant  $c$  for each test was determined using Equation 2 and is shown in Table 2:

$$c = P'/dtF_u n_b \quad (\text{Eq. 2})$$

where  $P'$  = tested tensile load at 6.35 mm (0.25 in.) connection deformation; and  $n_b$  = number of bolts.

The constant  $c$  varied from 1.493 to 2.478 for the different connections as shown in Table 2. However, the mean, considering all the tests in Table 2, was found to be 1.93. Therefore, a proposed bearing strength equation that would limit the deformation around the bolt hole to approximately 0.25 in. is given as follows:

$$P_n = 1.93dtF_u \quad (\text{Eq. 3})$$

where  $d$ ,  $t$  and  $F_u$  are previously defined.

The accuracy of Eq. 3 to provide a 6.35 mm (0.25 in.) deformation limit is indicated by the ratio of  $P'$  to Eq. 3 (Table 2); the ratio ranged from 0.774 to 1.284, with a mean of 1.001, a standard deviation of 0.127 and a coefficient of variation of 0.127.

## 6. CONCLUSIONS

Based on tests of single sheet bolted connections, a design equation for bearing and combinations that include bearing was developed for the serviceability limit state which was defined as 6.35 mm (0.25 in.) of connection deformation.

## 7. ACKNOWLEDGEMENTS

The authors gratefully acknowledge the financial support provided by the American Iron and Steel Institute. Thanks are also extended to the Institute's subcommittee on connections chaired by M. Golovin for providing technical guidance. Special appreciation is expressed to the technical staff of the Department of Civil Engineering at UMR, J. Bradshaw, J. McCracken, and S. Gabel.

Table 2 - Test Results for Serviceability Limit State

Assembly Number	P' (kips)	c	P'/Eq. 3
AY22-1	3.90	2.065	1.070
AY22-1	3.87	2.107	1.092
AY23-1	3.85	2.096	1.086
AY23-3	4.12	2.243	1.162
BY13-1	4.82	2.055	1.065
BY13-2	4.24	1.766	0.915
BY13-3	4.00	1.628	0.844
AN32-1	7.09	2.266	1.174
AN32-2	7.62	2.478	1.284
AN33-1	7.29	2.330	1.207
AN33-2	7.10	2.232	1.156
BN33-1	12.62	2.000	1.036
BN33-2	12.52	1.984	1.028
DN12-2	3.71	1.545	0.801
DN12-3	3.95	1.684	0.873
DN22-1	7.17	1.952	1.011
DN22-2	7.00	1.879	0.974
AY12-1	2.32	1.978	1.025
AY12-2	2.17	1.807	0.937
BY12-1	4.43	1.763	0.913
BY12-2	4.17	1.659	0.860
BY12-3	4.03	1.718	0.890
BY22-1	6.82	1.831	0.949
BY22-2	6.79	1.849	0.958
BY22-3	7.58	2.064	1.069
BN32-1	13.74	2.196	1.138
BN32-2	13.68	2.205	1.143
DN32-1	13.42	2.109	1.093
DN32-2	13.17	2.105	1.091
EN12-1	7.33	1.526	0.791
EN12-2	7.17	1.493	0.774
EN22-1	12.59	1.690	0.876
EN22-2	12.77	1.690	0.876
EN32-1	23.17	1.852	0.959
EN32-2	22.17	1.787	0.926
	Mean	1.930	1.001
	Std. Dev.		0.127
	COV		0.127

Note: 1 kip = 4.5 kN

## 8. REFERENCES

- Carril, J. L., LaBoube, R. A., and Yu, W. W. (1994), "Tensile and Bearing Capacities of Bolted Connections," First Summary Report, Civil Engineering Study 94-1, Cold-Formed Steel Series, Department of Civil Engineering, Center for Cold-Formed Steel Structures, University of Missouri-Rolla
- Frank, K. H. and Yura, J. A. (1981), "An Experimental Study of Bolted Shear Connections," FHWA/RD-81/148, December 1981
- Load and Resistance Factor Design Specification for Structural Steel Buildings (1993), American Institute of Steel Construction, Chicago, IL
- Specification for the Design of Cold-Formed Steel Structural Members (1986), 1986 Edition with 1989 Addendum, American Iron and Steel Institute, Washington, D. C.

# AN ATTEMPT OF CODIFICATION OF SEMIRIGIDITY FOR SEISMIC RESISTANT STEEL STRUCTURES

Federico M. Mazzolani<sup>1</sup>

Vincenzo Piluso<sup>2</sup>

## Abstract

In this paper, the attention is focused on the different behaviour of full-strength and partial strength connections from the seismic point of view. With reference to the most common types of connections, by considering the experimental data collected in the technical literature, the relation between the flexural strength and the ductility of partial strength beam-to-column joints is analysed. Successively, the main parameters governing the influence of beam-to-column joints on the seismic behaviour of steel frames are briefly summarized.

Finally, taking into account the above state-of-art, an attempt of codification for seismic design purposes is made.

## 1. INTRODUCTION

The recent earthquake of Northridge (California, January 17, 1994) has seriously compromised, at least in U.S.A, the image of steel structures as the solution to seismic design problems. In fact, immediately after the earthquake it was reported that no significant damage to steel buildings was occurred, but few weeks later alarming news began to be published regarding significant damages of steel members. Nowadays, it has been reported (Bertero et al., 1994) that these damages have concerned the fracture of column base plates leading to the failure of the anchor bolts, the overall buckling of lateral bracing members leading to the local buckling and in some cases to the fracture of their ends and, last but not least, the failure of welded beam-to-column connections of special moment resisting frames. This last is undoubtedly the most important type of failure occurred in steel structures during the Northridge earthquake. The investigations concerning the causes of this type of damage have given rise to a wide discussion within the scientific international community. On one hand, it can be assumed that poor workmanship is solely to blame and, therefore, it is necessary to tighten the site supervision and to improve the welding details and procedures; on the other hand, damage causes can be attributed to defective design guidance leading to a rotation ductility supply lower than the earthquake imposed demand. Even if we can content ourselves by considering the fact that there have been no cases of collapse of steel structures, this latter point of view seems nowadays the most supported (Elnashai, 1994).

By means of a review of the experimental tests carried out in USA and Japan, it has been evidenced (Bertero et al., 1994) that the types of failure occurring in welded beam-to-column connections during the Northridge earthquake have been already observed in experiments conducted in the laboratory. In addition, the numerical analysis of the seismic response of a six-storey steel framed building damaged during Northridge earthquake has pointed out that there were several ground motions, recorded during the earthquake, able to significantly lead the structure into the inelastic range. In many cases, the plastic rotation demand at the beam ends exceeded 0.02 rad, therefore, on the base of the available

---

1 Department of Structural Analysis and Design, University of Naples, Italy

2 Department of Civil Engineering, University of Salerno, Italy

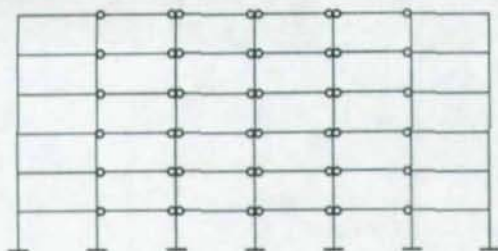


Fig.1 - Typical structural scheme used by California designers

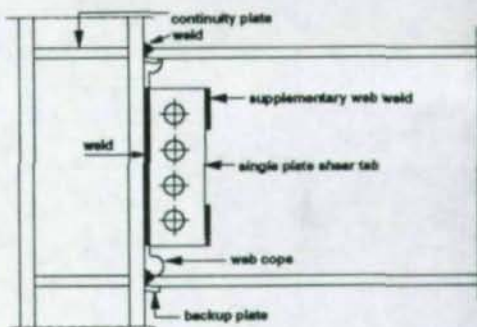


Fig.2 - Typical beam-to-column joint for moment-resisting frames in USA

experimental data (Tsai and Popov, 1988 - Engelhardt and Husain, 1992, 1993), it is clear that the cracking occurring in the connections cannot be considered unusual.

In the experimental tests carried out in USA, a plastic rotation supply equal to 0.02 rad has been used as a benchmark to judge the seismic performance of beam-to-column connections, because it was believed to be sufficient to withstand severe earthquakes (Tsai and Popov, 1988). As this limit value can be exceeded, it is clear that the attention should be focused on the design value of the  $q$ -factor which could be reduced in order to limit plastic rotation demands occurring during severe earthquakes or, as an alternative, on the improvement of the seismic performances of dissipative zones.

The following question can be raised: «Can the results of the american "on field" experience be applied to european practice?».

It has to be considered that the steel grade, the chemical composition and the mechanical characteristics of the steel can be different. Also the welding technique can be different. In addition, different strength requirements leads to different plastic rotation demands.

Regarding the strength requirements, it has to be remembered that the american code UBC91 (Uniform Building Code, 1991) provides for special moment resisting frames a reduction factor  $R_w$  equal to 12 which is equivalent to a value of the european  $q$ -factor equal to 8. On the contrary, Eurocode 8 (Commission of the European Communities, 1993) provides a  $q$ -factor value equal to 6 and the japanese code (AIJ, 1990) a structural coefficient  $D_s$  equal to 0.25 which corresponds to  $q = 4$ . Therefore, the strength requirement given in the american code is the least restrictive.

In addition, in the structural scheme used by California designers (Fig.1) the moment resisting frames do not involve all the bays (Bertero et al. 1994), thus reducing the number of dissipative zones and attracting more inertial forces.

Last but not least, it has to be considered that the beam-to-column connection detail used in USA for moment resisting frames does not correspond to the european practice (Fig.2).

The recent "on field" experience due to the Northridge earthquake has to be capitalized by the international scientific community, but local conditions and design practice have to be accounted for. Taking into account the above considerations and the available experimental data concerning the inelastic behaviour of beam-to-column connections, an attempt of codification of semirigidity is herein presented on the basis of previous studies carried out by the Authors' research group.

## 2. THE CODIFIED SEMIRIGIDITY CONCEPT IN EUROPEAN CODES

Beam-to-column joints have a fundamental importance in case of seismic resistant steel frames, because dissipative zones have to be located at the beam ends, so that their rotational ductility supply is strictly related to the detailing of connections.

In Eurocode 3 (Commission of the European Communities, 1990) particular attention has been paid to the joint classification, in which two main parameters are involved: the flexural strength and the rotational stiffness. On the basis of these parameters and excluding the case of nominally pinned connections, which do not correspond to the case of moment resisting frames, four fundamental cases can be recognized: a) full strength-rigid

joints; b) full strength-semirigid joints; c) partial strength-rigid joints and d) partial strength-semirigid joints.

From the seismic point of view, such a distinction is particularly important, because the seismic behaviour of moment resisting frames is considerably affected both by the strength and by the stiffness of the beam-to-column joints. Notwithstanding, the term semirigid frame is often undifferently used both for frames with full strength-semirigid joints (case b) and for frames with partial strength joints (cases c and d). On the contrary, the term rigid frame is often adopted to denote frames with full strength-rigid joints, but the distinction between cases a and c should be made.

It is evident that the case of full strength-rigid joints (case a) represents the reference case, i.e. the case in which the beam-to-column joints exhibit the ideal behaviour, so that they do not represent a frame imperfection (Cosenza et al., 1987).

In particular, from the point of view of the location of the dissipative zones, completely different behaviours are developed in case of full strength joints and in case of partial strength joints. In fact, three different types of behaviour can be recognized depending on the ultimate moment of the joint ( $M_{u,j}$ ) and on the plastic moment of the connected beam ( $M_{pb}$ ).

In the case of full strength joints ( $M_{u,j} > M_{pb}$ ), a possible plastic hinge will develop at the beam end, while the joint remains in elastic range. Plastic rotations involve only the beam end.

In the case of partial strength joints ( $M_{u,j} < M_{pb}$ ) the dissipative zone is located within the joint, while the beam remains in elastic range. In this case the joint has to be able to experience large plastic rotations.

Finally, in the intermediate case ( $M_{u,j} = M_{pb}$ ), representing a transition condition, the yielding occurs both in the joint elements and at the end of the beam.

In addition, Eurocode 3 gives in its Annex J (CEN/TC250/SC3-PT9, 1994) simplified rules for evaluating both the rotational stiffness and the flexural resistance of the most common types of beam-to-column joints, providing the operative tool to apply the semirigidity concept. Therefore, for static design, modern codes such as Eurocode 3, have already opened the door to the use of semirigid frames, either with full strength or partial strength joints, provided that all code requirements are met. This new development has not yet been considered by seismic code drafting committees.

In the European seismic codes (ECCS, 1988 - Eurocode 8, 1993), it is requested that joints in dissipative zones have to possess sufficient overstrength to allow for yielding of the ends of connected members. It is deemed that the above design condition is satisfied in case of welded connections with full penetration welds. On the contrary, in case of fillet weld connections and in case of bolted connections the design resistance of the joint has to be at least 1.20 times the plastic resistance of the connected member. This means that the use of full-strength joints is suggested and dissipative zones have to be located at the member end rather than in the connections.

The use of partial strength connections, i.e. the contribution of the connections in dissipating the earthquake input energy, is not forbidden. Notwithstanding, it is strongly limited because, in such a case, the experimental control of the effectiveness of such connections in dissipating energy is requested.

Concerning the above overstrength level (1.20) which is aimed at assuring the location of the dissipative zones at the beam ends, it is important to underline, since now, that the above level should be properly related to the width-to-thickness ( $b/t$ ) ratios of the beam section. In fact, the maximum flexural strength, that the beams are able to withstand is developed at the occurrence of local buckling.

In both cases, either of full-strength or of partial-strength semirigid frames, codified rules for evaluating the behaviour factor to be used in design are not still available.

### 3. REVIEW OF THE EXPERIMENTAL DATA ON BEAM-TO-COLUMN JOINTS

Despite numerous experimental tests dealing with the cyclic behaviour of beam-to-column joints have been carried out all over the world, simplified rules for estimating the rotational ductility of beam-to-column joints are not at all codified. This is probably due to the great number of joint typologies to be tested and to the fact that even a small modification of a structural detail can lead to a significant variation of the joint behaviour under both monotonic and cyclic loading conditions.

With reference to fully welded connections, it has been evidenced that the use of web copes at the beam end can reduce the ductility of the connections. Web copes are usually

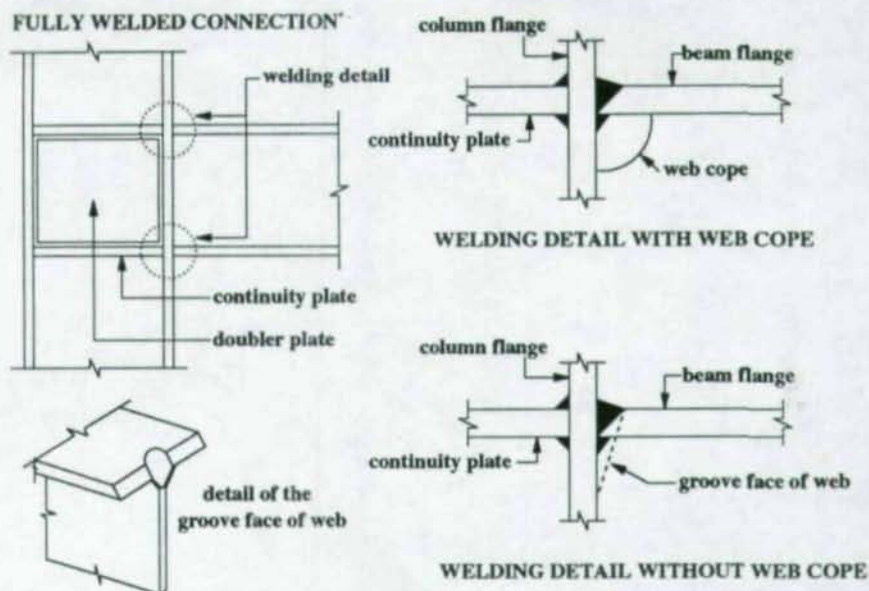


Fig.3 - Detailing of fully welded connections

located at the beam end in order to avoid the intersection of the fillet welding line of the beam web and the back running line of the beam flange. Recently, the influence of the web copes on the cyclic behaviour of welded connections has been experimentally investigated (Matsui and Sakai, 1992). Two groups of three specimens have been tested. A group was detailed with web copes and the second one without web copes. Each group was composed by a specimen designed to develop plasticity in the panel zone, a specimen able to develop the plastic hinge at the beam end and a specimen involving the plastic engage both of the panel zone in shear and of the beam end in bending. In case of specimens without web copes, a part of the web at the beam end was cut as a groove and butt welded to the column flange (Fig.3). The experimental tests (Matsui and Sakai, 1992) have pointed out that the use of web copes leads to the cracking of the welding portion of the beam flange and finally to the fracture of the beam flange at the heat affected zone. The specimens without web copes exhibited a significant improvement both of ductility and energy dissipation capacity. Only the specimens whose plastic zone was located in the panel zone in shear were practically insensitive to the presence of the web copes or not, developing a plastic rotation supply of about 0.06 rad. In the other cases, the plastic rotation supply was about 0.035 rad in specimens with web copes and about 0.055 rad in specimens without web copes.

The importance of the detailing was already evidenced during the experimental program developed some years ago within the activities of the technical committee TC13 «Seismic Design» of ECCS (Ballio et al., 1987). The experimental program was devoted to the analysis of the cyclic behaviour of the most common connection typologies designed in order to develop the full plastic resistance of the beam: connections with double web angles bolted to the beam web and to the column flange and with splices welded to the column and bolted to the beam flange, top and seat angle with double web angle connections, extended end plate connections and, finally, fully welded connections. From the experimental evidence, some general considerations were drawn about the use of additional stiffeners in the main connection types:

- if stiffeners are added to the parts of the connection which are the most responsible of its flexibility, the amount of energy absorption is decreased but the load carrying capacity is increased;
- if the added elements do not substantially modify the evolution of the deformation mechanism but, on the contrary, increase the local strength of the connection components (as for example an increase of thickness), then there will be an increase of energy absorption and strength, provided that the original type of collapse is ductile.

The plastic rotation supply ranged from 0.03 to 0.07 rad. In addition, by considering the measured yield strength of the material, it has been evidenced that welded connections provided the greatest energy dissipation capacity (Mazzolani and Piluso, 1995).

As the experimental results have evidenced that a very satisfactory ductility and energy dissipation capacity is obtained through the plastic hinge formation in the beam, some researchers have proposed to reduce the beam flange width near the beam-to-column connections in order to force the formation of the plastic hinge at the beam rather than in the connection and/or in the panel zone. An experimental program including also this type of beam-to-column connection detail has been recently developed (Ballio and Chen, 1993a, 1993b).

The complete experimental program has been devoted both to bare steel joints and to composite joints with and without slab (Schleich and Pepin, 1992). In particular, with reference to the case of bare steel joints, the cyclic behaviour of bolted web-welded flange connections, end-plate connections and fully welded connections has been investigated. In addition, both exterior and interior joints have been tested. All the specimens have developed a flexural resistance greater than the plastic moment of the beam. The plastic rotation supply ranged from 0.04 rad to 0.10 rad. In addition, the experimental results have confirmed that, in fully welded connections, the reduction of the beam flange causes a little loss of strength, but assures the formation of the plastic hinge in the beam leading to a very ductile behaviour.

The cyclic behaviour of partial strength connections has been experimentally investigated at the University of Trento (Bernuzzi et al., 1992 - Bernuzzi, 1992). The attention has been focused on the connection only. In fact, the specimen consists of a long beam stub attached through the connection to be tested to a rigid counterbeam, so that the testing conditions are able to represent the case of beam-to-column joints with negligible panel zone deformability. The test results show that this type of connections can provide a satisfactory ductility, but a significant reduction of the energy dissipation capacity is exhibited in comparison with the full strength rigid welded joint results, as it has been evidenced in (Mazzolani and Piluso, 1995) by means of a comparison, in nondimensional form, between these experimental tests and the ones of full strength connections (Ballio et al., 1987).

Even if monotonic tests do not provide any information about the stiffness and strength degradation which can occur under repeated plastic excursions, such as the ones developed during destructive earthquakes, they are able to give a first look insight into the ductility supply of beam-to-column joints. This is particularly interesting, because a significant number of experimental tests is collected in data banks, such as the SERICON data bank (Weinand, 1992) and the SCDB data bank (Kishi and Chen, 1986). With reference to the data collected in these data banks and to the tests performed by Aggarwal (1994), Zoetemeijer and Kolstein (1975), Zoetemeijer and Munter (1983), Simek and Wald (1991), Figs. 4, 5 and 6 show a comparison between the experimental data and the following formula, proposed by Bjorhovde et al. (1990), relating the ductility supply to the joint flexural resistance:

$$\bar{\varphi}_{uj} = \frac{5.4 - 3\bar{m}}{2} \quad (1)$$

where  $\bar{m}$  is the nondimensional ultimate moment of the joint and  $\bar{\varphi}_{uj}$  is the nondimensional ultimate rotation computed as the ratio between the joint ultimate rotation and the conven-

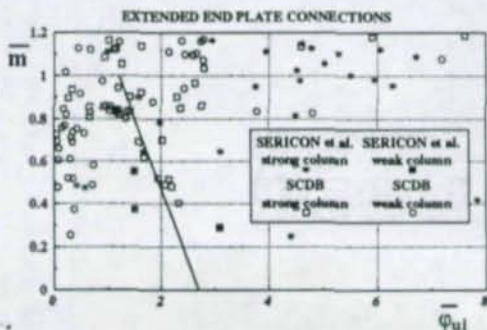
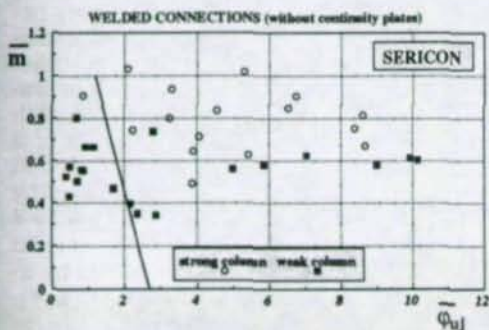


Fig.4 - Flexural strength versus ductility: unstiffened welded connections

Fig.5 - Flexural strength versus ductility: extended end plate connections

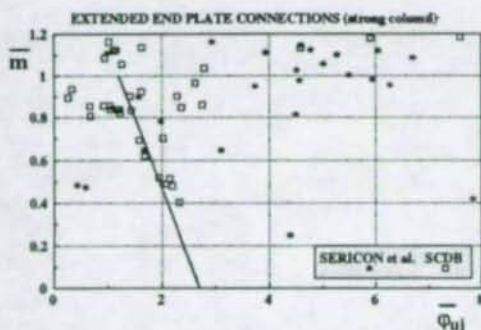


Fig. 6 - Flexural strength versus ductility: extended end plate connections satisfying the strong column-weak beam criterion

hierarchy criterion required for seismic design, excluding weak-columns. In addition, the great scatter of the available data points out the need of further experimental tests, at the light of new interpretation rules which have to define the basic parameters to be recorded. The existing gap is also testified by the fact that Annex J of Eurocode 3 (CEN/TC250/SC3-PT9, 1994) does not provide any rule regarding the ductility supply. It is only stated that if the flexural strength of the joint is at least 1.20 times the one of the connected member, the control of the joint rotation capacity is not requested.

#### 4. SEISMIC RESPONSE OF SEMIRIGID FRAMES

Despite numerous experimental tests on the behaviour of beam-to-column connections under monotonic and cyclic loads have been carried out by many researchers, the seismic behaviour of semirigid frames has not been exhaustively investigated.

For these reasons, aiming at a clarification of all parameters affecting the seismic inelastic behaviour of full/partial strength semirigid frames, a simplified model has been introduced (Faella et al., 1994a, 1994b) with reference both to full strength-semirigid connections and to partial strength-semirigid connections. This approach presents also the advantage to allow the use of the great amount of studies concerning the seismic response of the SDOF systems and, therefore, includes also the effects of the random variability of the ground motion.

The analysed model represents a subassemblage which has been extracted from an actual frame by assuming that beams are subjected to double curvature bending with zero moment in the midspan section and by considering each beam as contemporary belonging to two storeys, so that their mechanical properties have been halved. It is believed that this model is representative of frames failing in global mode. The flexural stiffness of the columns of the original frame, from which the substructure has been derived, is equal to  $EI_c/h$ , the flexural stiffness of the beams is equal to  $EI_b/L$ . The moment versus rotation curve of the joint is modelled with a bilinear relation which is completely defined by means of only two parameters: the elastic rotational stiffness  $K_\theta$  and the ultimate moment  $M_{uj}$ . It is evident that, with reference to the elastic range, the comparison between the semirigid substructure and the rigid one is governed by the following nondimensional parameters:

$$\zeta = \frac{EI_b/L}{EI_c/h} \quad (2)$$

and:

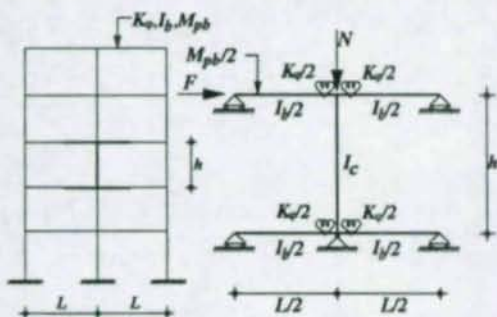


Fig. 7 - The simplified model

$$\bar{K} = \frac{K_q L}{E I_b} \quad (3)$$

being  $\zeta$  the beam-to-column stiffness ratio and  $\bar{K}$  the nondimensional rotational stiffness of the joint.

In addition, with reference to the inelastic behaviour, the nondimensional ultimate flexural resistance of the joint:

$$\bar{m} = \frac{M_{uj}}{M_{pb}} \quad (4)$$

provides the distinction between the two fundamental cases: the full strength connections for  $\bar{m} > 1$  and the partial strength connections for  $\bar{m} < 1$ .

By means of this model, closed form relations representing the connection influence of the elastic and inelastic behaviour of steel frames have been derived. In particular, in (Faella et al., 1994a) the connection influence of the period of vibration, on the frame sensitivity to second order effects and on the ductility of frames either with full strength or partial strength connections has been pointed out. In (Faella et al., 1994b) the parameters affecting the seismic response of the model have been underlined. The ideal case of model with full strength rigid joints, where the connection does not represent a frame imperfection, has been used as reference case. It has been recognized that the ratio between the q-factor of the model with full strength semirigid joints  $q_k^{(FS)}$  and the one of the reference case  $q_m^{(FS)}$  can be expressed as a function of four parameters:

$$\frac{q_k^{(FS)}}{q_m^{(FS)}} = f(\bar{K}, \zeta, \gamma_m, R) \quad (5)$$

being  $\gamma_m$  the frame sensitivity to second order effects computed for the model with rigid joints (equal to the inverse of the critical elastic multiplier of the vertical loads) and  $R$  the beam rotation capacity.

In case of partial strength connections, a significant increase of the number of parameters involved in the seismic behaviour of the model arises. In fact, the nondimensional value of the q-factor, i.e. the ratio between the q-factor of the model with partial strength semirigid joints  $q_k^{(PS)}$  and the one of the reference case, is affected by six parameters (Faella et al., 1994b):

$$\frac{q_k^{(PS)}}{q_m^{(PS)}} = f'(\bar{K}, \zeta, \gamma_m, R, \bar{m}, L/d_b) \quad (6)$$

being  $L/d_b$  the beam span-to-depth ratio.

In particular, this simplified model has evidenced that the ratio between the beam plastic rotation capacity and the joint rotational ductility supply is of paramount importance for evaluating the possibility to use partial strength joints in seismic resistant structures. As an example, with reference to extended end plate connections, Fig.8 represents the case  $R=4$ ,  $\gamma_m=0.025$  and  $L/d_b=15$ . It can be recognized a theoretical discontinuity corresponding

to the passage from partial strength to full strength connections. The location of this discontinuity mainly depends on the connection typology. The magnitude of the discontinuity depends on the ratio between the beam rotation capacity, governing the ductility of the model with full strength joints, and the joint rotation capacity, whose lower bound is given by equation (1), governing the model ductility in case of partial strength joints.

The reliability of the model for predicting the influence of beam-to-column joints on the seismic behaviour of actual frames has been demonstrated elsewhere (Mazzolani and Piluso, 1994).

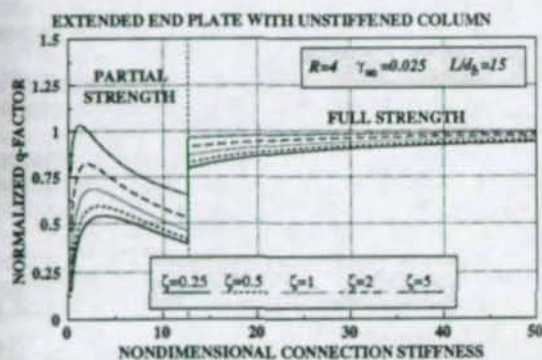


Fig.8 - Seismic response of the model: example

## 5. ATTEMPT OF CODIFICATION

On the basis of the existing background, whose main points have been briefly summarized in the previous sections, it is the Authors' opinion that the door can be opened to semirigid frames also for seismic design purposes, provided that dissipative zones are located at the beam ends. The use of partial strength connections, i.e. the participation of the connection in dissipating the earthquake input energy, should be avoided unless the capacity of the connection to dissipate the energy imposed by the design earthquake is demonstrated by means of experimental tests. This recommendation, which is already given in Eurocode 8, can be justified a posteriori by the great scatter of the available experimental data on the ductility supply of partial strength connections as testified in Section 3. However, in case of partial strength connections, the yielding should be forced to develop in steel elements which compose the connection, such as angles and plates. On the contrary, the elements providing the fastening action, such as bolts and welds, should be dimensioned to remain in elastic range (Astaneh and Nader, 1992b).

The following proposals for recommendations are aimed at the design of full strength semirigid connections.

First of all, it has been already said that the required level of overstrength, which the connections have to be able to develop in order to assure the plastic hinge formation at the beam ends, has to be related to the width-to-thickness ratios of the beam section.

As it has been pointed out in a previous paper (Mazzolani and Piluso, 1992), the maximum flexural resistance that the beams are able to develop is given by:

$$M_{max} = s M_{pb} \quad (7)$$

where the overstrength coefficient  $s$  ( $s \geq 1$  for first and second class sections) represents the ratio between the stress leading to local buckling and the yield stress. The coefficient  $s$  can be computed by means of the following relation:

$$s = \frac{1}{0.695 + 1.633 \lambda_f^2 + 0.062 \lambda_w^2 - 0.602 \frac{b_f}{L^*}} \leq \frac{f_u}{f_y} \quad (8)$$

where:

$$\lambda_f = \frac{b_f}{2 t_f} \sqrt{E_y} \quad \lambda_w = \frac{d_w}{2 t_w} \sqrt{E_y} \quad (9)$$

are the slenderness parameters of the flange and of the web respectively (being  $b_f$  the flange width,  $d_w$  the web depth,  $t_f$  and  $t_w$  the flange thickness and the web thickness respectively). In addition,  $L^*$  is the distance between the point of zero moment and the plastic hinge (approximately  $L^* = L/2$ , being  $L$  the beam span).

The above relation evidences that if the width-to-thickness ratios are strongly limited, the local buckling is practically prevented, so that  $s = f_u/f_y$ . In this case the value of 1.20 commonly used as overstrength factor for designing beam-to-column connections could not be sufficient to allow the development of the whole beam rotation capacity, due to the premature collapse of the connection.

It is also evident that the obtained overstrength level should be furtherly amplified to account for random material variability.

The above provision to use the parameter  $s$  (Eq.8) as overstrength factor instead of a given number (such as 1.20) should assure the complete development of the beam plastic rotation capacity, so that the control of the connection ductility is not requested.

Further provisions should account for the influence of the beam-to-column connection deformability on the period of vibration, the frame sensitivity to second order effects and the frame ductility supply. All these effects can be taken into account by properly reducing the design value of the  $q$ -factor (Mazzolani and Piluso, 1995).

Always with reference to full strength connections, the analysis of equation (5), representing the reduction coefficient  $\eta$  of the  $q$ -factor to account for the influence of the beam-to-column connection deformability, allows to recognize that the most significant variations of  $\eta = q_k^{(FS)} / q_c^{(FS)}$  are obtained by varying the beam-to-column flexural stiffness ratio  $\zeta$ . This is evidenced in Figs. 9, 10 and 11, where the influence of  $\zeta$ ,  $R$  and  $\gamma_w$  is analysed, respectively.

Taking into account that  $\zeta = 0.5$  provides a lower bound of the above reduction coefficient and that, at the same time, this value of  $\zeta$  is more close to the practical situations, the

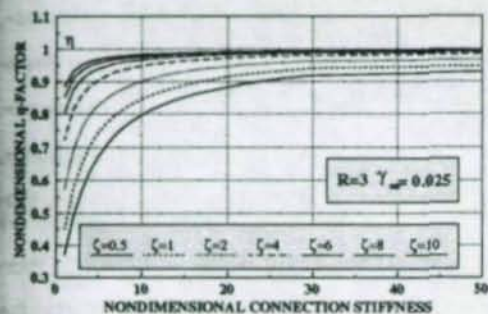


Fig.9 - Influence of  $\zeta$  on the reduction coefficient of the  $q$ -factor

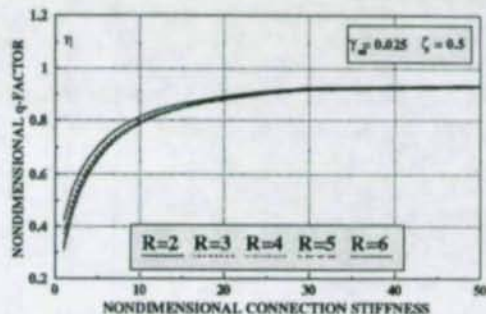


Fig.10 - Influence of  $R$  on the reduction coefficient of the  $q$ -factor

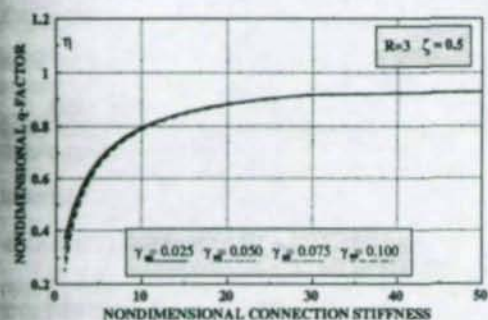


Fig.11 - Influence of  $\gamma_w$  on the reduction coefficient of the  $q$ -factor

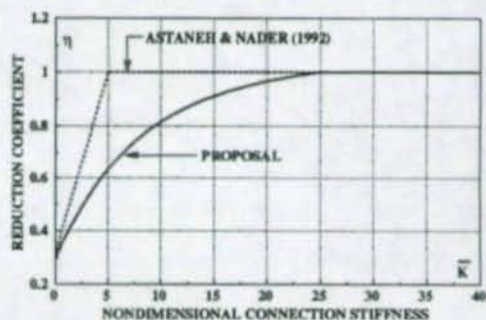


Fig.12 - Proposed reduction coefficient

following formula for evaluating the reduction coefficient  $\eta$  of the  $q$ -factor as a function of  $\bar{K}$  can be suggested:

$$\eta = 0.30 + \frac{0.08 \bar{K}}{\left\{ 1 + \left( \frac{\bar{K}}{10} \right)^{1.58} \right\}^{1/1.58}} \leq 1 \quad (10)$$

The above proposal accounts also for the fact that  $\bar{K} = 25$  is the limit value commonly used (Eurocode 3, 1990) to define conditions for which the influence of the beam-to-column joint behaviour is negligible and, therefore, the structure is considered as a rigid frame.

The comparison between the above relation and the one suggested by other Authors (Astaneh and Nader, 1992a, 1992b) is given in Fig.12. It can be noted that the Astaneh-Nader's proposal practically is limited to a very small range  $\bar{K} < 5$  for the connection stiffness. On the contrary, the physical meaning, also supported by an extended numerical analysis on the assumed model, is in favour of a continuous coverage of the semirigid range with a progressive reduction of the  $q$ -factor as far as  $\bar{K}$  decreases.

## 6. REFERENCES

- A.K. Aggarwal: «Behaviour of Flexible End Plate Beam-to-Column Joints», Journal of Constructional Steel Research, Vol.16, pp.111-134, 1990.
- AIJ: «Standard for Limit State Design of Steel Structures» (Draft), Architectural Institute of Japan, 1990 (English version, October 1992).
- A. Astaneh, N. Nader: «Shaking Table Tests of Steel Semi-Rigid Frames and Seismic Design Procedures», 1st COST C1 Workshop, Strasbourg, October, 1992.

- A. Astaneh, N. Nader:** «Proposed Code Provision for Seismic Design of Steel Semirigid Frames», Submitted to AISC Engineering Journal for review and publication, 1992.
- G. Ballo, L. Calado, A. De Martino, C. Faella, F.M. Mazzolani:** «Cyclic Behaviour of Steel Beam-to-column Joints: Experimental Research», *Costruzioni Metalliche*, n.2, 1987
- G. Ballo, Y. Chen:** «An Experimental Research on Beam to Column Joints: Exterior Connections», XIV Congresso C.T.A., Viareggio, 24-27 Ottobre 1993.
- G. Ballo, Y. Chen:** «An Experimental Research on Beam to Column Joints: Interior Connections», XIV Congresso C.T.A., Viareggio, 24-27 Ottobre 1993.
- C. Bernuzzi, R. Zandonini, P. Zanon:** «Semi-Rigid Steel Connections under Cyclic Loads», Proceedings of the 1st World Conference on Constructional Steel Design, Acapulco, Mexico, 6-9 December, 1992.
- C. Bernuzzi:** «Cyclic Response of Semi-Rigid Steel Joints», Proceedings of the 1st COST C1 Workshop, pp.194-209, Strasbourg, 28-30 October 1992.
- V.V. Bertero, J.C. Anderson, H. Krawinkler:** «Performance of Steel Building Structures during the Northridge Earthquake», Earthquake Engineering Research Center, Report No. UCB/EERC-94/09, University of California, Berkeley, 1994.
- R. Bjorhovde, J. Brozzetti, A. Colson:** «Classification System for Beam-to-Column Connections», *Journal of Structural Engineering, ASCE*, Vol.116, N.11, November, 1990.
- CEN/TC250/SC3-PT9:** «Eurocode 3, Part 1: Joints in Building Frames (Annex J)», 3rd Draft, CEN/TC250/SC3 meeting, Dublin, September 1993.
- Commission of the European Communities:** «Eurocode 8: Structures in Seismic Regions», Draft of October 1993
- Commission of the European Communities:** «Eurocode 3: Design of Steel Structures», 1990
- E. Cosenza, A. De Luca, C. Faella, F.M. Mazzolani:** «Imperfections Sensitivity of Industrial Steel Frames», In «Steel Frames Advances», edited by R. Narayanan, Elsevier Applied Science Publishers, 1987
- ECCS-CECM-EKS:** «European Recommendation for Steel Structures in Seismic Zones, Technical Working Group 1.3 (now TC13): Seismic Design», N.54, 1988.
- A. Elnashai:** «Comments on the Performance of Steel Structures in the Northridge (Southern California) Earthquake of January 1994», *New Steel Construction*, Vol.2, n.5, October 1994.
- M.D. Engelhardt, A.S. Husain:** «Cyclic Tests on Large Scale Steel Moment Connections», Tenth World Conference on Earthquake Engineering, Madrid, Balkema Rotterdam, pp. 2885-2890, 1992.
- M.D. Engelhardt, A.S. Husain:** «Cyclic-Loading Performance of Welded Flange-Bolted Web Connections», *Journal of Structural Engineering, ASCE*, Vol.119, pp.3537-3550, No.12, December 1993.
- C. Faella, V. Piluso, G. Rizzano:** «Connection Influence on the Elastic and Inelastic Behaviour of Steel Frames», International Workshop and Seminar on Behaviour of Steel Structures in Seismic Areas, STESSA 94, Timisoara, Romania, 26 June-1 July, 1994.
- C. Faella, V. Piluso, G. Rizzano:** «Connection Influence on the Seismic Behaviour of Steel Frames», International Workshop and Seminar on Behaviour of Steel Structures in Seismic Areas, STESSA 94, Timisoara, Romania, 26 June-1 July, 1994.
- N. Kishi, W.F. Chen:** «Data Base for Beam-to-Column Connections», I and II, Purdue University, West Lafayette, Indiana, 1986.
- C. Matsui, J. Sakai:** «Effect of Collapse Modes on Ductility of Steel Frames», Tenth World Conference on Earthquake Engineering, Madrid, 1992.
- F.M. Mazzolani, V. Piluso:** «Evaluation of the Rotation Capacity of Steel Beams and Beam-Columns», 1st COST C1 Workshop, Strasbourg, 28-30 October, 1992.
- F.M. Mazzolani, V. Piluso:** «Prediction of the Seismic Behaviour of Semirigid Steel Frames», Second COST C1 Workshop, Prague, 26-28 October, 1994.
- F.M. Mazzolani, V. Piluso:** «Theory and Design of Seismic Resistant Steel Frames», FN & Spon an Imprint of Chapman & Hall, 1995.
- J.B. Schleich, R. Pepin:** «Seismic Resistance of Composite Structures», Commission of the European Communities, Report EUR 14428 EN, 1992.
- I. Simek, F. Wald:** «Test Results of End Plate Beam-to-Column Connections», CTU, G-1121 Report, Prague, 1991.
- K. Tsai, E.P. Popov:** «Steel Beam-Column Joints in Seismic Moment Resisting Frames», Report N. UCB/EERC-88/19, Earthquake Engineering Research Center, University of California, Berkeley, November, 1988.
- UBC:** «Uniform Building Code», 1991 Edition, International Conference of Building Officials, Whittier, CA, 1991.
- K. Weinand:** «SERICON: databank on joints in building frames», 1st COST C1 Workshop, Strasbourg, October 28-30, 1992.
- P. Zoetemeijer, M.H. Kolstein:** «Bolted Beam-Column Connections with Short End Plate», Report 6-75-20 KV-4, University of Technology, Delft, 1975.
- P. Zoetemeijer, H. Munter:** «Extended End Plate with Disappointing Rotation Capacity: Test Results and Analysis», Report 6-75-20 KV-4, University of Technology, Delft, 1983.

## ADVANCES IN CONNECTION DESIGN IN THE UNITED STATES

Charles J. Carter<sup>1</sup>

### Abstract

This paper provides an overview of notable recent advancements in connection design practice in the United States. Topics to be addressed are: partially restrained (PR) moment connections, steel connections in high-seismic regions, blind bolting for tubular members, electronic data transfer, and tee shear connections. As noted herein, many of these topics are addressed in greater detail by other authors at this same conference.

### 1. PARTIALLY RESTRAINED (PR) MOMENT CONNECTIONS

The common approach to connection analysis and design in the United States has been to idealize the moment-rotation characteristics of connections as either simple or fixed. A double-angle simple-shear connection, for example, would be assumed to accommodate the simple-beam rotation while transferring shear, but no moment. A flange-plated moment connection would be assumed to fix the end of the beam, transferring shear and moment, while allowing no relative rotation of the beam end with respect to its support.

The assumption that a connection was either simple or fixed, as well as the construction of connections to approximate that assumption, were both necessary for two main reasons. First, the tasks of analysis and design were greatly simplified and could be accomplished with the tools available to the designer of yesterday: pencil, paper, and slide rule. Second, the actual non-linear moment-rotation behavior of the connection fell outside the assumptions of the elastic allowable stress design approach.

Current technology, however, allows innovative engineers to shed these limitations. Pencil, paper, and slide rule have given way to sophisticated computer-based second-order elastic analysis techniques wherein connections can be modeled as non-linear rotational springs. Furthermore, the advent of LRFD allows the designer to consider the actual behavior of the structure under ultimate loading to ensure its strength and stability.

---

<sup>1</sup>Senior Staff Engineer, American Institute of Steel Construction, One East Wacker Drive, Suite 3100, Chicago, IL 60601-2001, USA

One approach is to model today's standard simple shear connections as PR moment connections to quantify and utilize their inherent rotational stiffness. Swenson (1992) advocates the design of low-rise frames using bolted double-angle connections as the gravity and lateral system for the building, thereby eliminating the need for bracing or what would be considered today as a standard moment connection, i.e., flange welds, flange plates, etc. This system substantially reduced cost by eliminating field welding/inspection and column-web stiffeners while reducing foundation costs, simplifying beam-to-column connections, and reducing frame erection time. It is also noted that consideration of PR-connection behavior in the retrofit of existing structures often eliminates the need for additional bracing or other intrusive strengthening.

The greatest advantage of PR connections, however, is in the potential to develop new connections which need not approximate the behavior of either simple or fixed ends. One such innovation is the semi-rigid composite connection (SRCC). Leon (1993) documents the development of this PR moment connection, which combines a typical web connection with a bottom flange angle and rebar in the slab above (Figure 1). Since the cost to add the bottom angle is minimal and some rebar may be used in the slab anyway for crack control, this detail provides a very economical connection to carry both gravity and lateral load. Papers on this same subject will be presented at this conference by Leon, as well as Easterling and Rex.

## 2. STEEL CONNECTIONS IN HIGH-SEISMIC REGIONS

Traditional seismic design practice has utilized the prescriptive moment connection detail (illustrated in Figure 2) as the preferred connection for special moment frames in seismic regions. Given the perception that this connection offered both superior performance and economy, it is not surprising that it was used nearly exclusively in seismic steel construction. However, unexpected structural damage to more than 100 buildings in the Northridge earthquake demonstrated the susceptibility of the standard detail when large inelastic rotations are required.

An emergency research project at the University of Texas—Austin confirmed some of the damage patterns and resulted in preliminary guidelines in the interim period until further research results are available. This information is available in AISC (1994b) and is the subject of the paper to be presented by Engelhardt, et al, at this conference.

Other research efforts have also been launched to determine long term solutions, such as bolted extended end-plate moment connections and PR framing. Additionally, an innovative energy dissipating connection called the slotted bolted connection (SBC) is now being tested (Popov, et al, 1994).

Illustrated in Figure 3, the SBC utilizes slots in the main connection plate (parallel to the line of loading), which is sandwiched between the brass shims and outer steel plates which have standard holes. When the tensile or compressive force applied to the connection exceeds the frictional resistance, the main plate slips relative to the brass

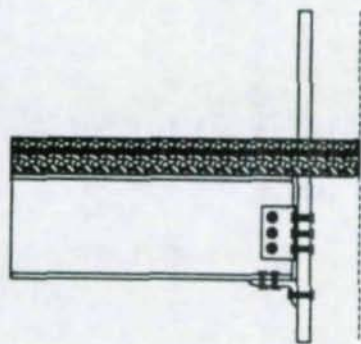
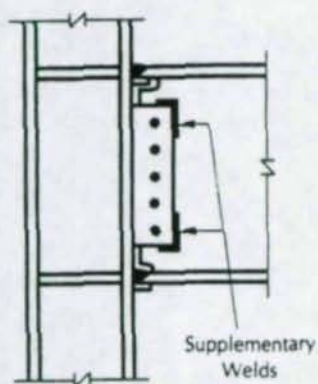


Figure 1. Typical semi-rigid composite connection



Current U.S. Code Requirement

- If  $Z_c/Z$  is less than 0.7:  
Provide supplementary welds with strength to develop 20% of  $M_{p,web}$ .
- If  $Z_c/Z$  is greater than or equal to 0.7:  
No supplementary welds required

Figure 2. Prescriptive seismic connection for special moment frame

shims and outer steel plates, thereby dissipating energy. This process is repeated with slip in the opposite direction upon reversal of the direction of force application.

The resulting approximately rectangular hysteresis loops in Figure 4 demonstrate an elastic-perfectly-plastic behavior with consistently repeatable energy dissipation. Calculations based upon test results showed that nearly 75 percent of the input energy is dissipated.

### 3. BLIND BOLTING FOR TUBULAR MEMBERS

While tubular members are less commonly used in the United States than in other countries, their use is increasing. Traditionally, connections to tubular members have been welded since bolting was possible only near the tube end due to inside inaccessibility. However, a product called the "twist-off blind bolt" or TBB (Figure 5) has been developed by Huck International, a fastener manufacturer in Irvine, CA. Initially, this product was devised to meet a need in the Japanese market.

Manufactured with no apparent head, a head is formed on the far (inaccessible) side of the grip in the initial phase of installation. Subsequently, the installation progresses through snug-tight and is fully tensioned when installation is complete. This fastener provides the strength equivalent of an ASTM A325 high-strength bolt. Refer to Sadri (1994).

### 4. ELECTRONIC DATA TRANSFER

There is a great variety of software available to automate the analysis, design, and fabrication of steel structures. The extent of coverage of any one program, however, is usually quite limited. Thus, in the course of the structure from conception/analysis through fabrication/erection, several different programs might be utilized.

To facilitate the exchange of information between these programs, AISC has formed a Committee on Software, which is responsible, among other things, to develop standards for such data exchange. As a pilot project, a link protocol called *DEL*ink was developed for AISC's connection design software *CONXPRT*.

The following is from the *DEL*ink User's Manual: "*DEL*ink is a data transfer protocol that allows structural design programs to export data to *DE*sign Advisor (the shell system in which AISC's *CONXPRT* runs). This data consists of a knowledge base specification and other information pertaining to the parameters being transferred; i.e., beam and column sizes, values of shear and moment, bolt and weld sizes, ... etc. *DEL*ink is a process in which a text file is generated then read, interpreted, and executed by *DE*sign Advisor. The file consists of a set of keywords and program code fragments. The keywords direct *DE*sign Advisor to perform certain tasks, and the program code fragments are interpreted and executed by the loaded knowledge base."

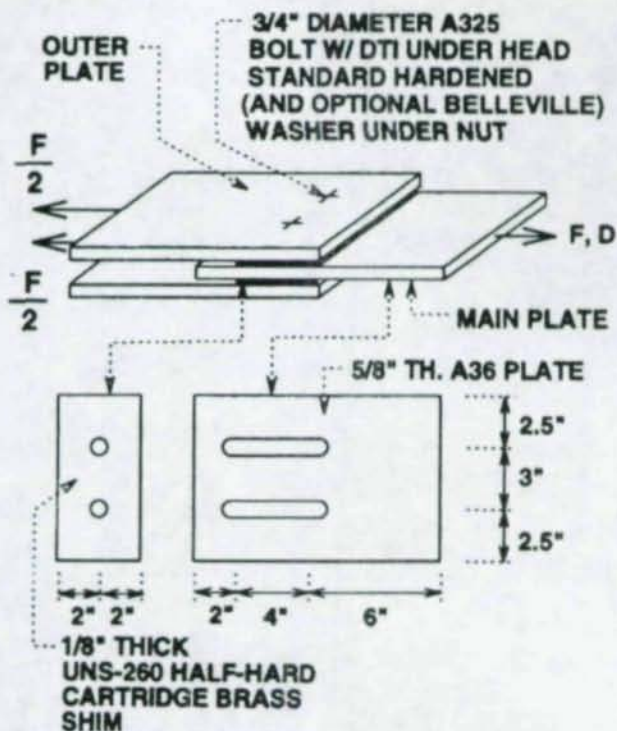


Figure 3. Slotted bolted connection (SBC) detail

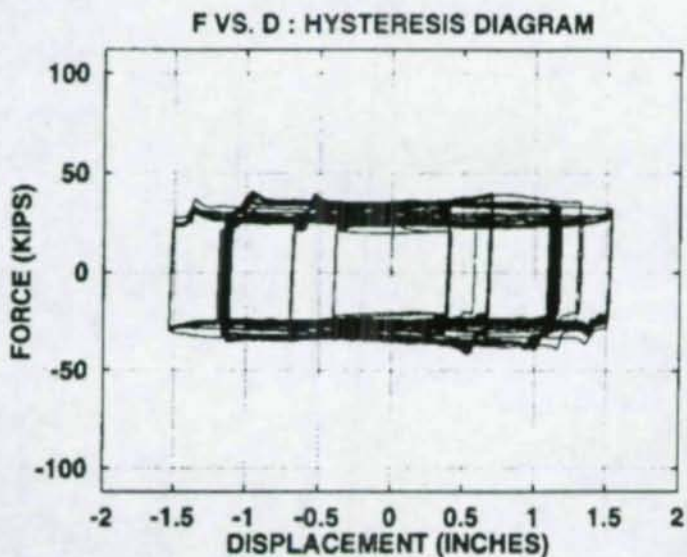


Figure 4. Force-displacement behavior of SBC

The pilot project for which this protocol linked gravity floor framing and column designs performed with RAM Analysis' *RAMSTEEL* to automated connection designs with AISC's *CONXPRT*.

## 5. TEE SHEAR CONNECTIONS

The Astaneh approach to design of tee shear connections (Nader and Astaneh, 1989) provided for ductile behavior through bending of the tee flange. Consequently, the use of many tee sections with thicker flanges was precluded by the assumed limitations. AISC (1994a) incorporates a new approach based upon requirements for ductile behavior (Thornton, 1995) which are also to be presented by Thornton at this conference.

When the tee is welded to the support and bolted to the supported beam, for ductility in the tee connection, the 70 ksi weld size  $w$  must be such that:

$$w_{\min} = 0.0158 \frac{F_y t_f^2}{b} \left( \frac{b^2}{L^2} + 2 \right) \quad (1)$$

but need not exceed  $\frac{3}{4}t_s$ . In the above equation,  $t_f$  is the thickness of the tee flange,  $t_s$  is the thickness of the tee stem, and  $b$  and  $L$  are as illustrated in Figure 6.

For a tee bolted to the support and bolted or welded to the supported beam, the minimum diameter for bolts through the tee flange for ductility must be such that:

$$d_{b \min} = 0.163 t_f \sqrt{\frac{F_y}{b} \left( \frac{b^2}{L^2} + 2 \right)} \quad (2)$$

but need not exceed  $0.69t_s^{1/2}$ . Additionally, to provide for rotational ductility when the tee stem is bolted to the supported beam, the maximum tee stem thickness should be such that:

$$t_{s \max} = \frac{d_b}{2} + 1/16 \text{ in.} \quad (3)$$

When the tee stem is welded to the supported beam, there is no perceived ductility problem for this weld.

Eccentricity is considered as follows: For a flexible support, the bolts or welds attaching the tee flange to the support must be designed for the shear  $R_v$ ; the bolts through the tee stem must be designed for the shear  $R_v$  and the eccentric moment  $R_v a$  where  $a$  is the distance from the face of the support to the centroid of the bolt group through the tee stem. For a rigid support, the bolts or welds attaching the tee flange to the support must be designed for the shear  $R_v$  and the eccentric moment  $R_v a$ ; the bolts through the tee

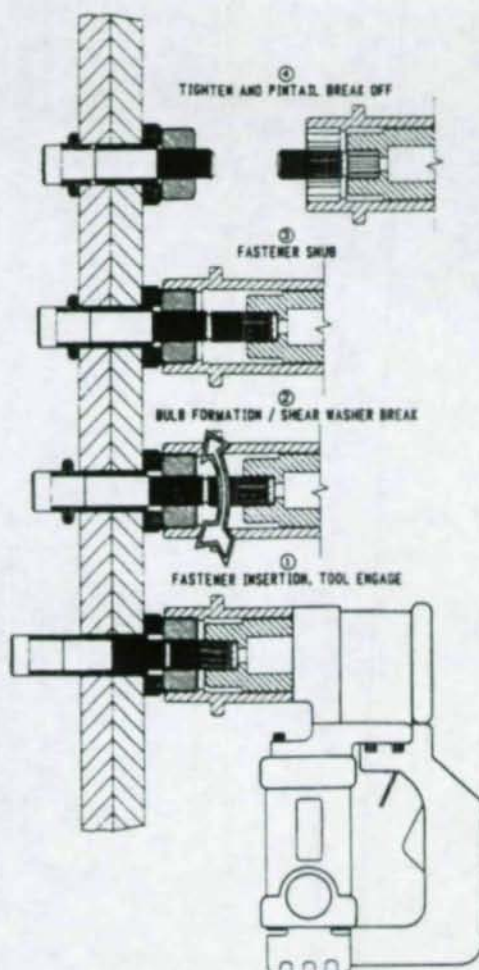


Figure 5. Blind bolt installation steps

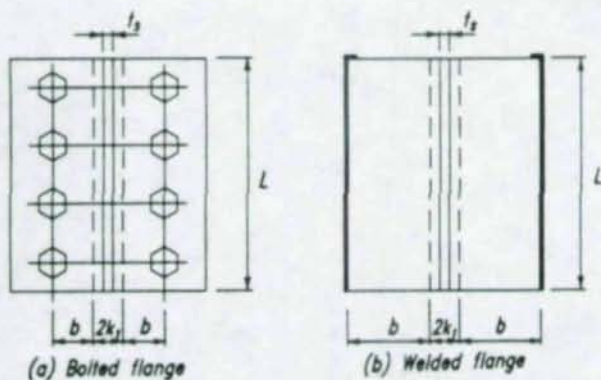


Figure 6. Variables for tee shear connections

stem must be designed for the shear  $R_v$ .

### REFERENCES

- American Institute of Steel Construction, 1994a, *LRFD Manual of Steel Construction*, 2nd Edition, AISC, Chicago, IL.
- American Institute of Steel Construction, 1994b, *Northridge Steel Update I*, AISC, Chicago, IL.
- Leon, R.T., 1993, "Design of Frames with Semi-Rigid Composite Connections," *Proceedings, 1993 National Steel Construction Conference*, pp. 24.1-24.21, AISC, Chicago, IL.
- Nader, M.N. and A. Astaneh, 1989, "Design of Tee Framing Shear Connections," *Engineering Journal*, Vol. 26, No. 1, (1st Qtr.), pp. 9-20, AISC, Chicago, IL.
- Popov, E.P., C.E. Gregorian, and T.S. Yang, 1994, "Cost Effective Energy Dissipating Connections," *Modern Steel Construction*, February, pp. 40-42, AISC, Chicago, IL.
- Sadri, S., 1994, "Blind Bolting," *Modern Steel Construction*, February, pp. 44-46, AISC, Chicago, IL.
- Swenson, K.A., 1992, "Unlocking the Inherent Stiffness of Low-Rise Buildings," *Modern Steel Construction*, (October), pp. 24-29, AISC, Chicago, IL.
- Thornton, W.A., 1995, "A Rational Approach to Design of Tee Shear Connections," *Engineering Journal*, Vol. 32, No. 2, (2nd Qtr.), AISC, Chicago, IL.

## CRITERIA FOR THE USE OF PRELOADED BOLTS IN STRUCTURAL JOINTS

J.W.B. (Jan) Stark <sup>1)</sup>

### Abstract

There are certain cases in which it is important to make sure that bolts in structural joints are so tightened that a minimum clamping force (preload) is ensured. In such cases controlled tightening is required. In practice there is no uniform opinion about the situations where preloading of joints is really necessary. Also there is not agreement on the tightening procedures. In this paper an attempt is made to formulate objective criteria for the use and installation of preloaded bolts.

### 1. INTRODUCTION

In ENV 1993-1 (Eurocode 3) and ENV 1090-1, rules are given for the design and execution of bolted connections. Depending on the required performance of the joint, the bolts may be used as preloaded or non-preloaded ("snug-tight") bolts. In some cases, the performance specifications can only be met when the bolts are so tightened that a minimum clamping force is ensured. In such cases, controlled tightening is to be requested. It should, however, be realised that procedures for control of preload are cost-intensive and have, in principal, a negative influence on the speed of fabrication and erection. So, preloaded bolts with controlled tightening should only be used in cases where it is absolutely necessary. In existing practice, controlled tightening is in the author's view unnecessarily required in many situations. This is of course not favourable for the use of steel. In the paper, a first attempt is made to objectively specify criteria for the use of preloaded bolts. If controlled tightening is necessary, a choice has to be made between different methods. In ENV 1090-1, four methods are specified. These methods will be shortly described and pros and cons discussed.

The subject of this paper has been intensively discussed in ECCS-TC 10 for a long time. Due to differences in tradition, quality level of the fabrication industry, control procedures and views on structural integrity in the various countries, it was, until now, not possible to reach full agreement on the best tightening procedure to be recommended.

So, although the contents of this paper is influenced by the discussions in ECCS-TC10, it does not necessarily reflect the common opinion of that committee.

---

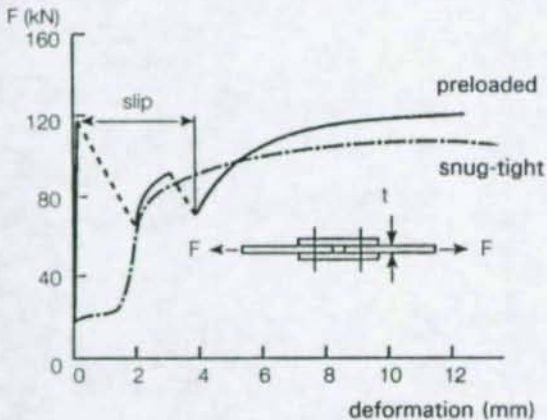
<sup>1)</sup> Professor Steel Structures, Delft University of Technology  
Deputy director, TNO Building and Construction Research  
P.O. Box 49, 2600 AA Delft, The Netherlands

## 2. WHY PRELOADING ?

By pretensioning of the bolts, a clamping pressure will develop between the connected parts. This clamping pressure influences the structural response. This will be illustrated for two basic load cases, e.g. shear and direct tension.

### Shear

To facilitate easy erection, the holes have a clearance with respect to the diameter of the bolt. The normal clearance is 2 mm. This hole clearance causes extra deformation due to slip if the joint is loaded in shear. The load-deformation response will be influenced by the preload in the bolts.



This is illustrated in figure 1, where the load-deformation diagram of a lap joint is given for a low and high preload.

The preload in the bolt causes clamping forces between the plates. Friction will prevent slipping of the connection.

Figure 1: Load-deformation diagram of a lap joint

The friction resistance for each friction interface is equal to the clamping force (= *preload*) times the *slip factor*. So if the preload is small, a relatively low shear load will cause some slip in the order of a few millimeters. The connection "sets" until the bolts are "bearing" against the sides of the holes. If the relatively small deformation due to slip is not acceptable, a high preload in combination with a good and reliable slip factor can be used to prevent the slip. Once slip occurs, a preloaded connection progressively becomes a bearing type and at larger slips both types of joints behave similarly. The load transfer mechanism in a non-preloaded and in a preloaded joint before slip is illustrated in figure 2.

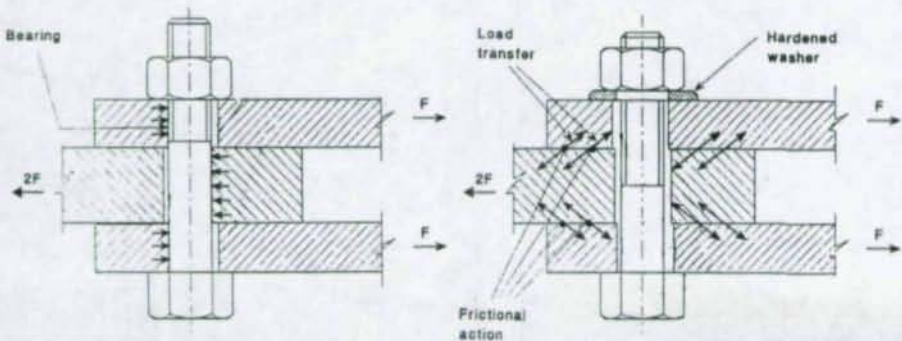


Figure 2: Load transfer mechanism in a non-preloaded and a preloaded joint

### Tension

If a joint with preloaded bolts is subjected to an external tension force, the response is often illustrated with the "force triangle" given in figure 3.

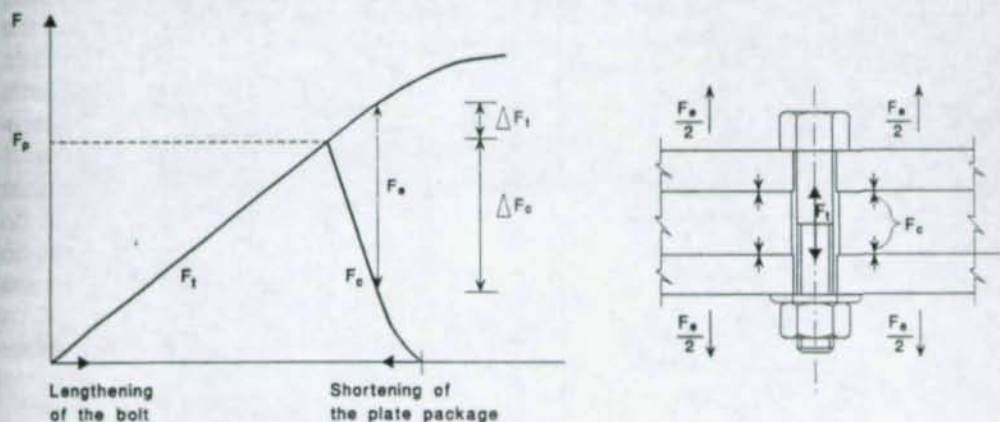


Figure 3: "Force triangle"

This triangle gives the relation between bolt elongation and the shortening of the plate assembly due to preloading. An external load  $F_e$  will cause an increase of the bolt elongation, but at the same time expansion of the plate assembly. As a result of that, the load in the bolt will increase by  $\Delta F_t$  and the clamping force will be reduced by  $\Delta F_c$ .

The external load  $F_e$  is the sum of  $\Delta F_t$  and  $\Delta F_c$ . The relation between  $\Delta F_t$  and  $\Delta F_c$  is dependent on the stiffness relation between bolt and plate assembly. Therefore the variation of the force in the bolt due to external load can be influenced by the location of the clamping force.

In figure 4, a T-stub connection is shown, where the contact is concentrated in the central "stiff" region. In this case, the bolt force will not increase until  $F_t = F_p$  and separation starts. So the location of the contact pressure is of crucial importance with regard to bolt fatigue. The right detailing as shown in e.g. figure 4 leads to static loading of the bolts, although the joint is subjected to fatigue loading.

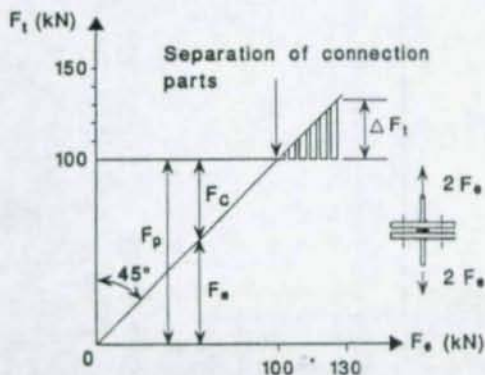


Figure 4: Development of bolt tension in a T-stub connection

### 3. WHEN PRELOADING ?

In some countries it was common practice to require that all high-strength bolts be installed, so as to provide a high level of preload, regardless of whether it was really needed or not. In North America this was the case until 1985 and the situation in Europe differs from country to country.

It may be that this practice was influenced by the use of the indication HSFG-bolts (high strength friction grip bolts). This suggests that "high strength" and "friction grip" are directly related.

As was noted in section 2, the ultimate strength of bolted joints is not dependent upon the amount of preload in the bolts. So if the joint has to conform with no other requirements than static strength ("resistance" in Euro-slang), there is no reason to require preloading. This is now accepted in Eurocode 3 by the introduction of 5 categories of bolted connections as given in table 1.

Use of non-preloaded high-strength bolts up to grade 10.9 is permitted for shear connections (Cat.A) as well as tension connections (Cat.D)

Table 1: Categories of bolted connections in ENV 1993-1 (Eurocode 3)

Shear connections		
Category	Criteria	Remarks
A bearing type	$F_{v,Sd} \leq F_{v,Rd}$ $F_{v,Sd} \leq F_{b,Rd}$	No preloading required. All grades from 4.6 to 10.9.
B slip-resistant at serviceability	$F_{v,Sd,ser} \leq F_{s,Rd,ser}$ $F_{v,Sd} \leq F_{v,Rd}$ $F_{v,Sd} \leq F_{b,Rd}$	Preloaded high strength bolts. No slip at the serviceability limit state.
C slip-resistant at ultimate	$F_{v,Sd} \leq F_{s,Rd}$ $F_{v,Sd} \leq F_{b,Rd}$	Preloaded high strength bolts. No slip at the ultimate limit state.
Tension capacity		
Category	Criterion	Remarks
D non-preloaded	$F_{t,Sd} \leq F_{t,Rd}$	No preloading required. All grades from 4.6 to 10.9.
E preloaded	$F_{t,Sd} \leq F_{t,Rd}$	Preloaded high strength bolts.
Key:		
$F_{v,Sd,ser}$	= design shear force per bolt for the serviceability limit state	
$F_{v,Sd}$	= design shear force per bolt for the ultimate limit state	
$F_{v,Rd}$	= design shear resistance per bolt	
$F_{b,Rd}$	= design bearing resistance per bolt	
$F_{s,Rd,ser}$	= design slip resistance per bolt at the serviceability limit state	
$F_{s,Rd}$	= design slip resistance per bolt at the ultimate limit state	
$F_{t,Sd}$	= design tensile force per bolt for the ultimate limit state	
$F_{t,Rd}$	= design tension resistance per bolt	

In North America the RCSC (Research Council on Structural Connections) introduced in 1985 the requirement that only fasteners that are to be used in slipcritical connections or in connections subject to direct tension, need to be preloaded. Bolts to be used in bearing-type connections need only be tightened to the snug-tight condition. This is hopefully a first step. The next step should be that also in North-America non-preloaded bolts may be used in connections subject to direct tension when the loading is predominantly static.

Now situations will be described where the use of preloaded bolts may be useful or even necessary.

### **Shear connections**

Reasons for preloading may be:

- a. To avoid reduction of stiffness due to slip in the joint.

When the deformation criteria are very stringent or when the deformation has to be determined very accurately it may be necessary to avoid slip in the joints. Normally this will concern a serviceability criteria so that category B is sufficient.

Deformation of joints may also influence the resistance as is the case for the stability of a slender unbraced frame (see figure 5). In this case category C connections are required.

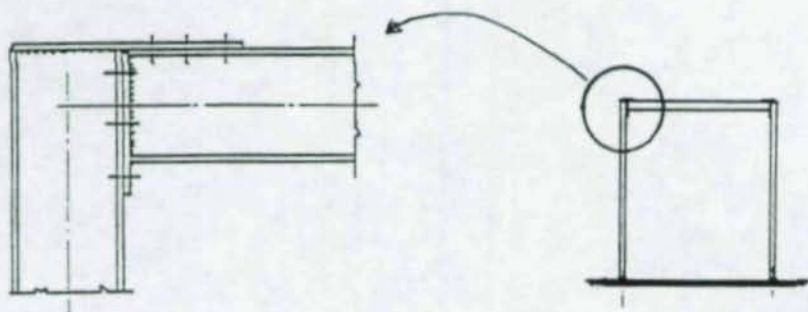


Figure 5: Beam-to-column connection in an unbraced frame

The designer should realise that use of slip resistant connections is very expensive and therefore seek for another solution. This may be to accept the additional deformation of the joint and compensate this by extra stiffness of the members. A bit more steel (relatively cheap!) will almost always be more economic than considerable increase of fabrication cost.

- b. Sometimes the normal clearance of holes is not sufficient to compensate the tolerances on site. The use of oversize or slotted holes may then be necessary to facilitate easy erection.

Oversize and slotted holes shall only be used in slip-resistant connections.

- c. When a connection is subject to frequent reversal of load, slipping is not acceptable and preloaded bolts in a slip-resistant connection, injection bolts or fitted bolts shall be used. An example is the bracing of a crane-runway.

For wind and/or stability bracing, bearing type connections may normally be used (EC3, clause 6.3 (3)). A possibility to avoid reversal of load in bracing connections is to pretension the brace member by a turn buckle or by other means.

- d. When a joint is subject to impact or significant vibration loosening of the nuts should be prevented. This may be by preloading the bolts but other locking devices are available and may be less expensive than controlled tightening.
- e. Preloaded bolts in slip-resistant connections may be used to improve the fatigue resistance.

For the decision to use slip-resistant connections the designer should realise that additional to cost-intensive controlled tightening procedures also special care for control of friction surfaces during fabrication and erection is required.

### *Tension connections*

Reasons for preloading may be:

- a. To improve the fatigue resistance.

The fatigue resistance of a single bolt in tension is rather poor. However, as explained in section 2, preloading in combination with the right location of the clamping force will reduce or even eliminate variation of bolt forces.

- b. By preloading of the bolts the stiffness will increase as illustrated by the load deformation diagram of a T-stub given in figure 6. The designer should consider whether the required stiffness can possibly be obtained by redesign of the connection components without using preloaded bolts. Alternatively he can also consider to increase the stiffness of other structural components, for example by taking somewhat heavier members. These measures will almost always give more economic designs than use of preloaded bolts.

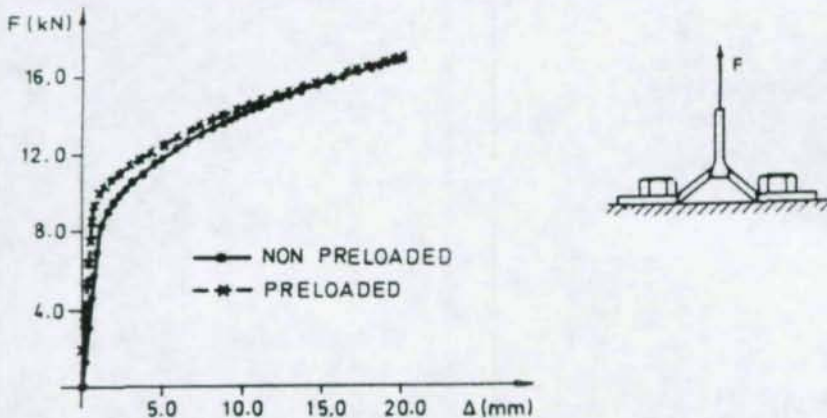


Figure 6: Effect of preloading on the response of a T-stub connection

In summary the need to use preloaded bolts is typically in bridges, cranes, crane girders and other structures loaded by fatigue or dynamic loading. They should rarely be applied in buildings and other predominantly static structures.

In the future the choice between preloaded and non-preloaded bolts should be based on quantitative performance specifications for the joints instead of general qualitative indications as given above.

#### 4. HOW PRELOADING ?

To provide the desired level of preload for bolts used in slip-resistant connections (cat. B and C) or preloaded connections subject to tension (cat. E) RCSC Specifications and Eurocode 3 require that the bolts be tightened such that the resulting bolt tension is at least 70% of the nominal tensile strength of the bolt.

$$F_{p,Cd} = 0.7 f_{ub} A_s$$

The installation of bolts should comply with the following two requirements:

- Tightening the bolts should result in at least the specified bolt tension (preload)
- Tightening should be stopped in time so that there is sufficient reserve against breaking of the bolt (overtightening).

In ENV 1090-1 the following installation methods are covered:

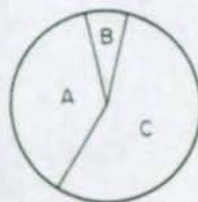
- Torque control method
- Turn of the nut method
- Torque and turn method (combined method)
- Direct tension indicator method
- Special devices/bolts

The first three "direct" methods and their pros and cons are now discussed.

##### **Torque control method**

When the high-strength bolt was introduced, installation was primarily by methods of torque control. Approximate torque values were suggested for use in obtaining the specified bolt tension.

For this method of tightening a calibrated torque wrench is required which may be hand operated or, for bolts of larger diameters, power operated.



- A = thread friction
- B = bolt tension
- C = nut face friction

The greater part of the torque applied is used to overcome the thread friction and the friction between the nut and the surface against which it rotates.

Only a small portion is effectively utilized to develop the bolt tension (see figure 7). If the geometry of the screw head and the coefficient of friction between the various mating surfaces were known, it would be possible to estimate the tension induced by a given torque.

Figure 7: Distribution of torque

The uncertainties concerning distribution of contact pressures, and the variabilities of coefficients of friction in practice, do not justify the use of anything other than a simple rule such as:

$$M_s = k d F_p$$

where:

$M_s$  is the applied torque (Nmm)

$d$  is the bolt diameter (mm)

$F_p$  is the preload in the bolt (N)

$k$  is the coefficient of friction between mating surfaces

In practice  $k$  values have been measured for new bolts which vary between 0,12 and 0,20.

Many tests showed the great variability of the torque-tension relationship as illustrated in figure 8.

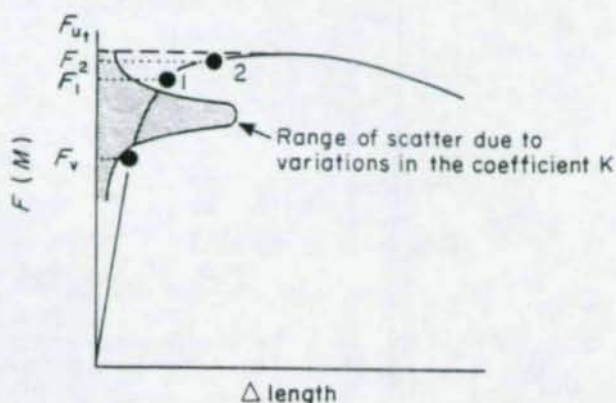


Figure 8: Preloading with the torque method

Even bolts from the same lot yielded extreme values of bolt tension  $\pm 30\%$  from the mean tension derived. The variance is caused mainly by the variability of the thread conditions, surface conditions under the nut and lubrication. The water-soluble lubricant supplied on bolts can be degraded by rain or moisture or threads can become contaminated on site with dirt or grease.

The result is an erratic torque-tension relationship.

Therefore, the torque method is not recommended by the ECCS and Eurocode 3. The best possible results will be obtained if the following recommendations are followed:

- the torque wrenches shall be checked at least every day using a bolt tension calibrator
- all bolts shall be from one manufacturer, at least per diameter group
- protect the bolts from contamination
- use a hardened steel washer under the part to be turned
- use reliable tightening tools

Even if these recommendations are complied with it is questionable whether 70% of the nominal tensile strength can be consistently and safely achieved.

It has been suggested to reduce the specified preload for this tightening method to as low as 50% of the nominal tensile strength [Bouwman and Piraprez, 1989]. In Germany 63% is common practice.

**Turn-of-the-nut method**

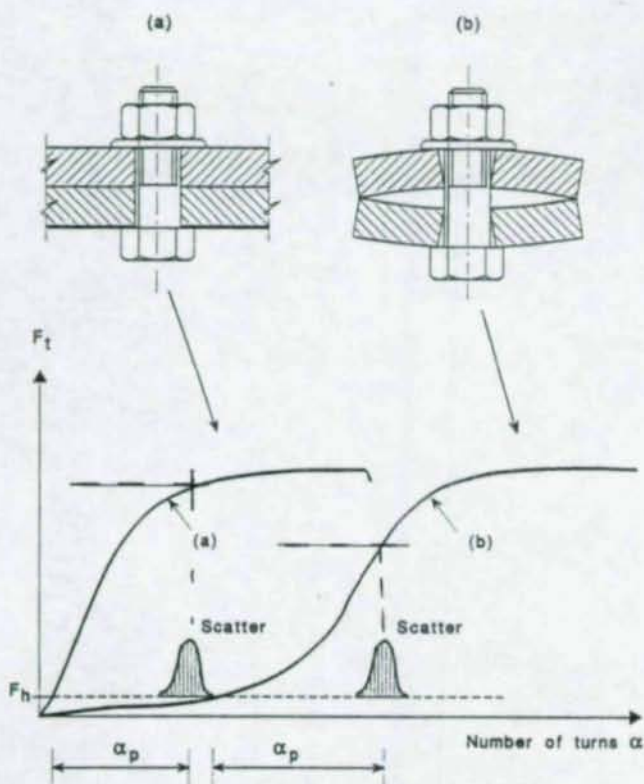
This method is based on a specified or predetermined rotation of the nut after initial tightening to "hand tight" or "snug tight" condition.

Controlling tension by the turn-of-the-nut method is primarily strain control (see figure 9).

The purpose is to rotate the nut sufficiently to take the bolt well into the inelastic region. In the inelastic region the load versus elongation curve is relatively flat, with the consequence that the bolt tension is comparatively insensitive to variation in the nut rotation, while a large reserve exists against breaking the bolt.

It should be noted that the ductility of the bolt largely depends on the length of the threaded portion. Care must be taken with short bolts which have only a small amount of thread in the grip (5 threads is a minimum).

Where the plates are not flat and parallel as indicated in Figure 9b, this method has the disadvantage that the preload will not be reached if not enough attention is paid to closing the gaps. A requirement of the method is therefore that the contact surfaces must fit snugly before the bolts are finally tightened.



(a) Plates are flat. After tightening ( $F_h$ ) the required preload is obtained ( $\alpha_p$  prescribed number of turns).

(b) Plates are stiff and not flat, after hand tightening ( $F_h$ ) the gap is not closed. The required preload is not obtained

Figure 9: Preloading with the turn-of-the-nut method

### Torque and turn method (combined method)

In this method the torque method and the turn-of-the-nut method are combined. It is the most reliable method and recommended by ECCS and CEN-TC135.

The bolts are tightened by a two step procedure :

Step 1: First tighten all the bolts to 75% of the specified preload (= 53% of the nominal tensile strength). As indicated in the discussion of the torque method the danger of overtightening due to unexpected low friction is sufficiently low at this level of the torque. On the other hand the bolt tension will be in most cases sufficiently high to close the gaps between the connected parts.

Step 2: Subsequently an additional further turn is applied. In ENV 1090-1 indicative values for the angle of the additional rotation are given (values between 60 and 120 degrees, depending of the bolt length). In case of doubt the required angle should be determined by testing.

This method is logical because it is based on force control in the elastic region and on deformation control in the inelastic region. The method is not very sensitive to variation in friction. At the same time it is not very sensitive to variation in stiffness of the plate assembly. This is illustrated in figure 10.

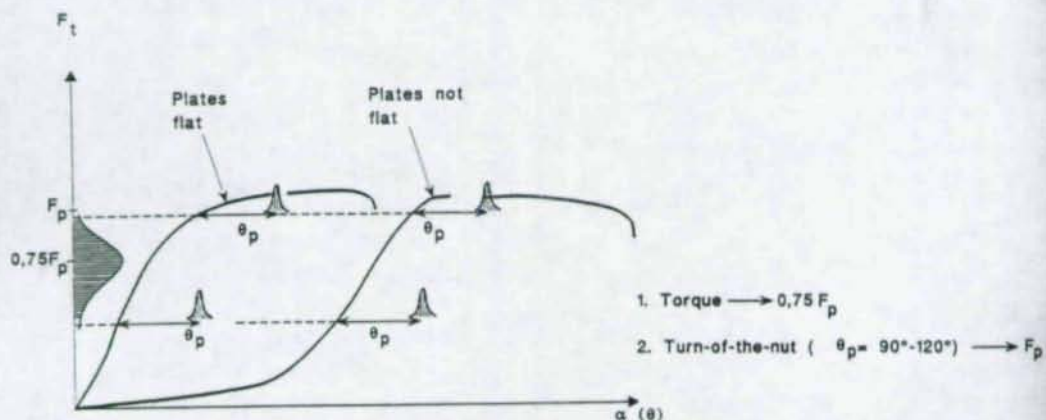


Figure 10: Preloading with the torque and turn method

### REFERENCES

- Kulak G.L., Fisher J.W., Struik J.H.A., (1987). *Guide to Design Criteria for Bolted and Rivetted Joints*. 2nd ed., John Wiley and Sons
- Bouwman L.P., Piraprez., (1989) *The tightening of high-strength bolts in Europe*. Steel Construction Today, 3
- ECCS, (1985), *European Recommendations for Bolted Connections in Structural Steelwork*. ECCS publication No. 38, Brussels
- Eurocode 3, ENV 1993-1-1, (1992). *Design of Steel Structures. Part 1.1 - General Rules and Rules for Buildings*. CEN, Brussels
- ENV 1090-1, (1995). *Execution of Steel Structures. Part 1 - General Rules and Rules for Buildings*. CEN, Brussels

## The Stiffness Model of revised Annex J of Eurocode 3

Klaus Weynand<sup>1</sup>

Jean-Pierre Jaspart<sup>2</sup>

Martin Steenhuis<sup>3</sup>

### Abstract

In 1994 a revised draft of Annex J of Eurocode 3 entitled 'joints in building frames' was approved by CEN. For this Annex a new model for the determination of the rotational stiffness was developed. This paper provides backgrounds to this new stiffness model and shows comparisons with test results.

### 1. INTRODUCTION

A major technical improvement in the revised Annex J of Eurocode 3 [1] (hereafter: Annex J) is the new model for the determination of the rotational response of joints. The objective of this paper is to provide backgrounds to this model. These are given in the first part of this paper. In the second part comparisons are made with test results.

In general, the moment rotation characteristic ( $M-\phi$  curve) of joints is non-linear. Although Annex J can be used to determine a simplified linear, bi-linear or multi-linear  $M-\phi$  curve, this paper will focus on its potential to predict a full non-linear curve. This is to enable a direct comparison between model and test results.

The test results are taken from the databank SERICON [2]. This databank forms a collection of  $M-\phi$  data from different laboratories all over Europe. The databank contains results for different types of joints (e.g. welded joints, joints with extended end

---

<sup>1</sup> Dipl.-Ing., Research Assistant, Institute of Steel Construction, RWTH Aachen, 52056 Aachen, Germany

<sup>2</sup> Dr. Ir., Research Associate, MSM Department, University of Liège, 4000 Liège, Belgium

<sup>3</sup> Ir., Research Assistant, Department of Structural Engineering, TNO Building and Construction Research, 2600 AA Delft, The Netherlands

plates, joints with flush end plates and cleated joints) and for different joint configurations (e.g. single sided, double sided).

Key differences between the model in the new Annex J and the old Annex J [3] are the following:

- 1) In the old Annex the calculated deformations of the components were those corresponding to the design resistance of these components (see chapter 3 for the definition of the word "component"). The elastic deformations were calculated back from these deformations by dividing with a factor 2,25. In the new Annex, the elastic deformations are calculated directly.
- 2) Unlike in the old Annex, these elastic deformations are now only dependent on the lay-out of the joint and the Young modulus and not any more on strength properties or safety factors.
- 3) The calculation of the full non-linear curve in the new Annex is simplified compared to the old one.
- 4) In the old Annex, the stiffness prediction of a stiffened end plated joint could be below the prediction of an unstiffened one. This problem is now resolved.

## 2. THE GENERAL MODEL

Provided that the non-linear  $M-\phi$  curve of the new Annex J is not limited by the rotational capacity ( $\phi_{Cd}$ ), this curve consists of 3 parts, see figure 1. Up to a level of  $2/3$  of the design moment resistance ( $M_{j,Rd}$ ), the curve is assumed to be linear elastic. The corresponding stiffness is the so-called initial stiffness  $S_{j,ini}$ . Between  $2/3 \cdot M_{j,Rd}$  and  $M_{j,Rd}$ , the curve is non-linear. After the moment in the joint reaches  $M_{j,Rd}$ , a yield plateau could appear. The end of this  $M-\phi$  curve indicates the rotational capacity ( $\phi_{Cd}$ ) of the joint. Since the determination of  $M_{j,Rd}$  and the rotational capacity in the new Annex J is not significantly different from the old Annex J and backgrounds are well documented [4, 5], this paper will not focus on these aspects.

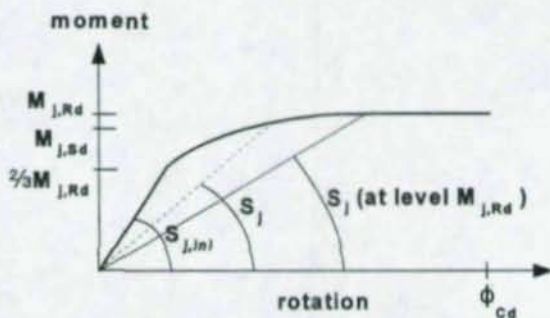


Figure 1: Non-linear  $M-\phi$  curve according to Annex J.

The model assumes a fixed ratio between the initial stiffness  $S_{j,ini}$  and the secant stiffness at the intersection between the non-linear part and the yield plateau ( $S_j$  at level  $M_{j,Rd}$ ). For end plated and welded joints, this ratio is equal to 3. For flange cleated joints, this ratio is 3,5, see figure 1. These values are simplified values and result from numerous parameter studies and test observations [5].

The shape of the non-linear part for  $M_{j,Sd}$  between  $2/3 \cdot M_{j,Rd}$  and  $M_{j,Rd}$  can be found with the following interpolation formula:

$$S_j = \frac{S_{j,ini}}{\left( \frac{1,5 M_{j,Sd}}{M_{j,Rd}} \right)^\psi} \quad (1)$$

where  $\psi = 2,7$  for end plated and welded joints and  $3,1$  for flange cleated joints.

In this interpolation formula, the value of  $S_j$  is dependent on  $M_{j,Sd}$ .

### 3. DETERMINATION OF THE INITIAL STIFFNESS $S_{j,ini}$

The Annex J stiffness model utilizes the so called "component method". The essence of this method is that the rotational response of the joint is determined based on the mechanical properties of the different components in the joint. The advantage of this method is that an engineer is able to calculate the mechanical properties of any joint by decomposing the joint into relevant components. Annex J gives direct guidance for end plated, welded and flange cleated joints for this decomposition. Table 1 shows an overview of components to be taken into account when calculating the initial stiffness for these types of joints.

Table 1: Overview of components for different joints

Component	Number	End plated	Welded	Flange cleated
Column web panel in shear	1	x	x	x
Column web in compression	2	x	x	x
Column flange in bending	3	x		x
Column web in tension	4	x	x	x
end plate in bending	5	x		
flange cleat in bending	6			x
bolts in tension	7	x		x
bolts in shear	8			x
bolts in bearing	9			x

In the model it is assumed that the deformations of the following components: a) beam flange and web in compression, b) beam web in tension and c) plate in tension or compression are included in the deformations of the beam in bending. Consequently they are not assumed to contribute to the flexibility of the joint.

The initial stiffness  $S_{j,ini}$  is derived from the elastic stiffnesses of the components. The elastic behaviour of each component is represented by a spring. The force-deformation

relationship of this spring is given by:

$$F_i = k_i \cdot E \cdot \Delta_i \quad (2)$$

where  $F_i$  = the force in the spring  $i$ ,  
 $k_i$  = the stiffness coefficient of the component  $i$ ,  
 $E$  = the Young modulus and  
 $\Delta_i$  = the spring deformation  $i$ .

Chapter 4 gives backgrounds of the formulae to determine  $k_i$ .

The spring components in a joint are combined into a spring model. Figure 2 shows for example the spring model for an unstiffened welded beam-to-column joint.

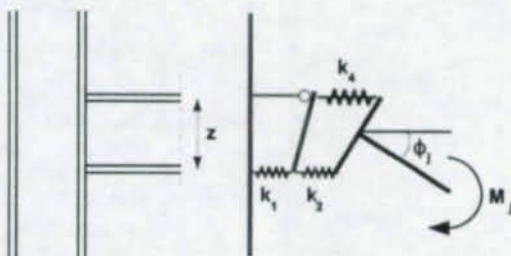


Figure 2: Spring model for an unstiffened welded joint.

The force in each spring is equal to  $F$ . The moment  $M_j$  acting in the spring model is equal to  $Fz$ , where  $z$  is distance between the centre of tension (for welded joints located in the centre of the upper beam flange) and the centre of compression (for welded joints located in the centre of the lower beam flange). The rotation  $\phi_j$  in the joint is equal to  $(\Delta_1 + \Delta_2 + \Delta_4) / z$ . In other words:

$$S_{j,ini} = \frac{M_j}{\phi_j} = \frac{Fz}{\frac{\Sigma \Delta_i}{z}} = \frac{Fz^2}{E \Sigma \frac{1}{k_i}} = \frac{Ez^2}{\Sigma \frac{1}{k_i}} \quad (3)$$

For an end plated joint with only one bolt row in tension and for a flange cleated joint the same formula yields. However, components to be taken into account are different, see table 1.

Figure 3a shows the spring model adopted for end plated joints with two or more bolt rows in tension. It is assumed that the bolt row deformations for all rows are proportional to the distance to the point of compression, but that the elastic forces in each row are dependent on the stiffness of the components. Figure 3b shows how the deformations per bolt row of components 3, 4, 5 and 7 are added to an effective spring per bolt row, with an effective stiffness coefficient  $k_{eff,r}$  ( $r$  is the index of the row number). In figure 3c is indicated how these effective springs per bolt row are replaced by an equivalent spring acting at a lever arm  $z$ . The stiffness coefficient of this

effective spring is  $k_{eq}$ . The effective stiffness coefficient  $k_{eq}$  can directly be applied in formula 3. The formulae to determine  $k_{eff}$ ,  $k_{eq}$  and  $z$  as given in Annex J can directly be derived from the sketches of figure 3. The bases for these formulae is that the moment-rotation behaviour of each of the systems in figure 3a, 3b and 3c is equal. An additional condition is that the compressive force in the lower rigid bar is equal in each of these systems.

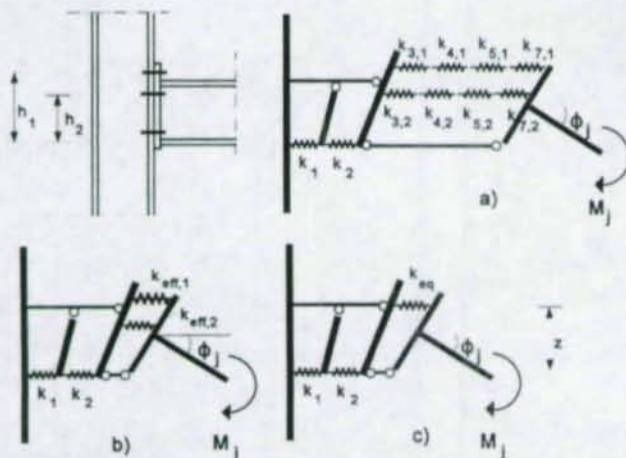


Figure 3: Spring model for a beam-to-column end plated joint with two bolt rows in tension.

#### 4. DETERMINATION OF THE STIFFNESS COEFFICIENTS $k$

##### 4.1 Plates in bending and bolts in tension

In the procedure for strength calculation included in Annex J, the three following components: (i) column flange in bending, (ii) end plate in bending and (iii) flange cleat in bending are idealized as T-stubs (see figure 4). These ones are assumed to be connected by means of bolts to an infinitely rigid foundation (figure 5 and 6.a). Their so-called "effective length  $l_{eff}$ " is such that the failure modes and the corresponding collapse loads are similar to those of the actual joint components. The concept of "equivalent T-stubs" for strength is easy to use and allows to cover the calculations of all the plated components with the same set of formulae.

The "T-stub concept" may also be referred to for stiffness calculation as shown in [5] and [6]. The equivalence between the actual component and the equivalent T-stub in the elastic range of behaviour (initial stiffness) is however to be expressed in a different way than at collapse and requires the definition of a new effective length  $l_{eff,ini}$ . In view of the determination of the related stiffness coefficients  $k$ , two problems have to be investigated:

- the response of the T-stub in the elastic range of behaviour;
- the determination of  $l_{eff,ini}$ .

These two points are successively addressed hereunder.

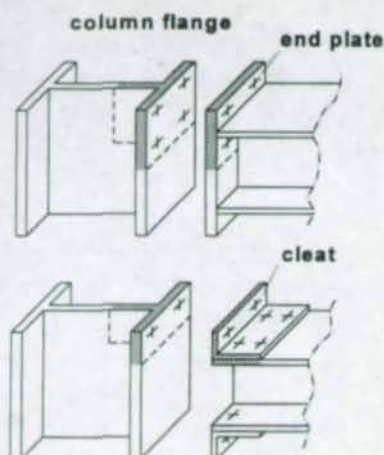


Figure 4: T-stub idealizations

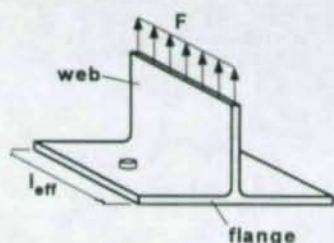


Figure 5: T-stub on rigid foundation

### a) T-stub response

When subjected to tension forces, the flange of the T-stub deforms in bending and the bolts mainly in tension (figure 6.a). The elastic response of this system has been studied first by YEE and MELCHERS [6]. A slight refinement related to the location of the prying effect has been proposed later in [5]. The corresponding expressions are rather long to apply so simplifications have been introduced by the authors:

- to simplify the formulae:  $n$  is considered as equal to  $1,25 m$  ( $m$  and  $n$  are indicated in figure 6.a)
- to dissociate the bolt deformability (figure 6.c) from that of the T-stub (figure 6.b).

Under these assumptions, it can be shown that:

- for the T-stub (figure 6.b):

$$k_{y,s,s} = \frac{l_{eff,ini} t^3}{m^3} \quad (4)$$

- for the bolts (figure 6.c):

$$k_y = 1,6 \frac{A_s}{L_b} \quad (5)$$

where  $A_s$  = bolt reduced area,  $L_b$  = bolt length including half thickness of the bolt head and of the nut and  $t$  = T-stub flange thickness. The indexes of the  $k$  coefficients relate to the component numbers listed in table 1. In equation (5), a factor 2,0 instead of 1,6 would be expected at first sight; in reality, the value 1,6 is defined in such a way that the prying effect is taken into consideration.

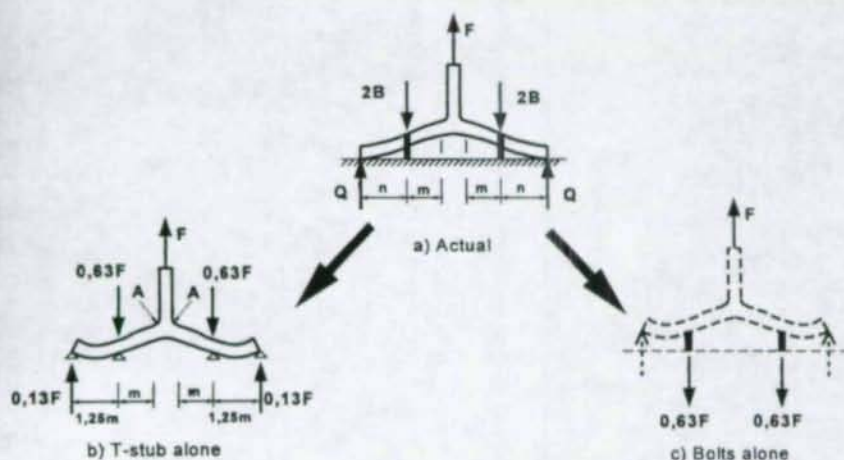


Figure 6: Elastic deformation of the T-stub

### b) Definition of $l_{eff,ini}$

In figure 6.b, the maximum bending moment in the T-stub flange (points A) is expressed as  $M_{max} = 0,322 \cdot F \cdot m$ . Based on this expression, the maximum elastic load  $F_{el}$  (first plastic hinges in the T-stub at points A) to be applied to the T-stub can be derived:

$$F_{el} = \frac{4 l_{eff,ini}}{1,288 \text{ m}} \frac{t^2 f_y}{4} = \frac{l_{eff,ini}}{1,288 \text{ m}} t^2 f_y \quad (6)$$

In Annex J, the ratio between the design resistance and the maximum elastic resistance of each of the components is taken as equal to 3/2 so:

$$F_{rd} = \frac{3}{2} F_{el} = \frac{l_{eff,ini}}{0,859 \text{ m}} t^2 f_y \quad (7)$$

As, in figure 6.b, the T-stub flange is supported at the bolt level, the only possible collapse mode of the T-stub is the development of a plastic mechanism in the flange. The associated collapse load is given by Annex J as:

$$F_{rd} = \frac{l_{eff} t^2 f_y}{m} \quad (8)$$

where  $l_{eff}$  is the effective length of the T-stub for strength calculation. By identification of expressions (7) and (8),  $l_{eff,ini}$  may be derived:

$$l_{eff,ini} = 0,859 l_{eff} = 0,85 l_{eff} \quad (9)$$

Finally, by introducing equation (9) in the expression (4) giving the value of  $k_{3,5,6}$ :

$$k_{3,5,6} = \frac{0,85 l_{eff} t^3}{m^3} \quad (10)$$

## 4.2 Column web panel in shear

In beam-to-column joints, column web panels are subjected to high shear forces  $V$  (see figure 7). The shear force  $V$  can be expressed as  $\beta \cdot F$  ( $F$  forces are statically equivalent to the applied moment  $M$ , see figure 7).  $\beta$  values are dependent on the joint configuration and loading; related values are given in Annex J.

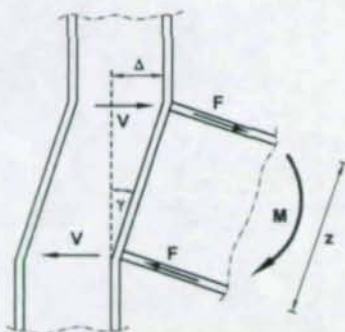


Figure 7: Column web panel in shear

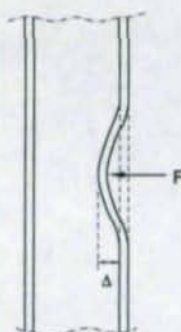


Figure 8: Column web in tension or compression

Through experimental and numerical research works e.g. [5], it has been shown that shear stresses  $\tau$  in column web panels are more or less uniformly distributed. The corresponding deformation  $\gamma$  is therefore such that  $\tau = G \cdot \gamma$ .  $V$  can be expressed as  $A_{vc} \cdot \tau$  and  $\gamma$  as  $\Delta/z$  so:

$$F = \frac{V}{\beta} = \frac{A_{vc} \tau}{\beta} = \frac{A_{vc} G}{\beta z} \Delta \quad (11)$$

As  $G = E/[2(1+\nu)]$  and  $\nu = 0,3$ , the following expression of  $k_1$  can be simply derived:

$$k_1 = \frac{A_{vc}}{2(1+\nu) \beta z} = 0,38 \frac{A_{vc}}{\beta z} \quad (12)$$

## 4.3 Column web in tension or compression

In [5], the elastic linear relationship between the tension or compression force  $F$  transversally applied to the column and the corresponding elongation or shortening  $\Delta$  of the web (see figure 8) is expressed as:

$$F = \frac{E t_{wc}}{d_c} \xi \Delta \quad (13)$$

$d_c$  is defined as the clear depth of the column web. The coefficient  $\xi$  depends on the relative stiffness of the column flange in bending and the column web in tension or compression; its expression - which differs for welded and bolted joints - is rather complicated so simplifications have been brought by the authors. These simplifications are based, as for the T-stub in section 4.1.b, on the ratio ( $= 3/2$ ) between the design resistance of the web defined in Annex J as:

$$F_{2,d} = b_{\text{eff}} t_{\text{we}} f_y \quad (14)$$

and the maximum elastic resistance of the web expressed (from equation 13) as:

$$F_{el} = \xi t_{\text{we}} E \frac{\Delta}{d_e} = \xi t_{\text{we}} E \epsilon_{el} = \xi t_{\text{we}} E \frac{f_y}{E} = \xi t_{\text{we}} f_y \quad (15)$$

From this ratio, an approximated value of  $\xi$  is derived:  $\xi = 2/3 b_{\text{eff}}$ . By introducing this value in equation (13), the following expression of the stiffness coefficient is obtained:

$$k_{2,d} = \frac{0,667 b_{\text{eff}} t_{\text{we}}}{d_e} = \frac{0,7 b_{\text{eff}} t_{\text{we}}}{d_e} \quad (16)$$

#### 4.4 Bolts in shear and bolts in bearing

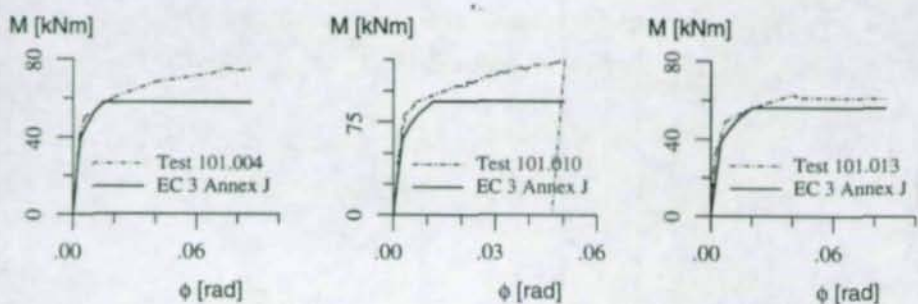
Formulae for stiffness prediction are proposed in [5]; they are based on previous works by PAVLOV and KARMALIN and are validated by comparisons with test results. Limited modifications (to avoid the use of specific units) have been brought to these formulae in Annex J. The reader is therefore asked to refer to [5] for background information.

### 5. COMPARISON WITH TEST RESULTS

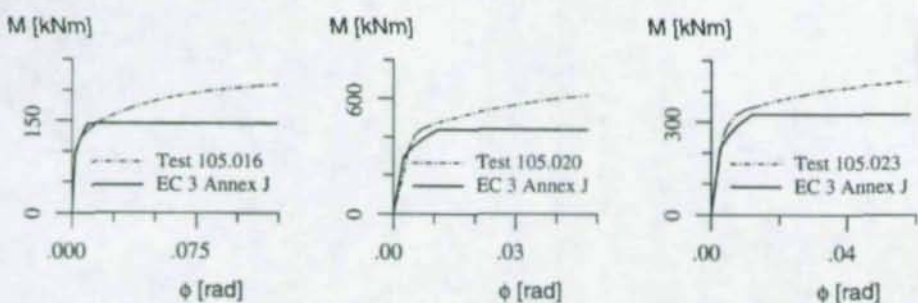
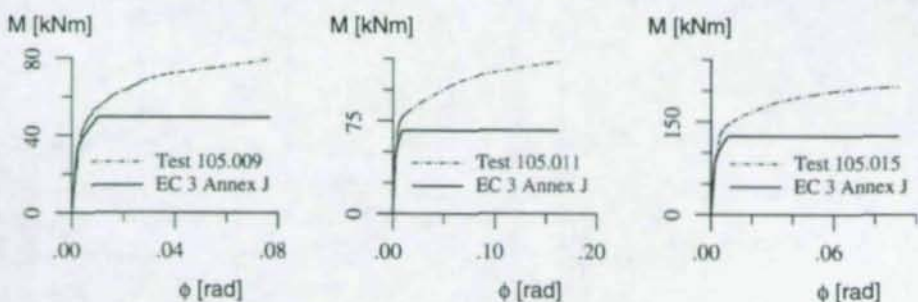
This section shows comparisons of the presented stiffness model with test results. The test data are taken from the databank SERICON [2]. In order to enable comparisons of the complete stiffness model with test results it is necessary to show the full non-linear curves which are obtained by using the application rules of Annex J.

For the determination of the joint properties, i.e initial stiffness and design resistance, measured material and geometrical data obtained from tests are used. The value of the moment resistance  $M_{j,Rd}$  is calculated with safety factor  $\gamma=1,0$ . The moment resistance is determined according to the most accurate model of Annex J, e.g. the alternative method to determine the resistance of the T-stub is used for joints with bolted end plates. Both the rotational stiffness and the moment resistance are calculated by taking into account the actual forces in the shear panel of the column web through the exact values of the  $\beta$ -coefficients.

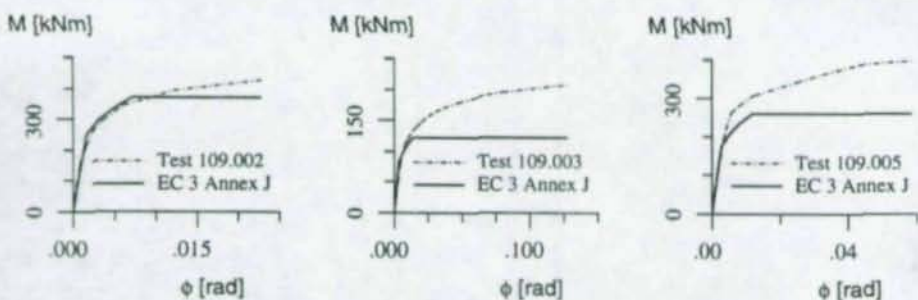
It can be seen from figure 9 that the prediction of the joint stiffness and resistance is in good agreement with the actual behaviour. The differences in the resistance are due to strain hardening and membrane effects which are not taken into account in the design rules of Annex J. In the stiffness model it is assumed that a joint remains elastic up to a level of  $2/3$  of  $M_{j,Rd}$ . This assumption is confirmed by the curves.



a) Liège, single sided, end plated joints

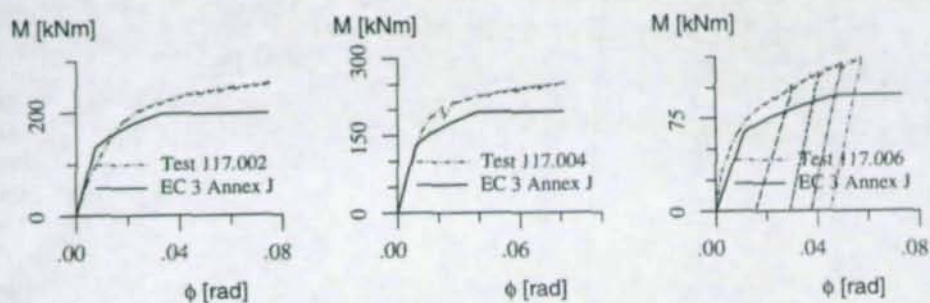


b) Innsbruck, single sided, welded joints

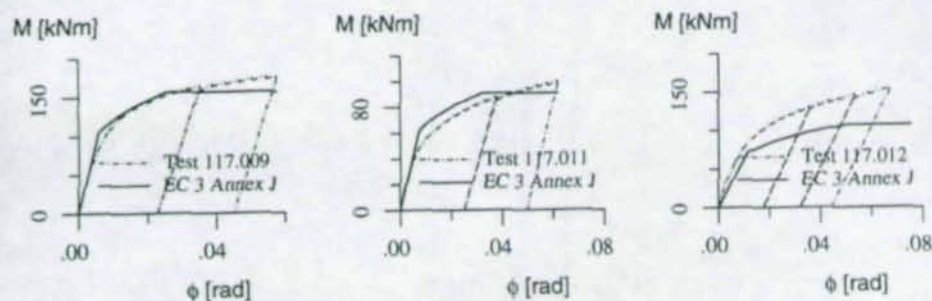


c) Innsbruck, double/single sided, end plated joints

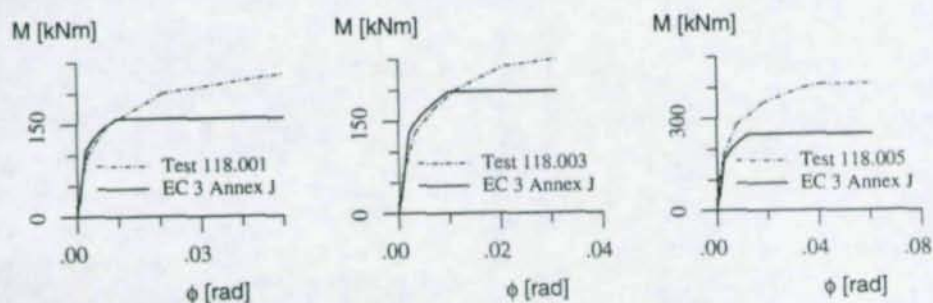
Figure 9: Comparison with test results



d) Leipzig/Aachen, single sided, end plated joints



e) Leipzig/Aachen, double sided, end plated joints



f) Dundee, double/single sided, end plated joints

Figure 9: Comparison with test results (continued)

## 6. CONCLUSION

The new stiffness model of the revised Annex J allows for the determination of the initial (elastic) stiffness of a joint independently of a strength calculation. It also gives design rules for the determination of a full non-linear  $M-\phi$  curve. Comparisons with test results show a good agreement between the predicted curves and the real ones obtained from tests.

The model for the stiffness calculation is based on the so-called component method. Therefore it can be applied for many types of joints and joint configurations. Moreover it can be easily extended to new types of joints as for example composite joints provided that on one side the deformation behaviour is known for all components (i.e. stiffness coefficients  $k$ ) and on the other side that the contribution of the different sources of deformability can be taken into consideration with the presented model by means of a set of springs.

## REFERENCES

- [1] EUROCODE 3, ENV - 1993-1-1, *Revised Annex J*, Design of Steel Structures, CEN, European Committee for Standardization, Document CEN / TC 250 / SC 3 - N 419 E, Brussels, June 1994.
- [2] SERICON, *International Databank System for SEMI-RIGID CONNECTIONS*, ECCS TC10 and COST C1, Version 1.5, RWTH Aachen, Germany, 1995.
- [3] EUROCODE 3, ENV - 1993-1-1, *Design of Steel Structures*, Commission of the European Communities, European Pre-norm, Brussels, Belgium, April 1992.
- [4] ZOETEMEIJER, P., *Summary of the Research on Bolted Beam To Column Connections*, Report 6-85-7, University of Technology, Delft, Netherlands, 1985.
- [5] JASPART, J.P., *Etude de la semi-rigidité des noeuds poutre-colonne et son influence sur la résistance et la stabilité des ossatures en acier*, Ph-D Thesis, University of Liège, Belgium, 1991.
- [6] YEE, Y.L. and MELCHERS, R.E., *Moment rotation curves for bolted connections*, Journal of the Structural Division, ASCE, Vol. 112, ST3, pp. 615 - 635, March 1986.
- [7] GOLEMBIEWSKI, D; LUTTEROTH, A.; SEDLACEK, G.; WEYNAND, K.; FELDMANN, M.: *Untersuchungen zum wirtschaftlichen Einsatz hochfester Stähle im Stahlbau - Rotationsuntersuchungen an Träger-Stützenverbindungen aus STE 460*, Abschlußbericht zum AIF-Projekt D 149, Leipzig/Aachen, January 1993.

## Safety considerations of Annex J of Eurocode 3

Markus Feldmann<sup>1</sup>  
Gerhard Sedlacek<sup>2</sup>  
Klaus Weynand<sup>3</sup>

### Abstract

The new Annex J of ENV 1993 -Eurocode 3 [1] presents rules for the design of joints both for stiffness and strength. Due to the different components and materials of which a joint may exist, the safety assessment of structural joints is rather complex and has so far not been thoroughly clarified. This paper gives some considerations of the influence of unexpected overstrength on the ductility and safety of joints. For seismic loading a method is suggested which allows an extension of plastic design to joints with alternating rotations.

### 1. INTRODUCTION

The ULS-design of a steel structure consisting of elements and joints may be performed with two options:

The first option is the consideration of the whole true moment-rotation characteristic of the joints. This means the use of the original  $M-\phi$ -curve from experiments or from FE-calculations, fig.1 (curve ①). It also means that both strength and rotations are considered in the most realistic way and model uncertainties are of no concern.

The second option is the use of a standardized model which describes the moment-rotation behaviour of a joint in a simplified way: the initial stiffness, the transition from the elastic part to the plastic part of the curve and the ultimate resistance level without an a priori limitation of the rotation. Annex J gives rules for such an approach, fig.1 (curve ②). Using this model in a plastic analysis with moment redistribution means *taking account of rotation on the resistance level  $M_{l,R}$  of a joint*. This necessitates an additional check whether the actual rotation-capacity of a joint is able to fulfil the rotation requirement determined from the calculation or not.

---

<sup>1</sup> Dr.-Ing., Institute of Steel Construction, RWTH Aachen, 52056 Aachen, Germany

<sup>2</sup> Prof. Dr.-Ing., Institute of Steel Construction, RWTH Aachen, 52056 Aachen, Germany

<sup>3</sup> Dipl.-Ing., Institute of Steel Construction, RWTH Aachen, 52056 Aachen, Germany

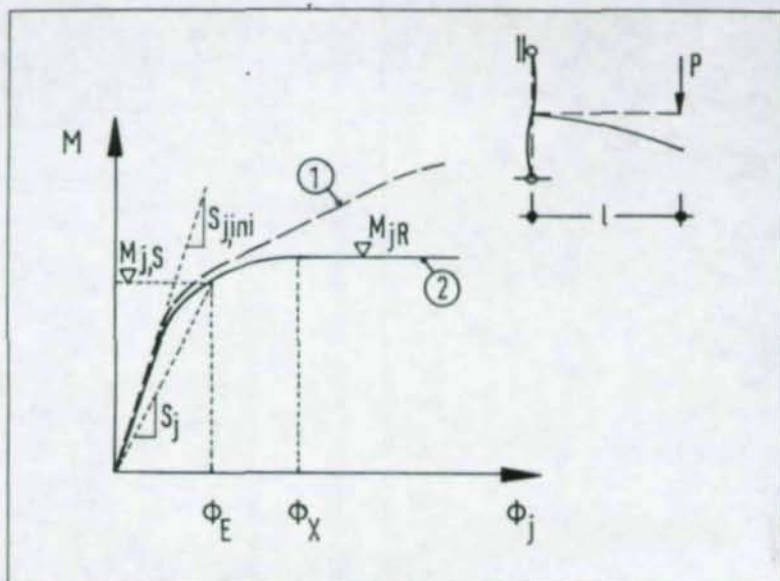


Fig. 1: Moment-rotation-curves: Original curve from the test (1) and model curve according to Annex J (2)

The model deviation of the moment-rotation behaviour in the initial elastic range and in the transition from the elastic-plastic to the full plastic range is fairly small whereas in the full plastic branch with great rotations the model deviation becomes significantly larger. However the model resistance level is below the real resistance and the actual stiffness of this full-plastic branch remains positive unless premature failure due to cracking or buckling occurs.

## 2. EFFECTS OF OVERSTRENGTH OF JOINT COMPONENTS

Performing a plastic analysis using Annex J of Eurocode 3 implies an additional check of the rotation-capacity of the joint on the level of  $M_{j,R}$ , *fig. 1*. However Annex J only provides lump rules for a check of the rotation capacity. Sufficient rules for determining the rotation capacity have not been established in Annex J so far.

This chapter deals with the consequences of overstrength phenomena of single components in the joint. These considerations refer to both the local moment-rotation behaviour of the joint and the global load-deflection behaviour of the structure and allows to determine the safety elements to be applied.

### 2.1 Effects of overstrength of joint components on the joint's behaviour

Taking the general moment-rotation behaviour of a joint according to Annex J, *fig. 2*, it is possible to identify several levels of resistance of each component of the joint. Following the positive stiffness of the full plastic branch of the actual moment-rotation curve (which Annex J reduces to a constant level  $M_{j,R}$ ) it is quite obvious that the

intersection of the actual  $M-\phi$ -curve with the resistance levels  $M_{R,comp,i}$  of the components limits the rotation capacity of the joints to  $\phi_{cap}$ , e.g. by the brittle failure of the bolts or welds. These rotation capacities might be calculated by

$$\phi_{cap} = \phi_{C,j} - \phi_X = \frac{M_{R,comp,i} - M_R}{S_{j,pl}} \quad (1)$$

provided that the plastic stiffness  $S_{j,pl}$  and the resistance levels  $M_{R,comp,i}$  are known and no premature failure due to buckling occurs.

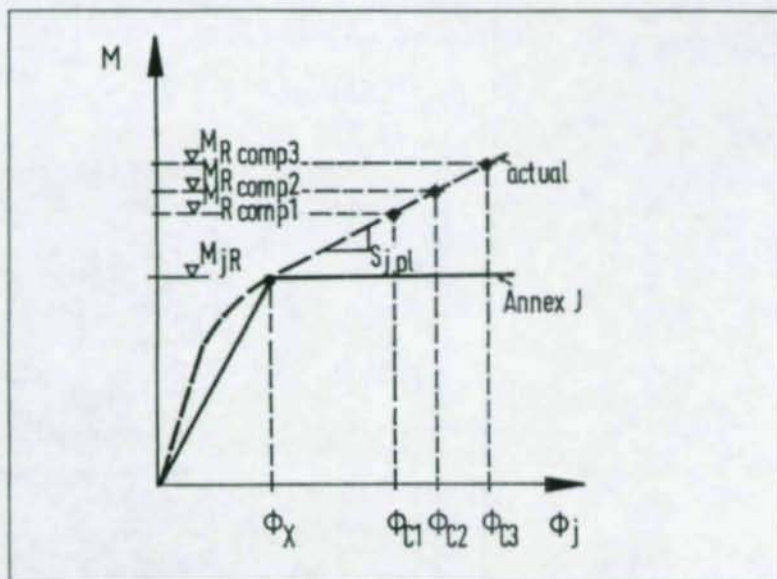


Fig. 2: Moment-rotation-curve according to Annex J and rotation capacities influenced by maximum strength  $M_{R,comp,i}$  of different components

The prediction of the characteristic behaviour of structural elements and joints is based on the nominal values for the yield stress  $f_y$ . The nominal value for  $f_y$  however is the lower 5%-fractile or less of the statistical distribution of the yield stress. The consequence is that the available rotation capacity becomes the smaller the more the actual yield stress exceeds the nominal one. Fig. 3 shows this significant reduction of available rotation capacity if the strength of one component of the joint (e.g. the bolts' strength of a joint with an endplate remains constant and also the stiffness  $S_{j,pl}$  remains constant).

By introducing the overstrength as  $\Delta f_y$  or, directly expressed, as  $\Delta M$  the rotation capacity becomes smaller. From the proportional relationship in the moment-rotation curve that reduction can be expressed as

$$\phi_{cap} = \phi_{C,j,over} - \phi_X = \frac{M_{R,comp,i} - (M_R + \Delta M)}{S_{j,pl}} \quad (2)$$

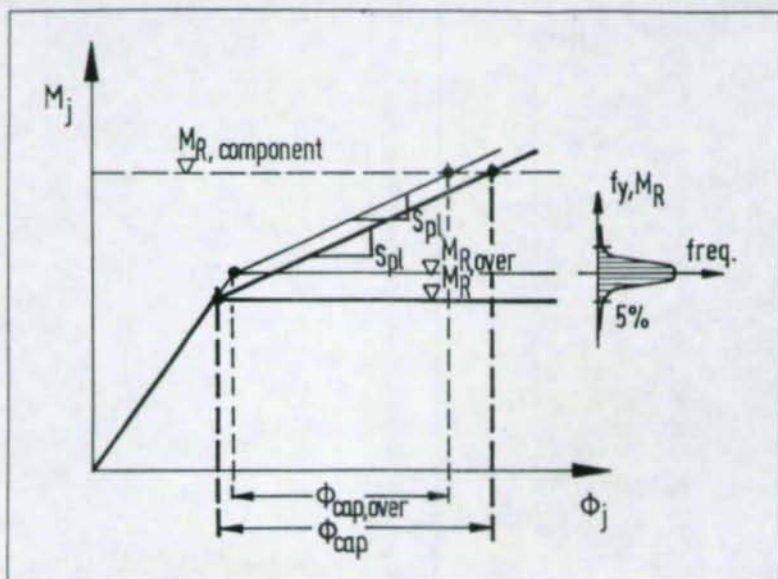


Fig. 3: Reduction of actual available rotation capacity of a joint introducing the actual yield stress

In *fig. 4a* the curves are shown which represent the dependence of the rotation capacity  $\phi_{cap}$  on the yield strength  $\Delta f_y$  with different hardening stiffnesses  $S_{i,pl}$  and constant  $M_{R,comp}$ . This sort of diagram may also be established for cases in which the rotation capacity is governed by local buckling phenomena, *fig. 4b* [2].

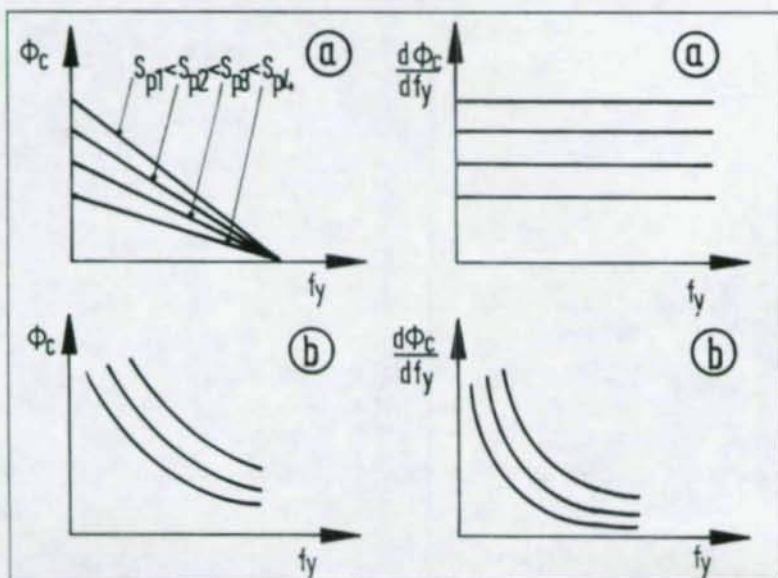


Fig. 4: Dependence of available rotation capacity of joints on the yield stress

## 2.2 Effects of overstrength of joint components on the structural behaviour

In fig. 5 a statically undetermined structure (continuous two span beam) with a partial-strength joint above the support is shown. In plotting the load-rotation diagram (referred to the rotation of the joint) the graph in fig. 5 applies (thick line).

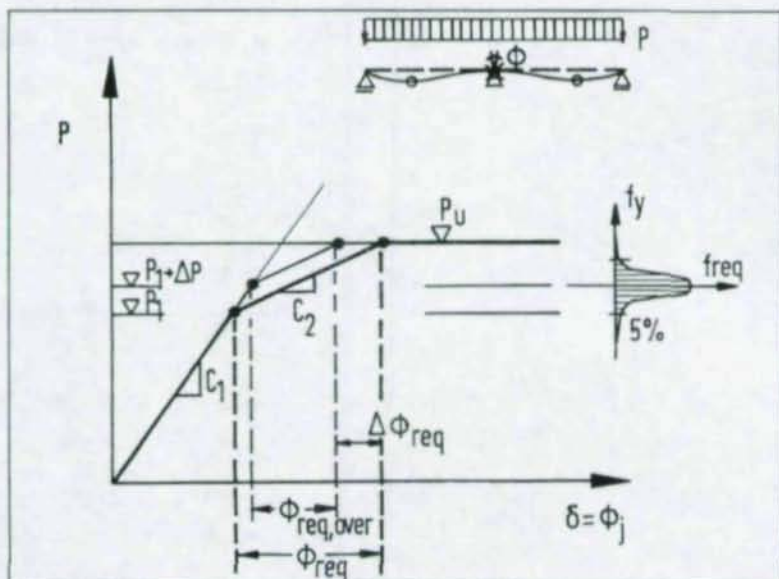


Fig. 5: Load-deformation behaviour of a statically undetermined structure without and with overstrength in the relevant plastic hinge (joint)

In the very first elastic part of the graph the deformation follows proportionally the load until the first plastic hinge occurs. In this case this plastic hinge is assumed to occur in the joint. Afterwards the load-rotation curve increases further with the remaining elastic stiffness  $C_1$  until the ultimate load  $P_u$  is reached by developing of the last plastic hinge. During the moment redistribution process the plastic hinge in the joint has to fulfil a certain plastic rotation.

However this load-rotation behaviour is based on an idealized bi-linear moment-rotation characteristics in the plastic hinges, see fig. 2. Assuming the actual moment-rotation behaviour of joints, the global load-rotation characteristic would become more smooth.

Let's now consider also in this graph an overstrength  $\Delta f_y$ . The first hinge would occur on the level  $P_1 + \Delta P$ . But the required rotation  $\phi_{req}$  is being significantly reduced from  $\phi_{req}$  to  $\phi_{req,over}$ , with:

$$\phi_{req,over} = \phi_{req} - \Delta \phi_{req} = \frac{P_u - (P_1 + \Delta P)}{C_2} \quad (3)$$

### 2.3 Comparison of the effects of overstrength of the joint components on the joint's behaviour with the effects on the structural behaviour

Considering a design situation in which the available rotation capacity is fully exploited, i.e.

$$\phi_{cap} = \phi_{req} \quad (4)$$

the question is whether an incremental change of strength towards larger yield strength of the material leads to actual rotation capacities greater than the required rotation (this would be a safe situation) or to actual rotation capacities smaller than the required ones (this would be an unsafe situation). To achieve the safe situation the following condition must be fulfilled, see [fig. 6](#):

$$\left| \frac{d\phi_{cap}}{df_y} \right| < \left| \frac{d\phi_{req}}{df_y} \right| \quad (5)$$

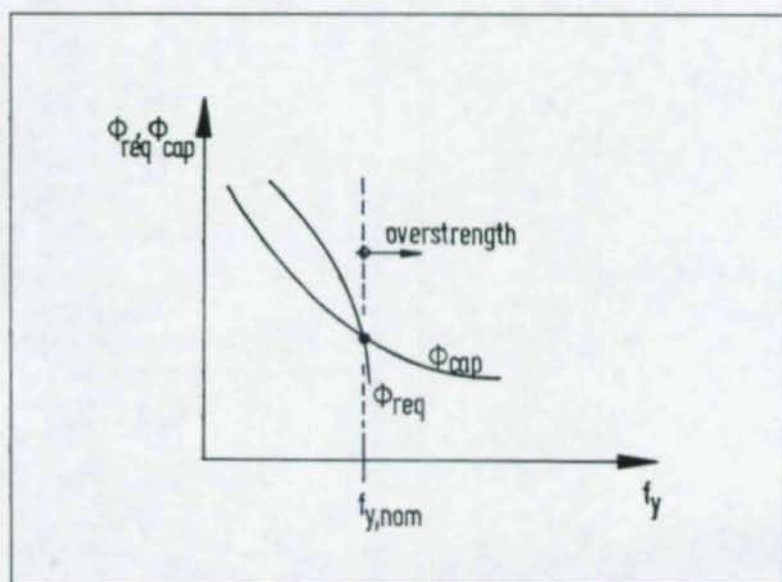


Fig. 6: Behaviour of required rotation and rotation capacity in view of overstrength

This condition can also be graphically shown for general cases. The  $\Delta\phi_{req}$  - distance in the graph of [fig. 5](#) can be derived for all levels of  $P_u$  which are possible, assuming that the calculated rotation requirement  $\phi_{req}$  remains the same. Then all  $\Delta\phi_{req}$  - values or  $d\phi_{req}$  - values for all possible  $P_u$  - levels for a certain overstrength  $\Delta P$  are obtainable. This is indicated in [fig. 7](#) (dashed hyperbola).

Introducing the value for  $d\phi_{cap}$  (dashed vertical line in [fig. 7](#)) the intersection of the  $d\phi_{req}$  - hyperbola and the  $d\phi_{cap}$  - vertical line gives the distinction between safe and unsafe ranges with respect to the overstrength phenomenon of a component in a joint.

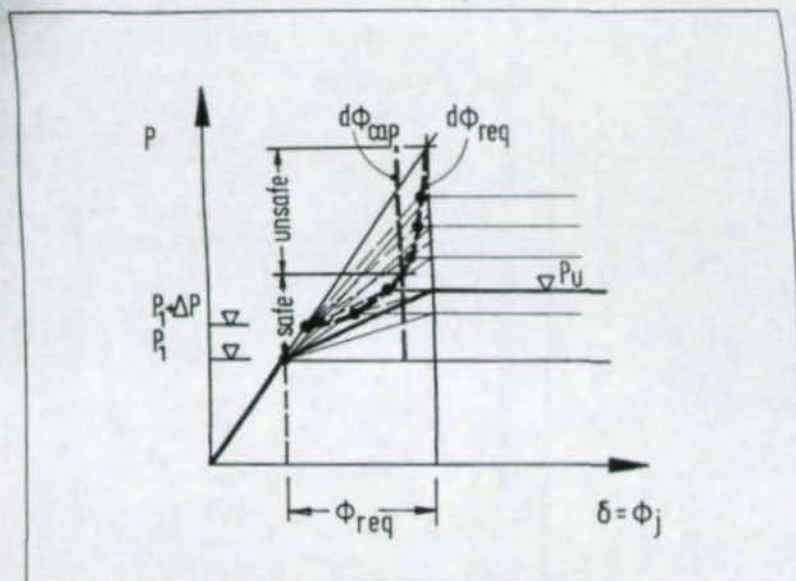


Fig. 7: Incremental change of the considered yield stress ( $=\Delta P$ ): Comparison of the effects side of requirement with the effects on the capacity side,  $\phi_{req}=\text{const}$

### 3. LOW-CYCLE FATIGUE ASSESSMENT FOR STRUCTURAL JOINTS

In this second part of this paper the effects of cyclic loading on the resistance of joints are considered. These considerations are necessary when repeated or alternating rotations could be applied during lifetime, e.g. for wind actions or seismic actions.

Having a joint with constant amplitude cyclic loading, see fig. 8, which can be modelled with Finite Elements [3], the strains and in particular the plastic strains were investigated during the cycling loading. It appeared, that the relationship between the plastic strains at the hot spot (strain at the relevant place where the first crack occurs) and the plastic rotations are linear. This linear relationship gives rise to estimate a "Wöhler-line-relationship" with logarithmic cycles on the abscissa and logarithmic plastic rotations on the ordinate, the slope of which is the slope of the Manson-Coffin-rule for steel material. The value for that slope was investigated [4] and determined to

$$m_{\epsilon} \cong 2,0 \quad (6a)$$

for low alloyed structural steels. Due to logarithm laws the slope of the rotational Wöhler-line is the same as the strain Wöhler-line assuming that one strain cycle is one rotational cycle:

$$m_{\phi} \cong 2,0 \quad (6b)$$

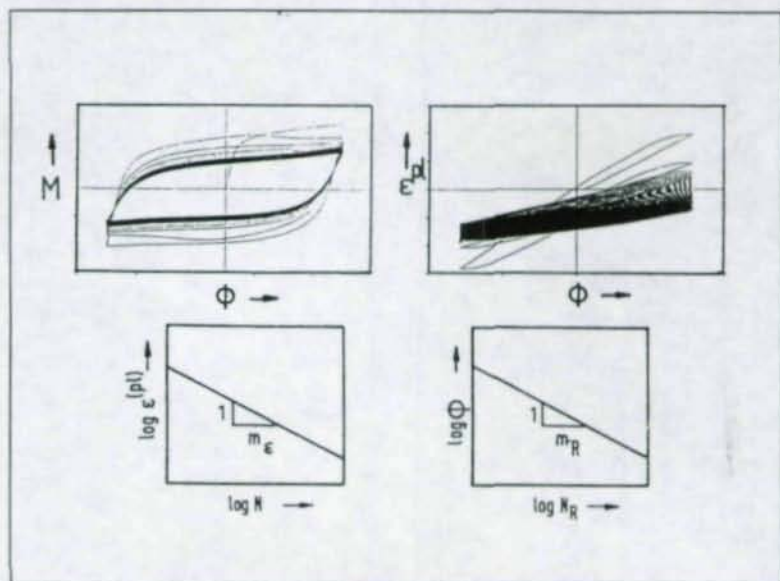


Fig. 8: Cyclic moment-rotation characteristic of a joint, cyclic plastic strain-rotation characteristic of the hot spot, strain Wöhler-line and rotational Wöhler-line

Having the slope of the rotational Wöhler-line, however the level of failure with  $N=1$  (static case) is so far being unknown, but is going to be determined by experiments [5][6].

If the value of  $\Phi_{N=1}$  is known then a life cycle assessment for joints with alternating loading can be derived allowing for plasticity i.e. energy dissipation in the joints. Using the Miner-rule, eq. (7), as a damage hypothesis, that has been already justified for beams [7][8][9], a damage equivalent quasistatic rotation capacity can be defined, fig. 9.

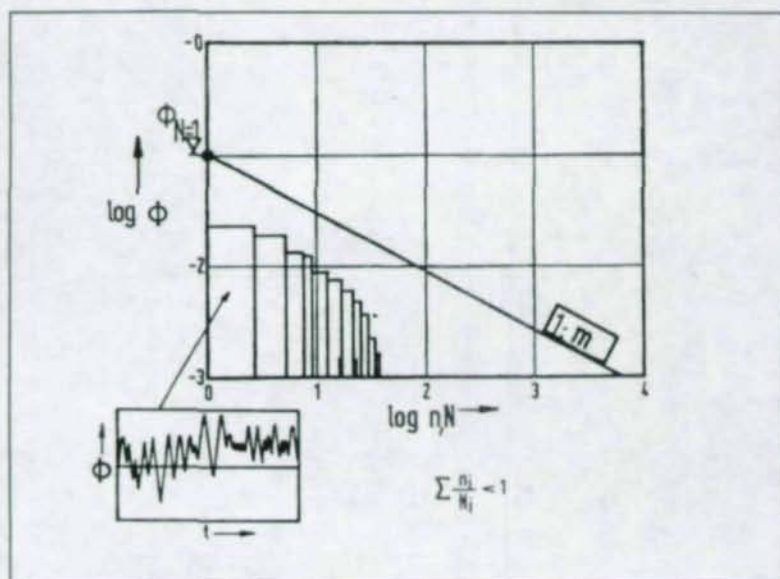


Fig. 9: Rotational Wöhler-line approach with starting value  $\phi_{N=1}$  and damage spectrum

The Miner-rule

$$\sum \frac{n_i}{N_i} \leq 1,0 \quad (7)$$

can be transformed into a comparison of damage using the slope of the rotational Wöhler-line  $m_\phi = 2,0$ :

$$\sum (\phi_i)^m n_i \leq (\phi_{N=1})^m \quad (8)$$

such that an equivalent rotation requirement for the static case can be formulated:

$$\phi_{\text{req,equi}} = \sqrt[m]{\sum (\phi_i)^m n_i} \quad (9)$$

With that rotation requirement a rotation check as for statically loaded structures can be allowed:

$$\phi_{N=1} \geq \phi_{\text{req,equi}} \quad (10)$$

This check limits the damage from alternating yielding to safe values and allows to extend the application of the plastic hinge method to joints subject to seismic loading.

## REFERENCES

- [1] EUROCODE 3, ENV - 1993-1-1, *Revised Annex J*, Design of Steel Structures, CEN, European Committee for Standardization, Document CEN / TC 250 / SC 3 - N 419 E, Brussels, June 1994.
- [2] FELDMANN, M.: *Zur Rotationskapazität von I-Profilen statisch und dynamisch belasteter Träger*, Ph.D. Thesis, Institute of Steel Construction, RWTH Aachen 1994.
- [3] SEDLACEK, G.; KONG, B.-S., WEYNAND, K.: *Das Rotationsverhalten von Riegel-Stützen-Verbindungen*, DFG Bericht Se 351/19-1, Aachen, 1995.
- [4] BOLLER, CH.; SEEGER, T.: *Materials Data for Cyclic Loading*, Vol. 42a/b, Elsevier Science Publishers B.V., 1987.
- [5] running DFG research project: *Untersuchungen der Grenzbeanspruchung für Stahlbaukonstruktionen in Erdbebengebieten, die alternierender Plastizierung ausgesetzt sind*, Se 351/27-1, Aachen, 1995.
- [6] running AIF research project: *Grenzen für alternierende Plastizierung für Stahlbauelemente*, Aachen and Leipzig, 1995.
- [7] BALLIO, G.; CASTIGLIONI, C.A.: *An Approach to the Seismic Design of Steel Structures Based on Cumulative Damage Criteria*, Journal of Constructional Steel Research, 1994.
- [8] BALLIO, G.; CASTIGLIONI, C.A.: *A Unified Approach for the Design of Steel Structures under Low and/or High Cycle Fatigue*, Journal of the Constructional Steel Research, 1994.
- [9] BALLIO, G.; CASTIGLIONI, C.A.: *Seismic behaviour of Steel Sections*, Journal of Constructional Steel Research, 1994.
- [10] KUCK, J.: *Anwendung der dynamischen Fließgelenktheorie zur Bestimmung der Grenzzustände für Stahlkonstruktionen unter Erdbebenbelastung*, Ph.D. Thesis, Institute of Steel Construction RWTH Aachen, 1994.
- [11] ZOETEMEIJER, P., *Summary of the Research on Bolted Beam To Column Connections*, Report 6-85-7, University of Technology, Delft, Netherlands, 1985.
- [12] COLSON, A., BJORHOVDE, R., *Connection Moment-Rotation Curves for Semi-Rigid Frame Design*, Connections in Steel Structures II: Behaviour, Strength, and Design, The Second International Workshop on Connections in Steel Structures, Pittsburgh, USA, 1991

## DESIGN OF FILLET WELDS IN RECTANGULAR HOLLOW SECTION T, Y AND X CONNECTIONS USING NEW NORTH AMERICAN CODE PROVISIONS

Jeffrey A. Packer<sup>1</sup>

### Abstract

The effective length and design of the perimeter weld around the branch member in axially-loaded Rectangular Hollow Section (RHS) T and X connections is examined experimentally. By means of 16 full-scale connection tests which were designed to be weld-critical, guidelines for the effectiveness of the heel, toe and side welds are developed in terms of the principal connection parameters. It is found that more of the weld perimeter is effective for lower branch member to chord member angles, and more weld is effective for smaller width branch members (relative to the chord member size). The effective weld length recommendations advocated are shown to result in weld designs with an adequate level of safety using the current AISC LRFD or CSA specifications.

### 1. INTRODUCTION

It is well known that the flexibility of RHS connections results in non-uniform loading of the welds around a joint. As a consequence, some recent international recommendations have required that welds to truss branch members develop the yield capacity of the member, to accommodate for any arrangement of loads in the member. Hence, on the basis of a 90° connection only, the International Institute of Welding (IIW, 1989) has recommended that the throat thickness ( $a$ ) of a fillet weld be  $\geq 1.07 t_b$ , where  $t_b$  is the thickness of the connected branch member, for tubes with a yield strength around 350 N/mm<sup>2</sup> regardless of connection angles. This was modified slightly to  $a \geq 1.10 t_b$  in

---

<sup>1</sup> Professor, Department of Civil Engineering, University of Toronto, 35 St. George Street, Toronto, Ontario M5S 1A4, Canada.

Eurocode 3 (1992). The safety level implicit in this recommendation is for the weld to have a safety index  $\beta^+ \geq 3.8$ . In North America, on the other hand, connectors (e.g. welds) are required to have a safety index  $\beta^+ \geq 4.5$  (Fisher et al., 1978).

Such a universal design provision for fillet welds, based solely on branch member thickness, will be excessively punitive for many applications. By proportioning the weld on the basis of acting member forces, however, a designer has the ability to justify potentially smaller weld sizes but the connection deformation and rotation capacity must be taken into account, typically by imposing a weld reduced effective length. The advantages of this weld design approach can be significant in situations where aesthetics have controlled the member selection, or only a restricted number of bracing (web) member sizes have been chosen for reasons of cost optimization, or a long compression bracing member causes the member to be loaded well below its full section squash load, or the bracing to chord member angle is low thereby producing a much longer weld around the member.

On the basis of extensive laboratory tests, both on isolated connections and complete trusses, recommendations have already been made for the effective length of welds in gapped and overlapped K (or N) connections between RHS members (Frater and Packer, 1992a, 1992b). These recommendations have been adopted in design guides published by the Comité International pour le Développement et l'Etude de la Construction Tubulaire (CIDECT) (Packer et al., 1992), the American Welding Society (AWS, 1994), and the Canadian Institute of Steel Construction (Packer and Henderson, 1992). As no information was available, at the time, for weld effective lengths in RHS T, Y and X connections, speculative formulae were provided in these same design guides. The purpose of this paper is therefore to report on a study of weld design for RHS T, Y and X connections and to give appropriate weld effective length rules for use in designing such joints.

## 2. EXPERIMENTATION

Four large-scale RHS 90° T connections and 12 X connections were fabricated, with plate attachments to the branch member ends for load application. All RHS members used were cold-formed to ASTM A500 Grade B. The connection parameters varied included the width ratio ( $\beta$ ), branch member to chord angle ( $\theta_1$ ) and weld size. As the failure mode of RHS T, Y and X connections depends on the  $\beta$  value, and changes around  $\beta = 0.8$  to 0.85 (Packer and Henderson, 1992), one set of branch members was selected to be around this transition ( $\beta = 0.80$ ) and another well below ( $\beta = 0.50$ ). Since the experiments were intended to examine weld behaviour, failure was designed to always occur in the weld rather than by some connection failure mode. With all test specimens being proportioned to fail locally in the welds it was considered that the results obtained from tension-loaded X connections would also be applicable to Y connections, since a Y connection resembles an X connection with one less branch member. The properties of the 16 test specimens can be found in Cassidy (1993).

Prior to fabrication of the test specimens, the perimeter lengths and individual side lengths were measured carefully for each branch member cut at different angles so that the actual weld length would be known accurately in evaluation of the test results. This is an important prerequisite to any eventual recommendation for effective weld length. Geometry dictates that the toe and heel of the RHS (sides *c* and *d* respectively) be of equal length and likewise the two branch member sides parallel to the direction of the chord (sides *a* and *b*) should be equal. These measured lengths are given in Cassidy (1993). A method has also been provided by AWS (1994) and adopted by CISC (1991) for determining the contact perimeter of an inclined RHS branch member. This assumes that a cold-formed member has an outside corner radius of  $2t_i$  and multiplies the  $90^\circ$  perimeter by a factor  $K_a$  to account for the sloping of the branch member. This gives the inclined RHS contact perimeter as:

$$\text{Perimeter} = K_a [ 4\pi t_i + 2(b_i - 4t_i) + 2(h_i - 4t_i) ] \quad \dots(1)$$

$$\text{where } K_a = \frac{\frac{h_i}{\sin\theta_i} + b_i}{(h_i + b_i)} \quad \dots(2)$$

Perimeters determined using Eqs. (1) and (2) showed that this " $K_a$  method" is sufficiently accurate for connection designers to use (Cassidy, 1993). In this paper the more precise measured lengths have been used in subsequent analysis of results.

The test welds were all made by the Welding Institute of Canada using flux-cored arc welding with a  $\text{CO}_2$  shielding gas. All final welds were checked and approved by a third party using magnetic particle inspection. For all connections having  $\theta_i < 60^\circ$  the toe of each branch member was bevelled then welded to form what is often considered a partial joint penetration butt (groove) weld. However, in this study all welds were considered fillets and measured as such.

Weld sizes were determined by making a negative mould of each test weld then cutting it at four or five locations along each branch member side and measuring the legs of the weld and throat size at each position. Over 1500 weld dimensions were taken for the 16 connections and the average measured values, along with the mechanical properties of the as-laid weld metal determined by tensile coupon tests, are given elsewhere (Cassidy, 1993).

Each of the four T connections was tested to failure in a quasi-static manner under tension loading on the branch member. This tension force was applied by a universal testing machine to a tongue welded into the branch member and to a special-purpose testing jig which applied a shear force to the chord. A typical testing arrangement is shown in Fig. 1. The 12 X connections were tested in a similar manner but with the two branch members loaded directly by the universal testing machine via tongue plates. Strain gauges were secured to the branch members of all test specimens to observe and record the strain distribution around the branch members adjacent to the welded joint. These

were positioned 10 to 15 mm away from the actual weld toe, to avoid the strain concentrations caused by the notch effect at the toe, and oriented in the direction of the branch member. Displacement transducers with a 50 mm stroke were used to monitor the overall connection deformation. (See Fig. 1). Strain gauges were also used on specimens to ensure proper alignment and therefore axial loading on the branch members, as well as to verify that the shear lag effect (caused by loading the RHS on only two sides via tongue plates) had disappeared well before the joint region. For the X connections, each specimen produced a test on two branch member "test welds" of similar size, so each X connection weld failure represents a lower bound of two samples. All test specimens failed in a sudden manner with fracture through the weld metal and/or base metal. A typical joint failure is shown in Fig. 2 and failure loads are given by Cassidy (1993).

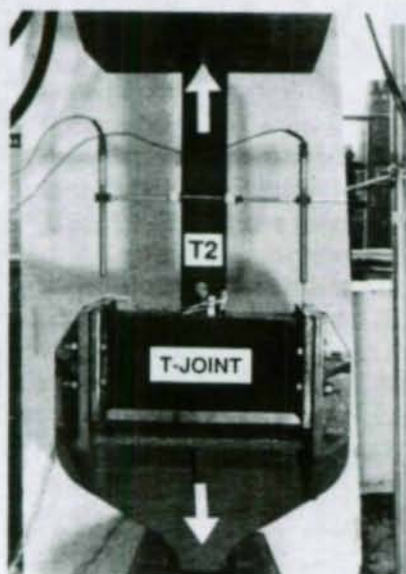


FIG. 1. T Connection in Testing Machine with Testing Jig Below

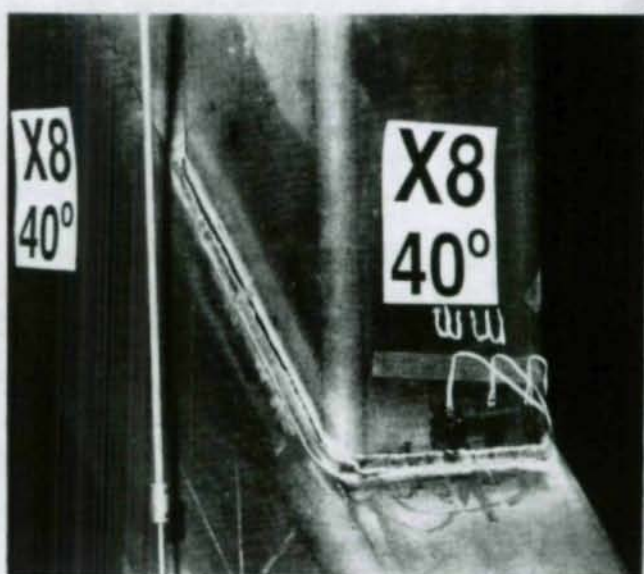


FIG. 2. Typical Weld Failure

### 3. DISCUSSION OF RESULTS

Graphs of load versus strain for the transverse and side welds of test T2 ( $\beta = 0.5$ ) are shown in Fig. 3. It can be seen that the side welds a and b are completely effective in resisting load whereas the transverse welds c and d are only effective at the corner locations until high loads are attained. If the width ratio ( $\beta$ ) is increased the transverse welds become even less effective, as is evident in Fig. 5(a). In this case only the corner region of the transverse weld resists the branch member tension load, with most of the transverse weld actually remaining in compression for the whole load range. One would expect the branch member load to be transmitted to the chord member walls primarily

through sides a and b at high  $\beta$  values, yet the ineffectiveness of sides c and d is rarely recognized by welding engineers leading to some instances of very unsafe design.

The X connection tests also confirmed that, for equal branch member angles, more of the perimeter was effective in resisting the applied tension load at the lower  $\beta$  value. However, for either  $\beta$  value (0.5 or 0.8) the X connections showed that a lower connection angle produces a larger effective perimeter length. This trend of more sides being effective at lower branch member angles is similar to the trend observed by Frater and Packer (1992b) for K and N connections, wherein the heel weld could only be considered fully effective for  $\theta_1 \leq 50^\circ$ . The influence of  $\theta_1$  on the effectiveness of the transverse welds in T and X connections, particularly the heel weld, can be seen by comparing Fig. 4 (T connection with  $\beta = 0.8$ ) with Fig. 5 (X connection,  $\theta_1 = 30^\circ$ ,  $\beta = 0.8$ ).

A study of the distributions of strain around the branch member adjacent to the "test welds" in all 16 T and X connections showed the trend for weld effectiveness given in Fig. 6. The side welds a and b (refer to Fig. 5) can be seen to be fully effective for all joints, but the toe and heel welds (sides c and d respectively) are generally only partially effective. These partially effective sides are designated  $c_e$  and  $d_e$  with the length of these portions estimated by an existing RHS effective width formula (Packer and Henderson, 1992):

$$b_e = \frac{10}{b_0/t_0} \cdot \frac{F_{y0}t_0}{F_{y1}t_1} \cdot b_1, \text{ but } \not\geq b_1 \quad \dots(3)$$

In view of the fact that only two width ratios were examined, and for a constant chord slenderness ( $b_0/t_0$ ) ratio which also influences the effective length of the transverse welds (see Eq. (3)), the behaviour illustrated in Fig. 6 was simplified to the recommended design model also shown in Fig. 6. This also acknowledges the large scatter of data that is inherent in welding research as well as the difficulty that welding engineers would encounter in applying Eq. (3) correctly. Thus, it is suggested that the weld effective length around a branch member be determined for all  $\beta$  values by:

$$\text{For } \theta_1 \leq 50^\circ : \text{ Effective length} = a + b + d = \frac{2h_1}{\sin\theta_1} + b_1 \quad \dots(4)$$

$$\text{For } \theta_1 \geq 60^\circ : \text{ Effective length} = a + b = \frac{2h_1}{\sin\theta_1} \quad \dots(5)$$

A linear interpolation is recommended between  $50^\circ$  and  $60^\circ$ . The lengths  $b_1$  and  $h_1$  should be based on the contact perimeter taking account of the rounded corners. For experimental analysis this can be done using the measured lengths, or in design practice using the  $K_a$  formula (Eqs. (1) and (2)). The consideration of the branch member as having square corners can produce unsafe weld lengths, particularly for small, thick-walled, RHS.

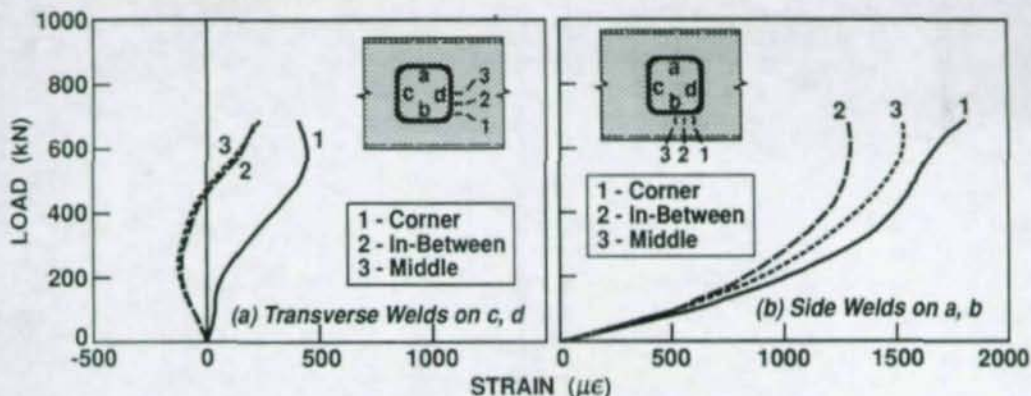


FIG. 3. Load v. Strain Relationship in Connection T2 for Transverse and Side Welds ( $\beta=0.5$ )

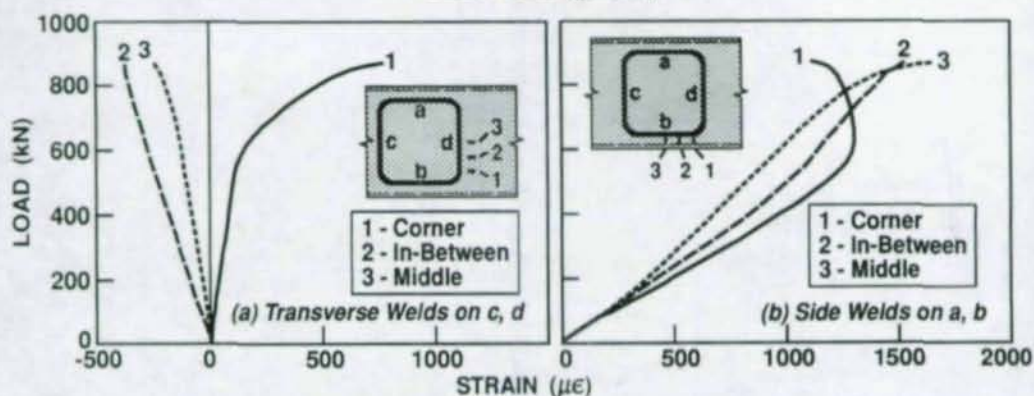


FIG. 4. Load v. Strain Relationship in Connection T4 for Transverse and Side Welds ( $\beta=0.8$ )

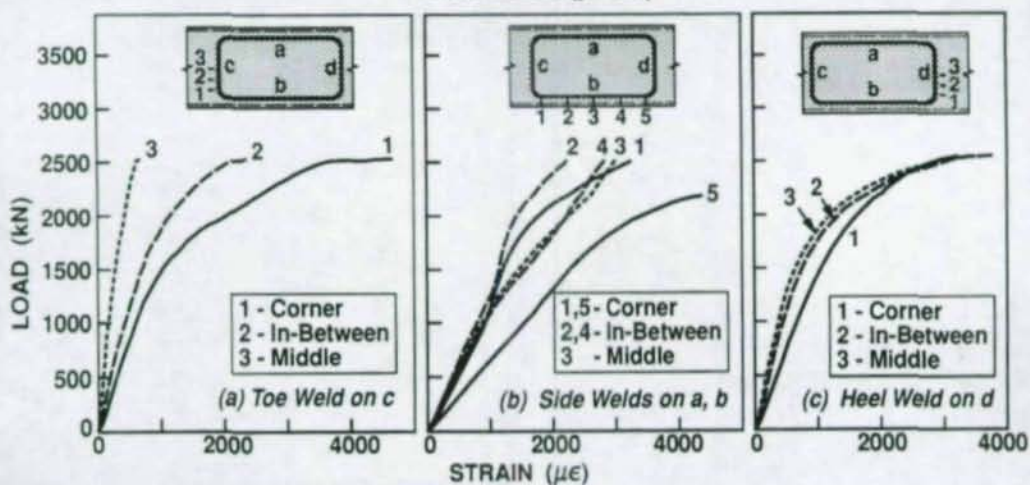


FIG. 5. Load v. Strain Relationship in Connection X7 ( $\theta_1=30^\circ$ ) for Transverse and Side Welds ( $\beta=0.8$ )

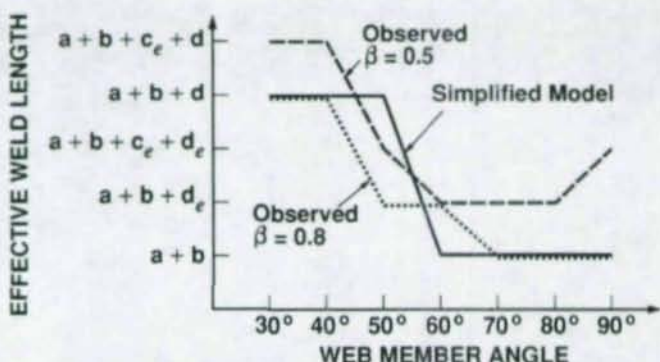


FIG. 6. Observed Effective Weld Lengths and Simplified Model for Effective Lengths, in T and X Connections.

#### 4. SAFETY LEVEL IMPLICIT IN RECOMMENDATION

Predicted resistances for the failed weld of each connection were calculated using the proposed effective length guideline (Eqs. (4) and (5)) in conjunction with both the AISC LRFD (1993) and CAN/CSA-S16.1-94 (CSA, 1994) steel specifications, along with measured material and geometric properties.

The Canadian Standards Association specification (CSA, 1994) gives the factored shear resistance of a fillet weld by the smaller of:

- For base metal
 
$$V_{r1} = \phi_w 0.67 F_{u1} A_{m1} \quad \dots(6a)$$

or

- For weld metal
 
$$V_{r2} = \phi_w 0.67 F_{u2} A_{m2} \quad \dots(6b)$$

- For weld metal
 
$$V_r = \phi_w 0.67 X_u A_w (1.00 + 0.50 \sin^{1.5} \theta) \quad \dots(7)$$

where  $\phi_w = 0.67$  for all of Eqs. (6a), (6b), and (7) and  $\theta$  in Eq. (7) is the angle between the axis of the weld and the line of action of the force ( $0^\circ$  for a longitudinal weld and  $90^\circ$  for a transverse weld). Conservatively, one is allowed to set the function  $(1.00 + 0.50 \sin^{1.5} \theta)$  to one. The latest American Institute of Steel Construction specification (AISC, 1993) replicates Eqs. (6a), (6b) and (7) although the  $(0.67)(0.67)$  term appears in the form  $(0.75)(0.60)$ , allowing for shear rupture of the base metal (Section J4), and the  $(1.00 + 0.50 \sin^{1.5} \theta)$  is only an optional function mentioned in Appendix J2.

The correlation between actual failure loads and predicted resistances using the CSA or AISC LRFD methods, in conjunction with the simplified model of Fig. 6, is shown in Fig. 7. The overall mean of the actual strength to predicted resistance ratios is 1.622 with a

coefficient of variation (COV) of 0.180. This mean appears to be conservative because the test strength is compared with the predicted resistance, which includes the  $\phi_w$  factor.

To assess whether an adequate, or excessive, safety margin is inherent in the correlation shown in Fig. 7, one can check to ensure that a minimum safety index of  $\beta^* = 4.5$  (Fisher et al., 1978) is achieved, using a simplified reliability analysis in which the resistance factor,  $\phi$ , is given by (Fisher et al., 1978; Ravindra and Galambos, 1978):

$$\phi = m_R \exp(-\alpha\beta^* \text{COV}). \quad \dots(8)$$

$m_R$  is the mean of the ratio: (actual element strength)/(nominal element resistance), COV is the associated coefficient of variation of these ratios, and  $\alpha$  is the coefficient of separation taken to be 0.55 (Ravindra and Galambos, 1978). Considering that a  $\phi$  factor was initially included in the predicted resistance calculations, the value determined by Eq. (8) - which can be considered a resistance factor adjustment or  $\phi_{adj}$  - would be greater than 1.0 if the required safety index of 4.5 was achieved. The  $\phi_{adj}$  is actually 1.039 for both the AISC LRFD and CSA specifications, indicating that both provide just adequate levels of safety when used in conjunction with the effective length recommendations made herein. It should be noted that  $\phi_{adj}$  values well below unity result if the total weld length ( $a + b + c + d$ ) is used. The effective length recommendations above should also prove conservative when applied in Europe, given previous cross-calibrations with Eurocode 3 recommendations for weld design (Frater and Packer, 1992a; 1992b).

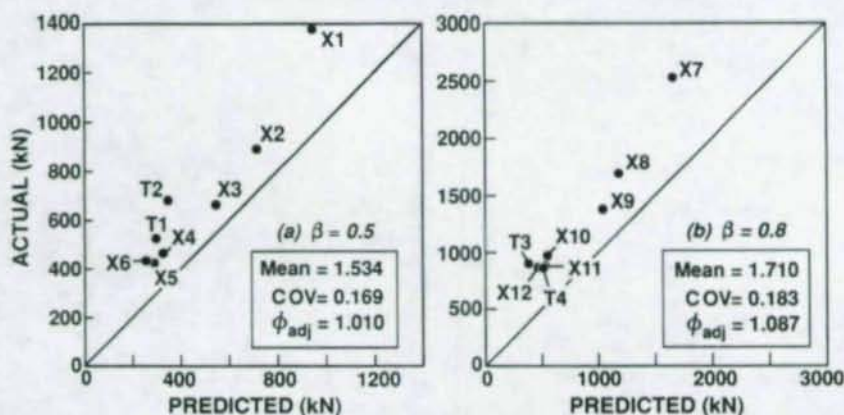


FIG. 7. Actual Failure Loads v. Predicted Resistances by CSA (1994) and AISC LRFD (1993), with Simplified Model for Effective Weld Lengths.

## 5. CONCLUSIONS

Based on a series of careful laboratory tests on weld-critical, isolated RHS T and X connections, it is recommended that an effective length for the branch member weld given by Eqs. (4) and (5) be used in the design of RHS, T, Y and X connections. This

recommendation has recently prompted a revision of the AWS D1.1 specification and is incorporated in the forthcoming AWS D1.1-96 (AWS, 1996). A speculative recommendation by Packer and Henderson (1992) also requires revision, as it is still unconservative for connections with  $\theta_1 \leq 50^\circ$ . Another recent pronouncement on this topic appears in a CIDECT Design Guide (Packer et al., 1992) and is overly conservative since it recommends the use of Eq. (5) for all  $\theta_1$  values.

## 6. ACKNOWLEDGEMENTS

Financial support for this project was provided by the Natural Sciences and Engineering Research Council of Canada (NSERC) and the Canadian Institute of Steel Construction's Steel Structures Education Foundation. Experiments were performed by Ms. C.E. Cassidy. The Rectangular Hollow Sections were provided by Ipsco Inc., Regina, Canada.

## 7. REFERENCES

*American Institute of Steel Construction*: "Load and resistance factor design specification for structural steel buildings", AISC, Chicago, U.S.A., 1993.

*American Welding Society*: "Structural welding code - Steel". *ANSI/AWS D1.1-94*, 13th edition, AWS, Miami, U.S.A., 1994.

*American Welding Society*: "Structural welding code - Steel". *ANSI/AWS D1.1-96*, 14th edition, AWS, Miami, U.S.A., 1996.

*Canadian Institute of Steel Construction*: "Handbook of steel construction". 5th. edition, CISC, Willowdale, Ontario, Canada, 1991.

*Canadian Standards Association*: "Limit states design of steel structures". *CAN/CSA-S16.1-94*, CSA, Rexdale, Canada, 1994.

*Cassidy, C.E.*: "Effective Weld Length for HSS T, Y and X Connections". M.A.Sc. thesis, University of Toronto, Toronto, Canada, 1993.

*European Committee for Standardization*: "Eurocode 3: Design of steel structures - Part 1.1: General rules and rules for buildings". *ENV 1993-1-1: 1992E*, British Standards Institution (BSI), London, U.K., 1992.

*Fisher, J.W., Galambos, T.V., Kulak, G.L., and Ravindra, M.K.*: "Load and resistance factor design criteria for connectors". *Journal of the Structural Division, ASCE*, 104(9), (1978), 1427-1441.

Frater, G.S., and Packer, J.A.: "Weldment design for RHS truss connections. I: Applications". *Journal of Structural Engineering*, 118(10), (1992a), 2784-2803.

Frater, G.S., and Packer, J.A.: "Weldment design for RHS truss connections. II: Experimentation". *Journal of Structural Engineering*, 118(10), (1992b), 2804-2820.

International Institute of Welding (IIW), Subcommission XV-E: "Design recommendations for hollow section joints - Predominantly statically loaded". *IIW Doc. No. XV-701-89*, 2nd. edition, Cambridge, U.K., 1989.

Packer, J.A. and Henderson, J.E.: "Design guide for hollow structural section connections". Canadian Institute of Steel Construction (CISC), Willowdale, Ontario, Canada, 1992.

Packer, J.A., Wardenier, J., Kurobane, Y., Dutta, D., and Yeomans, N.: "Design guide for rectangular hollow section (RHS) joints under predominantly static loading". CIDECT and Verlag TÜV Rheinland, Köln, Germany, 1992.

Ravindra, M.K., and Galambos, T.V.: "Load and resistance factor design for steel". *Journal of the Structural Division, ASCE*, 104(9), (1978), 1337-1353.

## 8. NOTATION

$A_m$	effective area of fusion in base metal number 1 ( $A_{m1}$ ) or 2 ( $A_{m2}$ ) = effective leg length of weld x length of weld;
$A_w$	effective throat area of weld = effective throat thickness of weld x length of weld;
$a$	theoretical throat thickness of weld;
$b_i$	external width of RHS member $i$ ( $i = 0, 1$ ), $90^\circ$ to plane of truss;
$F_u$	ultimate stress of base metal;
$F_{yi}$	yield stress of member $i$ ( $i = 0, 1$ );
$h_i$	external depth of RHS member $i$ ( $i = 0, 1$ ), in plane of truss;
$i$	subscript to denote member of connection; $i = 0$ designates chord; $i = 1$ refers to a branch member for T, Y and X connections;
$K_a$	relative length factor for weld around RHS branch according to AWS (1994, 1996);
$m_R$	mean of ratio: (actual element strength)/(nominal element resistance);
$t_i$	thickness of RHS member $i$ ( $i = 0, 1$ );
$V_r$	factored resistance of weld;
$X_u$	ultimate strength of electrode material;
$\alpha$	separation factor = 0.55;
$\beta$	width ratio between branch member and chord = $b_1/b_0$ ;
$\beta^*$	safety (reliability) index for LRFD and Limit States Design;
$\theta_1$	angle between branch member 1 and chord;
$\phi_w$	resistance factor used for base and weld metals.

# Requirements and Capabilities for Composite Connections in Non-Sway Frames

David A Nethercot<sup>1</sup>

## Abstract

Developments aimed at improving understanding of both the achievable levels of moment capacity, rotational stiffness and rotation capacity for composite connections and the values required from these quantities to achieve economy when using the semi-continuous approach to frame design are described. In both cases emphasis is on the provision of design expressions that link performance and requirements directly to the main physical parameters of the connections and the frame members respectively.

## 1 INTRODUCTION

The past 20 years have seen the development of a substantial body of knowledge on the behaviour of composite connections. This has led to a situation in which the role of variations to the principal items that make up a composite connection in controlling the key measures of the structural performance of the joint is now generally appreciated. Understanding the behaviour of the connection is, of course, not an end in itself; the real need is to be able to profit from this improved understanding by developing more realistic approaches to the design of composite frames, that by recognising the actual contributions of the joints give the designer a competitive edge.

The opportunity to use more advanced design approaches of this type and yet to operate within the framework of an accepted design code has been provided by the inclusion in EC4 (1) of the "Semi-Continuous" approach to frame design. This extends the concepts of "Partial Strength" and "Semi-Rigid" Joints that are currently rather more rigorously developed for bare steelwork via Annex J of EC3 (2) to composite construction. At present the approach is limited to non-sway frames, thereby reflecting the fact that almost all testing of composite connections has employed non-sway arrangements. Of the few exceptions to this, the most notable example is the work of Leon (3,4), who has utilised his findings in developing a design approach for composite sway frames employing U.S - style details

---

<sup>1</sup>Professor and Head, Department of Civil Engineering, University of Nottingham, University Park, Nottingham NG7 2RD, U.K.

In frame design the objective must be to match the levels of performance that are readily achievable from connections to the requirements of the joints necessary to achieve a competitive design. Essentially this centres around the need to redistribute high elastic moments from the beam to column support regions into the mid-span regions of the beams so as to utilise the large sagging moment capacity of the composite section. This must, of course, be achieved without exceeding the capability of the joint regions - either in terms of strength or of deformation. Thus complementary studies of the levels of performance required from connections when operating in a frame environment are just as important as work to investigate connection behaviour itself.

It is the purpose of this paper to bring together the findings of several recent studies of both connection behaviour and connection requirements as a way of demonstrating the progress that has been made towards the development of comprehensive design treatments for semi-continuous composite frames.

## 2 CONNECTION PERFORMANCE

It is now widely accepted that the important measures of connection performance as defined on Figure 1 are:

- $M_u$  - Moment Capacity
- $K$  - Rotational Stiffness
- $\phi_u$  - Rotation Capacity

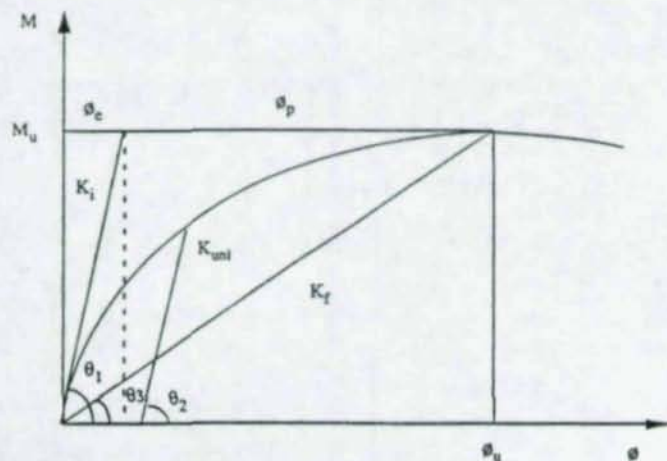


Figure 1 Simplified  $M-\phi$  curve for a composite connection

and that the most comprehensive representation of connection performance is its complete  $M-\phi$  curve shown as Figure 2. Compared with the equivalent bare steel detail, composite action generally increases  $M_u$  and  $K$  but because it changes the eventual mode of failure it normally significantly reduces  $\phi_u$ . Indeed, re-examination of the vast body of test data on steel joints

shows that in a large number of cases actual failure - in the sense of reaching a peak on the  $M-\phi$  curve - did not occur, the test being stopped once very large deformations had been achieved and/or the available rotation provided by the particular testing arrangement had been exhausted.

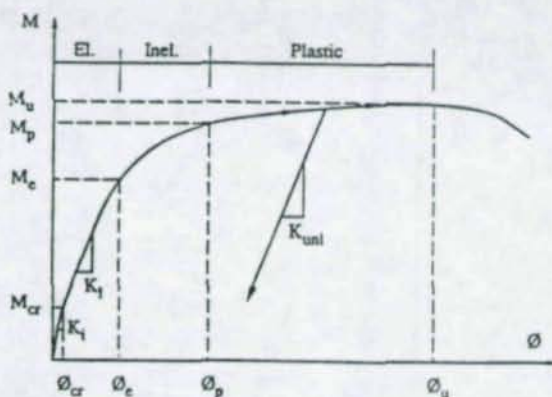


Figure 2 Most general form of moment - rotation characteristic

All available composite connection test data, amounting to some 150 test histories, have been included in a database linked to a spreadsheet calculation facility (5) that permits the verification of design approaches. Methods are now available (5) for predicting both  $M_u$  and  $\phi_u$  - the two properties whose values influence the ultimate load carrying capacity of the semi-continuous frame through their effect on the achievable final pattern of moments. The availability of these design models has, in turn, permitted the study of practically achievable levels of connection performance.

### 3 REQUIREMENTS

Compared with the extensive studies of connection performance referred to in the previous section, very little work had, until quite recently, been undertaken to study the relationship between frame properties e.g. support and span moment capacities, hogging and sagging beam stiffnesses, span lengths, pattern of moments etc., the percentage of moment redistribution necessary to achieve the desired final moment distribution and the support rotations needed to achieve this. Starting with the separate consideration of elastic and plastic behaviour illustrated in Figure 3 recent theoretical work at Nottingham (6,7) now permits the determination of the required support rotation  $\theta$ , for several different arrangements, linking this directly to the final level of design moments selected within the span. Exploratory calculations have been used to investigate the sensitivity of these rotations to the various problem parameters; from these the key quantities have been identified as:

$M/M_d$  - ratio of support i.e. connection, moment to span design moment.

$$R_m = (M_d - M_y) / (M_p - M_y) \text{ - relative moment ratio}$$

in which  $M_d$  = span design moment

$M_y$  = span yield moment

$M_p$  = span plastic moment, calculated using the stress block approach

$R_m$  implicitly includes the ratio  $M_d/M_p$ , the chosen level of span design moment.

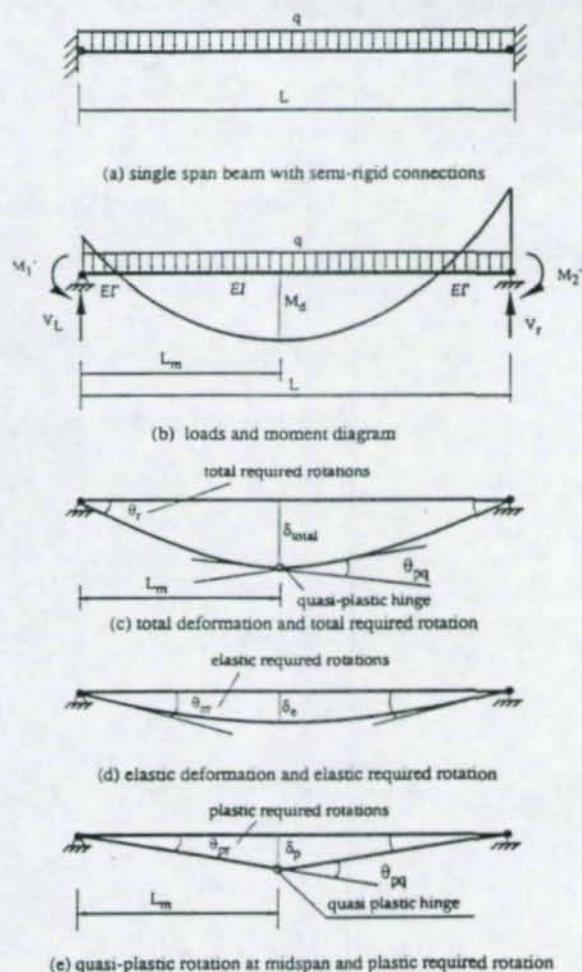


Figure 3 Subdivision of required rotation

Further work has permitted the "inversion" of these findings so that explicit formulae have been provided to give not just required rotations in terms of beam properties but, more usefully, the available percentage of moment redistribution (or the final value of  $M'/M_d$ ) for selected values of  $\theta$ , and  $M_d$ . Thus starting from an appreciation of reasonable levels of connection performance

-  $M'$  and  $\theta$ , - the designer can work directly with the final moment diagram. Alternatively, by ensuring that certain limits are observed, rather like the restrictions on cross-sectional geometry to give a "class I section" when using plastic design, a quasi-plastic approach (8) that parallels the mechanism method of simple plastic theory may be adopted.

#### 4 CAPABILITIES

Based on behaviour observed in the tests (5), including the 11 different, possible failure modes listed in Table 1, design models for  $M_u$ ,  $K$  and  $\phi_u$  have been established. In the case of  $M_u$  and  $\phi_u$  a consistent approach using the stress block concept and assuming:

- i no tensile contribution from cracked concrete
- ii all reinforcement at yield (but neglecting strain hardening)
- iii a uniformly distributed compressive force

has been employed.

Test terminated due to excessive joint deformation Excessive deformation of column flange Buckling of beam flange Shear connector failure Anchorage failure of reinforcement Failure of slab in shear Fracture of slab reinforcement Local buckling of column web Finplate twisting Bolt failure
---

**Table 1 Failure Modes Observed in Tests**

Using basic concepts of mechanics, the pattern of force transfer through each component in a composite connection may be constructed; Figure 4 illustrates the concept for an endplate for which the neutral axis (of the connection) falls between the level of the first and second bolt rows. Each of the component resistances - suitably linked to the possible modes of failure - may be expressed in terms of an appropriate formula, the neutral axis located, the lever arm determined and hence the moment capacity calculated.

Full procedures have been worked out within the context of the Procedure Guides and Engineering Bases approaches of the EUREKA CIMsteel project for the 4 cases:

- endplates
- fin plates
- web cleats
- web cleats plus seating cleat

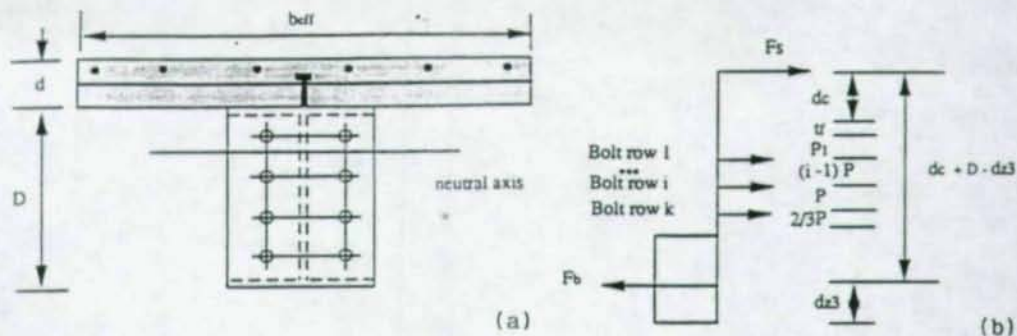


Figure 4 Model for determination of moment capacity;  
neutral axis below first row of bolts

Validation was by direct comparison with test data and Table 2 shows the findings to be generally on the safe side. More recently the approach has been extended to take account of unbalanced moment loading (9,10).

Connection types	Number of tests checked	Standard Deviation (SD)	Coefficient of Variation ( $\alpha$ )	$M_{test}/M_{pred.}$
Flush endplate	30	0.17	14%	1.18
Partial depth endplate	3 (top position)	0.04	4%	1.10
	5 (middle position)	0.04	4%	1.11
	7 (bottom position)	0.08	8%	1.03
Cleated	7	0.09	7%	1.25
Finplate	4	0.08	7%	1.26
Total	59	0.08	7.3%	1.16

Table 2 Summary of Comparisons for Prediction of Moment Capacity

A compatible method for calculating the available rotation capacity  $\phi_u$  has also been devised (5). Starting from the same determination of the location of the neutral axis, the elongation of the reinforcement together with any slip of the shear studs is calculated. Based on records of reinforcement strains from tests the assumption has been made that the region up to the second set of shear studs will be yielded. The model is illustrated in Figure 5. Validation has again been by direct comparison against test data and the results are summarised in Table 3. When studying this it should be borne in mind that the method is effectively attempting to predict the extent of

the plateau region on the  $M-\phi$  curve of Figure 2, an inherently more difficult task than to predict the peak of this curve i.e.  $M_u$ . It is also the case that the designer is interested in the question of adequate rotation capacity - not in using the precise value.

Availability of these design models permits the effect of changing certain key parameters in the connection to be readily studied. As an example, Figure 6 shows the influence on  $M_u$  of varying the percentage of slab reinforcement for a full depth endplate arrangement. For the 120mm deep slab 1.7% is required to develop a connection capacity equal to the hogging moment capacity of the beam, a figure that increases to 2.1% for a slab depth of 100mm. The different rates of increase of connection and beam moment capacity may readily be explained by considering the movements of the neutral axis.

Using these calculation methods it is possible to identify "sensible" arrangements i.e. levels of connection moment capacity and rotation capacity that are readily achievable with practical connection arrangements. It is also possible to identify unattainable levels of performance e.g. partial depth endplates welded to either the top or the middle of the beam cannot have their moment capacity increased beyond a certain level through the addition of ever more reinforcement or further increases in slab depth.

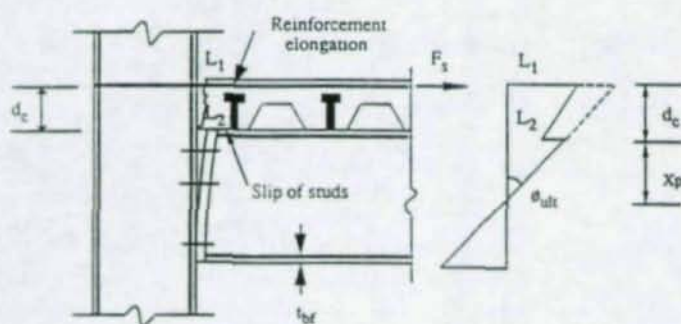


Figure 5 Beam-to-column rotation capacity model

Connection Type	No. of tests	Average $\phi_{test}/\phi_{pred}$	Standard Deviation
Flush endplate	19	1.29	0.54
Finplate	4	1.21	0.19
Cleated	6	1.10	0.35

Table 3 Connection Rotation Capacity Predictions

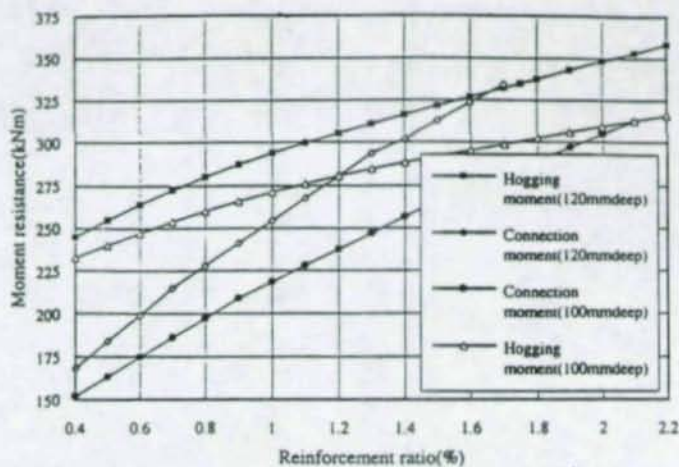


Figure 6 Influence of reinforcement ratio on moment resistance

## 5 CONCLUSIONS

The essential requirements of composite connections in non-sway frames designed according to the principles of semi-continuous construction have been identified as:

- i Sufficient moment capacity  $M'$  to reduce the design moment within the span of the beams.
- ii Adequate rotation capacity  $\theta$ , to permit the associated redistribution of support moments to the span.

Methods that link  $\theta$ , to  $M'$  and to the basic beam properties have been identified and coupled with methods to predict available levels of connection moment capacity  $M_u$  and rotation capacity  $\phi_u$ . These procedures may be re-arranged in a variety of ways e.g. to operate in terms of percentage redistribution of support moments as is commonly used in the design of continuous composite beams and frames or as justification for the use of a quasi-plastic design approach.

## 6 ACKNOWLEDGEMENTS

The work reported herein is a synthesis of the findings of several research projects supported over a number of years by BRE, SERC, British Steel and DTI. The author is grateful to these organisations and to those colleagues who have assisted with the work of individual projects.

**References**

1. Eurocode 3, Design of Steel Structures, Part 1.1: General rules and rules for buildings, DD ENV, 1993 - 1 - 1, BSI, London 1992.
2. Eurocode 4, Design of Composite Steel and Concrete Structures, Part 1.1: General rules and rules for buildings, DD ENV 1994 - 1 - 1, BSI, London 1994.
3. Leon, R T and Ammerman, D A (1987) "Behaviour of Semi-Rigid Composite Connections", Engineering Journal, AISC, 24 (4), pp 53-62.
4. Leon, R T et al, (1987) "Semi-Rigid Composite Steel Frames, Engineering Journal, AISC, 24(4), 1 pp 147-155.
5. Xiao, Y (1994) "Behaviour of Composite Connections in Steel and Concrete", Ph.D thesis, Department of Civil Engineering, University of Nottingham, UK.
6. Li, T Q, Choo, B S and Nethercot, D A (1995) "Determination of Rotation Capacity Requirements for Steel and Composite Beams", Journal of Constructional Steel Research, Vol. 32, pp. 303-332.
7. Nethercot, D A, Li, T Q, Choo, B S (1995) "Required Rotations and Moment Redistribution for Composite Frames and Continuous Beams, Journal of Constructional Steel Research, (in press).
8. Nethercot, D A (1995) "Semi-Rigid Joint Action and the Design of Non-Sway Composite Frames", Engineering Structures, (in press).
9. Li, T Q, Nethercot, D A and Choo, B S "Behaviour of Flush Endplate Composite Connections with Unbalanced Moments and Variable Shear/moment Ratios: Part 1: Experimental Behaviour, (under review).
10. Li, T Q, Nethercot, D A and Choo, B S ""Behaviour of Flush Endplate Composite Connections with Unbalanced Moments and Variable Shear/moment Ratios: Part 2: Prediction of Moment Capacity, (under review).

# THE USE OF THE ISO BOLTS, IN ACCORDANCE WITH THE EUROPEAN STANDARDS

Eugène PIRAPREZ <sup>1</sup>

## Abstract

The "ISO bolts" are now proposed, instead of the "DIN bolts", in the European pre-standards. The good quality of these bolts and their excellent behaviour during tightening are shown on base of nearly 500 tests results.

Consequently, the rotation applied during the tightening can be reduced and the different components of the bolts can be supplied by several manufacturers.

*In any case, the reliability is improved.*

## 1. INTRODUCTION

The so-called bolts "ISO Bolts" in contrast with the "DIN Bolts" were defined since several years but were considered in application standards of only in few countries. They are now included in the draft of the European Standards and the question is : are they compatible with the other norms relative to the execution of the steel structures ?

Several researches have been carried out to check the influence of the threaded length of the screw on the behaviour of the global bolt. But this larger length is adopted to reduce the stocks of bolts and to avoid problems due to a bad positioning of the nut; this threaded length cannot have an important influence on the preload of the bolt.

---

<sup>1</sup> Engineer at the CRIF, Steel Structures Department, LIEGE, BELGIUM.

On the other hand, it is often forgotten that the nut is also an element of the bolt and that its height is of the most importance on the tightening characteristics.

During the last years, the height of the nuts used in Europe increased significantly. Until recently, most of them were manufactured in accordance with DIN 6915 [1]; they were usually called "DIN nuts" and they had a height ( $m$ ) equal to  $0.8 d$  ( $d$  = the nominal diameter). Only nuts manufactured in U.K. had a height equal to  $0.9 d$  and in France equal to  $1.0 d$ . Now, in the European standards [2] [3], the values which have already been in the ISO standards, are considered (respectively  $m/d = 0.9$  and  $1.0$ ) and they are recommended in the pre-standard 1090 [4] concerning the execution of the structures.

Obviously, the height and therefore the "bending rigidity" of the nut can influence the global behaviour of the bolts not only during the tightening but also during all the life of the construction.

The determination of this possible influence was the goal of a very important research : 480 bolts were tightened and the main conclusions of the analyse of their behaviour are given below.

## 2. PARAMETERS

Three values were considered for the height of the nut :

- $m = 0.8 d$  in accordance with DIN 6915 [1].  
This value is the same for non-preloaded bolts;
- $m = 0.9 d$  (or a bit less) in accordance with prEN 783 [2] concerning the style 1 of nuts;
- $m = 1.0 d$  in accordance with prEN 780 [3] devoted to nuts for preloaded bolts.

It must be pointed out that for 8.8 bolts another parameter is linked to the height of the nut : it is the hardness of the material. The relation between the two factors is shown in figure 1. It will be very difficult to make a distinction between the influence of each of the two parameters. Meanwhile, we have already shown that a higher hardness of the nut improves the behaviour of the bolt [5].

The influence of the height of the nut has been evaluated by looking at several parameters, particularly :

- the validity of the tightening methods;
- the geometrical conditions when tapered washers are required;
- the use of components (screws and nuts) supplied by different manufacturers.

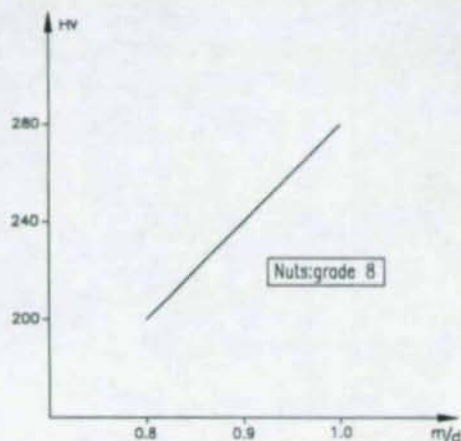


Figure 1 - Relation between height and hardness of the nuts.

### 3. INFLUENCE ON THE TIGHTENING CHARACTERISTICS

When the nut is higher, its bending rigidity is larger and the repartition of the forces on the thread is more uniform. Consequently, the plastic deformations along the thread are smaller and it is possible that the required rotation of the nut ( $\alpha$ ) to reach the nominal preload ( $F_v$ ) must be reduced. On the other hand, if the threaded part of the screw is larger, the zone with a small plastic deformation is also larger and it is possible that the required rotation must be increased.

In addition, the maximal preload is determined by the rupture of the net section and not by stripping of the thread. That means that the "reserve of rotation" ( $\alpha_u$ ) from the point reached by an usual tightening till the maximal load on the diagram ( $F_p - \alpha$ ) cannot be sufficient.

All these parameters have been considered during the evaluation of the tests results. It appears that when using nuts with a height equal to 1.0 d instead of 0.8 d :

- the value of the coefficient k is about 10 % lower.  
This coefficient links the applied torque to the preload by the relation  $M_a = k d F_v$ ; it depends upon the friction between the threads and between the rotated part and the washer.

- the maximal stress ( $\sigma_{\max}$ ) is about 10 % higher for 8.8 bolts and the same for 10.9 bolts;
- the stress induced by the combined method ( $\sigma_{\text{comb}}$ ) is 10 % higher for 8.8 bolts and the same for 10.9 bolts.

This method is defined by the relation :  $0.75 M_a + \alpha_c$ ;

it consists in applying a torque equal to 3/4 of the required torque to reach the full preload and then in applying a further rotation equal to  $\alpha_c$ ;

- the reserve of rotation ( $\alpha_u$ ) is much higher (between 10 and 40 %);
- the "ductility" of the bolt in the elastic range is a bit lower for 8.8 bolts;
- the stresses due to torsion are nearly the same in all cases.

The conclusions can be illustrated by the figures 2 and 3.

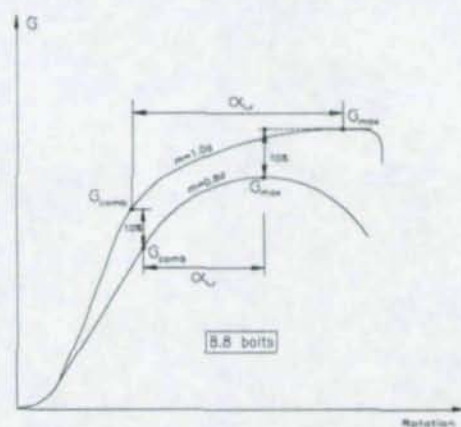


Figure 2 - Influence of "new" nuts on the behaviour of 8.8 bolts.

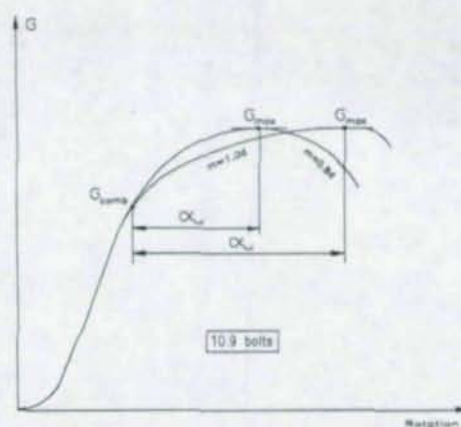


Figure 3 - Influence of the height of the nuts on the behaviour of 10.9 bolts.

If we compare the diagrams shown in these two figures, it seems that the behaviours of 8.8 and 10.9 bolts are different, but this difference is due to the hardness of the nut and not to its height. For 10.9 bolts, the hardness of all the nuts was the same and it is clearly shown on figure 3 that the height of the nut increases only the "capacity of rotation".

It is evident that the behaviour of a 8.8 bolt with an ISO nut is very similar and that the increase of the maximal stress and of the "rigidity" is due to the variation of the hardness of the nut. This phenomena was already remarked a few years ago, when the hardness of grade 10 nuts was modified [5].

About the calibration of the combined method of tightening, these results confirm the conclusions of previous researches [5,e.g.] : since the manufacturers have a quality control system, the quality of the bolts is higher and the angle of rotation ( $\alpha_c$ ) to apply on the nut during the second phase of the tightening can be reduced. The standardized values and the proposed values for  $\alpha_c$  are given in table 1, where  $\Sigma t$  is the total nominal thickness of parts to be joined (including all packs and washers).

Table 1 - Values of  $\alpha_c$

$\Sigma t/d$	2	5	6	10
Standardized values	60	90	120	?
Proposed values	60	90	90	?

If the values of  $\alpha_c$  are reduced in this way, the required preload can be guaranteed for all the bolts and the deformations of the thread are lower, which improves the long duration behaviour of the bolt, even if the "reserve of rotation ( $\alpha_u$ )" is very large.

#### 4. INFLUENCE ON THE USE OF TAPERED WASHERS

In accordance with the norms [4], ..., a taper washer must be used under the rotated part of the bolt when the surface is not normal to the bolt axis, without mentioning the limit angle. In the ECCS recommendations [6], it is stipulated besides that such a washer is also required under the non-rotated component when the taper is larger than 3°. These requirements are based on very few tests results. Moreover, only two types of taper washers are standardized : with a taper equal to 8 % ( $\cong 5^\circ$ ) and to 14 % ( $\cong 8^\circ$ ) which correspond to the tapers of the flanges of IPN and U profiles. It

was necessary to check if these values were still adequate for nuts with a larger rigidity, because the secondary effects could be larger too.

Tightening tests were carried out with uniform plates and washer(s) with a taper of 8%. A taper washer was installed :

- under the head
- under the nut
- under head and nut.

The diagrams of the figures 4 to 7 give an overview of the results.

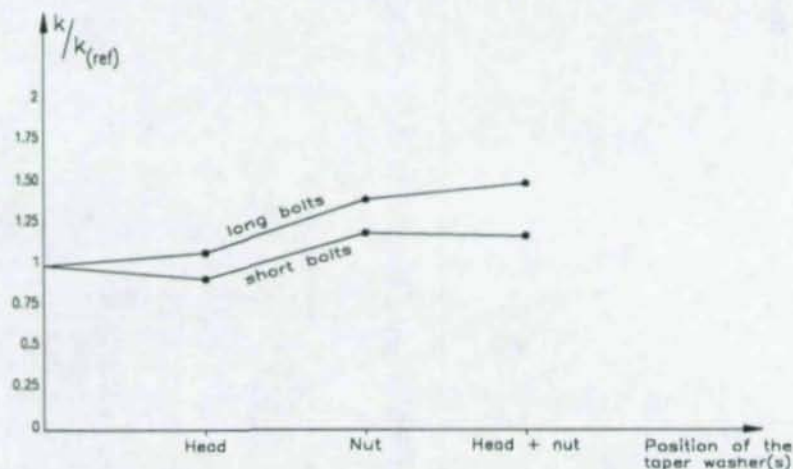


Figure 4 - Influence of the taper on the k value

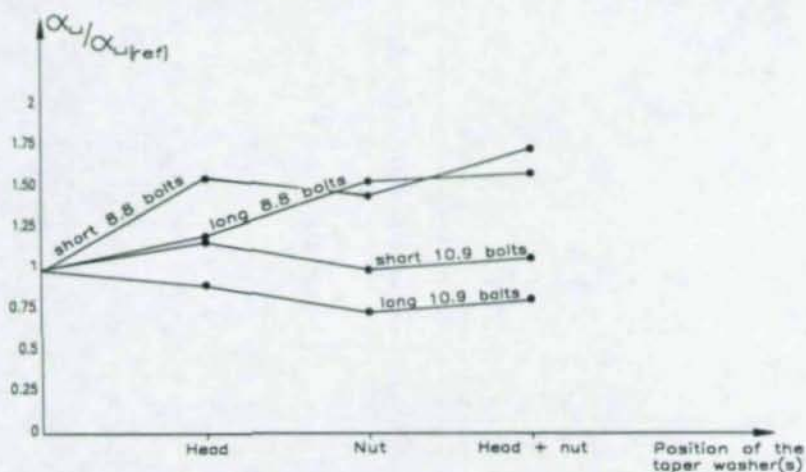
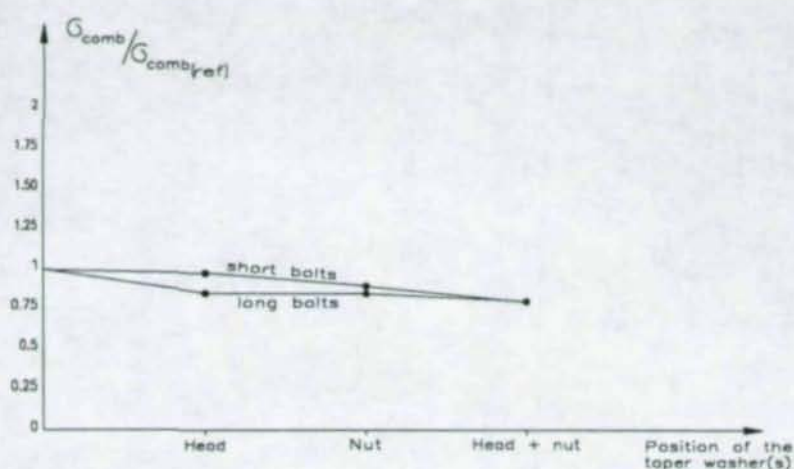
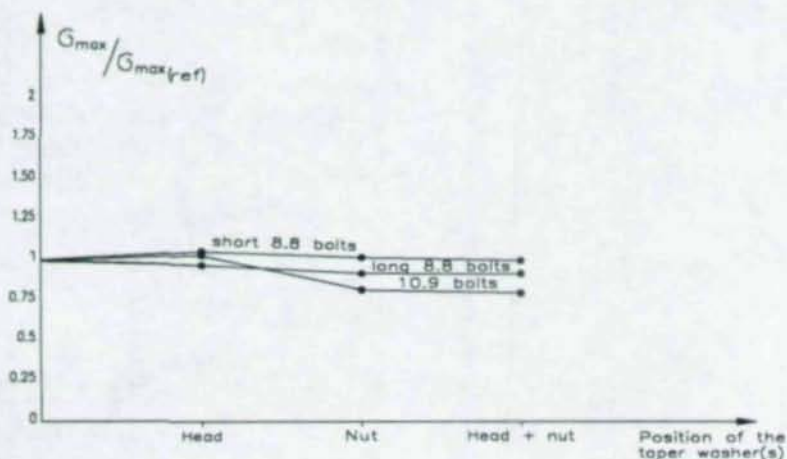


Figure 5 - Influence of the taper on the reserve of rotation ( $\alpha_u$ )

Figure 6 - Influence of the taper on  $\sigma_{comb}$ Figure 7 - Influence of the taper on  $\sigma_{max}$ 

It is evident that when the surfaces of the assembled parts are not parallel (8 %, in this case), the behaviour of the bolt can be very different. When using the torque method of tightening, the loss of preload can be larger than 30 %. When using the combined method, the preload is also lower ( $\approx 10$  %) but sufficient in any case. Nevertheless, if no taper washer is used when the angle between the surfaces is equal to 5° (or higher), the further rotation applied during the second step of the tightening must be increased. But the security is reduced.

The height of the nut has no influence on the effect of the non-parallelism of the surfaces, but the parallelism is a parameter to check carefully on site before the installation of the bolts and the limit value of  $3^\circ$  given in the standards about the permitted taper seems to be appropriate.

## 5. COMPONENTS FROM DIFFERENT SOURCES

It is usually stipulated in national standards that all the components of a bolt must be provided by the same supplier. But now, regarding to the high quality level of the fabrication, the question is: "Is this requirement still necessary?".

Screws and nuts coming from 3 different suppliers were combined and their behaviour characteristics during tightening were determined.

A very important conclusion can be established from this tests serie :

"The behaviour of the bolt is influenced by the nut and not by the screw" : the same nut applied on different screws gives exactly the same results, but on the other hand, the results obtained by the same screw with different nuts are scattered.

The general conclusions regarding to the use of different nuts are :

- the range of the preload obtained by the torque control method of tightening is more than 20 %;
- the range of the preload obtained by the combined method of tightening is about 10 % for 8.8 bolts and less than 2 % for 10.9 bolts.

The difference between the results obtained by the two methods of tightening is in line with the results of the previous researches and the values of the ranges of the preload are similar with the results obtained about 10 years ago when the controls during the fabrication were not so severe.

The rather large range of the results obtained with 8.8 bolts is not due to the height of the nuts; it proves again the very important influence of the hardness of the material. The scattering is maybe also due (for a small part) to the tolerances of fabrication which are not so closed for 8.8 bolts as for 10.9 bolts.

## 6. GENERAL CONCLUSIONS

The ISO bolts have a very good behaviour; the quality of their fabrication is now very high.

This level of quality is mainly due to the nut improvements.

The quality of the nut is much more influenced by its hardness than by its height.

The rotation applied during the second step of the combined method of tightening should be reduced.

The control of the parallelism of the surfaces of the assembled elements must be severe.

The source of the different components of the bolt (according to ISO standards) has no importance when the combined tightening method is used.

## 7. REFERENCES

- [1] DIN 6915  
"Sechskantmuttern mit grossen Schlüsselweiten für verbindungen mit HV-Schrauben in Stahlkonstruktionen"
- [2] prEN 783  
"Hexagon nuts for structural bolting with large width across flats  
- Style 1 - Product grade B - Property class 10".
- [3] prEN 780  
"Hexagon nuts for high-strength structural bolting with large width across flats  
- Product grade B - Property classes 8 and 10".
- [4] prENV 1090-1  
"Execution of steel structures - Part 1 : General rules and rules for buildings".

- [5] J.P. DEGUELDRE, E. DEHAN, E. PIRAPREZ.  
"Boulons à haute résistance de qualité 10.9 - Recherche des conditions optimales pour le serrage mixte".  
CRIF - MT179 - Décembre 1990.
- [6] ECCS - Technical Committee 10 - n° 38.  
"European Recommendations for bolted connections in structural steelwork".

Technical Papers on

**STATE OF PRACTICE**

## FROM DESIGN DRAWINGS TO STRUCTURE THE ROLE OF THE FABRICATOR'S ENGINEER IN DEVELOPING CONNECTIONS IN USA

LAWRENCE A. KLOIBER, P.E.<sup>1</sup>

### ABSTRACT

Traditionally the structural engineer establishes the strength and stiffness requirements for the connection on the design drawing along with the preferred method of force transfer. The fabricator's engineer is responsible for developing a constructable connection that complies with these guidelines. The Scope of this work may vary from merely establishing detail dimensions to selecting the type of connector and locating and sizing the connection material. Examples of the fabricator's role in developing connections are reviewed.

### 1. THE FABRICATORS ROLE

The structural engineer of record (EOR) is by law the person responsible for the design of a structure. His role is well established both by law and custom. Less defined and understood is the role of the fabricators engineer in converting the design into an actual structure. This is a multifaceted role that includes interpreting the design drawings, reviewing for conflicts and inconsistencies, checking constructability, serving as a technical resource, providing value engineering, developing connections, details, supervising quality control, preparing repair procedures for fabrication non-conformances and helping solve field problems. The fabricator assists the EOR by serving as a steel expert with knowledge of material properties, material availability, weld procedures, fabrication methods, and erection procedure. All of these roles are part of being a contractor and builder and are a complement to the EOR's role as designer.

Design drawings are intended to convey the EOR's concept of the structure to the builder. As in any communication there are always ample opportunities for misinterpretations or even a failure to communicate important information. The chance of a communication failure increases when constraints such as time or budget impact the drawing preparation and when the structural system involves unique, complex or

---

<sup>1</sup> Chief Engineer, LeJeune Steel Company, 118 W. 60th Street, Minneapolis, MN 55419

heavy members. Typically most of the engineer's design efforts involves positioning members, structural analysis and designing the members. Connections are often a last minute addition to the drawing. They are usually communicated by use of schedules and standard details or in the case of unique connections a representative detail. In a complex structure it is almost impossible for the designer's details to show all the variations required to accommodate the various connections. A world class structural consultant using the latest computer programs can analyze and design the structural frame for a complex 50 story high rise in a few weeks. A steel fabricator would need 6 months to prepare shop drawings, detailing all of the connections needed for this same structure.

Converting these design drawings into a structure requires a partnership between the EOR and the fabricator. Each has their role, the EOR as the designer and the fabricator as the builder. While they may assist each other they remain solely responsible for their separate duties. The fabricator may size connections and proposes changes in details and material but this is done as a builder not a designer. The engineer may help with construction by providing dimensional information but the fabricator remains responsible for the fit of the structure.

The fabricator begins the construction process with an overall review of the structural design drawings to understand the scope of work, sequence of construction and the structural system arrangement and function. This includes a review of specifications, structural notes, members sizes, loads and forces and connection details. The fabricator looks for conflicts, inconsistencies, missing information and anything that does not look right. Special attention is given to the lateral load resisting system.

Bracing systems usually involve some of the most complex shop details, require the most labor to fabricate and are the members most likely to have field fit-up problems. These members, however, are probably shown with the least detail on the design drawing. Typical bracing elevations show members sizes, the axial forces in the diagonal member and a standard connection with a concentric work point. The fabricator must be able to determine what the complete load path is from the origin of the force to the foundation in order to detail all of the connections for the appropriate forces. This includes knowing diaphragm shears and chord forces, collector forces and pass through forces at bracing connections. The designer's failure to provide a complete load path may require the application of the trickle theory of load transfer. The use of concentric work points at bracing joints makes the analysis of the frame and the design of members easier but may subject the detail material to eccentric loads or result in awkward details. This usually occurs when bracing slopes are extreme or member sizes vary substantially in size. It is important when reviewing bracing to determine if the work points shown will result in reasonable details.

Moment frame systems are usually very conservatively shown with notes calling for connections with a strength equal to the full section, often a complete joint penetration weld, along with column stiffeners equal in thickness to the beam flange. The fabricator

wants to know actual moments and shears in order to develop connections that are efficient and erectable. It is important when detailing connections for wind frames to know the size of the moment in each direction. Typically the reverse moments are less due to gravity load moments. When checking for stiffeners and detailing bottom flange moment connections the use of these reduced tension loads may provide simpler more economical connections.

Shear wall systems are simpler to detail and normally involve knowing only drag strut forces or diaphragm forces. Neither of these are usually clearly shown or detailed. When the structure depends on shear walls, precast panels, or horizontal diaphragms for lateral stability it is important that the general contractor and erector know this. The erector by standard practice only provides erection bracing for lateral loads on the bare frame. The construction sequence may require the general contractor or his erector to design additional temporary bracing because the permanent lateral load system is not complete.

Gravity load systems are reviewed to be sure all the needed connection information is given and seems reasonable. Any special conditions involving heavy loads or large eccentricities are studied. If typical connections are scheduled the fabricator reviews these to see if they can be efficiently built using the available equipment and provide easy safe erection.

Special framing systems such as long span trusses, arches or space frames get a preliminary constructability review along with a general review of forces, connection details and bracing.

The fabricator then usually contacts the EOR to verify his interpretations of drawings, to request additional information needed to prepare connection details, and to discuss how the various connections should be detailed. Preliminary sketches of some connections may be submitted at this time. This initial review by the fabricator is not a peer review but it is an effort by an experienced professional to understand the structural concept, verify whether all the needed information is shown, and determine if there are any obvious constructability problems.

Framing plans are then prepared for every member in the project. Even where the design drawings are used as the framing plans, all of the dimensions are reviewed and where possible checked. Point to point dimensions are calculated for all sloping or skewed members. Design drawings prepared by computer aided drafting can present special problems when down loaded. If the operator puts the cursor on the wrong point the machine will scale the wrong dimension. If manual changes have been made they may not be picked up. Because the fabricator is responsible for the fit of the structure it is essential that all of these dimensions be verified before connection detailing begins. It is during this stage that dimensional discrepancies and conflicts show up. Members shown in plan may conflict with members shown only in elevation. Columns may be rotated and members may not intersect as shown in connection details on the design

drawings. Each issue must be satisfactorily resolved before the connections can be detailed.

While framing plans are being prepared connection details are developed. The details and schedules shown on the designs are again reviewed for constructability and economy and where possible used as shown. Special connections are usually shown in concept only and actual detail dimensions, bolt sizes, and weld details are left to the fabricator to detail. When the EOR attempts to fully detail connections the fabricator often finds constructability problems or judges the connection to be uneconomical to fabricate. Standard competitive bidding practice dictates the fabricator anticipate using the most economical connections suitable for the structural needs unless more stringent requirements are indicated on the designs. In order for the owner to benefit from this practice it is necessary to clearly show what the minimum connection requirements are. Many EOR's are convinced that regardless of what type of shear connections they show, the fabricator will want to change them. What they should realize is that often the fabricator has to evaluate several options before deciding on the type of connection to use for a particular project. This should not be a real problem because it is easy to provide for these options. The EOR can simply specify the required reactions and allow the fabricator to use any of the standard connections in the AISC manual. This includes the use of single plate and single angle connection to improve economy and erection safety. Single side connections are becoming more important as erection safety rules get more restrictive.

The solution for special connections is for the EOR to show representative connections that have the type load path that is needed and then show all of the required connection forces. The fabricator then sizes connections for these forces and provides all of the detail dimensioning. The EOR can then review and verify the connections are adequate for his design. This method of developing connection details utilizes the knowledge and experience of both the EOR and the fabricator in the most efficient way.

Unique connections such as space frame connections, heavy plate connections and splices in Group IV and V shapes present special problems. Standard connections have been refined over the years and the problems are known. Every time you develop connections for new special systems you have to be on the alert for unforeseen problems. Heavy connections may have material and structural compatibility problems. Space frames connections have access and dimensional tolerance problems. The fabricator must be able to determine the strength and stiffness requirements for these unique connections before constructability problems can be solved. As loads or eccentricity increase, it becomes more difficult to develop flexible connections and this may change the forces on the member. The EOR and the fabricator have to share their knowledge to develop these connections.

Connection design does not stop with the approval of shop drawings by the EOR. The beginning of shop fabrication presents additional challenges. Material ordered for the project may not conform to specifications, fabrication errors may occur and unforeseen

constructability problems might be discovered. The fabricator must evaluate each problem to determine if a modification or repair is necessary. Even though shop supervision or quality control personnel may identify the problem it is important that the fabricator's engineer review and document any modification. Where it is determined that the connection even after repair or modification will not meet the original standards the proposed action must be submitted to the EOR to make the determination if the connection as fabricated will be fit for purpose.

The erection of the steel frame serves as a check of the fabricators efforts to detail and fabricate connections that fit perfectly. If the erector cannot put the bolt in the hole it may be necessary to modify the connection. Most minor fit up problems can be resolved with reaming, slotting, or shimming. Larger dimensional errors or other constructability problems may require the fabricator to develop a new connection detail that requires the approval of the engineer. Again, it may not be feasible to provide a connection that meets original design standard and the EOR will be called on to make a fitness for purpose determination.

## 2. EXAMPLES OF CONNECTIONS DEVELOPED

The fabricator's role in developing economical and constructable connections that fulfill all of EOR's structural design requirements can be further explained by some examples of this partnership.

The first project is a 42 story office building that uses a perimeter moment frame coupled with a braced core as the lateral load resisting system. When the fabricator began to detail connections for the braced core he realized that horizontal strut axial loads given in the connection schedule were substantially less than the horizontal component of the brace diagonal. When the fabricator asked about this difference it was discovered that when the structure was modeled an arbitrary stiffness was assigned to the floor to simulate the interaction between the moment frame and the braced core. In the model the floor was carrying part of the brace force. The EOR was not willing to rely on this type of composite action so all of the horizontal struts and their axial forces were increased in size. The fabricator then developed connections for these new forces.

The second project is a sports arena using a skewed chord space truss supported on 8 columns with the roof located at the bottom chord of the trusses. Each type of connection was clearly shown on the design drawing along with the forces to be used to determine the number of bolts and weld required for each connection. The fabricator in reviewing the forces given for the bottom chord discovered that the bottom chord members had been modeled as axially loaded pin ended members with end shears due to the transverse loading of the roof. The actual connection which consisted of double web plates welded between the flanges of W27 sections was extremely rigid. After reviewing this compatibility concern with the EOR the fabricator proceeded to size the connections for only the axial forces and shears given using N type values for all of the

bolts. A check of the connections for fixed end moments using an assumed stiffness and X type values for the bolts indicated there was adequate strength even if a rigid connection was assumed.

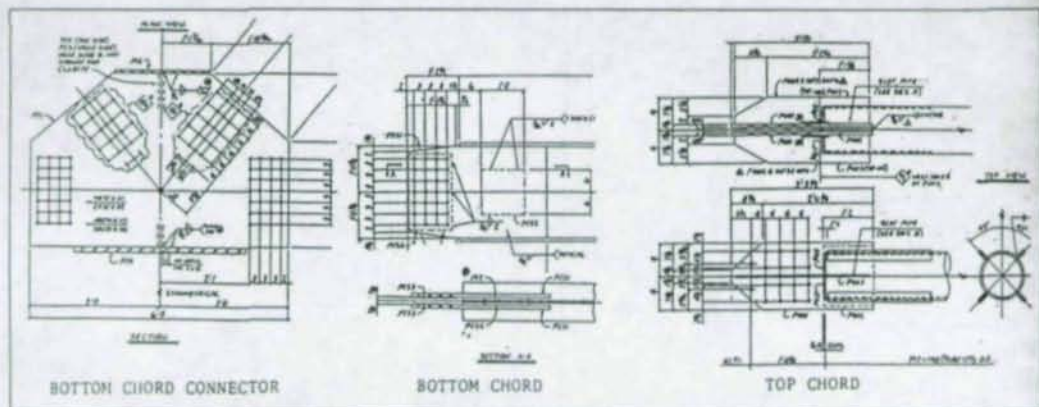


FIGURE 1. SKEWED CHORD TRUSS DETAILS

The top chord and all of the diagonals of this same truss were circular tubes of ASTM A588 material left unpainted to weather. While the fabricator was detailing the connections for these members the EOR became aware of a study (Brockenbrough, 1983) describing possible problems in weathering steel joints. The study indicated that under certain conditions where moisture had access to the inside of a joint the expansive pressure of continuing corrosion could over stress the connection bolts. Connection details were reviewed to make sure the material thickness and fastener spacing recommendations were complied with. Special restrictive fabrication tolerances were established for connection material flatness in order to insure that the connection bolts would be able to clamp the full surface together. The fabricator, by using techniques such as pre-bending, compensating heats, and special fixturing, was able to eliminate almost all of the weld shrinkage effects. The in-place connection fit tightly together with virtually no gaps.

The third project is a 57 story office building that uses a number of unique lateral load systems. The wind in the longitudinal direction is resisted by a series of 5 story bands of virendiel trusses spanning 97 ft to reinforced concrete super columns. The virendiel frames were designed as a series of horizontal trees with the verticals spliced at mid-height between floors. The design drawings called for the splices of these verticals to be partial penetration groove welds. The shop connection of these same verticals to the horizontal were CJP welds. Even if the verticals were milled to length after welding there was no way to maintain the alignment needed for the proper field weld joint. Since the field splice was at the inflection point the connection forces were rather modest axial and shear loads. The fabricator developed an end plate splice with slip critical bolts in oversize holes. All of the verticals were detailed short to allow for a standard

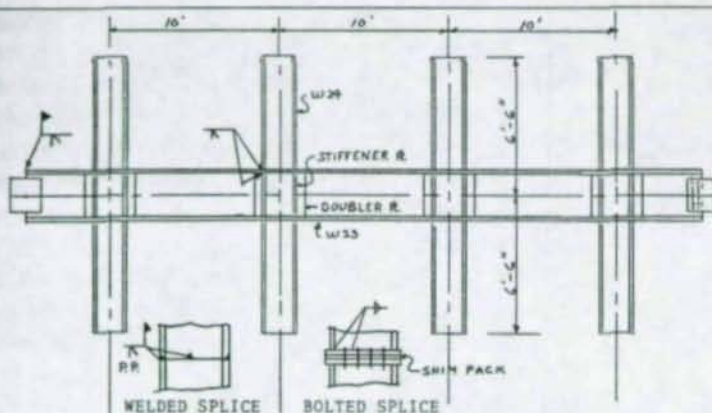


FIGURE 2. TREE BEAM DETAIL

3/8 inch shim pack. This connection allowed enough adjustment in all three directions to accommodate fabrication tolerances. This extensive reduction in field welding was one of the keys to completing erection ahead of schedule.

The fourth project is a 37 story mixed use structure that uses a mega truss bracing system for lateral loads. The bracing nodes are at 5 story intervals with wide flange diagonals sized for compressive loads. The EOR designed the connection of the diagonal to column and the horizontal strut as a groove welded butt splice. Because of past experience with poor fit up the EOR indicated joint fit up had to comply with AWS D1.1 tolerances with no buildout permitted. There was no way the combination mill, fabrication, and erection tolerances would allow the erector to achieve this type of fit between nodes. The fabricator added a splice at the midpoint of the diagonals utilizing field welded lap plates for adjustment. This allowed the erector to jack each segment to the exact required fit up at the nodes. Adding this splice also made it necessary to add a temporary column to support the lower half of the brace until the midpoint connection could be welded.

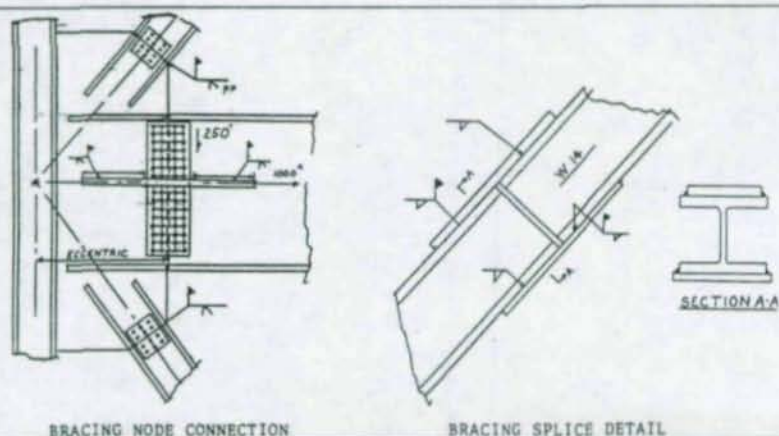


FIGURE 3. MEGA TRUSS CONNECTION DETAIL

The mega truss also serves as part of the gravity load structure where the building changes from a hotel to office use. One of the interior columns drops off and the truss diagonals carry the column load to the exterior columns. The horizontal tie at this level is a plate girder with an end reaction of over 200 Kips. The connection shown on the design drawings utilized a large gusset sized to accommodate the connections of the W14 diagonals and the plate girder without over lapping. Stiffeners were sized to match the flanges of each member. this detail placed the connection of the plate girder approximately 3 ft from the center of the column. The web splice of the girder consisted of lap plates in double shear. The EOR directed the fabricator to size this connection for the specified reaction with an eccentricity of 3 ft. This resulted in a connection with two rows of 16 - 1" diameter A490 bolts each side of the connection. The EOR then refused to allow the fabricator to transmit any of the 1000 Kips axial tension through the flanges because he did not want to make the connection too rigid. The final detail developed by the fabricator used a drag strut consisting of 2 plates 2 1/2" x 10" field welded at the mid depth of the girder.

The fifth project is an exhibition hall which consists of three lamella domes 210 ft in diameter surrounded by hollow structural tube (HST) space trusses. Each dome was supported by a series of sloping pipe struts from four columns. The domes vertically supported the inside edge of the space truss and the space truss laterally restrained the domes.

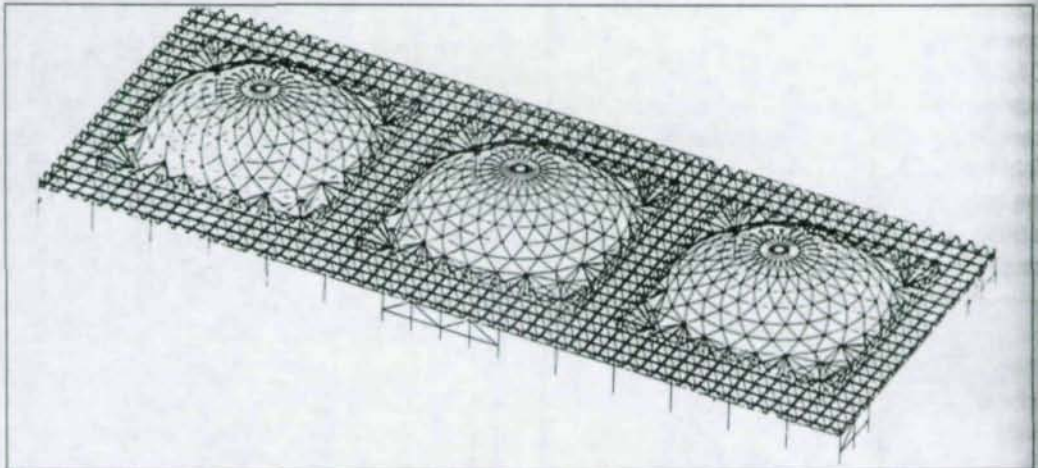


FIGURE 4. EXHIBITION HALL FRAMING SYSTEM

The EOR was directed by the owner to design all connections. The design specified for all space frame connections was a CJP weld. Many of the connections were "K" type joints where CJP welds could not be made because of restricted access. Even where access was adequate this type of detail required special welder certifications and was very difficult to inspect.

The fabricator's engineer working with industry experts Dr. Jeffrey Packer and Omar Blodgett developed weld details for each "K" type joint using fillet welds combined with partial penetration groove to provide the required strength. "T" type joints and butt joints were detailed with special internal backer bars so all welds could be made by welders with standard 2 and 3 G certifications.

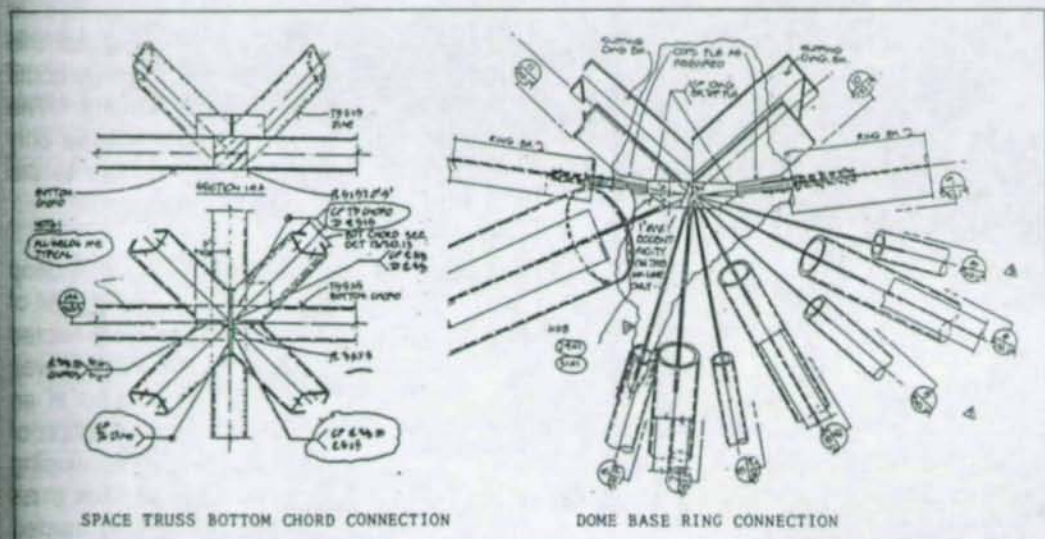


FIGURE 5. SPACE FRAME AND DOME CONNECTIONS

The dome base ring connections were complex welded heavy plate assemblies consisting of 6 inch plates with two wide flange diagonals and a series gusset plates CJP welded to opposite faces and tie plates welded to the edges. The EOR had previous experience with brittle fracture of heavy welded connections so he had specified ASTM A588 material with standard Charpy-V-Notch (CVN) testing in an effort to provide material toughness. When the fabricator reviewed material specifications with the producer it was determined that standard CVN testing would not provide assurance of through thickness toughness. The fabricator with the owners approval retained Dr. John Fisher and Dr. Alan Pense to work with Dr. John Barsotti to develop a specification for material properties needed to provide adequate through thickness properties.

A new test procedure calling for through thickness samples taken at the geometric center of the plate was developed. Yield stress was reduced to 46 KSI but a 20% reduction in area was specified for through thickness tension tests. CVN minimum values were set at 15 ft lbs @ 70° F in all three directions. The producer supplied a fully killed, low sulfur, vacuum de-gassed, and normalized material with inclusion shape control. All material was 100% ultra sonically inspected at the mill. There were absolutely no through thickness problems due to welding strains.

A different problem with these weldments was discovered during the erection stage. Each of these weldments had a series of gusset plates up to 4 ft long CJP welded to the 6 inch plate as described above. The angular alignment of the gussets required the CJP welds to be made from one side. The weld shrinkage from this type of joint caused the plate to rotate. Even with fixturing and compensating heat spots it was impossible to maintain the actual position of the ends of the gussets to a tolerance of less than 1 inch. Because of the flexibility of the plates the erector was still able to slide the slotted pipe struts over the gusset plate. The fabricator noted, however, that this misalignment resulted in an eccentricity in the gusset and thought this eccentricity could be enough to cause some of the gussets to buckle under compression loads. The fabricator notified the EOR of this problem and ultimately convinced him that the only reasonable solution to this problem was the addition of field welded stiffeners to the critical gusset plates.

The sixth project is a multi-use sports facility. The roof is framed with three 26 ft deep trusses spanning 206 ft and framed at one end to a jack truss spanning 185 ft. All of the truss members were W14 sections oriented with the flanges vertical and connected with lap type gusset plates. The work point of the connections of the roof trusses was shown at the neutral axis of the top chord of the jack trusses. This resulted in an eccentricity of 13 + inches to the center of the connection bolt group with reaction of 450 Kips. It was impossible to design a field bolted connection capable of developing these moments and shears. By moving the work point to the face of the jack truss gusset plate the connection eccentricity was reduced to 4 1/2 inch and a heavy framed angle connection was capable of developing the required strength. The eccentricity of the reaction in the jack truss was easily balanced by adding a 14 Kip horizontal force to the bottom chord connection of the truss to the jack truss.

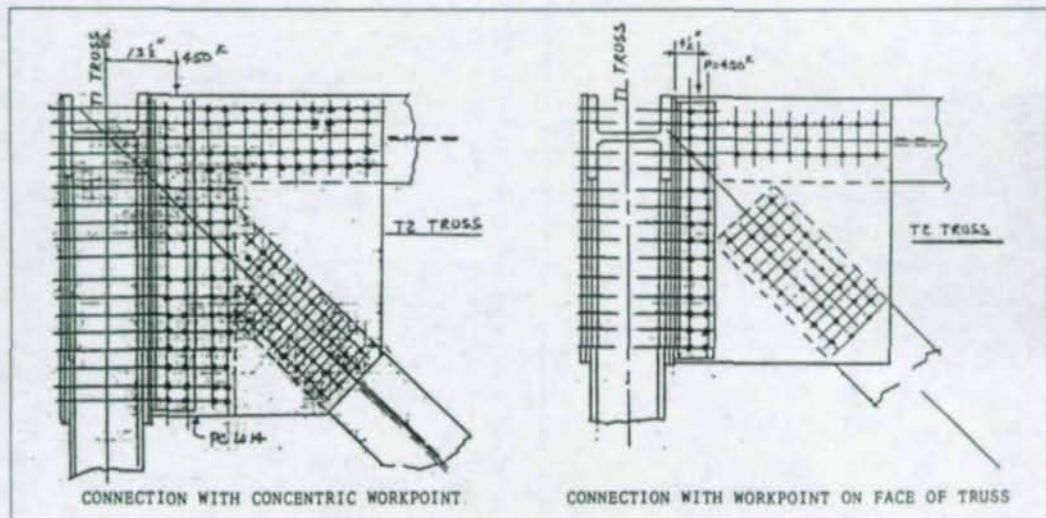


FIGURE 6. ROOF TRUSS CONNECTIONS

The seventh project is a discount store prototype that uses a moment frame to resist wind loads in one direction and shear walls in the other direction. The moment frame consists of a fixed base column and a continuous joist girder field welded to the column. The original design had the joist girder and intersecting joists supported by stiffened seats on the column. The joist girder top chords were tied together with field welded plates and the bottom chords were field welded to a heavy through plate. The fabricator revised the detail so the joist girder sat on the column cap plate and the joists sat on the joist girder thereby eliminating all of the stiffened seats. The top chords were then connected together using angles field welded under each side. Small connection plates transfer the wind moment force to the column cap plate. This redesign saved about \$7,000 per store and at approximately 90 stores per year the owner saves over \$600,000 annually.

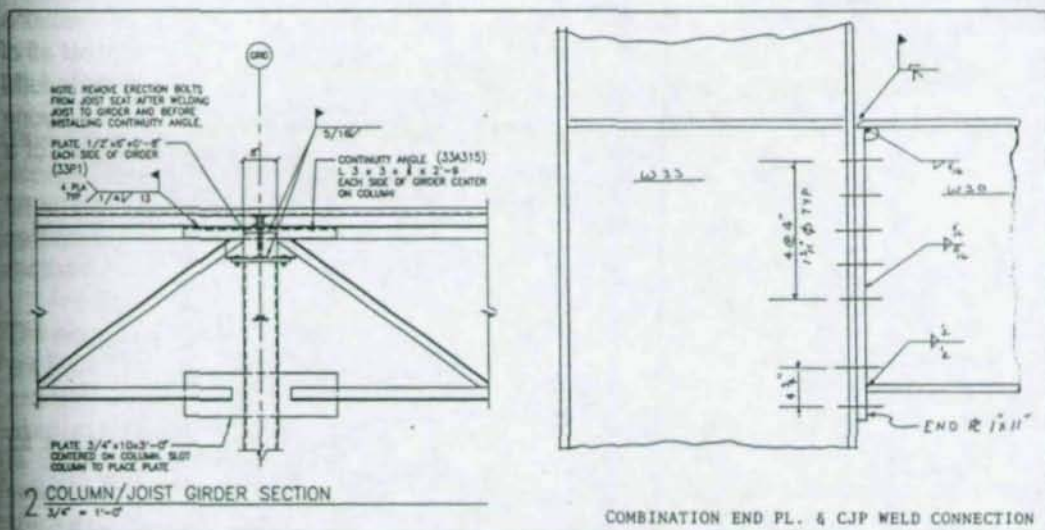


FIGURE 7. WIND MOMENT CONNECTION

FIGURE 8. MODIFIED END PLATE

The fabricator's knowledge of connection design coupled with his experience in solving fabrication and erection problems can give a unique insight into solving special connection problems. The eighth project is a recently built linerboard mill to recycle cardboard boxes. The main paper machine building is a conventional mill building using heavy wide flange step columns to support the crane runway and building roof. The operating floor girders which are designed for minimum floor load of 400 psf are moment connected to crane columns to provide lateral load support. All of this material is blast cleaned and receives a two coat paint system in the shop because of the corrosive operating conditions. Because of the special paint system every effort is made to avoid field welding.

The girder moments in several cases, however, were beyond the capacity of a stiffened 8 bolt end plate connection. Standard field welded moment connections would have

had to have the backer bars removed or seal welded prior to field cleaning and painting the connection area.

A review of the actual moments showed the reverse moment was only 1/3 of the maximum connection moment. A standard end plate connection could easily handle this reduced tension load at the bottom flange. The connection was then detailed with CJP weld for the top flange with an end plate serving as a permanent backer for this weld and also as the web and bottom flange connection. The use of an end plate for the bottom flange connection sized for the smaller tension load also eliminated the need for column stiffener plates at the bottom flange.

### 3. CONCLUSION

The fabricator, the erector and the EOR must work together to develop connections that can be fabricated and erected to the required tolerance and quality and meet all of the structural design requirements. Each party must be able to rely on the other to fulfill its role. When this partnership works well it is a win win proposition for everyone involved. There is nothing quite like the satisfaction that comes from being part of a successful team responsible for making an idea become a reality.

#### REFERENCES:

Brockenbrough, Roger 1983 -- "Considerations In The Design of Bolted Joints for Weathering Steel". Engineering Journal, Vol. 20 NO.1, AISC, Chicago, Illinois.

## PR Connections In Design Practice

Arvind V. Goverdhan, Ph.D.<sup>1</sup>

Stanley D. Lindsey, Ph.D., S.E.<sup>2</sup>

### Abstract

The use of PR connected unbraced frames is discussed from the viewpoint of design practitioners. The features of a computer program and a procedure designing PR frames using composite connections is presented with an example. Issues for further research to assist designers have been identified, based on this example.

### 1. INTRODUCTION

This paper outlines the design of unbraced frames with partially restrained (PR) connections as practiced in an engineering design office. At the very outset, it should be emphasized that the design of PR unbraced frames is only viable with computer software that specifically allows modeling the connection restraint. A computerized method for the design of PR frames eliminates tedium and encourages creativity.

The economic incentives for partially restrained connections in structural steel frames are found in the reduction of steel tonnage due to end restraint and in simpler and less expensive connection details. The idea is simple – make use of the inherent stiffness of connections that have traditionally been ignored, perhaps with minor modifications to details that enhance connection performance or improve the predictability of response. This approach is feasible for low to moderate height structures built in the United States. In the authors' experience, the best results require the mobilization of more (PR) frames than would normally be required with fully rigid (FR) frames. The lateral stiffness is, therefore, distributed over the floor plan as opposed to being isolated along a few column lines. Widespread use of PR frames in the U.S. is hindered by the absence of guidance on the moment-rotation response of connections in the design specification. There is also a lack of understanding of nonlinear analysis and software tools required for design.

---

<sup>1</sup>Associate, Stanley D. Lindsey and Associates Ltd., 2300 Windy Ridge Pkwy, Suite 1180 South, Atlanta, Georgia 30339, U.S.A.

<sup>2</sup>President, Stanley D. Lindsey and Associates Ltd., 2300 Windy Ridge Pkwy, Suite 1180 South, Atlanta, Georgia 30339, U.S.A.

The design engineer is concerned with the serviceability and strength of the unbraced system at specified combinations of loading. The questions that must be addressed include:

- 1) What does the design specification sanction?
- 2) Where is information obtained on connection stiffness and response?
- 3) What software tools are needed? What are the minimum analysis requirements and modeling guidelines?
- 4) How are the various elements of the frame designed— the beams, the columns and the connection elements?

These points are discussed in the following sections.

## 2. SPECIFICATION AND BUILDING CODE ISSUES

The use of partially restrained connections is explicitly permitted by the AISC Load and Resistance Factor Design (LRFD) Specification for Structural Steel Buildings. This is predicated on evidence of predictable end restraint by the connections and "... the capacity of the connections to provide the needed restraint shall be documented in the technical literature or established by analytical or empirical means." (LRFD 1993). There is no further guidance or reference to published works. The commentary cautions the designer to "take into account the reduced connection stiffness on the stability of the structure and its effect on the magnitude of second order effects." The limit states approach of the LRFD specification is better suited for the analysis and design of PR frames than the Allowable Stress Design (ASD) specification. While the ASD specification allows PR connected frames, it does not provide a rational basis for their analysis and design when nonlinear effects are dominant.

The use of PR frames in seismic zones is permitted; however, there is no codified design procedure. Minimum lateral forces which are a function of system ductility and lateral stiffness are specified by code for basic prequalified systems. Presently there is only limited published research upon which to draw. Until there is a codified procedure for design, the use of PR frames in regions of significant seismic risk is not recommended unless time history studies are used and the connections used do not exhibit severe degradation due to cyclic loading.

## 3. CONNECTION BEHAVIOR

Connection response is quantified by a characteristic moment-rotation relationship for each type of connection. Figure 1 shows a typical moment-rotation curve. This relation is nonlinear due to inelastic deformation of the connection components. The degree of nonlinearity is dependent on connection type. This characteristic moment-rotation relationship is an atomic input to the analysis and design of PR frames. Without access to this basic information it is not possible to pursue the design of PR frames. From the connection curve the following information is obtained:

- 1) The secant stiffness,  $K_s = M/\phi$
- 2) The tangent stiffness,  $K_t = dM/d\phi$
- 3) The unloading stiffness,  $K_u$
- 4) The ultimate moment capacity,  $M_u$
- 5) The ultimate rotation capacity,  $\phi_u$

A connection is said to be full strength when the ultimate moment capacity exceeds the moment capacity of the connected beam. Otherwise, the connection is classified as partial strength. Several researchers have also found use for the quantity,  $K_i$ , defined as the initial stiffness of the connection. Most of the experimental work on connections has focused on the monotonic loading response of the connections and there is insufficient data to quantify the unloading stiffness  $K_u$ . This is usually assumed to be equal to the initial loading stiffness  $K_i$ .

It was recognized in the early 1930's when research on the semi-rigid nature of connections was pursued in earnest that designers needed to know the characteristic moment-rotation relationship. Since then, substantial work has been undertaken to quantify this relationship for various types of connections. Currently the designer wishing to use PR connections must research the literature to determine the moment-rotation relationship and

document predictable end restraint. Experimental data from tests dating from 1936 were digitized by the first author (Goverdhan, 1983) to facilitate the study of the moment-rotation relationship of connections and the various attempts to quantify it. This data also appears in the connection data-bank established at the University of Purdue and is available in electronic form (Chen and Toma, 1994). There has been more experimental work on connection response since the initial compilation, but the authors are unaware of any attempts to keep the database up to date.

Ideally, connection behavior models should be established on the basis of geometrical and material parameters. Some calibration constants may be required to smooth the variation in nominally identical connections and deal with influences of material overstrength in seismic construction. The accuracy of representation of a moment-rotation relationship should be assessed from its influence on overall frame as well as individual element behavior. This involves basic research which should be the focus of institutions such as the AISC to promote the use of PR frames. Work is underway under the direction of the first author to collect and standardize connection models for design use.

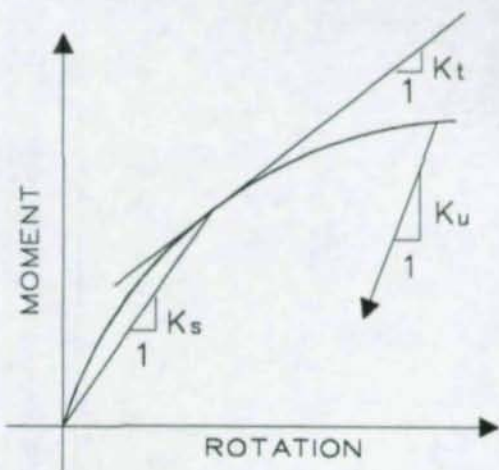


Figure 1 Typical Moment-Rotation Curve

#### 4. ANALYSIS AND DESIGN SOFTWARE

Several papers have outlined computer analysis techniques which incorporate the effect of PR connections. While some of the formulations include the consideration of large deformation theory and material inelasticity, these are not believed to be necessary for routine design office use. According to the LRFD specification, a first order linear elastic member response is acceptable to determine the distribution of forces in a structural framework. Higher order effects must, however, be considered in the design of a member of the framework. The specification outlines a method to convert first order linear elastic forces to design forces before applying the design interaction equation check to ensure adequate strength capacity. This method, called the  $B_1$ - $B_2$  method, may be avoided by considering  $P$ - $\Delta$  and  $P$ - $\delta$  effects directly in the analysis using a second order linear elastic member response.

There are other higher order effects which are significant to the response of the imperfect structural frame that cannot be practically or realistically modeled. Some of these effects, such as those due to residual stresses, member imperfections and lateral-torsional buckling, require computer resources beyond those that are readily available to the design engineer. These are best handled by empirical factors in the design equations from the specification. From a design office perspective, analysis software is needed that closely ties in the design specification.

The following is a list of features useful in the analysis and design of PR frames. These have been incorporated into a program used regularly in our design practice.

- 1) Three-dimensional modeling capability with or without rigid diaphragm assumption.
- 2) Explicit modeling of connections at member ends. Connection stiffness and response are internally evaluated from a library of connection models, e.g., piecewise linear, polynomial, power, modified exponential models etc. Connection response may be different under positive and negative moments. Unloading behavior may be specified.
- 3) Second order linear elastic element stiffness formulation. The member material obeys Hooke's law and the  $P$ - $\Delta$  formulation assumes that displacements are in the realm of small displacement theory. Bi-symmetric prismatic members are assumed thereby decoupling the bending effects about the two axes. The tension stiffening effect of axial forces is typically ignored. Member stiffness assignment is under the control of the user. Within a single model some elements may ignore the  $P$ - $\Delta$  effect (beams attached to a concrete floor) while others include it (columns).
- 4) Member in-span loadings are consistent with the stiffness matrix formulation.
- 5) Independent primary loading cases may be constructed from other primary loading cases input, as the principle of superposition may not be used to post-process the results.

- 6) Live load reductions may be computed internally for floor framing members and column members. The live load reduction is generally different for these members.
- 7) The solution algorithm allows incremental and/or iterative strategies and includes equilibrium correction. For research purposes staged loading can be considered and path dependent connection response can be traced.
- 8) Implementation of the LRFD design specification for member design and checks. Serviceability deflection checks are an integral part of member design.

## 5. DESIGN APPLICATION

To illustrate the various issues involved with designing PR frames a six-story structure is used as an example. A composite floor slab system is used with composite PR connections to develop resistance to lateral loads through frame action. The roof framing system is considered identical to the floor system to minimize the complexity of the example. Usually a noncomposite roof deck with lightweight insulating concrete and rigid insulation would be used introducing another connection type. Figure 2 shows the layout of a typical floor. The moment-rotation response for the composite connections is taken from Leon (Leon 1994). The "wet" loads at service level are assumed to cause no moments in the composite connections but are a major component of the axial loads and contribute to P- $\Delta$  effects which amplify the connection moments. Since lateral loading is due to wind only, the columns are oriented to provide more lateral stiffness in the north-south direction. For comparison to the FR design approach Figure 3 shows a framing layout with rigid frames.

A suggested procedure for the analysis and design of frames with PR composite connections is now outlined.

- 1) Set all composite PR connections as pinned and beams at "bare" steel inertia. Analyze the service level DL load case which consists of the "wet" loads on the frame. This provides information for cambering, ponding, etc.
- 2) Compute the live load adjustments for the columns. This requires one or more iterations of analysis of the live loads. A procedure similar to that described by Ziemian and McGuire (Ziemian and McGuire, 1992) is used. We choose to separate the live load into two distinct primary loadings, those that are reducible (LL) and those that are not (NRL), due to the different load factors applicable.
- 3) From the axial loads in the columns under the DL case create a new primary loading, DLJT. This new primary load consists of joint loads only which when applied results in the same axial forces in the columns as those due to the primary DL. Simplistically this can be a loading vector generated by summing the beam reactions with the applied joint loads and ignoring the fixed end moments.

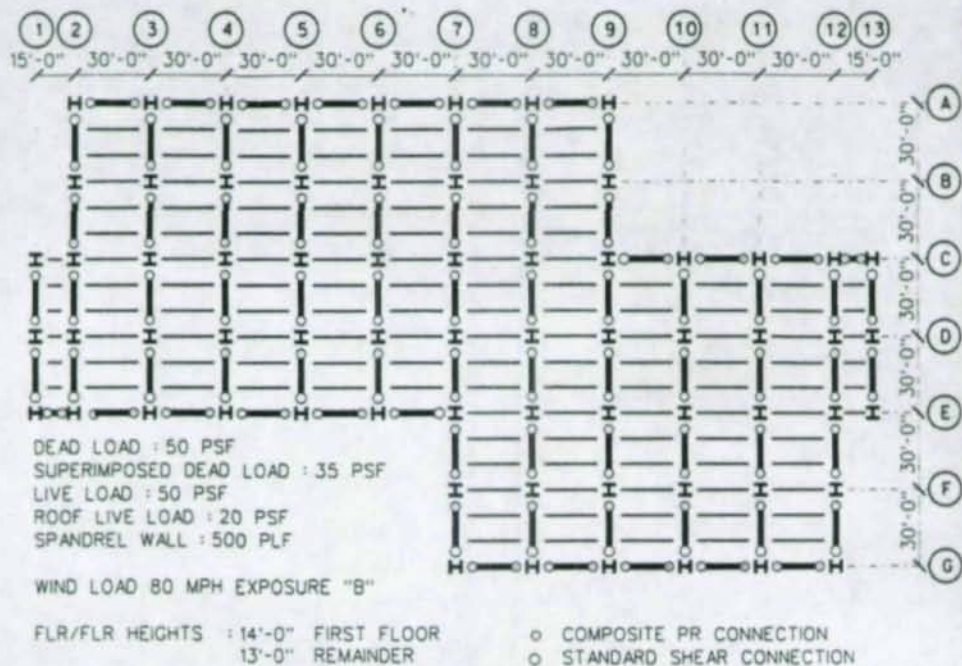


Figure 2 - PR System Framing

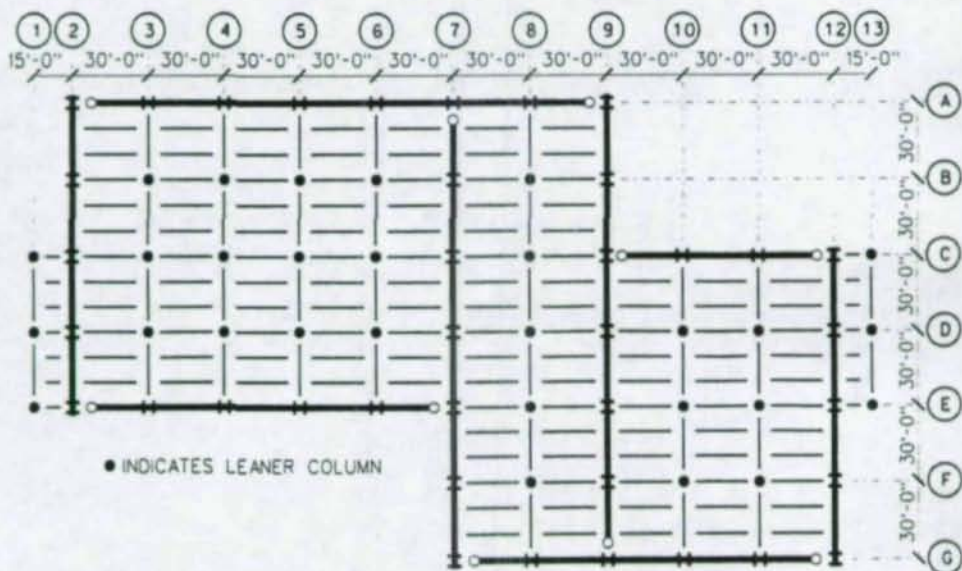


Figure 3 - FR System Framing

- 4) Analyze the factored "wet" load condition to check for strength under construction. If simple connections are assumed under these conditions design forces are related to service level forces by a simple factor.
- 5) Set all the composite PR connections to use the Leon model. Revise the cross-section moment of inertia of all composite beams to the effective composite inertia. The effective composite inertia is computed as a weighted average as described by Leon. Revise the column stiffness matrix formulation to include stability effects.
- 6) Analyze loading conditions to determine service level lateral displacements.

$$\begin{aligned}
 &1.0 \text{ DLJT} + 1.0 \text{ SD} + 0.5 \text{ LL} + 1.0 \text{ NRL} + 1.0 \text{ WX} \\
 &1.0 \text{ DLJT} + 1.0 \text{ SD} + 0.5 \text{ LL} + 1.0 \text{ NRL} - 1.0 \text{ WX} \\
 &1.0 \text{ DLJT} + 1.0 \text{ SD} + 0.5 \text{ LL} + 1.0 \text{ NRL} + 1.0 \text{ WZ} \\
 &1.0 \text{ DLJT} + 1.0 \text{ SD} + 0.5 \text{ LL} + 1.0 \text{ NRL} - 1.0 \text{ WZ}
 \end{aligned}$$

Since the PR connection stiffness is a function of the moment at the connection which is a result of the superimposed dead loads, live loads and lateral loads, all loads must be applied. In the absence of any guidance on a specific combination of these loads only one-half the live load is considered with full lateral and superimposed dead loads. If drift limits fail, revise beams, columns, connections, etc. and start again.

- 7) Analyze service level gravity loading conditions. As a minimum consider
 
$$1.0 \text{ SD} + 1.0 \text{ LL} + 1.0 \text{ NRL}$$
- 8) Analyze loading conditions to satisfy ultimate strength criteria. Consider the following combinations

$$\begin{aligned}
 &1.4 \text{ DL} - 1.0 \text{ DL} + 1.0 \text{ DLJT} + 1.4 \text{ SD} \\
 &1.2 \text{ DL} - 1.0 \text{ DL} + 1.0 \text{ DLJT} + 1.2 \text{ SD} + 1.6 \text{ LL} + 1.6 \text{ NRL} \\
 &1.2 \text{ DL} - 1.0 \text{ DL} + 1.0 \text{ DLJT} + 1.2 \text{ SD} + 0.5 \text{ LL} + 1.0 \text{ NRL} + 1.3 \text{ WX} \\
 &1.2 \text{ DL} - 1.0 \text{ DL} + 1.0 \text{ DLJT} + 1.2 \text{ SD} + 0.5 \text{ LL} + 1.0 \text{ NRL} - 1.3 \text{ WX} \\
 &1.2 \text{ DL} - 1.0 \text{ DL} + 1.0 \text{ DLJT} + 1.2 \text{ SD} + 0.5 \text{ LL} + 1.0 \text{ NRL} + 1.3 \text{ WZ} \\
 &1.2 \text{ DL} - 1.0 \text{ DL} + 1.0 \text{ DLJT} + 1.2 \text{ SD} + 0.5 \text{ LL} + 1.0 \text{ NRL} - 1.3 \text{ WZ} \\
 &0.9 \text{ DLJT} + 0.9 \text{ SD} + 1.3 \text{ WX} \\
 &0.9 \text{ DLJT} + 0.9 \text{ SD} - 1.3 \text{ WX} \\
 &0.9 \text{ DLJT} + 0.9 \text{ SD} + 1.3 \text{ WZ} \\
 &0.9 \text{ DLJT} + 0.9 \text{ SD} - 1.3 \text{ WZ}
 \end{aligned}$$

Other combinations specified by the code may be important as well. In the above combinations only the portion of dead load above the 1.0 factor is assumed to be carried by the composite section thereby generating moments in the connections. The full factored dead load is accounted for by including the primary DLJT so that  $P\Delta$  magnification is properly considered.

- 9) For strength design of the beams, the simple moment diagram due to 1.0 DL (or 0.9 DL as appropriate) is superposed on the results of the analyses in Step 8. The column design forces are directly available from Step 8.

The design of beams follows the provisions of Section I3, I5 and Chapter F of the LRFD Specification with supplementary serviceability deflection checks. Design engineers should be familiar with these provisions from traditional composite and rigid frame design. The location of inflection points is tracked so that the reinforcing steel in the negative moment region can be adequately anchored and the requirements of Section I5.5 on shear stud spacing satisfied.

Design of columns fall under the provisions of Chapter H of the LRFD Specification which requires that the design forces satisfy the interaction equation. To apply the interaction equation properly one needs to determine the nominal axial capacity of the column in the frame in the absence of moments and the nominal flexural capacity in the absence of axial loads. The effective length factor or K-factor method is one way to determine the nominal axial capacity of a column in a frame. The K-factor of a column is determined by using the solution of the nomograph equation. The traditional nomograph equation can be used with modified G-factors (Driscoll 1976). The modified G-factors are a function of connection restraint which is a function of connection moment. Thus, the K-factor is a function of the loading condition under consideration. For rigid moment frames in-span beam loading does not significantly alter the buckling load capacity of a frame. However, in PR frames this is not the case, in as much as the connection restraint is a function of in-span loading. The inelastic action of columns should be considered while computing the effective column stiffness. The effect of leaner columns on the nominal axial capacity of a column resisting lateral loads has been described (LeMessurier 1977). The commentary to the LRFD specification also describes a modification of the nomograph equation to approximate this effect. The second effect of leaner columns on the amplification of moments is easily accounted for by including them in the analytical model and performing a second order analysis.

The analysis of PR connected frames assumes that the connection stiffness is represented as the secant of the moment-rotation curve and that the response is path-independent. This is only an approximation of convenience to capture the global response of the frame. A connection unloads almost linearly and, therefore, the connection state is altered after the application and removal of load. The virgin loading path on the moment-rotation curve always represents the maximum moment state for the connection. The maximum positive moment in a beam, however, is obtained after a full cycle of application, removal, reverse application and removal of loading. The connection state can change further on continued cycling of the load. The first cycle of load represents the worst case condition for drift criteria as well as the end restraint for column buckling. A step-by-step path-dependent analysis is unsuitable for design purposes as the actual time sequence of the loading is unknown. In the case of frames with composite connections under quasi-static loading, the increase in positive design moment has been found to be insignificant to the design. Further studies on this phenomenon is suggested to provide a rational design procedure for the positive moment region for the general case.

### 5.1 Design Summary

The typical infill beam is the same in both design approaches. The interior typical composite girder is a W21X44 Gr 50 assuming simple connections. This section with composite PR connections is adequate to resist the lateral loads due to wind in the north-south direction. The sizes selected for the frame elements in the FR design are governed by drift criteria. A tradeoff is made by increasing the member sizes to limit the number of frames and welded rigid moment connections. In lieu of detailed design results, a summary of differences in total member weight is presented below in tons with reference to Figure 3. Infill E-W beams which do not participate in lateral resistance are not included in the member weights.

	FR	PR	Difference
N-S Girders	232.9	213.8	29.1
E-W Beams	80.4	63.0	17.4
Leaner Columns	56.5	59.0	(2.4)
N-S Columns	68.4	58.8	14.6
E-W Columns	<u>43.0</u>	<u>36.0</u>	<u>7.0</u>
TOTAL	491.2	430.6	65.7

The lateral drift criterion was set at a liberal 0.5 inches per floor (approximately  $h/300$ ). Despite the increased steel weights for the FR design, lateral displacements were marginal, and some further increase in steel weight is required.

#### LATERAL DISPLACEMENTS (inches)

LEVEL	EW-DIR		NS-DIR	
	PR	FR	PR	FR
ROOF	2.14	2.67	1.96	2.73
6	2.03	2.43	1.85	2.47
5	1.79	2.02	1.61	2.05
4	1.43	1.50	1.25	1.58
3	0.94	0.92	0.84	1.03
2	0.44	0.42	0.37	0.50

## REFERENCES

- Chen, W. F. and Toma, S. (1994), Editors, "Advanced Analysis of Steel Frames - Theory, Software, and Applications," ISBN 0-8493-8281-5, CRC Press Inc., 1994.
- Driscoll, G. C. (1976), "Effective Lengths of Columns with Semi-Rigid Connections," AISC Engineering Journal, Fourth Quarter, 1976, pp. 109-115.
- Goverdhan, A. V. (1983), "A Collection of Experimental Moment-Rotation Curves and Evaluation of Prediction Equations for Semi-Rigid Connections," M.S. Thesis, Vanderbilt University, 1983.
- LeMessurier, W. J. (1977), "A Practical Method of Second Order Analysis, Part-2 Rigid Frames," AISC Engineering Journal, Second Quarter, 1977, pp. 49-67.
- Leon, R. T. (1994), "Composite Semi-Rigid Construction," AISC Engineering Journal, Second Quarter, 1994, pp. 57-67.
- LRFD (1993), Load and Resistance Factor Design Specification for Structural Steel Buildings, American Institute of Steel Construction, December 1993.
- Ziemian, R. D. and McGuire, W. (1992), "A Method for Incorporating Live Load Reduction Provisions in Frame Analysis," AISC Engineering Journal, First Quarter, 1992, pp. 1-3.

## STRENGTH AND INSTALLATION CHARACTERISTICS OF TENSION CONTROL BOLTS

Geoffrey L. Kulak<sup>1</sup>  
Scott T. Undershute<sup>2</sup>

### Abstract

Tension control bolts are a configuration of high-strength bolt in which a splined end extends beyond the threaded portion of the bolt. To install the bolt, a special electrically powered wrench that has two coaxial chucks is used. The inner one slips over the splined end of the bolt and the outer one envelops the nut. The two chucks turn relative and opposite to one another to tighten the bolt. At some point, the splined end of the bolt shears off at an annular groove that is located between the threaded portion of the bolt and the spline. If properly calibrated, preload is achieved at this point. Factors that control the preload include bolt material strength, thread conditions such as lubrication, dirt, and thread damage, the diameter of the groove, and the surface condition at the nut-to-washer interface. The testing program reported herein measured the preload in a large sample of bolts (about 850) taken from several different manufacturers. Differing conditions of bolt age and exposure before installation were included.

### 1. INTRODUCTION

Preloaded high-strength bolts are required when slip of the joint would produce an unacceptable change in the geometry of the structure, when the joint is subject to load reversals, or when bolts are loaded in direct tension. In the case of a bolted joint in a bridge structure, for example, it would be required that the connection resist slip. In such an application, the capacity of the joint is a function of the slip coefficient of the faying surfaces and the clamping force provided by the high-strength bolts. While the condition of the faying surfaces may be reasonably apparent from a visual inspection, the preload in a bolt is not.

Specifications for the design of steel structures (Research Council on Structural Connections, 1988, Eurocode 3, 1993) generally permit the use of one or more of the following techniques for achieving the required preload in a bolt: turn-of-nut installation, calibrated wrench installation (control of torque), use of load-indicating devices, the use of alternative design bolts, or the part-tighten part-torque method. In North America, Japan, and elsewhere one of the so-called alternative bolt designs is the "tension control" bolt. This paper reports on a study of bolt tension achieved in a large sample of tension control bolts acting under a broad range of practical parameters.

<sup>1</sup> Professor, Dept. Civil Engrg. University of Alberta, Edmonton, Canada T6G 2G7

<sup>2</sup> Canam Manac, 270 Chemin du Tremblay, Boucherville, Quebec, Canada J4B 5X9

## 2. TENSION CONTROL BOLTS

Tension control bolts are a relatively new type of alternative design high-strength bolt. The bolt has a splined end that extends beyond the threaded length of the bolt and an annular groove between the threaded portion of the bolt and the splined end (Figure 1). A special electrically powered wrench is required to install the bolts. This wrench has two coaxial chucks—an inner chuck that slips over the splined end of the bolt and an outer chuck that envelops the nut. The two chucks turn relative and opposite to each other to tighten the bolt. At some point, the torque developed by the friction between the nut and bolt threads and at the nut-washer interface exceeds the shear resistance of the bolt material at the annular groove and the splined end of the bolt shears off. If the system has been properly manufactured and calibrated, preload (to some specified level) is achieved at this point. The installation procedure is carried out from one side of the joint only, is relatively independent of operator control, and use of the light-weight electric wrench can be economical as compared with an installation using an air-operated impact wrench.



Figure 1 Tension Control Bolt

Factors that affect the preload of a tension control bolt are bolt material strength, thread conditions (such as lubrication, dirt, and thread damage), the diameter of the annular groove at the splined end, and friction conditions at the nut-washer interface. Consider two hypothetical extremes for illustration. At one limit, friction will be assumed to be very large. In this case, torsion will build up rapidly and the splined end will shear off before any significant amount of preload is attained. At the other limit, friction can be assumed to be very low. Since the torsion in the bolt will therefore also be low, the bolt could fail in direct tension before the splined end has sheared off. Clearly friction will play a major role in determining the level of preload achieved.

The purpose of the testing program was to investigate the preload of tension control bolts as it may vary from manufacturer to manufacturer and under different conditions of aging and weathering. The results of the tests are used to evaluate the reliability of the bolts for use in high-strength bolting and to set out guidelines for the physical handling and care of tension control bolts.

There is very little literature available on the behavior of tension control bolts. The studies that have been reported generally were commissioned by manufacturers of tension control bolts and, moreover, are confined to a narrow range of test parameters. A summary of these studies can be found in Undershute and Kulak (1994). There are no national standards that address the tension control bolt.

## 3. EXPERIMENTAL PROGRAM

### 3.1 Specimen Description

Bolts were received from seven manufacturers or suppliers; five were American, one was Japanese, and one was a Japanese company that operates in the United States. In total, there were

13 lots tested. The target fastener was a 20 mm diameter by 70 mm long ASTM A325 bolt. (ASTM A325 and ISO Grade 8.8 are very similar bolts.) This size was suggested by the sponsor of the program, The Research Council on Structural Connections, as one in common use in fabricated steel construction. Eight of the 13 lots were of this size. Of the other five, four were 20 mm. diameter with lengths of 57 mm, 64 mm, 76 mm, and 83 mm, and one was 22 mm diameter with a length of 102 mm. The target age of the bolts was that they be as new as possible. Obtaining newly manufactured bolts was difficult, however, because it was not practical for the manufacturers to produce a keg of bolts just for this program. As a result, the age of the bolts at the start of the test program varied from approximately one month to two years. The suppliers, bolt sizes, quantities, and bolt ages upon receipt are given in Table 1. Suppliers or manufacturers are not identified by name, however.

Table 1 Bolt Lot Information

<i>Manufacturer</i>	<i>Lot Number</i>	<i>Bolt Size dia. x length mm</i>	<i>Quantity Supplied</i>	<i>Age Upon Receipt (months)</i>
A	2	20 x 70	250	3
B	3	20 x 70	75	21.5
	4	20 x 70	75	21.5
	5	20 x 83	120	5.5
C	1	20 x 70	130	30.5
	6	20 x 70	250	28.5
	7	20 x 76	130	4
	8	20 x 57	125	unknown
	9	22 x 102	59	unknown
D	10	20 x 70	125	2.5
E	11	20 x 70	125	5
F	12	20 x 70	100	unknown
G	13	20 x 64	125	0.5

### 3.2 Testing Regime

A typical testing regime consisted of the following:

- Hardness (Rockwell C) and direct tension characteristics (five bolts).
- Torqued tension characteristics (five bolts).

Measurement of bolt preload in each of the following categories (nine bolts tested in each category):

- As-delivered condition.

- Bolts aged in a sealed keg in the laboratory for two weeks and four weeks.
- Bolts exposed to outside humidity for two weeks and four weeks.
- Bolts weathered for two weeks and four weeks with full exposure to the elements.
- Bolts weathered for two weeks and four weeks in a joint with full exposure to the elements.

The numbers actually tested varied somewhat from lot to lot, depending on the number of specimens available in total in each lot. Most of the bolt lots were exposed to the weather during the month of September, but Lots 6, 7, 8 and 9 received their exposure during the months of July and August and Lot 13 was exposed during February.

Only the results of the as-delivered and exposure (aging) tests to establish preload will be presented in this paper. All bolts met the requirements of the relevant material specifications. Full details of these aspects can be found in Undershute and Kulak (1994).

### 3.3 Bolts Subjected to Various Conditions of Exposure

Bolts from each lot were tested upon arrival to obtain the preloads of the as-delivered product. Further tests were then performed on bolts from the same lots but which had been stored in a sealed metal keg in the laboratory environment in order to determine whether there was any tendency for the thread lubricant to deteriorate with time. Storage such as this is quite likely to occur. For example, one of the lots received was already over two years old.

Other bolts from each lot were subjected to the ambient outside humidity, but protected from direct contact with rainwater, in order to determine the effect of humid storage. This was considered to be representative of field storage conditions where the bolts may be stored in a shed but without a lid on the keg. Some of the bolts from each lot were given direct exposure to all of the atmospheric weathering elements (precipitation, humidity, wind and temperature). Again, this could be a possible field condition if bolts are left out in the open.

Often, an erector will initially install bolts in a connection only to a snug-tight condition and the final tightening will be done later. To examine the effect of this time delay, the weathered joints tests were established. The joints consisted of a three-plate assembly in which bolts were brought to snug-tight and then the joint put out to weather in direct exposure to the elements. After various periods of time, the final installation of the bolts was then completed.

Determination of preload was done in either a solid block, using a hollow (20-mm inner diameter) load cell, in a hydraulic bolt load indicator, or in the simulated joints, also using the hollow load cell. The solid blocks actually consisted of three plies, and they were proportioned to be representative of a symmetric splice. (Plates for the weathered joint tests were of the same thickness as those used for the solid block tests.) A bolt was first installed to finger-tight. Tightening then proceeded with the electric tension control installation wrench in a continuous, one-step process until twist-off of the splined end, thereby establishing the preload.

Bolts that were aged in the laboratory were placed in a metal keg with the lid securely fastened. After the specified amount of time (two or four weeks), the bolts to be tested were removed. In addition to these short-term indoor storage periods, long-term indoor storage periods were also

examined for Lots 1, 10, and 11. Lot 1 was stored for 32 weeks, while Lots 10 and 11 were stored for 24 weeks. After these periods of storage, the ages of the bolts were approximately 132 weeks for Lot 1, 46 weeks for Lot 10, and 34 weeks for Lot 11. Lots 1 and 11 were stored as previously described. Lot 10, however, was stored in a metal keg with the lid only loosely attached so that the bolts were exposed to the environmental conditions of the laboratory.

Bolts that were exposed to humidity were placed in a metal keg with the lid resting on top of the keg and the keg was then placed outside. In this way, the bolts were subjected to the ambient outside conditions but not exposed directly to rainwater. The bolts that were to be weathered with full exposure to the elements were laid out flat on a piece of plywood in a location that did not interfere with their exposure.

In the weathered joint tests, as-delivered bolts were placed in the connection with filler plates under the bolt head and then brought to snug-tight. The filler plates were a substitute for the load cell so that when the bolts were subsequently tested with the load cell in the grip length, the position of the nut on the bolt would be identical to its position when the joint was being weathered. Silicone was used to seal potential water entry points created by the presence of the filler plates within the grip length so that the only locations at which water could penetrate the joint were under the bolt head, between the plies of the plates, or under the nut. This corresponds to field conditions. The joints were then placed outside to weather, with the axis of the bolts in a horizontal position. After the specified period of exposure, the joints were brought inside and any rust that had accumulated on the bolt threads between the nut and the splined end was removed. This was done to avoid transfer of rust to the nut threads since, in practice, the nut would not be removed.

#### 4. TEST RESULTS, OBSERVATIONS AND DISCUSSION

##### 4.1 Bolt Material Properties

The ultimate tensile strength of all bolt lots met the requirements of the ASTM Standard (ASTM, 1992). The average value of the non-dimensional ratio of measured ultimate tensile strength divided by the specified minimum ultimate tensile strength is 1.21, with a standard deviation of 0.07. This is reasonably close to the published value for A325 fasteners (Kulak, et al., 1987), namely 1.183, standard deviation of 0.045. It was concluded that these A325 tension control bolts are substantially the same as regular A325 bolts, as would be expected.

##### 4.2 Bolt Preloads

Unless otherwise noted, when normalized preloads are given they have been normalized with respect to the specified minimum preload. This gives an explicit description of the bolt performance and allows the preload of bolts with different diameters to be grouped. In a broad sense, any normalized value of preload above 1.00 is acceptable since the result shows that the specified minimum preload has been exceeded. Of course, a preload of exactly 1.00 may not be very desirable, as will be discussed later.

In some cases it is useful to normalize a bolt preload with respect to the ultimate tensile strength of the bolt lot. This type of number is essentially an efficiency factor for the friction conditions on the bolt (lubricant, rust, thread damage, contamination) and calibration of the bolt (the annular groove diameter). Theoretically, in the best case a bolt preload would reach a value of 1.00 with respect to the tensile strength of its parent lot. This is unrealistic, however, and as will be seen later, most bolts reach a preload that is about 70% of its ultimate tensile strength.

Table 2 is a summary of the bolt preload results. There was considerable scatter within individual lots, but space does not permit inclusion of those data herein. Details are available in Undershute and Kulak (1994).

Table 2 Bolt Preloads for the Various Test Series

Item	As - Delivered	Stored Indoors		Exposed to Humidity		Full Exposure to the Weather		Weathered in a Steel Joint	
		2 Weeks	4 Weeks	2 Weeks	4 Weeks	2 Weeks	4 Weeks	2 Weeks	4 Weeks
Number Tested	81	79	105	79	105	76	105	93	124
Preload (kN)*	153	149	152	149	149	143	140	136	134
Standard Dev. (kN)*	14.6	23.1	14.9	18.9	17.5	14.5	14.3	17.9	17.1
Preload Specified Min. Preload	1.20	1.16	1.20	1.16	1.17	1.12	1.10	1.05	1.05
Standard Deviation	0.11	0.17	0.12	0.14	0.13	0.11	0.11	0.10	0.12
Preload Ult. Tens. Str. Direct Tens.	0.70	0.67	0.70	0.68	0.68	0.65	0.64	0.61	0.61

\* The values do not include Lot 9 since its diameter was different from all other lots.

## 5. SUMMARY AND CONCLUSIONS

### 5.1 Installation Characteristics and Delivered Preload

The preload that will be attained in a tension control bolt is controlled by the size of the twist-off groove, the conditions of lubrication, and the bolt material strength. The test program reported herein used bolts as supplied by the manufacturers. As such, the dimensions of the twist-off groove, the quality and location of the lubrication, and the strength of the bolt were already established. The preloads measured reflect the conditions of lubrication and different conditions of storage of the bolts. In the reports of preload that follow, the figures reported are average values for all lots. Examination of the specific data will show that there can be significant variations between lots (Undershute and Kulak, 1994).

## 5.2 Preload: As-Delivered Bolts

The average normalized preload for all the bolts tested as-delivered in this test program was 1.20, standard deviation 0.11.

The age of the various bolt lots upon receipt was not constant. Ideally, it would have been desirable to have all lots of bolts lubricated by the manufacturer and then immediately shipped to the laboratory. Examination of the data from individual lots shows, however, that the bolt age, *per se*, may not necessarily be important. For example, Lot 13, which was only one-half a month old upon receipt, reached 70% of its average ultimate tensile strength, whereas Lot 1, which was about 30.5 months old, attained 75% of its average ultimate tensile strength. It appears that lubricant quality and durability are more important than the age of the bolts.

The average normalized preload for the individual lots ranged from 1.05 to 1.31. Of the ten lots tested as-delivered (Lots 6, 7, and 8 were not tested in this condition), five attained a preload ratio greater than 1.20 and four reached values of between 1.12 and 1.17. Lot 9 reached a preload ratio of only 1.05. This range of values between bolt lots can be attributed to two factors: lubrication and, to a lesser extent, bolt strength.

Bolt strength can also affect bolt preload. Lot 2 attained an as-delivered preload of 1.17, corresponding to 77% of its ultimate strength. Lot 1 reached a much higher preload of 1.31, and this corresponds to 75% of its strength, which is nearly the same as the value for Lot 2. This reflects the fact that Lot 2 had a ratio of ultimate tensile strength to specified ultimate tensile strength of 1.06, while for Lot 1 this ratio was 1.23.

## 5.3 Preload: Indoor Storage

This study showed that indoor storage in a sealed metal keg for up to four weeks does not cause any significant decrease in bolt preload. The average normalized preloads for the as-delivered, two-week, and four-week indoor storage periods were 1.20, 1.16 and 1.20, respectively. These lie between the reported values of preload for the turn-of-nut and calibrated wrench methods (Kulak et al., 1987).

Long term indoor storage in an unsealed keg may be deleterious. For example, Lot 10, which was 2.5 months old upon receipt, had normalized preload values of 1.27, 1.34, and 1.31 in the as-delivered, two-week, and four-week indoor storage tests, respectively. After 32 weeks of indoor storage (in a metal keg with the lid loosely fitted), the normalized preload value dropped to 1.21.

## 5.4 Preload: Exposure to Humidity

Allowing bolts to be exposed to humidity for two and four weeks resulted in only slightly lower preloads than for the cases of as-delivered and the two and four-week indoor storage periods. The two and four-week average normalized preloads in a humid atmosphere (about 62% relative humidity) were 1.16 and 1.17, respectively (see Table 2). It can be anticipated that longer storage periods or higher humidity will lead to lower preloads.

### 5.5 Preload: Bolts With Full Exposure to the Weather

Subjecting individual bolts to full exposure to the weather had a measurable effect on the preloads attained, as seen in Table 2. The two and four-week average normalized preloads are 1.12 and 1.10, respectively. The bolts did rust, but less than might normally be expected for the periods of time involved. The amount of rust and lubricant degradation will affect the preload attained, of course, and the amount of degradation will depend on the local climate.

### 5.6 Preload: Simulated Joints

Tension control bolts in the simulated joints provided the lowest bolt preloads of all the different types of exposures. The two and four-week average normalized preloads were both 1.05. Obviously, these preloads are close to the specified minimum preload. The preloads are lower than those reported for calibrated wrench installations, and very much lower than those obtained by turn-of-nut installations (Kulak et al., 1987).

### 5.7 Slip-Critical Relationships and Slip Probability

In the case of a slip-critical joint, the probability of slip is a reflection of the slip coefficient of the connected material and the clamping force provided by the bolts. Both quantities have a dispersion about their mean value. Thus, the actual slip probability depends on the method used for bolt installation and on the condition of the faying surfaces in the joint.

The equation for the slip resistance of a joint given in the *Guide* (Kulak, et al., 1987) and the basis of design rules for North American specifications is:

$$P_s = m n \alpha T_{ispec} k_s \quad (1)$$

where  $P_s$  = slip load

$m$  = number of slip planes

$n$  = number of bolts

$\alpha = T_i/T_{ispec}$

$T_{ispec}$  = specified minimum preload

$k_s$  = slip coefficient of the connected material

The *Guide* provides information for a wide variety of cases: there are 54 combinations of slip coefficient, bolt grade, and slip probability level listed. It is impractical for design specifications to provide this much flexibility, however. In North American practice, for example, if the mean slip coefficient is 0.33 (clean mill scale) and A325 bolts are installed using the turn-of-nut method, then the design rules infer a slip probability level of 5%. For the same conditions except that a calibrated wrench installation is used, a 10% probability of slip is predicted. The rules reflect a desire for simplicity, and the difference in slip probability for these two cases is just an outcome of that philosophy.

The turn-of-nut method of installation produces normalized bolt preloads of 1.35 with respect to the specified minimum preload for A325 bolts installed to one-half turn in laboratory experiments. However, studies on real structures show that the actual preload in the field may be less. For example, Kulak and Birkemoe (1993) determined the ratio to be 1.27 for A325 bolts in bridges. The calibrated wrench method gives a normalized preload ratio of 1.13. For this case, only laboratory studies are available. It seems reasonable to expect that the preload attained by any installation method (e.g., tension control bolts, load-indicating washers) should attain preloads that are at least as high as those reported for the calibrated wrench installation. Otherwise, design specifications would have to make it clear that a greater probability of slip exists for these cases. Based on the study reported herein, the following comments can be made regarding the suitability of tension control bolts:

- **As-Delivered and Indoor Storage Bolts**

The tension control bolts tested in the as-delivered condition, after indoor storage in a sealed keg, and after exposure to ambient, indoor humidity had average non-dimensionalized preloads that were between the average values for the turn-of-nut and calibrated wrench method of installation. The lowest average value of measured preload to specified minimum preload in any of these categories was 1.16 (Table 2). It should be noted, however, that a few individual lots were much lower than this (Undershute and Kulak, 1994).

- **Bolts Exposed to Humidity**

The average preloads for the bolts exposed to humidity are only slightly less than those corresponding to the as-delivered and indoor storage cases. The lowest average preload measured was 1.16 with respect to the minimum specified preload (Table 2). However, detailed examination of the results (Undershute and Kulak, 1994) shows that humidity had a more pronounced effect on some lots: the preload ratios were as low as 1.03 in several cases. Overall, the preloads were slightly better than those provided by the calibrated wrench method in a laboratory environment, but much less than the preloads obtained from the laboratory turn-of-nut method results. The tension control bolt preloads can also be significantly less than turn-of-nut installations in the field (Kulak and Birkemoe, 1993).

- **Bolts Given Full Exposure to the Weather**

The tension control bolts that were given full exposure to the weather gave non-dimensionalized preloads significantly lower than those obtained by turn-of-nut and marginally lower than those delivered by the calibrated wrench method. After two and four weeks of exposure, the tension control bolts gave average preload to specified minimum preload ratios of 1.12 and 1.10, respectively (Table 2). As in all of these comparisons, the results for the individual lots should also be examined. Of the 23 lots in this category, five showed values of the preload ratio less than 1.0 and eleven lots were less than the figure 1.13 that pertains to calibrated wrench installations. However, field studies of bolts installed by calibrated wrench are not available, and the comparison with tension control bolts should be viewed in that light.

- **Bolts Weathered in a Simulated Steel Joint**

The tension control bolts that were weathered in the joints prior to final installation produced preloads that were much lower than those that would be obtained by the calibrated wrench

method and very much lower than those for the turn-of-nut method in a laboratory environment. After both two and four weeks of exposure, the average preload ratio was 1.05 (Table 2). Eight of the 23 lots tested had preload ratios that were less than 1.0, while another six reached preloads ranging between 1.00 and 1.05. In total, 16 lots gave preload ratios that were much less than the calibrated wrench method ratio of 1.13. Overall, the preloads seem to be much less than the preload of standard bolts installed in bridges using the turn-of-nut method (Kulak and Birkemoe, 1993).

Installation of tension control bolts in a way comparable to that used in the weathered joint tests, that is, installing bolts in a joint with a snug-tight load in the bolt and then later (two or four weeks) performing the final tightening, means that the majority of the tension control bolts will have a preload that is less than that for bolts installed by calibrated wrench. Furthermore, recalling that the average preloads for the two and four-week weathered joint tests were both 1.05, it is quite likely that a significant number of tension control bolts installed this way will have a clamping force that is even less than the specified minimum value. As previously noted, eight of the individual 23 lots in this category had values of this ratio less than 1.0.

## 5.8 Conclusions

Considering the results reported herein, the following conclusions are presented:

1. The as-delivered preloads of the tension control bolts fall between the preloads reported for laboratory studies of comparable A325 bolts installed by turn-of-nut and by calibrated wrench.
2. Thread and washer lubrication are important to the performance of tension control bolts. Torsional friction at the nut-washer interface accounts for as much as 90% of the total torsional friction. Thus, proper lubrication of the washer is a crucial factor for the attainment of preload.
3. Bolts stored indoors in a sealed metal keg for short periods (two and four weeks) produced preloads that are comparable to those for as-delivered bolts.
4. Depending on the age of a bolt at the start of a storage period, long-term indoor storage can have an effect on installed preload. Bolts stored in an unsealed keg attained lower preloads than those tested as-delivered.
5. Exposure to outdoor humidity for two and four weeks reduces the preload of a tension control bolt compared to its as-delivered preload. The preload after two or four weeks of exposure was comparable to that for standard bolts installed by the calibrated wrench method, although some individual lots were less than that value.
6. Bolts fully exposed to the weather for two or four weeks generally had preloads slightly less than those provided by the calibrated wrench method and significantly less than those produced by the turn-of-nut method.
7. Bolts exposed to the weather while snug-tight in a joint for two or four weeks and then installed suffered the most serious degradation in preload of all conditions tested. The average bolt preload after the exposure was only marginally greater than the specified minimum preload. The preloads measured here were less than those produced by the calibrated wrench method and

substantially less than those produced by the turn-of-nut method. Almost one-third of the bolt lots tested in this condition gave preloads that were less than the specified minimum value.

This test program has illustrated that the performance of a tension control bolt is strongly a reflection of the conditions of friction that exist on bolt threads and the washers supplied with the bolts. As the quality of the lubricant decreases, resulting in a higher coefficient of friction between the bolt and nut threads and at the nut-washer interface, the installed preload also decreases. Furthermore, as the effectiveness of the lubricant decreases, the preload attained after a given exposure type and length of time also decreases. Superimposed on this is the fact that the majority of frictional torque occurs at the nut-washer interface. If a proper amount of lubrication is not maintained on the washer (or the washer side of the nut face), clamping force will be less than otherwise. Since the preload attained is also dependent on the type of exposure, specific installation techniques may have to be dictated by specifications. Thus, proper manufacturing in combination with proper installation is required in order for this fastener system to perform satisfactorily.

## 6. REFERENCES

- Eurocode 3: Design of Steel Structures, European Committee for Standardisation, Brussels, 1993.
- Kulak, G. L., Fisher, J.W. & Struik, J.H.A., Guide to Design Criteria for Bolted and Riveted Joints, 2nd edn, Prentice-Hall, Englewood Cliffs, NJ, 1987.
- Kulak, G. L. & Birkemoe, P.C., Field Studies of Bolt Pretension, Journal of Constructional Steel Research, Vol. 25, Nos. 1 & 2, 1993
- Load and Resistance Factor Design Specification for Structural Joints Using ASTM A325 or A490 Bolts, Research Council on Structural Connections of the Engineering Foundation, June, 1988. (Available through the American Institute of Steel Construction, Chicago.)
- Standard Specification for Structural Bolts, Steel, Heat-Treated, 120/105 ksi Minimum Tensile Strength, ASTM A325-92a, American Society for Testing and Materials, Philadelphia, 1992.
- Undershute, S.T. & Kulak, G. L., Strength and Installation Characteristics of Tension-Control Bolts, Structural Engrg. Report No. 201, Dept. of Civil Engineering, University of Alberta, Edmonton, Canada, 1994

## ECONOMIC COMPARISONS BETWEEN SIMPLE AND PARTIAL-STRENGTH DESIGN OF BRACED STEEL FRAMES

David Anderson<sup>1</sup>

Mahmood Md Tahir<sup>2</sup>

### Abstract

Semi-continuous construction of braced frames is known to result in significant savings in frame weight. To be attractive to designers though, calculation methods need to be straightforward and savings are required in overall frame cost, not just weight. The paper describes the advantages of plastic design using partial-strength joints. This approach has been used in comparisons with simple design, resulting in average cost savings for planar frames of approximately 5.5%. Such savings are worthwhile in comparison with other opportunities available for reductions in the cost of fabricated steelwork.

### 1. INTRODUCTION

Steel frames for buildings have usually been designed on the basis that beam-to-column joints are either pinned or rigid. The actual stiffness though will often fall between these extremes, giving what is generally termed 'semi-rigid' behaviour. A joint may also have a moment resistance less than that of the connected beam; such behaviour is termed 'partial-strength'.

Frames which contain semi-rigid or partial-strength joints are termed 'semi-continuous' by Eurocode 3 (1992). This code has encouraged the use of this approach to design by including a method to predict both the rotational stiffness and moment resistance of some types of joint. Some national codes, for example BS 5950 (1990), also permit semi-continuous design but the British Standard fails to provide a method to predict the joints' properties.

End plates provide a common form of connection (Fig. 1). For semi-continuous unbraced frames they can be used without the stiffening associated with rigid design. It is widely accepted that this leads to total cost savings on a plane frame of the order of 20% (Bjorhovde and Colson, 1992; Anderson et al, 1993; Girardier, 1994). However, if it is possible to brace the frame against sidesway, designers will usually avoid unbraced construction.

- 
1. Reader, Department of Engineering, University of Warwick, UK
  2. Postgraduate Student, Department of Engineering, University of Warwick, UK

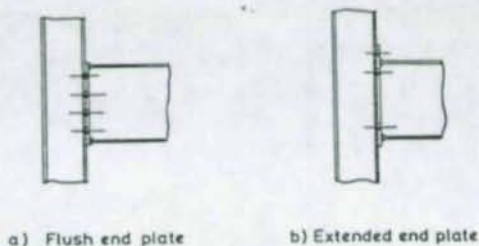


Fig.1. End plate connections

For braced frames the potential advantages of a semi-continuous approach compared to traditional "simple" construction are reductions in beam depth and an overall reduction in frame cost. These reductions vary from frame to frame though, partly due to the limited range of rolled sections.

The reductions in beam depth may be up to around 75mm. However, where a significant number of sections of different mass have the same nominal serial size, it is possible to find that no significant reduction in depth occurs. In such circumstances though an appreciable saving in beam weight would be expected.

This paper reports the first phase of a study being carried out to evaluate the likely reductions in cost for a range of planar frames within braced multi-storey buildings. By examining a range of structures, it is hoped to give designers better overall information on savings than are possible with more limited studies.

## 2. PLASTIC DESIGN OF SEMI-CONTINUOUS BRACED FRAMES

For ultimate limit states, plastic design provides an attractive approach, particularly if linked with partial-strength joints providing a moment resistance 30-50% of that of the connected beam. As will be shown, such resistance still provides worthwhile reductions in beam weight and overall frame cost. The advantages of this approach are:

- (i) The moment resistance required at the connection is readily determined from a beam-type plastic hinge mechanism (Fig. 2).

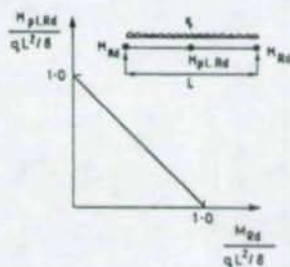


Fig.2. Plastic analysis of beam with partial-strength connections.

- (ii) Ductility can be provided through use of relatively thin end plates (12-15mm) in mild steel, in conjunction with appropriately strong bolts and welds (Bose and Hughes, 1995).
- (iii) For typical relative values of dead and live loading, pattern loading need not be considered because each joint will attain its design resistance  $M_{Rd}$  under the factored dead load (Fig. 3).

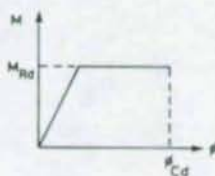


Fig. 3. Bi-linear  $M-\phi$  characteristic.

- (iv) Joint resistance will usually be independent of column size, thereby assisting the preparation of concise design tables for standard connections and permitting beam design to be completed before the columns are considered.
- (v) Although the beam's compression flange is unrestrained adjacent to the supports, the limited joint resistance will reduce the likelihood that lateral buckling will occur.

### 3. DESIGN RECOMMENDATIONS

The studies so far have been concerned with costs associated with fabrication in the UK, and use has therefore been made of British design rules (BS 5950, 1990) and resistance tables for joints (Steel Construction Institute, 1995). The latter are based on Eurocode 3's design model but with strength checks modified to suit BS 5950.

Two aspects of British practice favour semi-continuous design:

- (a) In "simple" design, beam end reactions are assumed to act at an eccentricity of 100mm from the face of the column (Fig. 4), to account very approximately for the observed semi-rigid nature of nominally-pinned joints. So unbalanced beam loading causes bending moment in columns, although the beams themselves are still designed as simply-supported. The eccentricity moment to some extent offsets the moments induced in columns with semi-continuous construction.

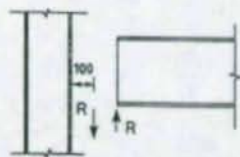


Fig. 4. Eccentricity moment

- (b) The deflection limits in BS 5950 apply under imposed load only. Consequently, serviceability calculations for semi-continuous design can be simplified, often by retaining the assumption of pinned joints, without sacrificing economy. Calculations of joint stiffness will not normally be necessary.

Another aspect of current British practice works against semi-continuous design, though. This concerns the type of connection used in "simple" design.

Flush end plates have been used extensively in the past as nominally-pinned joints, sometimes with designers specifying relatively thick plates. It is well-known that such joints possess significant strength and stiffness. On this basis, semi-continuous design can use these inherent characteristics to obtain "something for nothing". However recent guidance (Steel Construction Institute, 1991) has encouraged the use of partial-depth end plates with web welds only (Fig. 5). With such connections used for "simple" construction, it becomes more difficult to realise significant savings from semi-continuous design, whose connections are expected to be made with full-profile welds. The studies do still show worthwhile savings in cost, but these will be greater for those fabricators who continue to prefer full-depth end plates in simple joints.

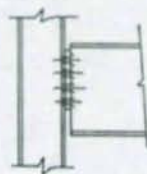


Fig. 5. Partial-depth end plate

## 4. THE STUDIES

### 4.1 Scope

A series of two bay and four-bay braced frames, of two, four, six and eight storeys, has been used to compare the two design approaches. The structure was assumed to comprise a series of plane frames at 6m centres. Floors and roof were assumed to span this distance between the plane frames, and therefore the longitudinal beams were designed only to tie the frames together and to provide lateral restraint to the columns at each floor level. Figure 6 shows a general arrangement for a typical plane frame of two bays, within a two-storey structure. Figs. 5 and 1(a) show typical arrangements for the two contrasting types of connection, namely a partial-depth flexible end plate for "simple" construction, and a full-depth end plate for the semi-continuous approach. Bolts were taken as M20 Grade 8.8. S275 steel was chosen for all end plates and the connected members. Typical plate thicknesses used for partial-depth flexible end plates were 8mm or 10mm thick. In order to achieve economy in the semi-continuous design, the columns were unstiffened at the joints, the forces transmitted to the columns being limited by the partial-strength nature of the connections. Beams spans were varied from 6m to 9m. The column height per storey was fixed at 5m for the bottom storey and 4m for each storey above. Dead load was based on precast concrete floor units with

finishes, giving a total characteristic dead load of  $4.0 \text{ kN/m}^2$ . Imposed load for the roof was  $1.5 \text{ kN/m}^2$  and for the floors  $4.0 \text{ kN/m}^2$ . Load due to cladding was taken as  $50 \text{ kN}$  applied to each external column at each storey. Reduction in live load was made when a column supported more than one level, in accordance with BS 6399 (1985).

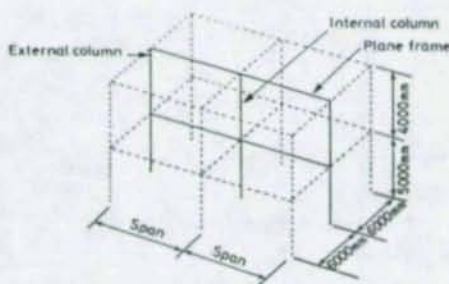


Fig 6. Typical frame layout.

#### 4.2 Simple Construction

This followed usual practice according to BS 5950. Hence, although the connections were designed for shear only, external columns were designed for a nominal moment due to an assumed eccentricity in the application of beam end reactions. This was taken as  $100 \text{ mm}$  from the face of the column. The effective length factor for the columns about the minor axis was taken as  $0.85$ .

#### 4.3 Design of the Beams in Semi-continuous Construction

These members were designed for a local plastic hinge mechanism, taking into account the design moment resistance of the joints. Beams were assumed to be laterally-restrained by the floor or roof units. Unlike conventional simple design, where the effective beam span is taken between centres of columns, in the semi-continuous design the beam was taken to span between column flanges. This was because accurate account was taken of the moment developed at the face of the column in the partial-strength connection. Beam sizes were selected from the list of Universal Beams in order to provide adequate resistance and stiffness for minimum depth.

#### 4.4 Design of the Columns in Semi-continuous Construction

For design of the columns the effective length factor about the minor axis was taken as  $0.85$  as for simple design. The moment applied to a column was taken as the moment resistance of the connection plus the additional eccentric moment arising from the presence of the joint at the face of the column. The latter moment was therefore determined using an eccentricity of half the depth of the column section. The external column thereby carried axial load and end moment whereas the internal columns carried only axial load. All column members were Universal Columns.

## 5. ANALYSIS OF RESULTS

In comparing the two forms of construction, the moment-resistance of the flush end plate connections meant that beams with partial-strength connections were of smaller depth. However, in this study there was no increase in weight of external columns because the beam end moment was limited by the connections. The internal columns were also not affected by moments being transferred from the beams because pattern loading did not result in unbalanced moments at ultimate limit state. Percentage weight savings and cost savings are shown in Fig. 7. The overall steel weight saving against "simple" construction ranged from 5% to 9%. The cost savings were determined by a UK fabricator. An overall cost saving for the fabricated plane frame delivered and erected within a 100 miles radius of the shops averaged about 5.5% against "simple" construction.

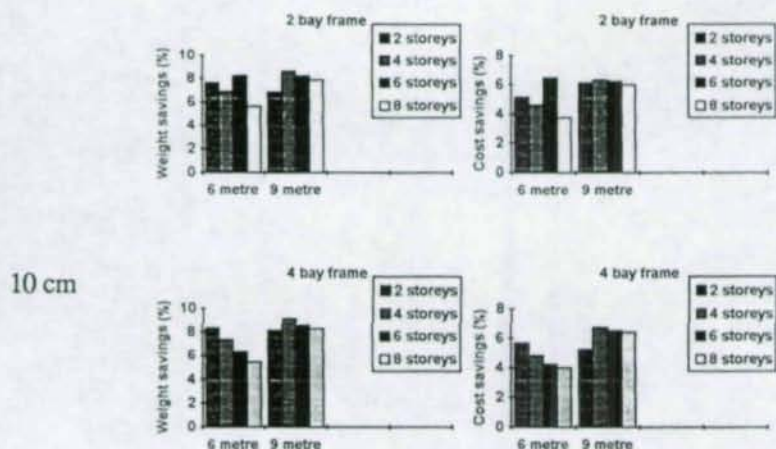


Fig. 7 : Percentage weight and cost savings

For the frames with 6m beam span, a reduction in the depth of the floor beam of 14% was achieved, although the percentage reduction of the total floor depth would be significantly less. For a 9m span, semi-continuous design resulted in a floor beam from the same serial size as for "simple" construction (both were from the 533 UB range), but the beam mass was reduced by 16%.

## 6. CONCLUSIONS

The benefits of semi-continuous construction are difficult to quantify because they depend upon what practice is followed in "simple" construction, and on the range of available sections.

Partial-depth end plates with only web welds provide a very economical form of connection for "simple" design. Even so, studies have shown an average overall cost saving for a planar frame of 5.5%. This was achieved using plastic design methods in conjunction with published

resistance tables for standard connections. With experience, design calculations therefore take little longer than those for "simple" design.

The flush end plate connections used for the semi-continuous designs were of limited moment resistance, with the result that the same column sections could be used for the two design approaches. Further studies are in progress to examine the economy of other design strategies. These include the use of extended end plate joints of greater resistance, the selection of the beam sections with the lowest mass/resistance characteristics (rather than sections of minimum depth), and the use of S 355 members.

## 7. ACKNOWLEDGEMENTS

The authors thank A. Hughes (Ove Arup and Partners) and N.D. Brown (University of Warwick) for providing tables of resistances for connections and M. Fewster (Caunton Engineering Ltd.) for costings.

## 8. REFERENCES

1. Anderson D., Colson A. and Jaspart J.-P., Connections and frame design for economy. *New Steel Construction*, 1 (1993) No. 6, 30-33.
2. Bjorhovde R. and Colson A., Economy of semi-rigid frame design. In *Connections in Steel Structures II : Behaviour, Strength and Design*. ed. Bjorhovde R., Haaijer G. and Stark J.W.B., American Institute of Steel Construction, Chicago (1992), 418-430.
3. Bose B. and Hughes A., Verifying the performance of standard ductile connections for semi-continuous steel frames. *Proc. ICE*, London (submitted for publication).
4. BS 5950, *Structural Use of Steelwork in Building Part 1. Code of Practice for Design in Simple and Continuous Construction : Hot-rolled Sections*. British Standards Institution, London. (1990).
5. BS 6399 *Design Loading for Buildings Part 1. Code of Practice for Dead and Imposed Loads*. British Standards Institution, London (1985).
6. ENV 1993-1-1 *Eurocode 3 : Design of Steel Structures Part 1.1 : General Rules and Rules for Buildings*. CEN, Brussels (1992).
7. Girardier, V., Cost reductions - semi-rigid construction put into perspective. *New Steel Construction*, 2 (1994), No. 2, 38-39.
8. *Joints in Simple Construction*, 1991. Steel Construction Institute, Ascot (1991).
9. *Joints in Steel Construction : Moment Connections*, Steel Construction Institute, Ascot (to be published 1995).

## A REVIEW OF CONNECTION RESEARCH AND DEVELOPMENT IN THE UK

D B Moore<sup>1</sup>

### ABSTRACT

The development of design methods for steelwork connections in the UK is described with the emphasis placed on the background research undertaken to validate and/or develop these methods. Research on the validation of the design rules for simple connections including work on fin plates and robustness is described in detail. A new procedure for the design of moment connections is introduced. This procedure is based on a combination of the rules given in BS5950:Part 1 and those given in EC3. Some of the main differences between this new approach and both EC3 and the UK's traditional method are identified and discussed.

It is concluded that both publications given recommendations that produce economic connections and give realistic estimates of strength.

### 1.0 INTRODUCTION

The cost of fabricating a typical steel structure is approximately two-thirds of the total cost of the complete steel frame. One might also expect the distribution of design effort to be weighted towards components such as the connections but all too often the design of the connections is neglected. Current UK Codes of Practice do little to redress this undesirable situation as many of them give little guidance on connection design. In many cases the engineer is not involved in the design and detailing process which is frequently left for the fabricator to complete.

Most connections have to be made and assembled by conventional fabrication and erection techniques. Therefore to reduce costs a connection should be as uncomplicated as possible to fabricate and erect and still satisfy the appropriate performance criteria.

In 1987 the Steel Construction Institute (SCI) and the British Constructional Steelwork Association (BCSA) set up the joint SCI/BCSA connection group. This group comprised

---

<sup>1</sup> Head of Metal Structures, Building Research Establishment, UK

engineers from all sections of the steel construction industry and was set up to achieve the following objectives:-

"The definition of a range of connection types whose behaviour and area of application will be clearly understood

The development and publication of standard methods for designing each of these connections

The laying of a framework which will lead to the widespread adoption of rationalized connections using standardized components"

During the past eight years this group has been very successful and has produced the following publications:-

Joints in Simple Construction  
Volume 1 : Design Methods<sup>(3)</sup>

Joints in Simple Construction  
Volume 2 : Practical Applications<sup>(4)</sup>

The first of these publications was revised in 1993. This revision included changes to the design procedures for both block shear and local notch stability. In the case of block shear the existing method was replaced by the method in Eurocode 3. Two changes were made to the procedure for checking local notch stability. The first change was an improvement in the method for checking the local stability of single notched sections and the second change was the inclusion of a new procedure for checking the local stability of double notched sections. Both of these improvements were based on the work of Cheng<sup>(5)</sup>.

The group is also preparing a single book on moment connections<sup>(6)</sup> which incorporates both design methods and practical applications.

## 2.0 CONNECTION PUBLICATIONS

All of the above documents can be used for both manual and computer-aided design and detailing. Although a number of computer detailing systems were in existence prior to the publication of these documents they employed different approaches. Therefore one of the aims of the publications was to present standard design methods for most commonly used connections.

The design methods in each publication are based on a combination of the latest design theories and practical aspects associated with current fabrication and erection techniques and produce realistic estimates of a connections strength.

None of the publications give the background information on which the design methods are based. Each provides design guidance in the form of an easy to use step-by-step check list

for a set of standard and commonly used connections. These design checks are supplemented by detailed examples for each connection type.

## 2.1 Joints in Simple Construction

All the technical work in the publications on joints in simple construction are based on the British Standard BS5950:Part 1:1990<sup>(7)</sup>. However, the design methods can be used with the ENV version of Eurocode 3<sup>(8)</sup> provided certain changes are made.

This set of publications gives design guidance for web angle cleats, flexible end-plates and fin-plate beam-to-column or beam-to-beam connections, bolted column splices and column bases. Figure 1 gives details of each of these connection types. The number of different connection types was deliberately limited to the most commonly used connections to encourage both designers and fabricators to use one of the preferred types, to increase standardization and improve economy.

### 2.1.1 Web Angle Cleat and End-plate Connections

Web angle cleats are a popular form of connection because they have the facility to provide for minor site adjustments when using untorqued bolts in 2 mm clearance holes.

The flexible end-plate connection consists of a single plate fillet welded to the end of the beam and site bolted to either a supporting column or beam. This connection is relatively inexpensive but has the disadvantage that there is no room for site adjustment. Overall beam lengths need to be fabricated within tight limits although packs can be used to compensate for fabrication and erection tolerances. The end-plate is often detailed to extend to the full depth of the beam but there is no need to weld the end-plate to the flanges of the beam. Sometimes the end-plate is welded to improve the stability of the frame during erection and avoid the need for temporary bracing. This type of connection derives its flexibility from the use of relatively thin end-plates combined with large bolt cross-centres. An 8 mm thick end-plate combined with 90 mm cross-centres is usually used for beams up to 457 x 191 UB's. For UB's of 533 x 210 and over a 10 mm thick end-plate combined with 140 mm cross-centres is recommended.

### 2.1.2 Fin-plate Connections

A more recent development which follows both Australian and American practice has been the introduction of the fin-plate connection. These connections are primarily used to transfer beam end reactions and are economical to fabricate and simple to erect. There is clearance between the ends of the supported beam and the supporting beam or column, thus ensuring an easy fit.

Figure 1 shows a typical bolted fin-plate connection. This connection comprises a single plate with either pre-punched or pre-drilled holes, that is shop welded to the supporting beam or column.

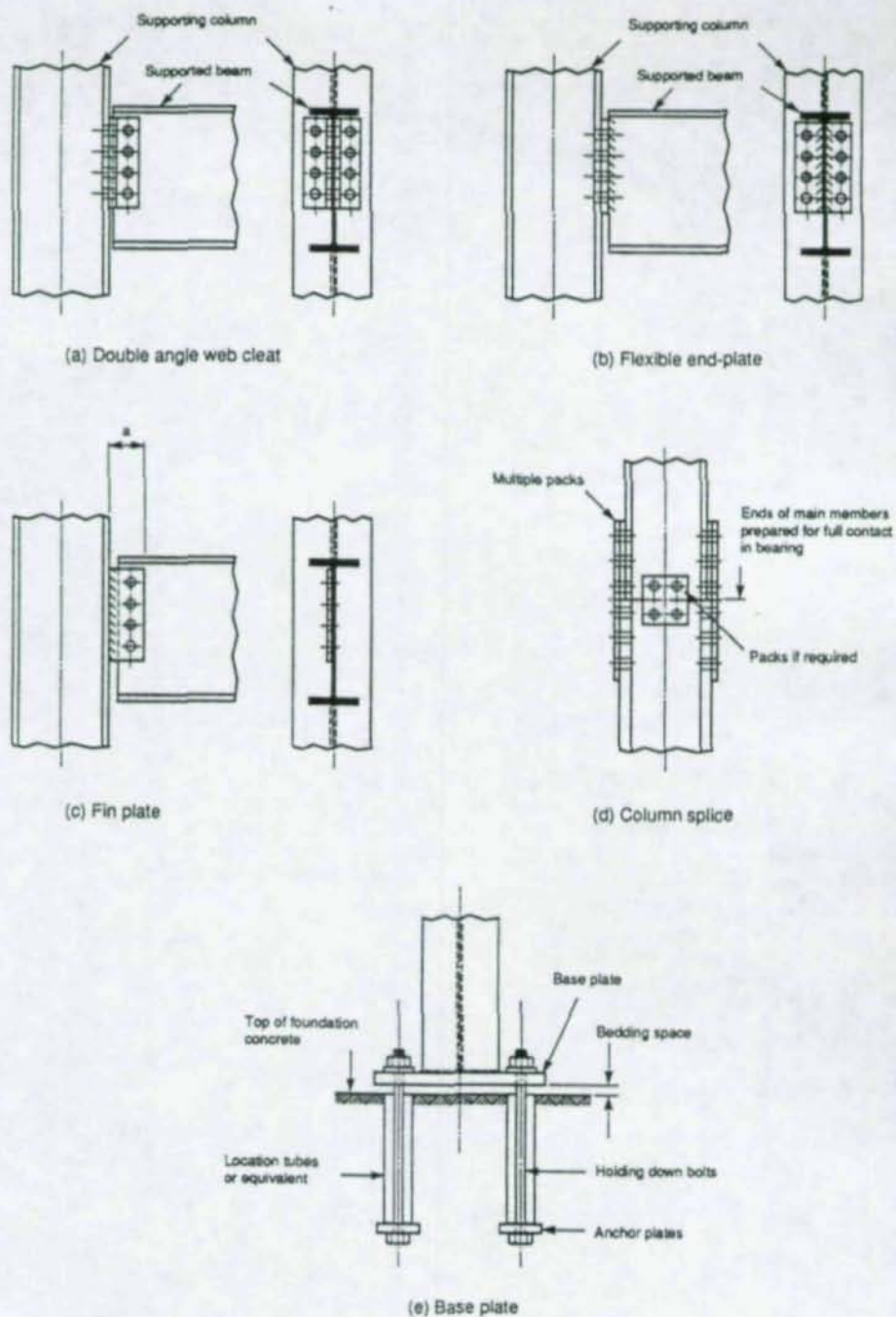


Figure 1 Simple connections

Before developing a design method for fin plates an extensive literature survey was carried out to identify practice in other countries. The most appropriate and best research design method was found to be that developed by AISC<sup>(9)</sup>. This was adopted as the starting point for the UK approach. The principal difference between the AISC method and that adopted in the UK concerns the line of action for the shear. Many researchers have invested considerable effort in trying to identify an appropriate line of action for the shear. This has necessitated classification of the support to the fin plate into flexible or stiff categories, with different design models for each category. This was considered to be unacceptable as it required a subjective judgement by the designer which may bring him into dispute with the checking authority. The solution was to require that all critical sections be checked for a minimum moment taken as the product of the vertical shear and the distance between the face of the column and the centre of the bolt group. The section was then checked for the resulting moment combined with the vertical shear.

The validation of this and other design assumptions were checked against a series of tests on fin plates undertaken by the UK's Building Research Establishment. A series of inverted 'H' frames with different fin-plate connections were tested. The results from these tests showed that the design method was conservative and gave adequate predictions of strength with safety margins varying between 1.57 and 3.57<sup>(10)</sup>. The tests also showed that long fin plates had a tendency to twist and suffer lateral torsional buckling. A check on this buckling mode was therefore introduced into the design procedure.

This check was based on theoretical work by Owens<sup>(11)</sup> who suggested the following limitation on the length of fin plates:-

$$t = \leq 0.15a$$

where

- t is the thickness of the fin plate
- a is the distance between the weld line and the centre of the bolt group

Fin plates which satisfy this limitation should be designed as short beams and checked for lateral-torsional buckling. In the absence of a detailed study into this mode of failure the following rationalized approach was recommended.

When checking a beam for lateral torsional buckling the following two parameters need careful consideration:-

- The effective length of the fin plate
- The shape of the bending moment diagram

At its connection to the column the fin plate is rigidly welded in position and it is reasonable to assume that this connection is capable of preventing both lateral deflection and twisting. The connection between the fin plate and the supported beam is more problematic. Most practical connections in which restraint is applied to the web of the beam only are capable

of preventing lateral deflections provided the connection is at least 0.6 times the depth of the beam<sup>(2)</sup>. Studies<sup>(12)</sup> on the amount of torsional restraint needed to assume that twisting at the end of the beam is prevented, suggest a figure of approximately twenty times the torsional stiffness of the supported beam. It is likely that fin plates would not normally satisfy this requirement. The design rules<sup>(3)</sup> therefore recommend that the beam is laterally restrained at its top flange immediately above the connection to the fin plate. This situation will normally be found to exist in the majority of floor constructions. In such cases the restraint against lateral deflections of the compression edge of the fin plate is provided by the bending stiffness of the beam web. However, for deep fin plates this may be inadequate to prevent buckling of the fin plate and cross-sectional distortion of the beam.

Provided the above recommendations are satisfied the fin plate is assumed to have an effective length equal to the distance between the weld line and the centre of the bolt group. That is:-

$$L_e = 1.0a$$

where

a is the distance between the weld line and the centre of the bolt group

The distribution of moment in the fin plate is difficult to predict with any degree of accuracy. A conservative approach is to assume uniform bending. However, tests<sup>(10)</sup> indicate that a linear varying distribution is more common. A triangular distribution of moment is therefore recommended as a reasonable compromise between safety and economy.

Adopting the above recommendations the lateral-torsional buckling resistance of a long fin plate can be calculated as follows:-

$$M_b = S_x P_b$$

where

$M_b$  is the lateral-torsional buckling resistance of a long fin plate  
 $S_x$  is the plastic modulus of the fin plate about its major axis

$$= \frac{t\ell^2}{4}$$

$P_b$  is the bending strength of the fin plate obtained from BS5950:Part 1, Table 12 and based on  $\lambda_{LT}$

$$\lambda_{LT} = n \times 2.8 \times \left[ \frac{L_e \ell}{t^2} \right]^{1/2}$$

n is the slenderness ratio correction factor which depends on the distribution of the bending moment. (Take as 0.77)

$$L_e = 1.0a$$

The lateral-torsional buckling of long fin plates has been the subject of a recent investigation by Dr Peebles of Dundee University<sup>(13)</sup>. The main aim of this study was to develop design rules for long fin-plate connections to either the minor axis of universal columns or beams without the need for notching. Tests were carried out on thirteen different fin-plate configurations using a propped cantilever arrangement.

A comparison of the experimental results with the design procedure given in the publication 'Joints in Simple Construction' showed that in every case where the fin plate was tested to either failure or the capacity of the laboratory floor the capacity of the fin plate exceeded the predicted failure load. Furthermore, none of the fin plates exhibited lateral-torsional buckling, even though all the fin plates had  $t/a$  ratios significantly smaller than the limiting value of 0.15. Peebles suggests two reasons for the difference in behaviour. Firstly the triangular moment distribution assumed in the design of the fin plate does not occur in practice and secondly the method of evaluating  $\lambda_{LT}$  assumes an effective length equal to the length of the fin plate between the centre of the bolt group and the weld line, which neglects the more complicated interactive buckling effects between the beam and the fin plate. Peebles concludes by suggesting that a better understanding of the buckling behaviour of long fin plates can be obtained by adopting an analysis which considers the interactive behaviour of the combined fin plate and supported beam.

The recommendations for fin plates given in the publication 'Joints in Simple Construction' are limited to connections to beams less than 610 mm deep. This is because it was thought that the deformations available from bearing failure of either the fin plate or beam web would give insufficient rotational capacity for beams larger than 610 mm deep. This limitation has also been the subject of a recent experimental investigation carried out by the UK's Building Research Establishment<sup>(14,15)</sup>. A series of six connection tests were carried out on fin plates connected to 914 mm deep beams. Each specimen consisted of two 914 x 305 x 224 Universal beams connected by a fin plates to the flanges of a 305 x 305 x 118 Universal column. A cruciform test arrangement was used to test each specimen. With this arrangement the applied loads and beam reactions were designed to vary the ratio of connection bending moment and shear to simulate a practical range of beam lengths and load configurations.

The results from the first four tests showed that the standard connection details given in the design guide<sup>(3)</sup> produced a connection with insufficient ductility to develop the full plastic collapse mechanism for many practical beam span to depth ratios. This is because the standard details have a 10 mm gap between the end of the beam and the column flange which limits the rotation capacity of the connection to approximately 0.02 rads. Once this gap is closed significant moments are developed in the connection. To overcome this problem the following modifications were made to the last two tests:-

- The gap between the column flange and beam was changed from 10 mm to 20 mm
- To eliminate bolt slip the bolts were not torqued up.

These tests had rotations up to 0.04 rads. However, Jarrett<sup>(15)</sup> points out that even with a large gap between the beam and column the moment in the connection can be significantly larger than the design moment  $Q_a$ . Jarrett goes on to say that because the existing guidelines are based on a conservative rule for the calculation of bearing failure in either the fin plate or beam web the existing procedure can still be used despite the higher than assumed connection moment.

### 2.1.3 Robustness of Simple Connections

In preparing the design rules for simple connections it was found that there was insufficient experimental evidence to develop sound design rules for simple beam-to-column connections subject to the tying forces recommended in BS5950:Part 1<sup>(7)</sup>.

A series of tests was therefore conducted by the Building Research Establishment in collaboration with the Steel Construction Institute<sup>(16)</sup>. The aim of this study was to investigate the robustness of simple connections and their ability to resist tying forces. The programme was devised to cover a representative range of practical buildings. The smallest test specimens were chosen as the lightest connection that would occur in practice and the largest are representative of medium-scale construction. The test programme comprised 11 tests on double web cleat beam-to-column connections and 10 tests on flexible end-plate connections.

Each specimen was tested in an inverted Tee arrangement to simulate the behaviour of a connection subject to accidental axial load and to allow the results to be compared directly with the recommendations for robustness given in BS5950:Part 1<sup>(7)</sup>.

The results of all the eleven tests on web cleat connections showed four different modes of failure :-

- bolt pulling through the web cleat
- bearing failure of the web cleat
- bearing failure of the beam web
- fracture of the web clear close to heel.

All of these connections had a failure load significantly greater than the 75 kN minimum tying force recommended in BS5950:Part 1 and had maximum axial displacements in excess of 30 mm.

The results of the ten end-plate tests showed two different modes of failure :-

- bearing failure of the end plate
- fracture of the end plate close to the toe of the weld.

The first mode of failure was observed in two of the single bolt pair specimens. All the multi bolt pair specimens failed by fracture of the end plates at the weld toe. Deformation of this mode of failure varied considerably.

In concert with this experimental work Owens<sup>(16)</sup> developed analytical procedures for calculating the tying resistance of both double web angle cleat connections and end-plate connections. Both procedures were based on a large displacement analysis and allowed for the changes in geometry observed in tests, membrane effects and the combined action of shear, tension and moment on the components of each connection.

The solution for the double web cleat produced a pair of simultaneous equations. However, because of certain approximations these equations cannot be satisfied simultaneously and an iterative approach must be used. Owens recognised the limits of this method and developed a safe and simple to use procedure for use in the design office. This approach recognises that in the limit the cleats would be pulled straight and all the tying force would be carried in membrane action. The tying force is, therefore, based on the net section of the cleats in tension. A comparison of this method with experimental results shows the method to be conservative with safety margins between 1.04 and 1.95.

The method for end-plate connections was based on the formation of plastic hinges in the end plate. This approach is considerably simpler than the iterative method developed for the double angle web cleat and has been adopted directly for design. Comparisons with experimental results show the method to be conservative with safety margins varying between 1.42 and 3.16.

From observations made on these tests and the analytical work, Owens and Moore<sup>(16)</sup> concluded that the minimum tying resistance required by BS5950:Part 1 can be achieved by all practical connections comprising double web cleats or end plates provided they satisfied the following simple rules:-

- The bolt cross-centres do not exceed 140 mm
- The connecting element thickness is not less than 8 mm
- At least two M20 grade 8.8 bolts are used to resist the tension.

## 2.2 Moment Connections

The publication for moment connections<sup>(6)</sup> gives three approaches for designing connections. These are:-

- "A rigorous and comprehensive method which should be used primarily as a reference and for the development of computer software
- A set of capacity tables based on the rigorous approach which can be used to determine the capacity for a standardised range of full-strength and partial-strength connections

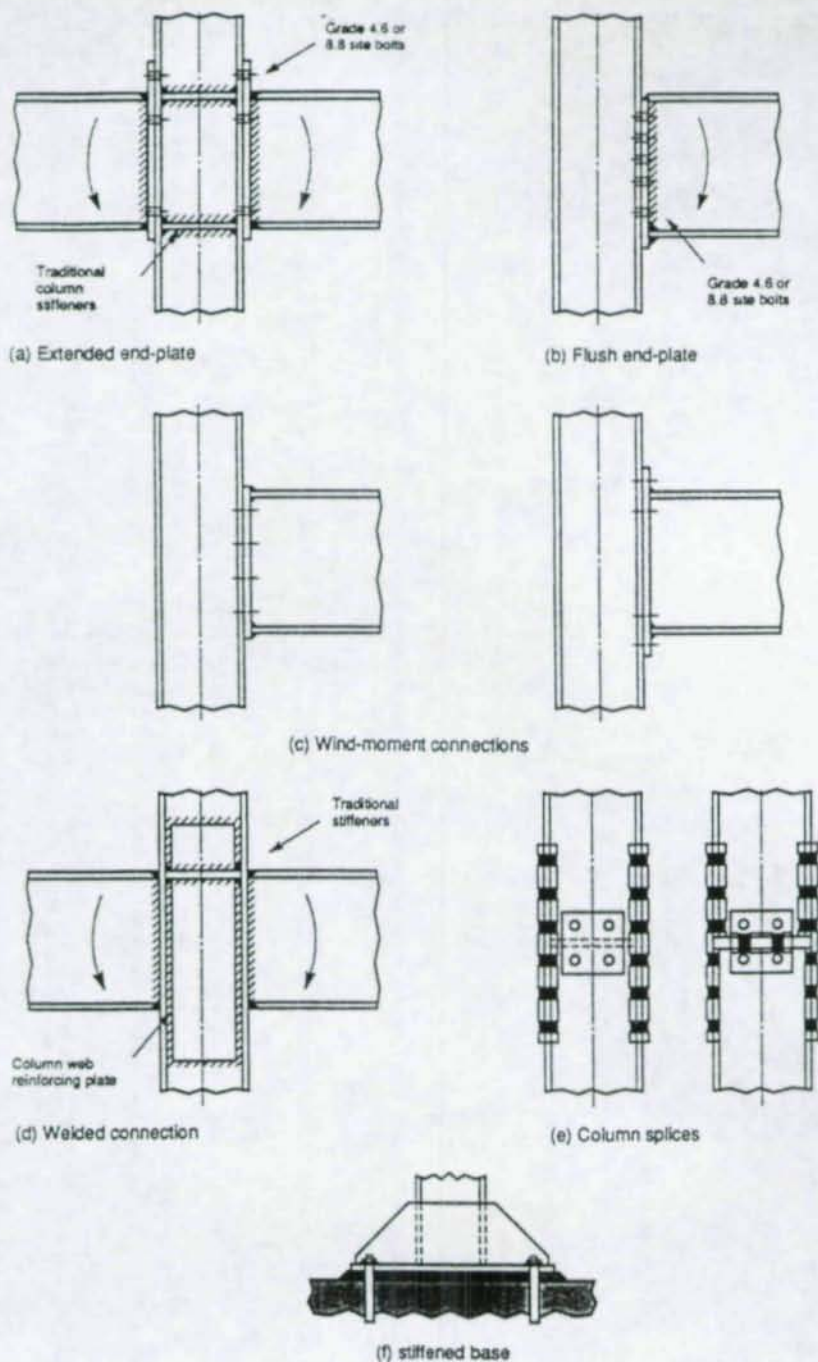


Figure 2 Moment connections

- An abridged method which is a simplified version of the more rigorous method and can be used to determine the capacity of a connection by hand calculation."

This publication gives guidance for bolted end-plate connections (both extended and flush end plates), wind moment connections, welded beam-to-column connections, bolt beam-to-column splices and column base connections. Figure 2 gives details of each of these types of moment connection.

The technical guidance on end-plate connections is based on a combination of the rules given in BS5950:Part 1<sup>(7)</sup> and those given in ENV Eurocode 3:Part 1.1<sup>(8)</sup>. The capacity checks for bolts, welds and sections are all based on BS5950:Part 1. However, the checks for calculating the capacity of either the end plate or column flange in the tension region of a bolted end-plate connection are based on the design model given in Annex J of ENV Eurocode 3:Part 1.1. Unlike the linear bolt force distribution used in traditional UK practice this method adopts a plastic distribution of bolt force. These two approaches are illustrated in Figure 3. In the traditional UK approach the centre of compression is assumed to be in line with the compression flange of the beam and a linear distribution of bolt force is also assumed, with the bolt row furthest from the centre of compression attracting the most tension. One disadvantage of this method is that to achieve the assumed bolt force distribution the designer often has to stiffen the column flange. In the Eurocode 3 approach no assumption is made about the distribution of bolt forces. Instead, each bolt row is allowed to attain its full design strength (on the basis of the strength of the column flange or end plate, whichever is the lowest). This model relies on adequate ductility of the connecting part in the uppermost bolt rows to develop the design strength in the lower bolt rows. To ensure adequate ductility an upper limit is set on the thickness of the column flange or end plate relative to the strength of the bolt. Where S275 steel is used with grade 8.8 bolts the maximum thickness of either end plate or column flange should not exceed 18.3 mm, 21.9 mm and 27.5 mm for M20, M24 and M30 bolts respectively. If this criterion is not satisfied then the force in the lower bolt rows is limited to a value resulting from the linear distribution shown in Figure 3.

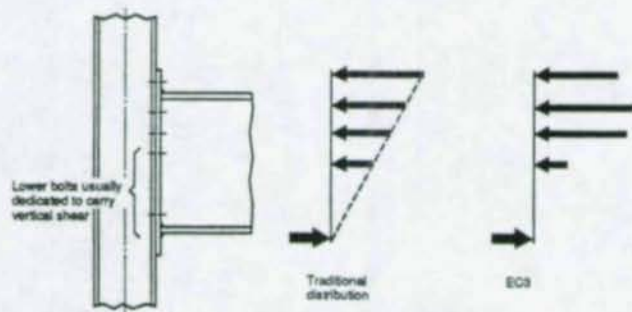


Figure 3 Distribution of bolt forces

A major difference between the guidance given in the publication on moment connections and Eurocode 3 is the way in which connections are classified as rigid.

Annex J of ENV Eurocode 3:Part 1.1 includes a procedure for classifying connections as either pinned, semi-rigid or rigid. The limits set by the Eurocode vary depending on whether the structure is braced or unbraced. This procedure is further complicated by the need to determine the stiffness of the connection before it can be classified, and although Annex J sets out a procedure for calculating the stiffness of end-plate connections the method is complicated and difficult to use. Furthermore, this method has been shown to give inaccurate results<sup>(17)</sup> and an improved version of Annex J is expected in 1995. For these reasons the publication on moment connections takes a more pragmatic approach and gives the designer simple rule-of-thumb guidelines which in most cases do not invalidate the assumptions used in the design of the frame. An example of one of these rules is 'Well proportioned connections designed for strength alone may be assumed to be rigid'. It is difficult to prove that this type of 'semi-intuitive' rule will produce satisfactory connections for all situations. However, test evidence has shown that connections which designers traditionally assume to behave as either pinned or rigid perform satisfactorily. The main reason for this is probably due to a combination of the inherent tolerance that steel structures have to large variations in connection behaviour, that buildings rarely receive their full design load and that buildings designed and constructed to normal commercial practice rarely behave as assumed in design.

There are also some significant differences between the new method and the traditional UK approach. Probably the most important difference concerns the treatment of prying forces. In end-plate connections prying forces are developed due to the flexural distortion of the end plate or column flange. The edge of the end plate bears against the column flange, which results in additional forces being induced in the bolts. The value of prying force varies widely depending on the geometry of the connection. But rather than give a general equation for calculating prying action the traditional UK approach<sup>(1)</sup> limits this action by limiting the geometry of the connection. Furthermore to avoid the need to calculate the prying forces in these connections the allowable bolt stresses in Table 32 of BS5950:Part 1<sup>(7)</sup> are reduced.

The rigorous method in the new procedure makes no specific mention of prying action nor are any equations given to calculate its value. This is because prying action is implicit in the equations for predicting the strength of either the column flange or end plate. For this reason the enhanced bolt tension capacities are used with the new design method (450 N/mm<sup>2</sup> in the traditional approach compared with 560 N/mm<sup>2</sup> in the new method for grade 8.8 bolts).

In Table 1 the new method for the design of moment connections<sup>(6)</sup> is compared with published experimental data on flush and extended end-plate connections. For the majority of tests the design model gives an adequate prediction of moment capacity with the safety margin varying from 1.19 to 2.56. However, for test 6 taken from reference 25 the value of the ratio  $M_E/M_D$  is below 1.0. This particular test failed by buckling of the column web in the compression zone. *Inspection of photographs and drawings of the test specimen indicates that the length of column below the compression flange of the beam was insufficient to develop the full buckling capacity of the column web. In most practical situations the column continues past the connection to the floor below and a higher buckling capacity would be expected.*

Ref No	Test No	Connection Type	Experimental Moment Capacity (kNm)	Design Moment Capacity (kNm)	$\frac{M_E}{M_D}$	Traditional UK Approach (kNm)
20	24	Flush	100	50	2.00	52
20	25	Flush	140	87	1.61	92
20	30	Flush	200	78	2.56	80
20	33	Flush	240	137	1.75	142
20	36	Flush	280	229	1.22	175
21	17	Flush	130	84	1.55	72
21	18	Flush	95.4	84	1.19	72
22	2	Flush	90	53	1.70	51
23	1	Flush	64	33	1.94	32
23	1	Extended	92	54	1.70	57
24	J1	Extended	97	60	1.62	54
24	J2	Extended	88	57	1.54	54
24	J3	Extended	79	33	2.39	29
25	6	Extended	100	117	0.85	132
25	9	Extended	210	98	2.14	86
25	10	Extended	228	134	1.70	132
25	14	Extended	268	146	1.84	132
25	15	Extended	186	74	2.51	55
25	18	Extended	243	134	1.81	131
25	22	Extended	192	111	1.73	108
25	28	Extended	158	111	1.42	108
25	28	Extended	161	122	1.32	108

**Table 1 Comparison between experimental results and design model for a range of flush and extended end-plate connections**

Table 1 also compares the UK's traditional approach with the new method. When the mode of failure is either yielding of the end plate or column flange both methods predict similar moment capacities. But when the failure mode involves the fracture of the bolts the new

method in general gives significantly higher moment capacities. This difference is a direct consequence of the difference in the treatment of prying forces and the enhanced bolt strengths used with the new method.

### 2.2.1 Wind-Moment Connections

The wind-moment method has been used for many years both in the UK and America to design unbraced multi-storey steel-framed buildings. In this method the connections are assumed to be pinned under gravity loads and under wind loads they are assumed to behave as rigid joints with points of contraflexure at the mid-height of columns and mid-length of beams. The advantage of this method is that the frame is statically determinate and the internal forces are therefore not dependent on the relative stiffness of the connected members. A full description of this method together with detailed design rules is given in the SCI publication 'Wind-Moment Design for Unbraced Frames'<sup>(18)</sup>.

The connections in a wind-moment frame will generally be only partial-strength with respect to the strength of the beams. A key requirement for such connections is that they should be ductile and must be able to form plastic hinges and participate in failure mechanisms. The moment connections publication<sup>(6)</sup> presents design rules which ensure that wind-moment connections have adequate strength and ductility. The connection is designed for strength using the methods outlined in the previous section. Adequate ductility is designed into the connection by ensuring that it fails in a ductile manner. These ductile modes include yielding of either the end plate or column flange (without bolt fracture) in the tension region of the connection (Mode 1 failure) and shearing of the column web. Non-ductile modes, particularly those involving failure of the bolts or welds in tension, should be prevented.

Four standard wind-moment connections are presented in the draft publication. These connections are based on Universal beams and are presented in simple look-up tables which give the designer a quick and easy method of designing connections for the majority of wind-moment frames. To ensure adequate ductility the geometry of the connection together with the bolt sizes and end-plate thicknesses have been chosen so that the connection fails in a ductile manner. A horizontal bolt spacing of 90 mm has been adopted for all bolt sizes (ie M20 and M24) to improve stiffness and still maintain adequate ductility. The end plate must be made from S275 grade steel and its thickness is approximately 60% of the diameter of the bolt.

To verify the ductile performance of these standard connections the SCI commissioned Dr B Bose of the Dundee Institute of Technology to carry out an experimental investigation<sup>(19,20)</sup>. Bose tested a total of fourteen cruciform connections. A summary of the results from these tests is given in Table 2. From these tests Bose<sup>(19,20)</sup> concluded that the rotation capacity of standard connections with beams up to 686 mm deep was well above the desired range of 0.02 to 0.04 radians. However, for deeper beams it is doubtful that the standard connections can be classified as ductile.

Test No	Experiment			Design Moment Capacity (kNm)	$\frac{M_e}{M_d}$
	Failure Moment (kNm)	Rotation at Failure (rads)	Mode of failure		
1	231	0.05	bolt stripping	102	2.26
2	425	0.034	bolt fracture	189	2.25
3	250	0.031	end-plate fracture	147	1.70
3	274	0.033	end-plate fracture	147	1.86
4	413	0.061	column web buckling	214	1.93
5	-	-	-	399	-
6	282	0.033	column web buckling	200	1.41
5B	689	0.019	column web buckling	306	2.25
7	413	0.039	bolt fracture	208	1.99
8	665	0.085	bolt fracture	389	1.71
9	125	0.036	bolt stripping	68	1.84
10	247	0.013	bolt stripping	182	1.36
11	185	0.034	bolt fracture		
12	557	0.007	column web buckling		

Table 2 Comparison between experimental results and design model for wind-moment connection

### 3.0 CONCLUSIONS

The background to the development of a series of design guides for a set of standardised and practical steelwork connections has been reviewed. The recommendations given in each publication are based on a combination of the latest design theories, current UK practice and engineering judgement, and have been validated against experimental data.

In general the recommendations produce economic connections and give realistic estimates of connection strength.

It is hoped that the general acceptance of the methods and standardised connections outlined in these publications will rationalise connection design within the construction industry.

### 4.0 REFERENCES

1. Pask, J W : "Manual on Connections for Beam and Column Construction conforming with the requirements of BS449:Part 2:1969", BCSA publication No. 9/82, 1982.
2. Pask, J W : "Manual on Connections, Volume 1 - Joints in Simple Construction conforming with the requirements of BS5950:Part 1:1985, BCSA publication No. 19/88, 1988.
3. BCSA/SCI : "Joints in Simple Construction, Volume 1 : Design Methods", SCI publication No. SCI-P-105, 1991.
4. BCSA/SCI, "Joints in Simple Construction, Volume 2 : Practical Applications", SCI publication No. SCI-P-105, 1991.
5. Cheng, J J R, Yura, J A and Johnson, C P : "Design and Behaviour of Coped Beams", B.M.F.S.E.L. report No. 841, University of Texas, Austin, Department of Civil Engineering, July 1984.
6. BCSA/SCI : "Joints in Steel Construction. Moment Connections". To be published.
7. BS5950 : "The Structural Use of Steelwork in Buildings. Part 1. Code of practice for design in simple and continuous construction : hot rolled sections", London, British Standards Institution, 1990.
8. Eurocode 3 : "Design of Steel Structures, Part 1.1 General rules and rules for buildings", DD ENV 1993-1-1, British Standards Institution, 1992.
9. Hogan, T J and Thomas, I R : "Design of Structural Connections", 3rd edition, Australian Institute of Steel Construction.
10. Moore, D B and Owens, G W : "Verification of Design Methods for Fin-plate Connections", Journal of the Institution of Structural Engineers, Vol. 70, No. 3, 1992.

11. Owens, G W and Malik, A : "A theoretical Investigation into the Lateral-torsional Buckling of Fin-plates". Private communication.
12. Kirby, P A and Nethercot, D A : "Design for Structural Stability", Constrado Monograph, Granada, 1979.
13. Peebles, K : "Behaviour of Long Fin-plate Connections", University of Dundee report submitted to the Steel Construction Institute, 1994.
14. Jarrett, N D : "An experimental investigation of the behaviour of fin-plate connections to deep beams", Building Research Establishment Client Report, September 1993.
15. Jarrett, N D : "An experimental investigation of fin-plate connections to deep beams", Draft Report No. 2, Building Research Establishment, February 1994.
16. Owens, G W and Moore, D B : "The Robustness of Simple Connections", The Structural Engineer, Vol. 70, No. 3, February 1992.
17. Moore, D B : "The Design of End-plate Connections", Paper No. 4 in Frame and Slab Structures, Edited by G S T Armer and D B Moore, Butterworths, London, 1989.
18. Anderson, D, Reading, S J and Kavianpour, K : "Wind-Moment Design for Unbraced Frames", The Steel Construction Institute publication No. 082, 1991.
19. Bose, B : "Tests to Verify the Performance of Standard Ductile Connections", Dundee Institute of Technology Consultancy Report No. DIT/CESB/HSRG/C1/93, 1993.
20. Bose, B : "Additional Tests of Standardized Ductile Connections", Dundee Institute of Technology Consultancy Report No. UAD/CESB/SRG/C1/94, 1994.
21. Zoetemeijer, P : "Semi-rigid Bolted Beam-to-column Connections with Stiffened Column Flanges and End-plates", Joints in Structural Steelwork, Edited by J H Hewlett, W M Jenkins and R Stansby, Pertech Press, 1981.
22. Zoetemeijer, P and Kolstein, M H : "Geboute balk-kolomverbindingen met korte kopplaat", Stevin Laboratorium, 1975.
23. Zoetemeijer, P : "A Design Method for the Tension Side of Statically Loaded Beam-to-column Connections", Heran, Vol. 20, 1974.
24. Chakrabarti, B : "Tests of Unstiffened End-plate Beam-Column Connections", Building Research Establishment Note N123/87, 1987.
25. Packer, J A and Morris L J : "A Limit State Design Method for the Tension Region of Bolted Beam-to-column Connections", The Structural Engineer, Vol. 55, 1977.
26. Prescott, A T : "The Performance of End-plate Connections in Steel Structures and their Influence on Overall Structural Behaviour", Doctor of Philosophy thesis, Hatfield Polytechnic, 1987.

## PERFORMANCE OF MOMENT RESISTING STEEL FRAMES IN THE JANUARY 17, 1994 NORTHRIDGE EARTHQUAKE

James O. Malley<sup>1</sup>

### ABSTRACT

Over one-hundred moment resisting steel framed buildings suffered structural damage in the M6.8 January 17, 1994 Northridge earthquake. The majority of damage documented to date occurred in the beam-to-column connections of these buildings. A small number of braced frame buildings also suffered structural damage. None of these buildings suffered collapse or caused any injuries as a result of the earthquake. This damage to steel frame buildings is important for the engineering community to consider, because of both the popularity of steel frame buildings in modern construction in areas of high seismicity, and the somewhat unexpected type and extent of damage which occurred. This paper will attempt to summarize the damage which occurred, describe the potential causes of the damage, discuss the difficulties encountered in assessing the damage to steel frames, and describe efforts which will attempt to improve the future performance of steel frame construction in areas of high seismicity.

### INTRODUCTION

The January 17, 1994 Northridge earthquake caused over sixty deaths and over \$15 billion in property damage. This total included significant damage to a large number of steel framed buildings. The extent of this damage was somewhat surprising to the engineering community, since steel frame buildings have exhibited excellent performance in past earthquakes. It should be noted that the Northridge earthquake, while of short duration, produced very intense ground shaking in a heavily urbanized area. As such, it was the first earthquake in the United States which subjected "modern" steel frame buildings to ground motions which approached or exceeded that anticipated in seismic design. Although none of these buildings collapsed, the structural damage was significant enough that many were evacuated

---

<sup>1</sup>Principal, Degenkolb Engineers, 350 Sansome Street,  
Suite 900, San Francisco, CA 94104

until necessary repairs could be made. In many cases, the cost of repairing these buildings has been significant, approaching the cost of the original structural system in a few instances. Even with this level of structural damage, many of the buildings were re-occupied following the earthquake because of the limited nonstructural damage which occurred. This damage presents a special challenge to engineers in determining appropriate repair procedures in the affected area, improved design methodologies for new construction, and a comprehensive approach for evaluating the thousands of similar existing steel frames structures located in areas of high seismicity.

### SUMMARY OF DAMAGE NOTED TO DATE

Over one-hundred moment resisting frames were reported to have suffered structural damage in the earthquake. This damage generally consisted of tearing at the welded connections between girder and column flanges. Most of the buildings were located in the San Fernando Valley near the epicenter of the event, although this type of damage has been reported in other areas, including West Los Angeles and Santa Monica. Buildings from one to twenty-seven stories have suffered damage, although the majority of damage has been reported to buildings of six stories or less. The majority of the affected buildings were constructed during the mid to late 1980s. Note that this was the era when the majority of large commercial buildings were built in the epicentral region.

Steel moment resisting frames have been a widely used form of construction in regions of high seismicity for a number of reasons. First, they were believed to be capable of reliable, ductile response in severe shaking. They also have less impact on building functions and programs than systems with bracing or shear walls. Finally, over the years, they have developed into an economical structural system. As a result of these considerations, moment resisting steel framing has become a predominant form of U.S. construction in regions of high seismicity.

The vast majority of steel moment resisting frames constructed since the mid-1970s have included connections consisting of complete penetration welds of the girder flanges to the column flanges and high strength bolting of the girder web for the design shear forces. Figure 1 shows this typical detail configuration. This detail came into widespread practice following research testing done on W18 and W24 girder sections at U.C. Berkeley (Popov and Stephen, 1972). This detail was "pre-qualified" in the 1988 Uniform Building Code (ICBO, 1988) as meeting the intent of providing a connection which is capable of developing the capacity of the girder.

Since the incorporation of this detail in the early 1970s, design practices have changed in an effort to make this system more economical. These changes have included reducing the number of frame bays which participate in the lateral force resisting system. This reduction in frame bays has resulted in member sizes in actual buildings which are much larger than any condition which had been tested in

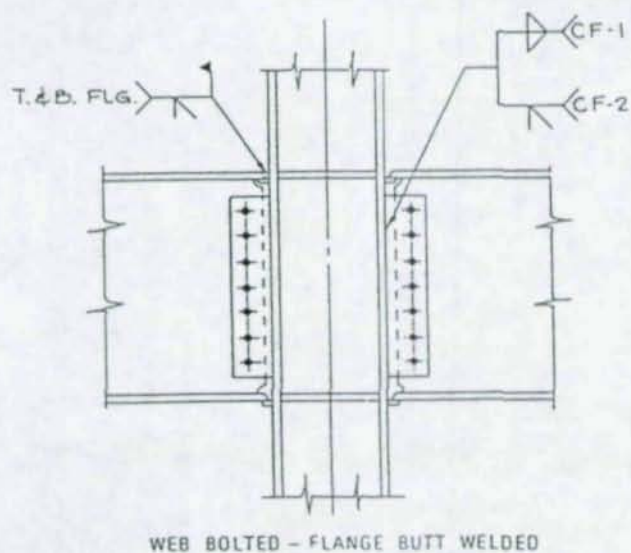


**Fig.1. Typical welded flange-bolted web moment connection joint detail.**

laboratory simulations (W36 girders and group 4 or 5 W14 columns, e.g.). Size effects and the reduction in frame redundancy which resulted from these design trends may have contributed to the extent of the damage which occurred.

As noted above, the damage to these frames consisted of the cracking or tearing of the complete penetration welded connections between the girder and column flanges. The extent of this tearing ranged from minor cracking in the weld material, to separation of the welded material from the column flange, to removal of "divots" of steel from the column flanges, to cracking through the flange(s) and web of the columns. The great majority of this damage occurred to the girder bottom flange connection, although there have also been a number of locations of top flange connection damage. In almost all cases, where damage to the top flange damage did occur, it was accompanied by similar and more extensive damage at the bottom flange. In some cases the flange connection damage led to cracking in girder web connection. See Figure 2 for a sketch of a typical damaged connection.

### POTENTIAL CAUSES OF DAMAGE

1. **Materials** - Damage to column members which was demonstrated in the form of removal of "divots" and cracking across the flange and web, is related to the material properties of the steel. In general, the material properties of the structural steel appears to have met the appropriate ASTM material specifications. Note that the materials typically used in building construction does not have minimum impact toughness requirements, nor special properties for ductility in the through thickness ("z") direction. This issue may be more significant for conditions with jumbo column sections, because of the difficulty encountered in obtaining ductile materials at the web-flange juncture.
2. **Welding Procedures** - A number of issues related to typical field welding procedures have been cited as possible contributors to the damage. Welding back-up bars that are left in place result in a notch condition which causes a stress concentration that can lead to a point of initiation for cracking to occur. Dam tabs were also noted at a number of complete joint penetration weld locations. Lack of fusion, both in the initial weld pass and between passes, has been observed in the damaged connections. Inadequate preheat, large diameter welding wires, welding wire material toughness, and other welding procedures have also been cited as potential contributors to the damage. In many cases, conditions which do not meet the standards of AWS D1.1 were observed.

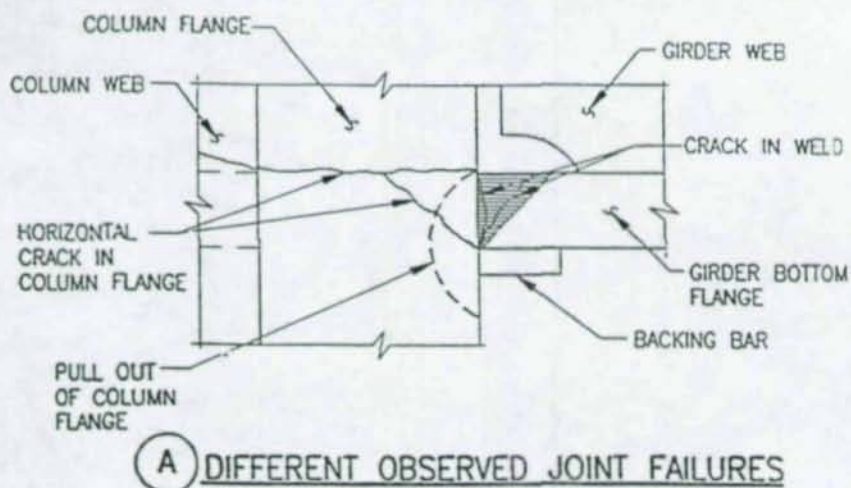
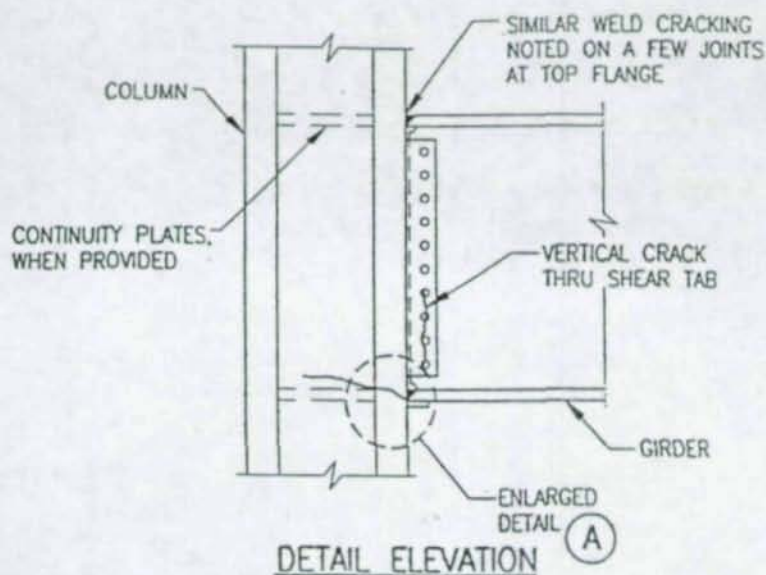


Fig.2. Sketch of typical connection damage experienced during the 1994 North-ridge earthquake.

3. Connection Detailing - Almost all of the damaged connections included the bolted web/complete penetration field welded flange detail which has been predominant in California steel moment frame construction for the last twenty years. Since the bolted web connection has little capacity to develop the web bending moment, increased stresses are required in the flange welds to develop the strength of the girder section. Provision, size and detailing of girder flange continuity plates may also have contributed to the damage.
4. Design Issues - Many of the damaged buildings relied on the moment resistance of only a small number of the frame bays. Use of these partial moment resisting frames leads to very large column and girder sizes in order to meet the strength and stiffness provisions of the building codes. Such designs reduce the redundancy of the lateral force resisting system, resulting in increased reliance on the competency of any one moment resisting connection. In addition, the large members and plate thicknesses in these frames result in other potential problems such as increased welding restraint and decreased material ductility.

### PROPOSED REPAIR TECHNIQUES

The repair techniques which have been and are presently being performed on the damage connections varies depending on the type and extent of the cracking and tearing, and the Engineer responsible for the repair work. In some cases, the repairs consist of simply gouging out the affected areas and rewelding. Other procedures are including the complete revision of the connection detail with reinforcing plates, haunches, etc. In general, undamaged connections have not been modified to be consistent with the repair of damaged locations.

#### Revised Details for New Construction

Engineers are presently attempting to develop alternate details and specifications for these moment frame connections. A wide variety of approaches are being considered to improve the performance of this connection, including revised details for both the girder web and flange connections, improved welding procedures, and a combination of both detail and procedure improvements. Some of the proposed detail improvements have been previously suggested by University researchers. There is presently no consensus for the revisions, and it may take a lengthy period of time before one is reached, since there are so many parameters which affect the performance of these connections.

Testing research on full scale connections occurred at the University of Texas at Austin led by Professor Michael Englehardt during the months which followed the earthquake. This research tested 16 full size sections (W36 girders and Group 4 W14 columns) similar to that of a building project which suffered damage from the Northridge earthquake. Various connection details and welding procedures were employed. A summary of the preliminary observations from this testing include the following:

- 1) Improved welding alone may not be adequate to assure satisfactory performance of the connection.
- 2) Reinforcing the connection to force the plastic hinging to form away from the connection appears to very beneficial.
- 3) Removal of run-off tabs and bottom flange back-up bar is likely to be beneficial.
- 4) Development and strict enforcement of a complete Welding Procedure Specification (WPS) appears to be very beneficial.
- 5) The need for weld filler metal with minimum specified impact properties is unclear.
- 6) The need for removal of the top flange back-up bar is unclear.
- 7) Passing an ultrasonic test does not necessarily indicate a weld which will exhibit ductile performance.
- 8) Column flange through thickness properties may be an important consideration in the connection design.

Note that these observations are based on the results of the tests on these large size connections. The general trends observed in these tests support the observations listed above. But, extrapolation of these observations to general conclusions for all forms of steel moment frame construction should only be made with extreme caution until future research is completed.

### **DAMAGE ASSESSMENT DIFFICULTIES**

In the first few days following the Northridge earthquake, there were very few reports of steel frame buildings which had suffered any structural damage. In fact, many of the buildings were reoccupied prior to the discovery of any structural damage. At the time of this workshop, sixteen months after the earthquake, the number of steel frame buildings identified with structural damage is still growing. The reasons that identification of this damage have taken such a long period of time include the following:

- A. The steel frame elements and their connections are almost always hidden from view by ceilings and or architectural cladding. In some cases architectural walls were separated by a distance large enough that they did not show any signs of the buckling to braced elements which they enclosed.
- B. These elements are also almost always covered with fireproofing materials. In many cases, there was no cracking or other damage to fireproofing which encased damaged moment frame connections.
- C. Many of the moment frame buildings which had damaged connections experienced very limited nonstructural damage. Initial post-earthquake damage inspectors would have typically concluded that the lack of nonstructural damage was a good indication that no structural damage occurred.

The California Seismic Safety Commission issued a warning to steel frame building owners of the potential for this "hidden" damage. The City of Los Angeles is presently considering requiring the owners of such buildings in areas which were subject to strong ground shaking to perform inspections of the moment resisting connections.

### ONGOING RESEARCH EFFORTS

The damage to steel moment resisting frame buildings has significantly reduced the confidence of the engineering community in this form of construction. In addition, in the United States there are thousands of existing buildings of similar construction which may be subject to similar damage in future strong earthquakes. As a result, the need for a major research effort was identified by the SAC Joint Venture. This joint venture is a partnership of the Structural Engineers Association of California, the Applied Technology and the California Universities for Research in Earthquake Engineering. The goal of this joint venture was stated to be the following:

*Develop professional practices and recommend standards for the repair, retrofit and design of steel moment resisting frame buildings so that they provide reliable, cost-effective seismic performance in future earthquakes.*

Three objectives will be met to achieve this goal:

1. Characterize and understand what has happened to steel moment frame buildings in the Northridge earthquake;

2. Prepare interim procedures for professional practices and standards application to:
  - a) identification of buildings that may have been damaged for investigation
  - b) characterize the safety condition of inspected buildings; and
  - c) rehabilitate damaged buildings to provide life safety;
3. Prepare recommendations for the repair, retrofit and design of buildings based on rational understanding of seismic behavior.

The SAC Joint Venture has developed a detailed work plan to develop interim guidelines for inspection and repair of damaged buildings and design of new buildings. Longer range tasks will focus on procedures for repair, retrofit and design of steel frame buildings. These tasks will include extensive analytical and testing research which will lead to the development of guidelines for these items.

The first phase included in the proposal to develop interim guidelines has been funded, and should be completed by the middle of 1995. The longer range objectives which will follow should be completed within the next few years. It is hoped that with the completion of this project, that the pre-Northridge confidence of the engineering community in the seismic resistance of steel moment resisting frame buildings can be restored.

#### REFERENCES

ICBO, Uniform Building, 1988 Edition, International Conference of Building Officials, Whittier, California, 1988.

Popov, E.P. and R.M. Stephen, "Cyclic Loading of Full Size Steel Connections," Bulletin No. 21, Washington, D.C., American Iron and Steel Institute, 1972.

Technical Papers on

**CONNECTIONS IN AUSTRALIA**

## CONNECTION RESEARCH, DESIGN AND PRACTICE IN AUSTRALIA

Gregory Hancock<sup>1</sup>

Arun Syam<sup>2</sup>

Bruce Chapman<sup>3</sup>

Tim Hogan<sup>4</sup>

### Abstract

Australian standards relevant to the design of connections in both hot-rolled and cold-formed steel structures are reviewed. Design manuals and publications used by design engineers in Australia for hot-rolled, cold-formed and hollow section member connections are summarised. Current research topics on connections in steel structures in Australia are summarised.

### 1. INTRODUCTION

Steel structures consisting of hot-rolled and fabricated members down to a thickness of 3 mm are designed in Australia to the limit states standard for Steel Structures AS 4100 (Standards Australia, 1990). Hollow section members including cold-formed hollow sections down to a thickness of 1.6 mm are also designed to AS 4100. Cold-formed steel structural members other than hollow sections are currently designed to the Cold-Formed Steel Structures Standard AS 1538 (Standards Australia, 1988) which is in permissible stress format. This standard is soon to be replaced by a limit states standard currently in committee draft form (Standards Australia/Standards New Zealand, 1994).

AS 4100 provides design rules for bolted and welded connections in Section 9.

- 
- 1 BHP Steel Professor of Steel Structures, University of Sydney, 2006, Australia
  - 2 Manager, Technical Services, Australian Institute of Steel Construction, 99 Mount Street, North Sydney, 2060, Australia
  - 3 Engineer, Technical Services, AISC (same address as 2)
  - 4 Director, Stigter Clarey and Partners, 70 Bathurst St, Sydney, 2000, Australia

Bolts are either of strength grade 4.6 to AS 1111 (Standards Australia, 1980) or more usually strength grade 8.8 to AS 1252 (Standards Australia, 1983). Grade 4.6 bolts may only be installed to the snug-tight condition (4.6/S). Grade 8.8 (ie high strength structural) bolts may be used in either the snug-tight condition (8.8/S) or fully tensioned bearing type (8.8/TB) and fully tensioned friction type (8.8/TF). Welds are designed to AS 4100 and welded and inspected to AS 1554.1 (Standards Australia, 1991a) and may be of two categories, SP (structural purpose) and GP (general purpose). The difference in the two categories lies in the level of permissible imperfections allowed. A higher level of weld quality may be specified for welded joints subject to fatigue loading (Standards Australia, 1989). AS 4100 also contains design provisions for the design of bolt groups and weld groups, as well as some general requirements for the design of connections.

AS 1538 gives design rules for bolted and welded connections in Section 5. This section is similar to Section E of the Specification for the Design of Cold-Formed Steel Structural Members (AISI, 1989). Design examples for connections to AS 1538 are given in Hancock (1994). The draft limit states cold-formed steel structures standard is based mainly on the Load and Resistance Factor Design Specification for Cold-Formed Steel Structural Members (AISI, 1991) except that design rules for screwed and riveted connections will be included using design information based on Eurocode 3, Part 1.3 (CEN, 1992).

The Australian Institute of Steel Construction (AISC) has published four editions of its manual "Design of Structural Connections" since 1978, the latest edition (Hogan and Thomas, 1994) being in limit states format. Further details of this manual are given in Section 2.1 of this paper. The Australian Institute of Steel Construction has published three editions of its manual "Standardized Structural Connections", the latest edition being 1985 (AISC, 1985), further details of which are given in Section 2.2 of this paper. The Australian Institute of Steel Construction is soon to publish a new limit states design manual entitled "Pre-engineered Connections for Structural Steel Hollow Sections". The basis of this manual is given in the paper "Development of Pre-Engineered Connections for SSHS" (Chapman *et al.*, 1994) and further detail is given in Section 2.3 of this paper.

Research into structural steel connections is being undertaken in Australia, mainly at the University of Sydney (USyd), Queensland University of Technology (QUT), Monash University (MonU) and the Commonwealth Scientific and Industrial Research Organisation (CSIRO). A brief summary of current projects is included in Section 3 of this paper.

## 2. DESIGN MANUALS

### 2.1 Design of Structural Connections

This section summarises the material in the manual "Design of Structural

Connections" (Hogan and Thomas, 1994). The manual contains recommended design models for a range of connections commonly used for structural steelwork in Australia. The recommended design models presented were originally developed as a necessary component of the manual "Standardised Structural Connections" (AISC, 1985) described briefly in Section 2.2 following. The design models presented in the first three editions of the manual were used to generate safe load tables for the range of standardised connections included therein, and were in permissible stress format. The latest edition is written in limit states format in conformity with AS 4100. Attention is given primarily to applications involving rolled steel channel and I-sections in orthogonal frameworks. The models have been developed with Grade 250 steel (250 MPa yield stress) in mind for the members and connection components but should be capable of extension to Grade 300, Grade 350 and Grade 400 steel although no test data is available for these grades at present.

The recommended design models are built up from general design recommendations for:

- bolts and bolt groups
- welds and weld groups
- components (cleats, gusset plates, brackets, etc)
- supported members at connections

The connection types covered in the manual and shown in Fig. 1 are:

#### FLEXIBLE CONNECTIONS (SIMPLE CONSTRUCTION)

- Angle seat
- Bearing pad
- Flexible end plate
- Angle cleat
- Web side plate
- Stiff seat
- Bracing cleat

#### RIGID CONNECTIONS (RIGID CONSTRUCTION)

- Welded moment connection
- Bolted moment end plate connection

#### SPLICES

- Welded splice
- Bolted splice

#### BASE PLATE

- Column base plate (pinned)

Two limit states require consideration in the design of bolted connections. These are:

**STRENGTH LIMIT STATE** (requires consideration for all bolted connections, 4.6/S, 8.8/S, 8.8/TB, 8.8/TF)

- Bolt in shear
- Bolt in tension

Bolt in shear and tension

Ply in bearing

Long bolt groups in lap splice connections

SERVICEABILITY LIMIT STATE (requires consideration only for that category of connection (8.8/TF) which is required not to slip under serviceability loads)

Bolt in shear

Bolt in shear and tension

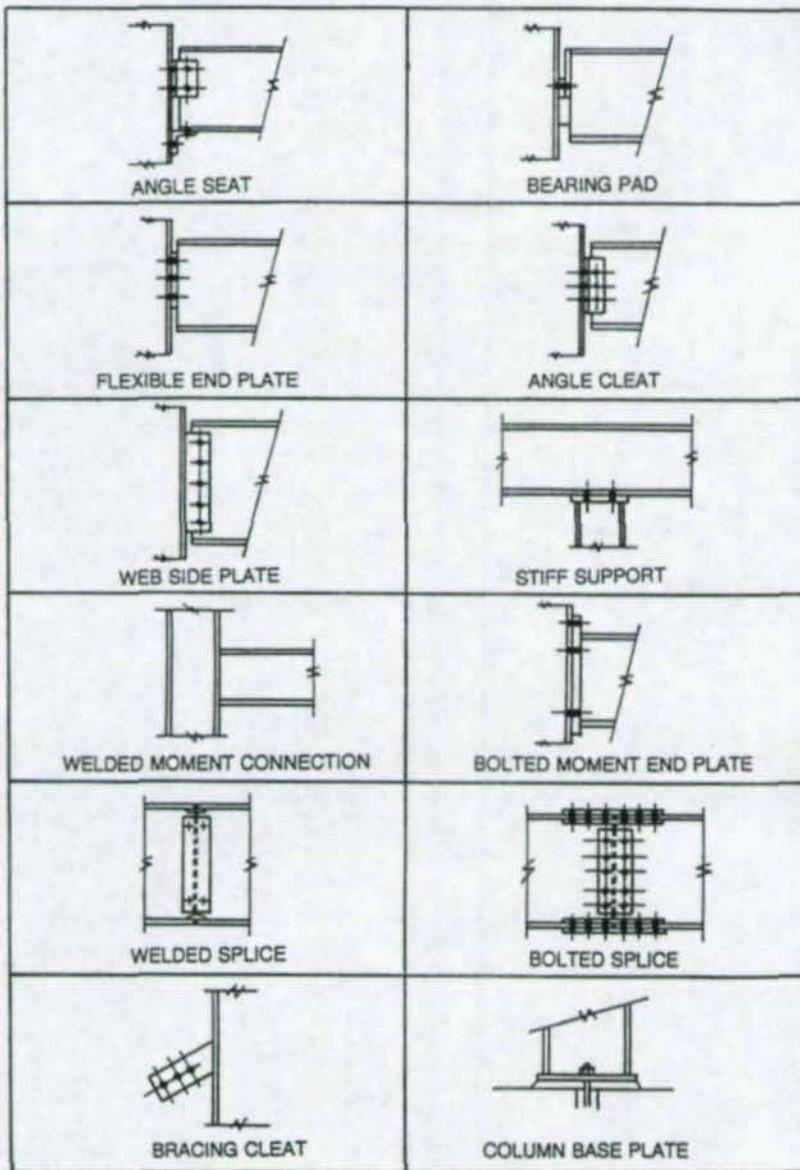


Fig. 1 Rolled Section Connection Types

The capacity factor (resistance factor),  $\phi$ , used in limit states design depends upon the limit state. For example, the capacity factors for bolt strength vary between 0.8 and 0.9, and are 0.7 for bolt serviceability.

The WELD TYPES used in AS 4100 include:

- Complete penetration butt weld
- Incomplete penetration butt weld
- Fillet weld
- Plug weld
- Slot weld
- Compound weld

For statically loaded welded connections, only the strength limit state needs to be considered. The capacity factor (resistance factor),  $\phi$ , depends upon the weld category type. For example, the capacity factors for a complete penetration butt weld are 0.90 for weld category SP and 0.60 for weld category GP.

Connection components (cleats, gusset plates, brackets) must also have their strength assessed in order to determine the strength of a connection as a whole. Clause 9.1.9 of AS 4100 specifies that connection components shall have their capacities assessed using the provisions of the member design Sections 5, 6, 7 or 8 as applicable. The component design covered in the manual includes shear capacity, moment capacity, axial compression capacity and axial tension capacity.

For the design of some connections, an assessment is required of the design capacity of the supported member in bending, shear, bearing, etc. The manual provides design recommendations for:

- Uncoped sections
- Single web coped sections
- Double web coped sections
- Block shear in coped sections

The computer program LIMCON has been developed by Engineering Systems Pty Limited in association with the Australian Institute of Steel Construction. The program runs on IBM compatible computers and has been designed to assist in the design and checking of connections according to the method set out in the manual. LIMCON is driven with pull-down menus. Data is entered into screen "forms" where it is grouped and displayed in context. Help information is provided for all data entry items. LIMCON can display and print 3D views of connection details. LIMCON provides printed reports with all design information.

## 2.2 Standardized Structural Connections

This section summarises the status of the manual "Standardized Structural Connections" (AISC, 1985). The first edition of this manual was published in 1978,

with subsequent editions in 1981 and the most recent in 1985 (AISC, 1985). The manual provides information on standard forms of connections, standard bolting configurations, standard components and designations.

The aim of the manual is to rationalise connections so that current economic design and fabrication practice can be incorporated. This permits increased efficiencies and a reduction of cost of fabricated connections in Australia. The manual also satisfies the requirement that 'design shall be on the basis of a recognisable method supported by test evidence'.

The first three editions of the manual were based on the permissible stress method of design. The connections considered within the manual are shown in Fig. 1. AISC is currently working on the fourth edition of the manual which is in limit states format and is also based on the design models of Section 2.1. Additionally, a change in the base grade of steel (from 250 MPa to 300 MPa) has highlighted the need to assess the details of these connections.

The standardised connections concept has been readily accepted by both designers and fabricators in Australia. With time, the following improvements have been made:

- (i) a reduction in the number of standard components
- (ii) a rationalisation of some dimensioning to improve design capacity
- (iii) a heavier rationalisation in simple connections to reflect the almost exclusive current use of 8.8/S bolting category and E48XX weld metal (tensile strength of 480 MPa) in the standardized connections
- (iv) the introduction of greater detail and standardization into the area of rigid connections, base plates and splices

### 2.3 Pre-Engineered Connections for Structural Steel Hollow Sections

This section summarises the material in the soon to be published manual "Pre-Engineered Connections for Structural Steel Hollow Sections" (PCHS). This publication was commissioned following requests to AISC from the steel construction industry for a publication which presents design models and corresponding tables of maximum design loads for a range of pre-engineered connections commonly used to connect structural steel hollow sections. In the last 30 years there has been extensive research and testing of hollow section joints, particularly welded connections. Much of this research has been sponsored and published by Comité International pour L'Étude de la Construction Tubulaire (CIDECT) and the International Institute of Welding (IIW). Despite the availability of design recommendations from these organisations, the design of connections for structural steel hollow sections can still be an area of uncertainty for practising engineers, and this uncertainty has restricted their use in structural applications. The PCHS has been prepared principally using the CIDECT and IIW research. This has been achieved by providing design models, detailing dimensions for each connection and tabulated maximum design loads for a range of common pre-

engineered hollow section connections as shown in Fig. 2.

The steel hollow sections which are considered within the PCHS comply with Australian Standard AS 1163 (Standards Australia, 1991b). The primary design reference is AS 4100. Until recently, AS 4100 only applied to sections of thickness 3 mm and greater, and AS 1538 had to be used for thinner sections. However, research at the University of Sydney, for member design (Key et al., 1988; Hasan and Hancock, 1989; Zhao and Hancock, 1991b) and for connection design described in Section 3 following, has shown that the weld design rules in AS 4100 are applicable to hollow sections in the thickness range 1.6 mm to 3.0 mm and so the recent Amendment No. 3 to AS 4100 has been made to allow hollow sections in this thickness range to be designed to AS 4100.

The presentation of information for each connection type follows a standard format as follows:

1. The reference for the design model.
2. A detailed explanation of the failure mode for each component in the connection.
3. The procedure for determining the maximum design load for the connection.
4. An example to illustrate the use of the tables.
5. Tables which contain the maximum design loads and detailing dimensions for the connection.

The pre-engineered connections are organised by member type. The PCHS has adopted standard parameters for materials, detailing and design criteria. However, the level of standardisation is kept to a minimum to provide structurally efficient solutions and to give the designer or fabricator the flexibility to further standardise components to suit individual situations. The connection types covered in the PCHS and shown in Fig. 2 are:

#### COLUMNS

Base plate

Cap plate

Side plate

Bracing cleat

#### TIES AND STRUTS

Flattened end

Welded tee end

Slotted end plate

#### BEAMS

Bolted moment end plate

Welded portal knee

#### WELDED JOINTS

K-connection

Y- and T- connections

Further areas for research are clearly identified in the paper describing the manual (Chapman *et al.*, 1994).

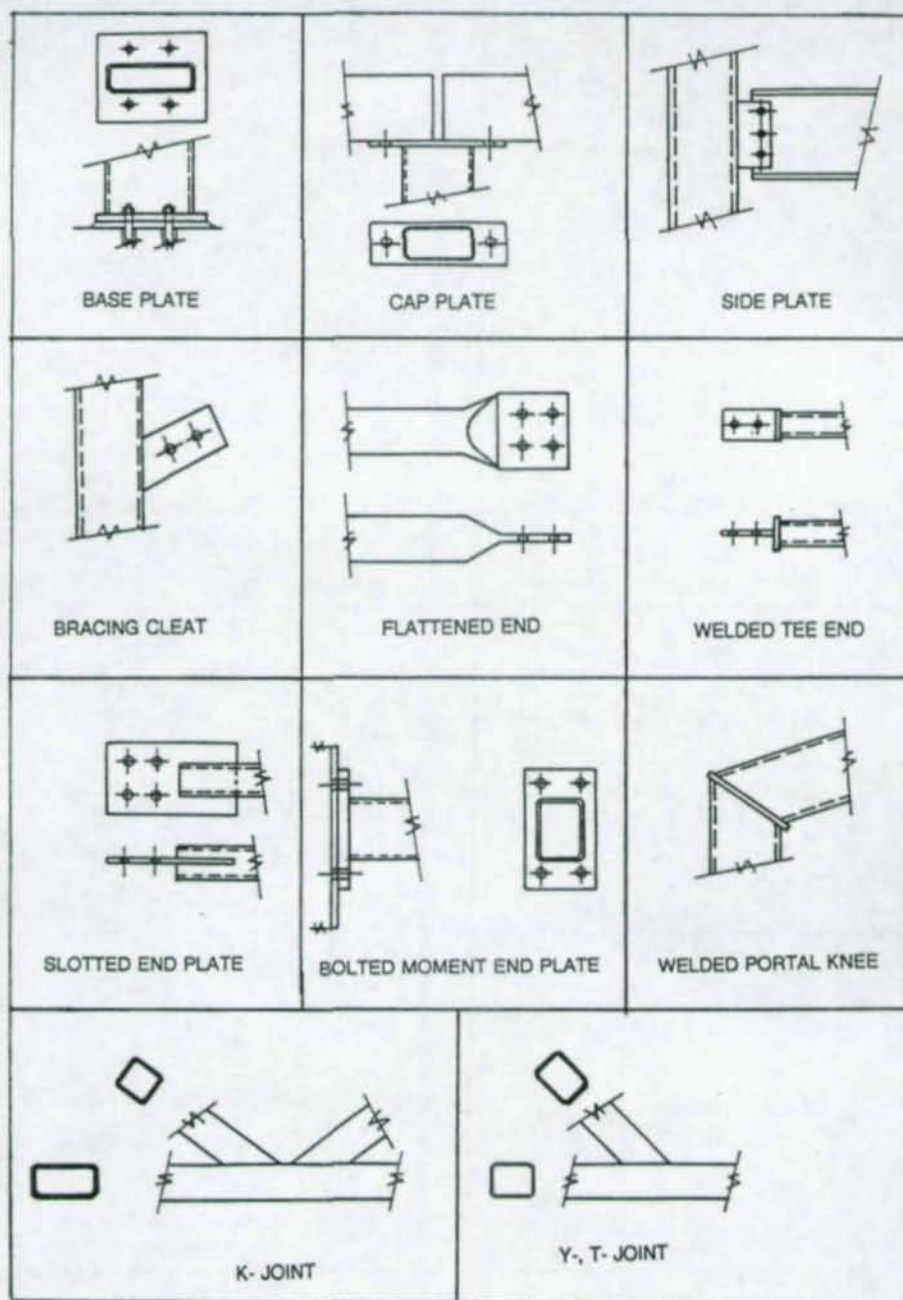


Fig. 2 Hollow Section Connection Types

### 3. RESEARCH

#### 3.1 Tubular Connections

Five substantial research programs are underway or have been recently completed in Australia on connections in tubular structures. These are being performed at the University of Sydney and Monash University.

As stated earlier, connections in tubular members in the thickness range 1.6 mm to 3.0 mm were previously required to be designed in Australia to the Cold-Formed Steel Structures Standard AS 1538-1988. A substantial test program (USyd) on butt welds and fillet welds (both longitudinal and transverse) in thin cold-formed RHS members was undertaken to show that these connections could be designed to AS 4100. The test program on cold-formed RHS sections of Grade C350L0 (350 MPa yield stress) is described in Zhao and Hancock (1994). The test program on cold-formed RHS sections of Grade C450L0 (450 MPa yield stress) is described in a paper at this 3rd International Workshop on Connections in Steel Structures (Zhao and Hancock, 1995). It is shown in the papers that existing capacity (resistance) factors can be used except for longitudinal fillet welds where the capacity factor has to be revised downwards from 0.80 to 0.70.

At Monash University, a detailed parametric study of local joint flexibility and stress concentration factors has been performed on connections in circular hollow sections. The joint configurations include Y-, YT-, K-, X- and KT-joints. For each of these configurations, four types of joints were considered, including profile-cut, flattened-end, grouted profile-cut and grouted flattened-end. The flattened-end and grouted joints are regarded as innovative. Results of the work are included in Ure et al. (1993).

At Monash University, tests on five types of X-joints have been performed (Eimanis and Grundy, 1993). Profile cut (with and without grouting), flattened end (with and without grouting), and flat plate insert joints were tested statically in both tension and compression and their strengths compared to identify the joint with superior strength.

At Monash University, an experimental program was devised to provide some relevant data on the capacity of tubular joints under slowly varying, high amplitude cyclic loading. Under such loading conditions, the tubular joint may achieve 'shakedown' in which the existence of permanent residual stress in the joints permits it to behave in a purely elastic manner. Conversely, the joint will undergo incremental collapse or alternating plasticity failure modes if it fails to achieve shakedown. The experimental program was carried out on CHS YT-joints. The shakedown limit was found to be less than the static collapse limit by up to 18%. Further details of this research can be found in Kwong and Grundy (1994).

A research program on bolted moment end plate connections is currently being

performed at the University of Sydney by Clarke and Wheeler. End plates are welded to SHS and RHS tubular sections which are then bolted together and subjected to pure moment. The major variables in the test program are the number and position of the bolts in the end plates and the plate thickness. The purpose of the test program is to provide strength and serviceability limit states data and to quantify the nonlinear moment rotation responses for this connection type. No publications have been produced at this stage.

### **3.2 Thin-walled and Cold-formed Sections**

As discussed in Section 1 of this paper, a new limit states cold-formed steel structures standard is being prepared jointly by Standards Australia and Standards New Zealand. Australian hot-dipped zinc-coated or aluminium-zinc coated steels to AS 1397 (Standards Australia, 1993) have yield strength values in the range 250 MPa to 550 MPa. For the highest strength grade (G550) which is similar to ASTM A449 and A611 Grade E Steel, tests on screwed and clinched connections for use in steel framed housing are currently being performed to see whether the design rules in the draft Australian Standard (Standards Australia/Standards New Zealand, 1994) are applicable to these steels. New standard tests for shear and cross-tension have been developed and are described by Macindoe and Hanks (1994). Research is continuing at the CSIRO in Australia on G550 steel connections.

### **3.3 Stainless Steel**

Research into the strength and behaviour of welded connections in stainless steel structural hollow sections has been undertaken at the University of Sydney. Tests were performed on planar X- and K-joints in square and circular hollow sections, as described in Rasmussen and Young (1994) and Rasmussen and Hasham (1994). The research on square hollow sections with and without superimposed loads in the chord is described in detail in Rasmussen *et al.* (1993) and Rasmussen (1994). Based on a reliability study, it has been shown that stainless steel SHS and CHS can be designed using the CIDECT Recommendations for carbon steel joints by replacing the yield stress by the 0.2% proof stress of stainless steel based on the properties of the finished hollow section.

### **3.4 Hollow Flange Beams**

A new structural steel section called a Hollow Flange Beam (HFB) has been developed in Australia by Palmer Tube Technology Pty Ltd. The section consists of two triangular flanges connected by a straight web, cold-formed from flat strip. The triangular flanges are closed by two electric resistance welds (ERW). The HFB is very different from conventional hot-rolled and hollow sections. A detailed design manual has been prepared to allow engineers to safely design structures from HFB sections (Palmer Tube Mills, 1993). The design manual contains an extensive section on connections.

Two research programs have been undertaken to investigate the structural

behaviour of HFB connections. These are bolted moment end plate connections (Dempsey, 1993) and web side plate connections (Syam, 1994).

#### 4. CONCLUSIONS

Limit states design information for connections between hot-rolled members in orthogonal frameworks has now been prepared in the form of design manuals in Australia for use by design engineers. Standardised structural connections have been detailed and are described in a manual. A computer program LIMCON is available to assist design engineers in performing the complex calculations required for connections.

A design manual for pre-engineered connections for structural steel hollow sections is in preparation. It will contain detailing information and maximum design loads as well as the design models used to compute the maximum design loads. There is considerable ongoing research in tubular connections for both RHS and CHS in Australia.

A limit states standard for cold-formed steel structures is in draft form and includes design rules for bolted, welded, riveted and screwed connections. Investigations are underway to ascertain the applicability of the connection rules in the draft standard to high strength steels such as Grade G550.

Innovative areas of research in steel connections include hollow flange beams and stainless steel tubular connections, as well as grouted and sleeved connections in circular hollow sections.

#### 5. REFERENCES

AISC, (1985), "Standardized Structural Connections", Australian Institute of Steel Construction, Sydney.

AISI, (1989), "Specification for the Design of Cold-Formed Steel Structural Members", Washington, DC.

AISI, (1991), "Load and Resistance Factor Design Specification for the Design of Cold-Formed Steel Structural Members", Washington, DC.

CEN, (1992), "Design of Steel Structures, Cold-Formed Thin Gauge Members and Sheeting", Eurocode 3 Part 1.3, Draft, CEN/TC250/SC3-PT1A, August.

Chapman, BG, Syam, AA, Dagg, HM and Dempsey, RI, (1994), "Development of pre-engineered connections for SSHS", Tubular Structures VI, AA Balkema,

Rotterdam, pp 93-100.

Dempsey, RI, (1993), "Development of Structural Connections for Hollow Flange Beams", ME Thesis, University of Queensland.

Eimanis, AM and Grundy P, (1993), "Load Capacity of Innovative Tubular X-Joints", Tubular Structures V, E & FN Spon, London, pp 485-494.

Hancock, GJ, (1994) "Design of Cold-Formed Steel Structures (2nd Ed.)", Australian Institute of Steel Construction, Sydney, Australia.

Hasan, SW and Hancock, GJ, (1989), "Plastic Bending Tests of Cold-Formed Rectangular Hollow Sections", J Aust Inst Steel Construction, 23(4), pp 2-19.

Hogan, TJ and Thomas, IR, (1994), "Design of Structural Connections (4th Ed.)", Australian Institute of Steel Construction, Sydney, Australia.

Key, PW, Hasan, SW and Hancock, GJ, (1988), "Column Behaviour of Cold-Formed Hollow Sections", J Struct Engng, ASCE, 114(2), pp 390-407.

Kwong, GT and Grundy, P, (1994), "Capacity of CHS YT-joints under high amplitude cyclic loading", Tubular Structures VI, AA Balkema, Rotterdam, pp 489-496.

Palmer Tube Mills, (1993), "Hollow Flange Beam Connection Design Manual", Queensland, Australia.

Macindoe and Hanks, P, (1994), "Standard Tests for Cold-Formed Steel Single Fastener Connections", Australasian Structural Engineering Conference, pp 253-257.

Rasmussen, KJR and Young, B, (1994), "Stainless Steel Tubular Joints - Tests and Design of X- and K-joints in Square Hollow Sections", Proceedings, 12th International Specialty Conference on Cold-formed Steel Structures, St Louis, pp 595-619.

Rasmussen, KJR and Hasham, AS, (1994), "Stainless Steel Tubular Joints - Tests and Design of X- and K-joints in Circular Hollow Sections", Proceedings, 12th International Specialty Conference on Cold-formed Steel Structures, St Louis, pp 621-640.

Rasmussen, KJR, Teng, F and Young, B, (1993), "Tests of K-Joints in Stainless Steel Square Hollow Sections", Tubular Structures V, E & FN Spon, London, pp 373-382.

Rasmussen, KJR, (1994), "Tests of K-Joints in Stainless Steel Square Hollow Sections with Superimposed Loads in Chord", Tubular Structures VI, AA Balkema,

Rotterdam, pp 457-464.

Standards Australia, (1980), "ISO Metric Hexagon Commercial Bolts and Screws", AS 1111.

Standards Australia, (1983), "High Strength Steel Bolts with Associated Nuts and Washers for Structural Engineering", AS 1252.

Standards Australia, (1988), "Cold-Formed Steel Structures Code", AS 1538.

Standards Australia, (1989), "SAA Structural Steel Welding Code, Part 5: Welding of Steel Structures subject to High Levels of Fatigue Loading", AS 1554.5.

Standards Australia, (1990), "Steel Structures", AS 4100.

Standards Australia, (1991a), "SAA Structural Steel Welding Code, Part 1: Welding of Steel Structures", AS 1554.1.

Standards Australia, (1991b), "Structural Steel Hollow Sections", AS 1163.

Standards Australia, (1993), "Steel Sheet and Strip - Hot-Dipped Zinc-Coated or Aluminium/Zinc Coated", AS 1397.

Standards Australia/Standards New Zealand, (1994), "Cold-Formed Steel Structures", Draft Limit States Code, Document BD/82/94/12.

Syam, AA, (1994), "Hollow Flange Beam Web Side Plate Connections", MES Thesis, University of Sydney.

Ure AJ, Grundy P and Eadie, I, (1993), "Flexible Coefficients of Tubular Connections", Tubular Structures V, E & FN Spon, London, pp 519-526.

Zhao, XL and Hancock GJ, (1991), "Tests to Determine Plate Slenderness Limits for Cold-Formed Rectangular Hollow Sections of Grade C450", J Aust Inst Steel Construction, 25(4), pp 2-16.

Zhao, XL and Hancock, GJ, (1994), "Tests and Design of Butt Welds and Fillet Welds in Thin Cold-Formed RHS Members", Tubular Structures VI, AA Balkema, Rotterdam, pp 465-472.

Zhao, XL and Hancock, GJ, (1995), "Welded Connections in Thin Cold-Formed Rectangular Hollow Sections", Proceedings, 3rd International Workshop on Connections in Steel Structures, Trento, May.

**CURRENT RESEARCH NEEDS**  
**FOR**  
**CONNECTIONS IN STEEL STRUCTURES**

## INTRODUCTORY COMMENTS

The research and development needs listed in this Section were determined from the technical papers that were presented at the Workshop, and from the extensive and lively discussions by the Workshop participants subsequent to the paper presentations. The list represents the essence of the work of the Research Reporters. Although no explanatory notes are provided with each topic, it is felt that the subjects give a realistic reflection of the work that needs to be done.

The research topics are categorized according to the areas of emphasis of the Workshop sessions, and are not prioritized in any way. Several of the topics are broad in scope, and may require multiple research projects.

Besides the gaps in the present knowledge of steel connection behaviour and the developments required to improve design approaches, the Workshop papers and discussions stressed an increasing demand of a closer collaboration among researchers, practitioners and fabricators. This would enable a finer identification of the priorities and goals of research projects, and would strongly enhance the practical effectiveness of the research outcomes.

## RESEARCH AND DEVELOPMENT NEEDS

### 1. *Composite Connections*

Modeling of interface slip between the steel beam and the concrete slab and its effect on the composite connection behaviour for various types of composite joint details.

Improvements of models of concrete tension stiffening effects prior to and at the ultimate capacity of the connection.

Determination of the available rotation capacity of composite semi-rigid connections under monotonic loads and the ductility under cyclic loads.

Analysis and testing of load history or load sequence effects

Study of long-term loading effects.

Analysis of shakedown and incremental collapse behaviour in composite semi-rigid frames.

Quantification of typical rotation demands on composite semi-rigid connections.

Development of design methods and criteria for partially-restrained beam-to-girder connections and partially continuous floor systems.

Testing of the load-deformation behaviour of bolts in single-shear and consideration of their influence on the moment-rotation behaviour of partially-restrained beam-to-girder connections.

Validation of theoretical work and analysis models on frames against suitable experimental tests of frame subassemblies, and comparison of connection performance when tested in isolation and when functioning as part of a complete structure.

## **2. *Special Connections***

Quantification of the effects of deformations of the lateral face of the column section in connections to concrete-filled RHS.

Study of fatigue performance of connections to concrete filled RHS.

Testing of the fatigue behaviour of mismatched welds (i.e., use of low-strength electrodes to improve the fatigue behaviour or resistance to crack initiation) for welds of large thickness sections with a minimum yield strength of 460 Mpa.

Study of the effect of the effect of welding sequence on fatigue behaviour for welds of large thickness sections with a minimum yield strength of 460 Mpa.

Execution of tests on connections of wide-flange beams to CFT columns to assess the force transfer mechanism, examining the effect of various structural details on the connection strength, stiffness and ductility.

Performance of subassemblage tests of wide-flange beams to CFT columns to assess cyclic load effects, beam attachment details, and contribution of the connection to the behaviour of the assembly.

Evaluation of deformation limit criteria for design of connections between I-shaped beams and RHS columns.

### 3. *Design Methods*

Development of approaches for selection of semi-rigid connections that generally give significant benefit by simplifying joint details, thus reducing shop and erection costs.

Assessment of the variability of connection properties.

Development of connection models for linear and nonlinear design analysis.

*Assessment and application of stiffness-based approaches for preliminary design of semi-rigid frames, with the ultimate strength checked by second order rigid plastic analysis.*

Evaluation of approaches to ensure an adequate margin of safety against loss of ductility in composite joints, including (a) applying a factor when comparing required capacity against that available, (b) relying on the reduced rotation capacity required at a joint when the moment resistance achieved in practice exceeds the design value.

Investigation of the economics of designing exterior beam-to-column connections as composite versus non-composite.

### 4. *Modelling of Connections*

Development and validation of FE models enabling a reliable approximation of the response of joints under more complicated situations than have been examined so far, for example unbalanced loading.

Refinement of the material models to be adopted in FE analysis, with particular reference to the properties of the confined concrete in composite joints.

Study of the mechanical models for approximating the cyclic response of joints in order to improve their accuracy and extend their range of applicability.

Development of standards for connection testing and reporting in order to provide suitable benchmark data for the calibration of the connection prediction models of connections under static and cyclic loading.

## 5. *Frame Behaviour*

Assessment of the need for shakedown analysis of frames with semi-rigid joints.

Evaluation of the potential use of semi-rigid construction to reduce or even eliminate bracings. This should also imply research to be carried out into the economics of semi-rigid unbraced frames in comparison with simple braced frames.

Investigation of the effect of the various aspects of structural behaviour (such as ductility demand to members and connections), which can be influenced by connection overstrength.

Reliability assessment of semi-rigid frames, based on a statistical calibration of partial safety factors for the joints.

Parametric study (numerical and experimental) of the influence of the response of column bases on the performance of frames.

Large-scale testing of subframes and full frames in order to provide benchmark data for calibration of joint models.

## 6. *Cyclic Response*

Extensive study of different welded connection solutions aimed at better defining effective and reliable detailing.

Development of retrofitting criteria and techniques of joints damaged by earthquakes.

Developments of assessment procedures for a realistic understanding of the actual behaviour of steel moment frames after their connections have been damaged by an earthquake.

Extensive investigation of bolted (rigid as well as semi-rigid) joints in order to provide design methods, and detailing and fabrication criteria, for their use in aseismic structures.

Validation of the proposed criteria for low cycle fatigue failure of joints.

## **7. Design Standards**

Development of comprehensive recommendations for the design of joints for thin walled cold-formed sections, including members in high strength steel grade.

Development of specifications for the use of innovative fasteners (e.g., the blind bolts) as well as for design of joints of innovative sections, as for example the Hollow Flange Beams.

Validation of design provisions for partial strength semi-rigid joints in aseismic frames.

Assessment of the different design criteria for the use of preloaded bolts in structural joints.

Refinement of the code specifications related to the design of fillet welds in RHS T, Y and X connections.

Development of simple design approaches consistent with Codes recommendations for the design of semi-rigid joints and frames.

## **8. State of Practice**

Cooperation among all parties involved in steel construction (i.e., scientists, designers, fabricators, erectors and engineers of record) in the "education" to new techniques and design concept.

Preparation of tools, in particular software and publications, enabling design guidance on the moment-rotation curve of connections.

Extensive site testing of pre-tensioned bolts in order to better understand the influence of various installation parameters.

Study of possible standardization of the most popular connection types.

Development of guidelines for the inspection and damaged assessment of connections in bui

APPENDIX

Attendees of the

*Third International Workshop*

*on*

*Connections in Steel Structures*

*Trento, Italy*

May 28 to 31, 1995

## WORKSHOP ATTENDEES

*Trento, Italy*

May 28 to 31, 1995

**Dr. David Anderson**

Department of Civil Engineering, University of Warwick, Coventry, United Kingdom

**Professor Jean Marie Aribert**

Laboratoire Structures, I.N.S.A. - Rennes, Rennes Cedex, France

**Professor Abolhassan Astaneh-Asl**

Department of Civil Engineering, University of California, Berkeley, California, U.S.A.

**Professor Reidar Bjorhovde**

Department of Civil Engineering, University of Pittsburgh, Pittsburgh, Pennsylvania, U.S.A.

**Dr. Ömer Bucak**

Versuchsanstalt für Stahl, Holz und Steine, Universität Karlsruhe, Karlsruhe, Germany

**Professor Luis Calado**

Department Decivil/CMEST, Instituto Superior Técnico, Lisboa Codex, Portugal

**Mr. Charles J. Carter**

American Institute of Steel Construction Inc., Chicago, Illinois, U.S.A.

**Professor André Colson**

Ecole Normale Supérieure des Arts et Industries de Strasbourg, Strasbourg  
Cedex, France

**Professor Michel Crisinel**

Ecole Polytechnique Fédérale de Lausanne, ICOM - Construction  
Métallique, Lausanne, Switzerland

**Professor Antonello De Luca**

Institute of Construction Technology, Faculty of Engineering, University of  
Naples, Naples, Italy

**Ir. Gerben D. de Winkel**

Faculty of Civil Engineering, Mechanics & Structures Division, Delft  
University of Technology, Delft, The Netherlands

**Professor Dan Dubina**

Department of Steel Structures and Structural Mechanics, Civil Engineering  
Faculty, Technical University of Timisoara, Timisoara, Romania

**Professor Lazlo Dunai**

Department of Steel Structures, Technical University of Budapest,  
Budapest, Hungary

**Professor Samuel W. Easterling**

Department of Civil Engineering, Virginia Polytechnic Institute and State  
University, Blacksburg, Virginia, U.S.A.

**Professor Duane S. Ellifritt**

Department of Civil Engineering, University of Florida, Gainesville, Florida,  
U.S.A.

**Professor Michael D. Engelhardt**

Department of Civil Engineering, University of Texas, Austin, Texas, U.S.A.

**Dr. Markus Feldmann**

Institute of Steel Construction, RWTH Aachen, Aachen, Germany

**Dr. Arvind Goverdhan**

Stanley D. Lindsey and Associates, Ltd., Marietta, Georgia, U.S.A.

**Ir. Nol Gresnigt**

Faculty of Civil Engineering, Mechanics & Structures Division, Delft University of Technology, Delft, The Netherlands

**Professor Gregory Hancock**

Centre for Advanced Structural Engineering, Civil Engineering, University of Sydney, Sydney, Australia

**Dr. Gerald Huber**

Institut für Stahlbau und Holzbau, Universität Innsbruck, Innsbruck, Austria

**Dr. Socrates A. Ioannides**

Structural Affiliates International, Inc., Nashville, Tennessee, U.S.A.

**Professor Miklos Ivanyi**

Department of Steel Structures, Technical University of Budapest, Budapest, Hungary

**Dr. Jean Pierre Jaspert**

MSM - Institut du Génie Civil, University of Liège, Liège, Belgium

**Mr. Lawrence A. Kloiber**

LeJeune Steel Company, Minneapolis, Minnesota, U.S.A

**Professor Geoff L. Kulak**

Department of Civil Engineering, University of Alberta, Edmonton, Alberta, Canada

**Professor Roger A. Laboube**

Department of Civil Engineering, University of Missouri Rolla, Rolla, Missouri, U.S.A.

**Professor Roberto T. Leon**

Department of Civil Engineering, University of Minnesota, Minneapolis,  
Minnesota, U.S.A.

**Mrs. Li Hua Lu**

Faculty of Civil Engineering, Section Mechanics & Structures, Delft  
University of Technology, Delft, The Netherlands

**Mr. James O. Malley**

H.J. Degenkolb Associates, Engineers, San Francisco, California, U.S.A.

**Professor Federico Mazzolani**

Institute of Construction Technology, Faculty of Engineering, University of  
Naples, Naples, Italy

**Dr. David Moore**

Building Research Establishment, Garston, Watford, United Kingdom

**Professor Thomas M. Murray**

Department of Civil Engineering, Institute and State University, Virginia  
Polytechnic, Blacksburg, Virginia, U.S.A.

**Professor David A. Nethercot**

Department of Civil Engineering, University of Nottingham, Nottingham,  
United Kingdom

**Professor Yasuhiro Ohtani**

Department of Architecture and Civil Engineering, Kobe University, Kobe,  
Japan

**Professor Jeff A. Packer**

Department of Civil Engineering, University of Toronto, Toronto, Ontario,  
Canada

**Professor Eugène Piraprez**

C.R.I.F. Section Construction Metallique, University of Liège, Liège,  
Belgium

**Dr. Clinton O. Rex**

Department of Civil Engineering, Virginia Polytechnic Institute and State University, Blacksburg, Virginia, U.S.A.

**Professor James M. Ricles**

Department of Civil Engineering, Fritz Engineering Laboratory, Lehigh University, Bethlehem, Pennsylvania, U.S.A.

**Mr. Ivor Ryan**

Centre Technique Industriel de la Construction Métallique, St. Remy Les Chevreuse, France

**Professor Jan W.B. Stark**

TNO Building and Construction Research, Delft University of Technology, Delft, The Netherlands

**Mr. Martin Steenhuis**

TNO Building and Construction Research, Delft University of Technology, Delft, The Netherlands

**Dr. William A. Thornton**

Cives Engineering Corporation, Roswell, Georgia, U.S.A.

**Professor Ferdinand Tschemmernegg**

Institut für Stahlbau und Holzbau, Universität Innsbruck, Innsbruck, Austria

**Professor Didier Vandegans**

C.R.I.F. Section Construction Metallique, University of Liège, Liège, Belgium

**Mr. Peter Verinder**

Australian Institute of Steel Construction, North Sydney, Australia

**Dr. Frantisek Wald**

Faculty of Civil Engineering, Czech Technical University, Praha, Czech Republic

**Dr. Klaus Weynand**

Institute of Steel Construction, RWTH Aachen, Aachen, **Germany**

**Professor Donal W. White**

School of Civil Engineering, Purdue University, West Lafayette, Indiana,  
**U.S.A.**

**Professor Joseph A. Yura**

Department of Civil Engineering, University of Texas, Austin, Texas, **U.S.A.**

**Professor Riccardo Zandonini**

Department of Structural Mechanics, Faculty of Engineering, University of  
Trento, Trento, **Italy**

# AUTHOR INDEX

- Aboutaha, R. S. 381  
Adány, S. 269  
Ahmed, B. 259  
Ales, Jr, J. M. 23  
Anderson, D. 223, 527  
Aribert, J.-M. 11  
Astaneh-Asl, A. 391
- Benussi, F. 57  
Bjorhovde, R. 331  
Borgsmiller, J. T. 169  
Bucak, Ö. 115
- Calado, L. 371  
Carril, J. L. 403  
Carter, C. J. 423  
Castiglioni, C. 371  
Chapman, B. 563  
Colson, A. 279, 331  
Crisinel, M. 33
- De Luca, A. 289  
de Winkel, G. D. 137  
Dubina, D. 349  
Dunai, L. 269
- Easterling, W. S. 1  
Ellifritt, D. S. 179  
Engelhardt, M. D. 381
- Feldmann, M. 453  
Frank, K. H. 381  
Fukumot, Y. 47  
Fukumoto, Y. 269
- Giusse, S. 321  
Goverdhan, A. V. 505  
Grecea, D. 349  
Gresnigt, A. M. 77
- Hancock, G. 89, 563  
Hoffman, J. J. 211  
Hogan, T. 563
- Ioannides, S. A. 191
- Iványi, M. 309
- Janss, J. 67  
Jaspart, J.-P. 159, 321, 441
- Kloiber, L. A. 493  
Kulak, G. L. 515
- LaBoube, R. A. 403  
Le-Wu Lu 99  
Leon, R. T. 211  
Li, T. Q. 259  
Lindsey, S. D. 505  
Lu, L. H. 127
- Malley, J. O. 553  
Mang F. 115  
Mazzolani, F. M. 413  
Md Tahir, M. 527  
Mébarki, A. 331  
Meng, R. L. 361  
Miller, A. S. 179  
Moore, D. B. 535  
Murray, T. M. 169, 361  
Nethercot, D. A. 57, 259, 473
- Ohtani, Y. 47
- Packer, J. A. 463  
Piluso, V. 413  
Ping Ren 33  
Piraprez, E. 483
- Queiroz, G. 237
- Rex, C. O. 1  
Ricles, J. M. 99
- Sabol, T. A. 381  
Sedlacek, G. 453  
Sellier, A. 331  
Sokol, Z. 249  
Sooi, T. K. 99  
Sputo, T. 179  
Stammet, L. 115

590 Author Index

Stark, J. W. B. 77, 431  
Steenhuis, M. 249, 441  
Syam, A. 563

Thornton, W. A. 149, 201  
Tschemmerneegg, F. 237  
Tsuji, B. 47

Undershute, S. T. 515

Vandegans, D. 67  
Vermaas, G. 99

Wai-Fah Chen 299  
Wald, F. 249  
Wardenier, J. 127, 137  
Wei-Wen Yu 403  
Weynand, K. 441, 453  
White, D. W. 299

Xiao-Ling Zhao 89

Yura, J. A. 23

Zaharia, R. 349  
Zandonini, R. 57

# KEYWORD INDEX

- 1-beam to RHS column connections 127
- Analysis 505
- Analytical approach 11
- Analytical model 137
- Analytical models 127
- Anchor bolts 249
- Annex J of eurocode 3 321, 441
- Axial force 201
  
- Beam flange buckling 57
- Beam-column connection 33
- Beam-to-column connections 371
- Beam-to-Girder 1
- Bearing 403
- Bolt 77, 403
- Bolted 563
- Bolted connection 77
- Bolts 1, 169, 515
- Bridge bearing 23
- Buckling 23
- Buildings 223, 527
- Butt welds 89
  
- Characteristic equations 299
- Codification 413
- Cold-formed 89, 403, 563
- Collapse load factors 211
- Column 179
- Column base 249
- Column-bases 309
- Comparison with tests 441
- Compatibility 493
- Component method 159, 441
- Component model 269
- Components method 279
- Composite 223, 505
- Composite beam 11
- Composite connections 33, 57, 67
- Composite construction 259, 473
- Composite joint 11
- Composite, 1
- Compressive strength 23
- Concentric workpoints 493
- Concrete 1
- Concrete bearing 23
- Concrete crushing 57
- Concrete filled profile 67
- Concrete filled tube (CFT) 99
- Connection 179, 279, 381, 403, 563
- Connection capacity 299
- Connection classification 299
- Connection modeling 269
- Connection stiffness 299
- Connections 89, 169, 191, 259, 289, 361, 371, 463, 473, 505, 553
- Connections, developing 493
- Constructability 493
- Constructional steelwork 279
- Corrosion 77
- Cost 527
- Curve 191
- Cyclic behaviour 289
- Cyclic load 381
  
- Damage 371, 391
- Damage assessment 553
- Deflections 191
- Deformation 403
- Degree of shear connection 11
- Design 169, 223, 299, 331, 463, 505, 527
- Design aids 159
- Design moment 159
- Design resistance 321
- Detailing 413
- Diaphragm 99
- Double angles 201
- Ductile shear connection 11
- Dynamic-rotational-check 453
  
- Earthquake 413
- Earthquake damage 553
- Earthquake fatigue 453
- Electronic data exchange 423
- End plate modified 493
- End rotation 201
- End slip 11
- End-plate 169, 361
- End-plates 535

- Endplate connections 259  
Equilibrium 149  
Eurocode 223, 527  
Eurocode 3 249, 441  
Experimental 99, 403  
Experimental analysis 57  
Experimental data 237, 413  
Experimental program 269  
Experimental research 127  
Experimental tests 137, 321, 371  
Experiments 23, 249  
Extension of rebars 11  
External column connections 57
- Failure 371  
Fatigue 23, 371  
FEM models 269  
Fillet welds 89  
Fin-plates 535  
Finite and infinite joint models 237  
Finite element 1, 11  
Finite element analyses 127, 137, 259  
Finite-element 279  
Fit for purpose 493  
Fitting 191  
Fracture 381  
Frame action 149  
Frame tests 57  
Frames 223, 473, 527  
Friction 515
- Global safety 453  
Gomez model 67  
Gravity load simulator 309  
Gussets 149
- Hardness 483  
High strength friction grip bolt 77, 431  
High-strength 515  
Hollow section 67  
Hot-rolled 89, 563  
Hysteretic loops 371
- I-beam to CHS column connection 137  
Induced moment 201  
Inelastic analysis 391  
Initial stiffness 441  
Injection bolt 77  
Instability 23  
Installation 515  
Interaction 321  
Iso bolts 483
- Joint 57, 349  
Joint deformations 237  
Joint models 237  
Joints 223, 463, 473, 527
- Large-scale tests 309  
Life safety 391  
Limit states 149, 331  
Load multiplier 349  
Low-cycle-fatigue 453  
LRFD 423  
Lubrication 515
- Manufacturer 483  
Mechanistic models 299  
Methods of preloading 483  
Mild steel 1  
Mixed connection 47, 269  
Modelization 279  
Modelling 289  
Moment 169, 361  
Moment connection 99  
Moment connections 159, 535  
Moment resisting frame (MRF) 99  
Moment rotation characteristic 441  
Moment-rotation behaviour 33, 269  
Moment-rotation curve 11, 279  
Moment-rotation equations 299
- New joint model 237  
Non-orthogonal 149  
Non-proportional loading 211  
Normal force influence 249  
Northridge earthquake 381, 391, 553  
Numerical analysis 259  
Numerical model 33  
Numerical simulation 11  
Numerical simulations 321  
Nut height 483
- Panel zone 99  
Partial strength connections 211  
Partial-strength 527  
Partially restrained connections 211, 423  
Partially-restrained 505  
Plastic analysis 211, 473  
Plastic design 211, 453  
Plate to CHS column connection 137  
Plate to RHS column connections 127  
PR frames 211, 505  
Prediction method 33  
Preliminary design 211  
Preload 515  
Preloaded bolts 431  
Prying action 201
- QST 115

- Rectangular hollow sections 89, 463
- Reference length 159
- Reinforcing steel 1
- Reliability 331, 463
- Reliability index 331
- Repair of bridges 77
- Repair techniques 553
- Resin 77
- Resistance 223
- Rivet 77
- Robustness 201, 535
- Rocker bearing 23
- Rolled beams 115
- Rotation 453
- Rotation capacity 33, 57, 223
- Rotation supply 413
- Rotation-waterline 453
  
- Safety 331
- Seat 179
- Second-order effects 211
- Seismic 99, 361, 381
- Seismic design 423, 553
- Seismic response 349, 413
- Semi rigid 289, 349
- Semi rigid connections 67
- Semi rigid design 249
- Semi rigid joints 237
- Semi-rigid 191, 279, 321, 331, 527
- Semi-rigid (PR) 211
- Semi-rigid connections 309
- Semi-rigid joints 57
- Semi-rigorous 191
- Serviceability 191, 403
- Shape parameter 299
- Shear connections 259
- Shear end plates 201
- Shear resistance 159
- Shear studs 1
- Simple connections 535
- Simplified approach 349
- Slip resistant 77, 431
- Slotted-bolted connections 423
- Snug-tight 431
- Software 505
- Specifications 463
- Spring 1
- Spring model 441
- Stability 391
- Standardized 563
- Static behaviour 127
- Static response 349
- Static strength 137
- Steel 169, 223, 331, 361, 381, 515, 527
- Steel framed buildings 553
- Steel frames 309, 349
- Steel joints 321, 441
- Steel members 47
- Steel spandrel beam 99
- Steel structures 249, 391, 463, 563
- Steel-concrete structure 269
- Stiffened 179
- Stiffness 67, 159, 191, 223
- Stiffness coefficient 441
- Stiffness model 441
- Stiffness of joints 441
- Stiffness prediction 249
- Stiffness variability 331
- Strain 1
- Strength formula 137
- Strength formulae 127
- Strength variability 331
- Stress 1
- Structural coefficient 413
- Structural design 473
- Structural frame design 33
- Structures 331
- Subassemblage tests 57
  
- Tapered washers 483
- Tee connections 201
- Tees 423
- Tests 149, 169, 361
- Threaded studs 67
- Tightening 431, 483
- Top & seat connections 289
- Toughness, through thickness 493
- Transformation problems 237
- Tree beam 493
- Truss 1
- Tubes 463
- Tubular connections 423
- Turn-of-nut method 431
- Torque and turn method 431
- Torque control method 431
  
- Uniform 149
  
- Validation 259
  
- Web 179
- Web angle cleats 535
- Weld 381
- Welded 179, 563
- Welded connections 391
- Welded steel moment frames 391
- Welding 463
- Welds 1, 89
- Width-to-thickness ratio 413
- Wind-moment corrections 535

Yield line 179

Yield strength 115

# **Connections in Steel Structures III**

**Behaviour, strength & design**

**Proceedings of the  
Third International  
Workshop**

**Italy  
29-31 May 1995**

**Composite Connections**

**Special Connections**

**Design Methods**

**Modelling of Connections**

**Frame Behaviour**

**Cyclic Response**

**Design Standards**

**State of Practice**

**Connections in Australia**

**Current Research Needs for**

**Connections in Steel Structures**

**Appendix**

ISBN 0-08-042821-5



9 780080 428215